THE GEOMECHANICAL AND HYDROGEOLOGICAL PROPERTIES OF WEATHERED CHALK.

A thesis submitted to Imperial College London in partial fulfilment for the Degree of Doctor of Philosophy and for the Diploma of Imperial College.

By

Anthony Maher

Department of Civil and Environmental Engineering

Imperial College London

London SW7 2AZ

April 2024

Abstract

The Upper Cretaceous Chalk Group of the UK covers a significant area of the south-east and east of England, and underlies several major cities, including London. This widespread distribution has led to several major infrastructure projects involving chalk. Weathering in chalk is difficult to identify and its distribution is poorly documented within current literature. Weathering is known to affect both geomechanical and hydrogeological properties but there are uncertainties as to the extent of these physical changes, both on the material and rock mass scale.

This study combines observational field techniques with industry best-practice to investigate chalk weathering. It introduces novel field-based uniformity surveys using non-destructive methods and develops novel sampling methods to enable laboratory testing. Laboratory testing underpins observations made in the field and allows characterisation of de-structured chalk.

Field measurements have shown that current industry standard methodologies produce consistently higher CIRIA density grades compared measured grades. Laboratory testing demonstrated that CIRIA D-grade chalks are observed to be one CIRIA grade lower than structured chalks and are not close to saturation like their parent material. Geomechanical testing showed that de-structured chalk is 11 – 12 times weaker than structured chalk and can behave as both a stiff soil or weak rock (exhibiting both brittle and ductile failure), while permeability testing identified a reduction in permeability with increasing effective stress.

This research has developed knowledge of the types of weathering present at select field sites and has characterised their extent. Novel methods of sampling and testing have been developed, which has enabled the characterisation of geomechanical and hydrogeological properties of de-structured chalk deposits. Laboratory testing has identified significant differences between de-structured chalk deposits compared to parent material, and has produced quantified useful parameters. This thesis lays a clear path for the further study of chalk weathering.

Statement of Originality

This thesis comprises work that is my own except where due referencing and acknowledgement is made.

Tony Maher

London, April 2024

Declaration

The copyright of this thesis rests with the author. Unless otherwise indicated, its contents are licensed under a Creative Commons Attribution-Non Commercial 4.0 International Licence (CC BY-NC).

Under this licence, you may copy and redistribute the material in any medium or format. You may also create and distribute modified versions of the work. This is on the condition that: you credit the author and do not use it, or any derivative works, for a commercial purpose.

When reusing or sharing this work, ensure you make the licence terms clear to others by naming the licence and linking to the licence text. Where a work has been adapted, you should indicate that the work has been changed and describe those changes.

Please seek permission from the copyright holder for uses of this work that are not included in this licence or permitted under UK Copyright Law.

Tony Maher

London, April 2024

Acknowledgements

Foremost, I am extremely grateful to my primary supervisor, Dr. James Lawrence, who set out this research problem and then subsequently supported me in my study of this. Without James' strong support and exceptional enthusiasm for chalk, I believe I would have lost momentum working on this project owing to challenges presented. Consequently, I have developed an exceptional enthusiasm for chalk myself.

I am grateful to my secondary supervisors; Dr. Phillipa Mason, Prof. Richard Ghail and Dr. Ken Vinck. Both Phillipa and Richard provided me with invaluable guidance, of which I am most appreciative of. My thanks to Ken for his generosity of expertise, time and patience with me in the laboratory.

The project was funded by EPSRC and ICO CDT. I would like to thank both Dr. Mike Bluck and Dr. Jon Tate for administering and supporting the program. I would also like to thank and acknowledge the late Prof Luc Vandeperre, who was the head of the ICO-CDT. Luc was instrumental in my undertaking this study, so for this I am grateful.

In terms of laboratory work, I must thank Messrs Prash Hirani and Steve Ackerley, whose patience, skill and knowledge were invaluable and have enabled my research to run smoothly. I really appreciate the time that both Prash and Steve extended to me.

I would like to thank Professor Catherine O'Sullivan for tuition on the MasterSizer and Dr. Marcus Yio for his tuition and insight on the SEM. Outside of Imperial College, I would like to thank Professor Rory Mortimore for his expertise in this area – one afternoon with Prof Mortimore was the equivalent of many days in the field. I would like to thank Dr Neill Hadlow for his advice on chalk ground models. I would like to acknowledge and thank Professor Bill Murphy and Mr. Kirk Handley, who kindly allowed me time at their laboratory at the University of Leeds.

I acknowledge and thank the MSc student researchers who I supervised and contributed to this research; Samuel Maclean, Tianren Shi, Suzie Marley, Erin Cullen and Elly Harmen.

My colleagues and friends; Ant Carpenter (who also served for scale in several field photos), Julia Hill and Alex Connelly, who took the time to proofread my work, despite protestations that they were not or 'no longer were geologists'. Their efforts are greatly appreciated.

Finally, I would like to acknowledge my parents and my family for their enduring support.

Contents

Abstract i
Statement of Originality ii
Declaration iii
Acknowledgements iv
Figures xi
Tables xvi
Equations xviii
List of abbreviations xix
1 Introduction 1
1.1 Project aim 2
1.2 Project objectives 2
1.3 Thesis structure 4
1.4 Chapter summary 6
2 Literature review 7
2.1 Introduction 7
2.2 Distribution of chalk in the UK 8
2.3 The formation of chalk 9
2.3.1 Deposition and sedimentation of chalk 10
2.3.2 Lithification and diagenesis of chalk 11
2.4 Stratigraphy 13
2.4.1 The development of a unified chalk stratigraphy 13
2.4.2 Stratigraphic framework of the Southern Province Chalk Formations 16
2.5 The geology of east Sussex 22
2.5.1 Geological map 22
2.5.2 Geological history 22
2.6 The classification of chalk 26
2.6.1 Classifications of carbonate lithofacies 26
2.7 The engineering classification of chalk 27
2.8 The physical properties of chalk material 35
2.8.1 Material properties of intact chalk 35
2.8.2 Material properties of de-structured Chalk 37
2.8.3 Permeability 40
2.9 Types of weathering in Chalk 41
2.9.1 Water weakening and karstification 41

2.9.2 Haloclasty 44
2.9.3 Cryoturbation and ice action 45
2.10 Chapter summary 49
3 Site selection 51
3.1 Introduction 51
3.2 Site reconnaissance 52
3.2.1 Sites visited 52
3.2.2 Itinerary 1: Brighton Marina to Peacehaven Steps 54
3.2.3 Itinerary 2: Newhaven Harbour, Splash Point, Cuckmere Haven 55
3.2.4 Itinerary 3: Birling Gap to Cow Gap 55
3.2.5 Itinerary 4: Holywell and Foyle Way 57
3.2.6 Itinerary 5: Breaky Bottom Farm (Lewes), 3 Ponds caravan site, Caburn Pit and Glynde Pit. 57
3.2.7 Summary of reconnaissance 58
3.3 Selection of research sites 59
3.4 The research sites 60
3.4.1 Roedean Access Point, Roedean (UK National Grid: TQ 34380 03182) 63
3.4.2 Portobello Outfall, Peacehaven (UK National Grid: TQ 39380 10173) 65
3.4.3 Newhaven Harbour, Newhaven (UK National Grid: TV 44620 99947) 67
3.4.4 Birling Gap, East Dean (UK National Grid: TV 55382 95990) 69
3.5 Chapter summary 70
4 Fieldwork methodology 71
4.1 Introduction 71
4.1.1 Aims of fieldwork 72
4.1.2 Previous weathering field studies 72
4.2 Field study methodology 81
4.2.1 Data collection and observation 81
4.2.2 Initial geological observations 82
4.2.3 Uniformity survey 82
4.2.4 Adapted CIRIA field density 84
4.3 Sampling methodology 85
4.3.1 Bulk sampling methodology 85
4.3.2 Undisturbed sampling methodology development 85
4.3.3 Developed sampling methodology 94
4.4 Chapter summary 95
5 Laboratory methodology 96

5.1 Introduction 96
5.2 Index tests 97
5.2.1 Natural moisture content (NMC) 100
5.2.2 Saturated moisture content (SMC) 100
5.2.3 Intact dry density (IDD) 101
5.2.4 Calculation of void ratio (e) and porosity (n) 103
5.3 The slake durability test 105
5.3.1 Samples 105
5.3.2 Slaking fluid preparation 107
5.3.3 Equipment 108
5.3.4 Sample preparation 109
5.3.5 Undertaking the slake durability test 109
5.3.6 Measurements after testing 110
5.3.7 Calculations 110
5.3.8 Reporting results 110
5.4 Permeability testing 111
5.4.1 Tests required 113
5.4.2 Equipment 114
5.4.3 Sample preparation 114
5.4.4 Testing 117
5.5 Unconfined compressive strength (UCS) 121
5.5.1 Samples 121
5.5.2 Equipment 122
5.5.3 Sample preparation 122
5.6 The Brazilian tensile test 127
5.6.1 Samples 127
5.6.2 Equipment 127
5.6.3 Sample preparation 127
5.7 Triaxial testing 129
5.7.1 Samples 130
5.7.2 Equipment 131
5.7.3 Sample preparation 131
5.8 Modification of the Bushinsky technique for Dm and Dc grade chalks 135
5.8.1 Samples 136
5.8.2 Equipment 137
5.8.3 Sample preparation 137

5.8.4 Data from processed image 137
5.9 Modified particle size distribution test 139
5.9.1 Equipment 139
5.9.2 Sample Preparation 139
5.9.3 Sieving the sample and particle separation 139
5.9.4 Proposed classification workflow 141
5.10 Chapter summary 142
6 Fieldwork observations 143
6.1 Introduction 143
6.1.1 Summary table of weathering observed at research locations. 145
6.2 Weathering characteristics 146
6.2.1 Roedean access point 146
6.2.2 Portobello Outfall, Peacehaven 157
6.2.3 Newhaven Harbour, Newhaven 168
6.2.4 Birling Gap, East Dean 174
6.3 Discontinuity survey 181
6.3.1 Scanline results 181
6.3.2 Scanline survey; Roedean 185
6.3.3 Scanline survey; Portobello outfall 188
6.3.4 Scanline survey; Newhaven Harbour 191
6.3.5 Scanline survey; Birling Gap 193
6.3.6 Discontinuity survey summary 195
6.4 Chapter summary 196
7 Uniformity Survey 198
7.1 Introduction 198
7.2 Results – Research site data 200
7.2.1 Roedean research site 200
7.2.2 Portobello Outfall research site 216
7.2.3 Newhaven Harbour research site 238
7.2.4 Birling Gap research site 255
7.3 Regional data summary 264
7.4 Chapter summary 271
8 Laboratory results 274
8.1 Introduction 274
8.2 Baseline index testing to establish the effects of weathering on chalk properties 276
8.2.1 Intact dry density testing results 276

8.2.2 Laboratory measured IDD versus Equotip derived IDD results 281
8.2.3 Moisture content 284
8.2.4 Void ratio and porosity 290
8.2.5 Water weakening of D-grade Chalk 292
8.2.6 Particle size distribution of D-grade chalk 294
8.2.7 Modification of the Bushinsky technique 296
8.3 Slake durability of Southern Province chalks 301
8.3.1 Standard slake durability procedure 302
8.3.2 Comparison of Seaford and Newhaven Chalk Formations from baseline testing 308
8.3.3 The effects of slaking fluid and moisture content on artificial chalk weathering 310
8.3.4 Slake durability of CIRIA chalk grades 316
8.3.5 Slake durability at I_d2 versus IDD 320
8.4 Permeability of de-structured chalk 322
8.5 Geomechanical properties of de-structured chalk 325
8.5.1 Unconfined compressive strength 325
8.5.2 Brazilian tensile strength of D-grade chalk 333
8.5.3 Triaxial strength testing of D-grade chalk 337
8.5.4 Mohr-Coloumb parameters 337
8.6 SEM analysis 343
8.7 Chapter summary 345
9 Summary and conclusions 350
9.1 Introduction 350
9.2 Summary discussion and conclusion of main findings 351
9.2.1 Fieldwork summary and conclusions 351
9.2.2 Uniformity Survey summary and conclusions 353
9.2.3 Laboratory testing summary and conclusions 356
9.2.4 Slake durability Summary and conclusions 359
9.2.5 Permeability summary and conclusions 360
9.2.6 Geomechanical testing summary and conclusions 362
9.2.7 SEM summary and conclusions 365
9.3 Strength and limitations of research 365
9.3.1 Strengths 365
9.3.2 Limitations 366
9.4 Future work 366
9.4.1 Proposed workflow classification as a predictive toolbox 367
9.4.2 Future fieldwork 371

9.4.3 Future laboratory work 372
9.4.4 Future modelling work 372
9.4.5 Future applications and implications for industry and academia 372
9.5 Conclusion 374
References 376
Appendix A - CIRIA grading 384
Appendix B - Quadrat photographs 390
Appendix C – Quadrat raw data 415
Appendix D - Index tests 429
Appendix E - Slake durability 441
Appendix F - Permeability 443
Appendix G - Brazilian tensile testing 444
Appendix H - SEM Analysis 447
Appendix I – Classification workflows 461

Figures

Figure 2-1 The distribution of Chalk in the United Kingdom and county borders (adapted from Lord et al. 2002 and Edina Digimap, 2024). 8
Figure 2-2 The development of chalk stratigraphy over time (BGS Earthwise, 2015)..... 15
Figure 2-3 Lithostratigraphy of the Southern Province of the UK Chalk (adapted from Lord et al. 2002). 17
Figure 2-4 Geological map of research area within east Sussex, with the extents of Roedean to Birling Gap (Digimap, 2023). 22
Figure 2-5 The Folk classification system for carbonate rocks (after Folk, 1959)..... 26
Figure 2-6 The Dunham classification system for carbonate rocks (after Dunham, 1962). 27
Figure 2-7 Structured and de-structured chalks reflecting CIRIA grades..... 31
Figure 2-8 NMC versus IDD with SMC line plotted (Mortimore et al. 2004). 37
Figure 2-9 Schematic of dissolution features (adapted from Lord et al. 2002). 42
Figure 2-10 Schematic of Quaternary glaciation limits with respect to the distribution of Chalk in the United Kingdom; Northern Ireland omitted (adapted from Gibbard and Clark (2011)). 46
Figure 2-11 A conceptual ground model of hill and valley deposits, with landform associated weathered deposits in cross section (Mortimore, 2014). 47
Figure 2-12 Brecciation types 1 & 2 (examples taken from (Murton, 2018a) (annotation of 'powdery chalk matrix' by Murton – chalk putty)..... 48
Figure 3-1 Site location map (adapted from Google-Earth (2021)). 60
Figure 3-2 Simplified cross-section of the coastal section between Brighton and Newhaven Harbour illustrating field locations 1-3 in relation to periclinal folds (adapted from Mortimore 2021). 61
Figure 3-3 Geological map of East Sussex showing site locations in relation to Anticlines and Synclines that control the distribution of Chalk formations (adapted from Mortimore (2021) and Digimap (2023)). 62
Figure 3-4 Site overview; Roedean Access Point (adapted from Edina Digimap 2021 (Maher, 2021c). 63
Figure 3-5 Photograph of Roedean Access Point (looking east). 64
Figure 3-6 Site overview; Portobello Outfall, Peacehaven (adapted from Edina Digimap (Maher, 2021b)). 65
Figure 3-7 Photograph of weathering at Portobello Bay, oriented west of Portobello Outfall, Peacehaven (looking east). 66
Figure 3-8 Site overview showing sample locations; Newhaven Harbour (adapted from Edina Digimap (Maher, 2021a)). 67
Figure 3-9 Dissolution features associated with faulting and discontinuities in the Tarrant Chalk Member, with overlying Tertiary sediments and Paleogene erosional surface, Newhaven Harbour (looking north). 68
Figure 3-10 Site overview; Birling Gap, East Dean (adapted from Edina Digimap (Maher, 2022a)). 69
Figure 4-1 The Proceq SilverSchmidt L-Type digital Schmidt hammer; 1 – traditional plunger, 2 – main body housing, 3 – USB and power port, 4 – digital display, 5 – power button, 6 – mushroom head plunger attachment (Proceq, 2021)..... 75
Figure 4-2 Proceq OS120-PT pendulum hammer; 1 – Outer semi-circular housing, 2 – rebound number gauge, 3 – operation switch, 4 – handle, 5 – operating mechanism with vertical to horizontal switch, 6 – pendulum with hammer face (Proceq, 2023). 77
Figure 4-3 Left - schematic of Equotip Leeb impact tester (left); 1 – loading tube, 2 – guide tube, 3 – induction coil and housing, 4 – operation switch, 5 – connection cable to data logger, 6 – support

ring, 6a – support ring, 7 – impact body, 8 – tungsten carbide test sphere, 9 – impact spring, 10 – loading spring, 11 – catch chuck and 12 – test material. Right - photograph of impact tester (adapted from Kompatscher (2004)).....79
Figure 4-4 Photograph of quadrat used for data collection constraint.....83
Figure 4-5 A 52 mm external diameter hollow drill core with attachment to fit SDS drill.....86
Figure 4-6 Mis-shaped and warped Culver Chalk sampled with 52 mm core barrel.....87
Figure 4-7 Press-in sampler adapted from a car exhaust pipe.....88
Figure 4-8 A – ELE branded U38 sampler, B – U38 sampler after cutting due to inability to extrude sample, C – highly oxidised surfaces of tuber inner wall.....89
Figure 4-9 Steel U38 sampling tube.....90
Figure 4-10 Left - aluminium sampling tube damaged by obstruction and retaining sample, right – steel sampling tube damaged by obstruction and retaining sample.....91
Figure 4-11 Ideal sampling equipment for de-structured grade chalks; 1 – 1.5kg hammer, 2 – jarring rig, 3 – aluminium sacrificial U38 sampling tube, 4- steel re-useable U38 sampling tube, 5 – head adapter.....92
Figure 5-1 Eureka jar and receptacle used for intact dry density testing.....102
Figure 5-2 Slake durability machine.....108
Figure 5-3 Slake durability drum (2.0 mm wire mesh).....108
Figure 5-4 Sampling locations Portobello Outfall, Telscombe (Maher, 2022c).....111
Figure 5-5 Sampling locations, Birling Gap, East Dean (Maher, 2022b).....112
Figure 5-6 Schematic of control board for the Bishop-Wesley triaxial cell; permeability configuration.....114
Figure 5-7 Bishop and Wesley triaxial cell.....130
Figure 5-8 Dc grade Seaford Chalk before and after the modified Bushinsky technique.....136
Figure 5-9 Seaford Chalk binarised for image processing after the modified Bushinsky technique..136
Figure 5-10 Proposed classification workflow for de-structured chalks (refined in future work section of Chapter 9).....141
Figure 6-1 Roedean Access Point.....146
Figure 6-2 Variability of weathering grade; Roedean access point (increasing grade with stratigraphic depth).....148
Figure 6-3 Roedean access point; cryoturbated involutions and changes in chalk textures.....149
Figure 6-4 aquiclude layers at Roedean, resulting in discrete laterally extensive weathering of beds.....150
Figure 6-5 Further slaking and material shedding of previously cryoturbated material, Roedean....151
Figure 6-6 Discrete weathering at proximity to the web of three intersecting discontinuities.....152
Figure 6-7 Younging relationships, Roedean.....153
Figure 6-8 Application of CIRIA grading to cryoturbated lobes; Roedean.....156
Figure 6-9 Map displaying areas of study at Portobello Outfall, Telscombe Cliffs.....157
Figure 6-10 Telscombe Cliffs – Portobello Bay; distribution of de-structured and structured chalk grades.....159
Figure 6-11 Discontinuity driven weathering observed at Portobello Bay, with A showing the distribution of faults and B and C showing blocky material loss.....161
Figure 6-12 Newhaven Chalk Formation observed to the west of Portobello Outfall.....162
Figure 6-13 Material loss from weathered dry valley during intense precipitation.....163
Figure 6-14 Younging relationships, Portobello.....164
Figure 6-15 Schematic map and cross-section of access to Portobello Outfall; A and B denote puttified dry valley deposits.....167
Figure 6-16 CIRIA grades at Castle Hill, Newhaven Harbour.....168

Figure 6-17 Overlying Woolwich Beds, fining up-sequence from glauconitic sands to lignitic clays, with sulphur-rich jarosite bands. 170
Figure 6-18 Culver Chalk Formation overlain by Tertiary deposits; Castle Hill, Newhaven Harbour. 170
Figure 6-19 Younging relationships, Newhaven Harbour. 172
Figure 6-20 Field photograph with schematic equivalent illustrating the distribution of the dry valley at Birling Gap (adapted from Adriano (2023)). 175
Figure 6-21 Schematic of weathered valley at Birling Gap, denoting the distribution of weathering grades (adapted from work by Asoni et al. 2018). 176
Figure 6-22 Dissolution features, Birling Gap, East Dean. 177
Figure 6-23 Younging relationships, Birling Gap. 178
Figure 6-24 Geological map of study sites with strike orientation data (adapted from Edina Digimap 2023). 184
Figure 6-25 Roedean scanline measurements. 187
Figure 6-26 Portobello Outfall scanline. 190
Figure 6-27 Newhaven Harbour scanline 192
Figure 6-28 Birling Gap scanline 194
Figure 7-1 Schematic cross-section of Roedean access point. 200
Figure 7-2 Roedean access point, SilverSchmidt quadrats 1 – 3 (white squares denote null readings). 202
Figure 7-3 Roedean access point, SilverSchmidt quadrat 4 (white squares denote null readings) 203
Figure 7-4 Roedean access point, SilverSchmidt quadrats 5 – 6 (white squares denote null readings). 204
Figure 7-5 Roedean access point, SilverSchmidt quadrats 7 – 8 (white squares denote null readings). 205
Figure 7-6 Roedean access point, Equotip quadrats 1 – 2 (white squares denote null readings) 208
Figure 7-7 Roedean access point, Equotip quadrats 3 – 4. 209
Figure 7-8 Roedean access point, Equotip quadrat 5 and descriptive statistics. Quadrat 5 is split into three discreet blocks based on texture; A – grade A1 competent chalk, B – diagonal discontinuity underlain by a widely spaced anastomosing flaser marl and C – a horizontal band of flaser marl with a tight anastomosing structure. Blocks are described by statistical distribution of IDD. 211
Figure 7-9 Roedean access point, Equotip quadrat 6. 213
Figure 7-10 Schematic cross section of Portobello Outfall, Telscombe Cliffs 217
Figure 7-11 Portobello Outfall, quadrat 1 (white squares denote null readings) 218
Figure 7-12 Portobello Outfall, quadrat 2 (white squares denote null readings) 219
Figure 7-13 Portobello Outfall, quadrat 3 (white squares denote null readings) 219
Figure 7-14 Portobello Outfall, quadrat 4 (white squares denote null readings) 220
Figure 7-15 Portobello Outfall, quadrats 1 - 4 and descriptive statistics. 221
Figure 7-16 Portobello Outfall, quadrat 5 (white squares denote null readings) 224
Figure 7-17 Portobello Outfall, quadrat 5 discrete blocks. 225
Figure 7-18 Portobello quadrat 6 – heat maps (white squares denote null readings). 228
Figure 7-19 Portobello Outfall, quadrat 7 (white squares denote null readings) 229
Figure 7-20 Portobello Outfall, quadrat 7 - discrete blocks. 230
Figure 7-21 Portobello Outfall, quadrat 8 (white squares denote null readings) 233
Figure 7-22 Portobello Outfall, quadrat 8 - discrete blocks. 234
Figure 7-23 Schematic field sketch 1; Newhaven Harbour. 239
Figure 7-24 Schematic field sketch 2; Newhaven Harbour. 240
Figure 7-25 Newhaven Harbour, quadrats 1 – 3 (white squares denote null readings) 241
Figure 7-26 Newhaven Harbour, quadrat 1 - discrete blocks. 242

Figure 7-27 Newhaven Harbour, quadrat 2 - discrete blocks. 244
Figure 7-28 Newhaven Harbour, quadrat 3 - discrete blocks. 246
Figure 7-29 Newhaven Harbour, quadrat 4. 247
Figure 7-30 Newhaven Harbour, quadrat 4 - discrete blocks. 248
Figure 7-31 Newhaven Harbour, quadrat 4 - discrete line of discontinuity and heat map. 252
Figure 7-32 Newhaven Harbour, quadrat 5. 253
Figure 7-33 Schematic cross-section; Birling Gap, East Dean. 257
Figure 7-34 Birling Gap, quadrat 1 versus quadrat 5 (de-structured chalk versus structured chalk – white squares denote null readings). 259
Figure 7-35 Birling Gap, quadrat 2 (white squares denote null readings). 260
Figure 7-36 Birling Gap, quadrat 3. 261
Figure 7-37 Birling Gap, quadrat 4 (white squares denote null readings). 262
Figure 7-38 Statistical summary of data by area. 265
Figure 8-1 IDD versus formation. 278
Figure 8-2 IDD of structured and de-structured Newhaven and Seaford chalk. 280
Figure 8-3 Lab derived IDD versus Equotip derived IDD; de-structured Newhaven and Seaford chalk formations. 282
Figure 8-4 Lab derived IDD versus Equotip derived IDD; Seaford Chalk Formation, grade Dc. 283
Figure 8-5 NMC versus formation. 285
Figure 8-6 SMC versus formation. 287
Figure 8-7 Average NMC versus SMC for Newhaven and Seaford de-structured chalk. 289
Figure 8-8 Natural moisture content of naturally occurring structured and de-structured chalks plotted into the IDD-SMC line (adapted from (Mortimore and Fielding, 1990)). 290
Figure 8-9 Collapse of D-grade material when submerged in water. 293
Figure 8-10 PSD curve for Seaford chalk, grade Dc and Newhaven chalk, grade Dm. 294
Figure 8-11 Particles after PSD completion. 295
Figure 8-12 Modified Bushinsky technique using wax; Seaford chalk, grade Dc. 296
Figure 8-13 Image binarisation for quantification of grade based on putty matrix/clast ratio. 299
Figure 8-14 Average slake durability of Southern Chalk Formations (less the Portsdown Chalk Formation). 305
Figure 8-15 Slake durability of Newhaven and Seaford chalk formations (4 cycles). 309
Figure 8-16 Comparison of Seaford and Newhaven chalk clasts after I_d2. 310
Figure 8-17 Slake durability using differing slaking fluids (A) Newhaven Chalk Formation, (B) Seaford Chalk Formation. 312
Figure 8-18 Newhaven chalk arisings after slaking (<2 mm). 313
Figure 8-19 Newhaven Chalk Formation disaggregation in response to slaking water change – upper figures show samples slaked in fresh water, lower figures show samples slaked in synthetic salt water. 315
Figure 8-20 Slake durability of CIRIA graded Newhaven chalk. 318
Figure 8-21 Slake durability of CIRIA graded Seaford Chalk. 320
Figure 8-22 Relationship between I_d2 and intact dry density - Newhaven and Seaford Chalk Formations. 320
Figure 8-23 Permeability of Seaford and Newhaven de-structured chalk. 323
Figure 8-24 Schematic of permeability reduction with increasing effective stress (arrows with greater thickness indicate higher flow rate). 324
Figure 8-25 Stress-strain plots of dried samples tested under UCS conditions. 328
Figure 8-26 Stress-strain plots of samples tested under NMC and UCS conditions. 329
Figure 8-27 Mean UCS of D-grade Newhaven and Seaford Chalk. 330

Figure 8-28 Lab derived UCS versus SilverSchmidt derived UCS (Structured chalk data taken from Lawrence et al. (2013)). 331
Figure 8-29 Tensile test of Newhaven Dc. 335
Figure 8-30 tensile strength; structured chalk versus de-structured chalk, Newhaven and Seaford Chalk Formations (Structured chalk data taken from (Lord et al. 2002, Marley, 2020, Lau, 2018, Mider and Lawrence, 2018)). 336
Figure 8-31 Deviatoric stress versus axial strain plots for WNC1 (A), WNC2 (B), WNC4 (C) and WSC1 (D) 338
Figure 8-32 Deviatoric stress versus axial strain of structured chalk by Maclean (2023). 339
Figure 8-33 modified Bushinsky technique on Newhaven (WNC4) and Seaford Chalk (WSC1) after triaxial testing (Maclean, 2023). 340
Figure 8-34 Mohr circle and failure envelope of de-structured Newhaven chalk. 341
Figure 8-35 Schematic of consolidation and deformation of a D-grade chalk sample. 342
Figure 9-1 Classification workflow for stages of field investigation of weathering. 368
Figure 9-2 Classification workflow for identifying weathering features 368
Figure 9-3 Classification workflow for structured chalks, grades A1-C5. 369
Figure 9-4 Classification workflow for use of slake durability and index testing to validate weathering in chalk. 370
Figure 9-5 Classification workflow 5. 371

Tables

Table 1-1 Overview of research objectives and where they are satisfied within this document. 3
Table 2-1 Southern and Northern Province stratigraphy of the UK Chalk Group (Adapted from Rawson et al. 2001)..... 9
Table 2-2 Contributing mechanisms of diagenesis, which may or may not have acted on the chalk, in varying degrees of extent (taken from Clayton and Matthews, (1987). 13
Table 2-3 Geological evolution of the Southern Chalk Province of Great Britain (adapted from Mortimore, 2021) 24
Table 2-4 The Mundford Grades, developed by Ward, et al. 1968, * - modification by Wakeling, 1970) 28
Table 2-5 Classification system by Spink and Norbury (1990). 29
Table 2-6 CIRIA discontinuity aperture grades (Lord et al. 2002). 30
Table 2-7 CIRIA discontinuity spacings (Lord et al. 2002). 30
Table 2-8 CIRIA density grading (Lord et al. 2002). 32
Table 2-9 Chalk gradings correlated with approximate permeabilities by Preene and Roberts (2017). 33
Table 2-10 Comparison of rock mass rating systems. 34
Table 2-11 Material properties of chalk published in CIRIA C574; Engineering in Chalk (Lord, et al. 2002). 35
Table 2-12 Select index properties of de-structured chalk by various authors 38
Table 2-13 Angles of shearing resistance taken from literature. 39
Table 3-1 Equipment list for reconnaissance. 52
Table 3-2 Details for sites reconnoitred in a coastal setting. 53
Table 3-3 Details for sites reconnoitred in-land. 54
Table 3-4 Itinerary 1 – Brighton Marina to Peacehaven, east Sussex (Mortimore, 2021). 55
Table 3-5 Itinerary 2 – Newhaven Harbour to Cuckmere Haven, east Sussex. 55
Table 3-6 Itinerary 3 – Birling Gap to Cow Gap (Mortimore, 2021). 56
Table 3-7 Itinerary 4 Holywell Retreat, Holywell Beach to Foyle Way, Holywell. 57
Table 3-8 Itinerary 5 – vehicle reconnaissance of four in-land sites. 57
Table 4-1 Mean and ranges of Schmidt hammer (R) values from other authors. 76
Table 4-2 Updated CIRIA density grading (adapted from Lord et al. 2002, Proceq, 2022 and Thrower et al. 2022). 84
Table 4-3 Equipment required for sampling. 85
Table 4-4 Overview of tube types and degree of success when sampling. 93
Table 5-1 Industry standards of index tests. 98
Table 5-2 Locations for sampling of Southern Province Chalk formations. 105
Table 5-3 Sampling locations for varying CIRIA chalk grades. 106
Table 5-4 Slaking fluid preparations 106
Table 5-5 Slake durability equipment. 109
Table 5-6 Pressures used during the accelerated permeability test. 113
Table 5-7 Equipment for the accelerated permeability test. 114
Table 5-8 Schedule of UCS testing for Newhaven and Seaford de-structured chalks at differing moisture contents. 122
Table 5-9 Equipment for unconfined compressive strength testing. 122
Table 5-10 Equipment for Brazilian tensile strength testing. 127
Table 5-11 Triaxial test schedule of Newhaven and Seaford D-grade chalks 131
Table 5-12 Table of equipment required for the triaxial test. 131

Table 5-13 Equipment for the modified Bushinsky technique. 137
Table 5-14 Equipment required for the PSD test. 139
Table 6-1 Weathering types and products encountered at each location. 145
Table 6-2 Soil description, Roedean. 147
Table 6-3 Geological history, Roedean. 155
Table 6-4 Soil description, Portobello Outfall, Telscombe Cliffs. 158
Table 6-5 Geological history Portobello Outfall. 165
Table 6-6 CIRIA density grading of dry valley deposits at Portobello either side of access route. 167
Table 6-7 Soil description, Newhaven Harbour. 168
Table 6-8 Geological history, Newhaven Harbour. 173
Table 6-9 Soil description, Birling Gap. 174
Table 6-10 Geological history, Birling Gap. 179
Table 6-11 Summary of scanlines. 183
Table 7-1 Roedean access point, SilverSchmidt descriptive statistics. 201
Table 7-2 Roedean; SilverSchmidt derived UCS against texture and weathering grade. 206
Table 7-3 Roedean access point; Equotip derived IDD descriptive statistics. 207
Table 7-4 Roedean access point, quadrat 5 degree of weathering. 212
Table 7-5 Roedean access point, quadrat 6 degree of weathering. 214
Table 7-6 Roedean, Equotip derived IDD against texture and weathering grade. 215
Table 7-7 Portobello Outfall, quadrats 1 - 4 descriptive statistics for SilverSchmidt. 222
Table 7-8 Portobello quadrat 5 - discrete blocks, SilverSchmidt. 226
Table 7-9 Portobello quadrat 5 - discrete blocks, Equotip 227
Table 7-10 Portobello quadrat 7 - discrete blocks, SilverSchmidt. 230
Table 7-11 Portobello quadrat 7 - discrete blocks, Equotip. 231
Table 7-12 Portobello quadrat 8 - discrete blocks, SilverSchmidt. 235
Table 7-13 Portobello quadrat 8 - discrete blocks, Equotip. 235
Table 7-14 Portobello, SilverSchmidt derived UCS and Equotip derived IDD against texture and weathering grade. 236
Table 7-15 Quadrat 1; SilverSchmidt descriptive statistics and CIRIA grades. 242
Table 7-16 Quadrat 2; SilverSchmidt descriptive statistics and CIRIA grades. 245
Table 7-17 Quadrat 3; SilverSchmidt descriptive statistics and CIRIA grades. 246
Table 7-18 Newhaven quadrat 4 - degree of weathering based on discontinuities, SilverSchmidt... 249
Table 7-19 Newhaven, quadrat 4 - degree of weathering based on discolouration, SilverSchmidt. . 249
Table 7-20 Newhaven Harbour, SilverSchmidt derived UCS against texture and weathering grade. 250
Table 7-21 Newhaven, quadrat 4 - degree of weathering based on discontinuities, Equotip. 251
Table 7-22 Newhaven, quadrat 4 - degree of weathering based on discolouration, Equotip. 251
Table 7-23 Newhaven, quadrat 4 - degree of weathering due to discontinuity 252
Table 7-24 Newhaven, quadrat 5 - degree of weathering, SilverSchmidt. 254
Table 7-25 Birling Gap, SilverSchmidt descriptive statistics and CIRIA weathering grades. 256
Table 7-26 Birling Gap, SilverSchmidt derived UCS against texture and weathering grade. 263
Table 7-27 SilverSchmidt correction ratio (data taken from Mider (2017), Lau (2018) and (Lawrence et al. 2013)). 267
Table 7-28 SilverSchmidt correction ratio – Culver Chalk Formation. 268
Table 7-29 SilverSchmidt correction ratio - Newhaven Chalk Formation. 269
Table 7-30 SilverSchmidt correction ratio - Newhaven Chalk Formation. 270
Table 8-1 List of tests undertaken to characterise weathering in chalk. 275
Table 8-2 IDD for Southern Province Chalks (less the Portsdown Chalk Formation). 277

Table 8-3 Comparison of IDD between structured and de-structured Newhaven and Seaford Chalk Formation.....279
Table 8-4 Laboratory measured IDD and Equotip measured IDD values. 281
Table 8-5 IDD of Dc grade Seaford Chalk. 283
Table 8-6 Mean IDD and NMC of Southern Province Chalks (less the Portsdown Chalk Formation).286
Table 8-7 Moisture contents of de-structured Newhaven and Seaford Chalks against structured counterparts (* – data taken from Mortimore and Fielding, 1990). 288
Table 8-8 Voids ratios and porosities of Southern Province Chalks. 291
Table 8-9 Voids ratios and porosities of D-grade Newhaven and Seaford chalk. 292
Table 8-10 Quantification of clasts versus putty matrix. 298
Table 8-11 Drying times of Newhaven and Seaford chalk. 302
Table 8-12 Slake durability of structured Southern Province chalks. 304
Table 8-13 Slake durability classification (Franklin and Chandra, 1972). 306
Table 8-14 Slake durability and classification of geomaterial based on Franklin and Chandra's methodology. 307
Table 8-15 Slake durability of Newhaven chalk. 308
Table 8-16 Slake durability of Seaford chalk. 309
Table 8-17 Slake durability using different slaking fluids. 311
Table 8-18 Formations and grades of Seaford and Newhaven chalk tested. 316
Table 8-19 CIRIA graded Newhaven chalk slake durability results (graded by Maher, slake testing by Shi, 2022). 317
Table 8-20 CIRIA graded Seaford chalk slake durability results (graded by Maher, slake testing by Shi, 2022). 319
Table 8-21 Permeability of de-structured Newhaven and Seaford chalks. 322
Table 8-22 UCS of D-grade Seaford and Newhaven chalk. 326
Table 8-23 UCS of de-structured Newhaven and Seaford chalks; dry and NMC. 327
Table 8-24 Tensile strength of de-structured Newhaven and Seaford chalk. 334
Table 8-25 UCS versus tensile strength; de-structured Newhaven and Seaford chalk. 336
Table 8-26 Triaxial test schedule of de-structured Newhaven and Seaford chalk. 337
Table 8-27 Triaxial test results for de-structured Newhaven and Seaford chalk. 340
Table 8-28 Mohr-Coloumb parameters (structured data taken from (Mortimore et al. 2004b). 343
Table 9-1 Research objectives; techniques and Chapters demonstrating satisfaction. 351
Table 9-2 IDD and UCS of structured and de-structured Seaford and Newhaven Chalk.....354

Equations

Equation 4-1 77
Equation 4-2 78
Equation 4-3 80
Equation 4-4 80
Equation 5-1 100
Equation 5-2 100
Equation 5-3 101
Equation 5-4 102
Equation 5-5 103
Equation 5-6 103
Equation 5-7 103
Equation 5-8 103
Equation 5-9 103
Equation 5-10 104
Equation 5-11 104
Equation 5-12 104
Equation 5-13 104
Equation 5-14 110
Equation 5-15 119
Equation 5-16 125
Equation 5-17 125
Equation 5-18 125
Equation 5-19 126
Equation 5-20 126
Equation 5-21 128

List of abbreviations

ASTM	American Society for Testing and Materials
BGS	British Geological Survey
BSI	British Standards institute
BTS	Brazilian tensile test
$CaCO_3$	Calcium Carbonate
C574	Engineering in Chalk, CIRIA publication
CIRIA	Construction Industry Research and Information Association
CV	Coefficient of variation
CUZ	Chalk unsaturated zone
Dc	Grade D chalk, clast dominated
df	Degrees of freedom
Dm	Grade D chalk, matrix dominated
EQ	Equotip Leeb device
HS1	High Speed Rail 1
HS2	High Speed Rail 2
ICL	Imperial College London
IDD	Intact dry density
ISSC	International Sub-commission on Stratigraphic Classification
KCl	Potassium chloride
MgCl2	Magnesium chloride
NaCl	Sodium Chloride
NMC	Natural moisture content
OS	Ordnance Survey
PPE	Personal protective equipment
PSD	Particle size distribution
SDS	Slotted drive shaft hammer drill
SH	Schmidt hammer (generic)
SMC	Saturated moisture content
SS	SilverSchmidt hammer
UCS	Unconfined Compressive Strength
UK	United Kingdom
U38	Standard 38 mm diameter core sample size

1 Introduction

The Chalk Group of the UK is distributed over a significant area of the south-east and east of England, with discrete deposits in Yorkshire and Scotland, covering approximately 21,500 km^2 (Bradford, 2002). The Chalk extends from Dorset eastwards along the south coast to the North Downs, with its in-land extent underlying Oxford, the Wessex Downs and the Berkshire downs (Lord et al. 2002)

The national distribution of the Chalk Group, means it is stratigraphically extensive under several overlying major cities, including London, resulting in multiple small to large scale infrastructure engineering projects sited either on or within this chalk geology (Preene, 2018). These include Tideway, Crossrail, HS1, HS2 and the Lower Thames Crossing. The implications of these coinciding factors are that engineering projects in chalk cannot be avoided owing to their increased frequency and that engineering challenges associated with chalk geology are likely to be a significant consideration during geotechnical investigation, design and construction (Preene, 2018).

Weathering and weathering products can be considered a significant hazard (Viles et al. 2011), and are associated with (and can exacerbate) these geotechnical challenges. Similarly, weathering can also modify the chalk, leading to significant uncertainty in terms of material and subsequent rock mass properties (Price, 1995). Weathering can be considered the degradation of a rock due to chemical, biological or physical processes, or a combination of all three. In chalk, weathering can alter the geomechanical properties and can be difficult to identify, which has implications for both design and practical construction within the chalk.

The processes that cause chalk weathering, the extent, spatial distribution as well as material properties are not well understood and are largely absent in current literature. Given the extensive coverage of the chalk within the United Kingdom, uncertainties of distribution and changes in material properties due to weathering, it is likely that a varied range of properties would likely be encountered, and therefore characterisation of these properties would be required in advance of engineering project.

Photographic examples of weathering are similarly limited and there is no single resource that documents how chalk weathers or the implications of weathering for infrastructure projects. The current classification system to grade chalk weathering has limitations in that it oversimplifies the variability encountered in chalk formations, is subjective, leading to inconsistencies between practitioners and has a limited quantitative criterion in assessing the degree of weathering. The implication of this is that, while the system can be used to assess chalk quickly and practically,

repeatability and precision can be inconsistent and therefore the classification system can only be relied upon as an approximation, requiring further geological context during investigation.

1.1 Project aim

The aim of the project is to further understand and characterise the development and distribution of weathered chalk (and subsequent various stages of weathering) in the Southern Province chalks of the UK Chalk Group. All formations of the Southern Chalk Province are focussed on in terms of evaluation of weathering susceptibility, however, the Formations focused on in terms of de-structured chalk grades are the Seaford and Newhaven Chalk Formations, due to their homogeneity, wide-spread distribution and likelihood of being encountered during infrastructure projects.

It is aimed to quantify and document weathering in both a field and laboratory setting, which will then be compared; densities and strength values will be collected in a field setting and compared to the geomechanical and hydrogeological properties of the chalk, characterised in the laboratory. By artificially weathering chalk samples in the laboratory, it is aimed that further insight of weathering processes that occur within the field setting will be achieved, and allow competing, concurrent processes to be identified separately.

1.2 Project objectives

The research objectives are to:

1. Qualitatively assess existing methods of grading of weathered chalk through practice within the field and comparison with differing localities.
2. Develop sampling and testing methodologies for weathered chalk.
3. Develop methodologies to measure the material and rock mass properties of weathered chalk.
4. Quantify chalk weathering and changes of grade through destructive and non-destructive field and laboratory techniques.
5. Develop a microtexture index or texture map for identification of chalk weathering types by correlating SEM analysis with field macrostructures.
6. Develop a predictive toolbox to assess weathering profiles in the chalk and provide consistency between engineers of varying levels of experience.

Table 1-1 Overview of research objectives and where they are satisfied within this document.

Objective	Chapter	Techniques used
1	3, 4, 5, 6, 7	Field observation, CIRIA grading methodology
2	4, 5, 6, 7, 8	CIRIA grading methodology, SilverSchmidt, Equotip, index testing, slake durability testing, geomechanical strength testing, permeability testing
3	7	SEM analysis, image processing
4	5, 6, 7, 8	CIRIA grading methodology, SilverSchmidt, Equotip, index testing, slake durability testing, geomechanical strength testing, permeability testing
5	6, 7, 8, Appendix	Sampling -- Chapters 6 and 7, validation - Chapter 8, results – appendix
6	4, 5, 6, 7, 8	CIRIA grading methodology, SilverSchmidt, Equotip, index testing, slake durability testing, geomechanical strength testing, permeability testing

Table 1-1 provides an overview of what Chapters satisfy the research objectives and summarises what techniques are required to do so. In terms of project scope, macrofeatures identified in a field setting will be considered to identify weathering trends, weathering types and distribution, while index properties, hydrogeological and geomechanical characterisation as well as artificial weathering experiments will focus on the material property scale. The microscale will also be investigated using scanning electron microscopy.

1.3 Thesis structure

- Chapter 1 introduces the PhD project, establishing the significance of weathering, omissions in literature and details the aims and objectives of the study.
- Chapter 2 is an in-depth review of the current literature on the formation of chalk, its distribution and weathering, identifying gaps within current understanding on chalk weathering and limitations of chalk classification systems. The literature review also covers the individual formations within the UK Southern Chalk Province, material properties intrinsic to the chalk and styles of weathering encountered within these chalk formations. Chapter 2 identifies important omissions within the literature required to be addressed to fulfil all objectives.
- Chapter 3 details site selection in relation to exceptionally preserved examples of weathering and covers all reconnaissance locations with brief evaluation of their suitability. Selected locations are summarised with the types of weathering encountered. Chapter 3 partially satisfies objectives 1, 2, 3 and 4.
- Chapter 4 provides detail on the development of the field methodology, providing information on non-destructive field testing and instrumentation, use of the CIRIA C574 weathering grade approach and a detailed commentary on the development of a sampling technique for D-grade chalks to produce core samples compatible with industry standard laboratory techniques. This chapter also sets out a strategy for measuring weathering on a field-scale basis utilising a uniformity survey methodology. Chapter 4 partially satisfies objectives 1 – 6.
- Chapter 5 is a detailed methodology for laboratory testing, including index tests, geomechanical tests, permeability tests and sets out a strategy for artificially weathering chalk using slake durability methods to assess the susceptibility of Southern Chalk Formations to weathering as well as evaluating CIRIA graded Seaford and Newhaven Chalks. Chapter 5 partially satisfies objectives 2, 3, 4, 5 and 6.
- Chapter 6 details field observations of weathering and assigns initial CIRIA grading from four selected research sites. Chapter 6 evaluates Younging relationships of weathering and geological features observed at these research sites to identify their geological history and interplay between each other. Chapter 6 partially satisfies objectives 2, 3, 4 and 5.
- Chapter 7 presents the results of a uniformity survey, comprising observations, measurements and statistical analysis, used to evaluate the distribution of weathering on a field-scale and at proximity to different geomorphological features. Chapter 7 evaluates novel use of non-destructive testing tools in the measurement of weathering in chalk. Chapter 7 partially satisfies objectives 1, 2, 3 and 4.

- Chapter 8 are the results from laboratory investigation, used to underpin observations made in chapters 6 and 7. This results chapter also characterises de-structured chalk in terms of index properties, geomechanical strength tests and permeability. Artificial weathering of CIRIA graded chalk is also presented and correlated with index properties. Chapter 8 partially satisfies objectives 2, 3, 4, 5 and 6.
- Chapter 9 is a summary and conclusions chapter highlighting the key finding of the research and makes recommendations future work.

1.4 Chapter summary

This chapter has provided brief background information, introduced the initial research question and set out the motivation for this research. In Section 1.1, the project aim is defined in more detail. Section 1.2 sets out research objectives, linked with Chapters and techniques, which are required to be achieved for this research to be considered successful (Table 1-1). Section 1.4 defined the thesis structure as a guide to the research and for ease of navigation of this thesis.

2 Literature review

2.1 Introduction

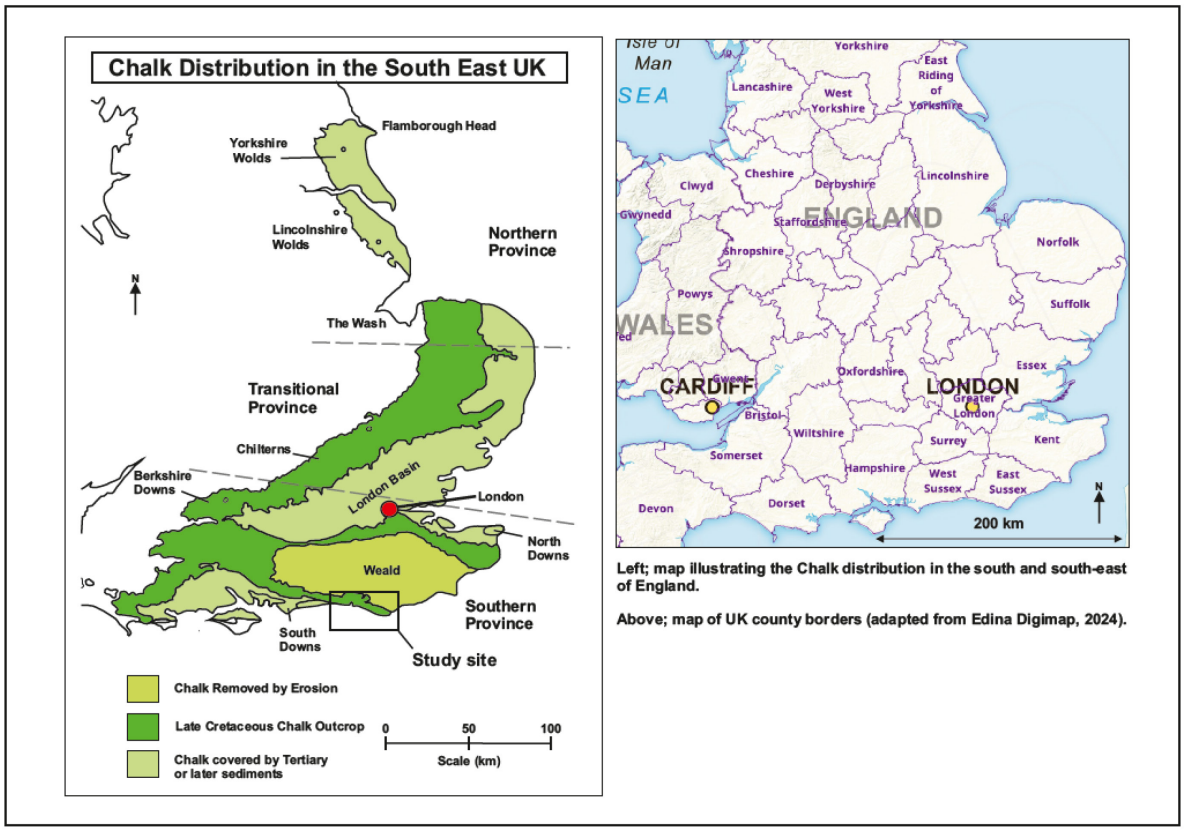
This Chapter presents an overview of literature relating to the deposition and lithification of chalk, its distribution across the southeast of Great Britain and the stratigraphic framework used to constrain the chalk through geological time. This Chapter also presents an overview of the classification systems used to grade chalk and their limitations as well as an overview of the types of chalk weathering encountered within a field setting. The importance of these topics cannot be understated; the implications of deposition and lithification of the chalk provides insight as to how the chalk may behave (and ultimately weather), while the distribution and stratigraphy of the chalk will indicate where and which formations of chalk will be encountered during engineering projects, while stratigraphic changes may indicate variation in chalk properties. A review of the classifications are important to this project as some are not considered fit for purpose when describing chalk weathering. The overview of weathering allows constraint of likely weathering types encountered in the field and allows identification of potential field sites.

The structure of this Chapter covers the distribution of chalk across Great Britain (section 2.2), the formation of chalk (including deposition, lithification and diagenesis - section 2.3), stratigraphy (section 2.4), the geology of east Sussex (section 2.5), the classification of carbonate lithofacies (section 2.6), the engineering classification of chalk (section 2.7), the physical properties of chalk relevant to weathering (section 2.8) and the types of weathering encountered in a field setting (section 2.9).

By establishing what is known within the current field of chalk geology, this Chapter contributes to this thesis by broadening understanding of which chalk formations may be more susceptible to weathering by virtue of their physical properties and geographical location. This Chapter frames the stratigraphical framework used for Southern Province chalk formations and puts this in a weathering context. This Chapter also provides important commentary on the current classification systems used to grade chalk weathering, including their limitations.

2.2 Distribution of chalk in the UK

The Chalk covers approximately 21,500 km^2 of the south and south-east of the United Kingdom (Figure 2-1) (Bradford, 2002). Given the extensive coverage of the chalk within the south of the United Kingdom, there is a clear requirement for robust characterisation of chalk properties in advance of project commencement. This is emphasised by the requirement of multiple engineering works within or on chalk strata, such as shaft sinking and tunnel boring for Crossrail, HS1, HS2, Thames Tideway and many others (Preene, 2018). Another important aspect of the UK Chalk is its role as a principal aquifer in the UK, providing 60% of total groundwater used and 20% of potable drinking water (Macdonald and Allen, 2001).



Left; map illustrating the Chalk distribution in the south and south-east of England.

Above; map of UK county borders (adapted from Edina Digimap, 2024).

Figure 2-1 The distribution of Chalk in the United Kingdom and county borders (adapted from Lord et al. 2002 and Edina Digimap, 2024).

The distribution of chalk on the mainland United Kingdom is in the south and the south-east of England. The chalk also outcrops in the Yorkshire and Lincolnshire Wolds. In the south of England, chalk extends from Dorset eastwards along the coast to the North Downs, through to East Anglia and Norfolk. The extent of the chalk in-land underlies Oxford, the Wessex Downs and the Berkshire Downs (Figure 2-1) (Lord et al. 2002). There is a presence of chalk in the Scottish Inner Hebrides, extending from Mull to Skye and equivalent chronostratigraphic non-chalk deposits in Northern Ireland, as well

as economically important chalks in the North Sea, however these groups fall outside of the remit of this thesis.

Stratigraphically, the Chalk group is split; the Grey Chalk subgroup (consisting of the division of Lower Chalk) and the White Chalk subgroup (consisting of the divisions of the Middle and Upper Chalk, with the Plenus Marl Member stratigraphically below the Middle Chalk) (Rawson et al. 2001) (Table 2-1). In terms of geographic locality, the Chalk is again split into three provinces – the Northern Chalk Province (including chalks outcropping in Yorkshire, Lincolnshire and the north of East Anglia), the Southern Chalk Province (including chalks outcropping from Dorset, in-land to Berkshire and the North Downs, with a significant amount of erosion in the Weald Basin, resulting in absent chalk) and an intermediate, Transitional Chalk Province (including part of the northern Chilterns and part of the London Basin) (Figure 2-1).

Table 2-1 Southern and Northern Province stratigraphy of the UK Chalk Group (Adapted from Rawson et al. 2001).

		Southern province		**Northern province**	
Stage	**Subgroup**	**Formation**	**Member**	**Formation**	**Member**
Campanian	White Chalk	Portsdown Chalk		Rowe Chalk	
		Culver Chalk	Spetisbury Chalk	Flamborough Chalk	
			Tarrant Chalk		
Santonian		Newhaven Chalk			
Coniacian		Seaford Chalk		Burnham Chalk	
Turonian		Lewes Nodular Chalk			
		New Pit Chalk		Welton Chalk	
Cenomanian		Holywell Nodular Chalk	Plenus Marls		Plenus Marls
	Grey Chalk	Zig Zag Chalk		Ferriby Chalk	
		West Melbury Marly Chalk			

2.3 The formation of chalk

The sedimentation (and type) of constituent material, lithification and subsequent diagenesis of chalk are important processes to discuss as they give rise to material properties that are unique to chalk as a rock (such as high porosity and permeability). Modification of the chalk via diagenesis and other processes (such as dissolution, resulting in hardgrounds) will affect these properties further depending upon the formation, member or bed's geological history, resulting in some chalks being more susceptible or resistant to weathering.

2.3.1 Deposition and sedimentation of chalk

Constituent material

Chalk is a highly pure, ultra-fine, biogenic micrite, comprised almost entirely from low-magnesium, skeletal calcite ($CaCO_3$) in both coarse and fine fractions. The lower chalk has been reported to have increasing calcium carbonate content, rising from 55 – 65% to 90 – 95% at the top of the stratigraphy, Middle Chalk has a calcium carbonate content of 95 – 99%, while the Upper Chalk has a calcium carbonate content of 97.5% or above (Lord et al. 2002). The fine fraction are the main constituent grains for all white chalks (contributing <95% of rock mass) and are derived from pelagic nanoplankton called coccolithophores and some foraminifera. The coarse fraction comprises biogenic material from marine macro-organisms, such as disaggregated molluscs, bivalves and echinoids (40 – 100 mm diameter range, accounting for 10 – 25% of the mass) (Hancock, 1975, Bell et al. 1999). There is also a fraction of clay material, accounting for <15% of the rock mass, depending on the Formation (Bell et al. 1999).

Coccolithophores are an autotrophic (i.e., self-feeding) phytoplankton (plankton that uses photosynthesis for energy), which assimilate (effectively 'fixing') inorganic carbon dissolved in the water column, converting it into calcite shields, known as coccoliths (Tyrrell and Young, 2009). These plates act as a protective exoskeleton. Coccolithophores themselves are spherical or ovoid in morphology and are approximately 20 µm in diameter. Coccoliths produced by the coccolithophore are in the range of 0.5 – 4.0 µm (Bell et al. 1999) and are shed over the coccolithophores life-cycle. This results in the deposition of a fine calcite fraction comprising both coccolithophore death assemblages and individual coccolith plates (Jordan, 2009).

Larger bioclasts and fragments of other calcareous, marine macro-organisms can be present in Chalk, and in sufficient quantity, can produce a wackestone texture in some chalks (Mortimore, 2014). This bioclastic fraction is reported to have negligible modification of the physical properties of chalk as a rock mass (Lord et al. 2002), although may prove useful for biostratigraphic correlation. The Dunham classification is discussed within Section 2.6.

Clay and clastic minerals within Chalk owe their provenance to several sources, and when in abundance form marl seams and stylolites. Laterally extensive clay concentrations, such as marl seams are reflective of episodic sediment input (resulting in thin layers with a grey to green colour) (Lord et al. 2002) and can be attributed to volcanic events, while clay and clastic minerals encountered within the chalk matrix can be attributed to minor terrigenous sediment input and authigenic mineral growth during diagenesis. In terms of mineralogy, illite has been identified as a constituent clay, although montmorillonite has also been observed (Lord et al. 2002).

Grain size and constituent mineralogy are important aspects of chalk as they control intrinsic material properties; fine grains control pore structure, which allows chalk the ability to retain high moisture content via capillary attraction (Lord et al. 2002). Flow of water through this fine matrix is via diffusion rather than advective flow (although this is observed in fractures), which makes chalk such an effective aquifer. The composition of chalk results in chalk being more vulnerable to acidic or aggressive ground water, which means that overlying deposits may induce chemical weathering depending upon their mineralogy.

Depositional environment

The Upper Cretaceous Chalk of the southeast of the United Kingdom was deposited over a significantly long period of geological time (30 million years), at rates of 10 mm/thousand years to 100 mm/thousand years (De Vargas et al. 2007) between 144 – 65 million years ago. Coccolithophores are pelagic, and formed in blooms in the photic zone (Morse, 2003) (between 0 – 200 m depth within a water column not exceeding 500 m) (Clayton, 1983). When coccolithophores shed their coccoliths or die, they settle to the sea floor, where they form a calcareous ooze, up to several kilometres in thickness.

The palaeoclimate during the late Cretaceous is considered a greenhouse period, with much higher temperatures than current. Sea temperature and levels were also higher, owing to a lack of sea ice and the occurrence of sea water expulsion onto continents as shallow, epicontinental seas. This formation of epicontinental seas was the result of ocean basin swelling due to mantle plume activity, known as the Cretaceous Superplume (Mortimore et al. 2001). Deposition coincided with the break-up of Gondwanaland, and the opening of the Atlantic Ocean, allowing chalk to be deposited in a continental shelf setting. In terms of palaeogeography, Britain was positioned between 30° and 40° N (Lawrence, 2007).

The depositional environment has implications for chalk in that relatively deep ocean settings, with significant distance to landmass, results in highly pure calcareous deposits. This is because the oceans are a low energy depositional environment, so there is little winnowing of fine-grained deposits and there is little terrigenous input associated with landmasses (Gale, 2012). The formation of coccoliths in blooms is also integral to the formation of chalk, as the settling of single, individual coccoliths under gravity conditions, has a lower likelihood according to Stoke's law, however when formed in a bloom, coccoliths may sink more rapidly (Tyrrell and Young, 2009).

2.3.2 Lithification and diagenesis of chalk

Initial gravity driven deposition results in a fine calcareous ooze with high porosity of approximately 70% at the chalk-water interface (Scholle, 1977). The ooze is effectively a granular deposit, with

porosity and strength attributed to intergranular contacts of detrital coccoliths, coccolithophore death assemblages and other bioclastic sediment input. Owing to this intergranular strength and prolonged periods of sedimentation, weak cementation occurs concurrently (via pressure solution, spot welding and re-precipitation) with deposition and sea floor compaction, rather than following compaction due to burial (Kirumakki, 1977). The result of this pre-burial diagenesis is that the calcareous sediments can withstand greater overburden before grain crushing and material collapse, resulting in the chalk maintaining high porosities.

Porosity and permeability are intrinsic properties of chalk material and correlate very closely with other index properties, such as saturated moisture content (SMC) and unconfined compressive strength (UCS) (Lord et al. 2002). This correlation allows some indication of how chalk will behave as an engineering material and will also indicate how resistant a chalk is to weathering.

These properties are modified and reduced by lithification and diagenesis; Scholle (1977) reports that porosity reduces as a function of burial depth, with a depth of 1 km reducing porosity to 35% and a depth of 2 km reducing porosity further to 15%, while Clayton and Matthews, (1987) postulate that chalks which have undergone earlier burial are more likely to be closely packed, having undergone consolidation prior to cementation. While burial and consolidation have been discussed as agents of lithification and diagenesis, there are other contributing mechanisms which may or may not have acted on the chalk, in varying degrees of extent (Table 2-2), set out by Clayton and Matthews (1987);

Table 2-2 Contributing mechanisms of diagenesis, which may or may not have acted on the chalk, in varying degrees of extent (taken from Clayton and Matthews, (1987).

Mechanism	**Influence in increasing Chalk density**	**Geographical extent**	**Stratigraphic extent**
Intrinsic diagenesis – (early lithification, prolonged seafloor exposure, bioturbation)	Potentially very strong	Very unpredictable	Very unpredictable
Consolidation (syn-sedimentary gravitational compaction)	Minor, except for high porosity chalks	Everywhere	Greater for more deeply buried chalks
Tectonism	Modest to strong	Around and including steeply dipping chalk	All levels
Late-stage solution	Strong to very strong	Lincolnshire and Yorkshire	All levels

It is important to understand both deposition and diagenetic mechanisms as these factors are responsible for some of the variation in rock mass properties observed in different chalk formations and will contribute to a chalk rock mass's susceptibility or resistance to weathering.

2.4 Stratigraphy

2.4.1 The development of a unified chalk stratigraphy

Figure 2-2 describes the evolution of chalk stratigraphy and nomenclature. Early lithostratigraphic schemes for Kent were produced by Phillips (Phillips, 1818) and Conybeare and Phillips (Conybeare and Phillips, 1822), Mantell for Sussex (Mantell, 1822) and Woodward for Norfolk (Woodward, 1833), based on the presence of flints and clay content. Phillips and Woodward subdivided the chalk into four lithological units, while Mantell subdivided his observations into three units, which combined Phillips and Woodward's' respective upper two units (Figure 2-2) (BGS-Earthwise, 2015, Bromley and Gale, 1982).

In 1870, Dowker produced a scheme for Thanet, Kent, which was followed by Whitaker, (1872), who produced a stratigraphic model of beds for the London Basin in 1872. In 1903 and 1904, Jukes-Brown and Hill presented an integrated biostratigraphic and lithostratigraphic model, this used as the basis of mapping, from publication up to the 1990's by the British Geological Survey (BGS) (BGS-Earthwise, 2015).

In 1986, Mortimore published 'The stratigraphy of the upper cretaceous white chalk of Sussex', which defined a high resolution lithostratigraphy for the Southern Province of UK chalk, detailing over 100 marker horizons (comprising flint bands, marl seams and hardgrounds) (Mortimore, 1986). This paper

is important as it utilised the International Stratigraphic Guide to focus specifically on the UK Southern Province and remain concise in terms of member nomenclature. The high resolution of marker beds allows for more ready identification of chalk formations in the field and demonstrates the degree of variation observed within chalks at formation level.

In 1997 Bristow, Mortimore and Wood published 'Lithostratigraphy for mapping the chalk of southern England', focussing on the Southern Province chalk members utilised as mappable units (Bristow et al. 1997). The Holywell Nodular Chalk Formation was also recognised as a distinct unit.

Significant work and discussion in the following years, such as the 1999 Chalk Lithostratigraphy meeting at BGS Keyworth, resulted in further refinement, and in 2001, Rawson et al. published 'The Chalk Group – a revised lithostratigraphy'. At this point, a lithostratigraphic framework was agreed upon, which detailed both the northern and southern chalk provinces and integrated previous models (Table 2-1).

The increase in stratigraphic resolution observed over time with further refinement has allowed identification and evaluation of variation within chalk facies, which subsequently reflects depositional environments, diagenesis and conditions. This has implications for chalk weathering as it would be expected that more dense chalks, or chalks with increased clay content, will likely be less susceptible or more resilient to weathering processes. This is speculated due to increased IDD correlating well with both reduced moisture content and increased material strength (Lord et al. 2002), associated with chalks of increasing stratigraphic age. The implication of reduced moisture content would be reduced water weakening effects and strength reduction associated with saturation, while intrinsic material strength would suggest greater durability. The mechanisms for reduced moisture content are uncertain, however Faÿ-Gomord et al. (2017) propose that increased clay content and cementation contribute to reduced porosity, while Clayton and Matthews (1987) suggest that overburden pressure has led to more compact chalk with lower porosities.

The clear benefit of a stratigraphic framework for the study of chalk weathering lies in that formations can be constrained lithologically, geographically and temporally, allowing evaluation and comparison of differing types of weathering in different formations.

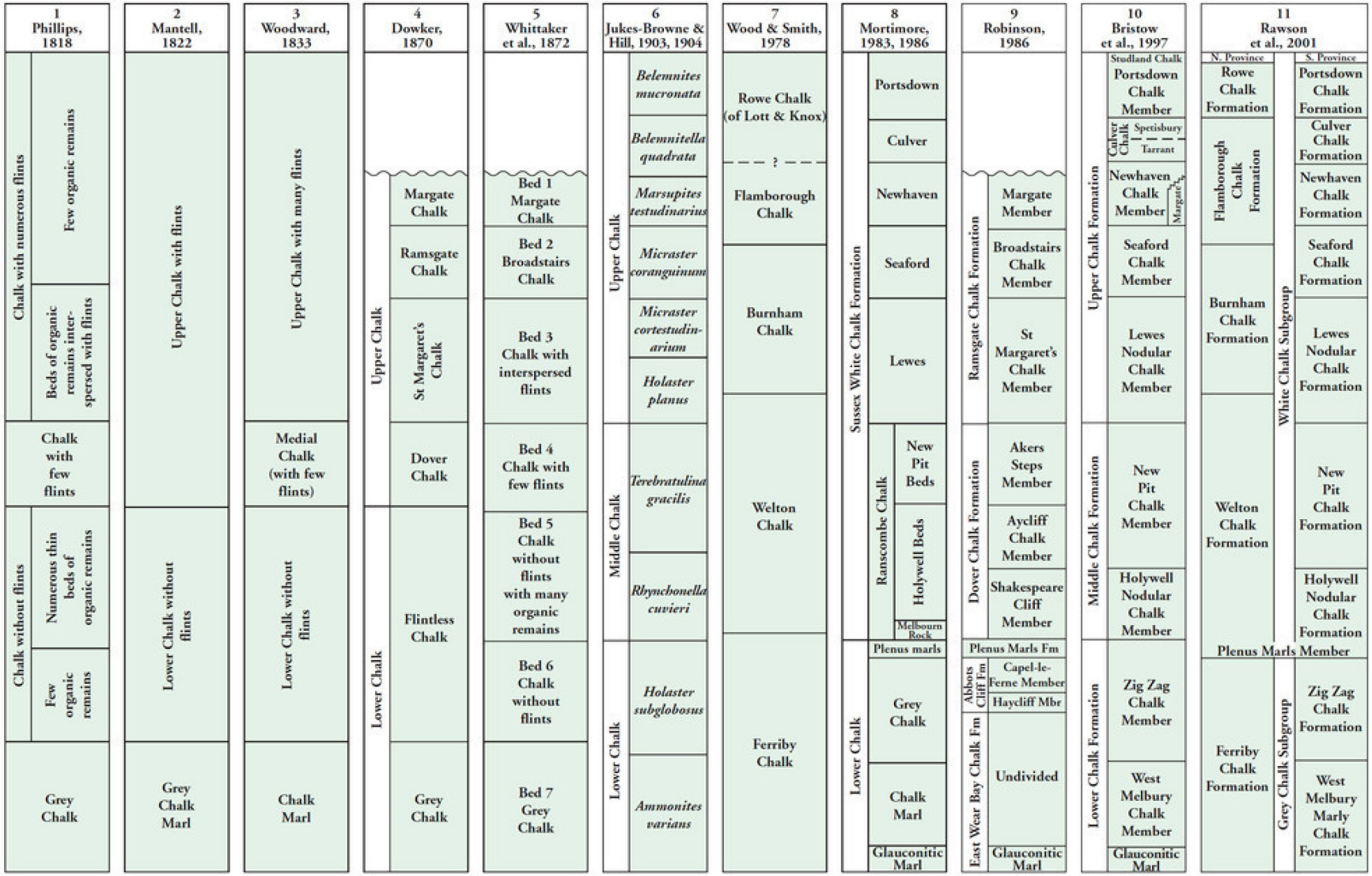


Figure 2-2 The development of chalk stratigraphy over time (BGS Earthwise, 2015).

2.4.2 Stratigraphic framework of the Southern Province Chalk Formations

The current stratigraphic framework of the southern province chalk formations was developed after Bristow et al. (1997) and Rawson et al. (2001). The base of the southern province is the West Melbury Marly Chalk Formation, deposited in the Cenomanian, while the top of the southern province stratigraphy is bound by the Portsdown Chalk Formation, deposited in the Campanian. The current nomenclature consists of the Grey Chalk Subgroup and the White Chalk Subgroup. The Grey Chalk Subgroup comprises the West Melbury Marly Chalk Formation and Zig Zag Chalk Formation. The White Chalk Subgroup comprises the Holywell Nodular Chalk Formation, New Pit Chalk Formation Lewes Nodular Chalk Formation, Seaford Formation, Newhaven Formation, Culver Formation and Portsdown Formation. These formations replaced the traditional Lower, Middle and Upper Chalk Formations (Figure 2-3).

Some formations have been reported more extensively than others, owing to the frequency in which they are encountered during previous engineering projects, degree of exposure and preservation. Examples include the well covered Seaford Chalk and Newhaven Chalk Formations, compared to the sparse information relating to the Portsdown and Culver Chalk Formations (Mortimore, 2014). The following sections describe the key sedimentological characteristics of each formation and their variations, working up through the UK Chalk stratigraphy of the Upper Cretaceous.

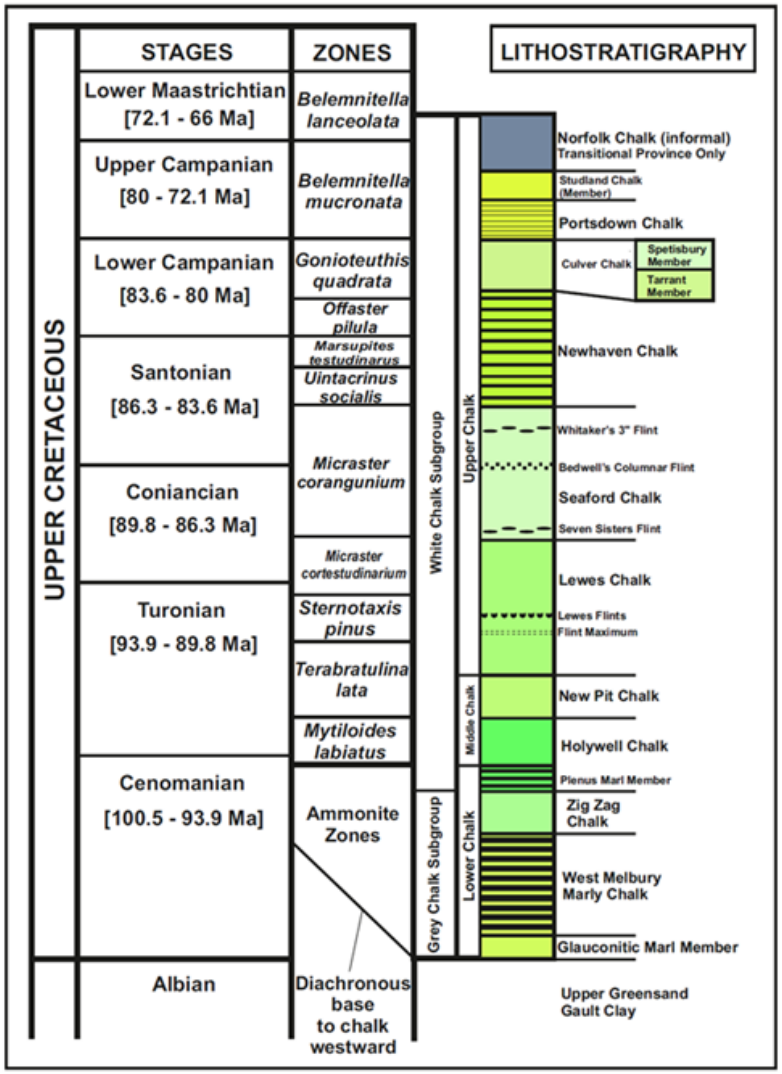


Figure 2-3 Lithostratigraphy of the Southern Province of the UK Chalk (adapted from Lord et al. 2002).

West Melbury Marly Chalk Formation

The West Melbury Marley Chalk Formation (early Cenomanian) comprises off-white, calcareous mudstones, soft grey marls and buff-grey, off-white limestones, rhythmically interbedded exhibiting cyclostratigraphy related to Milankovitch cycles (Newell et al. 2018).

In terms of marker beds, the West Melbury Marly Chalk comprises The Bank, which consists of white limestones with beds of marly chalk. The chalk above this, consists of marl and limestone couplets, which are stratigraphically below a hard, nodular sponge rich limestone called The Rib. The upper 5.0 m of this formation displays significant disturbance and reworking (Lawrence, 2007).

The reported average thickness of this formation is 15 – 30 m, with a maximum of 40 m in the northern Chilterns (Newell et al. 2018). Thicknesses, densities and strengths of the marl-limestone couplets vary; however, it has been reported that the older limestone beds have higher densities compared to that of younger chalks (Mortimore, 2014).

The lower boundary of this formation in the southern province is the erosional surface at the base of the Glauconitic Marl Member, and in the south-west, the Melbury Sandstone Member (BGS(a), 2022). The upper boundary is the erosional base of the overlying Zig Zag Chalk Formation (BGS(a), 2022).

Zig Zag Chalk Formation

The Zig Zag Chalk Formation (Mid-Late Cenomanian) comprises massively bedded, cyclical couplets of thin marls and limestone (Lawrence, 2007). The BGS describe the chalk of this formation as firm, pale grey to off-white chalk, with rhythmic alterations of firm white chalk and flaser marls in the lower sequence (BGS(b), 2022).

Average thicknesses of 35 – 50 m are recorded in the southern province (BGS(b), 2022) and the lower boundary is defined by the unconformable, erosional contact of the Cast Bed, above the Tenuis Limestone (BGS(b), 2022). Lithological markers within the Zig Zag Chalk Formation include the White Bed, the basal Jukes-Brown 7 Bed, Triple Marls, *Asham Zoophycos* 1 & 2 and the Cast Bed (Lawrence, 2007).

Holywell Nodular Chalk Formation

The Holywell Nodular Chalk Formation (Late Cenomanian – Early Turonian) is characterised by contrasting facies types of hard, nodular chalks with flaser marls and significant amounts of fossiliferous material in the upper sections (BGS(c), 2022). This formation includes the Plenus Marl Member at the base (overlying the Sub-Plenus Erosion Surface, making distinction between the Zig Zag Chalk and Holywell Nodular Chalk challenging), and is overlain by the stronger Melbourne Chalk Member (distinguished by the lack of fossiliferous material and inclusion of pebbly intraclast nodular layers (Lawrence, 2007).

The Melbourne Chalk Member is then overlain by 'Grit beds' – nodular chalk beds with a significant amount of inoceramid fossil assemblages (*Mytiloides* shell debris), although other fossils are also present, such as ammonites (Mortimore, 2014).

The lower boundary of this formation is defined by the base of the Plenus Marl member, while the upper boundary is the Gun Garden Marl. Thicknesses observed range from 25 – 35 m (BGS(c), 2022) and time of deposition has been constrained to the Cenomanian-Turonian boundary (Lawrence, 2007), during which, there was a period of significant late Cretaceous flooding and the beginning of the expansion of white chalk facies onto flooded continental margins (Newell et al. 2018).

New Pit Chalk Formation

The New Pit Chalk Formation (Mid-Turonian) is a smooth textured, firm to hard, white chalk (Mortimore, 2014) (BGS(d), 2022) with regular horizons of marl and marly chalks (Newell et al. 2018).

The chalk is blocky and has numerous marl seams, some of which are paired, and correlate over a large geographical range (Mortimore, 2014). The upper defining boundary of the New Pit Chalk Formation is the Glynde Marl 1, while the lower boundary is defined by the Gun Garden Marl.

Typical thicknesses observed are 35 – 50 m, however, it has been noted that this formation is more variable than most other chalk formations, with a trend of thinning in southerly regions. Observed thicknesses of 10 – 25 m are recorded in the Wiltshire area, thicknesses <65 m in the Chilterns, whereas in the transitional province, thicknesses of 75 – 80 m have been reported (Newell et al. 2018, Mortimore, 2014).

Lewes Nodular Chalk Formation

The Lewes Nodular Chalk Formation (Late Turonian – Early Coniacian) comprises hard chalk, marls, marly chalk and hardgrounds (Newell et al. 2018). Stratigraphically, the Lewes Nodular Chalk Formation divided into 12 beds (descending in increasing age); the Shoreham Beds, the Beachy Head Beds, the Light Point Beds, the Beeding Beds, Hope Gap Beds, Cliffe Beds. The Navigation Beds, the South Street Beds, Kingston Beds, Ringmer Beds, Caburn Beds and the Glynde Beds (Lord et al. 2002). These beds are separated by marl horizons, although, while marl horizons do define the bed stratigraphy, other marls also cross-cut bed members.

In terms of engineering behaviour, the Lewes Nodular Chalk Formation comprises hard to very hard nodular chalks (characterised by orange staining), interbedded with softer (soft to medium) grey, chalks, with a coarse texture (BGS(e), 2022, Mortimore, 2014). Harder nodular beds generally fracture with a curvilinear geometry, while the softer, lower density beds do not fracture easily and are less brittle (Mortimore, 2014). Variation in material density and fracture characteristics are reported throughout the beds, both laterally and vertically, giving rise to inhomogeneity (Mortimore, 2014).

The thickness of the formation is in the range of 35 – 40 m (Newell et al. 2018), with the thickest sections observed in areas of basinal succession in the southern province. The base of the Lewes Nodular Chalk Formation is also the base of the White Chalk Subgroup (Upper Chalk) (Lawrence, 2007), formations, overlying the White Chalk Subgroup (Middle Chalk), and Grey Chalk Subgroup (Middle and Lower Chalks).

Seaford Chalk Formation

The Seaford Chalk Formation (Mid-Coniacian – Early Santonian) is split into 3 beds; with the Haven Brow Beds uppermost, the Cuckmere Beds in the middle and the lower beds being the Belle Tout Beds (Lawrence, 2007). The formation is described as a ‘homogenous, firm, white chalk with nodular and

tabular flints' (BGS(f), 2022) however, there are marls and marly chalk units in the lower part (Newell, et al. 2018)**,** with distinctions between the three beds themselves.

The Haven Brow Beds are described by Mortimore (Mortimore, 2014) as pure white with burrow mottling with bands of flint and (lesser developed) pseudoflint, while the Cuckmere Beds are described as a very, fine grained, white chalk with an abundance of pseudoflints and nodular flints. The lower Belle Tout Beds are described as fossiliferous, with bands of fragmented inoceramid shells, as well as sponge beds (in differing stages of development).

The Seaford Chalk Formation is the most widely outcropping chalk unit in the southern province (Newell et al. 2018), meaning that while the reported formation thickness is in the range of 50 – 80 m, the formation's wide geographical extent has resulted in significant sub-Palaeogene erosion (BGS(f), 2022).

Newhaven Chalk Formation

The Newhaven Chalk Formation (Mid-Santonian – Early Campanian) comprises apparently homogenous, firm to medium hard chalk, with a smooth surface texture (BGS(g), 2022). Marl seams are relatively widely spaced (Mortimore, 2014) and separate out 5 constituent beds; the Splash Point Beds, the Old Nore Beds, the Peacehaven Beds, the Meeching Beds and the Bastion Steps Beds (Lawrence, 2007).

While appearing homogeneous, the formation has been observed to contain distinct phosphatic chalks which are not laterally extensive (BGS(g), 2022). Structurally, the chalk displays a high frequency of inclined conjugate faults, flint bands and inclined fractures compared to other chalk formations (Mortimore, 2014). The BGS reports the thickness of this formation as 45 – 75 m, but some locations have been subject to sub-Paleogene erosion, thus limiting observation of true thickness (BGS(g), 2022).

Culver Chalk Formation

The Culver Chalk Formation lies stratigraphically above the Newhaven Chalk, and below the Portsdown Chalk, with the upper boundary defined by the Portsdown Marl (Mortimore, 2014). The lithology is described as homogenous, soft, white chalk, relatively marl free with widely spaced, large flint bands, and has observed thicknesses of 65 – 70 m on average (<90 m in some locations) (BGS(h), 2022)**.** This formation comprises the Tarrant and Spetisbury Members respectively.

Portsdown Chalk Formation

The Portsdown Chalk Formation is described as a white chalk with numerous thin, grey, wavy marl seams (Mortimore, 2014), the frequency of these marls reduce up sequence, with the upper Studland

Chalk Member being relatively marl free compared to the lower members (Gale et al. 1987). Nodular flint bands are well developed in this formation, forming marker beds, however there is an absence of sub-horizontal and sub-vertical flint sheets, which are observed in association with marl bands in other chalk formations (such as the Newhaven Chalk Formation) (Mortimore, 2014).

The maximum thickness of the formation is reported as 62 m at Whitecliff, Isle of White, however it is likely that sub-Palaeogene erosion has limited the thickness of this formation in other locations (BGS(i), 2022).

2.5 The geology of east Sussex

2.5.1 Geological map

Figure 2-4 shows the distribution of geological units within the study area. To the west is the Roedean research site and to the east, the Birling Gap research site. The predominant chalk formations within the area are the Seaford and Newhaven Chalk Formations respectively.

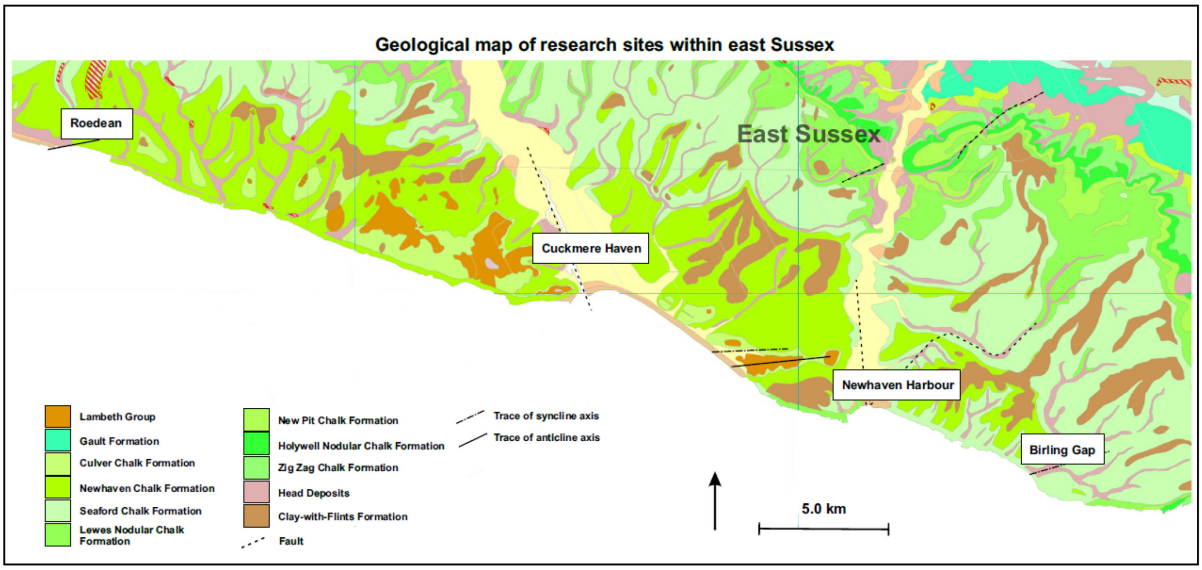


Figure 2-4 Geological map of research area within east Sussex, with the extents of Roedean to Birling Gap (Digimap, 2023).

2.5.2 Geological history

The early Cretaceous was characterised as a warm period in geological time, with high eustatic sea levels resulting in shallow, epicontinental seas (Scotese et al. 2025). In terms of sea level, the beginning and end periods of the Cretaceous were relatively low (estimated as +50 – 70 m), with the highest coinciding with the mid Cretaceous, with highest levels estimated as +150 m, resulting in high continental flooding (Scotese et al. 2025).

By this period of geological time, Pangaea had broken up, with gradual widening of the North Atlantic ocean as the American and Eurasian plates moved apart. In north-western Europe, significant amounts of chalk was deposited, resulting in the chalk formations observed in the United Kingdom, as well as the cliffs observed on the Normandy coast, and Belgium, Luxembourg, the Netherlands, Germany, Denmark and the North Sea. In addition to the Chalk, the biogenically favourable warm temperatures and epicontinental flooding led to the deposition of Limestone and carbonate platforms that became the Paris basin, the Juras mountain range and the Northern Alps. Towards the end of the Cretaceous, the convergence of the African and Eurasian plate led to marine transgression, reflected by deep water marine Flyshe deposits and shallow marine and continental Molasse deposits in the foreland basin (Scotese et al. 2025).

The geological evolution of the Chalk Group in southern England has been described in four phases of geological events by Mortimore (Mortimore, 2021) (Table 2-3). The first phase was characterised by extensional tectonics, known as the syn-rift phase (Mesozoic – Mid-Cretaceous). As Pangaea broke apart and the Atlantic Ocean opened due to extension, normal and strike-slip faulting occurred in response to induced tensile stresses, resulting in an extensive series of half-grabens and a considerable amount of accommodation space for sediment. These stresses resulted in reactivation of faults in the Hercynian basement and production of normal faults in the east, which led to the creation of the Wessex Basin and, further east, the Weald Basin (Mortimore, 2021).

Table 2-3 Geological evolution of the Southern Chalk Province of Great Britain (adapted from Mortimore, 2021)

Phase of geological evolution	**Geological age**	**Event**	**Mechanism**	**Impact on chalk landscape**
1	Mesozoic – Mid-Cretaceous	Syn-rift phase of sedimentation.	Extensional regime – strike slip faults and normal faults leading to extensive accommodation space for sedimentation. Reactivation of Hercynian faults.	Increased accommodation space for sediments. Reactivation of underlying basement faults led to the production of the Weald and Wessex basins.
2	Early – Late Cretaceous	Increased global sea levels and basin inversion.	Mid ocean ridge production increased, which resulted in a change to marine conditions within the Weald Basin as the basin flooded.	As sea levels progressively increased the deposition and lithification of the calcareous ooze on continental shelf settings occurred.
3	end-Cretaceous	Post-rift uplift, contemporaneous sea level fall and erosion of uplifted rocks.	Strike-slip generated periclinal fold belts causing protracted erosion, rendering the uplifted deposits topographically low-lying.	Campanian and Maastrichtian chalks eroded but preserved in low-relief synclinal structures in the South Downs. Topographic lows also in-filled. Palaeogene sediments laid down.
4	end-Miocene - Quaternary	Glaciation and periglaciation. Reactivation of strike-slip faults.	Glacial and periglacial processes, such as cryoturbation. Reactivation of strike-slip faults Weathering due to glaciation. Alluvial erosion.	Erosion of chalk. Oversteepening of *en-echelon* folds and Palaeogene periclines, Weathering due to glaciation events. Cryoturbation of chalk.

The second phase of geological evolution (Early – Late Cretaceous) was characterised by increased global sea levels, compressional reverse faulting and basin inversion. For the south-east of England, it also resulted in the deposition of the chalk. Mid-ocean ridge production increased, which resulted in a change to marine conditions within the Weald Basin as the basin flooded. Sea levels progressively increased through the Cretaceous, initially depositing greensands and ammonite-rich clays. Following this, deposition of calcareous oozes that would lithify to chalk occurred on continental shelves. The

inversion in tectonic stresses (i.e., extension to compression, known as the post-rift phase) resulted in normal faults becoming reverse thrust faults, and strike-slip faults became inverted, uplifting the Weald Basin into the Weald Anticline (Mortimore, 2021).

A third phase of evolution occurred at the end-Cretaceous comprising further uplift and folding driven by post-rift tectonic processes, sea-level fluctuation (but the general trend is sea level fall) and subsequent erosion of the uplifted rocks (Mortimore, 2021). As strike-slip generated periclinal fold belts, protracted erosion occurred, rendering the uplifted deposits topographically low-lying and planar (Mortimore, 2021). In the north, Campanian and Maastrichtian chalks are eroded completely, but preserved in low-relief synclinal structures in the South Downs. Topographic lows are also in-filled with sediment generated in the northeast up-lands. Throughout this period, folding and erosion of the chalk occurred, and Palaeogene sediments were laid down, reflecting both climatic and sea-level fluctuations (Mortimore, 2021).

The fourth phase occurred at end-Miocene through the Quaternary and was dominated by erosion and modification due to glacial and periglacial processes. Reactivation of strike-slip faults resulted in oversteepening of *en-echelon* folds and Palaeogene periclines, significantly increasing their dip. Weathering due to glaciation events and alluvial erosion caused significant loss of Palaeogene deposits and cryoturbation resulted in reworking of the upper layers of chalk.

The geological evolution of the south-east of England is important as both tectonics and periglacial action contribute to weathering. This framework for geological evolution indicates the likely distribution of tectonic controlled weathering (i.e., stress distribution, joint and fracture sets, as well as increased frequency of fractures at proximity to larger faults). This geological evolution also provides a crude itinerary of rocks not observed (i.e., those part of the stratigraphy, but are absent due to erosion) (Mortimore, 2021). The fourth sequence in the geological evolution of the south-east of England is particularly important to this study as large drainage systems developed as meltwater from periglacial environments drained towards the English Channel, the remnants of which are preserved as truncated, hanging, dry valleys, filled with Quaternary sediments – these dry valleys and periglacial re-working in the upper surface layers of chalk are effectively evidence of Quaternary weathering encountered in the field today.

2.6 The classification of chalk

Classification of chalk for engineering purposes has been developed over several years owing to the unique material properties of the chalk itself. It is also important to acknowledge how chalk is classified in the broader carbonate context to identify limitations of these systems and why schemes for engineering behaviour are required.

2.6.1 Classifications of carbonate lithofacies

Two classification systems have been widely adopted for describing carbonate lithofacies and textures; the Folk classification system (figure 2-5 - developed in 1959) (Folk, 1959) and the Dunham classification system (figure 2-6 - developed in 1962 (Dunham, 1962)**,** later modified in 1971 (Embry and Klovan, 1971)).

The basis for the Folk system is to describe the relative proportions of allochems (transported grains) to matrix in thin section (Perras and Diederichs, 2011)**.** The classification was initially used for classifying marine sandstones, and later adapted to marine limestones, where the matrix comprises sparry cement (>10 µm) or calcareous ooze (1 – 4 µm), hosting allochems (also described as sparry or micritic) (Perras and Diederichs, 2011).

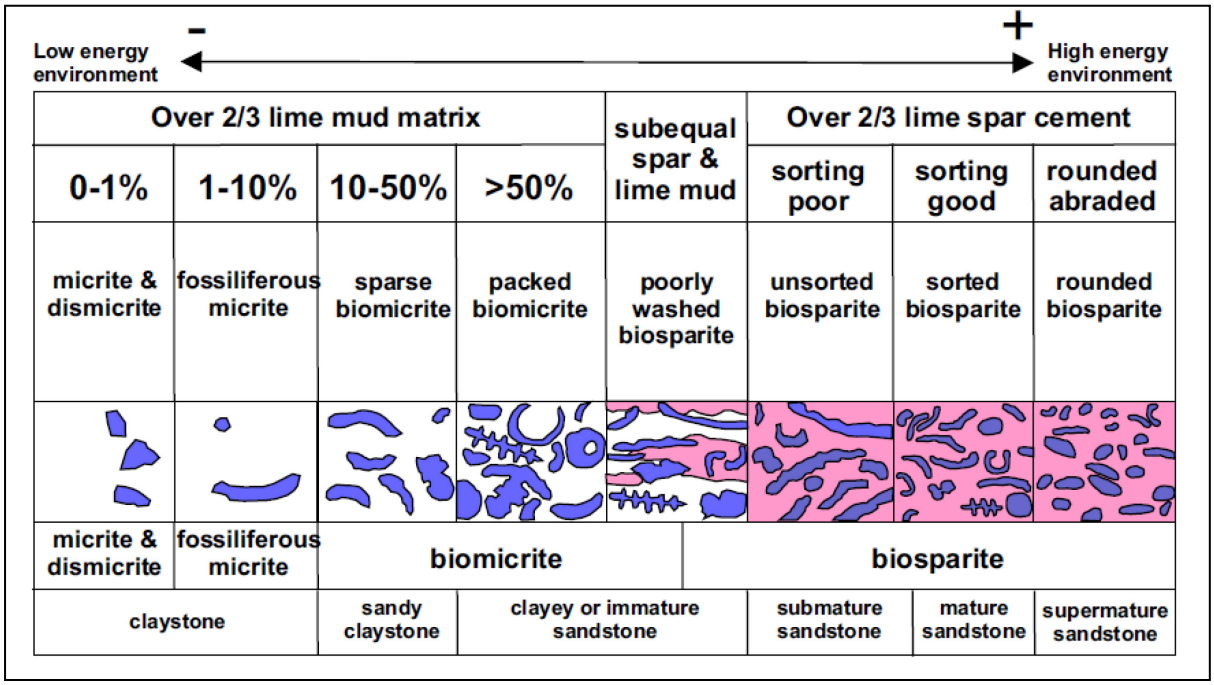


Figure 2-5 The Folk classification system for carbonate rocks (after Folk, 1959).

As the initial basis for the Folk classification was intended for sandstones, there is a considerable grainsize difference compared to coccoliths. This is significant in terms of how appropriate this classification is for classifying chalk textures on this scale. This is supported by the typical homogeneity of grainsize observed within lithified chalks. This implies that, when using the Folk classification

system, a true, apparently homogenous chalk would be categorised as micrite, dismicrite or fossiliferous micrite, with little requirement for other textures within the Folk system (figure 2-5). The Dunham classification system (figure 2-6) is also based on the ratio of matrix content to larger clasts or grains, however, unlike the Folk classification system, can be employed using either a microscope in the laboratory or hand lens in the field (Perras and Diederichs, 2011).

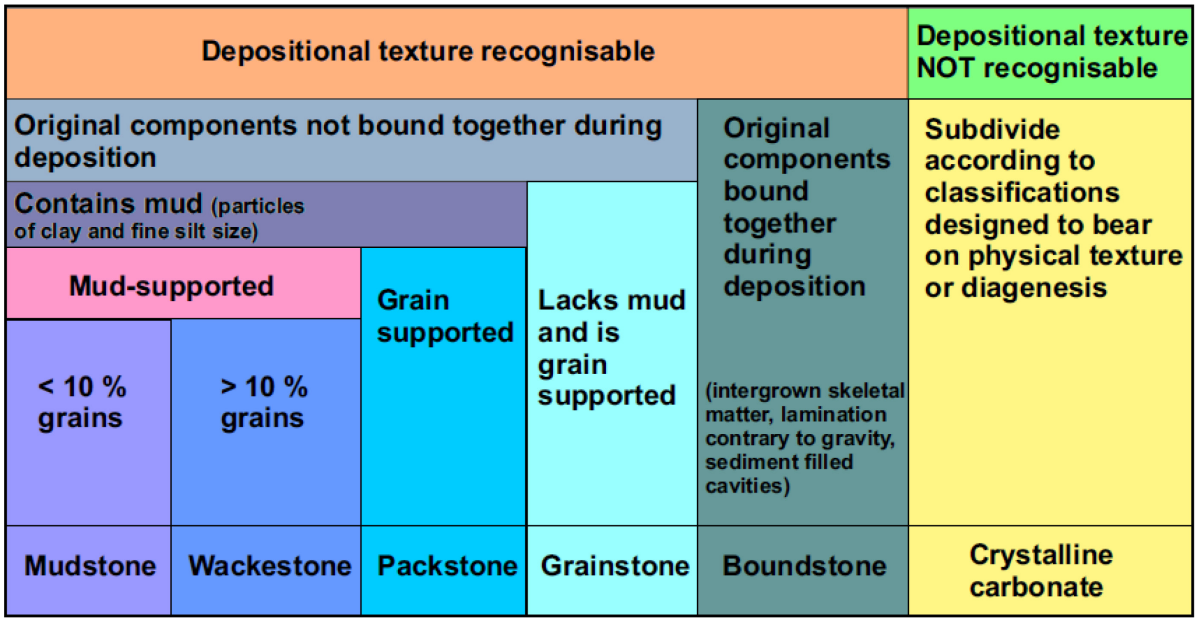


Figure 2-6 The Dunham classification system for carbonate rocks (after Dunham, 1962).

In terms of classification based on grainsize and texture as per the Dunham classification, homogenous chalk would be categorised as a mudstone, while fossiliferous chalks may move into the wacke and packstone categories, with little use of the rest of the classification system. Given this limited scope, both systems would be considered to be inappropriate for engineering classification.

Another limitation, as identified by Lokier et al. (2016), is that, while these schemes are well established, there is still a wide disambiguation between practitioners (both academic and industry based) in terms of accurate and repeatable description (Lokier and Al Junaibi, 2016). This could be interpreted as each of the systems being either too complex in terms of their components, or the material yields too little detail, or details which may easily be misinterpreted by practitioners.

2.7 The engineering classification of chalk

In 1968, a grading system based on weathering and the presence or absence of structures (bedding and jointing) was devised by Ward et al. (1968) for a site in Mundford, United Kingdom, as part of a site investigation for a proposed proton accelerator (Ward et al. 1968). This system is commonly referred to as the Mundford Grade system.

In the absence of an engineering classification system for chalk, and the fact that the attributes used in the system were applicable to most other chalks, the Mundford grades were widely adopted by other practitioners. Grades IV, V and VI in this system are specifically the result of weathered texture and are therefore independent of chalk lithology (Ward et al. 1968). In 1970, Wakeling then adapted the Mundford Grades to include very soft, saturated grade V chalks, referring to them as grade VI (Table 2-4) (Bell et al. 1999, Wakeling, 1970).

*Table 2-4 The Mundford Grades, developed by Ward, et al. 1968, * - modification by Wakeling, 1970)*

Grade	Brief description	Approximate range of E (kg cm^{-2})	Bearing pressure causing yield (kg cm^{-2})	Creep properties
VI*	Saturated, structureless remoulded chalk containing lumps of intact chalk	< 5,000	< 2	Exhibits significant creep
V	Structureless remoulded chalk containing lumps of intact chalk	< 5,000	< 2	Exhibits significant creep
IV	Friable to rubbly chalk with open joints often infilled with soft remoulded chalk	5,000 – 10,000	2 - 4	Exhibits significant creep
III	Medium to hard rubbly to blocky chalk with closely spaced, slightly open joints	10,000 – 20,000	4 - 6	Pressures not exceeding 4 kg cm^{-2}
II	Medium hard to hard chalk with widely spaced tight joints	20,000 – 50,000	> 10	Negligible creep for pressures of at least 4 kg cm^{-2}
I	Hard brittle chalk with widely spaced, tight joints	> 50,000	> 10	Negligible creep for pressures of at least 4 kg cm^{-2}

In 1990, Spink and Norbury published a grading of the Middle and Upper Chalks in the Proceedings of the International Chalk Symposium (Table 2-5) (Spink and Norbury, 1990) based on the presence of structures, descriptions of structures and visual estimation of the ratio of fines to coarse material. Concurrently, Mortimore et al. (1990) also produced a hardness scale for chalk, related to intact dry density (Mortimore and Fielding, 1990).

Table 2-5 Classification system by Spink and Norbury (1990).

Structure	Grade	Colloquial description of grade	Definitions of grade		Typical features of grade	
			% comminuted chalk matrix	% coarser fragments	Weathering of coarser fragments	Strength of coarser fragments
Structureless chalk, bedding & jointing absent	VI	Putty chalk with small lumps	Greater than ca 35%	Less than 65%	Moderately, highly or completely weathered	Very weak or weak
	V	Chalk lumps in comminuted matrix	Less than ca 35%	Greater than ca 65%	Moderately or highly weathered	Very weak or weak
			Fracture spacing (mm)	**Fracture width (mm)**	**Material weathering**	**Material strength**
In situ structured chalk, with bedding & jointing	IV	Rubbly chalk	Extremely closely to very closely spaced <60	Open or infilled ≥5	Moderately or highly weathered	Very weak or weak
	III	Rubbly to blocky chalk	Closely spaced 60-200	Open or infilled ≤3	Slightly or moderately weathered	Weak or moderately weak
	II	Blocky chalk	At least medium spaced >200	Tight & clean	Fresh or slightly weathered	Moderately weak
	I	Brittle & massive chalk	At least medium spaced >200	Tight & clean	Fresh or slightly weathered	Moderately weak or moderately strong

In 2002, the Construction Industry Research and Information Association (CIRIA) published C574: Engineering in Chalk (Lord et al. 2002), which includes a classification designed to be used with BS5930 code of practice for ground investigations (BSI, 2015).

This classification comprises three categories; fracture aperture, fracture spacing and density (assumed to be the most important properties which influence the behaviour of a chalk as a rock mass); The chalk is initially given a grade based on degree of structure (Table 2-6), grades A, B and C are structured chalk, differentiated by fracture aperture; A grades correspond to closed fractures, B grades correspond to discontinuity apertures <3 mm, while C grades have discontinuity apertures of 3 mm or greater. D grades signify de-structured chalk, with two further sub-classifications based on ratios of matrix to clasts - Dm assigned for deposits with a matrix component of 65% or greater, or Dc, where clasts are 65% or greater. Figure 2-7 presents typical fracture apertures and corresponding CIRIA grades.

Table 2-6 CIRIA discontinuity aperture grades (Lord et al. 2002).

CIRIA chalk grade	Typical discontinuity aperture	Subdivision
Grade D	Structureless or remoulded melange	
D_m		D_m = comminuted matrix >35% (matrix dominated)
D_c		D_c = comminuted matrix <35% (clast dominated)
Grade C	>3mm	Suffix 1-5 – BS5930 discontinuity spacing 't'
Grade B	<3mm	Suffix 1-5 – BS5930 discontinuity spacing 't'
Grade A	Closed	Suffix 1-5 – BS5930 discontinuity spacing 't'

The second component in this system (Table 2-7) is based on fracture spacing and assigns a numerical suffix (1 – 5), with grade 1 having the widest fracture spacing (600 mm or greater), while grade 5 have fracture spacings of less than 20 mm**.**

Table 2-7 CIRIA discontinuity spacings (Lord et al. 2002).

Suffix	Typical discontinuity spacing 't'
1	T > 600mm
2	200mm < t < 600mm
3	60mm < t < 200mm
4	20mm < t < 60mm
5	T < 20mm

The third component is density grading (Table 2-8), where the chalk is classified as low (<1.55 Mg/m^3), medium (1.55 Mg/m^3 ≤ IDD ≤ 1.70 Mg/m^3), high (1.70 Mg/m^3 ≤ IDD ≤ 1.95 Mg/m^3) or very-high density (>1.95 Mg/m^3) (Lord et al. 2002). This component is based initially on intact dry density measurements in the laboratory but provides alternative field identification methods based on the authors' experience. These methods include ease of breaking fragments by hand, penetration of a 150 mm nail and penetration of both used and new geological hammer picks. The authors have also correlated these density categories with approximate UCS values as well as strength terms from BS5930 (BSI, 2015).

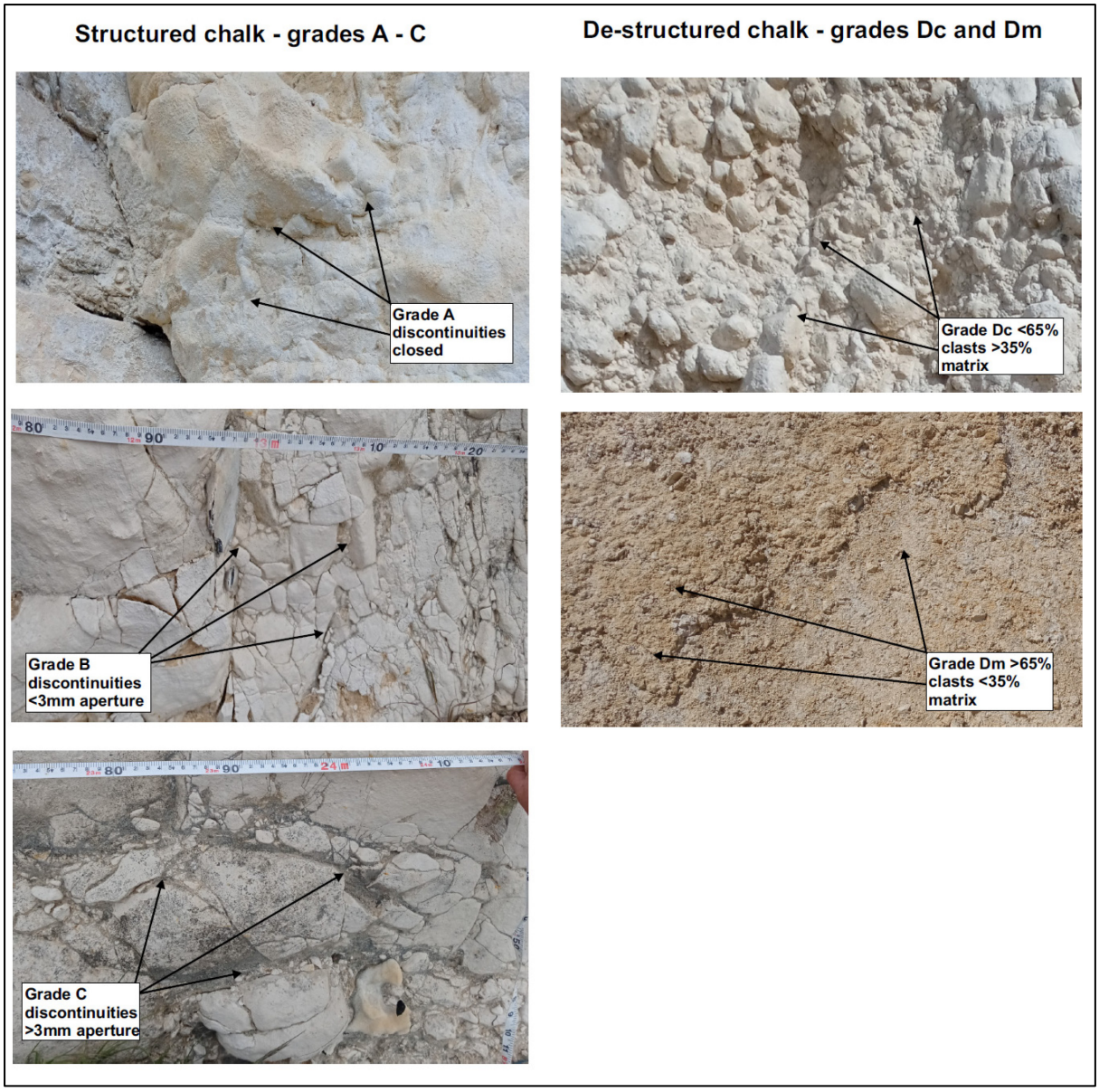


Figure 2-7 Structured and de-structured chalks reflecting CIRIA grades

Table 2-8 CIRIA density grading (Lord et al. 2002).

Identification method	Low density	Medium density	High density	Very high density
Intact dry density	<1.55 Mg m^{-3}	1.55 – 1.70 Mg m^{-3}	1.70 – 1.95 Mg m^{-3}	>1.95 Mg m^{-3}
Approximate UCS	<3 MN m^{-2}	3 – 5 MN m^{-2}	5 – 12.5 MN m^{-2}	>12.5 MN m^{-2}
BS5930:1999 *Amendment 1 (December 2007)* strength terms	Extremely weak to very weak	Very weak	Weak	Weak
Ease of breaking fragments	30 – 40mm fragments can be crushed between finger & thumb, and be remoulded to putty	30 – 40mm fragments can be broken in two using both hands but cannot be crushed between finger and thumb	30 – 40mm thick fragments cannot be broken in two. Only thin slabs <10mm thick, and corners and edges of lumps can be broken with difficulty using both hands	Cannot be broken by hand. 100mm diameter lump can be broken with a single hammer blow when held in the palm of the hand
150mm nail penetration	>25mm, putty forms around nail	15-25mm	6-15mm	<6mm
Used hammer pick penetration	>30mm, chalk splashes	11-30mm	2-11mm	<2mm
New hammer pick penetration	>35mm, chalk splashes	18-35mm	6-18mm	<6mm

In 1990 (subsequently updated in 2017), Preene and Roberts produced guidance on dewatering methods in chalk for construction. The guidance provided approximate permeabilities of chalk, relating them to the CIRIA grades, Mundford grades and the Spink colloquial rock descriptions (Preene and Roberts, 2017) (Table 2-9), however these are heavily caveated and are not intended to replace a grading scheme or site-specific hydrological investigation. This is because depending on chalk structures (or their absence) within the matrix, fractures and their frequency, there is disparity in how the Chalk transmits water and, how the Chalk behaves (either as rock, or a geotechnical soil). While approximate permeabilities may be useful, they are approximations and would not reflect how water is transmitted.

Table 2-9 Chalk gradings correlated with approximate permeabilities by Preene and Roberts (2017).

CIRIA Grade	Mundford Grade	Chalk type (after Spink 2002)	Approximate permeability range (m/s)
A	I & II	Structured; bedding and/or jointing	Erratic due to presence of fissures
B & C	III & IV	Structured; bedding and/or jointing	10^{-5} to 10^{-3}
Dc	V & VI	Structureless; clast dominated	10^{-7} to 10^{-9} in relatively soft Chalk; 10^{-5} to 10^{-3} in relatively harder Chalk, where they form chalk bearings or frost shattered Chalk
Dm	V & VI	Structureless; matrix dominated	10^{-7} to 10^{-9}

While the CIRIA grading system has been called a weathering grade system, there are limitations in their use. Using the CIRIA grades exclusively, without a rock description, would not provide an accurate representation of the chalk and the system does not quantify weathering by exclusively assigning a grade – it is necessary to use other observations and engineering judgement to define what fractures sets are sedimento-tectonic in origin (i.e., not weathered) and fracture sets whose provenance are weathering processes.

Table 2-8 (used for field density approximation) can be considered semi-quantitative, while the tables used for characterising aperture (Table 2-6) and spacing (Table 2-7) are based on quantitative measurements. The approximation of density in a field setting is considered a limitation in that the prescribed method of using hammer pick or 150 mm nail penetration is subjective, with repeatability and precision being inconsistent between users with differing physiology and levels of experience. To constrain the uncertainty posed by this component of the CIRIA C574 methodology. a suitable standardised method would be required, such as an instrument that could be used in the field.

Other limitations of the system, which underpins the case for review include the fact that the system does not measure or identify weathering types; each of the three aspects measured are not co-dependent on each other, therefore does not measure weathering as a process (e.g., fracture frequency is not controlled by density), while another limitation is that the system does not characterise D-grade chalks except for an approximation of the ratio of clasts to matrix. It does not quantify clast size, angularity or degree of clast interlocking, which may affect engineering behaviour.

Several systems have been developed for classifying rock masses, with CIRIA C574 being specific to chalk geology. Table 2-10 shows a breakdown of components for the CIRIA weathering grades,

Bieniawski's RMR system (developed in 1974), the Q-system (developed by Barton at NGI in 1974) and the GSI system, developed by Hoek and Brown in the 1990's. Some of the components within the latter three rock mass rating systems are similar to the CIRIA method in that they semi-quantify discontinuity characteristics and spacings. The RMR, Q-system and GSI rock mass systems are designed to provide an 'index number' on rock mass quality, with the intention of this number being used within numerical designs, while the CIRIA grading system provides a descriptive result.

Table 2-10 Comparison of rock mass rating systems

CIRIA C574 weathering grades (Lord et al. 2002)	RMR system (Bieniawski, 1974)	Tunnel Quality system (Q-system) (Barton et al. 1974)	Geological strength index (GSI) (Hoek, 1994)
(i) Description of chalk to BS5930 (ii) Density grade estimation (iii) Discontinuity aperture (iv) Discontinuity spacing	(i) Uniaxial compressive strength of rock material (ii) Rock quality designation (RQD) (iii) Discontinuity spacing (iv) Discontinuity conditions (v) Groundwater conditions (vi) Discontinuity orientation	(i) Rock quality designation (RQD) (ii) Number of joint sets (Jn) (iii) Roughness of most poor joint (Jr) (iv) Degree of alteration and infilling (Ja) (v) Water inflow (W) (vi) Stress reduction factor (SRD)	Estimation of rock mass strength based on physical appearance of the structure of the rock mass and the surface conditions of discontinuities Designed to be implemented within the Hoek-Brown failure criterion.

The strength of rock mass rating systems lie in standardisation, practicality and ease of use, versatility and compatibility with design methods, while limitations include subjectivity, oversimplification of geological regimes and empirical nature of their application. Of the four systems considered, only the CIRIA C574 method is chalk geology specific, and none measure weathering quantitatively, with some comment on alteration. The RMR and Q systems, unlike the CIRIA C574 weathering grades and GSI, provides rock mass reinforcement guidance, while GSI is not appropriate for highly disturbed rock masses (Hoek et al. 2005), which a CIRIA D-grade chalk and chalk grades B3 – C5 (discontinuity spacing and aperture) chalk would be considered.

2.8 The physical properties of chalk material

Chalk can present itself as an apparently homogenous material but can be considered a complex rock type to characterise, with variation occurring on the material scale, as well as on a formation scale. Chalk can be characterised as a rock mass using engineering classification but can also be characterised using material properties – both for intact chalk and for de-structured chalk.

2.8.1 Material properties of intact chalk

The physical properties of chalk are assessed to provide an insight as to how the chalk will behave mechanically as an engineering material (Mortimore et al. 2004b) and can be used to inform an engineering geologist of the chalk's behaviour under working conditions (Head, 2006).

Preliminary index tests include intact dry density (IDD), natural moisture content (NMC) and saturated moisture content (SMC). Values for intact chalks have been published by CIRIA (Table 2-11) (Lord et al. 2002). These material properties correlate well with geomechanical tests, such as point load index, strength tests and porosity (Mortimore et al. 2004b), which gives some indication as to the behaviour of chalk from small scale testing.

Table 2-11 Material properties of chalk published in CIRIA C574; Engineering in Chalk (Lord, et al. 2002).

Property	**Symbol**	**Unit**	**Range**
Dry density	γ_d	Mg/m^3	1.29 – 2.46
Porosity	n*	%	9 – 52
Voids ratio	e*	-	0.10 – 1.10
Saturated moisture content	m_{sat}	%	4 – 40
Calcium carbonate content		%	55 – 99
Specific gravity	G_s	-	2.69 – 2.71
Liquid limit	w_L	%	18 – 53
Plasticity index	I_p	%	4 – 30
Liquidity index		-	-2.25 – +2.50
Point load index	$I_{s(50)}$	MPa	0.01 – 1.15
Unconfined compressive strength	q_u	MPa	0.7 – 40
Slake durability index	I_{d2}	%	13 – 96

IDD and SMC are considered the most important index tests for chalk (Lamont-Black and Mortimore, 1996), with IDD consistently correlating with strength (Lamont-Black and Mortimore, 1996) and the degree of porosity (Bloomfield et al. 1995). Moisture content can be sub-divided into two properties; NMC, which reflects insitu moisture conditions, and SMC, which reflects the maximum amount of moisture a sample can hold.

Chalk as an engineering material has the capacity to retain a high NMC (close to saturation) (Higginbottom, 1966)**,** which has implications for engineering applications, such as the use of chalk as an engineering fill and use in embankments (Lord et al. 2002)**.** Chalks with a high moisture content tend to be more susceptible to frost action, more easily crushed and puttified during engineering works and weaker (in terms of strength) by virtue of this high moisture content (Lord et al. 2002)**.**

Natural moisture content in this context is effectively the amount of moisture preserved within the matrix of a specimen in its natural condition (i.e., conditions in which the specimen is found). Variability in natural moisture content is observed and can arise for several reasons, including specimen provenance (i.e., coastal or in-land), depth of sampling with respect to the chalk unsaturated and saturated zones and other ground water conditions, time of year and meteorological input (Lord et al. 2002).

SMC is the maximum amount of moisture a rock can hold at saturation, where pore spaces are filled with water, expressed as a percentage. Lamont-Black et al. demonstrated a relationship between IDD and moisture content (Lamont-Black and Mortimore, 1996)**,** whereby higher density chalks retained water more readily, while lower densities had variation in measured NMCs (Molyneux, 2012)**.** Figure 2-8 demonstrates that Chalks with density less than the 1.70 Mg/m^3 have a greater deviation from the IDD-SMC line presented by Mortimore et al. Chalks above this density value have much less deviation and NMC can be considered to be equivalent to SMC (Mortimore et al. 2004b)**.** This relationship between IDD, NMC and SMC can be considered significant (as identified by Molyneux) in that chalks with an IDD of 1.70 Mg/m^3 and below are able to gain and lose water more readily/easily (Molyneux, 2012)**,** which would indicate that regardless of strength, lower density chalks were more susceptible to water weakening processes.

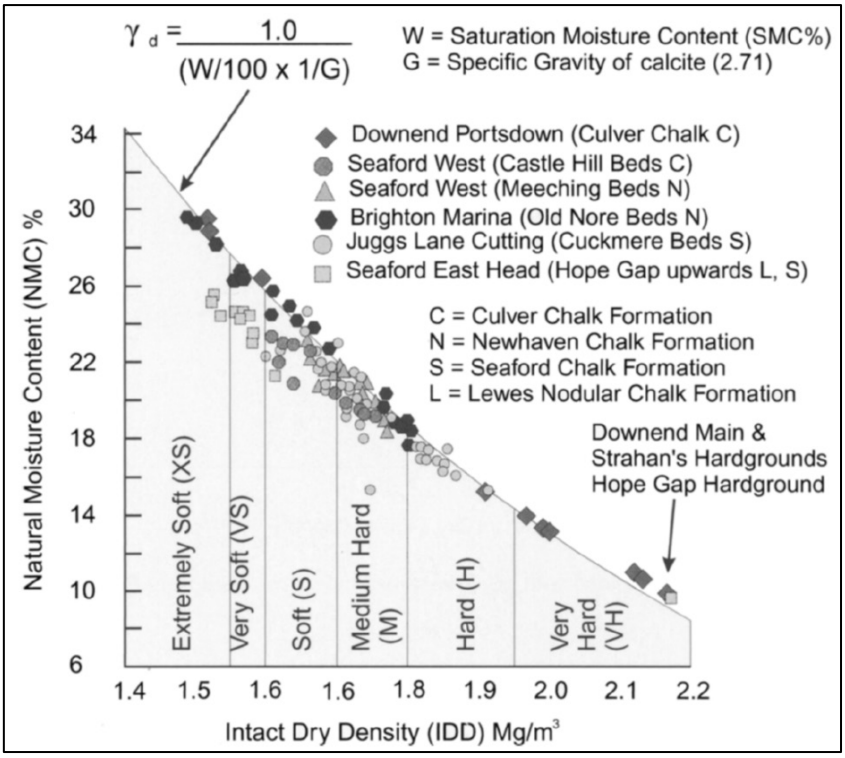


Figure 2-8 NMC versus IDD with SMC line plotted (Mortimore et al. 2004).

While it is possible to establish physical characteristics, there are limitations as to what this information can provide in that understanding of processes that occur within the chalk material are limited in some areas (such as that of diagenetic history or weathering processes). The implication of this is that index testing alone is not sufficient for true classification, without some geological context, however, as the index tests can be closely correlated with other geomechanical tests, index tests should remain an integral part of the preliminary investigation.

Index tests would be necessary when investigating weathering in the chalk as they would allow a baseline index of the behaviour competent chalks, whereby any changes in physical properties due to weathering could be measured and compared against. It is likely that mechanical properties will dictate how a chalk will be more susceptible or resistant to weathering.

2.8.2 Material properties of de-structured Chalk

Investigations of the material properties of insitu D-grade chalks (i.e., Dc and Dm) are sparse and there is little in terms of specific guidance relating to construction in these materials (Williamson and Solera, 2018)**.** CIRIA C574 states that de-structured chalks should be approached as engineering soils rather than weak rocks, with Dm grades likely to behave as fine cohesive soils and Dc grades likely to behave as coarse granular soils (Lord et al. 2002). While studies relating to formally graded chalks are sparse, there are a number of studies that relate to de-structured, re-constituted chalk putties (Clayton (1978)**,** Razoaki (2000)**,** Spearing-Bundy (2013), Doughty et al. (2016), Bialowas, (2017), Alvarez-

Borges, (2019) and Liu et al. (2021)), which have been prepared in laboratory settings with the aim of ascertaining their material properties in the context of putty production through excavation, pile driving and other engineering works (Table 2-12).

Table 2-12 Select index properties of de-structured chalk by various authors

Author	**Formation**	**IDD (parent material) (Mg/m^3)**	**Liquid limit (%)**	**Plastic limit (%)**	**Mean grain size**	**$CaCO_3$ content (%)**
(Clayton, 1978)	Seaford	1.43	-	-	<2 mm	-
(Razoaki, 2000)	Newhaven	1.65	28	22	425 µm	97.12
(Spearing-Bundy, 2013)	Culver	1.78	22.1 – 24.7	18.3 – 20.8	0.2 - 2 µm	98.61
(Spearing-Bundy 2013)	Newhaven	1.65	21.9 – 22.9	25.3 – 26.8	0.2 - 2 µm	99.34
(Doughty, 2016)	Maastrichtian	1.50	33 – 38	23 – 25	-	-
(Bialowas, 2017)	Margate	-	30	22	-	-
(Alvarez-Borges, 2019)	Seaford	1.57	28 – 29	22	-	98.2
(Alvarez-Borges, 2019)	Seaford	1.47	30 – 31	22 – 23	-	98.5

The effective angle of shearing resistance observed within this range of tests is 29° - 39°, with samples exhibiting contractive behaviour initially, before reaching a critical point where dilation occurs. Work by Razoaki (2000) suggests that the behaviour of chalk slurry during shear is similar to a granular or low plasticity material, with peak strength ratios corresponding to a shear resistance of 31.2° (Table 2-13), while Spearing-Bundy (2013) identified that de-structured chalk can be classed as an ML soil as per BS5930 (i.e., a silt) with limited thixotropy and plasticity. Bundy prepared putties from both Culver Chalk and Newhaven Chalk and found that shear angles vary between 29° - 38°.

Table 2-13 Angles of shearing resistance taken from literature.

Author	**Test type**	**Ø°**
(Lake, 1975)	Undrained triaxial	33° (critical state)
(Clayton, 1978)	Drained triaxial	31° – 33°
(Fletcher and Mizon, 1984)	Drained triaxial	39°
(Twine and Wright, 1991)	Shear box	39°
(Razoaki, 2000)	Consolidated Drained triaxial	31.2°
(Spearing-Bundy, 2013)	Unconsolidated Undrained triaxial	29° - 38°
(Bialowas, 2017)	Consolidated Drained triaxial	33°
(Le et al. 2014)	Shear box and ring shear	26° (undrained) 30° (drained)
(Doughty, 2016)	Consolidated Undrained triaxial	31°
(Alvarez-Borges, 2019)	Consolidated Undrained triaxial	31.8° - 31.5° (critical state) 33.2° – 36°
(Liu et al. 2021)	Consolidated Undrained triaxial	30.1° – 31.6°

Stabilisation of compacted, de-structured chalks, and subsequent increase of strength over time has been observed (Lord et al. 2002), which could have significant implications for field recognition and construction in insitu D-grade chalk deposits. This increase in strength has been used to explain increase in pile capacity over time and has been attributed to (i) consolidation due to excess porewater dissipation and overgrowth of $CaCO_3$ (released during compaction) providing additional cementation (Clayton and Matthews, 1987). Given that both excess pore water pressure and release of $CaCO_3$ are associated with an increase in energy due to construction processes, the question which arises here is whether insitu D-grade chalks (having formed from weathering processes rather than excess energy input) behave in a similar fashion to idealised re-constituted chalks (i.e., de-structured chalk due to compaction and construction). Another key question is whether D-grade chalks should be treated as a weak rock or a stiff soil.

Thixotropy is a term relating to shear thinning and occurs when a soils behaviour changes from that of a gel (where the material will flow subject to an applied shear force of a specific value), to a sol (where the material will flow under any applied shear force). The unit used to define thixotropy is the 'N' value, which is the void ratio that corresponds to a soil sample which behaves thixotropically in an inverted test tube when tapped with a finger (Boswell, 1948)**.** It must be noted that while soils require a certain moisture content, flow is induced by the input of energy and not the addition of water. Boswell (1948) observed 'N' values of 1.5 – 2.6 in Senonian chalks, while Spearing-Bundy (2013) observed values of 2.1 – 2.3. In terms of shear strength increase over time Doughty et al. (2016) observed shear strength increasing from 2.4 kPa to 7.4 kPa after 28 days.

The difference between Dm and Dc chalk is largely their grain size and sorting, with Dc chalk being clast dominated. The experiments discussed here using re-constituted chalk largely rely on processes that have homogenised the chalk and would therefore be more representative of Dm grade, rather than Dc grade chalk.

2.8.3 Permeability

Permeability can be defined as the ease of which a fluid can flow through a porous medium (i.e., permeable rock). When insitu the chalk is split into a lower saturated zone underlying a higher unsaturated zone near the ground surface. In the saturated zone, the matrix of the chalk is saturated as are the discontinuities, while in the unsaturated zone, only the matrix is saturated. Owing to this, the chalk is considered as a dual porosity aquifer and reservoir rock, therefore it is important that the permeability of intact chalk is considered as well as that of chalk rock mass.

Preene et al. (2017) produced guidance based on field tests for permeabilities and related these to CIRIA C574 weathering grades. Permeabilities by Preene et al. (2017) range from 10^{-3} to 10^{-9} m/s for structured chalks (with higher permeabilities corresponding to increased fracture density), while permeability of de-structured chalks (Dm grades) are markedly lower in the range of 10^{-7} to 10^{-9} m/s, and Dc chalks in the range of 10^{-5} to 10^{-9} m/s. It is speculated that the increased permeability of Dc grades is attributed to the microstructure of clasts and surface areas of clasts acting as preferential flow paths, while Dm chalks cannot maintain discontinuities as flow paths.

Similarly, Molyneux (2012) reports values for intact chalk of 10^{-7} to 10^{-9} m/s from field tests. While CIRIA grades are not assigned and fracture distribution has not been considered in this study, it is assumed that the figures reported by Molyneux reflect permeability of a chalk mass, rather than the material properties of the constituent chalk.

Laboratory testing on Dm and Dc grade chalks are limited but (Mider and Lawrence, 2018) identified a minor, vertical-horizontal anisotropy in intact Newhaven and Seaford Chalk material in the ranges of 1.07 – 1.11 x 10^{-8} m/s and 1.07 – 2.4 – 2.5 x 10^{-8} m/s respectively. Work by Spearing-Bundy (2013) on the permeability of reconstituted, homogenised chalk putty has produced permeability ranges of 2.5 – 12.5 x 10^{-9} m/s at a confining pressure of 0 – 400 kPa. This may reflect insitu D-grade chalks in the field. Spearing-Bundy reports that permeability reduces linearly with an increase in confining stress.

Al-Jaf et al. (2022) used a hydraulic permeameter centrifuge to measure permeability and reported values of 1.62 x 10^{-8} to 8.00 x 10^{-8} m/s for Seaford and Lewes chalk although there was no commentary on the degree of weathering of the material at the time of testing.

2.9 Types of weathering in Chalk

Weathering in chalk is dependent on location, topography, depositional and diagenetic history, and other environmental factors, such as the palaeoenvironment (i.e., climate in the Quaternary), current environmental setting (i.e., in-land or coastal), mechanical weathering (such as relaxation via isostasy, or deformation due to tectonics), meteoric input, presence of groundwater and groundwater chemical composition. One of the key challenges within this study is identification of differing weathering processes and the elucidation of the predominant process, which will affect the chalk in terms of physical properties.

2.9.1 Water weakening and karstification

Several mechanisms have been proposed for water weakening of chalk, including chemical dissolution, changes in capillary forces and increased pressure on chalk grains caused by Van der Waals attraction of water molecules to the chalk surface (Lawrence et al. 2018b)**.** These processes may contribute to the weathering of chalk.

Chemical dissolution and karstification

As chalk is a pure $CaCO_3$ deposit, it is vulnerable to acidic water. Owing to this, there are significant dissolution and karstic features within the chalk as a rock mass, which generally form where there are preferential flow paths (Lord et al. 2002). While dissolution can be the cause of material softening, reduction in shear strength, bulk density and material loss (Gallois, 2006), it can also cause hardening, where leached $CaCO_3$ is moved within groundwater, percolating through the rock mass. Subsequent re-precipitation and recrystallisation results in harder calcrete horizons.

Spatial distribution and extent of dissolution is difficult to predict, however there are three types of dissolution features, which are associated with both perched water tables and discontinuities, which allow the flow of water through the chalk (Maurice et al. 2006) (Figure 2-9). The three features are;

- Sinkholes (commonly referred to as dolines)
- Dissolution pipes
- Stream sinks or swallow holes

Sinkholes are associated with increased discontinuity density, which allows vertical flow of water through the rock**.** Increased fracture density would allow greater flow and has implications for block size – more fractures would result in smaller blocks but have a greater surface area allowing dissolution to act on more of the rock than in a single discontinuity.

Dissolution pipes occur on the intersection of major joints and discontinuities and are most common in calcium rich chalks. They are generally infilled with material, either transported by water or from

overlying collapsed sediment (Maurice et al. 2023). In terms of morphology, these pipe-like structures are not uniform and can be complex, with subsidiary pipes joining, giving rise to large voids.

Stream sinks or swallow holes form in a similar fashion to sinkholes, however, they are not infilled and transport water underground. These occur when areas of increased discontinuity density are subject to a concentrated flow of water and can be the result of differences in rock properties (i.e., less soluble material) which concentrates water flow, or man-made structures, such as drainage systems and soakaways (Lord et al. 2002; Maurice et al. 2023). Karstic stream sinks are most likely to occur when adjacent or overlying deposits produce acidic soils, leading to dissolution of the chalk.

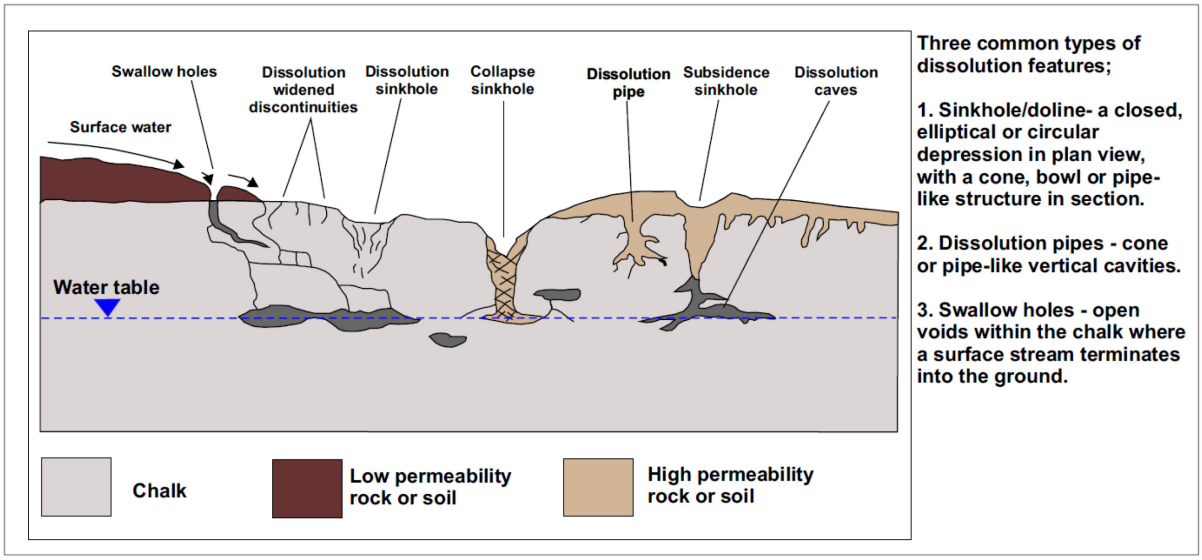


Figure 2-9 Schematic of dissolution features (adapted from Lord et al. 2002).

While dissolution features are obvious in a field setting, dissolution occurs on the material scale of chalk, resulting in increased permeabilities and weakening of intact chalk mass. Dissolution is one of several proposed (and potentially concurrently active) water-weakening mechanisms, therefore it is important to identify to what extent dissolution contributes to weathering processes.

Studies on the dissolution of terrestrial chalks are limited, with recent focus of research relating to the distribution of dissolution features, aquifer protection, and geological hazards, such as work by Maurice et al. (2023) and Rigby-Jones et al. (1994).

Studies of marine chalk dissolution have been undertaken to identify the causes of subsidence and weakening of chalk oil reservoirs, identifying mechanisms of dissolution and discounting other water-weakening mechanisms. Heggheim et al. (2005) investigated chemically induced weakening of chalk by seawater in response to oil recovery from the Ekofisk Formation, Norway sector of the North Sea. During their experiments, 3 fluids were used; (i) an artificial brine with constituent chemical composition as that of the brine taken from the Ekofisk Formation for reference (EF-Brine), (ii) a

synthetic seawater (SSW) and (iii) a synthetic seawater with 4 x sulphate amount of that of the SSW brine (SSW1) (Heggheim et al. 2005).

The mechanism of dissolution is the dilution of the initial brine in the chalk reservoir (high in Ca^2+ ions) with seawater (lower concentrations of Ca^2+ ions), causing chemical disequilibrium. This results in the dissolution of $CaCO_3$ as the CO_3 is partially removed. Results showed that chalk cores saturated with SSW1 were 20-25% weaker than cores saturated with EF-Brine and SSW, which the authors reason is due to induced dissolution.

As all cores were saturated with a saline water, the weakening effect of SSW1 could not be explained by capillary weakening as capillary pressures between the water saturated cores would have been similar (Heggheim et al. 2005)**.** The authors also identify that correlation between water activity and weakening due to water adsorption on grain surfaces was not easily observed using the methods employed (Heggheim et al. 2005)**.**

Capillary forces and degree of saturation

Delage et al. (1996) investigated oil reservoir collapse and subsidence in marine chalks by modelling the chalk at varying degrees of saturation. Delage et al. (1996) modelled chalk oil reservoir weakening using unsaturated soil collapse through capillary action as an analogue. The mechanical behaviour of an unsaturated soil was considered with simplified, spherical grains and air-water menisci acting as bridges at grain contacts. These menisci exert an increasing attraction of grains when suction is increased. When saturated, the menisci are no longer present, no capillary action is exerted, and the chalk structure is lost (Delage et al. 1996)**.** This study demonstrated that this analogue provided a reasonable prediction and order of magnitude for chalk collapse (Delage et al. 1996), and utilised SEM in their methodology to quantify (i) chalk grain size (1 - 2 µm) and (ii) pore sizes (0.1 – 10 µm) to constrain their model using chalk- based data (Delage et al. 1996).

This would suggest that saturated and water inundated chalk was weaker than chalk with a moisture content lower than SMC, such as those observed within the chalk unsaturated zone (an unsaturated profile of chalk below ground level but above the water table; 20-80 m thickness (Price et al. 2000, Al-Jaf et al. 2021). This may also have implications for de-structured deposits found insitu, as they are effectively a biomicritic silt, retain a relatively high moisture content, display an apparent cohesion and are fairly brittle when desiccated and may indicate that partial saturation is a significant contributor to strength in these deposits.

Molecular bonding

In 2003, Risnes et al. (2003, 2005), investigated if the activity of water (i.e., water bonding on the molecular level) was the main contributor to water weakening (Risnes et al. 2003, Risnes et al. 2005). Further work on the activity of water was followed by Korsnes et al. (2006). Risnes et al. investigated chalk-fluid interactions using glycol and brine solutions and undertook four types of mechanical tests; low confining pressure triaxial tests, high confining pressure triaxial tests, hydrostatic tests, and Brazilian tensile tests (Risnes et al. 2005).

Ethylene glycol, when used as a saturate in chalk, elicits a similar behaviour to that of an oil and does not dissolve calcite, which allows the consideration of chemical dissolution (as observed with water) to be disregarded. Ethylene glycol also is miscible with water and has a similar specific gravity, therefore when saturated, the chalk will not exhibit any capillary effects (Risnes et al. 2003). The water weakening mechanism proposed by Risnes et al. involves additional external pressure applied to grains via water molecule attraction to the grain surfaces. This attraction acts in a similar fashion to increased pore pressure, which reduces the cohesion of the chalk (Risnes et al. 2005).

Korsnes et al. (2006) used modified seawaters and identified that water composition had an impact on mechanical strength at higher temperatures, with dolomitization occurring at inter-granular contacts. The authors suggest that this substitution reaction increases with greater temperatures and the greater solubility of $MgCO_3$, compared to that of $CaCO_3$, would have a greater weakening effect on chalk stability (Korsnes et al. 2006).

2.9.2 Haloclasty

Studies of the effect of fresh and saline water on chalk weakening have focused on their role on chalk cliff stability in coastal environments, such as experimental work by Duperret et al. (2005), Lawrence et al. (2013) and Lawrence et al. (2018).

Duperret et al. (2005) studied groundwater and seawater weathering cycles on chalk strength using a combination of unconfined compressive strength tests (UCS) and SEM techniques**.** The study tested dry chalk samples, chalk samples with differing moisture contents and dry samples subjected to wetting and drying cycles using distilled water and salt water (Duperret et al. 2005). The study linked chalk strength relative to coastline position (and to some extent vertical cliff position), with the greatest decrease of UCS (70%) at the base of the cliff. subject to sea spray but not reached by high tide. A decrease in UCS of 40% on the shore platform was observed, where the chalk matrix is weathered by seawater but is not subject to halite crystallisation (Duperret et al. 2005).

SEM observation of chalk artificially weathered by distilled water allows the determination of weathering degree and indicates that strength reduction in these samples was likely due to the

occurrence of microcracks, particle disaggregation and the detachment of particles from the weathered rupture surface of the chalk (Duperret et al. 2005). In chalk weathered by artificial seawater, the presence of salt crystals in the matrix was identified via SEM (Duperret et al. 2005).

Lawrence et al. (2013) investigated the impact of sea water weathering on cliff stability. Methods employed include index testing, salinity tests to determine the amount of sea salt in chalk pores, triaxial tests to establish changes in rock strength and SEM analysis for mechanical, chemical and texture analysis (Lawrence et al. 2013). SEM techniques identified the weakening of the rock structure by the nucleation of cubic salt crystals within the pores. These crystals then outgrow pore space, into the surrounding matrix, altering it mechanically (Lawrence et al. 2013).

The studies undertaken by Duperret et al. and Lawrence et al. provide good examples of how comprehensive investigation can be used effectively to evaluate weathering as well as the extent of weathering. The approaches used also allow some constraint in terms of active processes, given the numerous proposed mechanisms of weathering and the uncertainty of which is most dominant, dependent on setting. While each of the methodologies discussed have been applied to assess chalk integrity with relation to petroleum exploitation or coastal cliff instability, there is merit in their approaches for the evaluation of weathering for engineering geology purposes. These techniques may be suitable to be used with experimental methods, such as slake durability and index testing, to identify the mechanisms of chalk weathering, allowing some inference of their distribution.

By using deaerated water, synthetic sea water and ethylene glycol as slaking fluids, and by changing the degree of saturation of the chalk being tested, it would be possible to evaluate if capillary forces, chemical dissolution, or molecular bonding have significant effects on the resistance of the chalk to wetting and drying cycles, with periods of abrasion.

By preparing samples of chalk from the same block, and by preparing the chalk in such a way that salt crystal may nucleate (from both saturation and analogous spray) within the chalk matrix, it would be possible to evaluate if haloclasty has a significant effect on chalk resistance to weathering.

Given that lower density chalks can take on and lose water in terms of moisture content, and the models for weakening detailed above, with water being the main agent for weakening and also solute transport (i.e., salt), it is possible to speculate that lower density chalks have an increased natural susceptibility to the mechanisms of weakening discussed.

2.9.3 Cryoturbation and ice action

In the Pleistocene, glaciers covered a significant proportion of the British mainland. The maximum limit of the icesheet formed a broadly east west line across Southern England during the Anglian Glaciation, however stopped short of the UK Southern province chalks under investigation (Figure 2-

9). This indicates that periglacial or permafrost weathering was predominant in the chalk at these localities during this time period, with little denudation (Murton and Ballantyne, 2017), thus preserving deeper weathered profiles. An alternative hypothesis is that extensive overlying Quaternary deposits in the Northern Province protected the underlying chalk from periglacial weathering (Catt and Hodgeson, 1976).

Water held within the chalk rock mas was subject to cyclic temperature changes, affecting upper surface layers (Collings, 2018), resulting in cryoturbation, weathering and brecciation, which is apparent in chalk macrotextures observed in the field, such as ice wedges and cryoturbation lobes. This has implications for distribution in that these weathering products manifest in a semi laterally extensive distribution at the near surface and are characterised by ice disturbance.

Areas subject to periglacial processes or within the permafrost thermal regime preserve deeper weathered profiles, which have been subsequently subject to non-periglacial, near-surface weathering processes after periods of periglaciation have ended (Murton and Ballantyne, 2017). Figure 2-10 details where the glacial maximum was located during the Albion and the Caledonian, with relation to both the non-glaciated province and Southern UK Chalk. The Southern province of the UK Chalk was not covered by glaciers during these periods.

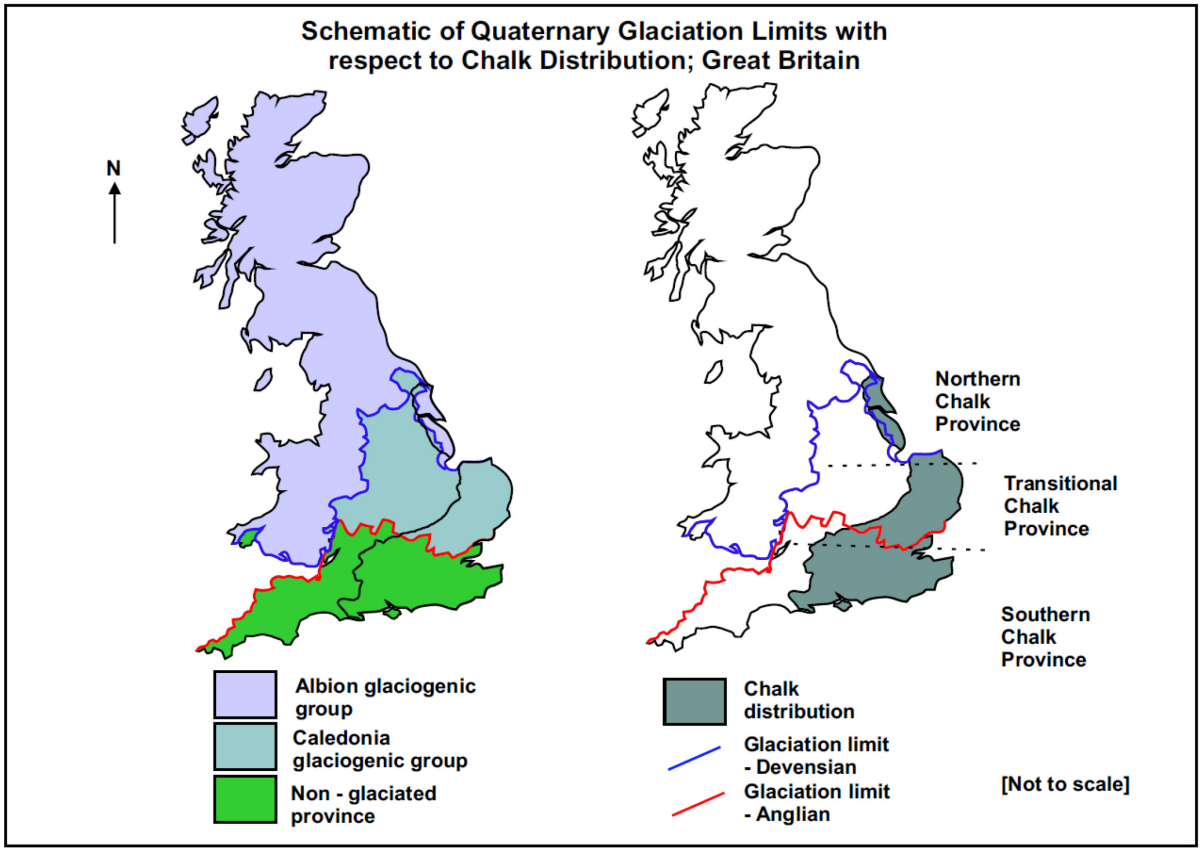


Figure 2-10 Schematic of Quaternary glaciation limits with respect to the distribution of Chalk in the United Kingdom; Northern Ireland omitted (adapted from Gibbard and Clark (2011)).

Periglacial processes in frost susceptible bedrock with high saturation levels, subject to cyclic temperature changes, such as chalk, include ice segregation, ice wedges, frost heave and thaw consolidation (Berry et al. 2020). These processes can give rise to relic features within the subsurface, such as thermokarsts, brecciation and cryoturbation involutions (Collins 2018).

Thermokarsts form when ice wedges develop within the bedrock, and upon thawing, material collapses into the void. These processes are considered relic as these do not occur within modern settings. Thermokarsts provide challenges in terms of identification as they may closely resemble dissolution features in the field (Collins 2018).

Laboratory and field studies by Murton have identified two types of brecciation attributed to periglacial processes: type 1 brecciation and type 2 brecciation (Murton, 2018a), both of which indicate weathering processes. Type 1 brecciation is observed in the relatively shallow, near-surface (1.5 – 3.0 m (Mortimore, 2014, Murton and Ballantyne, 2017) and is associated with brecciation observed underlying plateaux land systems (Figures 2-11 and 2-12) (Murton, 2018b). These observations indicate that in areas with relatively flat topography, the thickness of severe weathered profiles due to periglacial action is likely to be thinner and constrained to the upper 3.0 m.

Type 2 brecciation is observed in plateaux and dry valley land systems and can be up to 30 m deep in some dry valleys (Figure 2-12). The rock texture produced by this form of brecciation is that of a diamicton, with sub-angular to rounded lithorelicts within a fine-grained matrix (Murton and Ballantyne, 2017).

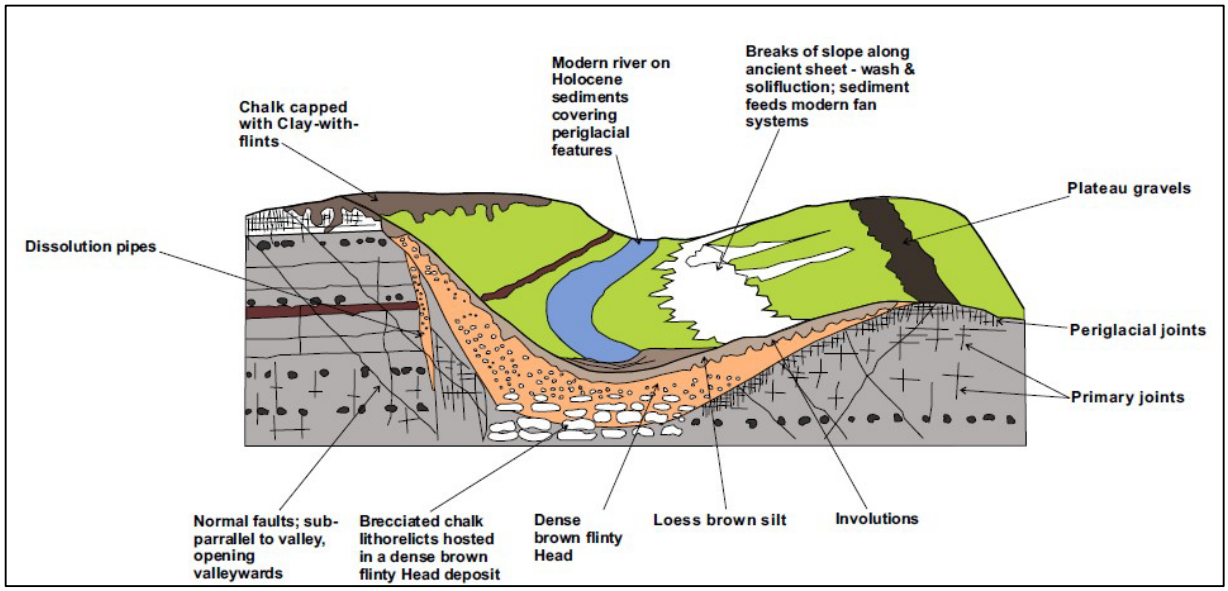


Figure 2-11 A conceptual ground model of hill and valley deposits, with landform associated weathered deposits in cross section (Mortimore, 2014).

Murton (2018a) demonstrated that multiple freeze-thaw cycles weather chalk to a fine-grained silt-chalk matrix with larger chalk clasts, therefore it is hypothesised that type 2 brecciation has undergone extensive freeze-thaw cycles compared to that of type 1. The classification of these grades would be Dc chalk for less effected breccias of type 1, while type 2 breccias may be either Dc or Dm. Generally, type 2 brecciation occurs in the uppermost sections of the bedrock, transitioning into type2 brecciation before further transitioning to competent bedrock, characterised by primary discontinuities (Berry, et al. 2020).

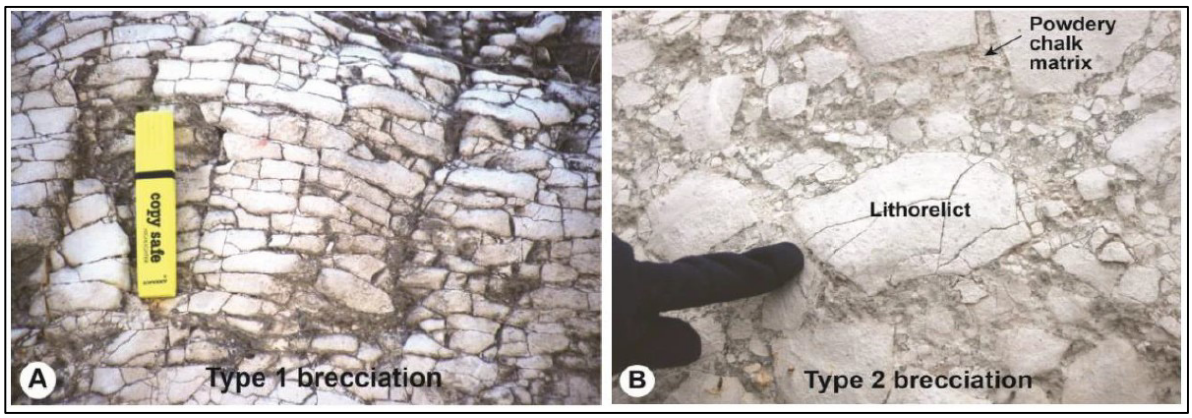


Figure 2-12 Brecciation types 1 & 2 (examples taken from (Murton, 2018a) (annotation of 'powdery chalk matrix' by Murton – chalk putty).

The mechanism(s) of action of freeze-thaw weathering in chalk are not well understood, however chalk can be considered a rock susceptible to freeze-thaw action owing to its relatively low strength (particularly in tension), high water saturation and high percent of void space, with freezing causing expansion of water when changing to ice and spalling of the material.

In terms of spatial constraint of weathering, given the extent of glaciation during the Quaternary (Figure 2-10), the southeast of the UK is likely to exhibit the deepest weathered profiles geographically. Murton's data suggests that the extent of weathering due to periglacial action is limited to <30 m, based on ground freezing. Type 1 brecciation identified by Murton was stated to reach depths of <3 m and be exhibited as cryoturbation lobes and would be expected to be a relatively uniform profile across flat topography, with deeper weathered profiles associated with topographic lows, exhibiting type 2 brecciation. This has implications for the distribution of periglacial weathering in that topography may be indicative of the extent of weathering, which allows some separation of competing and concurrent weathering processes.

2.10 Chapter summary

This Chapter has presented a detailed literature review of the deposition and formation of chalk, its geographic distribution and stratigraphy of the Southern Province Chalk Group of Great Britain in the context of chalk weathering. Aspects which are key are;

- The distribution of Chalk within Great Britain (Section 2.2) is significant for a study on chalk weathering in that it is extensive (covering approximately 21,500 km^2), split into 3 provinces, located in the south and southeast, and underlies several major cities (including London) where engineering infrastructure projects have and will be undertaken. The implications of this distribution is that is that weathering will highly likely be encountered in an engineering context and may pose engineering challenges.
- Section 2.3 presented a review of the formation of chalk, with Section 2.3.1 detailing deposition and sedimentation. These are important aspects in that the sedimentation of coccolithophores as blooms control the very material ($CaCO_3$) that chalk comprises. The implications of this constituent material is that it is physically soft, therefore vulnerable to physical weathering, and due to chemical composition, vulnerable to acidic weathering processes. Section 2.3.2 covers the lithification and diagenesis of chalk, which are also two important aspects of the formation of chalk; prolonged sedimentation has led to lithification with an absence of significant cementation, meaning that the chalk retains a unique high porosity, which is recognised as a controlling factor in chalk physical properties. Diagenesis details how the chalk has been further modified, with reductions in porosity and increased hardness, which has implications in that this may decrease chalk susceptibility to weathering.
- The stratigraphy of the chalk is presented in Section 2.4. Section 2.4.1 details the evolution of chalk stratigraphy, which effectively mirrors the increase in knowledge of chalk (differences in chalk formations and beds and their distribution) with prolonged study over time. The implication of this increase in resolution of chalk types for a weathering study is that it enables constraint of weathering to specific chalk formations. Similarly, Section 2.4.2 details the current stratigraphic framework of the Southern Province, which allows the constraint of this weathering study geographically to formations exclusively found within this province, such as London, or east Sussex. This informs which study areas may be most suitable for this study.
- Section 2.5 detailed the geology of east Sussex, with Section 2.5.1 detailing the geological history, within four defined stages by Mortimore (2021); (i) extensional tectonics, (ii) increased global sea levels coinciding with basinal inversion, (iii) uplift and then (iv) erosion. These periods are significant in that they control the deposition and lithification of chalk, then the modification of the chalk through tectonics, uplift and erosion, all of which have significant

effects on chalk as a material as well as chalk as a rock mass. The effects of geological history on chalks cannot be understated. In the context of weathering, the geological history ultimately controls which chalks are most susceptible to weathering.

- Section 2.6 presents a review of the classification of carbonate lithofacies and identifies why these descriptive schemes are not suitable for describing (i) chalk, (ii) the engineering grade of chalk and (iii) the description of weathering in chalk – this is due to the apparent homogeneity of chalk and lack of description within chalk as a material itself. This highlights how these schemes would be inappropriate for describing chalk weathering.
- Section 2.7 detailed the engineering classification schemes of chalk, starting with the Mundford grades (developed in 1969 by Ward et al.), Spink and Norbury's classification (1990) and the current CIRIA C574 grading system. This section highlights the limitations of these classification systems, particularly the current C574 system, identifying that this classification cannot be used without other standards, does not exclusively quantify weathering (and is semi-quantitative in its approach), does not identify weathering type and repeatability is questionable. These limitations further justify the research aims.
- Section 2.9 presented types of weathering observed in chalk with water weakening, chemical dissolution, karstification, haloclasty, cryoturbation and ice action identified as agents of weathering. This section informs Chapter 3 and ultimately, subsequent Chapters, as it links the physical appearance of weathering in the field with weathering type, which enables observation within a field setting.

The physical properties of structured chalk and classification systems were reviewed as well as weathering types encountered in the field to inform the direction of this investigation. Following this, Chapter 3 presents a detailed reconnaissance plan for site selection, while Chapters 4 and 5 detail methods of field and laboratory investigation respectively, based upon previously reported literature reviewed in this Chapter.

3 Site selection

3.1 Introduction

The selection of sites to investigate the weathering of chalk was dependant on geology, contemporary and historic environmental processes, and accessability. This chapter is important as it sets out the rationale of site selection and introduces the site locations – field results from subsequent investigation are detailed in Chapters 6 and 7. Without the work undertaken in this Chapter, field studies would not have been possible. This Chapter therefore partially satisfies objectives 2, 3 and 4.

Four sites were selected for field study, while many others were reconnoitred but discounted as viable field sites. While some of these sites were not used for prolonged field studies, they were used for sampling of geological material for laboratory testing. Many of the sites are detailed in Mortimore's 1997 field guide (Mortimore, 1997), later refined in a new guide by Mortimore (2021).

This chapter demonstrates the importance of undertaking preliminary study (i.e., desk study, literature reviews and map reviews) to inform reconnaissance, as it allows more efficient identification sites for reconnaissance and allows the development of a site selection criteria. By identifying the geology, stratigraphy, geological history of the site and access points, it was possible to focus more closely on areas with excellent examples of evidence of weathering processes, while maintaining safe access and egress.

From a geological perspective, this chapter demonstrates the link between weathering and geological history and tectonics, with periclinal features (i.e., synclines and anticlines) controlling the stratigraphy of rocks, and the topography, resulting in specific weathering features, such as dry valleys and more intense fracturing in valley bottoms.

In this Chapter, section 3.2 details site reconnaissance, section 3.3 details research site selection, section 3.4 introduces the research sites and describes why these sites were selected and section 3.5 summarises the Chapter.

3.2 Site reconnaissance

Site reconnaissance was undertaken periodically (i.e., non-consecutive days) to assess the suitability of sites, to find good examples of weathering in the field for future study and to observe geology and geomorphology on a regional scale. All grid references are from the UK National Grid system. Personal protective equipment (PPE) and basic field equipment are listed in Table 3-1.

Table 3-1 Equipment list for reconnaissance.

Hard hat	30 m measuring tape
High visibility vest	Estwing 0.9 kg geological hammer
Safety glasses	Compass clinometer
Safety gloves	Binoculars
Outdoors clothing	Camera
Geological notebook and stationery	Vehicle for remote access
Hand lens	

3.2.1 Sites visited

Coastal sites

Site reconnaissance was undertaken at 21 sites, which included coastal and in-land sites to evaluate their suitability to study weathering in the field. Table 3-2 details 17 coastal sites visited during reconnaissance.

Table 3-2 Details for sites reconnoitred in a coastal setting.

Location	Grid	Geology
Roedean	534497, 103103	Newhaven Chalk Formation; quaternary weathering features (Stavrou et al. 2011)
Rottingdean	537014, 102118	Newhaven Chalk Formation (Stavrou et al. 2011)
Portobello	539616, 102278	Newhaven Chalk Formation; Culver Chalk Formation; quaternary weathering features (Bristow et al. 1997)
Bastion Steps	540252, 101804	Newhaven Chalk Formation overlain by basal Culver Chalk Formation (Bowden, 2013)
Newhaven Harbour	544592, 99953	Culver Chalk Formation; Tertiary deposits (Woolwich and Reading Beds); karstic weathering processes (Robinson, 2020)
Splash Point	548813, 98208	Culver – Newhaven Chalk Formation boundary (Mortimore, 2021)
Seaford Head	549459, 97754	Newhaven Chalk Formation overlain by Head deposits (Bristow et al. 1997)
Hope Gap	550976, 97380	Seaford Chalk Formation overlying Lewes Chalk Formation. Quaternary loess and Head deposits, with karstic pipe-infill (Mortimore, 2021)
Cuckmere Haven	552181, 100550	Seaford Chalk Formation (Mortimore et al. 2004a)
Birling Gap	555311, 96003	Seaford Chalk Formation with a significant, well preserved dry valley (Asoni et al. 2018)
Belle Tout	556339, 95481	Seaford Chalk Formation overlain by Newhaven Chalk Formation (Mortimore et al. 2004a)
Beachy Head	558328, 95218	Holywell Nodular Chalk Formation; New Pit Chalk Formation (Mortimore, 1986)
Falling Sands/Head Ledge	559391, 95544	West Melbury Marly Chalk Formation; Zig Zag Chalk Formation; New Pit Chalk Formation; Lewes Chalk Formation (Mortimore, 1986)
Cow Gap	559718, 95911	Rotational landslip system of West Melbury Marly Chalk and Upper Greensands moving on the underlying Gault clay (Mortimore et al. 2004a)
Whitebread Hole	559888, 96524	Holywell Nodular Chalk Formation and dry valley system (Mortimore, 2013)
Holywell Retreat	560333, 97262	Holywell Nodular Chalk Formation; Zig Zag Chalk Formation (Mortimore, 1997)
Foyle Way	55984, 96894	New Pit – Lewes Nodular Chalk boundary (Mortimore, 1997)

In-land sites

Table 3-3 details the remining four in-land sites visited for reconnaissance. Each of the in-land sites were private property, therefore reconnaissance was limited.

Table 3-3 Details for sites reconnoitred in-land.

Location	**Grid**	**Geology**
Breaky Bottom Vineyard	540661, 105116	Lewes Nodular Chalk Formation (British Geological Survey - Strange, 2006)
3 Ponds Caravan Park, Tarring Neville	550976, 103404	Seaford Chalk Formation – excavated previously. (British Geological Survey - Strange, 2006)
Caburn Pit	544700, 108904	New Pit Chalk and Lewes Chalk Formations (Mortimore, 2021)
Glynde Pit	544984, 109514	Holywell Nodular Chalk and New Pit Chalk Formations (Mortimore, 2021)

3.2.2 Itinerary 1: Brighton Marina to Peacehaven Steps

Initial reconnaissance was undertaken on foot – the undercliff walk, starting at Brighton Marina, allows semi-continuous access to the cliff faces, punctuated by some requirement to walk along the clifftop should the tide be non-permitting. Table 3-4 details grid references, distance between points and description of the route. This route is detailed in Mortimore's 2021 guide (Mortimore, 2021).

Table 3-4 Itinerary 1 – Brighton Marina to Peacehaven, east Sussex (Mortimore, 2021).

From	To	Distance (m)	Notes
Brighton Marina [533714, 103357]	Roedean Access Point [534497, 103103]	950	Beginning of route. Moving east along the undercliff walk. Roedean allowing cliff access.
Roedean Access Point [534497, 103103]	Ovingdean Beach [535992, 102545]	1600	East along undercliff walk.
Ovingdean Beach [535992, 102545]	Telscombe Cliffs [538879, 181738]	2850	East to end of undercliff walk in this locality.
Telscombe Cliffs [538879, 181738]	Portobello Outfall, Telscombe [539616, 102278]	1300	Walk westwards and exit beach at access point [grid 539616, 102276], then head eastwards along clifftop footpath to Portobello Outfall – follow safety instructions and signs.
Portobello Outfall, Telscombe [539616, 102278]	Peacehaven Access Point [540252, 101804]	970	Following clifftop path eastwards to Peacehaven Access Point – follow safety instructions and signs.
Peacehaven Access Point [540252, 101804]	Bastion Steps [541133, 100719]	900	East along undercliff walk.
Bastion Steps [541133, 100719]	Peacehaven Steps [542455, 100368]	1400	East along undercliff walk until end of promenade – end of route.

3.2.3 Itinerary 2: Newhaven Harbour, Splash Point, Cuckmere Haven

Between the eastern bound of the area of working (Roedean – Peacehaven) and the western bound area of working (Holywell), there are locations where vehicular access provides significant advantage to on-foot reconnaissance. At these sites however, on-foot observation was required (Table 3-5).

Table 3-5 Itinerary 2 – Newhaven Harbour to Cuckmere Haven, east Sussex.

Location	Grid	Notes
Newhaven Harbour	544592, 99953	Basal Culver Chalk Formation. Access via public car park.
Splash Point, Seaford	548813, 98208	Basal Culver Chalk Formation, Access via public car park. Tide dependent.
Cuckmere Haven, Cuckmere	552181, 100550	Parking at Exceat public car park [grid 551976, 99518].

3.2.4 Itinerary 3: Birling Gap to Cow Gap

Birling Gap to Cow Gap allows access to unprotected coastal sections but is restricted by limited egress points. This is significant for personal safety in that excursions must be undertaken on a falling tide, less becoming trapped by the sea (Table 3-6). This route is detailed in Mortimore's 2021 guide (Mortimore, 2021).

Table 3-6 Itinerary 3 – Birling Gap to Cow Gap (Mortimore, 2021).

From	To	Distance (m)	Notes
Birling Gap [555311, 96003]	Belle Tout Lighthouse [556339, 95481]	1250	Limited egress points – only undertake on a falling tide, allow 6 hours.
Belle Tout Lighthouse [556339, 95481]	Shooters Bottom [557546, 95267]	1300	Waypoint in-line with Shooters Bottom.
Shooters Bottom [557546, 95267]	Beachy Head Lighthouse [558328, 95218]	770	Uneven underfoot owing to historic cliff collapses.
Beachy Head Lighthouse [558328, 95218]	Falling Sands/Head Ledge [559391, 95544]	1170	Earliest egress point from beach area – egress via steep chalk slopes, slippery in wet weather.
Falling Sands/Head Ledge [559391, 95544]	Cow Gap [559718, 95911]	500	Egress via steep chalk slopes, slippery in wet weather.

3.2.5 Itinerary 4: Holywell and Foyle Way

Access to Holywell Retreat is easy-going, however, upon moving across the beach, the going becomes more difficult with blocks and groynes to manoeuvre. Access to Foyles Way is facilitated by steps (Table 3-7).

Table 3-7 Itinerary 4 Holywell Retreat, Holywell Beach to Foyle Way, Holywell.

From	To	Distance (m)	Notes
Parking; King Edwards Road [560296, 97366]	Holywell Retreat [560333, 97262]	430	Walk to the beachfront via the Italian Gardens.
Holywell Retreat [560333, 97262]	Holywell Pinnacle [560243, 97080]	180	Follow steps to study the Holywell Pinnacle, immediately north-east of Holywell Quarry (historic).
Holywell Pinnacle [560243, 97080]	Bede's Preparatory School [560111, 97220]	510	Head south-west along road toward Foyle Way.
Beeds Prep School [560111, 97220]	Foyle Way [55984, 96894]	525	Follow Foyle Way, with chalk outcropping on path embankments.

3.2.6 Itinerary 5: Breaky Bottom Farm (Lewes), 3 Ponds caravan site, Caburn Pit and Glynde Pit.

Itinerary five requires a vehicle to drive between points. Access to all but one of these sites is restricted by private ownership. Parking away from the location and cross-country walking was required. Table 3-8 provides grid references and locations.

Table 3-8 Itinerary 5 – vehicle reconnaissance of four in-land sites.

Location	Grid	Notes
Breaky Bottom Vineyard	540661, 105116	Breaky Bottom Vineyard privately own pit – permission given to access to pit for reconnaissance purposes.
3 Ponds Caravan Park Tarring Neville	550976, 103404	Caravan Park is privately owned – permission given to visit site for reconnaissance purposes.
Caburn Pit	544700, 108904	Caburn Pit is fenced off and extremely overgrown – care should be taken when accessing the site
Glynde Pit	544984, 109514	Glynde Pit is extremely overgrown.

3.2.7 Summary of reconnaissance

From 17 potential sites listed above, four were selected for further field study;

- Roedean Access Point, Roedean.
- Portobello Outfall, Peacehaven.
- Newhaven Harbour, Newhaven.
- Birling Gap, East Dean.

In-land sites were disregarded for field study purposes for two reasons; inappropriate geology for the study and private ownership. Breaky Bottom Farm hosted a shallow chalk pit in the Lewes Nodular Chalk Formation, and is located on private land, therefore permission would be required for access. The chalk pit was still in use, providing aggregate to fill potholes on the access road, meaning that the weathering profile of the site was subject to excavation and modification. The weathering profile was observed to be approximately 300 mm and it was difficult to distinguish between discontinuities due to weathering and those due to excavation.

3-ponds caravan park, while situated on the Seaford Chalk Formation, is the site of a former quarry, and is used as a caravan park. While the geological setting would have been useful to this investigation, permission for access was required. Current land use meant that there was a high likelihood of holiday makers, with fieldwork disturbing their respective holidays. As the site was a former quarry, insitu weathering profiles were not preserved and rock texture was modified by excavation.

Both Caburn and Glynde Pits are privately owned, with permission required. Caburn Pit is extremely overgrown, with access to the rock faces restricted. Glynde Pit sits on a working estate, requiring the correct permissions.

From the five itineraries planned, itineraries 1, 2 and 5 provided access to the required geology and satisfied the site selection criteria. The completion of all itineraries was integral to understanding the geology of the area, as well as identifying opportunities for study. During reconnaissance, material for laboratory testing was collected from each of the geological formations, except for the Portsdown Chalk.

3.3 Selection of research sites

Site selection was significantly important for this study as it was necessary to access geology which accurately represented weathering in the field, depicted their distribution (remaining easily and safely accessible) and allowed the aims of the project to be evaluated before significant time was invested in field study. Four sites on the south coast met these requirements.

Preliminary study for site selection included map surveys, literature review and desk studies undertaken to inform reconnaissance. Site walk-over reconnaissance was undertaken on a regional scale to identify sites which had exceptional examples of weathering and associated geomorphology. This process proved that no single site was sufficient for this study exclusively owing to a wide geographical distribution of weathering features, which were absent in some locations, but present in others.

It was identified that studying weathering of all chalk formations would pose significant time constraints and that focussing on a smaller number of formations would be of most benefit. To that end, three formations were selected based upon their material properties and distribution. The Seaford and Newhaven Chalk Formations were selected based on their wide occurrence and geographical spread, meaning that these formations would be encountered more often on construction and engineering projects.

The benefit of focusing on the Seaford Chalk formation is that it is the most widely outcropping chalk, and it is one of the most consistent chalks in terms of material properties. The Seaford Chalk also hosts a large dry valley at Birling Gap. Similarly, the Newhaven Chalk is also considered to be homogenous, although is more fractured than the Seaford Chalk Formation. The Culver Chalk Formation, while considered to be a lower strength chalk, is also homogenous and hosts a dry valley at Portobello Outfall, Peacehaven, which could be compared to the dry valley at Birling Gap.

The sites were selected based on

(i) Geology – the Seaford, Newhaven, and Culver Chalk Formations respectively.
(ii) Presence and preservation of weathering features within the chalk at these sites.
(iii) Ease of access – safe accessibility of sections, both vertically to assess change in grade with depth with respect to the CUZ, and horizontally, across weathering features.

All sites selected were coastal, therefore all sites demonstrated weathering associated with coastal processes to some degree, however areas of interest at some sites were markedly different in terms of stratigraphy. Birling Gap allows the study of a dry valley exposed to coastal and tidal processes,

while Portobello Outfall allows the study of a dry valley that is truncated and positioned at the cliff top, meaning that tidal processes are not active and coastal processes are active to a lesser extent. Periglacial cryoturbated involutions at Roedean are more developed than those observed in other locations and the access slope leading to the underlying undercliff walk makes this location excellent for closer inspection and study of these features. Newhaven Harbour has excellent examples of dissolution features and access, and egress are particularly good. The overlying Tertiary deposits also allows for the study of evidence of chemical weathering.

In-land, alternative sites were considered and reconnoitred, however these were deemed unsuitable; quarries and chalk pits were deemed to have weathered material removed and modified through excavation, while rail and road cuttings had inherent danger due to moving vehicles, as well as modification of the chalk structure due to reprofiling.

3.4 The research sites

Based on site selection criteria and reconnaissance, four research sites were selected on the south coast of the United Kingdom; (i) Roedean access point, Roedean, (ii) Portobello Outfall, Peacehaven, (iii) Newhaven harbour, Newhaven and (iv) Birling Gap, East Dean (Figure 3-1).



Figure 3-1 Site location map (adapted from Google-Earth (2021)).

All locations are serviced by the A259, and each have carparking facilities for vehicle access. This was an important consideration for sample collection and carriage of equipment into the field. Roedean access point and Portobello Outfall afford access to the base of the cliff via concrete footpaths from the cliff top, with Portobello Outfall having a limited undercliff walk and access to unprotected cliffs. Newhaven Harbour is accessed from the carpark at the cliff base, with undulating ground and an absence of concrete apron. Birling Gap is approached by the A259, however, at this point the road is situated further in-land and access is via Birling Gap Road, through The Wish Valley. The site is also unprotected but is accessed from the clifftop, via a metal staircase (Mortimore, 2021).

Three site locations (Roedean, Portobello Outfall and Newhaven Harbour) are within the same 10 km along the south coast, however, the lithologies of interest differ at each site by virtue of the underlying structural geology, comprising en echelon periclinal folds (axes-oriented east-west), including the Old Steine Anticline. Newhaven Syncline and Friars' Bay Anticline (Figures 3-2 and 3-3).

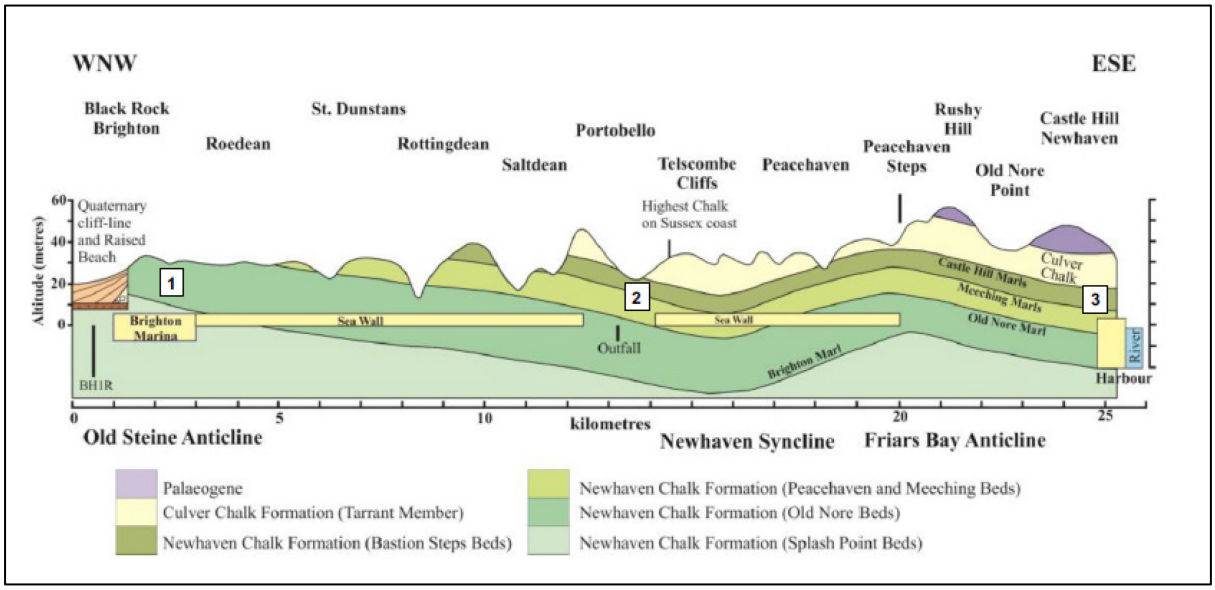


Figure 3-2 Simplified cross-section of the coastal section between Brighton and Newhaven Harbour illustrating field locations 1-3 in relation to periclinal folds (adapted from Mortimore 2021).

The effect of tectonics on the distribution of observed geology results in more Culver Chalk preserved in the Newhaven Syncline (as observed at Portobello Outfall – location 2) compared to that at Newhaven Harbour (location 3 - on the easterly limb of the Friar's Bay Anticline), and secondly, a westerly trending thickening of the Newhaven Chalk from Old Nore Point, towards Brighton, resulting in a significant outcrop of Newhaven Chalk at Roedean Access Point, Roedean (location 1) (Figures 3-2 and 3-3) (Mortimore, 2021).

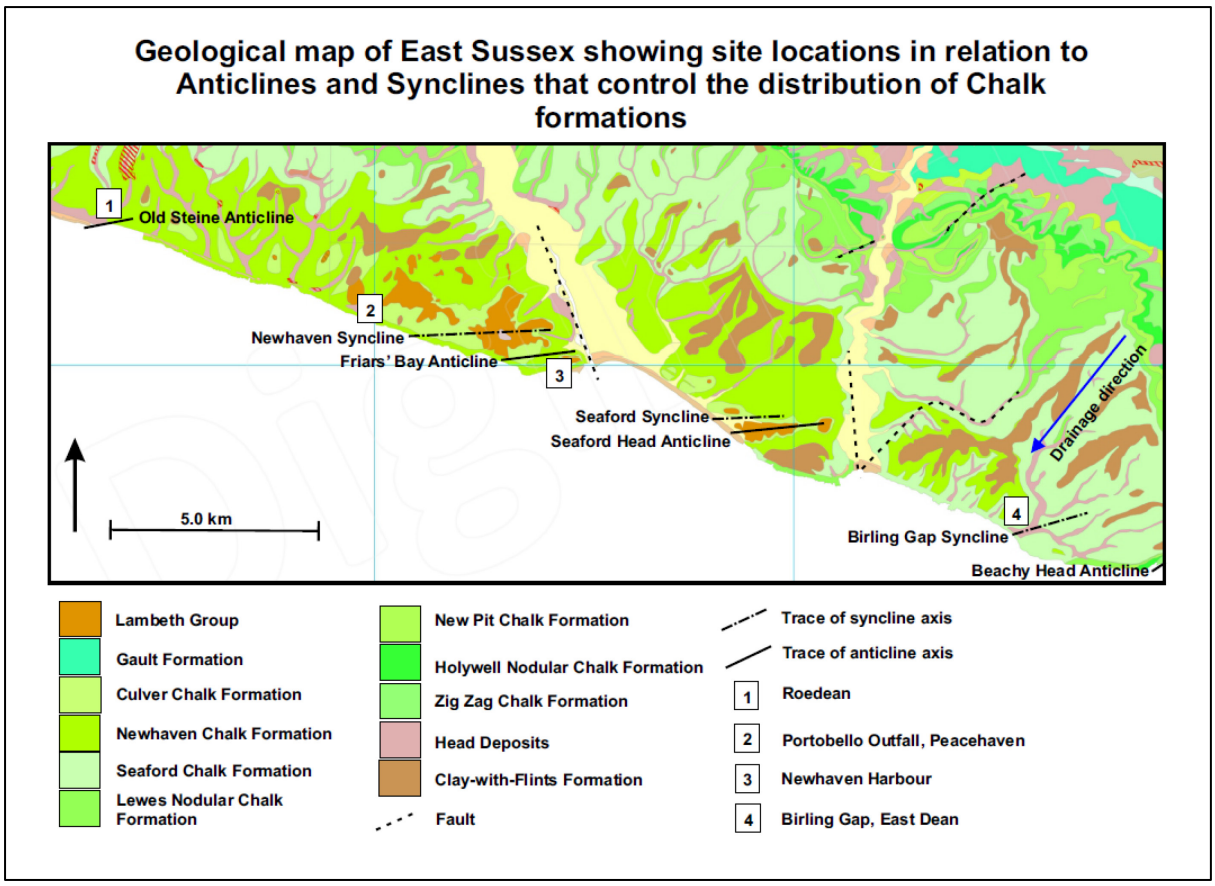


Figure 3-3 Geological map of East Sussex showing site locations in relation to Anticlines and Synclines that control the distribution of Chalk formations (adapted from Mortimore (2021) and Digimap (2023)).

The fourth site is Birling Gap, East Dean (Figure 3-3). Situated approximately 23 km ESE of Roedean Access Point, Birling Gap is situated in a topographic low containing a Devensian dry valley, oriented ENE-WSW, which is reflective of typical secondary drainage dictated by the topography of the South Downs. The dry valley at Birling Gap is the axis of the Birling Gap Syncline (north westerly dipping at 10 – 12°), which is part of the tectonic en echelon line that includes the Old Steine, Seaford and Newhaven anticlines. Further east, there is the minor Shooters Hill Syncline and the Beachy Head Anticline (Mortimore, 2021).

Topographic highs, some of which have since been eroded, have contributed to D-grade chalks and Head deposits hosted in dry valleys, such as the examples seen at Portobello Outfall, Peacehaven and Birling Gap, East Dean (locations 2 and 4).

3.4.1 Roedean Access Point, Roedean (UK National Grid: TQ 34380 03182)

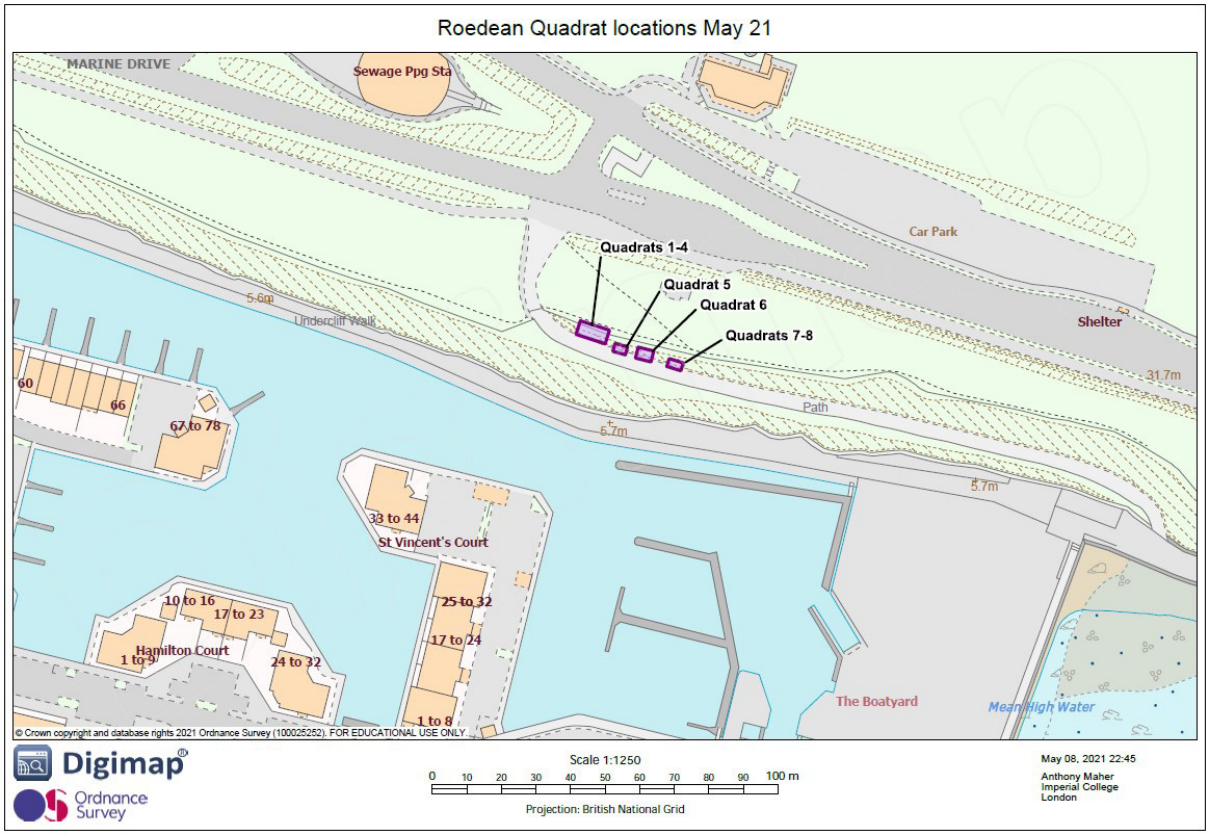


Figure 3-4 Site overview; Roedean Access Point (adapted from Edina Digimap 2021 (Maher, 2021c).

Roedean access point (and concrete access ramp) (Figures 3-4 and 3-5) provides excellent access through the Newhaven Chalk, starting with degraded Old Nore Beds and markers including the Roedean Triple Marls, Rottingdean Pair of Marls and the Saltdean Marl. At the base of the cliff (above the protective concrete apron) is the Friars' Bay Marl 1 (representative of the Santonian-Campanian boundary).



Figure 3-5 Photograph of Roedean Access Point (looking east).

Notable weathering features at this site are well-preserved Quaternary cryoturbation lobes and extensive degree (and depth) of periglacial weathering (controlled by the Friars' Bay Marl 3). This is reflected in weathering profiles from Dm grades, through to more competent chalk grades, with retained bedding structures (Mortimore, 2021). The chalk increases in competency, with fracture frequency, spacing and aperture reducing with depth. To the west of this site is Black Rock (at proximity to Brighton Marina), where there is a preserved raised beach, while to the east, the chalk grades from competent A-grade chalks to de-structured D-grade chalks in a truncated dry valley at Saltdean.

3.4.2 Portobello Outfall, Peacehaven (UK National Grid: TQ 39380 10173)

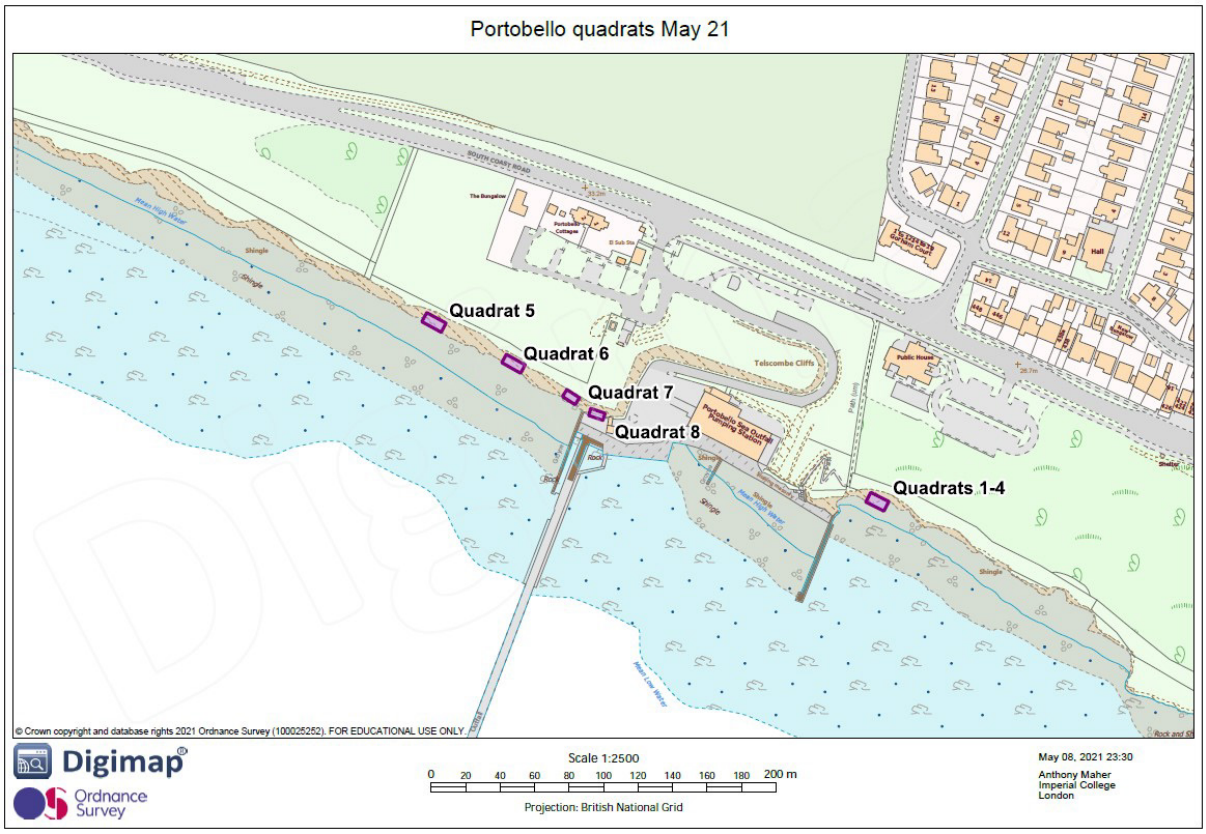


Figure 3-6 Site overview; Portobello Outfall, Peacehaven (adapted from Edina Digimap (Maher, 2021b)).

Portobello Outfall, Peacehaven (Figure 3-6) is the site of a truncated dry valley (denoted as dry valley 2 – DV2 by Mortimore (2021)) to the east of the access path, with thick Quaternary sediments relative to the dry valley at proximity. Further east from this, after the groyne, is Portobello Bay, which has excellent examples of in-filled dissolution features in the upper layers of the Culver Chalk, however due to their stratigraphic height, they are unable to be reached from the beach platform (Figure 3-7). At the intersection of the groyne and the cliff face, there is evidence of marine erosion and increased sub-vertical discontinuity frequency.

Marker beds observed on the east side include the Meeching Marl pair at the base of the cliff (which rises westward through the cliff face), with a significant number of flint bands within the cliff. To the west of Portobello are unprotected chalk cliffs comprising the Peacehaven Beds of the Newhaven Chalk Formation, which are noticeably more competent than those observed in the east side of the site.



Figure 3-7 Photograph of weathering at Portobello Bay, oriented west of Portobello Outfall, Peacehaven (looking east).

The Culver Chalk Formation hosts the truncated dry valley and has excellent examples of complex weathering features within the chalk. The underlying geology is the Newhaven Chalk Formation and there is access through the Quaternary sediments to competent chalk bedrock. This allows observation of changes in weathering grades as well as structures associated with periglacial weathering.

3.4.3 Newhaven Harbour, Newhaven (UK National Grid: TV 44620 99947)

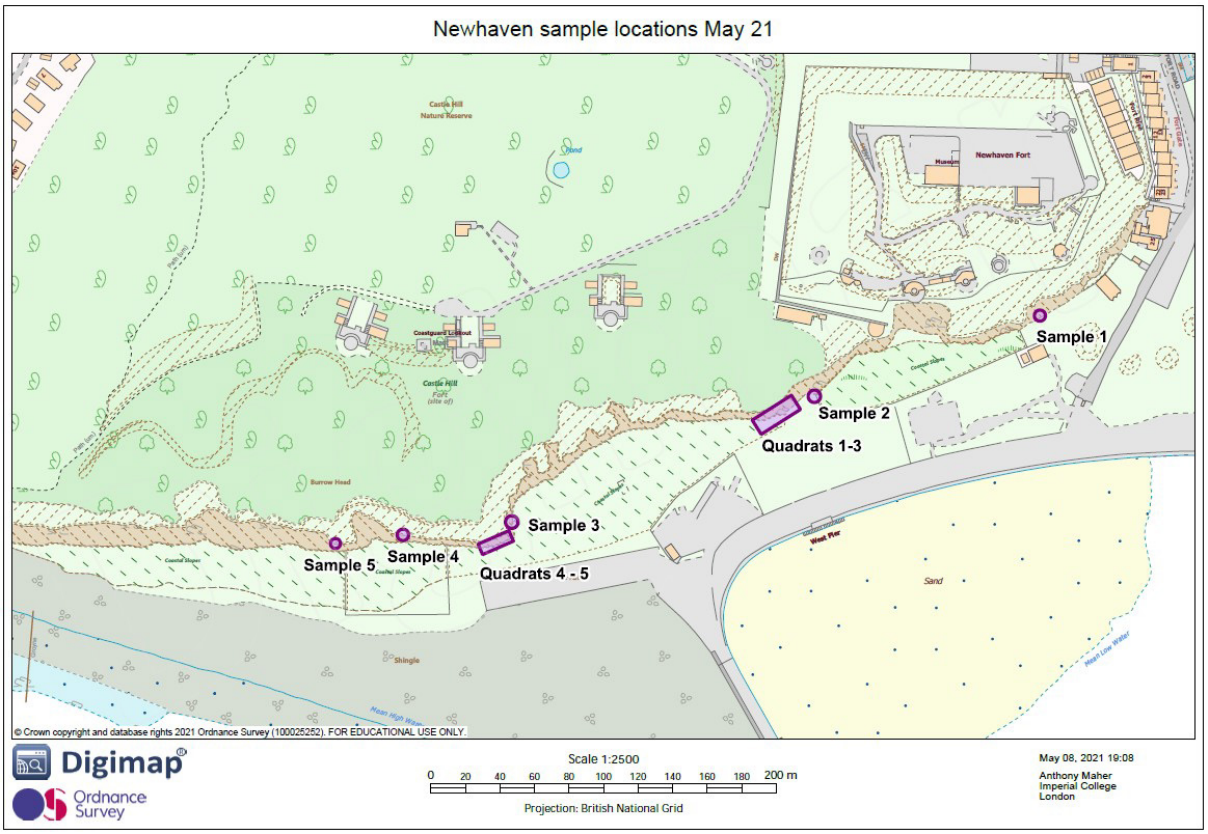


Figure 3-8 Site overview showing sample locations; Newhaven Harbour (adapted from Edina Digimap (Maher, 2021a)).

Newhaven Harbour (Figure 3-8) allows the study of the Tarrant Member of the Culver Chalk Formation (early Campanian), with Tertiary sediments (Woolwich and Reading Beds) lying unconformably above. Further west along the coast, the Newhaven lies stratigraphically below the Culver Chalk Formation.



Figure 3-9 Dissolution features associated with faulting and discontinuities in the Tarrant Chalk Member, with overlying Tertiary sediments and Paleogene erosional surface, Newhaven Harbour (looking north).

The Culver Chalk Formation is considered a soft chalk and is cross-cut in this location by the Castle Hill Flints. Dissolution features follow discontinuities and flint filled fractures. The sub-Palaeogene erosional surface is observed at this site and has karstic dissolution pipes sitting below (Figure 3-9).

Further west along the coast, the Newhaven Chalk has steeply inclined conjugate fractures at regular intervals and has developed horizontal dissolution pipes, indicating how rock structure has controlled karst development at this locality (Mortimore 2021). The overlying Palaeogene beds are undisturbed, with the erosion surface marked by a flint filled cobble bed, moving up through chemically active, iron and glauconite rich sands. The presence of lignites, lignitic clays with selenite and jarosite within these deposits suggest that percolating ground water is sulphate-rich (Mortimore 2021).

3.4.4 Birling Gap, East Dean (UK National Grid: TV 55382 95990)

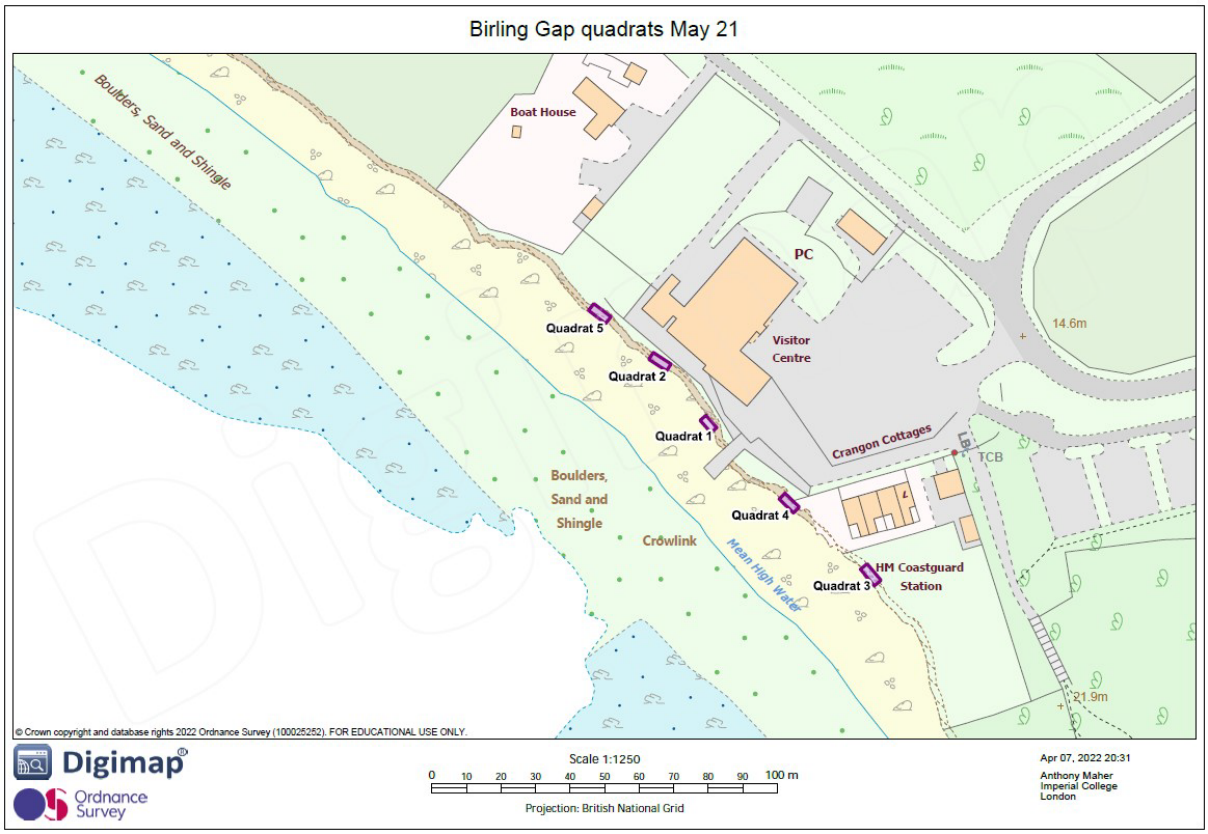


Figure 3-10 Site overview; Birling Gap, East Dean (adapted from Edina Digimap (Maher, 2022a)).

Birling Gap, East Dean, forms part of the Seven Sisters cliffs and is a Site of Special Scientific Interest (SSSI) owing to the geological and geomorphological features at this location (Figure 3-10). Birling Gap hosts a significant, asymmetric dry valley truncated by erosion, formed in the Birling Gap syncline within the Seaford Chalk formation (Mortimore 2021).

The dry valley comprises highly weathered chalk, with the most intense weathering at the valley axis. Below the valley, chalk is described as blocky and intensely fractured with D-grade chalks infilling fracture openings, while at shallower depths in the valley, the chalk is comminuted to silty fines, reflecting a significant number of freeze-thaw cycles in the sites' geological history. To the east and west of the dry valley, chalk increases in competency (and grade).

The D-grade chalks within the dry valley show distortion, reflected in deformed flint bands, indicating episodes of gravity-driven slump and solifluction. The Seven Sisters Flint Band is within the shore platform at the dry valley but rises to be exposed in the east and west, and can be traced through the more competent chalks aside the valley. Flint bands demonstrate evidence of preferential flows along their impermeable horizons, with dissolution processes indicated by voids, infilled with brown sediment. Owing to this degree of weathering, Birling Gap is subject to significant erosion >400 mm/year, while the surrounding cliffs are subject <300 mm/year (Moses and Robinson, 2011),

with a significant cliff collapse occurring within 2 weeks of writing, resulting in the National Trust centre atop of the cliff being relocated.

3.5 Chapter summary

This chapter has set out a criterion by which sites were selected for study to evaluate the aims of this project. Of four in-land sites and 17 coastal sites considered, four coastal sites were selected for field studies. This was selection process was based upon geology, tectonics, stratigraphy they type(s) of weathering observed at these locations and access.

The sites selected were;

- Roedean Access Point, Roedean – where it was possible to observe extensive periglacial weathering of the Newhaven Chalk Formation evidenced by cryoturbated involutions, and the change of weathering grade with both depth and location. This site is affected by coastal weathering to a limited degree owing to the concrete undercliff walk.
- Portobello Outfall, Peacehaven – at this site, it was possible to observe a dry valley truncated by erosion within the Culver Chalk Formation, along with significant dissolution and solifluction features. It was also possible to observe the change in weathering grade with depth.
- Newhaven Harbour, Newhaven – at this location, there are extensive dissolution and karst features associated with structural geology, such as sub-horizontal and subvertical discontinuities and flint in-filled discontinuities. It was possible to observe the Palaeogene erosional surface, as well as study the thick Tertiary deposits lying unconformably above the Culver Chalk Formation. The contact between the Tertiary deposits and underlying Tarrant Member is associated with dissolution pipes and evidence of karstic dissolution.
- Birling Gap, East Dean – it was possible to observe an exceptionally preserved, asymmetric Devensian dry valley in a topographic low at this location. Hosted in the Seaford Chalk Formation, the dry valley and surrounding Seaford Chalk are subject to meteorological, coastal and tidal processes, and has evidence of both periglacial and karstic weathering.

During reconnaissance, all formations were sampled, except for the Portsdown Chalk Formation, due to there being no outcrop in this geographical region. To constrain site selection, and to make most efficient use of time and resources, three Chalk formations were considered; the Culver Chalk Formation, the Newhaven Chalk Formation, and the Seaford Chalk Formation. The selection of these formations was based on the likelihood of being encountered on engineering projects, their wide geographical abundance, and their material properties.

4 Fieldwork methodology

4.1 Introduction

Chapter 3 detailed the reconnaissance phase undertaken in this study with the aim of identifying field sites with exceptional examples of weathering. Further field study was undertaken, with a total of 45 field days in the East Sussex area, specifically between Brighton and Eastbourne. The selection of sites for the investigation of weathering in chalk was based on;

(i) Geology.

(ii) Types of weathering encountered and their degree of representation.

(iii) Ease of access.

(iv) Safety.

In terms of geology, this work concerns itself with one rock type, which is Chalk, but focuses on differing formations. While weathering in all the Formations of the Southern Province Chalk have been observed, more emphasis has been placed on the Culver, Newhaven and Seaford Chalk Formations, owing to their stratigraphic proximity, and for Newhaven and Seaford Chalks, their frequent occurrence in engineering works and wide geographic distribution. The types of weathering considered are confined to the upper 30 m of the chalk (the CUZ) and include Quaternary weathering processes, as well as those associated with tectonics and environment. Ease of access and safety are considered paramount in fieldwork, with ease of access being key to observing variation in weathering grade, formation change with depth as well as being able to measure these with specialist equipment. Safety considerations meant that working quarries and road and rail cuttings were avoided, and that consideration of tides and access and egress points was required at coastal sites.

This chapter focusses on how previous field research of weathering and rock characterisation inform the field methods used in this study, the field methods employed and the rationale behind the techniques selected. In terms of structure, section 4.1 introduces the aims of fieldwork and details previous field studies relating to weathering. Section 4.2 details the data collection, geological observation, and uniformity survey methods respectively, introducing an adaptation of the CIRIA C574 field density card. Section 4.3 lists equipment required for sampling and field observations, and details the development of a procedure for sampling U38 cores in de-structured Chalk. Section 4.4 is the chapter summary. This Chapter partially satisfies objectives 1 – 6.

4.1.1 Aims of fieldwork

The aims of fieldwork are to

- Test and evaluate the hypotheses of this study.
- Identify sites that have good examples of weathering types.
- Characterise weathering types and their distribution.
- Collect data for the development of a ground model.
- Identify macrotextures in the field indicative of weathering.
- Assign CIRIA C574 weathering grades to site locations and evaluate the grading method effectiveness.
- Develop sampling methodologies.
- Collect samples for laboratory testing.

Fieldwork was broken down into three phases;

- Reconnaissance.
- Physical data collection and observations.
- Sample collection.

Twenty-one locations were visited on foot and by vehicle for reconnaissance to assess suitability for field studies. Of which, four locations have been used for data collection, while several other localities for study have been visited to provide context and for sample collection.

4.1.2 Previous weathering field studies

The weathering of chalk is a significant issue in an engineering context as it can change the Chalks' mechanical properties, modify permeability and porosity attributes, affect the stability of engineering structures built on the chalk and can pose risk by developing into geological hazards, such as karst environments and drift-filled hollows. Field studies allow weathering processes to be studied insitu, and to identify weathering products and their distribution.

Field studies of weathering of chalk are limited, however, the study of weathering of rocks in a field setting is multidisciplinary, with practitioners having varied backgrounds, including engineering geology, geomorphology, building conservation, environmental and soil sciences. The implication of this is that techniques used in different disciplines are applicable to the study of weathered chalk.

Previous field studies of chalk weathering include work by Duperret, et al. (2005), focussing on ground and sea water weathering cycles on unstable cliffs (Duperret et al. 2005), Moses & Williams (2008), who measured weathering of chalk spheres produced from Lewes Nodular Chalk for an art installation

(which could be considered a good analogy for exsitu erratics and boulders) (Moses and Williams, 2008) and Asoni, et al. (2018)**,** who looked at rates of erosion at Birling Gap, therefore focussing on the Seaford Chalk Formation (Asoni et al. 2018). While these studies focussed on weathering of chalk and employed laboratory testing, they did not measure the degree to which chalk is modified due to weathering processes in the field.

Moses (2014) produced a critical review of methods for measuring rock surface weathering and erosion in 2014. Their paper identified methods of measuring rates of surface change (i.e., erosion) using contact measurement (such as micro-erosion meters) and non-contact measurement (such as remote sensing, including laser scanning and photogrammetry) (Moses, 2014). The paper also covers methods for measuring sub-surface change in rocks, including the use of equipment, such as triaxial testing in a laboratory setting, and in a field setting, Vickers microhardness testers, Schmidt test hammers and Equotip hardness testers.

It is important to distinguish between weathering and erosion as, while these two processes occur simultaneously, they are very different. Weathering occurs insitu and changes the properties of a rock via mechanical, biological or chemical breakdown, either weakening, hardening or reducing density of the rock, ultimately producing sediment. Erosional processes remove and transport these sediments, and may result in geomorphological features (i.e., weathering products), such as infilled dry valleys as observed in the Chalk. The implication of this distinction is that weathering features in the field may be the result of insitu weathering or the result of weathering and subsequent erosion and transport, which is reflected in the geomorphology of the landscape.

Given that weathering is an insitu process, and results in modification of the properties of insitu rock, it was identified that it is more appropriate to focus on material properties of chalk that have been modified, rather than focus on rates of erosion. In terms of material properties, the two key properties to characterise competent chalk and allow inference of susceptibility to weathering are intact dry density (IDD) and moisture content, both of which are closely linked and correlate well. A previous review of C574 weathering grades (Maher, 2019) identified that density estimation in the field is unreliable with repeatability and precision being questionable. From this review, it was clear that the C574 grading system would benefit from a standardised method of measuring IDD in the field, which was also precise in terms of operation, with little error between users. To address this discrepancy, the Schmidt hammer (SH), OS-120 pendulum hammer and Equotip hardness tester were used to measure hardness and density in the field.

Initially developed by E. Schmidt in 1948 (Schmidt, 1950) as a non-destructive concrete hardness tester, the Schmidt hammer has been used extensively by engineering geologists, geotechnical

engineers and geomorphologists for characterising the hardness of rocks and contributing to rock mass classification systems.

Goudie (2006) evaluated the contribution of the Schmidt hammer to geomorphological research, identifying that the Schmidt hammer has numerous roles in the study of weathering. The roles detailed by Goudie that are relevant to chalk include measuring the changing rates of weathering over time, measurement of karstic forms of weathering in limestone (including case hardening and calcrete strength), measurement of the degree of weathering associated with glacial limits and periglacial processes, and contribution to weathering classifications, allowing the ability of quantitatively assigning a value for weathering (Goudie, 2006).

The Schmidt hammer gives an empirical indication of the elastic properties of a rock by measuring the rebound of a controlled impact on the rocks' surface. The Schmidt hammer comprises an outer case, with a plunger and a rebound gauge on the side of the instrument. Internally, the Schmidt hammer has a piston loaded into a spring, which strikes the plunger when the plunger is depressed against the rock surface. When the plunger is struck by the piston, the impact energy is transferred through the plunger, with some energy lost via plastic deformation of the rock beneath the plunger (this energy is converted to heat and sound). The portion of remaining energy causes the internal piston to rebound within the instrument, and the distance of rebound recorded by the rebound gauge on the side of the device, giving a number referred to as the rebound value (R) (Viles et al. 2011)**.** Harder rocks have a higher R value than weaker rocks (Table 4-1), and this R value can be empirically correlated with UCS.

There are two main types of traditional Schmidt hammer; the N-type Schmidt hammer, with an impact energy of 2.207 Nm, suitable for weak to very strong rocks with UCS values in the range of 20 – 250 MPa. The second type of Schmidt hammer is the L-type, with an impact energy of 0.735 Nm (Figure 4-1). This hammer is suitable for weak rocks and rocks with thin weathered surfaces with UCS values in the range of 5 - 30 MPa. The plunger on the L-type Schmidt hammer can be changed from the standard cylindrical plunger (with a diameter of approximately 10 mm), to a 'mushroom' plunger with a diameter of 25 mm. Electronic versions of these hammers exist; SilverSchmidt hammers with the notation of BN as the counterpart to the N-type Schmidt hammer an BL as the counterpart of the L-type Schmidt hammer (which was used in this study).

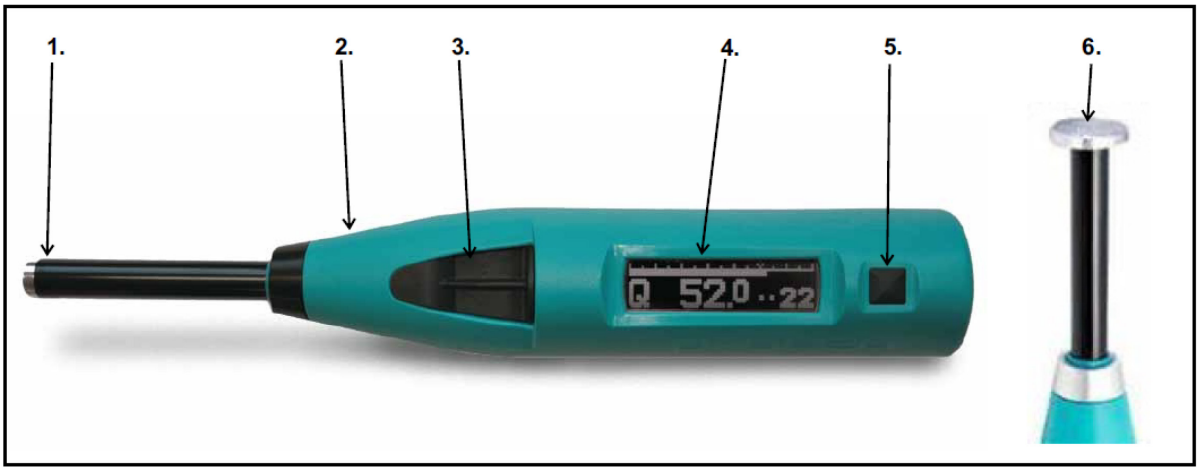


Figure 4-1 The Proceq SilverSchmidt L-Type digital Schmidt hammer; 1 – traditional plunger, 2 – main body housing, 3 – USB and power port, 4 – digital display, 5 – power button, 6 – mushroom head plunger attachment (Proceq, 2021).

After evaluation of each of these rebound hammer types, it was considered that the N-type would be inappropriate as the impact energy would be excessively high for weaker rocks and the plunger would likely punch through weak or weathered material. The range of measurement was also higher than the lower readings required for study of Chalk. The benefit of using the L-type Schmidt hammer is that the impact energy is approximately 3 times lower than the N-type and is designed for the measurement of weak rocks, making this type of hammer fit for the purpose of this study. The addition of the 'mushroom' plunger means that the likelihood of the plunger punching through weaker material was lower as the energy would be distributed over a greater surface area.

(R)-value data of Chalk are limited; however, Table 4-1 illustrates values for a small range of Chalks from the literature. In terms of UK Chalk, Goudie (1989) reports mean R values of 20 for Middle Chalks, which are reflective of the relatively harder New Pit Chalk Formation and underlying Holywell Nodular Chalk Formation, and 9.0 for Upper Chalks, which are applicable to the relatively softer Culver, Newhaven and Seaford Chalk Formations considered in this study. The work by Moses et al. was an experimental study of platform down-wearing of various rock types, and identified that of all the rock types considered, both the British and French Chalks were the weakest and most susceptible to experimental weakening designed to emulate down-wearing.

Table 4-1 Mean and ranges of Schmidt hammer (R) values from other authors.

Material	**Rebound number (R)** (r – range, m – mean)	**Author**
Maresha Chalk	23.9 (m)	(Katz et al. 2000)
Chalk (Israel)	14.0 (m)	(Yaalon and Singer, 1974)
Middle Chalk (UK)	20.0 (m)	(Goudie et al. 1989)
Upper Chalk (UK)	9.0 (m)	(Goudie et al. 1989)
Austin Chalk (Texas, USA)	29.13 (m)	(Lewis, 2022)
Austin Marly Chalk (Texas, USA)	27.67 (m)	(Lewis, 2022)
Lower Chalk (Speeton, UK)	21 (m)	(Bell, et al. 1999)
Middle Chalk (Thornwick Bay, UK)	24 (m)	(Bell et al. 1999)
Upper Chalk (Selwicks Bay, UK)	20 (m)	(Bell et al. 1999)
Lower Chalk (Hunstanton, UK)	14 (m)	(Bell et al. 1999)
Melbourn Rock (Burnham Market, UK)	20 (m)	(Bell et al. 1999)
Newhaven-Seaford Chalk Formations (undifferentiated) (East Sussex, UK)	14.3 – 22.6 (r)	(Moses et al. 2006)
Eletot and Le Grande Dalles (Pay de Caux, Normandie)	11.7 (m)	(Moses et al. 2006)

The benefits of the Schmidt hammer in the study of weathering are clear; the device is portable and can be used to rapidly take many readings with little physical effort, they are financially inexpensive and there is little variance between operators. This final point would address the variability and lack of precision associated with the CIRIA C574 field approximation of density however, this would be within the UCS range of 5 – 30 MPa, therefore Chalks with a weaker UCS of 5 MPa or less could not be measured with this device.

Limitations of the Schmidt hammer include sensitivity to discontinuities, with impact energy loss occurring (Viles et al. 2011) – this would have implications for structured chalks that are intensely weathered, with close discontinuity spacings. Another limitation is surface texture. Similar to the impact energy loss due to discontinuities, irregular rough surfaces are likely to give lower readings as the undulations on the surface of the rock are likely to be crushed before the plunger fully comes into contact with competent rock. Again, this may have implications when testing highly weathered Chalk where the surface may have exfoliated clasts of material, leaving a pitted surface.

Repeated testing of the same sampling site on a rock face may result in modification of the rock in question. Chalk may be more susceptible to modification owing to its inherent relative weakness; therefore, it would be necessary to alternate the position of the Schmidt hammer plunger.

Sumner and Nel identified that rebound values decrease with increasing moisture content, indicating that high moisture content could influence field results (Sumner and Nel, 2002). As Chalk has an exceptionally high moisture content and, in association with this high moisture content, has been demonstrated to be weaker, this may affect the R values produced by this methodology.

To estimate compressive strengths, the R number (denoted as Q for a Silver Schmidt) was used in a prepared curve, where;

$$fck = aQ^3 + bQ^2 + cQ \qquad \textit{Equation 4-1}$$

Q = SilverSchmidt number, a = 0.0, b = 0.0108, c = 0.2236

The Schmidt OS-120 pendulum hammer (Figure 4-2) was designed to test lower strength, softer materials compared to the N and L-type rebound hammers (with UCS values in the range of 1 – 5 N mm^{-2}), with an impact energy of 0.833 Nm (Proceq, 2021). Materials include light weight concrete, mortar, gypsum board and fresh, incompletely cured concrete.

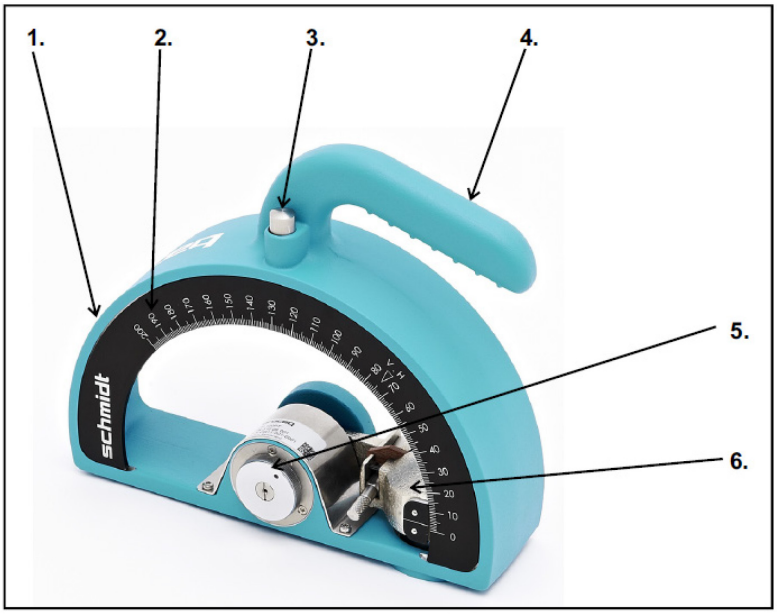


Figure 4-2 Proceq OS120-PT pendulum hammer; 1 – Outer semi-circular housing, 2 – rebound number gauge, 3 – operation switch, 4 – handle, 5 – operating mechanism with vertical to horizontal switch, 6 – pendulum with hammer face (Proceq, 2023).

The hammer comprises a large half-circular frame, with a rebound gauge on the side. The frame houses a pendulum with a hammer face that is 40 mm in diameter. To operate this rebound hammer, the pendulum is locked into place at the top of the half-circular housing, and the test surface is placed on a vertical or horizontal surface. The hammer is then engaged, where the pendulum falls freely in the arc of the half-circle, strikes the material in question, and upon rebounding, the pendulum is locked into place, indicating this hammer types (R) value (Proceq, 2023).

Prepared conversion curves by Proceq are used to convert to compressive strength, where;

$$y = 1.05 * (0.0015x2 + 0.0615x - 0.3585) \quad \textit{Equation 4-2}$$

To date, this method is limited to construction material testing, with little application in a geological or geomorphological context. Tudor, (2019) used this methodology as part of a study to evaluate mine stability in a historic chalk mine. The study identified that while the test can be performed vertically and horizontally, inclined test surfaces mean that the hammer is operated sub-vertically, which places an undue load on the pendulum, leading to affected results (Tudor, 2019).

The Equotip hardness tester (Figure 4-3) is an electronic rebound device which was developed in the 1970's by Dietmar Leeb (Leeb, 1979). It was initially developed fort testing metallic machine components but in 1993, it was first used by Verwaal and Mulder to estimate rock strength of a variety of rocks, including sandstone, limestone and granite (Verwaal and Mulder, 1993). Since then, the Equotip has been used more frequently on geological and geomorphological applications, such as the work by Kawasaki et al. (2002) in testing rock hardness (Kawasaki et al. 2002), Aoki & Matsukura (2007) on the effect of weathering on rock hardness (Aoki and Matsukura, 2007), and (more relevant to this study) the rapid estimation of the IDD of chalk by Thrower et al. (2022)**.**

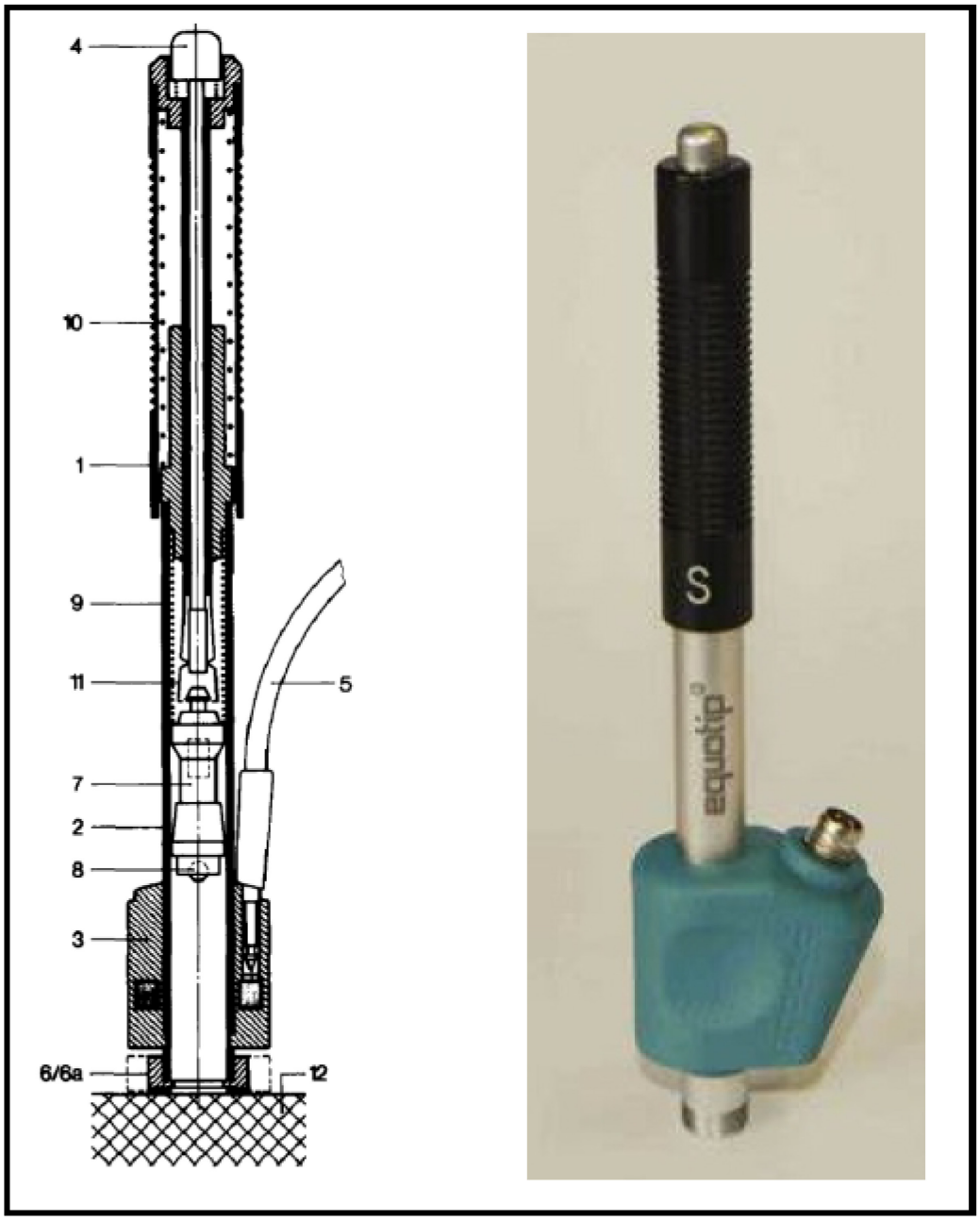


Figure 4-3 Left - schematic of Equotip Leeb impact tester (left); 1 – loading tube, 2 – guide tube, 3 – induction coil and housing, 4 – operation switch, 5 – connection cable to data logger, 6 – support ring, 6a – support ring, 7 – impact body, 8 – tungsten carbide test sphere, 9 – impact spring, 10 – loading spring, 11 – catch chuck and 12 – test material. Right - photograph of impact tester (adapted from Kompatscher (2004)).

The work by Thrower et al. tested Newhaven Chalk from both a coastal setting (Peacehaven) and in-land (Falmer, East Sussex). Thrower et al. found that in terms of IDD, inland samples were higher than coastal, which the authors interpreted as being due to coastal processes weakening the rocks. When correlated with IDD, the hardness values yielded regression curves (R^2 values) of 0.73 for coastal samples and 0.57 for in-land values (Thrower et al. 2022).

The device operates by firing the tungsten carbide ball (via spring force) through an induction field. The impact force produced is 0.011 N m^{-1} and the tungsten carbide ball has a diameter of 3 mm. The

velocity of the tungsten carbide indenter is measured upon firing, and upon rebound to produce a Leeb Hardness number (HL value). This value is equal to the ratio of rebound velocity (V_r) divided by the impact velocity (V_i), multiplied by 1000;

$$HL = \frac{V_r}{V_i} \times 1000 \qquad \textit{Equation 4-3}$$

The Leeb Hardness number was then converted to an intact dry density value using an equation produced by work by Thrower et al. (2022) based on correlation of IDD with HL values in the laboratory. Regression analysis by Thrower et al. results in an R^2 value of 0.73 for coastal settings, and the slope of the regression described as;

$$y = 0.0030HL + 0.9223 \qquad \textit{Equation 4-4}$$

The advantages of the Equotip include light-weight portability and non-destructive, low impact testing, while the limitations include relatively high expense, sensitivity to moisture content and susceptibility to flouring (i.e., the indenter becomes clogged with chalk dust). Owing to this final point, single impact methods (SIM) are more appropriate to repeated impact methods (RIM).

4.2 Field study methodology

4.2.1 Data collection and observation

Initially, 30 m scan lines were set out and geological observations were made, including measurement of discontinuities, rock descriptions as per BS5930 and the application of CIRIA C574 grades. This allowed an initial detailed assessment of the site to base observations of weathering types and weathering products.

Measurement of discontinuities allows characterisation of the orientation, frequency and density of joints and larger faults, which, while potentially sedimento-tectonic and not exclusively weathering related, may control weathering by allowing preferential water flow, leading to increased water weakening, karstic features or case-hardening in the Chalk. The distribution, aperture and frequency of fractures also contribute to the C574 weathering grade, therefore; this survey allows the distribution of grade to be approximated.

There is a distinction made between the classification and description of chalk. C574 was developed to be used in conjunction with descriptions based on BS5930, rather than an exclusive system, without description. Discolouration, strength, density and fracture characteristics are required to be described.

As discussed previously, field density estimation using the CIRIA C574 method is subject to imprecision and error. To address this error and to improve repeatability in a novel fashion, the CIRIA hammer penetration method was used in conjunction with a low strength L-type SilverSchmidt hammer, an OS-120PT pendulum hammer and an Equotip Leeb hardness tester to measure relative hardness. In conjunction with these methods, published values were taken from the CIRIA field density method and correlated with manufacturer prepared curves and regression work by Thrower et al. This allowed the novel production of an updated CIRIA table to be used in the field.

The use of C574 weathering grades is important as it allows quantification of weathering. That said, the question arises as to when should chalk be described as weathered? Sedimento-tectonic (or primary) discontinuities do not fall within the remit of C574 as the product of weathering. The focus when evaluating if a chalk is weathered should be (i) density (either reduced or significantly increased density) and (ii) the degree of secondary fracturing (such as from frost action). These two aspects reflect chemical alteration and mechanical disaggregation of the chalk respectively.

4.2.2 Initial geological observations

To set up the site for study, it was necessary to undertake initial observations to effectively constrain areas of interest.

1. Set up scanline using a 30 m tape.
2. Move along scanline making geological observations.
    - Description to BS5930.
    - Application of CIRIA C574 weathering classification.
    - Application of CIRIA C574 field density approximation.
    - Identification of weathering and weathering products in the field.
    - Determination of the style of weathering encountered and observe any cross-cutting weathering relationships.
3. Structural geology measurements.
4. Identification of suitable sites for relative weathering survey.

4.2.3 Uniformity survey

To constrain sampling at outcrop, a 500 mm x 500 mm quadrat (Figure 4-4) was used, split into a 10 x 10 grid, and positioned at intervals along the scanline where possible. CIRIA C574 classification and rock descriptions were then applied to the area within the quadrat and hardness and density readings were measured and recorded. An updated CIRIA C574 density grading was produced to aid in grading this aspect with the Schmidt hammer and Equotip devices (Table 4-2).

The quadrat was used to eliminate bias and isolate a standard and consistent unit of area for the study of the distribution of fractures as well as density and hardness across the square area covered. Unlike the scientific fields of biology where quadrats are used, the use of the quadrat in this study was to spatially constrain the rock, rather than count a sample size.

From quadrat observation and photography, it was possible to quantify;

- The number of fractures.
- Length and persistence of fractures.
- Fracture geometry.
- Aperture of fractures.
- Degree and percent of discoloration over the square area.
- Distribution of strength and density readings.



Figure 4-4 Photograph of quadrat used for data collection constraint.

In terms of positioning the quadrats, these were placed across the field sections to constrain a spatial distribution of weathering. At a number of sites, the quadrats were placed next to identified weathering features to enable comparison of weathered chalk with unweathered chalk from the same sites. The sites where this was undertaken was (i) Roedean Access Point to investigate cryoturbation lobes, (ii) Portobello Outfall, to investigate weathering at proximity to a large-scale conjugate fault and (iii) Newhaven Harbour, where discontinuities with karstic features was investigated.

4.2.4 Adapted CIRIA field density

Table 4-2 Updated CIRIA density grading (adapted from Lord et al. 2002, Proceq, 2022 and Thrower et al. 2022).

Adapted from CIRIA C574 (Lord et al. 2002, Proceq, 2022 and Thrower et al. 2022)				
Identification method	**Low density**	**Medium density**	**High density**	**Very high density**
Intact dry density	<1.55 Mg/m^3	1.55 – 1.70 Mg/m^3	1.70 – 1.95 Mg/m^3	>1.95 Mg/m^3
Approximate UCS	<3 MN/m^2	3 – 5 MN/m^2	5 – 12.5 MN/m^2	>12.5 MN/m^2
BS5930 strength term	Very weak and lower end of weak	Upper end of weak	Moderately weak	Moderately strong
Ease of breaking fragments	30 – 40 mm thick fragments can be crushed between finger and thumb and remould to putty	30 – 40 mm thick fragments can be broken on two using both hands, but cannot be crushed between finger and thumb	30 – 40 mm thick fragments cannot be broken in two. Only thin slabs < 10 mm thick, and corners and edges of lumps can be broken with difficulty using both hands	Cannot be broken by hand. 100 mm diameter lump can be broken by a single blow when held in the palm of the hand
150 mm nail penetration	>25 mm. Putty formed around nail	12 – 25 mm	6 – 15 mm	<6 mm
Used hammer pick penetration	>30 mm chalk splashes	11 – 30 mm	2 – 11 mm	<2 mm
New hammer pick penetration	>35 mm chalk splashes	18 – 35 mm	6 – 18 mm	<6 mm
SilverSchmidt L-Type Q number (correlated with UCS, after Proceq (2022))	<9.5	9.5 – 14	14 – 25	>25
Equoptip Leeb HL number (correlated with IDD, after Thrower (2022))	<210 kg/mm^2	211 – 260 kg/mm^2	261 – 327 kg/mm^2	>327 kg/mm^2

4.3 Sampling methodology

Bulk and hand samples used for index testing, slake durability and other laboratory analysis were selected on formation type, CIRIA grade and apparent degree of weathering. Methods of sampling undisturbed samples were developed in the field and the workshop, with effectiveness continuously evaluated. The methods developed during this study allowed the collection of U38 samples of de-structured Dm and Dc grade chalk as well low-density chalks, suitable for geomechanical and permeability laboratory testing. Equipment required for sampling is presented in Table 4-3.

Table 4-3 Equipment required for sampling.

Hard hat	Handsaw
High visibility vest	U38 jarring rig
Safety glasses	U38 coupling head
Safety gloves	U38 steel sample tubes
Outdoors clothing	Adapted aluminium U38 sacrificial sampling tubes
Geological notebook and stationery	U38 extension rod
Plastic bags	Flathead screwdriver
Aluminium foil	Wooden chock
Labels and markers	Piston extruder
Camera	U38 membranes
Estwing 0.9 kg geological hammer	U38 membrane stretcher
1.5 kg sledge hammer	Storage boxes
Bolster chisel	Vehicle

4.3.1 Bulk sampling methodology

Bulk samples were selected based on chalk formation, degree of homogeneity and C574 grade to evaluate insitu weathering at location and the amount of material was dictated by test type. The amount of material required for bulk sampling was estimated to be a minimum of 10 kg of material.

Samples were removed from the rockface or outcrop using a geological hammer, 1.5 kg hammer, bolster chisel and handsaw, exploiting discontinuities where practical and suitable. Samples were then wrapped in aluminium foil, labelled and then sealed in plastic bags before being transported to the laboratory.

4.3.2 Undisturbed sampling methodology development

Without the capability of a full-sized drill rig to undertake geotechnical sampling, it was identified that hand sampling methods would be required to procure materials for laboratory testing. After a significant number of failed attempts, eventually a novel method was developed whereby D-grade de-structured chalk could be sampled, stored, transported and tested in the laboratory.

A significant amount of time, field days and physical effort was expended on developing a solution to sample weak structured and completely de-structured chalk. Major challenges in the development of sampling solutions included the relatively weak and damage-susceptible material properties of the Chalk, a lack of current, in-service sampling methodologies and the fact that many sampling methods either destroyed the chalk completely or modified its inherent material properties to the point that the samples were no longer representative of field conditions.

The first attempt of sampling weak structured and completely de-structured chalk utilised a cordless 36 kV slotted drive shaft (SDS) Hilti hammer drill in conjunction with a 52 mm external diameter hollow drill core (Figure 4-5). The rationale behind using this piece of equipment was that the drill was portable, therefore easily carried into the field, it had a 36 kV battery, negating the requirement for a diesel generator and the fact that it was an SDS drill, meant that the drill had sufficient torque to bore through weak and de-structured chalk, with a high-water content. The core barrel, while not corresponding to standard test sizes (such as U38, U50 or U100's), was considered to allow enough material to be sampled, at which point, laboratory tests would be adjusted to cater for the non-standard dimensions of the sample.



Figure 4-5 A 52 mm external diameter hollow drill core with attachment to fit SDS drill.

After several attempts of sampling the Culver Chalk Formation at Newhaven Harbour, it became apparent that this methodology was not suitable. Initially, the SDS drill became stuck within the bore as the surrounding chalk puttified on drilling due to high moisture content and excess vibration. This created a putty annulus which, owing to thixotropy, held the core barrel steadfast upon cessation of drilling and subsequent relaxation. A water or air flush was considered, however, the presence of water in the rock matrix meant that an air flush would not be effective, and the introduction of more water would exacerbate puttification and induce further weakening of the rock material. During later attempts, the bore was successfully drilled, however, extruding the chalk from the solid core barrel proved challenging, with many cores becoming stuck in the barrel and breaking. Removal of the cores using tools damaged many of these cores. The cores which were liberated from the core barrel were

not to full length, highly disturbed, with porewater exacerbated. This resulted in the cores being misshapen and their material properties significantly modified (Figure 4-6).



Figure 4-6 Mis-shaped and warped Culver Chalk sampled with 52 mm core barrel.

The next methodology attempted was push sampling with a non-standardised tube sampler (Figure 4-7). The fact that de-structured chalk could be considered a stiff soil or a weak rock, led to the concept that the material could be sampled as a stiff soil, and that push sampling would be a viable sample methodology The tubes were produced from chromed exhaust pipe and the rationale was that the unstandardised dimensions (approximately 75 mm internal diameter, with a wall thickness of 3 – 4 mm) was sufficiently large to cause minimal, undue disturbance to the sample, yet smaller than a standard 100 mm U100 sample, therefore require less energy to drive the sampler into the chalk.

The sample tubes were easily driven into de-structured Culver Chalk at Portobello Access Point using a 1.5 kg hammer, and easily extracted from the ground by hand. This was inferred to be due to the low friction chromed outer tube. After sampling, extrusion of the sample in the field was attempted but unsuccessful, with the sample remaining steadfast within the tube. The samples and tubes were then wrapped in tinfoil and placed in a plastic bag and returned to the laboratory at Imperial College.



Figure 4-7 Press-in sampler adapted from a car exhaust pipe.

In the laboratory, a mechanical extruder was used to extrude the sample, but again was unsuccessful, with the extruder becoming damaged. The sample tube was then cut axially by the ICL technicians to inspect any processes or interactions between the sample and the tube, preventing extrusion. Upon inspection, it was possible to observe that clumps of de-structured chalk accumulated in areas on the inside of the tube and that a significant amount of oxidisation had occurred on the interface between the sample and the inner wall of the tube. This indicated that the soil skeleton, while containing a significant amount of moisture, also contained a significant amount of air, leading to oxidisation of the metal.

After it was identified that sampling with a larger tube was successful, but extrusion was problematic, it was postulated that by reducing the skin friction between the sample and the tube by using a tube with a smaller internal diameter, extrusion may be more successful. Given the success of previous soil sampling and using the approach that de-structured chalk should be treated like a stiff soil, a Shelby soil sampler was considered for further sampling.

The Shelby sampler comprises a 38 mm internal diameter, thin-walled steel tube with a chamfered cutting edge. This type of sampler is used to sample soils that are sensitive to sample disturbance. This, and the fact that chalk is particularly sensitive to damage through sampling, indicated that this method may be more suitable than those approaches used previously. Advantages of this test are that it is suitable for firm to stiff soils and that samples can be driven in by percussive means or by continuous means (such as via a hydraulic jack).

The Shelby tubes initially used were proprietary tubes from ELE, constructed from steel. Initial driving of the tubes with the supplied jarring rig was not successful. The weight of the jarring rig was not

sufficient to overcome the strength of the de-structured chalk without the tube deviating or requiring a substantial number of blows to enable advancement of the tube, which was considered to affect the material properties of the chalk considerably. Material sampled using these tubes was again difficult to extrude requiring the tubes to be cut (Figure 4-8), but there was more success in extruding samples compared to the sampling procedure with the chromed pipe.



Figure 4-8 A – ELE branded U38 sampler, B – U38 sampler after cutting due to inability to extrude sample, C – highly oxidised surfaces of tuber inner wall.

Upon inspection, oxidisation was an issue within the ELE produced sample tubes, as with the chromed pipe, resulting in the chalk material clinging to the walls of sampling tube. Driving of the tubes using a 1.5 kg hammer was markedly more rapid than the jarring rig, although the sample extrusion results were similar in terms of successful extrusion. This indicated that the problem of extruding the samples was linked to the material of which the tubes were made, rather than the sampling procedure.

Owing to observations of sampling using the ELE Shelby tubes, it was identified that the same sampling method could be successful if the material of the tubes was changed. Stainless steel U38 tubes were sourced from the Imperial College lab and were bespoke made for sampling undisturbed soil samples (Figure 4-9). These proved to be robust enough to be driven into the de-structured chalk via a hammer, without significant issue. When taken back to the laboratory for extrusion, these sample tubes, while requiring physical effort, allowed the extrusion of chalk samples.

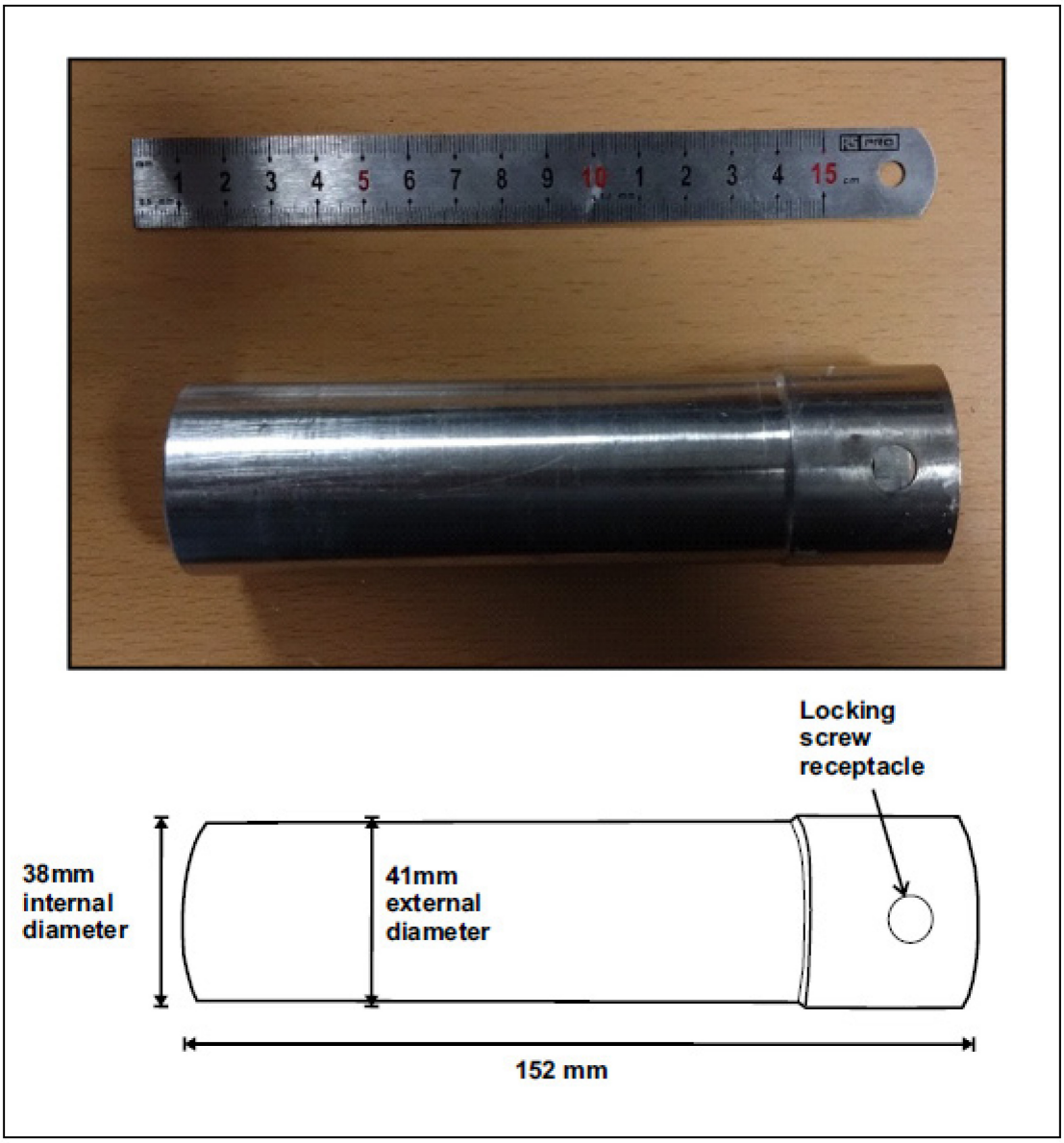


Figure 4-9 Steel U38 sampling tube.

A significant challenge encountered when sampling with stainless steel, thin-walled tube was obstructions, such as hard clasts and flints. In 5 out of 10 samples, the sample tubes encountered obstructions and became visibly deformed and damaged (Figure 4-10), resulting in the inability to (i) extrude samples without cutting the tubes and (ii) re-using the tubes for future sampling. This meant that a suitable, more cost-effective methodology was required. The degree of effort required to extrude samples from non-deformed or damaged sample tubes in the laboratory (and previous experience of oxidisation of the metal at the soil-sampler interface) also indicated that time was a factor when extruding, and that a method of extruding the samples in the field was required. This meant that a method of storage and transportation of the material was also required, which maintained both water content and the sample integrity.



Figure 4-10 Left - aluminium sampling tube damaged by obstruction and retaining sample, right – steel sampling tube damaged by obstruction and retaining sample.

Given the expense of stainless-steel sample tubes, aluminium was selected as an alternative material. 38 mm internal diameter aluminium tube was procured, and bespoke U38 Shelby tubes were prepared by the technicians at Imperial (Figure 4-11), ensuring that reciprocal holes for the driving mount and chamfered cutting edge were machined onto the aluminium sample tubes. Trials of driving the aluminium sample tubes proved successful, and the relative in-expense of the aluminium material meant that the aluminium sample tubes could be considered sacrificial if damaged but re-used where sampling and extrusion was successful. Extrusion trials proved that sampled material could be extruded from the aluminium with a greater degree of ease compared to that of stainless steel, however it was still considered that time was a critical factor in extruding material and that a method of field extrusion was still required.

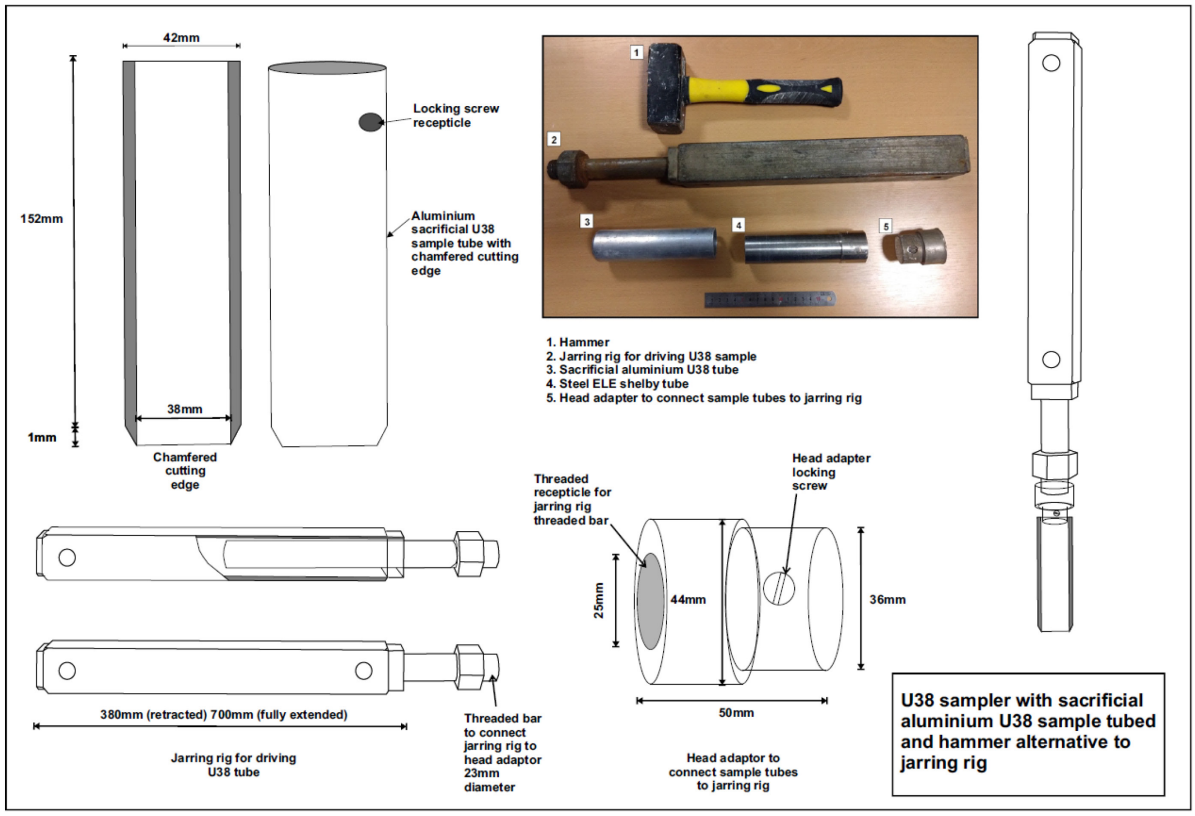


Figure 4-11 Ideal sampling equipment for de-structured grade chalks; 1 – 1.5kg hammer, 2 – jarring rig, 3 – aluminium sacrificial U38 sampling tube, 4- steel re-useable U38 sampling tube, 5 – head adapter.

In terms of in-field extrusion, it was identified that the main challenges were that samples would lose moisture as well as deform easily. As the initial test for these samples was likely a permeability test, requiring a latex membrane, the samples were extruded directly into latex membranes in anticipation. This meant that samples would more readily retain their moisture content and integrity, but, owing to the disposability of membranes, were easily accessible should test requirements differ (i.e., UCS testing). To further ensure against moisture loss, samples were wrapped in tin foil, then placed in zip-lock bags. Upon return to the laboratory, samples within tin foil were waxed.

Given that samples were driven into de-structured chalk with a hammer, it was anticipated that there would be some degree of disturbance to the sample. To avoid this disturbance, an alternative method of driving the sample tubes via jacking was trialled. Based on pile testing methods for compression testing, a four-ground anchor arrangement was selected, with the use of lifting straps and a scissor jack to drive the sample. The four ground anchors would act in tension, while the lifting straps would act as a fulcrum and the scissor jack would apply compressive force to the sample tube.

Initially, penetration into the outcrop by the sample tube was successful, however, when tested on sub-vertical faces (i.e., inclined faces), the anchors failed before the sample tube was driven to the required depth. This was attributed to the heterogeneity of the de-structured chalk and

discontinuities. While this driving method was considered unsuccessful, further trial and development of this method would be of merit. Comparison of percussive sampling versus jacked sampling would allow quantification of the degree of disturbance to percussive samples. While percussive methods are likely to cause some disturbance, they should not be discounted as ultimately, they have enabled de-structured chalk to be successfully sampled and tested, as opposed to having not been sampled and remaining insitu.

This anchor method has scope for further development and would be particularly suited to vertical sampling from level ground. There is potential with this method to develop press-in methodologies utilising vehicles or kentledge as required weight, however the success of this method would depend significantly on the topography, geomorphology and position of de-structured chalk deposit.

A significant number of U38 sample tubes were damaged during this development of methodology and investigation. This could be considered as a mark of reliability of a technique or could reflect the development of experience. A summary is presented in Table 4-4 of number of successful and unsuccessful sampling attempts.

Table 4-4 Overview of tube types and degree of success when sampling.

Sample tube type	**Constituent material**	**Initial number of tubes**	**Remaining number of intact, undamaged tubes**	**Number of samples successfully cored and extruded**
ELE tubes	Non-stainless steel	6	2	3
Stainless steel tube	Stainless steel	10	5	18
Sacrificial aluminium tube	Aluminium	8	6	34

4.3.3 Developed sampling methodology

Undisturbed sampling was undertaken with steel and aluminium tubes with a 38 mm internal diameter.

1. Inspect area of sampling for obvious heterogeneities and/or obstructions (such as fossils, or flint clasts).
2. Remove 50 mm of cover from the face of the deposit using a trowel or chisel, removing loose material.
3. Inspect sampling tube, ensuring the cutting edge is true, without burrs, and there is no loss of integrity or shape in the body of the tube.
4. Ensure the internal surfaces of the tube are clean and free from particles that may impede sampling.
5. Fit the U38 coupling head to the sample tube using the flathead screwdriver.
6. Attach the jarring rig and drive the U38 tube into the deposit if resistance allows.
7. Failing the jarring rig, driving was achieved by hammer. Using the wooden chock as a dampener, drive the sample tube into the deposit using the 1.5 kg hammer, with the force of blows dictated by the weight of the hammer to avoid undue forces on the sampling tube.
8. Screw the extension rod to the coupling head and remove the sample from the deposit.
9. Check the sample hole walls for any undue disturbance or collapse.
10. Refill voids from sample with puttied chalk material surrounding the area.

4.4 Chapter summary

This chapter has introduced the fieldwork component of this study, stated the aims of the field investigations and detailed the phases of field investigation undertaken. The chapter provides commentary on previous field studies of weathering across several disciplines, highlighting that weathering studies of chalk in the field for engineering purposes are limited. This commentary provides the rationale behind the approach taken to field studies as well as introduces specialist equipment used for measuring hardness and density in the field, while effectively highlighting the omissions in CIRIA C574 and linking how these tools may supplement this classification system.

In section 4.2, a detailed field methodology is presented, introducing methods of data collection, bias reduction and spatial constraint of observations, lending techniques from cross-disciplines. This section also provides an update CIRIA C574 density estimation, adjusted for the Equotip and SilverSchmidt hammer respectively, which effectively increases the robustness of this approach in the field by reducing imprecision and improving repeatability.

Section 4.3 detailed the equipment required for an effective investigation of weathering and weathering products in chalk. This section also provided a methodology for bulk sampling. In section 4.3.3, there is a commentary on the trial and development of a novel method of sampling based on U38 samples for stiff soils. This section detailed the approaches undertaken, highlighted which methods were successful and which were not. It also provided detail on the development and refinery of a successful method using 38 mm diameter sampling tube, and how propriety equipment was not suitable. By adapting this design and changing material to that of stainless steel and aluminium, an efficient and suitable methodology was developed.

Section 4.3.4 detailed a best practice methodology developed during this study and was used throughout for sampling.

5 Laboratory methodology

5.1 Introduction

Chapter 4 described the methods used for data and sample collection to enable characterisation of structured chalk, de-structured chalk, and weathering products within a field setting. The field sites were chosen primarily for their preservation of excellent case examples of weathering types, including periglacial cryoturbation, weathering associated with sedimento-tectonic features (such as at proximity to conjugate faulting), varying chalk fracture states with depth, weathered horizons, dry valleys and karstic weathering features. Chapter 4 also detailed the development of a sampling methodology for de-structured Dc and Dm grade chalks which were compatible with standard laboratory testing.

Chapter 5 details laboratory methods used to characterise both structured and de-structured chalks collected from targeted sample sites and includes adaptations of traditional methods to assess de-structured chalk. The aim of this laboratory work is to compliment and underpin field studies and further augment the CIRIA C574 grading system, while developing techniques to characterise sampled Dm and Dc graded chalk to reflect field conditions. This laboratory work does not aim to characterise homogenous chalk putties prepared in controlled laboratory settings as an idealised geoengineering material, but to characterise undisturbed, heterogeneous de-structured grade chalks. The corresponding results Chapter to this methodology is Chapter 8. Chapter 5 partially satisfies objectives 2, 3, 4, 5 and 6 of this study.

The objectives of this laboratory testing are to

- Test and evaluate the hypothesis of this study.
- Assess which chalk formations of the Southern Province Chalks are most susceptible to weathering by undertaking slake durability tests (inducing artificial weathering) in combination with index testing and CIRIA weathering grades.
- Assess if gradings given in accordance with C574 correlate with degree of weathering and durability.
- Evaluate water weakening and salt weakening processes on chalk by using an adapted slake durability methodology with prepared slaking fluids.
- Adapt methods of geotechnical testing for Dc and Dm graded chalk.
- Develop a strategy of geotechnical testing that compliments the C574 grading methodology and characterises de-structured chalks.
- Undertake microscopy to evaluate if weathering has any effect on the microstructure of chalk.

The importance of laboratory testing of both structured and de-structured chalk cannot be overstated; laboratory testing allows the characterisation of soil and rock properties required for geotechnical analyses, the development of geotechnical models and allows some prediction of the materials engineering behaviour under working conditions. This is significant as weathering processes alter the physical properties of the parent rock, resulting in insitu chalks that have varying physical properties. De-structured chalks also pose challenges in terms of characterisation as to whether they should be approached as a very weak rock, or a stiff soil. Currently, there are little data of the physical properties of Dm and Dc chalks within the literature. This research project aims to develop a classification strategy and begin the development of a database of physical properties of Dm and Dc chalks as an engineering material.

Initial laboratory testing undertaken comprises index testing of chalk to characterise material properties and provide reference values, including natural moisture content (NMC), intact dry density (IDD) and saturated moisture content (SMC), with porosity and void ratio calculated. Geomechanical testing includes unconfined compressive strength testing (UCS), Brazilian tensile strength testing and triaxial testing, while hydrogeological characterisation is undertaken by an accelerated permeability test procedure. Complimentary tests have also been undertaken, such as particle size distribution (PSD) and the Bushinsky technique (with the aim of inspecting and quantifying internal fabric of Dm and Dc graded chalks).

5.2 Index tests

Index tests are preliminary tests undertaken within the laboratory to provide insight into the behaviour of a chalk. Correlation of index tests allow characterisation of the material, which provide a framework for quantitative prediction. Every formation of chalk was tested except for the Portsdown Chalk Formation. Table 5-1 provides a list of index tests and corresponding references in literature.

Table 5-1 Industry standards of index tests.

Test	Definition	Industry standard / reference used
NMC	Natural moisture content	BS 1377-2:1990 superseded by BS 1377-2:2022 (BSI, 1990, BSI, 2022a)
SMC	Saturated moisture content	BS 1377-2:1990 superseded by BS 1377-2:2022 (BSI, 1990, BSI, 2022a)
IDD	Intact dry density of material	BS 1377-2:1990 (BSI, 1990) superseded by BS 1377-2:2022 (BSI, 1990, BSI, 2022a, BSI, 2022b)
Voids ratio	Ratio of void space volume and solid particle volume	Craig and Knappet (2012)
Porosity	Ratio of bulk volume to mass particle volume	Craig and Knappet (2012)

It is anticipated that chalks with high natural moisture content and lower density chalks (i.e., less than 1.70 Mg/m^3) are likely to be most susceptible to and affected by weathering processes (Lord et al. 2002). The rationale behind this hypothesis is due to the significance of water in terms of weathering. Water acts as a solvent for weathering agents (i.e., NaCl), acting as transport, allowing these agents to penetrate the chalk, has weakening properties on chalk in its own right and upon freezing, the formation of ice crystals are postulated to damage the low tensile strength, internal structure of chalk, resulting in cryoclasty. Chalks that have a high moisture content are likely to be more susceptible to cryoclasty, while chalks with densities lower than 1.70 Mg/m^3 have been observed to take on and lose water more easily (Lord et al. 2002). This would indicate that chalks with lower densities may be more susceptible to the deposition of higher concentrations of weakening agents within their internal structures, as well as being susceptible to water weakening processes.

Terms used for index testing;

Notation	***Definition***	***Units***
m_1	Mass of container	(g)
m_2	Mass of container plus wet chalk sample	(g)
m_3	Mass of container plus dry chalk sample	(g)
W	Natural water content of chalk	(%)
w_s	Saturated water content of chalk	(%)
ρ_d	Intact dry density	(Mg/m^3)
v_s	Volume of chalk specimen	(cm^3)
m_w	Mass of chalk specimen and wax coating	(g)
m_g	Apparent mass of chalk specimen with wax coating in water	(g)
m_s	Mass of chalk specimen	(g)
ρ_p	Density of paraffin wax	(Mg/m^3)
P	Bulk density	(Mg/m^3)
E	Voids ratio	Dimensionless
v_{void}	Volume of voids	(cm^3)
v_{solid}	Volume of solids	(cm^3)
V	Volume	(cm^3)
N	Porosity	Dimensionless
G_s	Specific gravity of chalk	Mg/m^3
ρ_w	Density of water	Mg/m^3
ρ_{sat}	Sample density	Mg/m^3

5.2.1 Natural moisture content (NMC)

Natural moisture content is determined by measurement and comparison of both the natural mass of a specimen and the dry mass, achieved by oven drying. A minimum sample size of 30-50 g was used for this test. The methodology for determining NMC is presented in BS 1377-2:2022;

Undertaking the test

1. The mass of a suitable container is measured and recorded (m_1)
2. The wet specimen is then placed within the container, and the mass of the container plus wet specimen is then measured and recorded (m_2).
3. The container and wet specimen are then placed in an oven with a controlled temperature of 105 °C for a minimum period of 24 hours.
4. The container and dry specimen are removed from the oven and allowed to cool to room temperature.
5. The mass of the container plus dry specimen is then measured and recorded (m_3).

Calculation of NMC as a proportion of dry soil mass;

$$NMC = \left(\frac{m_2 - m_3}{m_3 - m_1}\right) \quad \textit{Equation 5-1}$$

Where

NMC = moisture content (g), m_1 = mass of the container (g), m_2 = mass of the container and wet specimen (g) and m_3 = mass of the container and dry specimen (g).

Calculation of NMC as a percentage of dry soil mass;

$$w = \left(\frac{m_2 - m_3}{m_3 - m_1}\right).100\ (\%) \quad \textit{Equation 5-2}$$

Where

w = moisture content (%), m_1 = mass of the container (g), m_2 = mass of the container and wet specimen (g) and m_3 = mass of the container and dry specimen (g).

5.2.2 Saturated moisture content (SMC)

Saturated moisture content (SMC) is the maximum amount of moisture a rock can hold at saturation, where pore spaces are filled with water, expressed as a percentage. SMC is an important index test as it correlates well with IDD, and, when used in conjunction with other index tests, can be used to provide a useful insight into the behaviour of the material (Mortimore et al. 2004b).

Calculation of SMC;

The methodology for determining saturated moisture content is presented in BS 1377-2 (1990);

$$w_s = \left(\frac{1}{\rho_d} - \frac{1}{2.7}\right).100\ (\%) \qquad \textit{Equation 5-3}$$

Where ρ_d = Intact dry density (IDD) (Mg/m^3) and 2.7 = assumed specific gravity of chalk (Mg/m^3)

5.2.3 Intact dry density (IDD)

Intact dry density (IDD) is a measure of the density of cylindrical or irregularly shaped lumps of chalk which have been dried under controlled conditions. Specimens are selected on their apparent homogeneity, with larger macro-foliations, such as trace fossils and discontinuities, acting as markers for sample unsuitability (due to introducing material heterogeneity), thus omitted from testing.

The standard used to determine the densities of intact chalk lumps is BS 1377-2:2022; volume is measured by water displacement, whereby a sealed chalk sample is immersed in de-aerated water, held in a vessel with an outlet pipe (to allow water displacement). Bulk density is subsequently calculated and used with moisture content to calculate intact dry density. A modified method for determining the intact dry density of irregularly shaped lumps of chalk was proposed by Lamont-Black and Mortimore (1996);

Sample preparation of irregular intact lumps for the measurement of IDD;

1. The chalk is cut or broken into lumps of no less than 30 g in mass.
2. The samples are then placed within an oven with a controlled temperature of 105 °C for a minimum of 24 hours.
3. The chalk is then removed from the oven and allowed to cool to room temperature. Upon cooling, the mass of the chalk is measured (m_s).
4. Suitable fine cordage is used to tie each chalk sample securely.
5. Each sample is then submerged in paraffin laboratory wax, melted at a 60 °C temperature, and removed instantaneously.
6. Upon quenching of the wax in air, the mass of the chalk specimen plus wax is measured (m_w).

Undertaking the test;

1. A eureka jar (Figure 5-1) is filled with de-aerated water to above the siphon tube, with excess water allowed to drain under gravity.
2. The mass of the receptacle is weighed and recorded. The receptacle is then positioned below the siphon tube to receive displaced water.
3. The chalk sample is then placed carefully into the eureka jar, ensuring there are no bubbles attached to the surface of the wax encasing.
4. The mass of the receptacle plus displaced water is then measured and recorded (m_g).



Figure 5-1 Eureka jar and receptacle used for intact dry density testing.

Calculation of IDD;

The volume of the test sample (cm^3) was calculated using the following method;

$$v_s = \frac{(m_w - m_g)}{\rho_w} - \frac{(m_w - m_s)}{\rho_p} \qquad \textit{Equation 5-4}$$

Where:

v_s = volume (cm^3), m_w = mass of specimen and wax coating (g), m_g = apparent mass of specimen and wax coating when suspended in water (g), m_s = mass of chalk specimen (g) ρ_w = density of water (Mg/m^3) and ρ_p = density of paraffin wax* (Mg/m^3)

* Or other sealing agent

Bulk density (Mg/m^3);

$$\rho = \frac{m_s}{v_s}$$ *Equation 5-5*

And dry density (ρ_d) (Mg/m^3);

$$\rho_d = \frac{100\,\rho}{100 + w}$$ *Equation 5-6*

Where ρ = bulk density (Mg/m^3) and w = moisture content of the chalk (%)

5.2.4 Calculation of void ratio (e) and porosity (n)

Voids ratio (*e*) is the ratio between the volume of void space and the volume of solid particles in a specimen of intact rock (Craig and Knappet, 2012). Interrelated to voids ratio is porosity (*n*). Porosity is the ratio of bulk volume to mass particle volume and indicates how much of the total volume consists of particle mass.

Calculation of both voids ratio and porosity is presented by Craig et al. (2012);

Voids ratio (*e*);

$$e = \frac{V_{void}}{V_{solid}}$$ *Equation 5-7*

Where *e* = voids ratio (dimensionless), V_v = volume of voids (cm^3) and V_s = volume of solids (cm^3).

Porosity (*n*) can be calculated from;

$$n = \frac{V_{void}}{V}$$ *Equation 5-8*

Where V = total volume (cm^3)

Given $V = V_{void} + V_{solid}$, the interrelation of void ratio and porosity can be shown as

$$e = \frac{n}{1 - n}$$ *Equation 5-9*

And

$$n = \frac{e}{1+e}$$ *Equation 5-10*

Bulk density can be expressed as;

$$\rho = \frac{m_s}{v_s} = \frac{G_s \times (1+w) \times \rho_d}{1+e}$$ *Equation 5-11*

Where G_s = specific gravity of chalk = 2.7, w = moisture content (%) and ρ_d = particle density (Mg/m^3)

When fully saturated, the sample density (ρ_{sat}) (Mg/m^3) will take the form of

$$\rho_{sat} = \frac{G_s + e}{1+e} \times \rho_w$$ *Equation 5-12*

Where ρ_w = density of water.

Void ratio can then be expressed as

$$e = G_s \times (1+w) \times \frac{\rho_w}{\rho} - 1$$ *Equation 5-13*

5.3 The slake durability test

The slake durability test is a method that measures a rocks resistance to alternative cycles of wetting and drying with a period of abrasion. The test was first proposed by Franklin and Chandra in 1972, and was initially used to measure durability in shales, mudstones and other clay bearing rocks. The standard used to test shales and similarly weak rocks is ASTM D4644-08, which was adopted in this research project (ASTM, 2008)

5.3.1 Samples

Individual samples to characterise Southern Province Formation Chalks were collected from eight coastal locations (Table 5-2) – all samples were index tested prior to more advanced testing. Specific locations are detailed in Chapter 3.

Table 5-2 Locations for sampling of Southern Province Chalk formations.

Formation	**Location**	**Grid**
Culver Chalk Formation	Splash Point, Seaford	548807, 98204
Newhaven Chalk Formation	Roedean Access Point, Roedean	534618, 103106
Seaford Chalk Formation	Birling Gap, East Dean	555318, 96034
Lewes Chalk Formation	Foyle Way, Holywell	559975, 96901
New Pit Chalk Formation	Beachy Head, East Sussex	558713, 95597
Holywell Nodular Chalk Formation	Holywell Beach Promenade, Holywell	560321, 97232
Zig Zag Chalk Formation	Falling Sands, Beachy Head	559197, 95525
West Melbury Marly Chalk Formation	Falling Sands, Beachy Head	559340, 95518

Samples to characterise CIRIA graded chalks for the Newhaven and Seaford Formations respectively were taken from three locations; Roedean, Telscombe Cliffs and Birling Gap (Table 5-3).

Table 5-3 Sampling locations for varying CIRIA chalk grades.

Formation	CIRIA grade	Location
Newhaven Chalk Formation	A 1 – 5	Roedean Access Point, Roedean; 534618, 103106
	B 1 – 5	
	C 1 – 5	
	Dc, Dm	Portobello Outfall, Telscombe Cliffs; 539313, 101394
Seaford Chalk Formation	A 1 – 5	Birling Gap, East Dean; 555318, 96034
	B 1 – 5	
	C 1 – 5	
	Dc, Dm	

Sample collection also included local measurement of field density approximation using the C574 grading system (i.e., Estwing hammer penetration and six-inch nail penetration), as well as measurement of moisture content and field observations. In terms of sample selection and storage, small cobble to boulder sized lumps of intact chalk were selected. The samples are wrapped twice in aluminium foil (to retain natural moisture content), labelled, and then wrapped in cellophane or zip-lock bags, where permissible.

To assess the effects of water weakening, capillary action and haloclasty on Newhaven and Seaford Chalks, three different slaking fluids were used. These tests are detailed in Table 5-4.

Table 5-4 Slaking fluid preparations

Slaking fluid	Rationale
De-aerated water	To assess the weakening action of water on chalk samples
Synthetic salt water	To assess the mechanical weakening action of haloclasty on the microstructure of chalk
Ethylene glycol water mix	To remove the water weakening aspects of the slake fluid and establish the chalk's mechanical resistance

5.3.2 Slaking fluid preparation

Synthetic seawater

Synthetic sea water was made using Peacock Salt's 'Seamix', an off-the-shelf salt mix designed to emulate British sea water, approved for use in the aquiculture industry. The typical composition of the mix is sodium chloride (NaCl 66.1%), magnesium sulphate (Mg SO4 16.3%) (heptahydrate), magnesium chloride (MgCl2 12.7 %), calcium chloride (CaCl2 3.30 %) and potassium chloride (KCl 1.60%).

Ethylene glycol

A 50% mix of laboratory grade ethylene glycol ((CH2OH)2) was mixed with de-aerated water to reduce the weakening effects of water on the chalk clasts. Ethylene glycol was considered suitable owing to its miscibility with and similar relative density to water, negating any buoyancy effects.

Each trough holds 2.5 litres of slaking fluid, and the ethylene glycol was added directly to 1.25 litres of water in the trough after being decanted into a measuring cylinder. The solution was then mixed to ensure full miscibility.

5.3.3 Equipment

The slake durability apparatus consists of a motorised drive unit, which is mounted on a base plate and connected to four drums, set inside water tanks. The overall unit weight (including 4 test drums) is 33.5 kg (Figure 5-2).

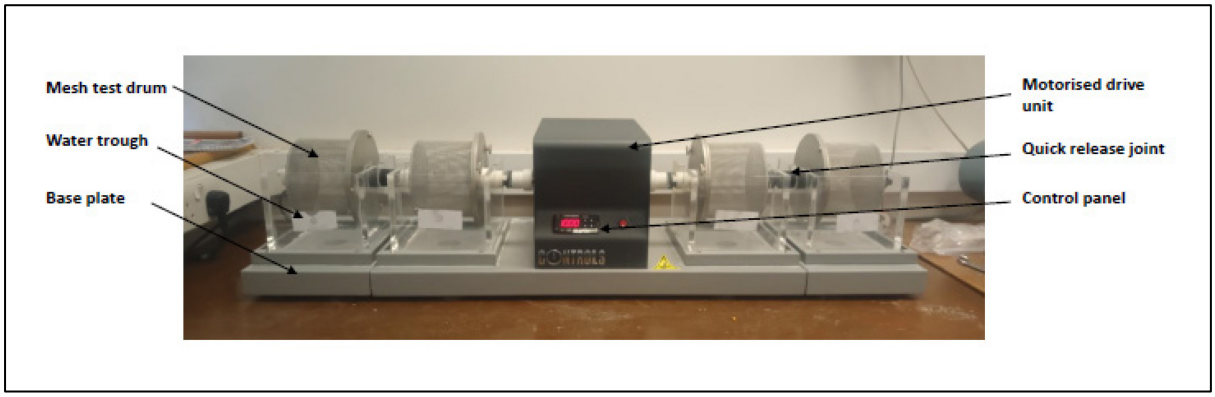


Figure 5-2 Slake durability machine.

The test drums are manufactured with a 2.0 mm wire mesh walls and are 140 mm in diameter and 100 mm long (Figure 5-3). The drums can be assembled using the quick-release joints and a maximum of four drums can be used at any one time. The machine operates for a period of 10 minutes at a rate of 20 RPM. In terms of settings, the duration of the abrasion can be modified, however the RPM at which the drums turn cannot be modified.

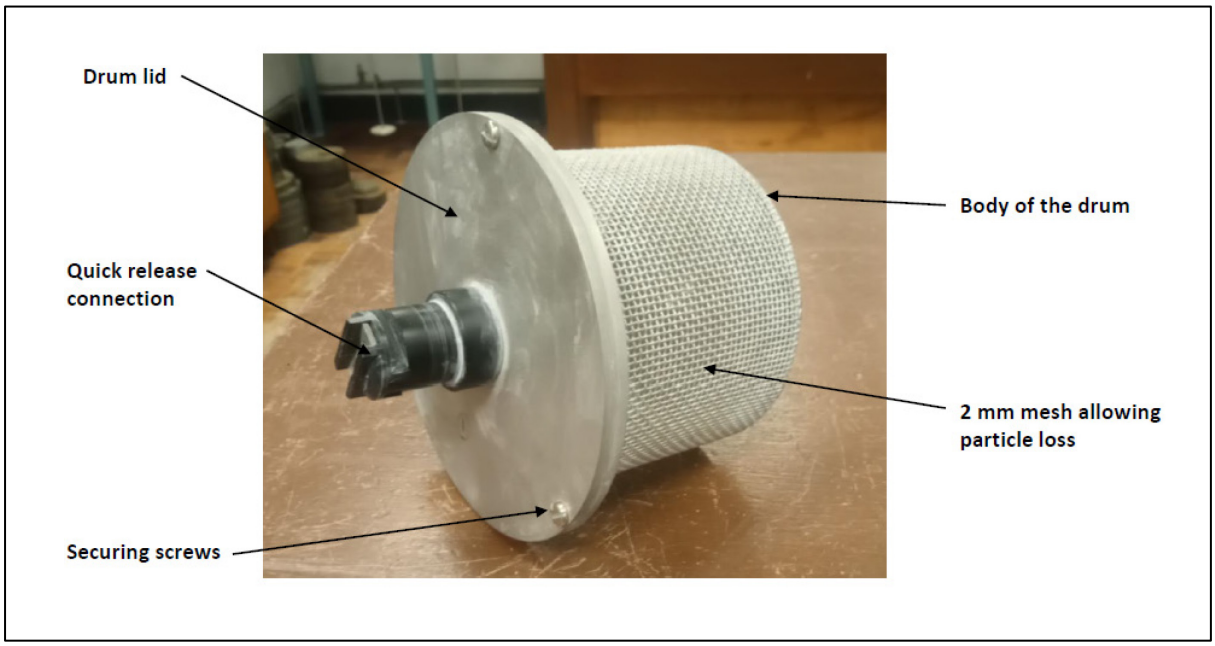


Figure 5-3 Slake durability drum (2.0 mm wire mesh).

The equipment required for the slake durability test are specified in ASTM D4644-08 (ASTM, 2008) and comprise;

Table 5-5 Slake durability equipment.

Laboratory tools for cutting and preparation	Balance (+/- 0.01 g)
Drying oven – 105 °C	Slaking fluid
Slake durability machine	Drying oven trays

5.3.4 Sample preparation

1. A single block of chalk is broken or cut into 10 representative, intact fragments, weighing between 40 – 60 g.
2. Angular edges are broken from the fragments to ensure no preferential breakage of sharp corners.
3. The samples are then placed in an oven with a controlled temperature of 105 °C for a minimum of 12 hours, or until the sample no longer loses mass when measured on a balance.
4. For samples subject to artificial haloclasty, samples are saturated in synthetic sea water within a vacuum desiccator prior to oven drying. Upon oven drying, to promote halite crystal nucleation, the samples are to be oven dried for a period of 48 – 72 hours.
5. Once removed from the oven, samples are brushed free of any chalk dust and weighed. The total specimen weight should be between 400 – 550 g.

5.3.5 Undertaking the slake durability test.

1. Photograph samples prior to placing within the drum.
2. Weigh empty drum and record.
3. Weigh empty drum with dried sample mass.
4. Fill slaking trough with required slaking fluid and measure the temperature.
5. Mount the drum in the trough and couple to the drive shaft.
6. Turn the programmed timer on and rotate the drum at 20 RPM for a period of 10 minutes.
7. Remove the drum from the trough and place in the oven for a period of 4 – 6 hours. Upon completion, measure the oven-dried mass of the drum and the sample.

5.3.6 Measurements after testing

1. Qualitatively describe turbidity of slaking fluid.
2. Describe the nature of arisings collected in the bottom of the trough, indicating grain size and angularity.

5.3.7 Calculations

$$I_d = \left(\frac{W_f - C}{B - C}\right) \times 100 \qquad \textit{Equation 5-14}$$

Where I_d = slake durability index, B = mass of drum plus oven dried specimen before first cycle (g), W_f = mass of drum plus oven dried slaked sample (g), C = mass of the drum (g)

5.3.8 Reporting results

1. Description of the specimen and location collected.
2. Slake durability index.
3. Water temperature
4. Description of fragments retained in drum.
5. Appearance of slaking fluid
6. Description of arisings collected in trough.

5.4 Permeability testing

In the previous sections, index testing to characterise material properties and slake durability testing to assess material durability were detailed. This section details the methodologies used to characterise the permeability and geomechanical properties of Dm and Dc graded chalk. Two locations were used for sampling Dm and Dc grades of chalk from two formations; the Seaford and Newhaven Chalk Formations, respectively (Chapter 3).

Portobello Outfall, Telscombe Cliffs, Grid 539276, 101430

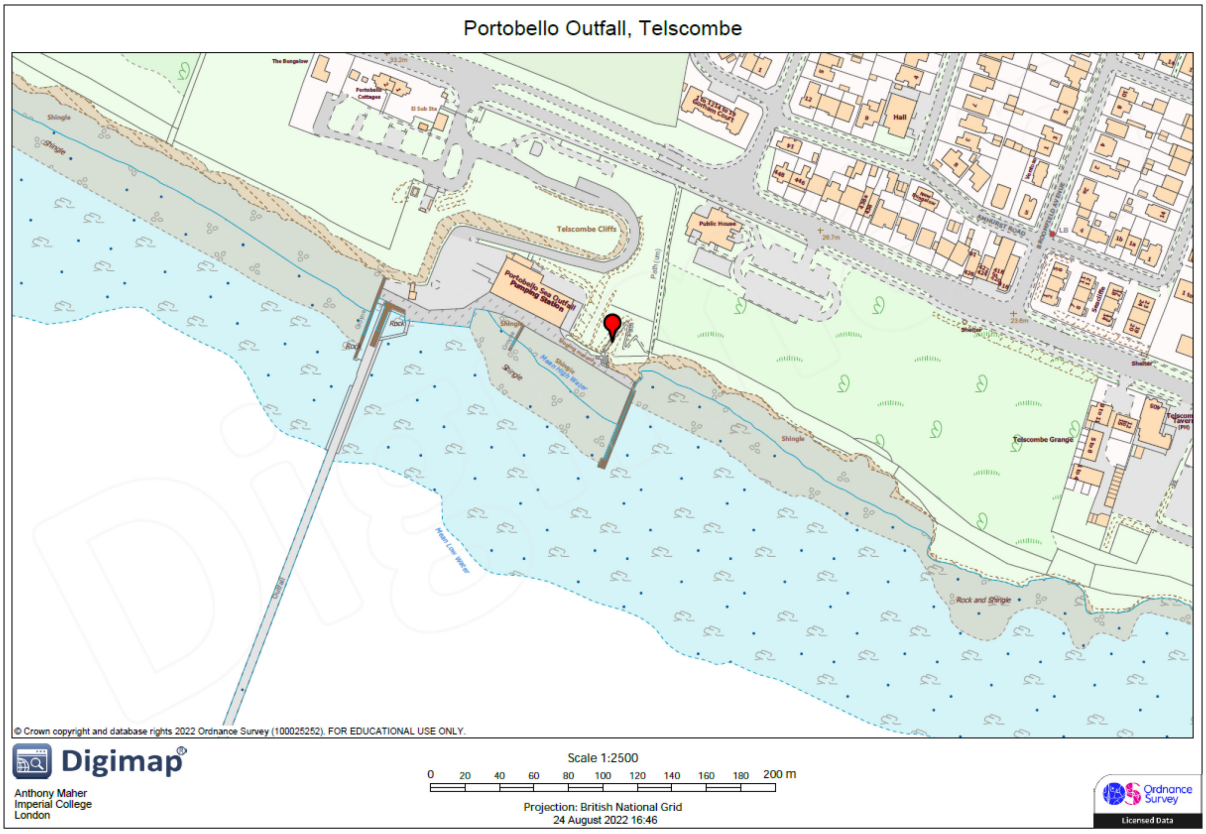


Figure 5-4 Sampling locations Portobello Outfall, Telscombe (Maher, 2022c).

Birling Gap, East Dean, Grid 555318, 96034

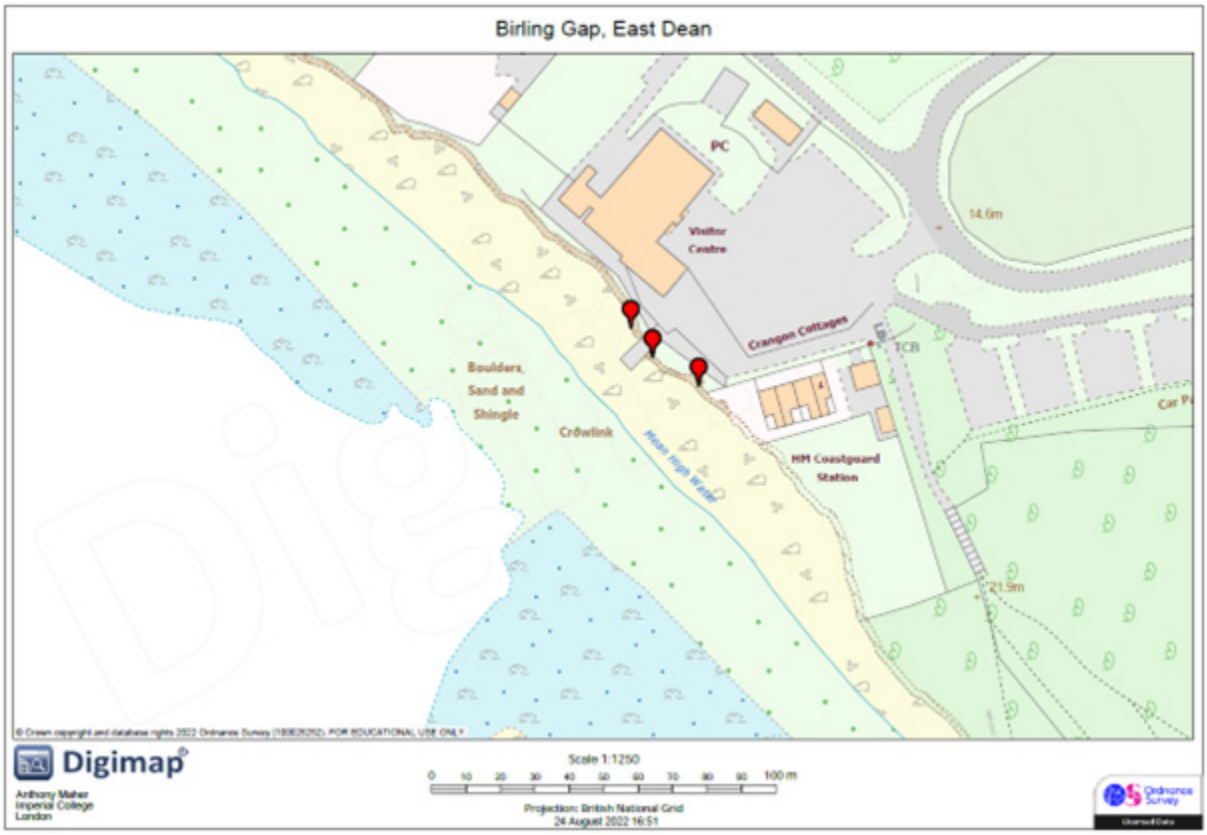


Figure 5-5 Sampling locations, Birling Gap, East Dean (Maher, 2022b).

The accelerated permeability test is a non-standard test (i.e., does not conform to British Standards), which uses the Bishop and Wesley triaxial cell and the procedure for this permeability test was taken from Murray (2003). The test is also prescribed within BS1377-6; method 6, for determining permeability. The test is considered as an alternative to the British Standard Triaxial Permeability test and allows for the permeability to be measured at a quicker rate by inducing a pressure differential, which has implications for low permeability deposits. This method was used to determine the coefficient of permeability of Dm and Dc grade chalks. Initially, the falling head method was attempted, however after three days, water flow through the chalk was negligible, and therefore this method was abandoned.

As reported in Chapter 3, permeability has been measured for both structured chalk and laboratory prepared idealised putty chalk samples, however, the measurement of permeability for Dm and Dc graded chalks has not been undertaken, which makes this approach novel.

Measurements taken along with sampling included field density approximation as per C574 field density method as well as sample collection for index testing. Samples were collected in the field using the methods detailed in Chapter 4. The samples were extruded in the field, directly into 38 mm

membranes to ensure that their integrity and shape were maintained. The samples were then wrapped in aluminium foil, labelled, and then placed in zip-lock bags. Where samples could not be extruded in the field, owing to sample competence or refusal to extrude from the sampling tubes, the samples were kept in the tube, with end caps placed on. The tubes were then wrapped in aluminium foil, labelled, and placed in zip-lock bags. These samples would then be brought back to Imperial College laboratories for tube cutting and extrusion.

5.4.1 Tests required

Three to four samples of Dm and Dc grades of both the Seaford and Newhaven Chalk were initially specified, however, sourcing Dm grade Seaford Chalk in field settings proved challenging, therefore samples of Dm grade Seaford Chalk Formation were omitted from the test schedule.

In terms of test conditions, the initial effective stress was calculated based on the depth of the samples in relation to ground level. Owing to the capabilities of the permeability rig, and the requirement to have three stages, the maximum effective stress that could be maintained was 480 kPa (Table 5-6).

Table 5-6 Pressures used during the accelerated permeability test.

Cell pressure (kPa)	**U_{bottom} (kPa)**	**U_{top} (kPa)**	**ΔU (kPa)**	**P'effective (kPa)**	**Equivalent depth (mbgl)**
370	120	125	5	120	4.5
490	120	125	5	240	9.5
510	120	125	5	480	18.0

Table 5-6 shows how the pressures are distributed within the triaxial system. The cell pressure provides confining pressure (measured in kPa), while U_{bottom} corresponds to the back pressure bottom tap (120 kPa), and U_{top} corresponds to the back pressure top tap (125 kPa). The differential (ΔU in kPa) between the two back pressure taps allows a flow of fluid from the back pressure top tap, with drainage at the back pressure bottom tap. $P'_{effective}$ is the effective pressure acting on the sample (kPa), while the equivalent depth (m) is calculated from overburden pressure. Samples were taken from approximately 5.0 mbgl, allowing an initial pressure of 120 kPa to be used as the first stage. This was then increased, with equivalent depths stated in Table 5-6.

5.4.2 Equipment

Equipment required for undertaking the accelerated permeability test (Table 5-7);

Table 5-7 Equipment for the accelerated permeability test.

Sample trimming tools	Filter paper
Balance (+/- 0.01 g)	O rings
Drying oven	Sealant grease
Vernier callipers	Bishop and Wesley triaxial cell
Latex membrane	Porous disks

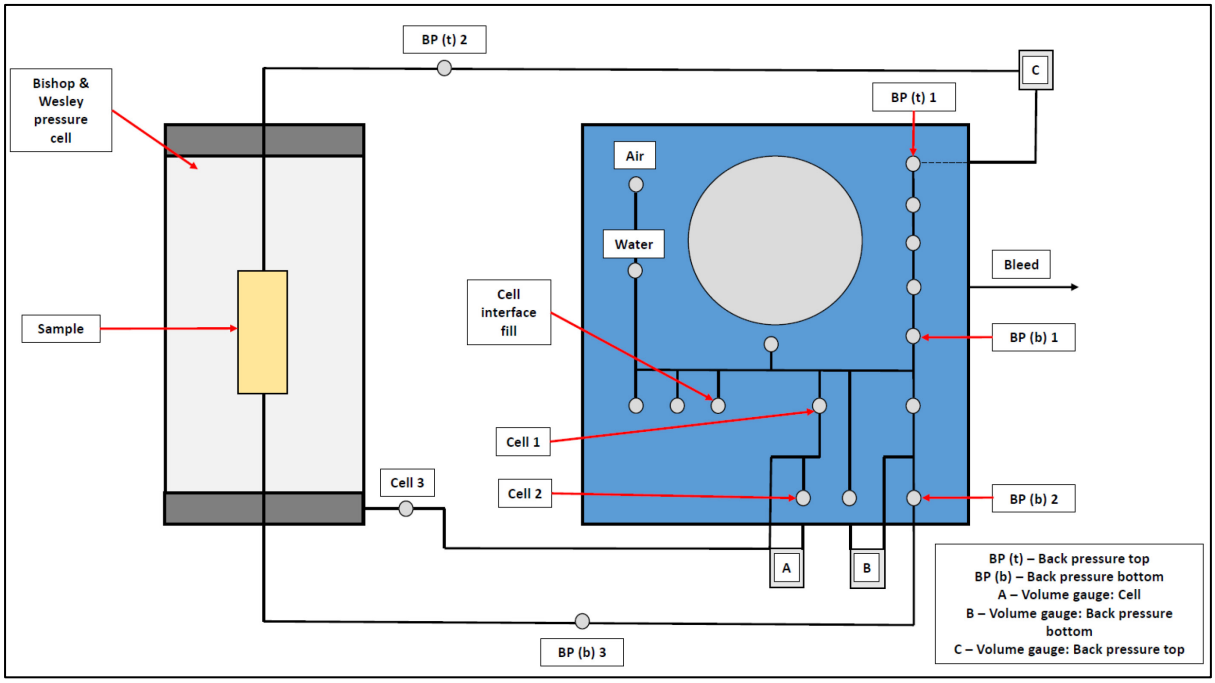


Figure 5-6 Schematic of control board for the Bishop-Wesley triaxial cell; permeability configuration.

5.4.3 Sample preparation

1. Trim & prepare sample in membrane:
    A. If the sample is competent, remove the sample from the membrane and use a fine saw to trim the ends of the sample square to the correct length.
    B. If the sample is incompetent and soft, keep the sample within the membrane and place a 2-part, split mould around the sample. With the use of a razor, trim the ends square to the correct length. Care should be taken to not to pluck any clasts from the sample, nor should excessive force be used when cutting, leading to sample material loss.
2. Take measurements of mass.
3. Take measurements of length (x3) at 120° apart.
4. Take measurement of diameter (x3 at three intervals: top, middle and bottom).

5. Add filter paper and porous disks on top and bottom.
6. Take initial moisture content from trimmings for comparison with site measurement.

Setting up the sample:

1. Clean pedestal, & top cap, including drainage feeds, apply a thin layer of grease.
2. Open pressure gauge and ensure back pressure (top and bottom) and cell pressure on board are closed.
3. Flush water through bottom entry line and slide sample onto pedestal.
4. Fix the base with two O-rings.
5. Flush water through the top drainage line.
6. Slide top drainage line into place, fold up membrane and fix two O-rings in place.
7. Place the cell on the apparatus.
8. Tighten bolts in diametric pairs.

Setting up the cell:

Fill volume gauges and check Cell and Back pressure(s) are in normal range (prior to connecting to sample):

1. Check all valves on the apparatus are closed.
2. Set air to closed, set water to open, use the back pressure top tap on the board to fill the volume gauge half-way, using the transducer lever as an indicator, then close.
3. Open back pressure bottom tap to fill back pressure bottom volume gauge to full, using the transducer lever as an indicator.

Filling the cell:

1. Close both back pressures (top and bottom).
2. Open air bleed on top of cell.
3. Open cell taps in consecutive order.
4. Fill the cell to the top.
5. Close cell taps in reverse order.

5.4.4 Testing

Saturate sample:

1. Check both back pressure drainage lines and cell taps are closed
2. Switch to SATURATION stage in TRIAX, check the CELL PRESSURE is at the correct setting and that the back pressure bottom is at the correct setting.
3. Write in notes on TRIAX that SATURATION IS ABOUT TO START.
4. Open the Back Pressure bottom drainage line.
5. Open the Cell taps.
6. Press RUN/START in TRIAX.
7. Make a note that SATURATION HAS STARTED in TRIAX.
8. Wait.
9. Undertake a B-Test.
10. Upon completion of Saturation stage, isolate the cell by shutting off cell taps and press STOP.
11. Record in TRIAX that SATURATION HAS STOPPED.

Consolidate sample:

1. Check both Back Pressure drainage lines and cell taps are closed.
2. Switch to CONSOLIDATION stage in TRIAX, check the CELL PRESSURE is at the correct setting and that the back pressure bottom is at the correct setting.
3. Write in notes on TRIAX that CONSOLIDATION IS ABOUT TO START.
4. Open the Back Pressure bottom drainage line.
5. Open the Cell taps.
6. Press RUN/START in TRIAX.
7. Make a note that CONSOLIDATION HAS STARTED in TRIAX.
8. Wait.
9. Upon completion of Consolidation stage, isolate the cell by shutting off cell taps and press STOP.
10. Record in TRIAX that CONSOLIDATION HAS STOPPED.

Undertake permeability test:

1. Switch to PERMEABILITY stage in TRIAX.
2. Make a note in TRIAX that PERMEABILITY STAGE IS ABOUT TO START.
3. Turn Bottom Pressure Top tap to open at a pressure of 120 kPa to induce a pressure differential between back pressure inlet and outlet, causing flow from bottom to top.
4. Change Cell pressure to required pressure.
5. Press START on TRIAX.
6. Make a note in TRIAX that the TEST HAS STARTED.
7. Wait for test completion. Upon completion, close back pressure taps and the cell pressure tap, press STOP on TRIAX.

Data management:

For data management, split down the test to individual files;

1. Saturation.
2. Consolidation.
3. Permeability stage 1.
4. Permeability stage 2.
5. Permeability stage 3.

Calculations

Coefficient of permeability:

1. Calculate the cross-sectional area of the chalk specimen (A) in mm^2.
2. From the steady state, linear portions of the cumulative flow plot (taken from TRIAX recordings), determine the mean rate of flow, q, in mL/mm.
3. Calculate the pressure difference between back pressure bottom and back pressure top (P_1 - P_2) (kPa).
4. Calculate the coefficient of permeability (k) (m/s):

$$k = \frac{(1.63 \times q_a \times L)}{A(p_1 - p_2) - p_c} \times R_t \times 10^{-4} \qquad \textit{Equation 5-15}$$

Where k = coefficient of permeability (m/s), q_a = mean rate of flow through specimen (mL/min coverted to m/s), L = length of specimen (mm), A = cross sectional area (mm^2), P_1 = back pressure top (kPa), P_2 = back pressure bottom (kPa), P_c = pressure loss in the system (taken from a calibration graph = kPa)), 1.63 = empirical constant for vertical permeability tests and R_t = temperature correction factor for the viscosity of water.

Measurement of sample after testing:

1. Take measurements of wet mass, oven dry and take measurement of the dry mass.
2. Take measurements of length (x3) at 120° apart.
3. Take measurement of diameter (x3 at three intervals: top, middle and bottom).

Reporting of results:

1. Initial measurements of dimensions and mass.
2. Initial trace of the specimen.
3. Initial volume of the sample.
4. Moisture content.
5. Coefficient of permeability (k).
6. Mean effective stress at which the sample was tested, detailing cell and back pressures.
7. Hydraulic gradient across the specimen during the test.
8. Final measurement of dimensions and mass.
9. Final volume of the sample.

10. Final moisture content.
11. Description of the specimen after the test.
12. Saturation test results.

5.5 Unconfined compressive strength (UCS)

The uniaxial compressive strength (UCS) test is a method for testing the strength of intact rock. The test consists of a cylindrical core of rock of defined dimensions, subject to axial loading, with an absence of radial loading or constraint, hence the uniaxial nature of the test (Hoek and Brown, 2019).

5.5.1 Samples

Dm and Dc grade chalks were sampled at both Portobello Outfall, Peacehaven and Birling Gap, East Dean (Figure 5-5). Other measurements included density approximation to CIRIA C574 field density methodology, along with moisture content and field observations.

Samples were extruded in the field, directly into 38 mm membranes to ensure that their integrity, shape and moisture content were maintained. The samples were then wrapped in aluminium foil, labelled, and then placed in zip-lock bags. Where samples could not be extruded in the field, owing to sample competence or refusal to extrude from the sampling tubes, the samples were kept in the tube, with end caps placed on. The tubes were then wrapped in aluminium foil, labelled, and placed in zip-lock bags. These samples would then be brought back to IC laboratories for tube cutting and extrusion.

Dc grade chalk samples were sampled using sacrificial aluminium U38 tubes. Upon extraction, the samples were wrapped in aluminium foil and labelled, prior to being placed in a zip-lock bag to maintain moisture content. The samples were then cut and extruded in the laboratory to maintain sample competency and control of sample trimming without plucking of clasts.

The material was tested at two moisture contents – oven dried (therefore moisture content assumed to be negligible) and at natural moisture content for field conditions. The rationale behind these tests is that there are strength changes with the loss of moisture, with dried cores likely to have higher tensile and unconfined compressive strengths compared to their undried NMC counterparts. It was considered to undertake a sample with increased moisture; however, this would likely require a membrane to hold the material together for testing purposes as the material collapses upon saturation. Table 5-8 lists a schedule for testing as well as the number of tests completed.

Table 5-8 Schedule of UCS testing for Newhaven and Seaford de-structured chalks at differing moisture contents.

Formation	Grade	Moisture content	Scheduled number of samples	Actual number samples tested
Newhaven Chalk Formation	Dm	NMC	3	1
Newhaven Chalk Formation	Dm	Dry	3	1
Newhaven Chalk Formation	Dc	NMC	3	2
Newhaven Chalk Formation	Dc	Dry	3	5
Seaford Chalk Formation	Dc	NMC	3	3
Seaford Chalk Formation	Dc	Dry	3	3

5.5.2 Equipment

Equipment required for undertaking the unconfined compressive strength test (Table 5-2);

Table 5-9 Equipment for unconfined compressive strength testing.

Sample trimming tools	UCS stiff testing frame (25 kN)
Balance (+/- 0.01 g)	Drying oven
Vernier callipers	Camera
2x Linear variable displacement transducers (LVDTs)	External displacement transducer

In terms of monitoring instrumentation, load is measured by 2x ferromagnetic linear variable transducers (LVDT) (accurate to 5µm), which are attached to the sample parallel to the long axis. A third LVDT was attempted to be mounted perpendicular to the long axis to monitor volume change, however, in some instances, owing to the fragile nature of the samples, this could not be achieved successfully. Similarly, care was taken with the vertical LVDT in that when glued to the sample, they had sufficient weight to pluck clasts out or damage sample integrity. A fourth displacement transducer was attached as contingency. This transducer was affixed to the load frame, with the plunger on the base plate. This transducer displaced at an equal rate to the sample, acting in a parallel orientation.

5.5.3 Sample preparation

To ensure repeatability of both tests conducted at natural moisture content and when dry, sample storage best practice of wrapping in aluminium foil and then stored in zip-lock bags under temperature-controlled conditions should be undertaken, with testing to be undertaken as quickly as reasonably practicable (generally within 24 hours of sampling). To verify the moisture content of each

test, NMC samples should be tested for moisture content as per Section 5.2.2, while dry samples should be tested as per Section 5.2.2 while they are being desiccated, to ensure that moisture content is driven off by laboratory grade ovens.

Trimming at natural moisture content:

Trim & prepare sample with natural moisture content:

A. If the sample is competent, remove the sample from the membrane and use a fine saw to trim the ends of the sample square to the correct 76 mm length.
B. If the sample is incompetent and soft, keep the sample within the membrane, but roll back the end. Place a 2-part, split mould around the sample. With a razor blade, trim the ends square to the correct 76 mm length. Care should be taken to not to pluck any clasts from the sample, nor should excessive force be used when cutting, leading to sample material loss.
C. For Dc samples, the material is to be sampled in an aluminium tube and retained in this until trimming. The tube is sawn at the ends to the required 76 mm length using a fine bandsaw to avoid accidental removal of clasts. The sample is extruded out of the tube when testing is required. Samples should not stay within aluminium tubes for longer than 48 hours to prevent corrosion of the metal.

Trimming a dry sample:

1. Remove sample membrane with care.
2. Oven dry-for a period of 24–48 hours, or until the sample ceases to lose mass when weighed.
3. Trim and prepare sample by using a split mould and fine hacksaw to trim ends square to a length of 76 mm.

After trimming:

1. Take measurements of mass.
2. Take measurements of length (x3) at 120° apart.
3. Take measurement of diameter (x3 at three intervals: top, middle and bottom).
4. Take initial moisture content from trimmings for comparison with site measurement.

Testing:

1. Samples with a height to diameter ratio of 2:1, are placed onto a base platen.
2. A second platen is then placed at the top, capping the sample.
3. Two linear vertical displacement transducers (LVDT) are placed on the sides of the sample to measure vertical displacement.
4. The sample is then placed in the UCS test frame.
5. The sample is then tested using a loading frame with a maximum load of 25 kN at a rate of 0.1 mm/min.
6. During loading, load and displacement data is measured by two axial LVDT's and one external transducer. Data was recorded using the 'Triax' software.

Calculations:

From the data collected, axial strain (ε_{ax}), UCS, Young's modulus and Poisson's Ratio can be calculated.

Axial strain is calculated by:

$$\varepsilon = \frac{\Delta L}{L_0} \qquad \textit{Equation 5-16}$$

Where ΔL = change of sample length taken from LVDT (mm) and L_0 = initial sample length (mm).

UCS is calculated from the axial load (in Newtons) by:

$$\sigma_1 = \frac{P}{A_0} \qquad \textit{Equation 5-17}$$

Where σ_1 = maximum principal stress (in this case, UCS = MPa), P = load applied to specimen (N) and A_0 = cross sectional area of specimen (mm^2).

Young's modulus (E) (modulus of elasticity) is a ratio of axial stress ($\Delta\sigma_1$) to axial strain ($\Delta\varepsilon$) is calculated by:

$$E = \frac{\Delta\sigma_1}{\Delta\varepsilon} \qquad \textit{Equation 5-18}$$

Poisson's Ratio can be calculated by:

$$v = -\frac{\varepsilon_{diametral}}{\varepsilon_{axial}} \qquad \textit{Equation 5-19}$$

Where $\varepsilon_{diametral}$ = diametric strain, calculated below:

$$\varepsilon_d = \frac{\Delta L_d}{L_d} \qquad \textit{Equation 5-20}$$

Where ΔL_d = change of sample length in the diametric dimension (mm) and L_d= initial sample length in the diametric dimension (mm).

Measurements after testing:

1. Moisture content of the sample (particularly important for saturated samples).
2. Sketch of failure mode.
3. Photograph of failure mode.
4. Measurement of length change.
5. Measurement of diameter change.

5.6 The Brazilian tensile test

The Brazilian tensile test is an indirect method used to determine the tensile strength of a geomaterial. Stresses are induced in a disk of prepared material by platens that exert a load on the outer diameter of the disk. These stresses act in a perpendicular direction to which the load is applied acting in a tensile fashion.

5.6.1 Samples

Dm and Dc grade chalks were sampled at both Portobello Outfall, Peacehaven and Birling Gap, East Dean (Figure 5-5). Other measurements included density approximation to CIRIA C574 field density methodology, along with moisture content and field observations.

Dm and Dc chalk material was trimmed from the samples collected for UCS testing and were also tested at two moisture contents – oven dried (therefore moisture content assumed to be negligible) and at natural moisture content for field conditions. The rationale behind the moisture contents used in these tests was the same as that for UCS testing; strength changes with the loss of moisture, with dried samples likely to have higher tensile strengths compared to their undried NMC counterparts.

5.6.2 Equipment

Table 5-10 Equipment for Brazilian tensile strength testing.

Sample trimming tools	UCS stiff testing frame (25 kN)
Balance (+/- 0.01 g)	Drying oven
Vernier callipers	Camera
Frame-mounted external displacement transducer	

Owing to the geometry of the samples (i.e. thick discs) LVDT's were not suitable. A frame mounted external displacement transducer was used to measure displacement equal to the sample displacement. The external transducer was frame mounted, with the transducer plunger reacting with the test anvil below the sample. The transducer was zeroed when the upper platen was touching the sample, prior to commencement of the test. The test was complete upon observed failure of the sample.

5.6.3 Sample preparation

Trimming:

1. Carefully remove membrane.
2. If sample is required to be dried, place in a drying oven for no less than 24 hours.

3. Place the sample in a split mould and use a fine-toothed hacksaw to cut square ends of the disks.
4. Undertake moisture content tests on trimmings to further characterise material.

After trimming:

1. Take measurements of mass.
2. Take measurements of thickness (x3) at 120° apart.
3. Take measurement of diameter (x3) at 120° apart.
4. Take initial moisture content from trimmings for comparison with site measurement.

Testing:

1. Prepared sample disks are placed onto a base platen.
2. A second platen is then placed at the top, capping the sample.
3. Photographs are taken of the sample prior to testing.
4. The sample is then placed in the UCS test frame.
5. The sample is then tested using a loading frame with a maximum load of 25 kN at a rate of 0.1 mm/min.
6. During loading, load and displacement data is measured using an external displacement transducer and recorded using the 'Triax' software.

Calculations:

The data recorded by Triax comprises frame load and displacement data. The tensile strength of the specimen σ_t (MPa), is calculated using the maximum applied load, P (N), the thickness, t (mm) and the diameter, D (mm) of the specimen:

$$\sigma_t = \frac{2P}{\pi t D} \qquad \textit{Equation 5-21}$$

Measurements after testing:

1. Moisture content of the sample (particularly important for saturated samples).
2. Sketch of failure mode.
3. Photograph of failure mode.
4. Measurement of length change.
5. Measurement of diameter change.

5.7 Triaxial testing

The triaxial test is a fundamental technique used to determine the mechanical behaviour of rocks and soils, such as stress-strain behaviour, cohesion and angle of shear (shear values for structured chalk are presented in Chapter 2). During the test, a core of rock or soil is subjected to controlled stresses to simulate analogous insitu stresses to those in the field.

The test comprises three stages;

- Saturation.
- Isotropic consolidation of samples to an effective stress of P'0 = 50 kPa.
- Shearing at 1, 5 and 50% strain rate per day.

The British Standard for this test is BS EN ISO 17892-9:2018. This standard is entitled 'Geotechnical investigation and testing. Laboratory testing of soil'. Consolidated triaxial compression tests on water saturated soils' (BSI, 2018). All stages are the same as the accelerated permeability test (utilising the Bishop and Wesley triaxial cell – figure 5-7) except for the permeability stage. The permeability stage is substituted for a shearing stage, where the sample is sheared by a piston (σ_1), while under effective stress (σ_3) at low confining pressures. Similarly, sample preparation and sample dimensions are the same as the permeability test.

Triaxial testing was undertaken by a MacLean (Maclean, 2023), who tested weathered chalk for strain-rate dependency. The results of which are included within this thesis. These results were then combined with UCS results to plot Mohr circles to ascertain cohesion and angle of shearing resistance.

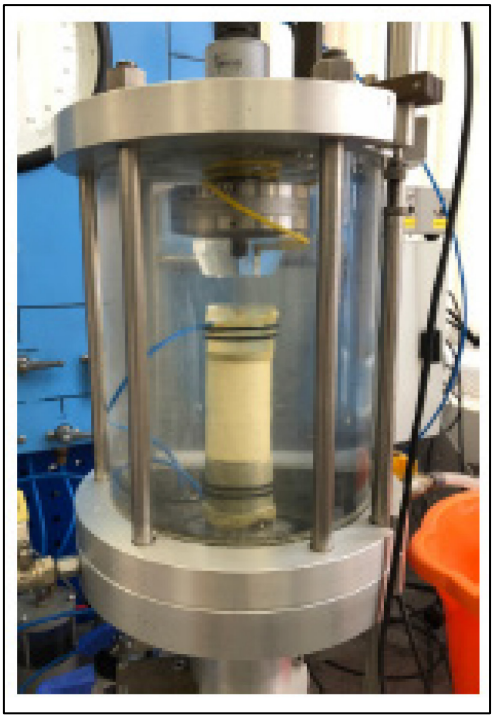


Figure 5-7 Bishop and Wesley triaxial cell.

5.7.1 Samples

Samples were sourced from locations detailed in Figures 5-4 for Seaford Chalk D-grades and Figure 5-5 for Newhaven Chalk D-grade samples. Four samples of both the Newhaven and Seaford Chalk types were collected for sampling but owing to sample preparation difficulties, three Newhaven samples and one Seaford sample were tested successfully (Table 5-11).

Table 5-11 Triaxial test schedule of Newhaven and Seaford D-grade chalks

Sample	Formation	Consolidation stage		Consolidation effective stress (kPa)	Shearing stage		Strain rate (%/day)
		Cell pressure (kPa)	Back pressure (kPa)		Cell pressure (kPa)	Ram pressure (kPa)	
WNC1	Newhaven	550	500	50	550	550	5
WNC2	Newhaven	550	500	50	550	550	5
WNC3	Newhaven	550	500	50	550	550	1
WNC4	Newhaven	550	500	50	550	550	50
WSC1	Seaford	550	500	50	550	550	5

5.7.2 Equipment

The equipment required to undertake the triaxial test is detailed in Table 5-12.

Table 5-12 Table of equipment required for the triaxial test.

Latex membrane	4 Rubber O-rings
Filter paper	Super glue
Steel half-ball	Vacuum grease
Top Cap	Membrane Stretcher
Suction Cap	O-ring Stretcher
Porous Stone	Vernier callipers
2x ferromagnetic Linear vertical displacement transducers (LVDT)	External displacement transducer

The test comprises the Bishop-Wesley pressure cell, which provides confining pressure, along with a piston ram, which applies axial stress (Figure 5-7). The sample itself is confined within a latex membrane, which serves to distribute stress uniformly around the sample, while still maintaining integrity as a barrier between the fluid within the sample and that within the pressure cell, which applies the confining stress. Measurement of the loads was undertaken by a total of three LVDTs; 2 LVDTs axially mounted, oriented vertically, to the sample to measure displacement, and a third LVDT positioned perpendicular to the vertical LVDTs to measure radial volume change. A fourth external, frame mounted displacement transducer was used to measure vertical displacement equal to the sample displacement.

5.7.3 Sample preparation

1. Trim & prepare sample in membrane:
    A. If the sample is competent, remove the sample from the membrane and use a fine saw to trim the ends of the sample square to the correct length.
    B. If the sample is incompetent and soft, keep the sample within the membrane and place a 2-part, split mould around the sample. With the use of a razor, trim the ends

square to the correct length. Care should be taken to not to pluck any clasts from the sample, nor should excessive force be used when cutting, leading to sample material loss.

2. Take measurements of mass.
3. Take measurements of length (x3) at 120° apart.
4. Take measurement of diameter (x3 at three intervals: top, middle and bottom).
5. Add filter paper and porous disks on top and bottom.
6. Take initial moisture content from trimmings for comparison with site measurement.

Setting up the sample:

1. Clean pedestal, & top cap, including drainage feeds, apply a thin layer of grease.
2. Open pressure gauge and ensure back pressure (top and bottom) and cell pressure on board are closed.
3. Flush water through bottom entry line and slide sample onto pedestal.
4. Fix the base with two O-rings.
5. Flush water through the top drainage line.
6. Slide top drainage line into place, fold up membrane and fix two O-rings in place.
7. Place the cell on the apparatus.
8. Tighten bolts in diametric pairs.

Setting up the cell:

Fill volume gauges and check Cell and Back pressure(s) are in normal range (prior to connecting to sample):

1. Check all valves on the apparatus are closed.
2. Set air to closed, set water to open, use the back pressure top tap on the board to fill the volume gauge half-way, using the transducer lever as an indicator, then close.
3. Open back pressure bottom tap to fill back pressure bottom volume gauge to full, using the transducer lever as an indicator.

Filling the cell:

1. Close both back pressures (top and bottom).
2. Open air bleed on top of cell.

3. Open cell taps in consecutive order.
4. Fill the cell to the top.
5. Close cell taps in reverse order.

Typical parameters for recording;

1. Sample identification
2. Test conditions: Record the test conditions, including the confining pressure applied, axial load applied, and the rate of application for both confining and axial pressures.
3. Specimen dimensions, before and after testing.
4. Deformation measurements: Record the axial strain, radial strain, and volumetric strain at intervals during the test.
5. Porewater pressure: Measure and record the pore water pressure within the soil specimen during the test.
6. Determine and record the mode of failure; axial stress at failure, the axial strain at failure, and any observable failure patterns (e.g., shear band development).
7. Record any additional observations or anomalies observed during the test, such as sample disturbance, equipment malfunctions, or unexpected behaviour.

Further analysis;

A principal stress analysis was performed using combined data and the proprietary computer program RocLab, which allowed the calculation of Mohr-Coloumb parameter, such as cohesion and the angle of friction.

5.8 Modification of the Bushinsky technique for Dm and Dc grade chalks

Bushinsky (1947) demonstrated a method to enhance the visualisation of structures in competent, structured marly chalk. The method comprised sanding of the competent samples, immersion for ten minutes to two hours in engine or mineral oil to enable incomplete impregnation of the chalk, then subsequent removal of the chalk and inspection. Bromley further developed this technique in 1981 by replacing the immersion in oil with the coating of a thin layer of engine oil on the objective and introducing high resolution photographs (Bromley, 1981). Lawrence et al. (2018a) further refined this technique by using propriety oil products (such as WD-40), which resulted in more rapid results and a higher resolution of enhancement.

This methodology is a proposed technique, like the Bushinsky method, although specifically developed for grade Dm and Dc chalks. When considering the Bushinsky technique, the author identified that two aspects of the applied oil were likely to be integral to enhancing structures not seen by the naked eye; the colour and the hydrophobic properties. Consideration of traditional oils had some merit, but the results were not permanent in de-structured chalk and samples lost integrity.

One significant challenge with grade Dm and Dc chalks are that they are delicate with a natural moisture content and friable when desiccated. Paraffin wax was then considered as it had a similar colour to the oils used in previous techniques and was hydrophobic. Two added benefits of paraffin wax was that the viscosity of the wax (and therefore degree of penetration) could be controlled by temperature, and when the wax cooled, it provided support to the delicate samples.

It was also identified that samples were required to be dried out to enable cutting and polishing of surfaces. Working of de-structured chalk with a natural moisture content resulted in further puttification and break down of sample integrity.



Figure 5-8 Dc grade Seaford Chalk before and after the modified Bushinsky technique.

It was identified that paraffin wax was successful at elucidating the internal structure of Dm and Dc chalks, and with the use of high-resolution photography and image processing, it was possible to estimate the degree of clast or matrix domination of the sample, as well as quantify clasts within the sample (Figures 5-8 and 5-9).

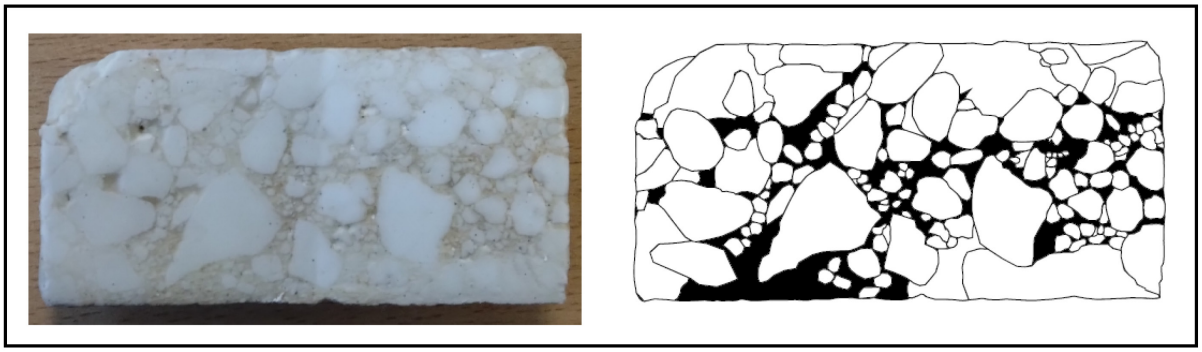


Figure 5-9 Seaford Chalk binarised for image processing after the modified Bushinsky technique.

5.8.1 Samples

The samples used for this experiment were cores used for permeability testing. The rationale behind this was to look for links between internal structure of the core and permeability. Samples were taken from the permeability rig, with moisture content measurements taken. They were then placed in the oven for desiccation for a minimum of 12 hours.

5.8.2 Equipment

The equipment required for this test is presented in table 5-13;

Table 5-13 Equipment for the modified Bushinsky technique.

Drying oven	Fine brush
Hacksaw/fine-toothed saw	Moisture content tin(s)
Coarse sandpaper	Wax and melting pot
Fine sandpaper	Labels and marker
Set square	Ruler

5.8.3 Sample preparation

1. Oven dry core for a minimum of 12 hours.
2. Remove core and allow to cool. Using the set square and ruler, identify and mark the centre axis of the core and mark a cutting template line.
3. Using the fine-toothed hacksaw, bisect the sample along the axis.
4. Upon cutting the sample in two, use the fine brush to brush away excess chalk dust from the sample required to be impregnated with paraffin.
5. Use the coarse sandpaper to ensure that the sample face is flush and repeat with the fine sandpaper to smooth off the sample face.
6. Brush the sample face with the fine brush to remove all fine chalk powder.
7. Heat the paraffin wax to 60°, immerse one half of the sample in the wax, ensuring no air bubbles are entrained and remove sample.
8. Repeat step 7 but for the uncoated end of the sample.
9. Place sample in a moisture content tin to cool.
10. Take high resolution photographs for inspection and image processing.

5.8.4 Data from processed image

To binarise the image of the cores, it was necessary to utilise CorelDRAW to individually sketch out clasts. These prepared images were then further processed using ImageJ and JMicrovision, where it was possible to quantify pore-space from clasts. JMicrovision also allowed the measurement of clast dimensions.

1. Number of clasts
2. Size of clasts
3. Percentage of clasts to percentage of matrix
4. Orientation of clasts
5. Evidence of any bimodality of clasts

6. Identification of potential preferential flow pathways
7. Character of microfractures

5.9 Modified particle size distribution test

BS EN ISO 17892-4:2016 (BSI, 2016) is the British Standard for determining particle size distribution of a soil using sieving, sedimentation, or a combination of both. It was identified that the standard was not suitable for weathered chalk, owing to apparent cohesion when at NMC and its more brittle behaviour when completely dry, therefore the standard was modified to facilitate de-structured chalk grades.

5.9.1 Equipment

The equipment required for the test remains the same as the British Standard (Table 5-14);

Table 5-14 Equipment required for the PSD test.

Sieves 0.63 µm – 10 mm mesh size	Conical flask
Balance (+/- 0.01 g)	Water bottle with nozzle
Drying oven	Scoops or spatulas
Soft and stiff brushes	Large metal bowl
Sample containers	Workspace: equipped with adequate lighting, ventilation and water source

5.9.2 Sample Preparation

1. Measure the mass of the sample at NMC and container.
2. Place in drying oven for 12 hours to remove excess moisture.
3. Remove from oven and measure the dry sample and container. Calculate NMC
4. Disaggregate chalk sample – place in distilled water in a conical flask, allowing the chalk to collapse and disperse under gravity.
5. The sample immersed in water is then mixed in continuous suspension but not so vigorously that particles are lost or fractured

5.9.3 Sieving the sample and particle separation

1. Weigh and record the mass of each sieve and metal bowl when dry.
2. Place the sieves in ascending order over the metal bowl.
3. Pour the sample in suspension through the top sieve.
4. Use the water bottle with nozzle to disperse the material through to the next sieve.
5. Weigh the mass of the first sieve and retained chalk when wet.
6. Repeat until all samples are dispersed, with excess suspension of grains <63 µm has been collected in the metal bowl.
7. Weigh the mass of the bowl with chalk suspension

8. Place all sieves and bowl into the drying oven and dry sieves for 12 hours and the metal bowl until all moisture has been driven off.
9. Record the mass of soil retained on each sieve and metal bowl.
10. Plot a particle size distribution curve using the percentage of material retained on each sieve versus sieve mesh size.

5.9.4 Proposed classification workflow

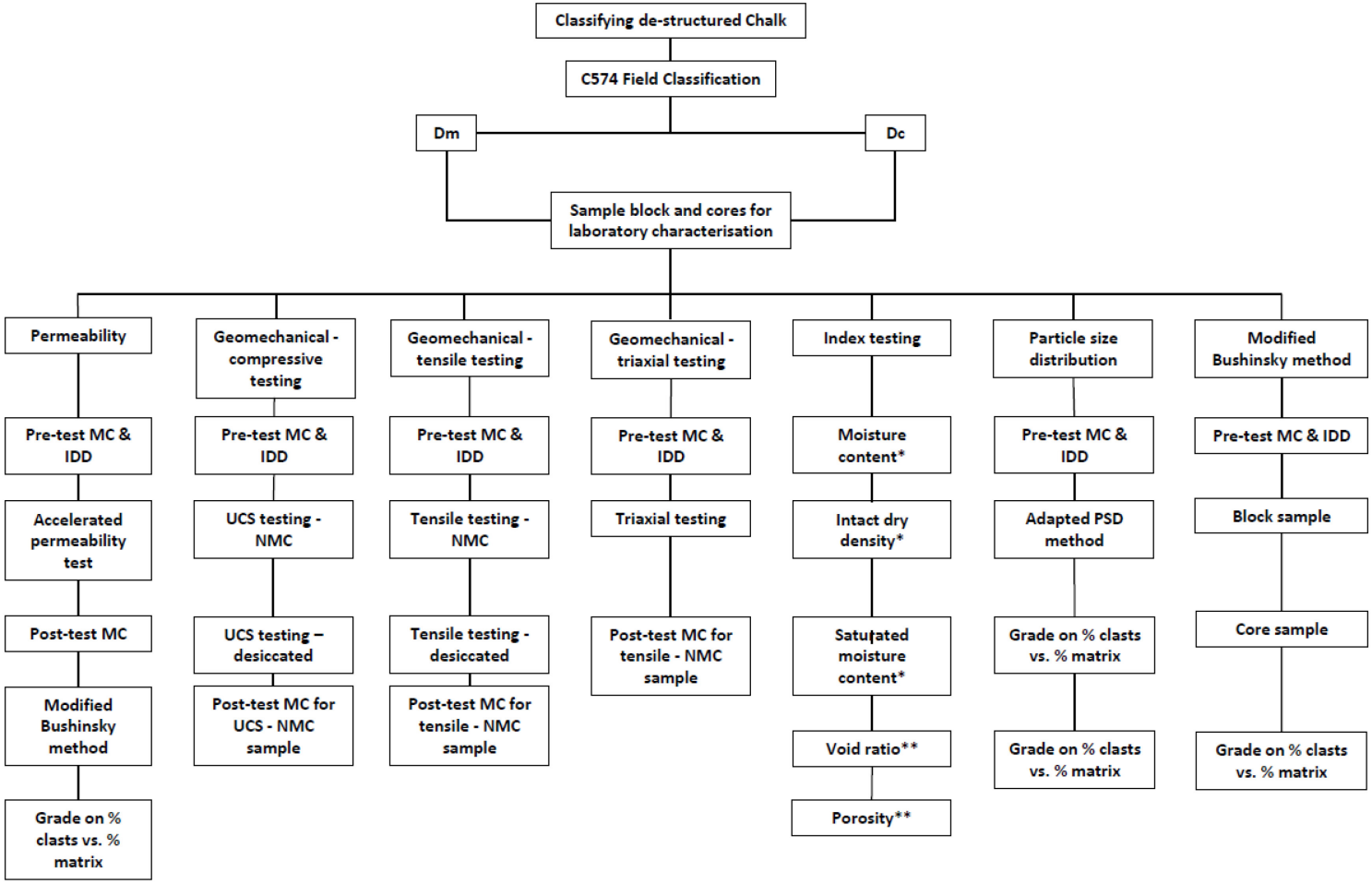


Figure 5-10 Proposed classification workflow for de-structured chalks (refined in future work section of Chapter 9)

5.10 Chapter summary

This chapter has detailed the laboratory methodologies used during the material testing component of this research project, stating the aims of laboratory testing, provenance of material tested, tests required and proposed a novel methodology to elucidate the internal structure of Dm and Dc grade chalk, providing a method for further quantification.

This chapter has also presented a workflow methodology of characterising weathered chalk, building on the CIRIA C574 chalk classification system, which will enable further constrained classification of Dm and Dc grade chalks.

Section 5.2 presented index testing methods to characterise chalk as a material, followed by section 5.3, which provided a method to assess durability. This method also allowed examination of the roles of water as a weakening agent. Permeability testing methods were presented in section 5.4, with geomechanical testing of Dm and Dc grade chalk were presented in section 5.5 (UCS), 5.6 (tensile testing) and 5.7 (triaxial testing).

Section 5.8 is a proposed update of the Bushinsky methodology, which uses physical experiments and image processing to quantify the internal structure of D-grade chalk. This Chapter concludes with Section 5.9 detailing a destructive method to measure particle size distribution of clasts within D-grade chalks.

6 Fieldwork observations

6.1 Introduction

This chapter summarises extensive field investigation at four research sites (detailed in Chapter 3), presenting results from geological observation and measured scanline data, and partially satisfies objectives 2, 3 4 and 5. The aim of the project is to further understand and characterise the development and distribution of weathered chalk (and subsequent various stages of weathering) in the Southern Province chalks of the UK Chalk Group. The objectives of fieldwork in this context were;

- Qualitatively assess existing methods of grading of weathered chalk through practice within the field and comparison with differing localities.
- Identify historic, contemporary and ongoing weathering processes and products.
- Develop a catalogue of images of weathering and weathering products to inform practitioners.
- Assign preliminary CIRIA grades.
- Quantify discontinuities by undertaking scanline surveys, bolstering the CIRIA C574 methodology.

Chapter 4 and 5 detailed the methodologies employed to investigate chalk weathering, while Chapter 3 detailed the sites selected for study. Selected research sites for case studies comprised Roedean access point, Portobello Outfall, Newhaven Harbour, and Birling Gap.

Weathering in chalk is graded using the CIRIA C574 methodology (described in Chapter 2) and comprises three aspects; a density measurement (or estimation, depending on method selected), measurement of fracture spacing and measurement of the degree of openness of the fracture aperture. This method does not fully address all diagnostic features of weathering in chalk, such as colour and textural changes, nor is the method adequate for describing weathering products, such as cryoturbation lobes or dry valleys, and therefore needs to be supported with field descriptions and observation. Chapter 4 details the field methodology, with results split into Chapter 6 – initial field observations using traditional CIRIA grading methods (i.e. Estwing hammer and 150 mm nail) and Chapter 7, a uniformity survey that employs the specialist instruments (i.e. Equotip Leeb and SilverSchmidt test hammer) described in Chapter 4 to measure the density aspect of the CIRIA grading system.

Geological observation results comprise CIRIA grading within the field and the quantification (where possible) of the weathering and weathering features encountered. Scan line and discontinuity surveys

comprise orientation data of large-scale faults and relatively smaller scale joints and fractures, to link their orientation and distribution with weathering features observed in the field.

This chapter advances knowledge in this area by providing a comprehensive catalogue of weathering and weathering products (summarised in Table 6-1), while providing high resolution photographic examples. This means that geotechnical engineers and geologists do not rely solely on text-based descriptions, thus reducing uncertainty in identifying weathering and associated products. Practitioners who would find this work useful include geotechnical engineers and geologists who are involved with logging, coastal engineers and coastal management specialists. In terms of approach taken, this chapter provides an example of an initial assessment of weathering, in such detail that has not been undertaken in any previously published studies.

6.1.1 Summary table of weathering observed at research locations.

Table 6-1 Weathering types and products encountered at each location.

Location	Formation	Type or trend of weathering	CIRIA grade	CIRIA density	Proposed mechanism	Physical indication
Roedean	Newhaven Chalk Formation	Cryoturbated involutions	Dm – Dc	Low to medium	Cyclic periglacial conditions	Discoloured (buff – light brown), fine grained, low to medium density, Dm – Dc grade involuted chalk, separated by medium density, Dc chalk
Roedean	Newhaven Chalk Formation	Decreasing weathering with section depth (i.e., cliff height)	Dm – Dc to A1-5	Variable	Reduction in tectonic stress at the top of the section, increased exposure to water and cyclic ground freezing	Increasing CIRIA grade (i.e., de-structured Dm and Dc grades at the top, moving to grades A 1- 5) with depth, indicating increasing rock competency
Roedean	Newhaven Chalk Formation	Cataclastic brecciation of chalk webs at proximity to faults	C3-5 to B3-5	Medium to high	Extensional and compressional movements within the chalk resulting in brecciation	Increased fracture frequency at proximity to faults, particularly where three or more discontinuities intersect
Roedean	Newhaven Chalk Formation	Artesian periglacial brecciation followed by contemporaneous slaking	C3-5 to B3-5	Variable but generally medium	Aquiclude horizons leading to artesian conditions in discrete beds. Historic and contemporary freeze-thaw leads to brecciation, with contemporary slaking	Highly brecciated beds with over and underlying material less weathered. After periods of intense rainfall followed by hot dry periods, significant slaking and loss of material is observed.
Portobello outfall	Culver and Newhaven Chalk Formation(s)	Weathered dry valley	Dm – Dc	Low to medium	Erosion and transport of chalk material (chalk clasts, cobbles, and putty, with disturbed nodular flints) to area of low topography, further water weakening and slaking of particulate material within dry valley leading to comminution.	Buff, de-structured putty chalks, which change colour when wet (from buff cream to a darker brown). Metastable soil that has significant movement when moisture content is increased.
Portobello outfall (east)	Culver Chalk Formation	Rubification and chemical weathering	C1-5 to B1-5	Low to medium	Percolation of iron rich minerals from overlying soils into underlying culver chalk, indicative of chemical-rich ground water and associated weakening	Rubification and oxidisation leads to iron staining of both chalk matrix and fractures, indicating water is the mechanism of transport.
Portobello outfall (east)	Newhaven Chalk Formation	Water weakening, haloclasty, chemical weathering and material loss driven by discontinuities	C1-5 to B1-5	Low to medium	As above, with cross-cutting discontinuities driving material loss within webs of high angled faults	Fresh angular material loss between faults observed, with heavily stained joints and rounding at the base of the cliff
Portobello outfall (east)	Overlying tertiary deposits and Culver Chalk Formation	Dissolution features and solifluction of weathered material	Not applicable	Not tested due to stratigraphic height	Dissolution of preferential flow pathways within the chalk and increased moisture content within puttified deposits leading to gravity driven solifluction.	Observable dissolution features infilled with overlying sediment and irregular soliflucted lobes leading to disturbed bedding features
Portobello outfall (west)	Newhaven Chalk Formation	Decreasing weathering with section depth (i.e., cliff height)	Dm-Dc C4 to B2	Variable	Reduction in tectonic stress at the top of the section, increased exposure to water and cyclic ground freezing	Increasing CIRIA grade (i.e., de-structured Dm and Dc grades at the top, moving to grades A 1- 5) with depth, indicating increasing rock competency
Portobello outfall (west)	Newhaven Chalk Formation	Small scale cryoturbation involutions	Dm – Dc to C5	Not tested due to stratigraphic height	Cyclic periglacial conditions	Discoloured Dm – Dc grade involuted chalk, separated by Dc chalk. Observably whiter in colour compared to Involutions observed at Roedean
Newhaven harbour	Culver Chalk Formation	Chemical weathering and reduction of density	Not applicable	Medium	Percolation of sulphate enriched water with provenance from overlying Woolwich Beds.	Yellowed chalk. Rounded surfaces and fractures.
Newhaven harbour	Culver Chalk Formation	Dissolution tubes	C5	Not tested	Percolation of sulphate enriched water with provenance from overlying Woolwich Beds causing dissolution of preferential flow pathways	Dissolution within the Tarrant Chalk, with dissolution tubes in continuity with the overlying Woolwich Beds and infilled with Upnor Formation material
Newhaven harbour	Culver Chalk Formation	Dissolution of sub-vertical and sub-horizontal discontinuities	C5	Not tested	Percolation of sulphate enriched water with provenance from overlying Woolwich Beds causing dissolution of preferential flow pathways	Dissolution within the Tarrant Chalk, with discontinuities in hydraulic conductivity with the overlying Woolwich Beds
Newhaven harbour	Culver Chalk Formation	Spatial weathering variation	Dm-Dc C1-5 to A1-5	Medium	Distribution of CIRIA weathering grades – De-structured grades observed where landslips are present with the grade improving away from slip surfaces	Landslips of overlying non-chalk Tertiary deposits, driven by discontinuities within the chalk, which have become increasingly weathered by overlying sulphate rich soils
Birling Gap	Seaford Chalk Formation	Extensive dry valley	Dm – Dc	Low to medium	Erosion and transport of chalk material (chalk clasts, cobbles, and putty, with disturbed nodular flints) to area of low topography, further water weakening and slaking of particulate material within dry valley leading to comminution. Significant material loss via wave action and meteoric activity (i.e., wet and dry periods)	Extensive dry valley with significant disturbance and solifluction within the valley itself. Flint nodules show gravity driven disturbance. De-structured chalks dominate, with primary grade of Dc. Weathering decreases away from valley axis and returns to C and B grade chalks at the flanks of the valley. Weathering also decreases with depth within the dry valley, although the valley base is not observed under the shore platform. Weathering is likely a combination of water weakening, haloclasty, wave action and meteorological action on an already puttified deposit.
Birling Gap	Seaford Chalk Formation	Discontinuity driven material loss	C1-5 to A1-5	Low to medium	Intensely spaced joint sets which are intersecting hosted by chalk, with weathering overprinting these primary structures and inducing weakness	Off-white chalk with significantly intense fracturing, leading to small scale blocky material loss.
Birling Gap	Seaford Chalk Formation	Dissolution features within the dry valley	Dm – Dc	Not measured	Dissolution of preferential flow pathways within the chalk and increased moisture content within puttified deposits leading to gravity driven solifluction.	Observable dissolution features infilled with overlying sediment and irregular soliflucted lobes leading to disturbed bedding features

6.2 Weathering characteristics

Observation of geology, weathering trends and weathering products was undertaken at each site. It is important that geological history, event history, younging relationships, and competing and concurrent weathering processes are taken into consideration as this is an important aspect of the weathering study, allowing identification of processes that may be occurring (or have previously occurred) in one study site, but are absent in others, producing significantly different styles of weathering. A reference table summarising weathering and physical indications is presented in Table 6-1.

Some observations can be linked to other data collected in this investigation phase, such as the influence of discontinuities on rock mass grading as well as the effect of chemically active overlying soils and the resulting karstic weathering from water percolation.

6.2.1 Roedean access point

Roedean access point provides access from the cliff-top at Roedean Café, to the undercliff walk at the cliff base (Figure 6-1). This ramp allows observation of the Newhaven Chalk Formation (including the Roedean Triple, Rottingdean Pair and Saltdean Marls, with the Santonian – Campanian boundary at the base) from the top of the cliff to the base (Mortimore, 2021).

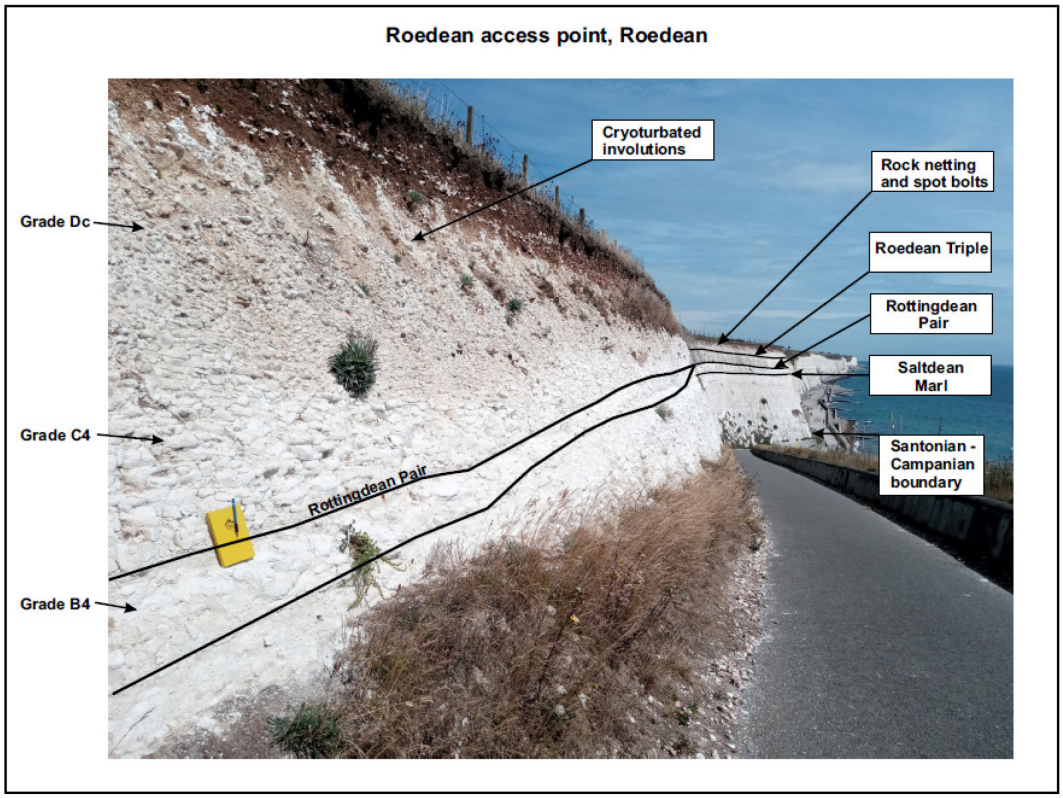


Figure 6-1 Roedean Access Point.

At the cliff-top section, there are soil deposits (figure 6-1), approximately 0.75 m thick, comprising orange-brown to brown, silty clay with calcareous clasts as well as flint clasts hosted in horizons. A detailed description of the soil is presented in Table 6-2;

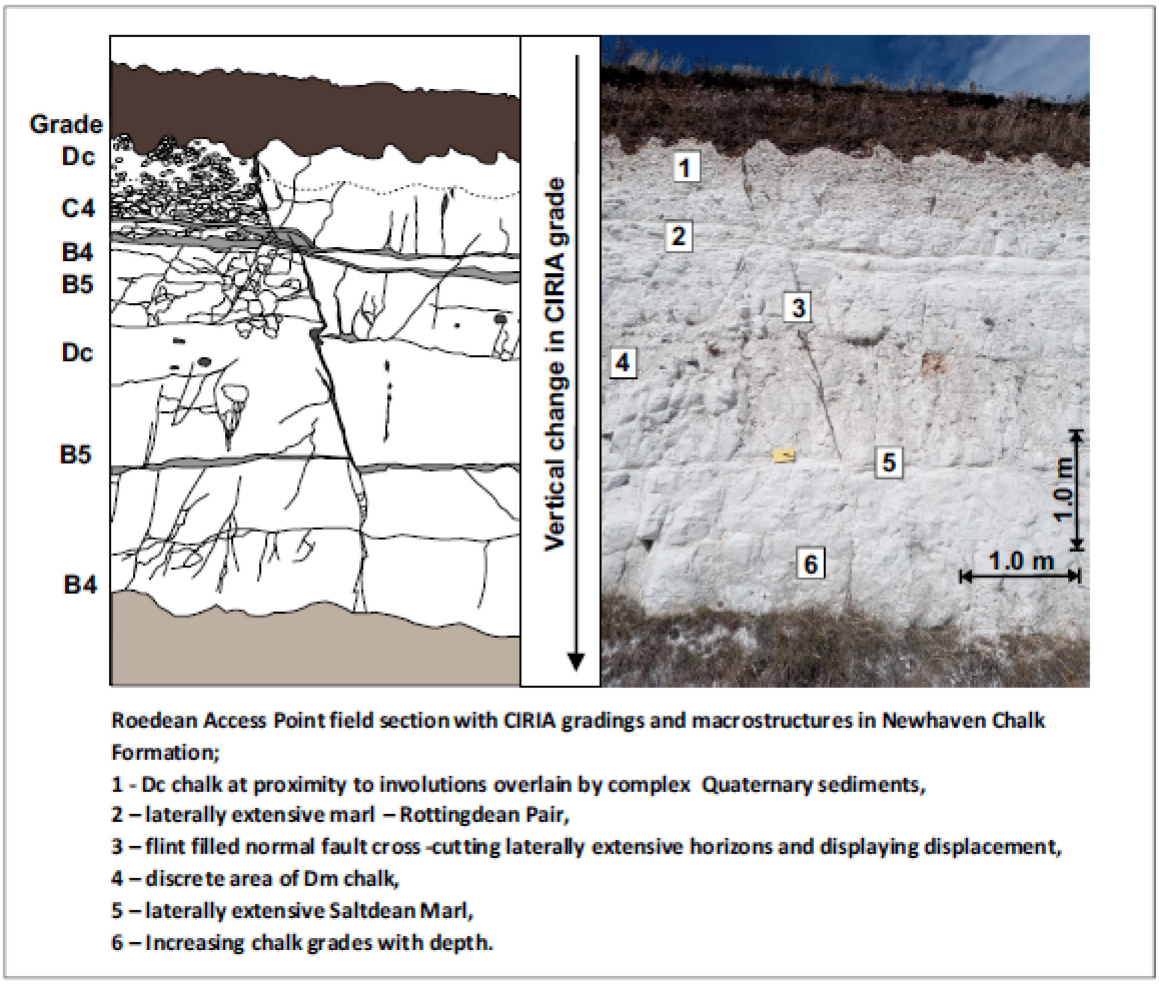
Table 6-2 Soil description, Roedean.

Depth (mbgl)	Description
0.0 – 0.10	Brown, firm silty CLAY; with a fine layer of angular to sub angular chalk clasts <10 mm. Cryoturbation lobes present, comprising soil-chalk disturbed ground.
0.10 – 0.30	Orange-brown, firm silty CLAY, <30% angular flint clasts, 10 – 40 mm.
0.30 – 0.55	Orange-brown firm silty CLAY, absence of clasts.
0.55 – 0.75	Horizon of angular to sub-angular, patinated chalk clasts, 80 – 90%, 10 – 50 mm diameter.
0.75	Weathered CHALK, white where less weathered, orange-white within lobes; irregular contact with underlying cryoturbated lobes. NEWHAVEN CHALK FORMATION.

The contact between the soil deposits and underlying chalk is observed to be undulating and irregular due to disturbed involution, with involuted material comprising a soil-chalk mixture. These involutions are lobe-like in morphology and are laterally extensive, occurring along the cliff line (Figure 6-2).

The underlying chalk at this location is the Newhaven Chalk Formation, observed as medium density, fine grained chalk, which is grey-white to brilliant white in colour. The stratigraphy of this site comprises the Old Nore beds at the base of the cliff (representing the Santonian-Campanian boundary), moving up into the Peacehaven beds. Markers at this location include the Saltdean Marl, Rottingdean Pair Marls and the Roedean Triple Marl (Mortimore, 2021) (Figure 6-1).

Several types of weathering (and weathering products) are present at Roedean (Table 6-1). From the CIRIA weathering classification scheme, it is possible to observe that the CIRIA grade of this lithology improves with cliff depth. Figure 6-2 shows the change in weathering grades. Starting as de-structured, Dm and Dc grade chalk at the top of the cliff, brecciation and fracture intensity reduces over approximately 0.6 m depth, with the Rottingdean Pair acting as a break between de-structured chalk and competent structured chalk. As depth increases, fracture spacings of grades 1 – 5 are observed, but generally increasing from grade 5 (intensely spaced) to grade 1 (widely spaced) with depth, although this improvement is not uniform due to individual beds having undergone discrete weathering (such as the bed stratigraphically above the Saltdean Marl). Similarly, the fracture aperture grading increases with depth (grades C to A; from open to closed fractures), but again the improvement is not uniform. The general trend, however, is that fractures observed are becoming tighter with depth.



Roedean Access Point field section with CIRIA gradings and macrostructures in Newhaven Chalk Formation;
1 - Dc chalk at proximity to involutions overlain by complex Quaternary sediments,
2 – laterally extensive marl – Rottingdean Pair,
3 – flint filled normal fault cross -cutting laterally extensive horizons and displaying displacement,
4 – discrete area of Dm chalk,
5 – laterally extensive Saltdean Marl,
6 – Increasing chalk grades with depth.

Figure 6-2 Variability of weathering grade; Roedean access point (increasing grade with stratigraphic depth).

The first type of discrete weathering encountered at this site (at the top of the cliff) is cryoturbation lobes and involutions, linked to periglacial processes (Figure 6-3). Cyclic ground freezing and thawing has resulted in brecciation and disturbance of the underlying chalk and overlying superficial deposits in distinct, bulb-shaped lobes. The distribution of these lobes appear to be laterally extensive and can be observed extending east in the cliff line for hundreds of metres. The thickness of this horizon and dimensions of the lobes varies along the cliff section. The lobes themselves are infilled with Dm grade chalk, or soils with a high chalk content, while the competent chalk material which separates them are graded as Dc grade.

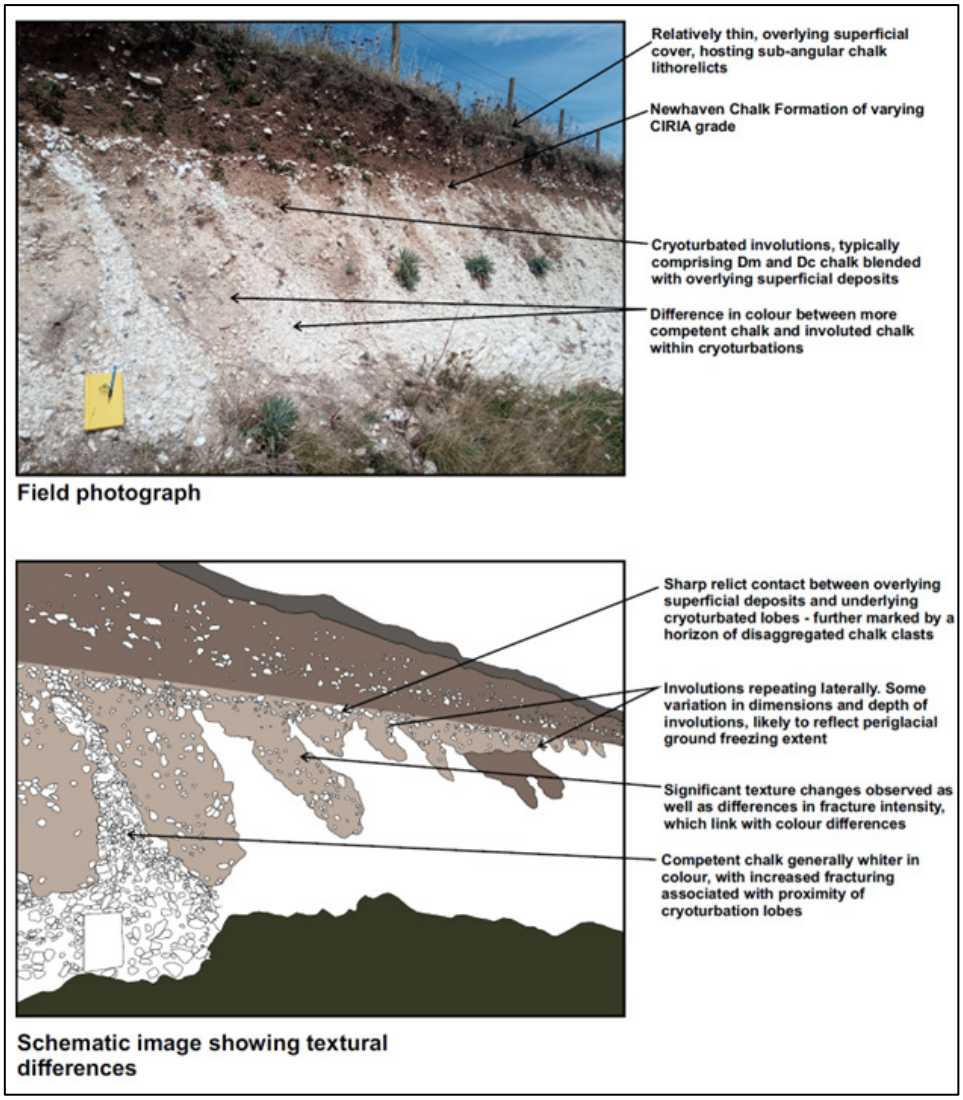


Figure 6-3 Roedean access point; cryoturbated involutions and changes in chalk textures.

Below the cryoturbation lobes, the chalk grade increases from Dc chalks to structured chalk with a C574 discontinuity spacing of grade 5 - 4. In terms of aperture, the grades here are C to B, with a distinct absence of competent A grade chalk. When struck with a used hammer pick, the chalk is estimated as high density, and while the fracture intensity is relatively high, the chalk appears more structured and less brecciated. The presence of cryoturbated lobes and intensely fractured chalk in the upper section of the cliff has resulted in the requirement for coastal and rock fall protection, with discrete rock bolting and rock netting where required. This indicates the extent of the distribution of this poorly structured chalk and the lower stability of this rock mass, associated with weathered rock.

There is evidence of discrete weathering in laterally extensive horizons within the cliff face, whereby low permeability horizons (such as marls or flint bands) are overlain by horizons of intensely brecciated chalk are observed (Figure 6-4). It is likely that these discrete weathering horizons are the

result of perched water tables, whereby the underlying low permeability horizon acts as an aquiclude, effectively trapping water in the chalk unit stratigraphically above.

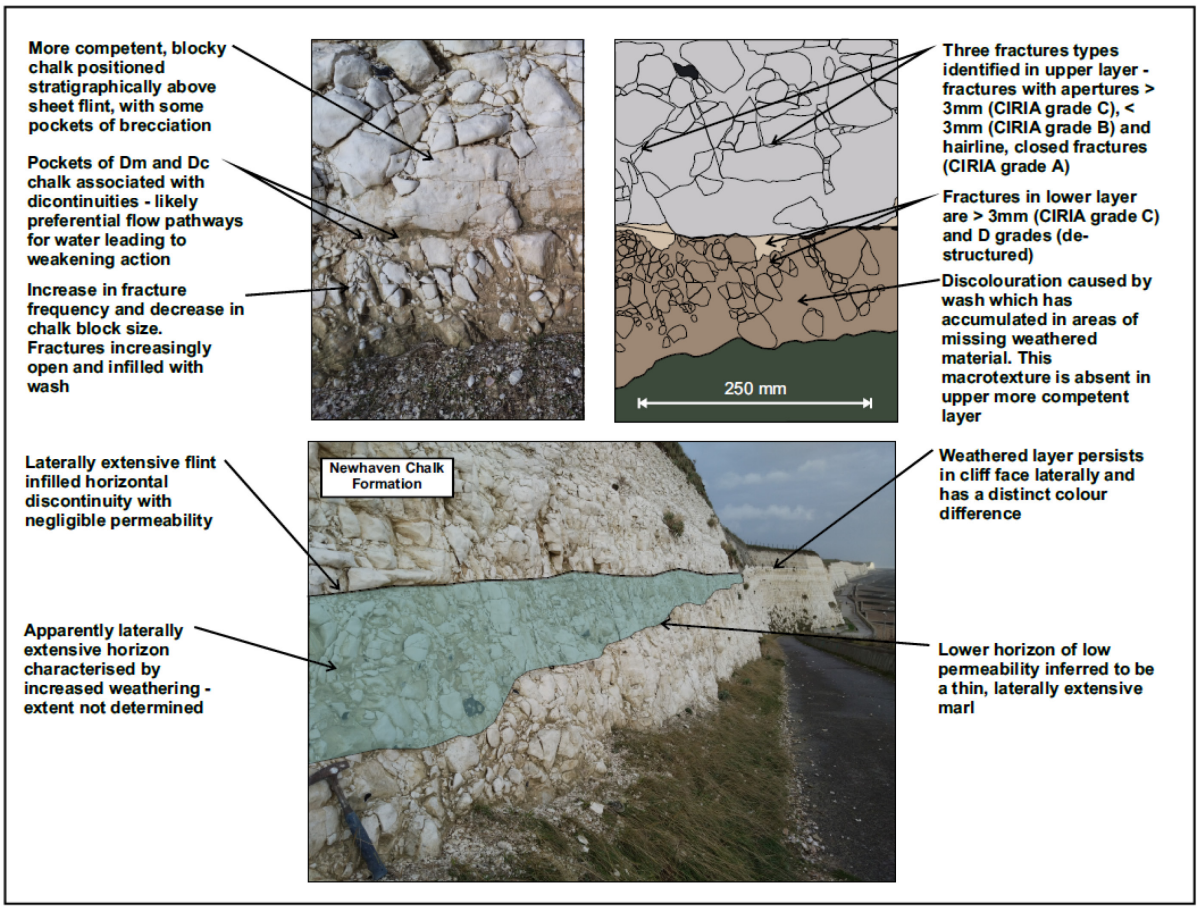


Figure 6-4 aquiclude layers at Roedean, resulting in discrete laterally extensive weathering of beds.

Cyclic freeze-thaw events during the Devensian (Mortimore, 1997) and contemporaneous freeze-thaw events are likely to have caused brecciation within this layer. Rainfall and drying events further accelerates this weathering, where freshly slaked material (clasts <120 mm diameter) from this layer are shed from the cliff face after periods of heavy rainfall and subsequent drying (Figure 6-5).

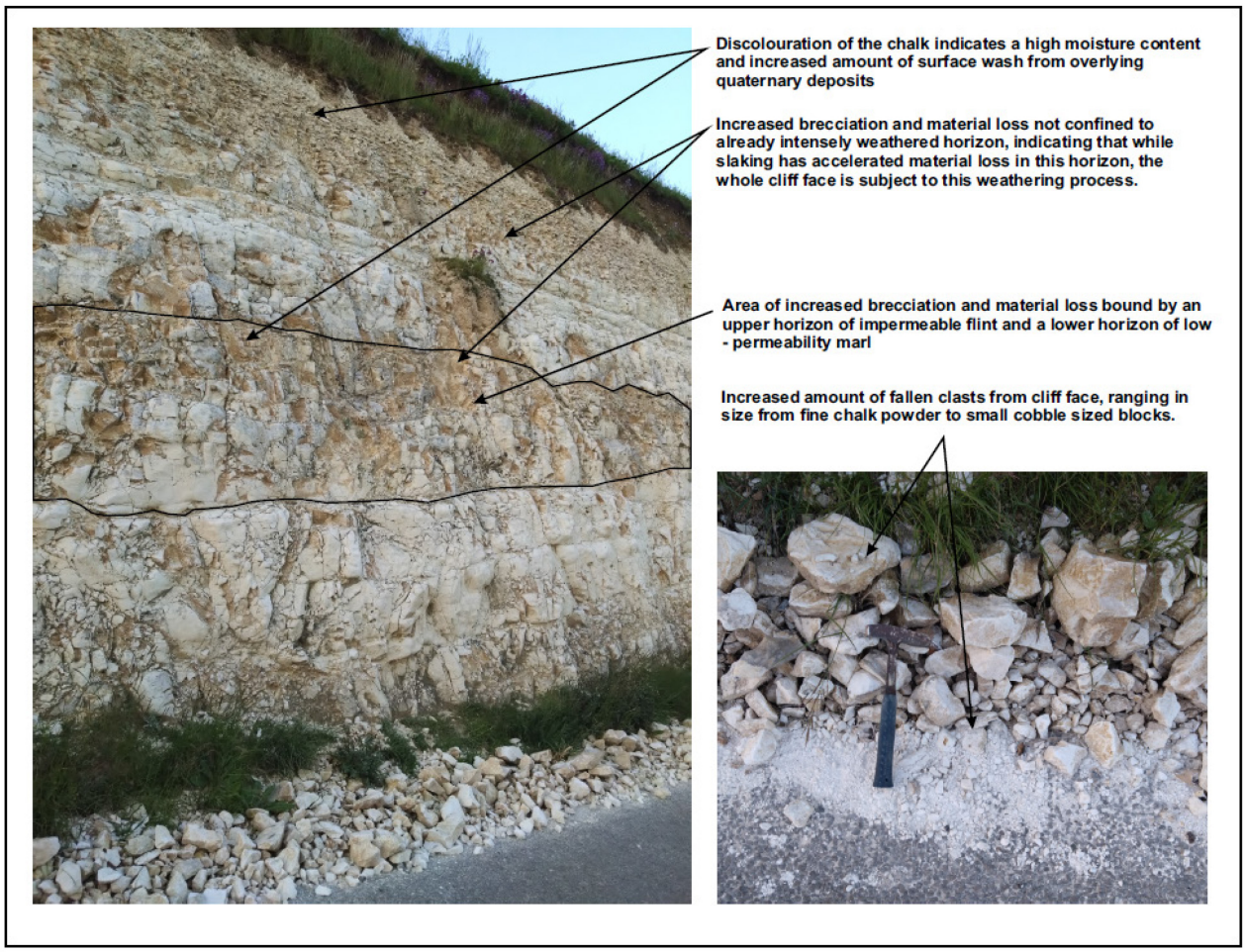


Figure 6-5 Further slaking and material shedding of previously cryoturbated material, Roedean.

Increased weathering is observed close to faults (Figure 6-6). Where large scale faults are conjugate, or discontinuities are closely spaced and parallel, there is more intense brecciation observed, although brecciation is associated with any significant slip. This indicates cataclastic processes, whereby mechanical degradation and fracturing of the chalk has been caused by movement of the fault. It is likely that this weathering is facilitated by the faults and discontinuities acting as preferential flow pathways for water, giving rise to water weakening and dissolution, with smaller clasts leading to an increased surface area for which dissolution processes to act upon.

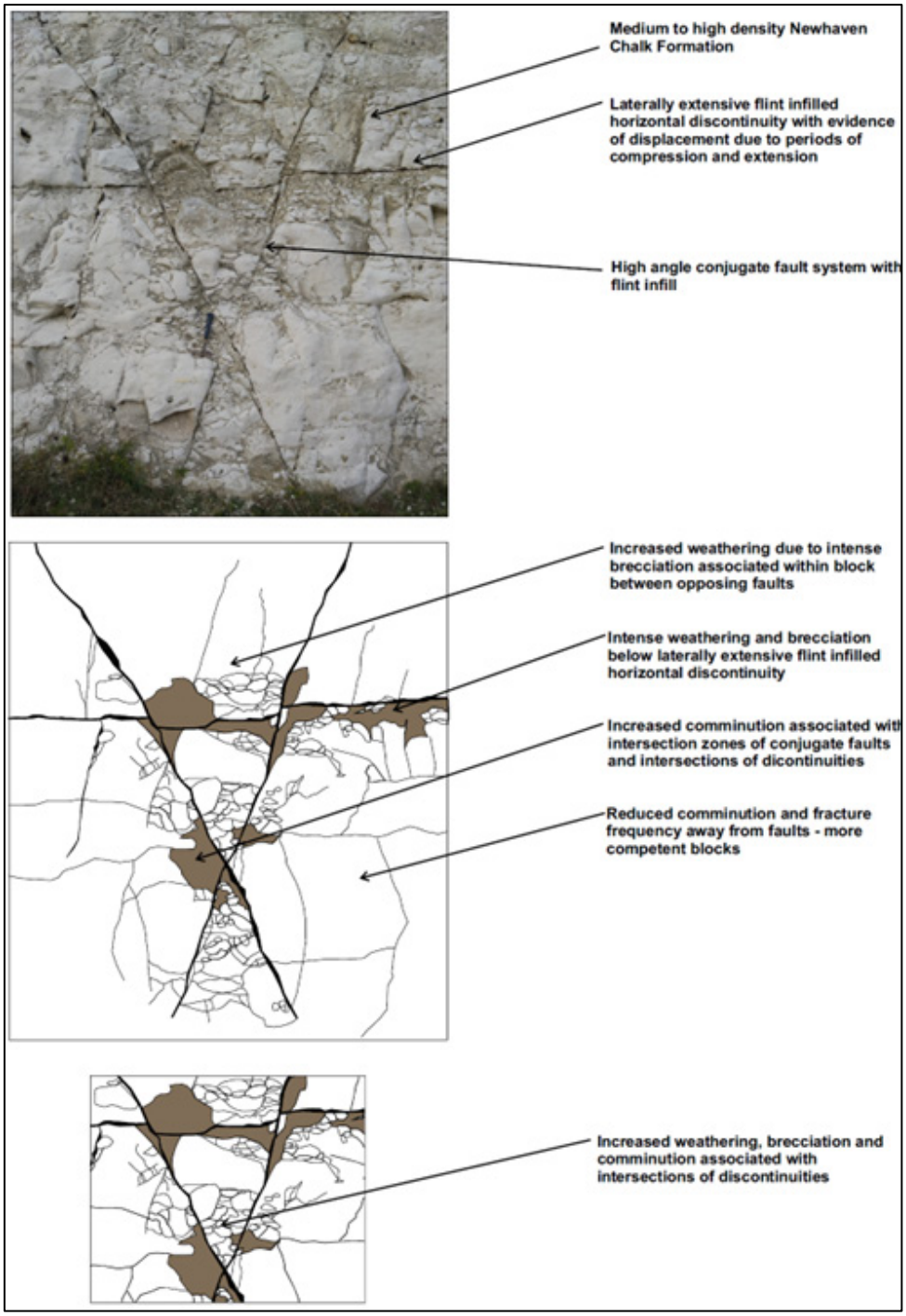


Figure 6-6 Discrete weathering at proximity to the web of three intersecting discontinuities.

At the Roedean research site, it is possible to observe cross-cutting and over-printing relationships between geological features and weathering. This allows some constraint of relative ages of the events which have occurred at this location and can be used to identify which weathering processes occurred relative to each other.

Younging relationships

In terms of geological events at Roedean, a basic history using the law of superposition can be described as deposition and lithification of bed A1, then deposition and lithification of the Saltdean Marl, A2, followed by the deposition and lithification of A3 chalk bed, then the deposition and lithification of the Rottingdean Pair (A4), finally the deposit of the overlying chalk bed; A5 (Figure 6-7 and Table 6-3).

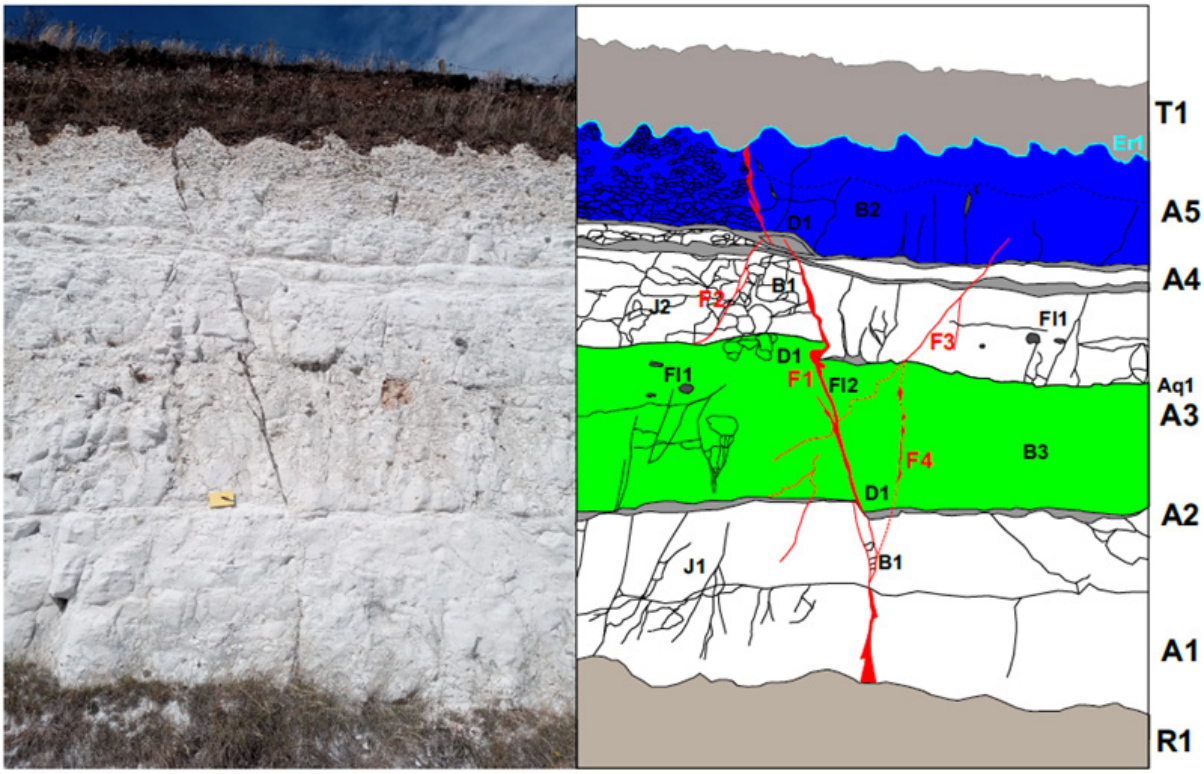


Figure 6-7 Younging relationships, Roedean.

Cross-cutting relationships further constrain the history. Nodular flints (denoted as Fl1) overprint bed A3, demonstrating that Fl1 are younger than bed A3 (and subsequently beds A1 and A2). A3 must have been subject to anoxic conditions enabling the formation of flint, conditions that could have arisen through deep burial and compaction or increased sea-level. The likelihood is that these flints formed when the sediment was still soft, while undergoing lithification.

F1 denotes a relatively large-scale fault, which cross-cuts all chalk and marl units, but terminates before the overlying superficial deposits (denoted T1). The fault is infilled with flint (Fl2), showing that the Fl2 is younger than F1 and that the fault was open, or sediment still unlithified, during a period of burial or anoxia, indicating an extensional tectonic regime. The deformation of this fault and conchoidal fracture of the in-filled sheet flint (denoted D1) indicates inversion of tectonics, leading to a compressional regime and the development of reverse faults. Areas of brecciation, denoted as B1,

overprint chalk units as well as J1 and J2. This is inferred as tectonic movement causing brecciation, which is later exploited by water.

At the top of the sequence, chalk bed unit A5 is cross-cut by an undulating erosive surface (denoted as Er1), which is infilled by Tertiary material. Below, cryoturbated involutions and brecciation (denoted B2) are observed, reducing with depth and terminating at A4. This brecciation also overprints F1 and J1 in chalk bed unit A5, indicating that this occurred after the formation of F1, infill of F1 by Fl2 and the joints of J1.

Brecciation (denoted B3) observed in the lower half of chalk bed unit A3 is observed. B3 overprints F1, Fl1, Fl2 and F4, but terminates at Saltdean Marl (A2) below, and above at an aquiclude horizon (Aq1). This discrete brecciation has no relationship with features above the aquiclude horizon (Aq1) above, or below the Saltdean Marl (A2). At the base of the cliff, there is a deposit of Rendzina, which is the youngest deposit of all observed. This deposit is considered a weathering product as it comprises transported material eroded from the cliff face.

Table 6-3 Geological history, Roedean.

Feature	Denotation	Process	Mechanism
Rendzina formation	R1	Landslip/hill wash	Exsitu hill wash/landslip material.
Brecciation	B3	Discrete brecciation	Observed in the lower half of chalk bed unit A3. B3 overprints F1, Fl1, Fl2 and F4, but terminates at Saltdean Marl (A2) below, and above at an aquiclude horizon (Aq1). This discrete brecciation has no relationship with features above the aquiclude horizon (Aq1) above, or below the Saltdean Marl (A2).
Brecciation	B2	Periglacial processes	Cryoturbated involutions with a typical lobe-like morphology and brecciation reducing in frequency with depth. Overprints F1 and J1 in chalk bed unit A5.
Erosion	Er1	Erosion	Erosion surface subject to periglacial processes, resulting in undulation, overlying intense brecciation (B2).
Joint formation	J1	Sedimento-tectonic jointing	Penecontemporaneous with D1 as well as the formation of J1 and J2.
Joint formation	J2	Sedimento-tectonic jointing	Penecontemporaneous with D1 as well as the formation of J1 and J2.
Brecciation	B1	Brecciation in web of fault	Penecontemporaneous with D1 as well as the formation of J1 and J2.
Deformation of fault conchoidal fracture of infilled flint	D1	Tectonic inversion from extensional to compressional regime	Penecontemporaneous with B1 as well as the formation of J1 and J2.
Fault infill with flint	Fl2	Formation	Fault infill Penecontemporaneous with fault formation.
Main fault – likely to be extensional	F1	Formation	Fault terminates at T1, indicating T1 younger than F1 and Fl2.
Nodular flints	Fl1	Deposition and lithification	Stratigraphic position(s).
Chalk beds	A1 – A5	Deposition and lithification	Stratigraphic position(s).

CIRIA weathering grades

Measurement and analysis of weathering in the upper part of the section, focussed on the cryoturbated involutions, shows that the infill within the cryoturbated involutions is Dm to Dc grades, separated by more competent but highly fractured chalk (Figure 6-8).

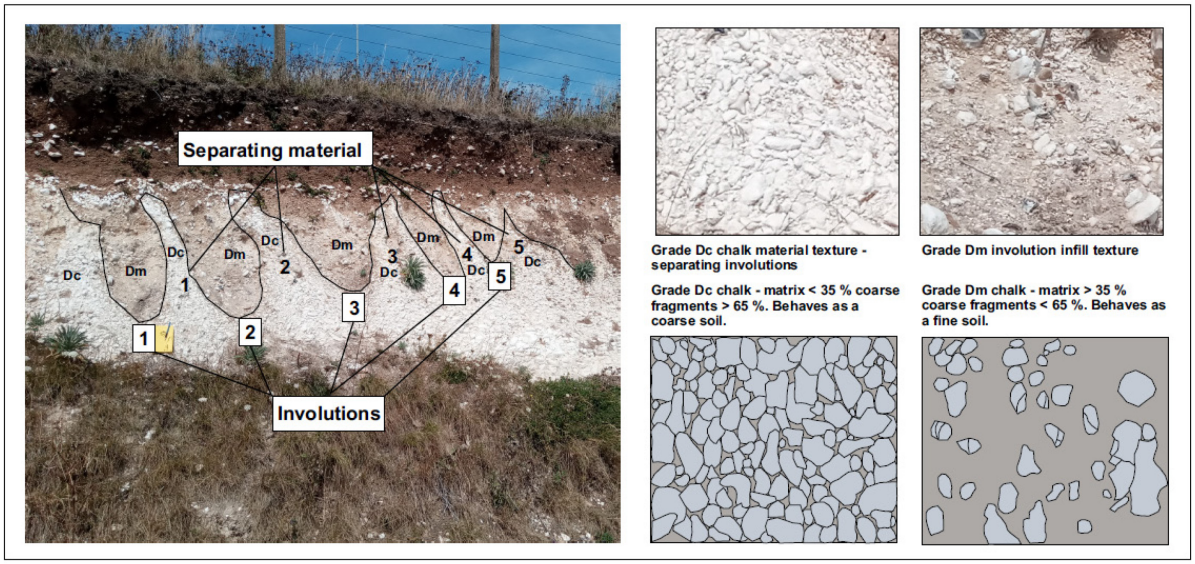


Figure 6-8 Application of CIRIA grading to cryoturbated lobes; Roedean.

Of the many cryoturbated involutions observable in the cliff, five representative cryoturbated lobes were selected for their accessibility to the features themselves. The five cryoturbated lobes are separated by five areas of chalk material, with measurement of dimensions, depth of hammer penetration and assignment of a CIRIA grade of both the lobes and intervening chalk material. Involution lobes were graded as Dm and their density was graded as low, with average penetration ranging 20 – 38 mm between the involutions. The intervening material was graded as medium density Dm, with average penetration ranging from 10 – 32 mm across the sample points (Figure 6-8).

Further CIRIA density sampling was undertaken to quantify weathering. Sampling started 2.0 m below the observed cryoturbated involutions, and moved down the access ramp at this location, where the chalk was not subject to intense fracturing due to this type of periglacial weathering. A total of 72 hammer penetrations were undertaken, with 12 tests per sample position. Hammer penetration ranged 3 – 24 mm, resulting in high CIRIA density grades. Each sample point was spaced at 5.0 m intervals moving down slope, with mean hammer penetration ranging 17 mm at the uppermost part of the slope, reducing to 8.0 mm at the lower sample point, corresponding to a high-density CIRIA grade. Average fracture spacing remains within the range of 20 – 60 mm across all sampling points, while fracture aperture is greater than 3 mm for the first four sample points, before reducing to less than 3 mm at the fourth sample point before becoming closed at the final sample point. This results in CIRIA discontinuity grade of C4 to B4. This trend reflects a reduction of weathering and an increase in rock competency with depth, as expected in an area subject to periglacial weathering, where ground freezing is the greatest at the ground surface and diminishes with depth (Table 6-1).

6.2.2 Portobello Outfall, Peacehaven

Portobello Outfall, Peacehaven was selected as a research site due to the presence of an accessible dry valley (through which a footpath has been incised), access to unprotected, competent Newhaven Chalk to the west of the outfall, and extensive unprotected, weathered deposits of Telscombe Cliffs to the east of the outfall, where Newhaven Chalk is overlain by Culver Chalk (Mortimore, 2021). Three localities were studied; a scanline to the east and west respectively, and the valley sides located at the access point (Figure 6-9).

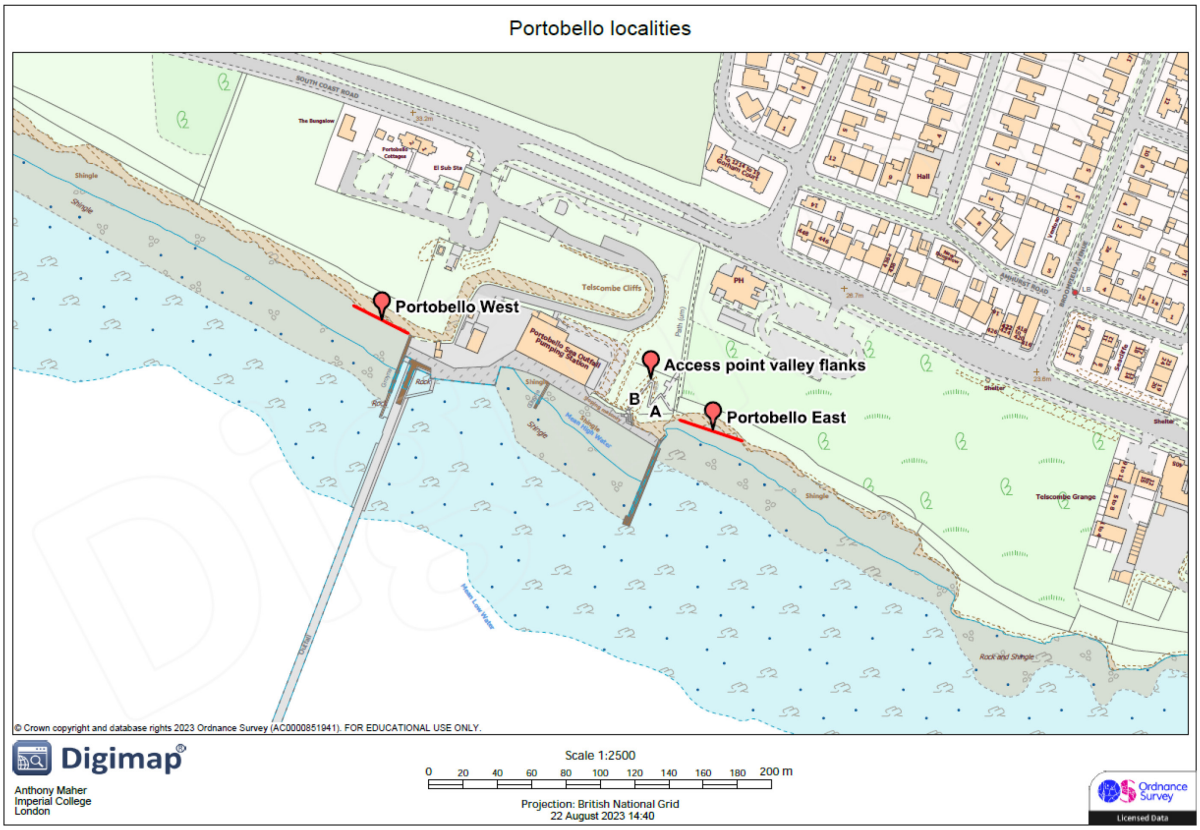


Figure 6-9 Map displaying areas of study at Portobello Outfall, Telscombe Cliffs.

A dry valley to the east of the outfall comprises complex Quaternary sediments (Table 6-4), overlying structured chalk, with evidence of rubification.

Table 6-4 Soil description, Portobello Outfall, Telscombe Cliffs.

Depth (m)	Description
0.0 – 0.25	Orange-brown silty CLAY.
0.25 – 0.40	Orange-brown silty CLAY with sub-angular flint clasts, 10%, 10 – 40 mm.
0.4 – 0.65	Orange-brown SILT; fine grained, firm silt with sub-angular flint and calcareous clasts 10 – 50 mm.
0.65 – 0.70	Orange-brown SILT; fine, firm silt with sub-angular flint and calcareous clasts, 40%, 10 – 50 mm.
0.70 – 1.0	Orange-brown SILT; fine, firm silt with sub-angular flint clasts, 10%, 10 – 50 mm.
1.0 – 2.5	Brown SILT wit 60% angular flint clasts 10 – 120 mm and 20% subangular calcareous clasts, 10 – 30 mm.
2.50	Reddish-white, weathered, de-structured CHALK, contact is undulating due to dissolution and ground disturbance. CULVER CHALK FORMATION.

At this location, the Newhaven Chalk is overlain by a <3 m thick section of Culver Chalk. Both the Culver and Newhaven Chalks are heavily discoloured, with fractures in the Newhaven Chalk-stained orange by the overlying Loess deposit. This is indicative of the presence of iron within the ground water at this location, with staining occurring in both the matrix via diffusive flow (resulting in overall orange discolouration), and focused discolouration at proximity to discontinuities, which have acted as preferential flow pathways (Figure 6-10).

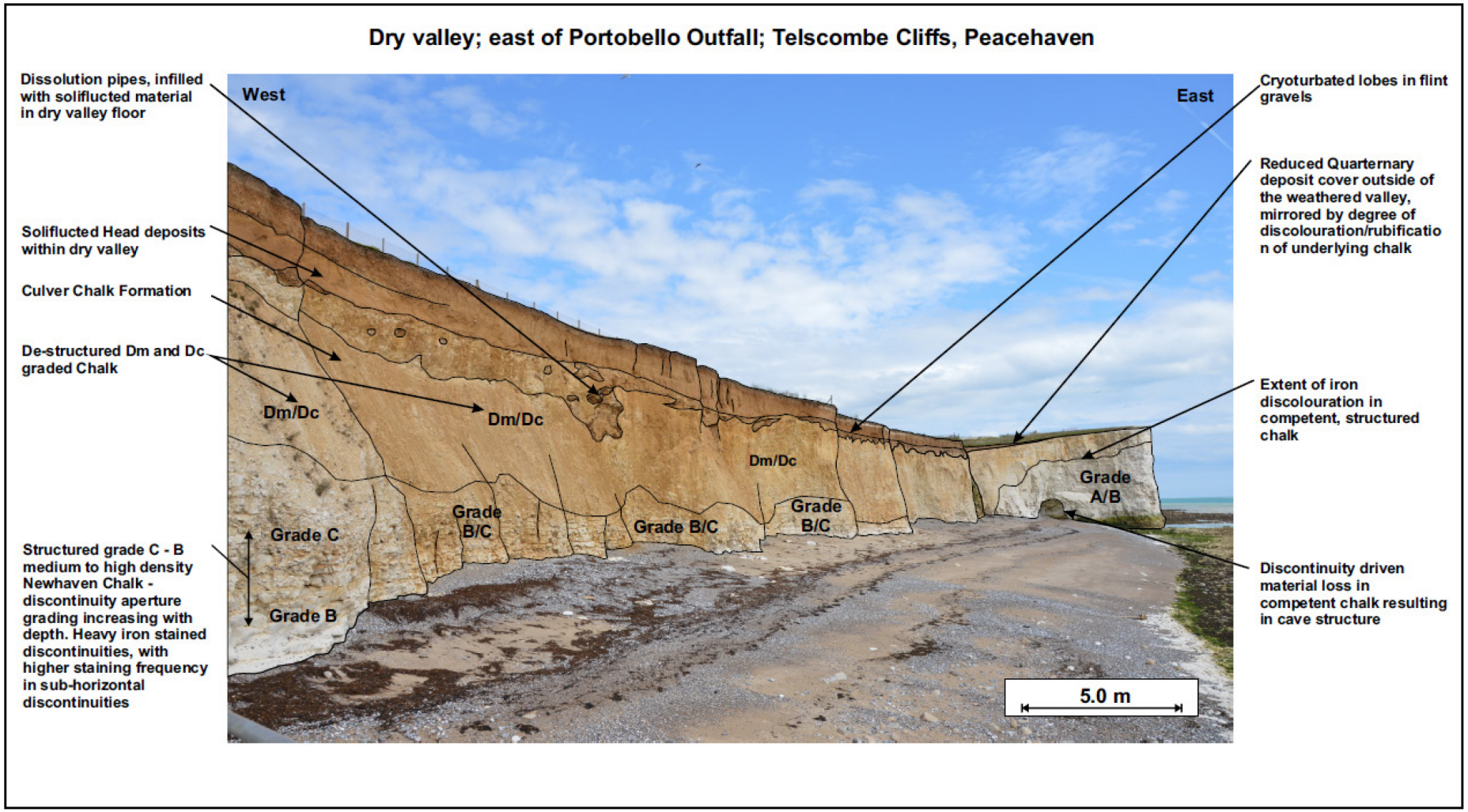


Figure 6-10 Telscombe Cliffs – Portobello Bay; distribution of de-structured and structured chalk grades.

There is significant weathering observed east of Portobello Outfall, with several types of weathering identified within different formations. A weathered valley with de-structured chalk (grades Dm and Dc) in the overlying Culver Chalk Formation contains valley-fill deposits and significant dissolution features. These dissolution features are infilled with soliflucted overlying Quaternary sediments, with lobe-like geometries reflective of mass movement and disturbance within the sediment.

The underlying Newhaven Chalk Formation is characterised by structured grade C chalk, overlying grade B chalk, and has primary inclined conjugate faults, crosscut by sub-horizontal discontinuities. These cross-cutting discontinuities have led to the discontinuity-controlled weathering whereby chalk material in the webs of the conjugate faulting has been lost. It is estimated from observation that, Approximate 1.25 m^3 of chalk loss was observed from conjugate fault 1 (Figure 6-11) between 2019 and 2021.

The brecciation observed between conjugate faults (Figure 6-11 A) is likely to be the product of jointing due to extensional and compressive regimes of tectonics inducing shear within the graben between these faults. The central graben between the two conjugate faults is highly fractured (Figure 6-11 B and Figure 6-11 C). The high angle of each conjugate fault indicate that they were formed during an extensional regime. The orientation of the joints indicates that there are two or more generations of discontinuities, with at least one attributed to a compressional regime – this is supported by the literature in that during the Mesozoic to mid-Cretaceous (syn-rift phase), the regime was initially extensional. By the mid-Cretaceous (beginning post-rift phase), basinal inversion had initiated and the regime was compressional (Mortimore, 2021). These generations of joints, with other discontinuities, such as bedding planes, intersect resulting in the formation of blocks. While this itself is not considered weathering, the brecciated nature of the chalk mass gives rise to vulnerability to water weakening processes and, in a coastal environment, to sub-aerial and coastal weathering processes.

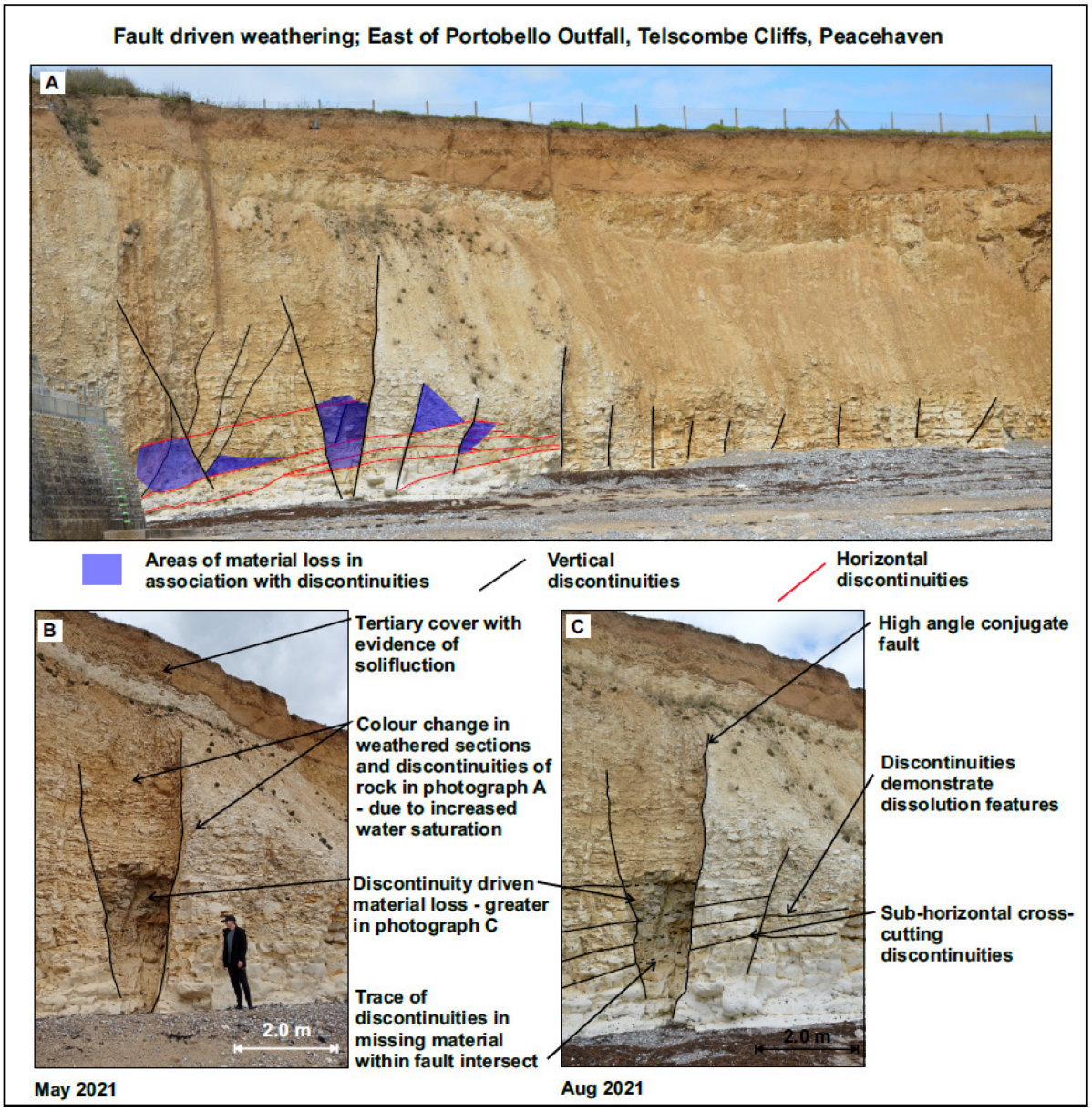


Figure 6-11 Discontinuity driven weathering observed at Portobello Bay, with A showing the distribution of faults and B and C showing blocky material loss.

The geology to the west of Portobello pumping station comprises the Newhaven Chalk Formation, which appears more competent than the chalk observed to the east of the pumping station. The chalk is grey to brilliant-white in colour, is characterised by high angled, high persistence conjugate faults and cross-cut by horizontal discontinuities, in some cases infilled with flint.

When tested using a used hammer pick, this chalk is medium to high density. The CIRIA grading varies spatially, with the grade decreasing with cliff height – predominantly grades A to C in the main cliff section, with grades Dc and some Dm chalks observed in the upper 1.0 - 1.5 m of the cliff face. These de-structured grades are overlain by a thin veneer of Quaternary deposits that exhibit cryoturbation lobes (comparatively smaller in scale than Roedean) (Figure 6-12).

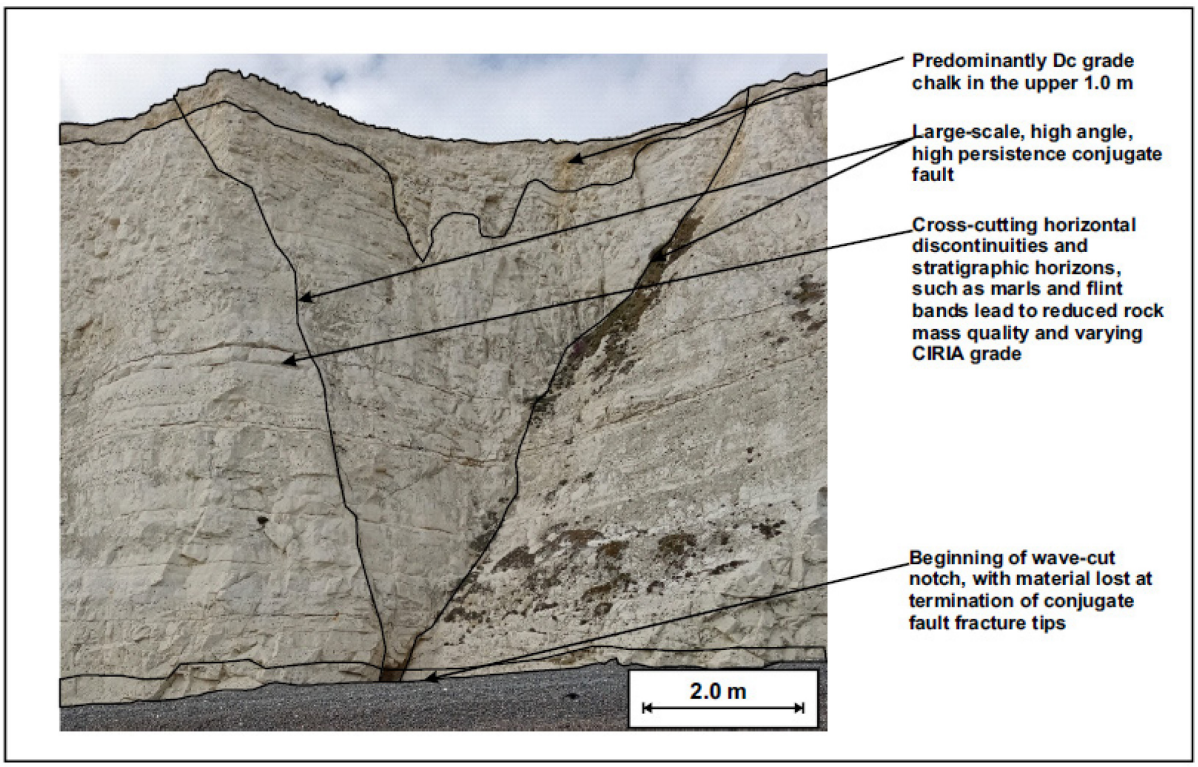


Figure 6-12 Newhaven Chalk Formation observed to the west of Portobello Outfall.

Discontinuity-driven material loss at this location is apparent from blocks lost from the cliff-face due to intersecting discontinuities. Rounded boulders on the beach platform indicate that the scale of the material loss (i.e., block size) in this location is greater than that observed east of Portobello outfall, and is attributed to both discrete, individual block loss and larger scale cliff collapse. At the cliff-base, a wave-cut notch is observed, where the chalk is incised into the cliff with rounded surfaces (in contrast to the angular character above), indicating weathering via discontinuity interaction with salt-water weakening and hydraulic wave action.

Weathered chalk and dry valley deposits are observed in the slopes that flank the access path to Portobello outfall. Down-sequence, the weathered chalk grades here are low to medium density, Dm and Dc, with Dc grade frequency increasing with depth. Within the de-structured matrix, larger clasts and disturbed flints are observed. In some instances, these clasts and flints are fractured, remaining in place with matching sides. During excessive rainfall periods, it is possible to observe transport and material loss of these de-structured chalks (Figure 6-13). This would indicate that these deposits are metastable and continually losing material via dissolution and entrainment of chalk rock flour in water, which has implications for the stability and longevity of dry valleys.

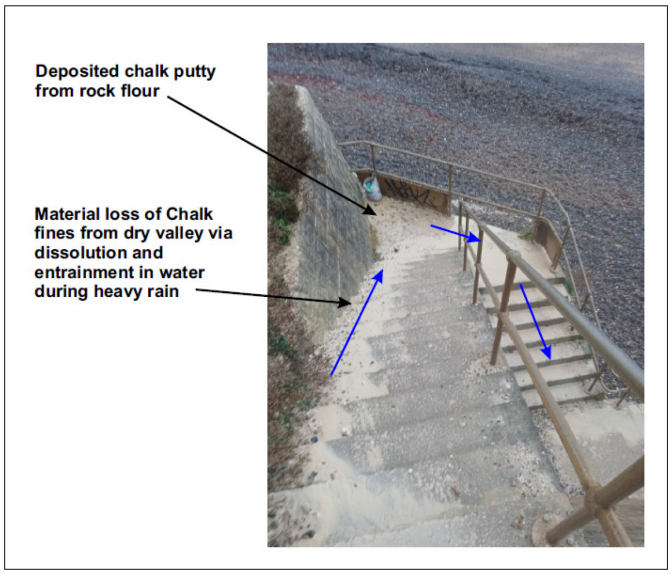


Figure 6-13 Material loss from weathered dry valley during intense precipitation.

The implication of this material loss is significant as it demonstrates de-structured weathered chalk is lost in water entrainment, which does not occur in unweathered, competent chalks on this scale.

Younging relationships

At Portobello (Figure 6-14 and Table 6-5), stratigraphic relationships show that the Newhaven Chalk formation (NC1), Telscombe Cliff Marl (TcM1) and Culver Chalk Formation were deposited and lithified in sequence.

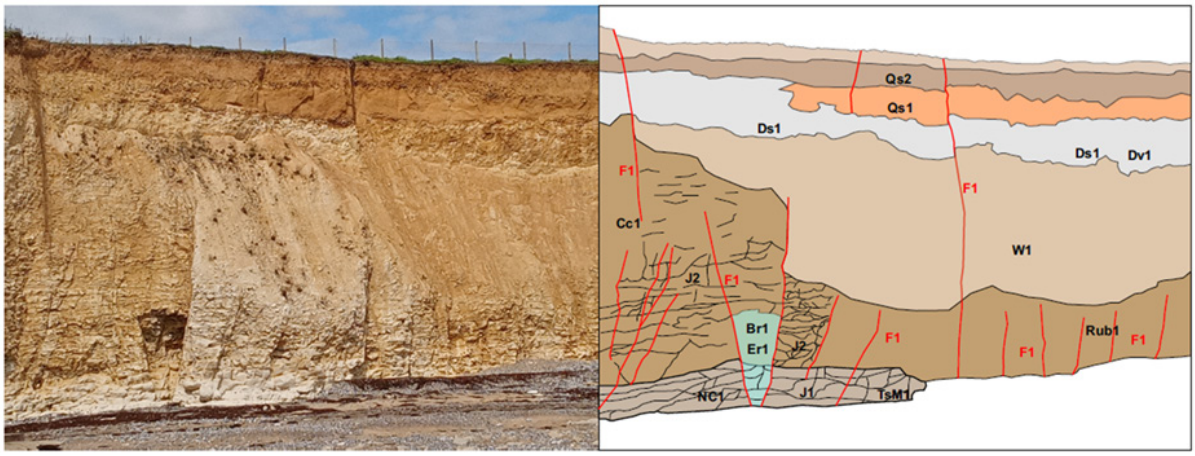


Figure 6-14 Younging relationships, Portobello.

Faulting (F1) cross-cuts each deposit. The faults are high-angled and small-scale, dipping west indicative of an extensional regime, resulting in small-scale half-graben structures, the development of accommodation space, and in this case, resulting in the formation of a shallow dry valley (Dv1). Penecontemporaneously, three or more joint sets formed (Br1). These joints are subject to increased material loss due to erosional processes. The combination of intersecting jointing with coastal action has resulted in accelerated, localised material loss within the web of a conjugate fault (denoted Er1).

Table 6-5 Geological history Portobello Outfall.

Feature	Denotation	Process	Mechanism
Production of wash	W1	Coastal weathering processes	Formation of sediment on cliff face, obscuring underlying geology from view.
Rubification of underlying soils and chalk	Rb1	Coastal weathering processes	Discolouration of underlying soils and chalk.
Dissolution of valley surface	Ds1	Periglacial, weathering and transport processes	Irregularly shaped contact between Qs1 and Qs2.
Dry valley development	Dv1	Periglacial, weathering and transport processes.	Irregularly shaped lobes of Quaternary sediment overlying CC1.
Material loss due to brecciation and subsequent weathering and erosion.	Er1	Sedimento-tectonic and coastal weathering processes	Blocky material loss within the web of F1 conjugate fault, overprinting the Culver Chalk Formation. This overprinting relationship could have occurred after the deposition of overlying deposits and have overprinting relationships with J2, and CC1 only.
Brecciation of 3 or more joint generations	Br1	Sedimento-tectonic	Jointing 2 contributing with unobserved joint sets leading to discontinuity driven material loss. This overprinting relationship could have occurred after the deposition of overlying deposits and have overprinting relationships with J2, and CC1 only.
Jointing	J2	Sedimento-tectonic	Cross-cuts CC1 resulting in discontinuity driven failure within the Culver Chalk. Jointing frequency observed to be greater than the J1, overprinting NC1.
Jointing	J1	Sedimento-tectonic	Cross-cuts NC1.
Main fault	F1	Tectonic activity – extensional	Small scale half graben structures, extensional regime, leading to thinning of dry valley and rotation of blocks giving rise to accommodation space.
Culver Chalk Formation	CC1	Deposition and lithification	Stratigraphic position; overlies Nc1 and TsM1 stratigraphically.
Telscombe Cliff Marl	TsM1	Deposition and lithification	Stratigraphic position(s).
Newhaven Chalk formation	NC1	Deposition and lithification	Stratigraphic position(s) – penecontemporaneous with the deposition of the (TsM1).

In the dry valley deposits overlying the lithified chalk, dissolution features (Ds1) are observed, indicating that dissolution occurred after deposition of Quaternary sediments. Orange staining of the underlying chalk and the orange hue of the overlying sediments indicates that rubification has occurred and joints are in hydraulic conductivity with the overlying soils. The production of wash is reflective of the overlying deposits being unlithified and subject to processes such as dissolution in response to meteoric input.

CIRIA weathering grades

Given the various Chalk formations and weathering types at Portobello outfall, four sub-locations were used for CIRIA grading; the base of the cliffs to the east and west of the outfall and two opposing sections within the dry valley to grade the de-structured chalks observed.

East side of Portobello outfall – Culver Chalk Formation

Six sampling points at 6.0 m intervals were undertaken for density estimation, with an average of six blows with a new hammer pick (i.e., two CIRIA density tests) undertaken at each sampling point. Measurement of discontinuity spacing, and aperture was undertaken every 2.0 m for a 28.0 m line, producing fifteen sample points. Mean hammer penetration varies across the section in a non-uniform trend, ranging from 4 to 8 mm, corresponding to high CIRIA density grades.

Discontinuity spacing varies significantly across the research site. In some locations, fractures are intense with spacings between ranging 20 – 100 mm, while in other locations spacings are <600 mm. CIRIA discontinuity grades range between A2 – C4.

West side of Portobello outfall – Newhaven Chalk Formation

Four sampling points along the west side of Portobello outfall were undertaken, with twelve penetrations per sample point. Mean penetration per sample point across the data set ranged between 4.8 and 6.4 mm (high CIRIA density grade) with discontinuity spacings of predominantly 200 – 600 mm with one occurrence of 60 – 200 mm. Apertures are generally open >3 mm. Discontinuity grades range from A2 to C3.

Portobello dry valley

Two sections were sampled within the dry valley at Portobello, with the east flank being more extensive than the west owing to access (Figure 6-15). On the east flank, there are twelve sample points where density estimation was undertaken using the hammer penetration method (both old and new picks for comparison) and the 6-inch nail penetration method. This was repeated on the western flank of the dry valley for six sample points (Table 6-6).

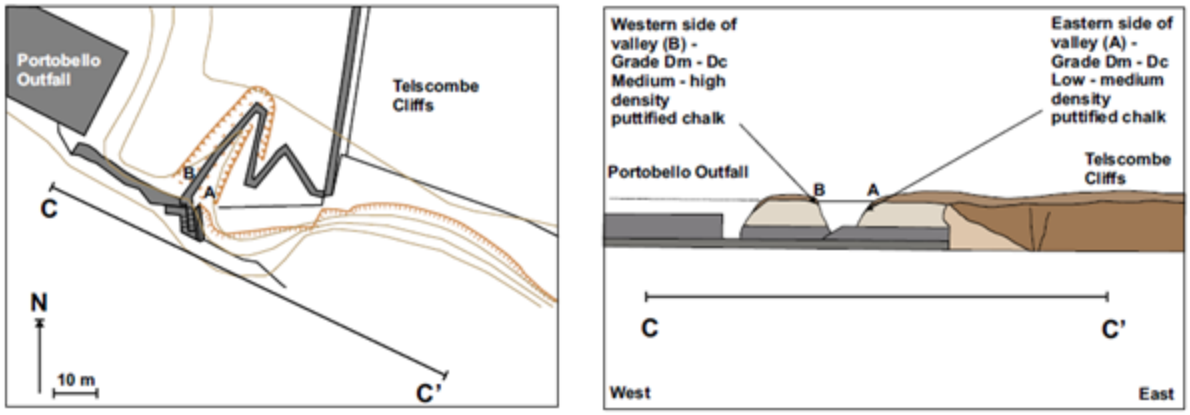


Figure 6-15 Schematic map and cross-section of access to Portobello Outfall; A and B denote puttified dry valley deposits.

All CIRIA discontinuity grades were Dm to Dc, with Dc increasing with depth (i.e., down slope of the valley), which indicates an improvement of grade and is likely the result of either density driven material sorting, or in situ weathering, where competent chalk has been weathered in situ leaving a brecciated rock mass.

Table 6-6 CIRIA density grading of dry valley deposits at Portobello either side of access route.

Valley flank	Number of sample points	CIRIA density from new hammer pick penetration	CIRIA density from old hammer pick penetration	CIRIA density from 6-inch nail penetration	Average discontinuity grade
East (A)	12	Medium - high	Low - medium	Low – medium	Dm - Dc
West (B)	6	Medium - high	Medium	Medium	Dm

6.2.3 Newhaven Harbour, Newhaven

Castle Hill, Newhaven Harbour was selected as a research site owing to the occurrence of karstic weathering features and interaction between the overlying superficial deposits and underlying chalk. The soils observed at this location are complex, and chemically active (Table 6-7).

Table 6-7 Soil description, Newhaven Harbour.

Depth (m)	Description
0.0 – 0.20	TOPSOIL
0.20 – 0.50	Organic rich blue-purple black CLAY (lignite) with orange jarosite streaks. Surface is covered with powdery white basaluminite (likely weathering product). WOOLWICH FORMATION.
0.50 – 2.0	Organic rich blue-purple black CLAY (lignite) with orange jarosite streaks. Clear well-formed gypsum crystals observed. WOOLWICH FORMATION.
2.0 – 2.25	Organic rich orange-black CLAY (lignite). Increasingly Fe-rich. WOOLWICH FORMATION.
2.50 – 3.25	Green-yellow, fine to coarse, well sorted, glauconitic GREENSAND, yellow-orange where weathered, exhibiting cross-stratification. WOOLWICH FORMATION.
3.25 – 3.55	Patinated green flints and cobbles, 65 %, within a clayey, green sand matrix, 35%. Thickness is observably variable on a site basis. UPNOR COBBLE BED.
3.55	Yellow-white, karstic, weathered CHALK, with irregular contact due to dissolution. CULVER CHALK FORMATION.

The geology observed is the Newhaven Chalk Formation comprising the shore platform (and therefore obscured from study), with the cliffs comprising the Tarrant member of the Culver Chalk Formation, overlain by a Palaeogene flint-cobble bed, which is then overlain by the Woolwich formation (Mortimore, 2021) (Figure 6-16).



Figure 6-16 CIRIA grades at Castle Hill, Newhaven Harbour.

Figure 6-16 is a field photograph of large-scale fault within the Tarrant Member, in hydraulic continuity with overlying Woolwich Beds, leading to karstification. The Tarrant Chalk Member at Castle Hill is observably more yellow in hue compared to previous locations studied, with rounded surfaces (i.e., less angular and lacking conchoidal fracture characteristics compared to the Newhaven Chalk observed in both Roedean and Portobello west), indicating that there is some staining of the chalk matrix by chemically enriched water percolating from the overlying superficial deposits, reflective of chemical weathering. The rounded character of the chalk indicates that the hardness of this chalk is lower than chalks observed at Roedean and Portobello, which is likely the result of sulphate-enriched water weakening the chalk (initially suggested by Mortimore (1997)). The fracture frequency at joint intersections is lower than within the Newhaven Chalk, suggesting that cataclastic processes are less important here.

Fracture frequency at this location is lower than observed in previous locations, with horizontal discontinuities separating the chalk into beds and near vertical jointing present within these beds. Large scale, high angle faults cross-cut the chalk and have hydraulic continuity with the overlying Tertiary deposits. The Castle Hill flints can be observed at this site and form key marker horizons. These are nodular flint bands and cross-cut the chalk and can be traced through the cliff for many miles (Mortimore 2021). In terms of CIRIA density estimation, the chalk is estimated to be medium to high density.

Overlying the chalk is a thin veneer of the basal Upnor Formation (Thanetian in age), which represents an unconformity, comprising a flint-cobble bed. The flints are green-black in colour, indicating a glauconitic coating. The deposit is up to 1.5 m in thickness and is irregular in terms of unit thickness. Above this are the Woolwich and Reading Beds, formed of fluvio-deltaic channel fill, fine to medium, glauconitic sands, fining up to lignitic clays (Figure 6-17).

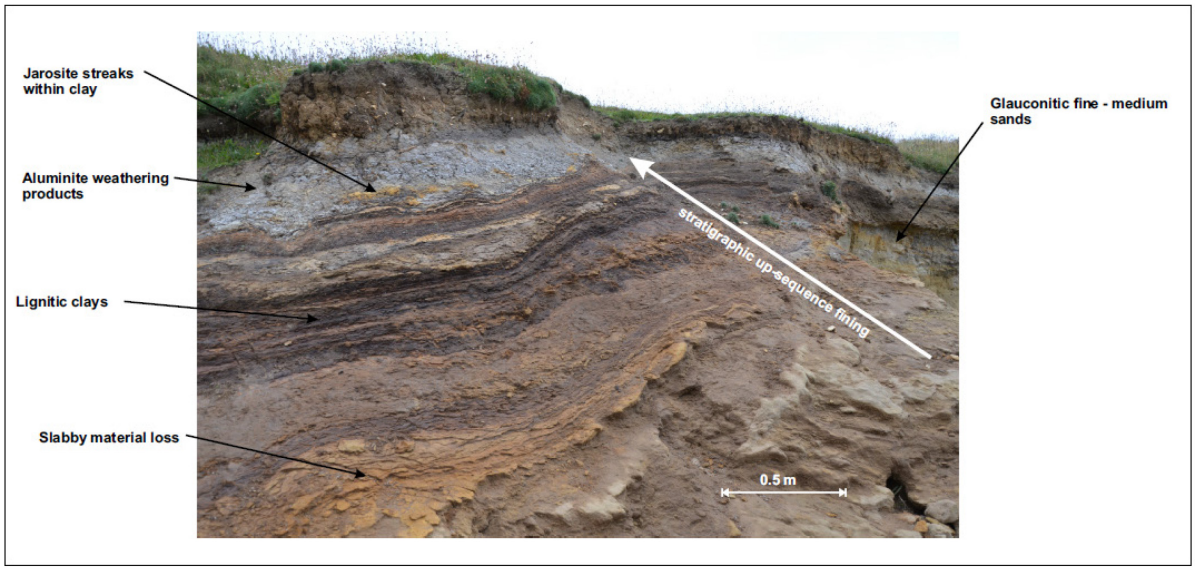


Figure 6-17 Overlying Woolwich Beds, fining up-sequence from glauconitic sands to lignitic clays, with sulphur-rich jarosite bands.

The channel fill sandstones exhibit strong cross-stratification and are yellow (when weathered) to green (unweathered) in colour. Figure 6-18 shows the stratigraphic position of the Woolwich beds (Figure 6-17) in relation to the underlying Tarrant Chalk Member. In the overlying lignitic clays, there are yellow sulphurous bands, indicative of the mineral jarosite, as well as the presence of gypsum crystals (both sulphate rich).



Figure 6-18 Culver Chalk Formation overlain by Tertiary deposits; Castle Hill, Newhaven Harbour.

Dissolution tubes are observed at the contact between the Upnor cobble bed and the underlying Tarrant Chalk, with the infill comprising material from the Upnor cobble bed, as well as white powdery authigenic aluminite or basaluminite as weathering products. (reported by Mortimore (1997)). There are significant karst features in both the high angle normal faults in hydraulic continuity with the

overlying Woolwich beds, as well as along horizontal discontinuities. This indicates that discontinuities act as preferential flow pathways for sulphur rich (and therefore chemically aggressive) ground water from the overlying Woolwich beds. The yellowish colour of the chalk is also indicative of weathering and reflects the percolation of chemically rich groundwater from the overlying Tertiary deposits through to the chalk, which is likely to have reduced the chalk density and hardness.

Weathering is not exclusive to the chalk, with the Tertiary deposits also affected, with cross bedding in sands showing significant erosion, and discolouration of both the glauconitic sand and the organic clays. This is significant in that weathering of these deposits will modify the geochemistry of groundwater, which will then accelerate chemical weathering of the underlying chalk.

Younging relationships

The younging relationships at Newhaven are complex and play a significant role in the weathering processes that are observed at this site. Figure 6-19 and Table 6-8 shows that deposition and lithification of the Tarrant Chalk (denoted A1 – A6), along with the penecontemporaneous formation of the Castle Hill flint nodules occurred first (CH1 – CH5). Faulting and jointing overprint the chalk (denoted F1), and likely occurred while the chalk was unlithified as some faults are infilled with flint. The faults do not cross-cut the overlying Woolwich formation, indicating that these were deposited after faulting.



Figure 6-19 Younging relationships, Newhaven Harbour.

By virtue of superposition, deposition of the Upnor cobble beds (UP1) and the Woolwich Formation occurred next in the sequence of events. The erosional surface at the top of the chalk does not exhibit cryoturbation, however there is fracturing. This indicates that the Woolwich Formation was likely deposited before the periglaciation of the Devensian, and acted as a barrier, protecting the chalk beneath. There is brecciation observed at the contact between the underlying chalk and the Upnor cobble beds and Woolwich Formation (where the Upnor is absent). Fracture frequency reduces with depth, indicating that this weathering is in response to an input from the overlying deposits.

Associated with F1 are subvertical karst features and sub-horizontal karst features associated with chalk beds. This is inferred to have occurred after the deposition of the Woolwich Formation, as weathering of sulphate rich minerals into groundwater, then exploiting sub-vertical discontinuities would provide a mechanism for karstification. Karstification of bed horizons could be due to preferential flow of groundwater down sub-vertical discontinuities, and then along bedding horizons, or the concentration of sulphate rich waters after percolation through the overlying chalk. Given the inconsistent occurrence of these karsts, the mechanism is thought to be the former, owing to rapid recharge, rather than gradual, consistent water percolation.

Occurring most late are contemporary processes, such as erosion of the cliff and landslip of the overlying deposits, resulting in the deposition of Rendzina at the base of the cliffs (R1).

Table 6-8 Geological history, Newhaven Harbour.

Feature	Denotation	Process	Mechanism
Rendzina formation	R1	Landslip/hill wash	Exsitu hill wash/landslip material.
Erosion of cliff surface	Er2	Erosional processes	Material loss penecontemporaneous with Rendzina formation.
Sub-horizontal karstification	K2	Karstification	Lack of vertical hydraulic conductivity – requires a conduit from overlying Woolwich beds.
Sub-vertical karstification	K1	Karstification	Inferred as earlier than K2 due to faults in hydraulic conductivity and size of karst voids.
Woolwich formation	WF1	Deposition	Stratigraphic position.
Upnor Cobble Beds	UP1	Formation	Stratigraphic position and lack of Upnor in some areas.
Erosion	ER1	Erosion	Erosion surface not subject to periglacial processes, indicating that the Tertiary acted as protection.
Main fault	F1	Formation	Hydraulic conductivity; upper Woolwich beds to chalk; faults not observed in the Woolwich beds.
Castle Hill Flints	CHF1 – CHF5	Deposition and lithification	Stratigraphic position(s).
Chalk beds	A1 – A6	Deposition and lithification	Stratigraphic position(s).

CIRIA weathering grades

Five discrete sampling locations were used for CIRIA density grading, where 12 penetration tests were undertaken. The rationale for discrete points was that the apparent degree of weathering was not sufficiently varied enough to undertake a section survey, as this would not capture the heterogeneity in terms of weathering.

CIRIA density grades across the research site were low – medium based on a hammer penetration range of 9 – 15 mm. Fractures were open (<3 mm) to closed, resulting in A and B grades in terms of aperture. Spacing varied significantly across the sampling points, ranging from 60 - >600 mm, resulting in spacing grades ranging from 1 – 5 across the research site.

6.2.4 Birling Gap, East Dean

Birling Gap, East Dean, is a site of specific scientific interest (SSSI) owing to exceptionally preserved geological features; (Mortimore 2021, Mortimore, 1997) the geological formation observed at this location is the Seaford Chalk Formation (Mortimore, 2021). The weathering features observed are complex, with the main focal point being an exceptional example of a low amplitude weathered valley within the Birling Gap syncline (Mortimore, 2021).

The soils observed at Birling Gap are much thinner than those observed at previous locations, which are attributed to the geomorphological and topographic setting. Table 6-9 provides descriptions of the soils observed.

Table 6-9 Soil description, Birling Gap.

Depth (m)	Description
0.0 – 0.25	White-brown, carbonate-rich rendzina, some irregular clasts of chalk <50 mm.
0.25 – 1.50	Flint gravel 10 – 100 mm, 60% with a carbonate clay matrix, 30%. Thickness observably variable at this site, with irregular lobe morphology.
1.50	Heavily de-structured, cream-brown weathered CHALK, with some flint clasts <150 mm. Total thickness not observed. SEAFORD CHALK FORMATION.

The competent Seaford Chalk observed at the site is buff to white, fine grained with nodular flint bands, and is horizontally bedded with widely spaced sub-vertical joint sets. These joint sets are oriented sub-perpendicular and sub-parallel to the cliff face and intersecting, leading to blocky material loss and evidence of numerous cliffs collapses at this locality (Mortimore, 2021).

The jointing observed at Birling Gap and subsequent material loss is interpreted to be exfoliation jointing, whereby the chalk has flaked away from the cliff face in sheet-like blocks. The mechanism for this is postulated to be due to rock expansion resulting from relaxation and a reduction in pressure due to isostatic rebound after erosion of previous overburden (in this case, the chalk units stratigraphically above the Seaford Chalk Formation).

The dry valley is approximately 200 m wide, and its brown colour contrasts with the surrounding white Seaford Chalk. There is significant disturbance within the fabric of the dry valley, with the present of sheet flints and tabular flint bands that have become fractured and deformed (attributed to gravity driven involution of material during periglacial cyclic ground freezing). The base of the dry valley is not observed as it lies below flint storm gravel deposits (Mortimore, 2021). Chalk grades within the dry valley are Dc and Dm owing to a lack of structure. At falling tide, it is possible to observe the footprint

of the syncline in the shore platform, identified by pooling sea water (Figure 6-20), which has not been identified before the work presented in this thesis.

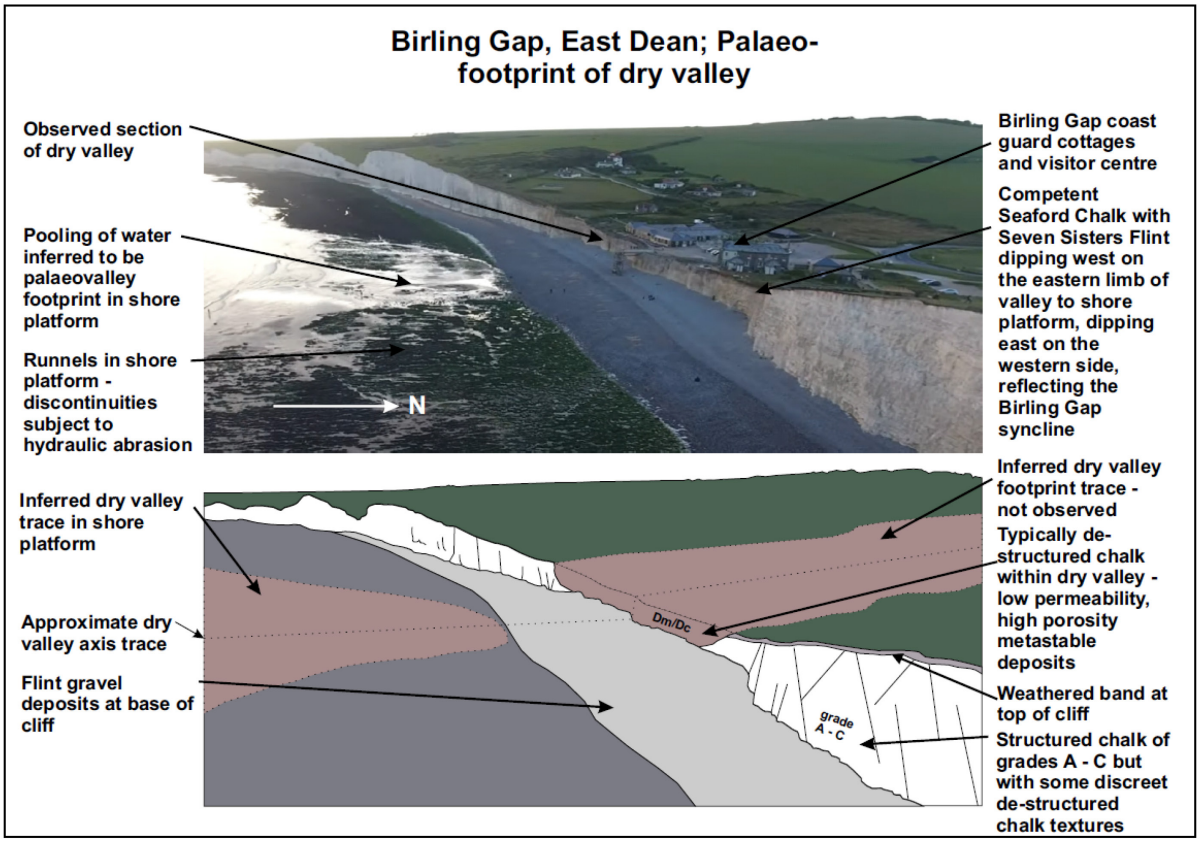


Figure 6-20 Field photograph with schematic equivalent illustrating the distribution of the dry valley at Birling Gap (adapted from Adriano (2023)).

Figure 6-20 shows the dry valley extent at Birling Gap. The platform in front of the terrestrial dry valley has a concave, valley-like morphology, where the sea is observed to pool. This is inferred to be the trace of the dry valley paleo-position both spatially, extending out to sea and within the chalk stratigraphy, extending lower than the Seaford Chalk Formation – effectively truncated by erosion processes. The rate of erosion at Birling Gap has been reported as 0.54 m/year (Mortimore, 2021), which is very similar to values presented by Asoni et al. (2018) for chalk in general, of 0.49 m/year for cliffs and 3.99 mm/year for platforms. This differential between the two erosion rates would explain why the paleo-valley within the platform has markedly less chalk material lost and is truncated from the overlying terrestrial chalk. The key structural controls of the dry valley remain, however the valley within the platform has not been subject to later weathering processes that the terrestrial valley has, therefore the chalk within the dry valley at sea is not comminuted to true de-structured chalk, making it more resistant to weathering processes.

The competent Seaford chalk is characterised as A1 CIRIA grade in the cliffs flanking the dry valley, however, the grade reduces to B – C grade at proximity to the valley sides, with fracture frequency intensifying towards the valley axis, where the chalk is graded as Dm and Dc grades of Chalk (following a similar distribution to that of the dry valley observed at Portobello) (Figure 6-21). Estimated densities are low to medium, with density increasing both from the syncline axis as well as with grade (i.e., Dc grades and structured chalk give higher density values).

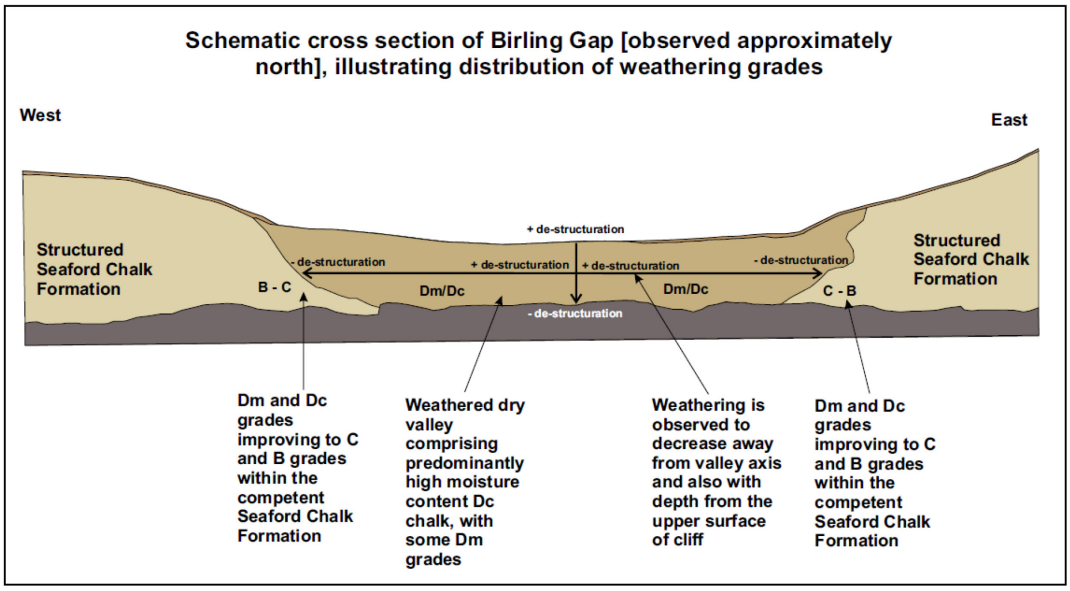


Figure 6-21 Schematic of weathered valley at Birling Gap, denoting the distribution of weathering grades (adapted from work by Asoni et al. 2018).

In the upper 2 – 3 m of the cliff section, there are dissolution tubes observed as well as involutions and lobes filled with Loess and flint gravels, and sometimes unfilled (Figure 6-23).

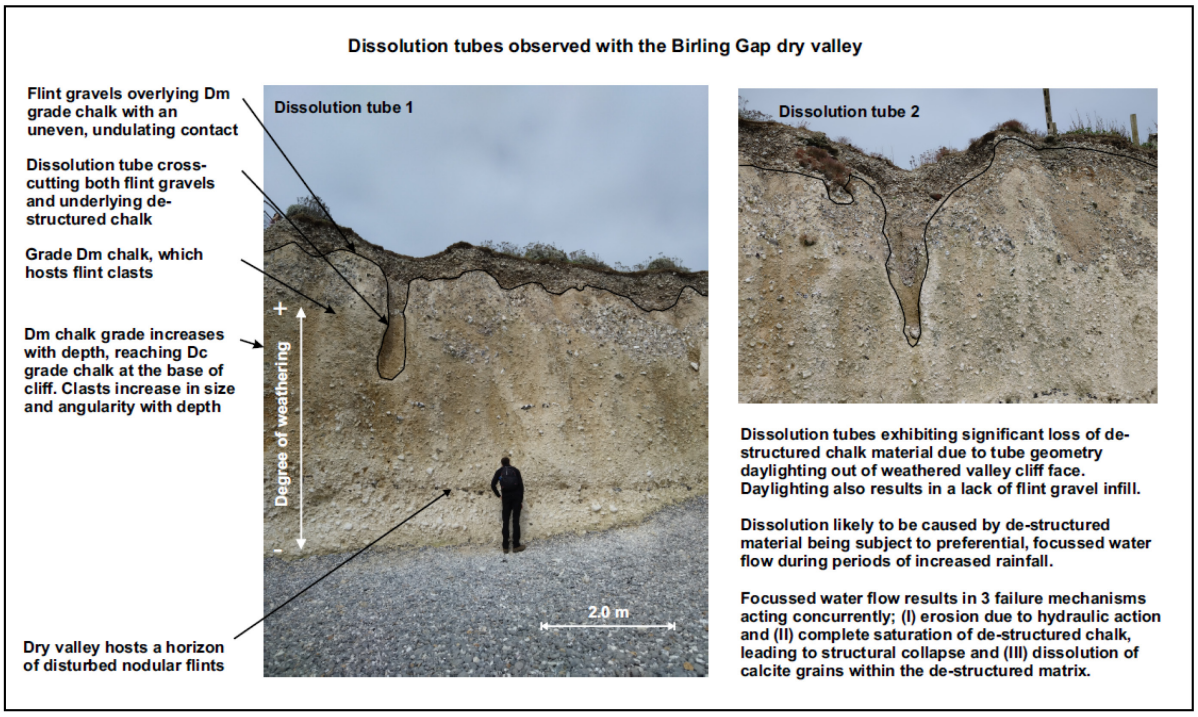


Figure 6-22 Dissolution features, Birling Gap, East Dean.

The formation of these lobes and tubes is attributed to periglacial weathering, with later dissolution processes and solifluction resulting in movement of the sediment. The magnitude of the dissolution tubes observed is attributed to preferential water flow causing dissolution. In the tubes observed at Birling Gap, the cross section of these tubes daylight onto the cliff face.

Younging relationships

The geological events at Birling Gap have given rise to the Seven Sisters and an example of an extensive dry valley (Figure 6-23 and Table 6-10). Initial geological events would have been the deposition and lithification of the Seaford Chalk Formation (Sc1), along with the formation of nodular flints (Fl1).

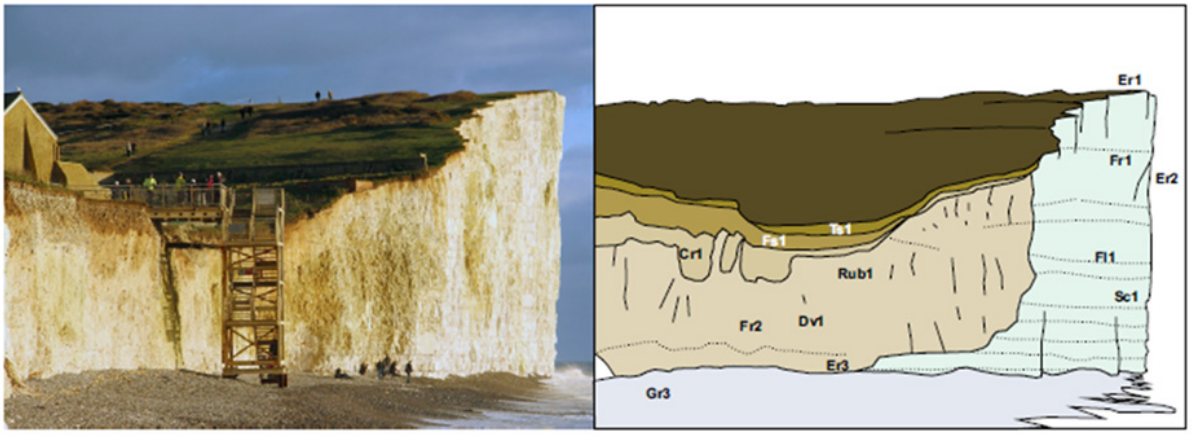


Figure 6-23 Younging relationships, Birling Gap.

The development of the Birling Gap syncline (Fr1), which cross-cuts the Seaford Chalk Formation, as well as the topographically high areas (Fr2) are representative of modification of the geomorphology due to tectonic regime. The generation of faults and joints within the topographic low ground has given rise to highly brecciated chalk, with preferential flow pathways. This means that the area within the dry valley (Dv1) was susceptible to both water weakening processes as well as cyclical freeze thaw action (Cr1), which resulted in the comminution of chalk to the weathered deposits observed currently.

Erosion of overlying chalk (Er1) has resulted in the liberation of relatively harder flint fragments, which have then been deposited in the dry valley (Fs1) and are present within soil deposits. Further erosion action and cliff collapse (Er2) of the cliff face has contributed both chalk and flint gravel material for the flint gravel deposit beach (Gr1). Owing to Dv1's relative de-structured character (compared to that of the surrounding competent Seaford Chalk), accelerated material loss is associated with the dry valley (Er3).

Table 6-10 Geological history, Birling Gap.

Feature	Denotation	Process	Mechanism
Flint gravel beach	Gr1	Coastal processes	Exsitu flint material provenance from eroded cliffs.
Accelerated erosion of dry valley	Er3	Erosion	Mechanism is likely de-structuration of the chalk via discontinuity driven fracturing followed by ice-age cryoturbation.
Erosion of cliff face	Er2	Material loss through meteorological weathering, wave action and cliff collapse	Penecontemporaneous with Er3 but at a lower rate. Er1 contributes to material carried within wave load of the sea.
Flint gravel deposition in dry valley	Fs1	Erosion and transport	Stratigraphic position(s), concentration at base of dry valley - material has travelled downslope. Provenance is chalk previously eroded away.
Erosion of overlying chalk	Er1	Erosion	flint gravels which form in the base of the dry valley.
Cryoturbated lobes	Cr1	Cryoturbation	Modification of dry valley sediments.
Formation of dry valley	Dv1	Weathering, erosion and transport	Topographic low with weathered material within.
In-land main tectonics, resulting in the Birling Gap Syncline	Fr1, Fr2	Syncline generation and topography modification	Resulting high topography east and west of the Birling Gap Syncline (topographic low); fracturing of the base of the valley syncline axis and topographic highs.
Nodular flints	Fl1	Deposition and lithification	Stratigraphic position(s). Penecontemporaneous formation with lithification.
Chalk beds	Sc1	Deposition and lithification of Seaford Chalk	Stratigraphic position(s).

CIRIA weathering grades

Three sections across Birling Gap were measured to characterise to CIRIA C574 standards. Four sample points from west to east on the eastern side of the valley and four samples east to west on the western flank of the valley were undertaken to characterise the competent chalk, while a final section was undertaken across the de-structured deposits of the dry valley itself. CIRIA grading was undertaken with a new hammer pick, a used hammer pick and a 6-inch nail for comparison.

Either side of the dry valley, the chalks are considered competent, with grades to the west comprising medium – high density, grade C – B chalk with spacings of 200 – 300 mm, corresponding to grades of 2 – 4. Grades to the east are medium to high density, with fractures open >3 mm aperture and below, leading to B and C grades. Fracture spacing ranges of 10 – 150 mm, corresponding to grades of 3 – 5. The dry valley is characterised as medium to high density, de-structured chalk, dominated by Dc grades, with some discrete Dm areas.

6.3 Discontinuity survey

Scanlines of varying lengths were undertaken at the four research sites. The data collected is summarised in Table 6-11. The importance of characterising discontinuities in a weathering context cannot be understated – this is because discontinuity provenance may be due to tectonic activity or through non-tectonic, weathering processes, such as frost action (Mortimore et al. 2004). It must also be noted that certain types of weathering may be the direct result of tectonic activity, including discontinuity driven material loss (such as the processes observed at Portobello outfall – Figure 6-11) and cataclastic brecciation at proximity to large scale discontinuities with associated movement (such as the cataclastic processes observed at Roedean – Figure 6-6).

Conjugate faults indicate a complex stress regime, and this is also reflected by intricate fracture patterns observed at Roedean and Portobello. Fractures perpendicular to fault surfaces are reflective of extension or displacement of a normal fault, while reverse faults exhibit mixed fracture patterns comprising a combination of parallel and perpendicular fractures relative to the fault surface, indicative of a compressive stress regime (Twiss and Moores, 2006). Faults at Roedean and Portobello exhibit both fracture types. From these observations, it is inferred that extensional stresses caused during the Mesozoic – Mid-Cretaceous Syn-rift phase induced the first generation of perpendicular fractures, then later, during the Mid-end Cretaceous, basin inversion began, and the extensional regime switched to a compressive regime, inducing a second generation of parallel and perpendicular fractures. By the end of the Miocene, uplift and erosion was occurring, leading to the reactivation of strike-slip faults (Mortimore, 2021). While not technically a true form of weathering, the implication of these fracture networks is that they enhance current weathering processes by providing conduits for fluid flow, leading to water weakening and material loss.

Uncertainty of discontinuity provenance is therefore an important, key aspect of identifying weathering and inferring likely weathering processes.

6.3.1 Scanline results

Scanline survey results from each research site as well as further analyses of geomorphology, weathering distribution and field observations are discussed in this section. Primary data is summarised in Table 6-11 and Figure 6-24.

In terms of discontinuity characteristics, each formation has individual styles of fracturing that are the result of formation material differences, tectonic history, and stratigraphy. The Seaford Chalk Formation (observed at Birling Gap in this study) is characterised as a creamy-white to white, medium

density chalk with sub-vertical and sub-perpendicular discontinuity sets and has numerous flint bands (>100 mm thickness).

Stratigraphically overlying is the Newhaven Chalk Formation, which is characterised as medium density chalk, with marl seams and repeated layers of flint. The Newhaven Chalk has sub-horizontal bedding, dipping south and has well defined, high angle (60 - 70°) shear fractures, which have been observed to be associated with increased localised brecciation, such as Roedean. This formation is also observed at Portobello, on the west side of the outfall during this study.

The final formation observed is the Culver Chalk Formation (basal member – Tarrant Chalk Member) and is characterised as a soft white chalk, with little marl seams but well-developed flint bands. In terms of discontinuity character, the Culver Chalk has clean, sub-vertical joint sets and more persistent, larger scale, sub-vertical faults.

In terms of nomenclature and convention in this report, discontinuities and fractures refer to both joints and faults. Where distinction is required, the discontinuities are described as

- Joint – a discontinuity where there is no evidence of visible displacement.
- Fault – a discontinuity where there is evidence of visible displacement.

In terms of measurement convention, this report will present dip and dip direction, unless specified where strike direction is an important parameter.

Table 6-11 Summary of scanlines.

Locality	Cliff height (mAOD)	Formation	Number of readings	Strike of scanline (°)	Length of scanline (m)	Mean dip (°)	Mean fracture spacing (m)	Mean persistence (m)	Types of weathering and weathering products encountered
Roedean	24.0 mAOD	Newhaven Chalk Formation	112	110	40.4	59.57	0.36	Not measured	Cryoturbation lobes, cryoturbated horizons within cliff formation, cataclastic weathering at proximity to faulting, cataclastic weathering at the intersection of three discontinuity types, Type 1 brecciation, type 2 brecciation; decreasing weathering with depth from cliff top, meteorological induced slaking, bioturbation in the upper layers at proximity to soil and chalk interface, microbial bioturbation on the chalk surface.
Portobello – West	17.0 mAOD	Newhaven Chalk Formation overlain by Culver Chalk Formation	65	120	19.5	63.41	0.30	3.4 +	Portobello East and West separated by a small-scale dry valley with head deposits, which are metastable and wash out during rainfall events. Cryoturbation lobes and solifluction in the upper layer below cliff face, wave cut notch present at base of cliff indicating weathering by hydraulic action, salt weathering, discontinuity driven weathering (i.e., intersecting, closely spaced discontinuities leading to material loss), minimal discoloration, indicating less chemical weathering than Portobello East.
Portobello – East	10.0 mAOD	Newhaven Chalk Formation overlain by Culver Chalk Formation	64	115	15.3	63.10	0.23	3.4 +	Portobello East and West separated by a small-scale dry valley with head deposits, which are metastable and wash out during rainfall events. Extensive cryoturbation lobes and solifluction in the upper layer below cliff face as an extension to the dry valley observed at access point, wave cut notch present at base of cliff indicating weathering by hydraulic action, salt weathering observed at base of cliff in SEM analysis, significant discontinuity driven weathering in larger scale conjugate faults (i.e., intersecting, closely spaced discontinuities leading to material loss), highly discoloured to reddish-orange indicating the presence of iron and increased likelihood of chemical weathering.
Newhaven Harbour	23.0 mAOD	Tarrant Member; Culver Chalk Formation	50	88	18.5	57.73	0.39	6.42	Fault cataclastic weathering, karstic weathering, chemical weathering, limited discontinuities observed at this site.
Birling Gap	7.0 mAOD at lowest topographic point (dry valley floor), 45.0 mAOD at highest (Seven Sisters)	Seaford Chalk Formation	169	74	68.5	73	0.37	3.25	Site comprises large-scale weathered valley deposits (Head/Coomb rock), cryoturbation and solifluction in the upper layers of chalk, extensive material loss due to intersecting discontinuities, salt weathering, hydraulic wave action.

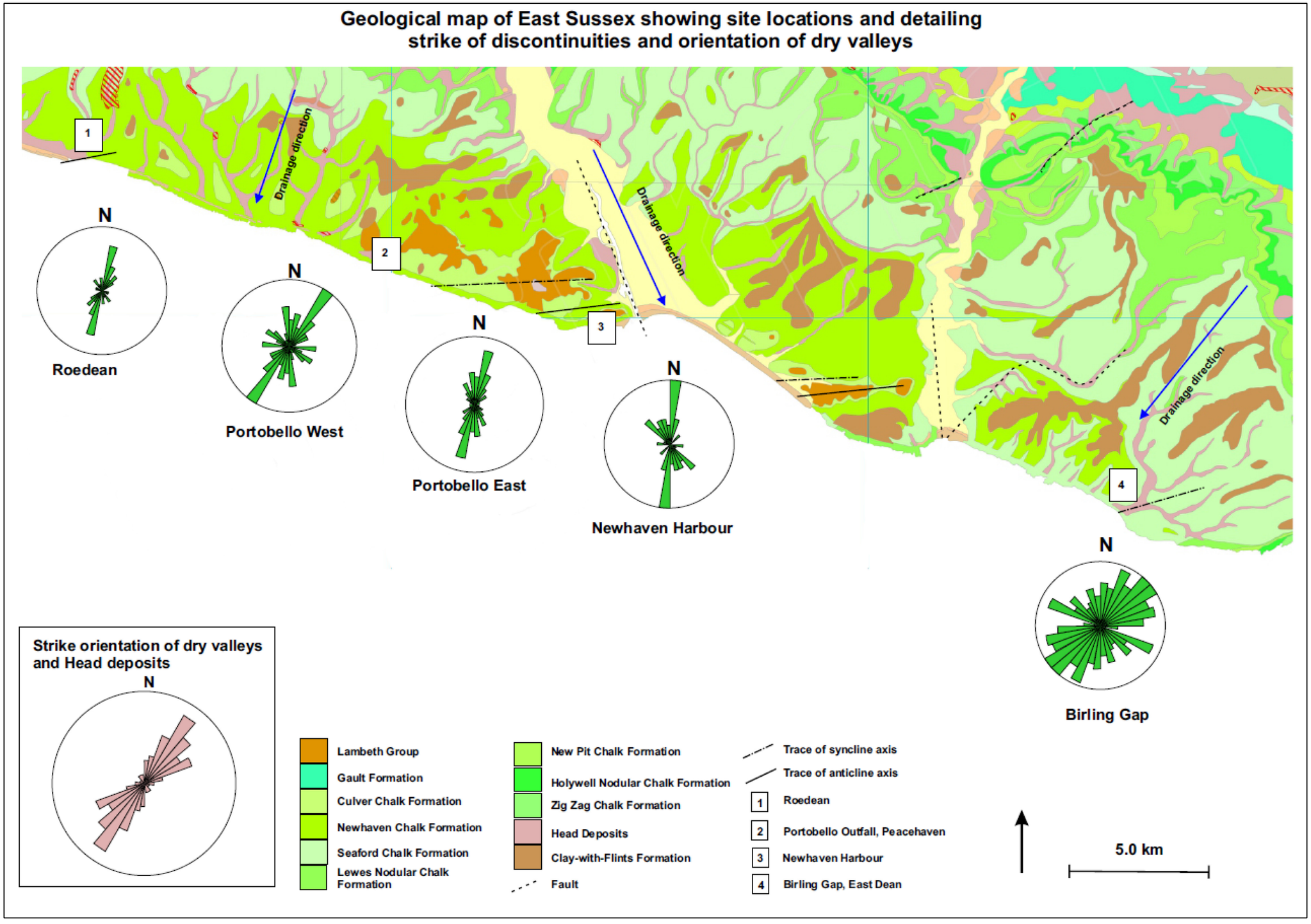


Figure 6-24 Geological map of study sites with strike orientation data (adapted from Edina Digimap 2023).

6.3.2 Scanline survey; Roedean

At Roedean, one scanline was undertaken (40.4 m in length), with discontinuity types split into faults (i.e., which displayed displacement), smaller fractures and joints. The scanline orientation was not horizontal, owing to the access ramp acting as a platform, and therefore are affected by reducing fracture frequency with depth, which is a trend attributed to weathering decreasing with depth away from the ground surface. A total of 111 discontinuity orientation readings were taken at Roedean, comprising 86 measurements of smaller scale fractures and joints and 26 measurements of primary faulting (which display evidence of displacement) (Table 6-11).

Within the measured data set for joints, there are four conspicuous joint sets, which vary in terms of intensity (Figure 6-25); joint set 1 – 51°/293°; joint set 2 – 53°/125°; joint set 3 – 90°/174° and joint set 4 – 74°/264°. For the 26 fault measurements, there are also 2 conspicuous sets, which also vary in set size (Figure 6-25); fault set1; 62°/126°, which is the largest set, and fault set 2; 60°/266°, which is the smallest of the two fault sets.

Fracture frequency was measured along the section, with the majority of spacings falling below 0.3 m, which places these within the CIRIA fracture spacings grade of 2 – 3 (Figure 6-25). The number of fractures which were greater spaced, reduced as frequency increased, i.e., the greater the spacing the lower the frequency. The mean fracture frequency of the scanline was 0.36 m. The scan-line approach shows how the CIRIA fracture spacing grade is not suitable as statistically, the frequency is averaged over a set distance, which may result in erroneous reporting of CIRIA grades. The actual mean spacing is likely to be much closer, as fine, intensely spaced fractures were not considered for this study.

Closer fractures implies that the rock mass is both considered more weathered by the CIRIA C574 standard (albeit sedimento-tectonic discontinuities require engineering judgement as to classification) and more vulnerable for further weathering processes with discontinuities act as preferential flow pathways leading to water weakening. Closer discontinuities imply that the block sizes within the rock mass are smaller and are therefore more likely to weather out at the cliff face.

Persistence was not measured owing to the research site being on a slope – this would mean that true persistence could not be estimated. The persistence of large conjugate fractures was observed to cross-cut the entire cliff height at the bottom of the slope, indicating that these faults have a persistence of at least 27.0 m where not subject to displacement from cross-cutting horizontal discontinuities.

The dip of the joints measured at Roedean range between 22° – 90°, with a mean dip of 59.3°. These average values are split based on 4 intersecting joint sets, with joint sets 1 and 2 being the dominant

joint sets and orientated conjugate to each other (Table 6-11). The dips for these joint sets were similar, with joint set 1 having an average dip of 51°, while joint set 2 had an average dip of 53°. Joint set 3 had the highest dip of the four sets measured and represents vertical to subvertical jointing within the rock mass, with an average dip of 90°, while joint set 4 was shallower than the subvertical joints of set 3, but higher than the dips observed in sets 1 and 2 at 74°.The dips measured for the faults at Roedean were very similar at 62° for joint set 1 and 60° for joint set 2. Spatially, these joints are conjugate to each other (Figure 6-25 and Table 6-11).

With the observations made within the first part of this chapter and this scan line survey, it is possible to infer that the main faults and subsequent cataclastic processes at their peripheries has increased weathering vulnerability within the rock mass as well as further weathering the rock in discrete areas, such as within the graben portions of conjugate faults, where brecciation is intensified.

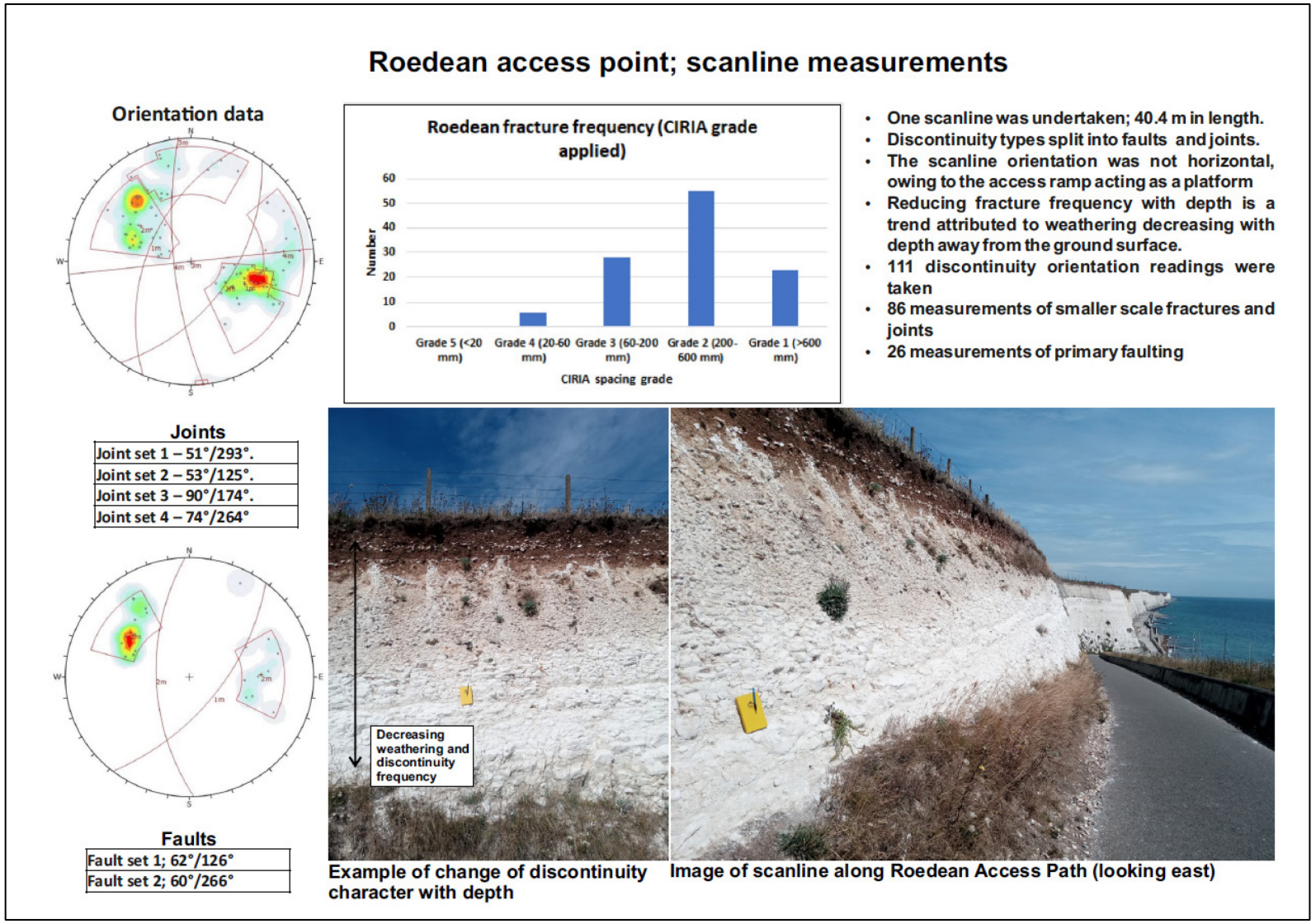


Figure 6-25 Roedean scanline measurements.

6.3.3 Scanline survey; Portobello outfall

West of Portobello outfall, 65 measurements were made in the Newhaven Chalk Formation over 19.5 m. 3 discontinuity sets were identified, but faults and joints were not defined (Table 6-11 and Figure 6-26). The largest discontinuity set had mean values of 56°/292°; the intermediate discontinuity set had a mean orientation of 66°/120°; while the smallest discontinuity set had a mean orientation of 82°/244°.

To the east of Portobello outfall, 64 measurements were made over 15.3 m at the base of the cliff, within the Newhaven Chalk, which identified 3 intersecting joint sets, which supports the observation of discontinuity-driven material loss and would result in small, block chalk masses to be lost (Figure 6-26). The mean orientation for the largest discontinuity set was 66°/132°; the intermediate discontinuity set had a mean orientation of 54°/299°, while the smallest discontinuity set had a mean orientation of 81°/223°.

The identification of 3 joint sets at each locality at Portobello indicates that material loss via weathering and exfoliation of blocks is possible. The likelihood of this would increase with more intense fracture spacings.

At Portobello west, the fracture frequency ranged from 0.1 – 0.56 m and had a mean of 0.30 m (Figure 6-26). Discontinuities below 20 mm were not measured due to the length of the scanline. At Portobello east, the mean fracture spacing observed was 0.23 m (CIRIA grade 4), ranging from 0.05 – 0.5 m. The average spacing observed at this location is misleading as it is possible to observe that that majority of measurements fall between grade 3 and grade 2 of the CIRIA spacing grades.

Field observations (Section 6.2.1) have shown that Portobello west is more competent than Portobello east in terms of weathering, with Portobello east being the site of significant weathering features related to blocky material loss. By comparing the two fracture spacings, Portobello west has wider spacings than Portobello east, which supports the observation of weathering vulnerability due to closely spaced discontinuities. While this may be a contributory factor to weathering at the Portobello east site, it is not the exclusive cause of weathering.

The persistence measured at Portobello differed between Portobello West and Portobello East, with Portobello West having a maximum persistence of 12.0 m, reflected in the high angled conjugate faults which cross-cut the extent of the cliff face. In Portobello East, vertical fractures were difficult to measure due to the proximity of the dry valley and significant material loss. Sub-horizontal fractures were estimated as 25.0 m+ at the base of the cliff, which the mean persistence of sub-vertical fractures was 3.4 m. Dips observed in the west of the site had a mean value of 68°, with the east being similar

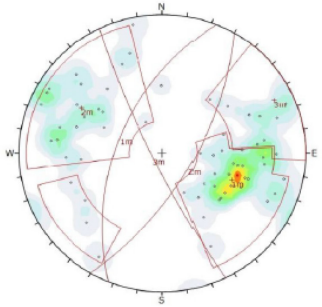
at 67°. These measured values were then interpreted to belong to 3 discrete joint sets for each part of the site (Table 6-11).

By characterising the orientations, spacings and persistence at these two sites, it is possible to observe that while fracture frequency and persistence differ, the orientations of both sites are similar, indicating that they were initiated by the same tectonic events.

Portobello Outfall; scanline measurements

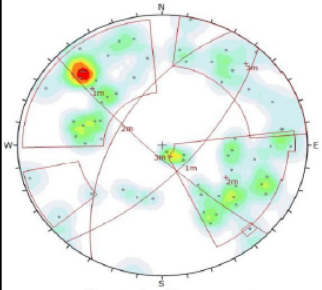
- West of Portobello outfall, 65 measurements made in the Newhaven Chalk Formation over 19.5 m.
- 3 discontinuity sets identified.
- Faults and joints were not defined.

Orientation data



Portobello - west

Joint set 1 – 55°/292°.
Joint set 2 – 66°/120°.
Joint set 3 – 82°/244°.



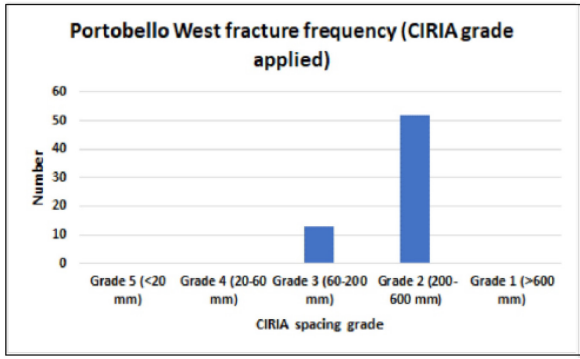
Portobello - east

Joint set 1 – 66°/132°.
Joint set 2 – 54°/299°.
Joint set 3 – 81°/233°.

- East of Portobello outfall, 64 measurements made over 15.3 m at the base of the cliff, within the Newhaven Chalk.
- 3 intersecting discontinuity sets identified.
- Discontinuity-driven material loss resulting in small, block chalk masse loss.



Left: Portobello East displaying 3 intersecting sub-horizontal joint sets and high angled, high persistence vertical to sub-vertical discontinuities, resulting in blocky material loss. Note: rubification and discolouration of the overlying Culver Chalk Formation



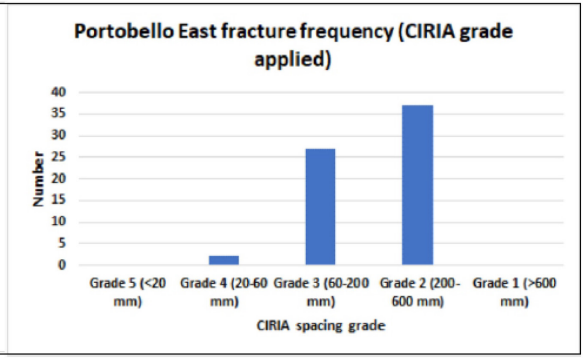


Figure 6-26 Portobello Outfall scanline.

6.3.4 Scanline survey; Newhaven Harbour

49 orientation measurements were taken over 18.5 m at Newhaven Harbour, within the Culver Chalk Formation (Table 6-11). 2 discontinuity sets were identified (Figure 6-27), with the largest joint set having mean orientation values of 56°/259° and the smallest set having mean orientation values of 59°/112°.

The mean fracture frequency measured at Newhaven was 0.39 m, using the CIRIA C574 spacing grades. Spacings ranged 0.05 – 1.5 m (Figure 6-27) and most measurements fell within the 200 – 600 mm range, which is categorised as grade 2 using the CIRIA discontinuity spacing scheme. The mean persistence of low angled conjugate faults in this research area was 6.42 m. Conjugate fracture sets were well developed and closely spaced, with some sub-horizontal discontinuities cross cutting. Large scale faults were observed to cross-cut the entire rock mass and were in hydraulic continuity with the overlying Tertiary deposits.

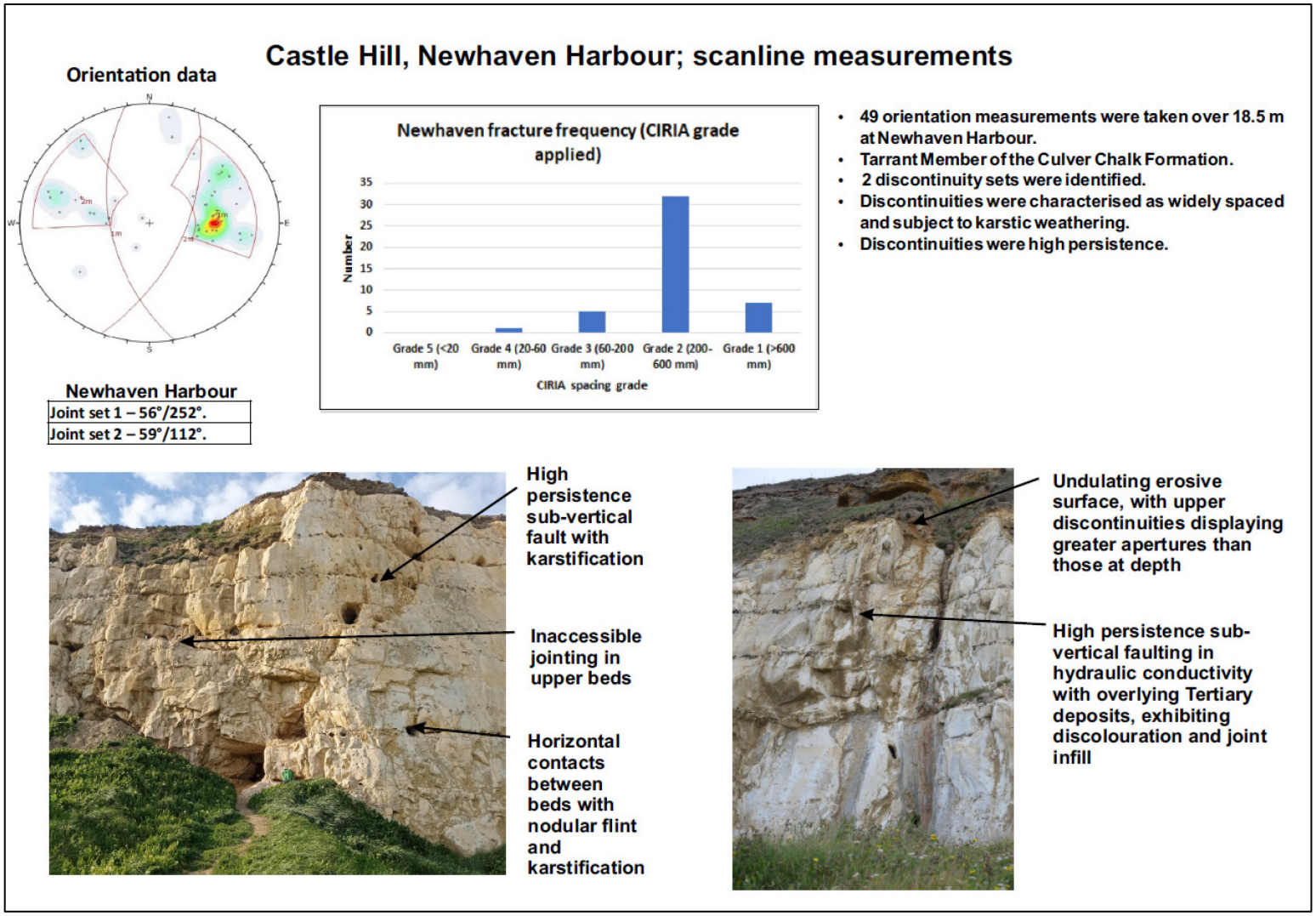


Figure 6-27 Newhaven Harbour scanline.

6.3.5 Scanline survey; Birling Gap

Birling Gap hosts a significant exceptionally preserved dry valley, with complex discontinuity character at proximity to the valley flanks, demonstrating exfoliation surfaces as well as de-structuration of the Seaford Chalk Formation. 168 measurements were taken over 68.5 m at Birling Gap, within the Seaford Chalk Formation, and 3 discontinuity sets were identified (Table 6-11). Discontinuity set 1 was the largest, with a mean orientation of; 72°/297°, discontinuity set 2 was intermediate in terms of significance, oriented 80°/166°, with a third smaller discontinuity set, with a mean orientation of 78°/226° (Figure 6-28).

Fracture spacings ranged 0.02 – 1.2 m at Birling Gap, which reflects the complex structural geology associated with the site (Figure 6-28). The mean fracture frequency measured at Birling Gap was 0.37 m, which is categorised as grade 2 using the CIRIA C574 spacing grades. Spacings ranged 0.02 – 1.2 m.

Birling Gap is complex in terms of discontinuities and mean persistence was estimated to be 3.25 m. Discontinuities are sub-vertical and sub-parallel and breaks in fracture form occur on bedding planes as well as fractures.

The dip at Birling Gap ranged from 09° – 90°, and the area mean dip was measured as 76.7°. Three intersecting joint sets were identified; two of which were conjugate to each other (joint sets 1 and 2) and a joint set 3, which was sub-perpendicular (Figure 6-28). Joint set 1 and 2 had mean dips of 72° and 80 ° respectively, while joint set 3 had a mean dip of 78°.

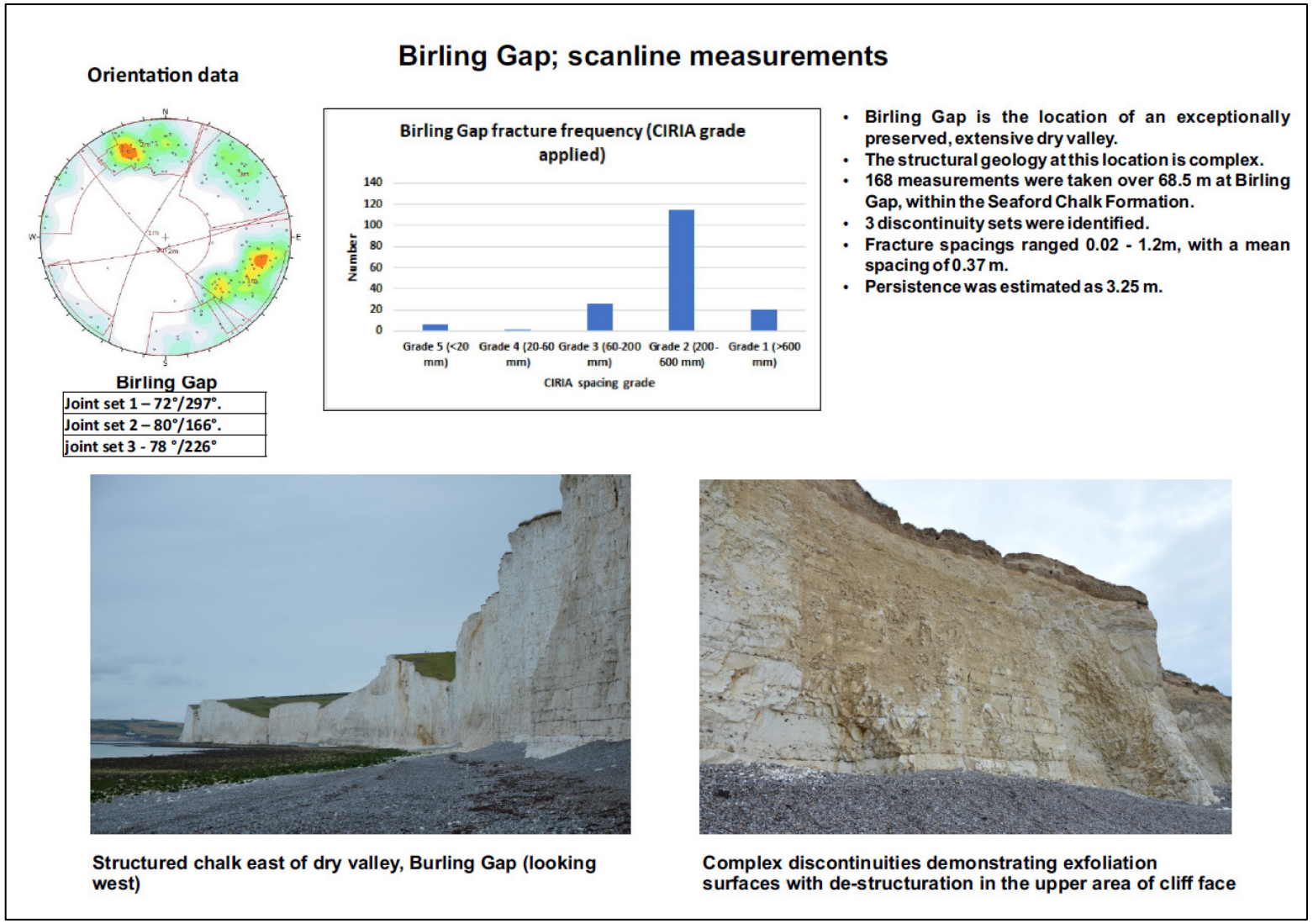


Figure 6-28 Birling Gap scanline.

6.3.6 Discontinuity survey summary

Discontinuities contribute to the characterisation of the hydrogeological and mechanical behaviour of chalk. Both intrinsic aspects have implications on weathering; high persistence, high frequency distributions of fractures modify the hydrogeology of a chalk mass significantly by providing preferential flow pathways for water. The implications of this are that secondary permeability is increased, allowing water to infiltrate the chalk mass more easily. This results in the chalk being more vulnerable to water weakening processes and aggressive ground water, leading to karstification (such as the dissolution pipes observed and karstification observed at faults in Newhaven – Figure 6-27).

Modification of the mechanical properties of chalk has implications for weathering, with the reduction of strength and density of a chalk due to micro-fracturing, leading to increased likelihood of mechanical disaggregation. This would lead to further vulnerability to weathering processes, such as cryoclasty (i.e., freeze-thaw) and physical weathering due to external aspects, such as wind and rainwater.

Undertaking scanline surveys in conjunction with the CIRIA C574 grading system allows further quantification and constraint of the identification and interpretation of weathering types. Two main components of the C574 grading system are based upon discontinuity characteristics – discontinuity spacing and discontinuity aperture, which means that the measurement of discontinuities on an engineering scale are significant to weathering studies; C574 allows quantification of weathering, while the scanline survey provides context and interpretation. There are limitations however in that statistical approaches in applying the CIRIA grades may lead to erroneous gradings, and may miss discrete, acutely weathered areas.

Another important aspect of undertaking scanline surveys in conjunction with weathering grading is that this combination of analyses allows identification and distinction between sedimento-tectonic discontinuity families, discontinuities caused by weathering and elucidates links between the two.

6.4 Chapter summary

In this section, analysis of field observations and measurements made in the identification of weathering processes and products have been presented, as well as an examination of geological relationships and events, intended to elucidate historic and contemporary, concurrent and competing weathering processes for four research sites.

Key outcomes include;

- Field observation allows the identification of weathering, weathering products and predisposing conditions to weathering vulnerability, and provides significant context prior to applying CIRIA grades.
- Younging relationships are vital in the identification of weathering types and their sequence in geological history, as well as identifying if some beds or formations are more susceptible to weathering than others.
- There are several different concurrent and competing weathering processes ongoing at any location at any one time and differ between locations.
- Weathering can be divided into historic and contemporary processes, which require identification to fully characterise weathering in the field.
- Brecciation via cataclastic processes at proximity to faults increases weathering vulnerability by inducing preferential flow pathways, leading to exacerbated water weakening and the production of small chalk blocks.
- Fracture intensity reduces with depth from cliff tops through the chalk unsaturated zone (CUZ), indicating a top-down weathering process, inferred to be periglacial ground freezing.
- Chalk horizons with aquiclude layers stratigraphically above and below have entrapped water, which is inferred to have allowed localised, acute cryoclasty during periods of ground freezing – both historic (i.e., periglacial) and contemporary. This then makes the horizon more susceptible to later weathering processes, such as slaking during wetting and drying episodes.
- Areas which have significant cover in the form of superficial deposits are likely to have less pronounced periglacial weathering effects owing to the overlying deposits protecting the chalk from permafrost conditions.
- Where 3 or more intersecting discontinuities are intensely spaced, accelerated weathering and material loss is more likely. While this confirms previous trends within the weathering of any rock, in some instances this has been identified to have occurred penecontemporaneously with chalk deposition. This is significant as it results in some chalks being more susceptible to

weathering from or close to the point of deposition, and where fractures are induced, more susceptible to water weakening processes in particular.

- Metastable, de-structured chalk deposits (dry valleys) lose constituent material upon water inundation via entrainment and run-off.
- Rubification is observed to be associated with highly weathered areas and overlying soil deposits have a significant impact on the degree of weathering of the underlying chalk.
- Chalk deposits with large-scale faults in hydraulic continuity with overlying chemically active soils give rise to sub-vertical and sub-horizontal karstic features, with chalk discolouration acting as a significant indicator of chemical weathering.
- Dry valleys are observed to extend out into the shore platform; a difference between platform and cliff erosion rates explains truncation of the dry valley, leading to cliff formation. Given that dry valleys lose de-structured material when saturated (as observed at Portobello Outfall), it is inferred that the mechanism of dry valley fill production is absent within the valley trace observed in the shore platform.

This chapter contributes to the research question by identifying sites with exceptional examples of weathering which enables field studies and sampling to be undertaken. Field studies are integral to identifying the distribution of weathering and weathering products, the type and extent of weathering on a site-scale basis. Sample collection is integral to laboratory testing and characterisation of chalk weathering.

7 Uniformity Survey

7.1 Introduction

Following from Chapter 6 where field observation and analysis of weathering was undertaken, Chapter 7 summarises the results from a survey in which UCS and IDD were measured in the field using both the SilverSchmidt test hammer and the Equotip Leeb 550 – UCS values were derived from a prepared Proceq curve and IDD from work by Thrower et al. (2022) at the University of Sussex. These were later compared to laboratory measured values (Chapter 8). Chapter 6 quantified the discontinuity characteristics of weathering, while this Chapter quantifies the distribution of strengths and densities in relation to weathering, allowing quantification of CIRIA density grades. Chapter 7 partially satisfies objectives 1, 2, 3 and 4 of this study. The aim of this survey is to measure the distribution of weathering (assessing uniformity), the effects of weathering and subsequent material property changes within the Chalk. The objectives of this uniformity survey are;

- To evaluate the SilverSchmidt and Equotip tools' effectiveness in measuring weathering.
- To evaluate the effects of different weathering types on UCS and IDD within the surrounding Chalk.
- Quantify and measure the CIRIA density component within a field setting.
- Characterise each quadrat with a CIRIA weathering grade.
- Characterise each research site and develop a statistically significant database for comparison.

A methodology to measure uniformity and the instruments used are presented in Chapter 4. The instruments are the SilverSchmidt low-strength rebound hammer (referred to as the SilverSchmidt) and the Equotip Leeb device (referred to as the Equotip) respectively. The same four research sites as Chapter 6 were used; Roedean access point, Portobello Outfall, Newhaven Harbour, and Birling Gap (described in Chapter 2).

Studies of weathering using the Schmidt Hammer and Equotip are also reviewed in Chapter 4. The use of the Schmidt hammer is more prevalent in the study of weathering and geomorphology than the use of the Equotip, such as studies undertaken by Goudie (2006), Olsen et al. (2020) and Matthews and Winkler (2022). There are few studies that use both the Schmidt rebound hammer and Equotip at the same time for the evaluation of UCS and IDD (such as Viles, et al. (2011), for heritage science), and there are no studies that use these instruments in conjunction with each other when measuring Chalk. Similarly, there are no studies that have focused on geomorphological features in a weathering context that have produced statistically significant data sets as generated within this study, nor have any employed a method of constraining measurements around these features (i.e., such as the use of a

quadrat, adapted from the fields of ecology and biology). Studies which employ the Schmidt hammer to evaluate weathering in carbonate rocks include Arman et al. (2019), with discrete, individual measurements used, while studies which utilise the Equotip are limited to those by Goudie (2006) (not specifically chalk) and Thrower et al. (2022), however their study is concerned with the measurement of IDD, and not weathering exclusively.

In terms of Chapter structure, Section 7.3 presents the results of the analysis of individual quadrats from 4 research sites, comprising section 7.2.1 Roedean research site, 7.2.3 Portobello Outfall research site, 7.2.3 Newhaven Harbour research site and 7.2.4 Birling Gap. Section 7.3 presents the results of a statistical analysis on a regional scale. Section 7.4 summarises this Chapter.

7.2 Results – Research site data

Data collected and analysed from each of the research sites are presented in detail within this section.

7.2.1 Roedean research site

At the Roedean access point research site, 14 quadrats were measured, resulting in 1400 readings in total; 800 readings (eight quadrats) were measured using the SilverSchmidt, yielding 480 valid readings, and 600 readings (six quadrats) were measured using the Equotip, yielding 591 valid readings. The aim of the quadrat measurements at this location was to evaluate strength and density changes occurring down-sequence of the cliff face in response to weathering, while also evaluating the suitability of both the SilverSchmidt and Equotip tools for measuring this variability. Figure 7-1 provides an overview of the measurements undertaken at this location.

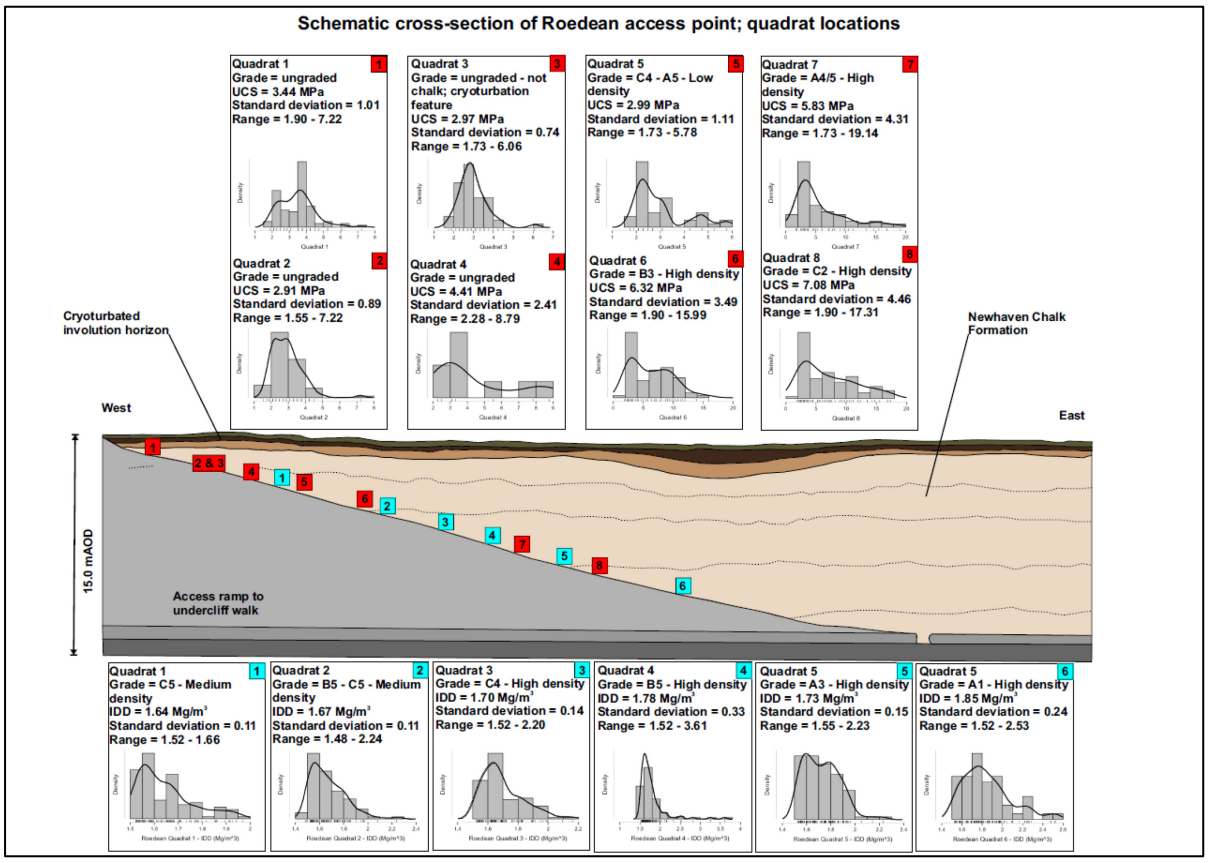


Figure 7-1 Schematic cross-section of Roedean access point.

SilverSchmidt measurements

Eight quadrats were set out along the access ramp to measure UCS using the SilverSchmidt in variable weathered sections (Figure 7-1); the first four (quadrats 1 – 4) were within cryoturbated and brecciated deposits considered to be soil rather than chalk, allowing evaluation of the tool on

weathering products. Mean UCS measured per quadrat ranged from 2.91 – 4.41 MPa, with a mean standard deviation (SD) of 0.74 – 2.41 MPa (Table 7-1).

While the SilverSchmidt provided valid readings from quadrats 1 - 4, they were highly variable. It was observed that repeated measurements in the same position improved readings produced by the SilverSchmidt. This was inferred to be modification of the material being tested, with compression leading to densification. This meant that the tool was unsuitable for de-structured deposits due to modification of the material by crushing of matrix structure and reduction of pore space.

Table 7-1 Roedean access point, SilverSchmidt descriptive statistics.

Silver Schmidt	**Quadrat 1**	**Quadrat 2**	**Quadrat 3**	**Quadrat 4**	**Quadrat 5**	**Quadrat 6**	**Quadrat 7**	**Quadrat 8**
Number of valid readings	92	80	51	9	42	68	48	89
Mean UCS (MPa)	3.44	2.91	2.97	4.41	2.99	6.32	5.83	7.08
Standard deviation	1.006	0.887	0.737	2.405	1.114	3.489	4.305	4.455
Range (MPa)	1.9 – 7.22	1.55 – 7.22	1.73 – 6.06	2.28 – 8.79	1.73 – 5.78	1.9 – 15.99	1.73 – 19.14	1.9 – 17.31
Variance	1.012	0.786	0.542	5.782	1.241	12.173	18.532	19.844
Skewness	0.851	1.69	1.639	1.17	1.232	0.594	1.532	0.727
Kurtosis	1.525	5.857	5.222	-0.167	0.469	-0.438	1.667	-0.589
CIRIA density grade	N/A	N/A	N/A	N/A	C4 – A5	B3	A4 – A5	C2
CIRIA fracture grade	N/A	N/A	N/A	N/A	Low	High	High	High

SilverSchmidt quadrat 1 (Figure 7-2), located at the top of the section, comprises a buff brown soil with disaggregated flints and angular coarse chalk clasts (<50 mm diameter). The chalk clasts increase in size and frequency to the lower part of the quadrat (grid squares A6-10, B7-10, C8-10, D9 and E9). The mean UCS is 3.44 MPa, ranging 1.9 – 7.22 MPa, with relatively high SilverSchmidt UCS values coinciding with chalk clasts, while low UCS values and invalid results coincide in areas of soil fabric. There is apparent change in relief on the surface of the deposit, which is likely a slip plane. The deposit observed within this quadrat was not considered to be chalk.

SilverSchmidt quadrat 2 (Figure 7-2) is located on the upper section of cryoturbation lobe and covers graded Dm infill (if considered chalk). The infill comprises a churned Newhaven chalk and Head matrix,

light brown in colour with brilliant white clasts. The surface relief is concave, with an increased frequency of chalk clasts at the upper boundary with soil. Clasts grade down in size. In the separating chalk material in between the lobes, the frequency of chalk clasts is greater, assigned a Dc grade. The mean UCS measured is 2.91 MPa, ranging 1.55 – 7.22 MPa. Low and invalid readings are associated with the distal edge of the cryoturbated lobe – the Dc separating chalk material, while relatively higher values are associated with the low relief infill.

SilverSchmidt quadrat 3 (Figure 7-2) covers the base of a cryoturbated lobe, encompassing more developed Dc chalk that separates the cryoturbation lobes. The lobe infill consists of a brown chalky Head, with minor occurrences of Newhaven chalk clasts. The separating Dc chalk material is more developed, comprising chalk clasts with increasing frequency. The mean UCS is 2.97 MPa, ranging 1.73 – 6.1 MPa. Invalid and low UCS readings are associated with the separating Dc material, while higher readings are associated with soil that appears more homogenous, indicating that increased fracture frequency and spacing results in rebound energy loss.

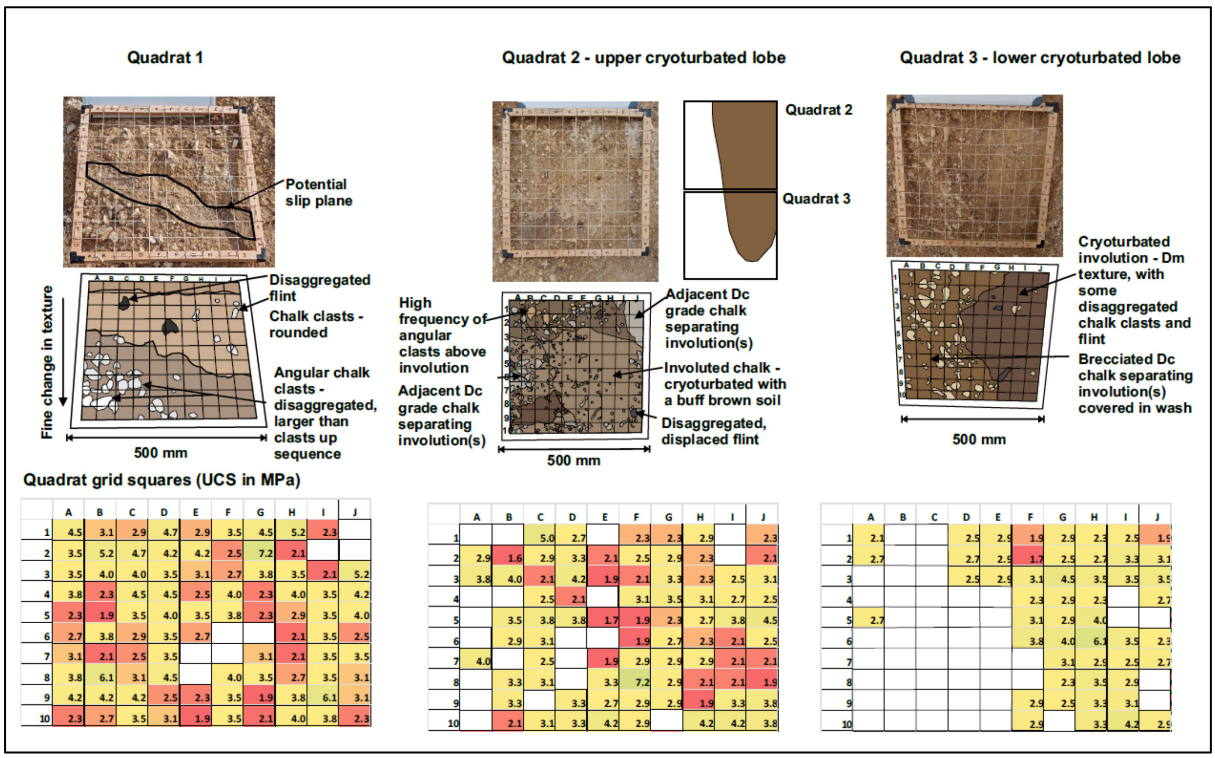


Figure 7-2 Roedean access point, SilverSchmidt quadrats 1 – 3 (white squares denote null readings).

SilverSchmidt quadrat 4 comprises a disaggregated, incompetent assemblage of buff white, Newhaven chalk breccia, set within a red-brown matrix (Figure 7-3). The mean UCS is 4.41 MPa ranging 2.28 – 8.79 MPa. Measurements are taken only from chalk clasts and are therefore subject to movement within the hosting matrix. This is reflected in the heat map of Figure 7-3, which illustrates that only

nine measurements were valid from 100 attempted. Chalk clast size increases with depth, indicating an increase in chalk competency.

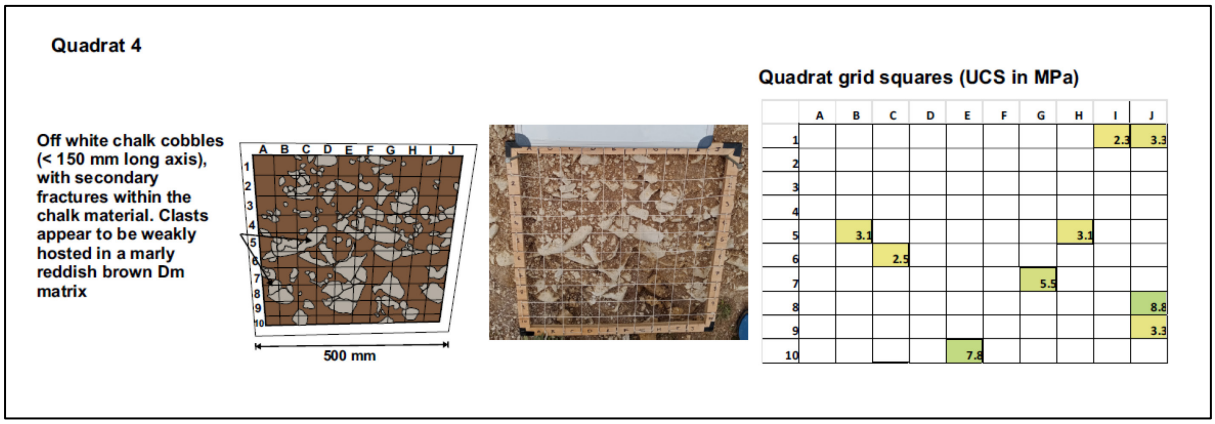


Figure 7-3 Roedean access point, SilverSchmidt quadrat 4 (white squares denote null readings).

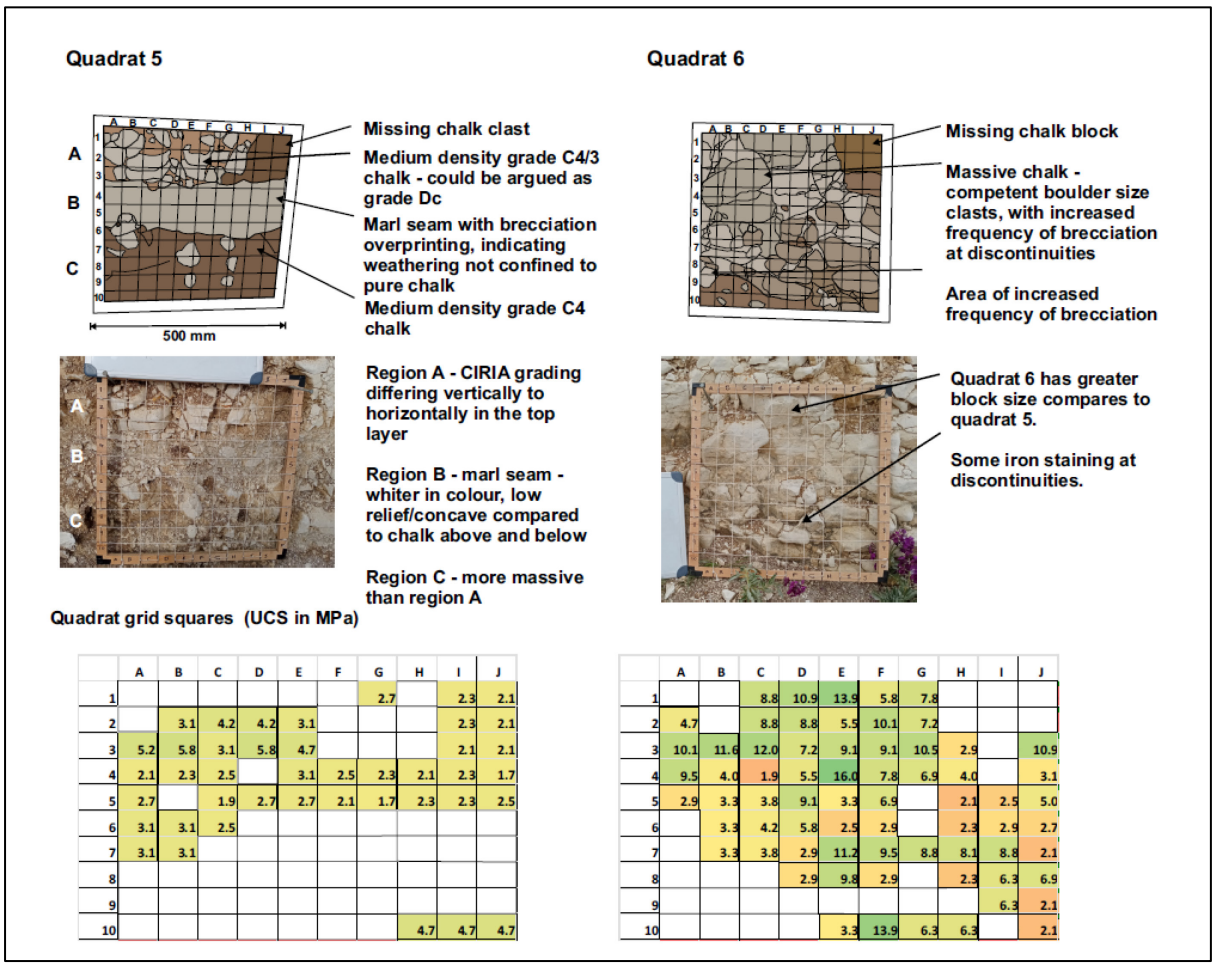
SilverSchmidt quadrats 5 - 8 were lower down-section, measuring structured chalk exclusively, covering CIRIA grades of A4 to C2. Mean UCS was 2.99 – 7.08 MPa, with mean SD ranging 1.11 – 4.46 MPa. These measurements increased down-section, with a non-uniform increase, and corresponded with low to high density CIRIA density grades (Table 7-1). The increasing UCS trend indicates that weathering grade improves with depth, however there is localised variation resulting in non-uniform increase in UCS, reflective of discrete pockets of weathering.

SilverSchmidt quadrat 5 (Figure 7-4) was located 7.0 m along section and comprises highly brecciated, buff-white, Newhaven Chalk (CIRIA grade C4 above, A4 below – open fractures), cross-cut by a low-relief, brecciated, altered marl layer (CIRIA grade A5 – closed fractures). The mean UCS of this quadrat is 2.99 MPa, with a range of 1.73 – 5.78 MPa.

The brecciation overprints both the Newhaven Chalk and the marl. This is interpreted as being cryoturbated through historic and contemporary freeze thaw processes (Murton, 2018a). The brecciation is reflected in the heat map (Figure 7-4), with invalid readings coinciding with heavily brecciated areas of chalk with open fractures, while the higher readings are taken from the less blocky marl layer, which has closed fractures.

SilverSchmidt quadrat 6 was located 13.0 m along section, stratigraphically below quadrat 5. The quadrat hosts more competent, off-white Newhaven chalk compared to quadrat 5, with a mean UCS of 6.32 MPa, ranging 1.9 – 15.99 MPa (Table 7-1). The chalk has iron staining and discontinuities are open <3 mm and filled with wash material in some instances. Discontinuity spacing varies horizontally and vertically in this quadrat; horizontally; grade B3 with discontinuities spaced at 60 – 100 mm and vertically; B3 with spacings of 60 – 120 mm.

Invalid readings coincide with missing blocks and areas of brecciation with open discontinuities and are reflected within the heat map (Figure 7-4) (such as grid squares A6-10, B8-10, C8-10, and D9-10). Where chalk blocks are larger with no apparent discontinuities, UCS readings are significantly greater (such as grid squares C1-4 to G1-4).



	A	B	C	D	E	F	G	H	I	J
1							2.7		2.3	2.1
2		3.1	4.2	4.2	3.1				2.3	2.1
3	5.2	5.8	3.1	5.8	4.7				2.1	2.1
4	2.1	2.3	2.5		3.1	2.5	2.3	2.1	2.3	1.7
5	2.7		1.9	2.7	2.7	2.1	1.7	2.3	2.3	2.5
6	3.1	3.1	2.5							
7	3.1	3.1								
8										
9										
10								4.7	4.7	4.7

	A	B	C	D	E	F	G	H	I	J
1			8.8	10.9	13.9	5.8	7.8			
2	4.7		8.8	8.8	5.5	10.1	7.2			
3	10.1	11.6	12.0	7.2	9.1	9.1	10.5	2.9		10.9
4	9.5	4.0	1.9	5.5	16.0	7.8	6.9	4.0		3.1
5	2.9	3.3	3.8	9.1	3.3	6.9		2.1	2.5	5.0
6		3.3	4.2	5.8	2.5	2.9		2.3	2.9	2.7
7		3.3	3.8	2.9	11.2	9.5	8.8	8.1	8.8	2.1
8				2.9	9.8	2.9		2.3	6.3	6.9
9									6.3	2.1
10					3.3	13.9	6.3	6.3		2.1

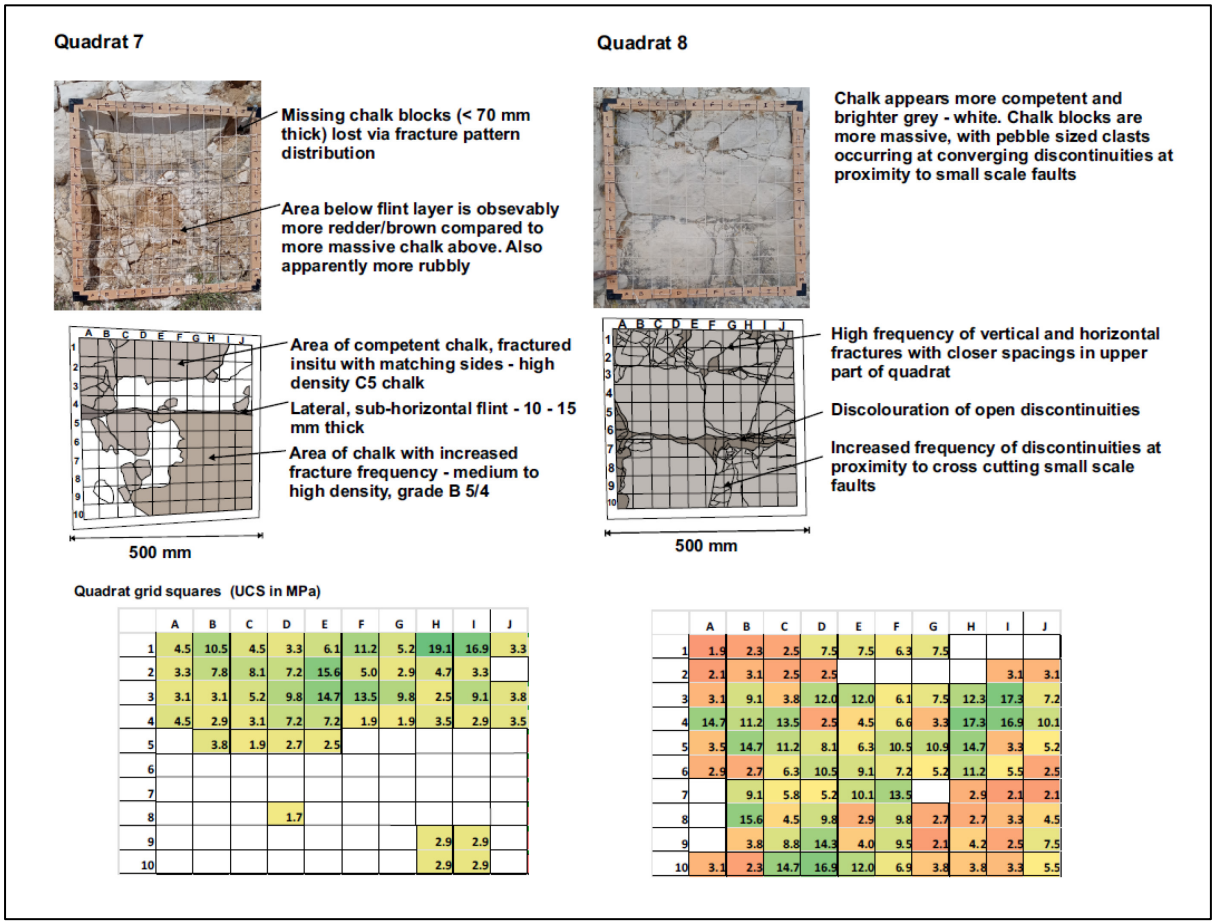
Figure 7-4 Roedean access point, SilverSchmidt quadrats 5 – 6 (white squares denote null readings).

SilverSchmidt quadrat 7 (Figure 7-5) was located 25.0 m along section and comprises white to buff-white Newhaven chalk cross-cut by a horizontal sheet flint (<15 – 20 mm thick). The chalk above the sheet flint is more massive compared to that below. Discontinuities are open (<3 mm) with spacings averaging 50 – 60 mm vertically (grade B4) and 50 mm horizontally (grade B4). The chalk below the sheet flint is highly brecciated and fractured with spacings <20 mm and fractures generally closed (grade A5). The mean UCS is 5.83 MPa, ranging 1.73 – 19.14 MPa (Table 7-1).

Invalid measurements are associated with the area below the flint layer. The chalk below this horizon is observably more weathered; red-brown in colour with increased brecciation (grade B5-4). Valid

measurements are associated with the more competent chalk above the flint horizon, which is graded as C5, high density chalk.

SilverSchmidt quadrat 8 was located 35.0 m along section and was the least weathered quadrat with a mean UCS of 7.1 MPa, ranging 1.9 – 17.31 MPa. Off-white Newhaven chalk; more competent than chalk observed in previous quadrats. This chalk is considered more massive despite the presence of discontinuities. Horizontal fractures are open >3 mm, with spacings of 200 – 250 mm, and are infilled, whereas vertical fractures are closed, with spacings of 150 – 200 mm. Horizontal; grade C2, vertical; A3. Invalid readings can be observed within the heat map as being associated with open discontinuities (Figure 7-5).



	A	B	C	D	E	F	G	H	I	J
1	4.5	10.5	4.5	3.3	6.1	11.2	5.2	19.1	16.9	3.3
2	3.3	7.8	8.1	7.2	15.6	5.0	2.9	4.7	3.3	
3	3.1	3.1	5.2	9.8	14.7	13.5	9.8	2.5	9.1	3.8
4	4.5	2.9	3.1	7.2	7.2	1.9	1.9	3.5	2.9	3.5
5		3.8	1.9	2.7	2.5					
6										
7										
8				1.7						
9								2.9	2.9	
10								2.9	2.9	

	A	B	C	D	E	F	G	H	I	J
1	1.9	2.3	2.5	7.5	7.5	6.3	7.5			
2	2.1	3.1	2.5	2.5					3.1	3.1
3	3.1	9.1	3.8	12.0	12.0	6.1	7.5	12.3	17.3	7.2
4	14.7	11.2	13.5	2.5	4.5	6.6	3.3	17.3	16.9	10.1
5	3.5	14.7	11.2	8.1	6.3	10.5	10.9	14.7	3.3	5.2
6	2.9	2.7	6.3	10.5	9.1	7.2	5.2	11.2	5.5	2.5
7		9.1	5.8	5.2	10.1	13.5		2.9	2.1	2.1
8		15.6	4.5	9.8	2.9	9.8	2.7	2.7	3.3	4.5
9		3.8	8.8	14.3	4.0	9.5	2.1	4.2	2.5	7.5
10	3.1	2.3	14.7	16.5	12.0	6.9	3.8	3.8	3.3	5.5

Figure 7-5 Roedean access point, SilverSchmidt quadrats 7 – 8 (white squares denote null readings).

Table 7-2 Roedean; SilverSchmidt derived UCS against texture and weathering grade.

SilverSchmidt quadrat	Texture	UCS (MPa)	UCS range (MPa)	SilverSchmidt CIRIA density grade	Hammer penetration (mm)	Hammer penetration range (mm)	Hammer CIRIA density grade	CIRIA fracture grade
5A	Highly brecciated chalk; open discontinuities	1.83	0 – 5.8	Low	11.83	9 – 15	Medium	B2 (block A)
5B	Highly brecciated marl; open and closed discontinuities	1.41	0 – 3.1	Low	14.16	5 – 20	Medium	C3-4 (block B)
5C	Brecciated; open discontinuities	0.47	0 – 4.7	Low	17.3	15 – 20	Medium	C4 (block C)
6	Jointed chalk; open discontinuities, blocky	6.32	1.9 – 15.99	High	7.7	5 – 12	High	B3
7	Brecciated chalk; above flint infilled horizon, open discontinuities	5.9	0 – 16.0	High	5.83	3 – 8	High	C5
	Brecciated; open discontinuities coalescing around flint infilled horizon	3.3	0 – 13.9	Medium	12.6	9 – 15	Medium	B5-4
8	Brecciated; open discontinuities	2.59	0 – 7.5	Medium	10.3	9 – 12	High	C5
	Jointed chalk; open discontinuities, blocky	8.57	2.5 – 17.3	High	6.3	5 – 8	High	B2
	Jointed chalk; open discontinuities, blocky	5.88	0 – 16.9	High	7.3	9 – 9	High	C3

Table 7-2 summarises CIRIA gradings based on lithological observations, SilverSchmidt-derived UCS and density estimated from the CIRIA hammer penetration test. The CIRIA hammer method yields consistently higher estimations of density compared to the SilverSchmidt. This is likely due to the presence of discontinuities within the rock mass, and their effect on rebound energy attenuation.

Equotip measurements

Six quadrats were set out to measure IDD with the Equotip, exclusively within structured chalk, graded C5 – A1. Measurement of de-structured grades was attempted, with Dm grades providing invalid readings and Dc providing relatively low readings. It was identified that as the Equotip sampler uses a small tungsten carbide ball, brecciated Dc chalk could be tested, but as Dc clasts are hosted in a puttified matrix, was considered ineffective as the clasts were likely mobile and subject to movement given external disturbance. Table 7-3 provides a summary of descriptive statistics and CIRIA gradings for each quadrat.

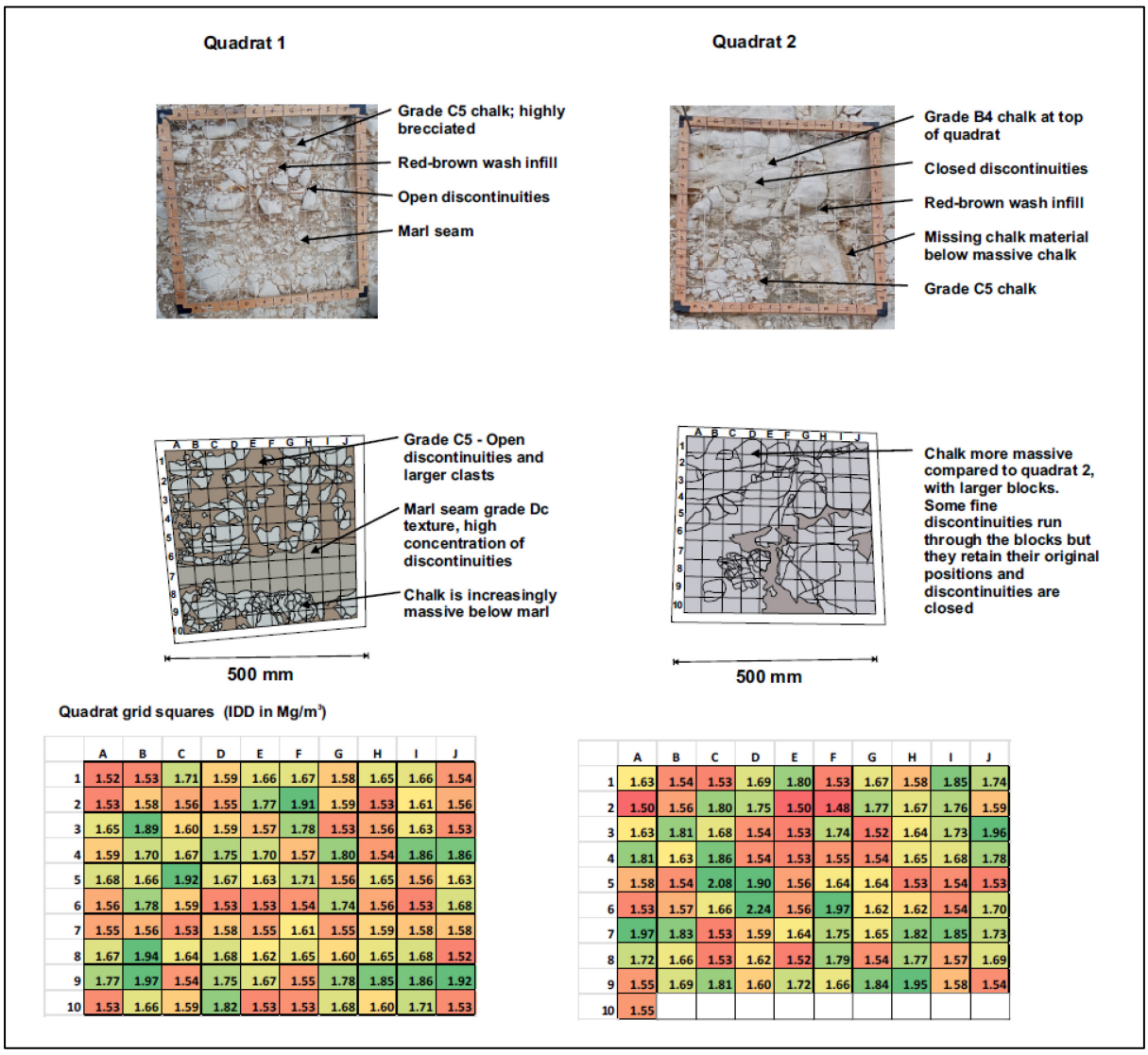
Table 7-3 Roedean access point; Equotip derived IDD descriptive statistics.

Equotip	Quadrat 1	Quadrat 2	Quadrat 3	Quadrat 4	Quadrat 5	Quadrat 6
Number of valid readings	100	91	100	100	100	100
Mean IDD (Mg/m^3)	1.65	1.67	1.70	1.78	1.73	1.85
Standard deviation	0.113	0.144	0.137	0.327	0.147	0.237
Range (MPa)	1.52 – 1.97	1.48 – 2.24	1.52 – 2.16	1.52 – 3.61	1.53 – 2.23	1.52 – 2.53
Variance	0.013	0.021	0.019	0.107	0.022	0.056
Skewness	1.109	1.225	1.098	3.349	0.697	0.985
Kurtosis	0.474	1.9	0.925	13.793	0.394	0.659
CIRIA density grade	Medium	Medium	High	High	High	High
CIRIA fracture grade	Dc to C5	B4 top C5 bottom	C3 – C/B5	C5 with A2 at base of quadrat	B5 – A5	A4

IDD increases down-section, with mean IDD ranging 1.64 – 1.85 Mg/m^3 (medium – high CIRIA density grades), which is evidence of improving CIRIA grade and reduced weathering with depth away from the cliff-top. Standard deviation appears low, ranging from 0.11 – 0.33 Mg/m^3, meaning the Equotip has provided relatively consistent readings at this site.

Equotip quadrat 1 frames brecciated Newhaven Chalk, overlying a brecciated marl. The chalk has discontinuities (<3 mm aperture) infilled with red-brown soil. 100 valid readings were measured,

yielding a mean IDD of 1.65 Mg/m^3, ranging 1.52 – 1.97 Mg/m^3. This chalk is graded as C5, with discrete areas of Dc grade material, while the IDD values correspond to a medium-density chalk. Figure 7-6 illustrates the position of the marl relative to the overlying chalk and the heat map demonstrates a highly variable IDD range within the quadrat area.



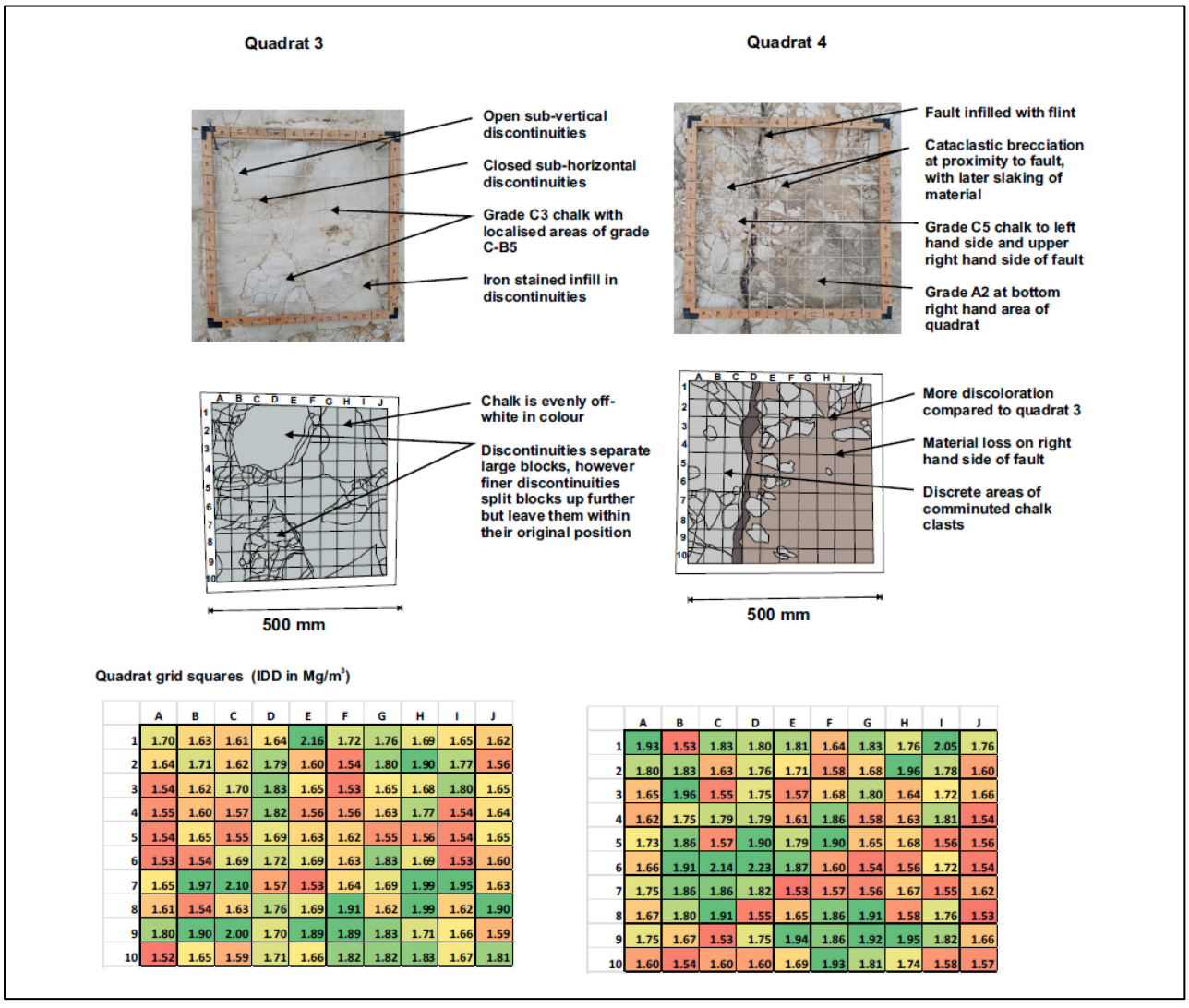
	A	B	C	D	E	F	G	H	I	J
1	1.52	1.53	1.71	1.59	1.66	1.67	1.58	1.65	1.66	1.54
2	1.53	1.58	1.56	1.55	1.77	1.91	1.59	1.53	1.61	1.56
3	1.65	1.89	1.60	1.59	1.57	1.78	1.53	1.56	1.63	1.53
4	1.59	1.70	1.67	1.75	1.70	1.57	1.80	1.54	1.86	1.86
5	1.68	1.66	1.92	1.67	1.63	1.71	1.56	1.65	1.56	1.63
6	1.56	1.78	1.59	1.53	1.53	1.54	1.74	1.56	1.53	1.68
7	1.55	1.56	1.53	1.58	1.55	1.61	1.55	1.59	1.58	1.58
8	1.67	1.94	1.64	1.68	1.62	1.65	1.60	1.65	1.68	1.52
9	1.77	1.97	1.54	1.75	1.67	1.55	1.78	1.85	1.86	1.92
10	1.53	1.66	1.59	1.82	1.53	1.53	1.68	1.60	1.71	1.53

	A	B	C	D	E	F	G	H	I	J
1	1.63	1.54	1.53	1.69	1.80	1.53	1.67	1.58	1.85	1.74
2	1.50	1.56	1.80	1.75	1.50	1.48	1.77	1.67	1.76	1.59
3	1.63	1.81	1.68	1.54	1.53	1.74	1.52	1.64	1.73	1.96
4	1.81	1.63	1.86	1.54	1.53	1.55	1.54	1.65	1.68	1.78
5	1.58	1.54	2.08	1.90	1.56	1.64	1.64	1.53	1.54	1.53
6	1.53	1.57	1.66	2.24	1.56	1.97	1.62	1.62	1.54	1.70
7	1.97	1.83	1.53	1.59	1.64	1.75	1.65	1.82	1.85	1.73
8	1.72	1.66	1.53	1.62	1.52	1.79	1.54	1.77	1.57	1.69
9	1.55	1.69	1.81	1.60	1.72	1.66	1.84	1.95	1.58	1.54
10	1.55									

Figure 7-6 Roedean access point, Equotip quadrats 1 – 2 (white squares denote null readings).

Equotip quadrat 2 (Figure 7-6) comprises more competent, blocky chalk compared to quadrat 1, however, yielded less valid results, with 99 valid measurements recovered. The chalk is noticeably whiter, with less red-brown wash and an absence of infill within discontinuities. Discontinuities are open <3 mm in the top half of the quadrat, leading to an assigned grade of B4, while at the bottom of the quadrat, the chalk has more intense brecciation and discontinuities are open >3 mm, assigned grade C5 (Figure 7-6). The measured mean IDD value of quadrat 2 is 1.67 Mg/m^3, corresponding to a medium density chalk, and ranging 1.48 – 2.24 Mg/m^3, (medium to high density) (Table 7-3).

Equotip quadrats 3 and 4 are less weathered than quadrats 1 and 2, and comprise significantly more competent, intact chalk. Equotip quadrat 3 (Figure 7-7) hosts competent, white Newhaven chalk, with infilled open fractures, with iron staining. There are two generations of discontinuities; wider spaced joints <250 mm, leading to a CIRIA fracture grade of C2, and secondarily, more tightly spaced discontinuities which coalesce around conjugate jointing, leading to a CIRIA fracture grade of C – B5. Measured mean IDD of the quadrat was 1.70 Mg/m^3, ranging 1.52 – 2.16 Mg/m^3, leading to a high CIRIA density grade (Table 7-3).



	A	B	C	D	E	F	G	H	I	J
1	1.70	1.63	1.61	1.64	2.16	1.72	1.76	1.69	1.65	1.62
2	1.64	1.71	1.62	1.79	1.60	1.54	1.80	1.90	1.77	1.56
3	1.54	1.62	1.70	1.83	1.65	1.53	1.65	1.68	1.80	1.65
4	1.55	1.60	1.57	1.82	1.56	1.56	1.63	1.77	1.54	1.64
5	1.54	1.65	1.55	1.69	1.63	1.62	1.55	1.56	1.54	1.65
6	1.53	1.54	1.69	1.72	1.69	1.63	1.83	1.69	1.53	1.60
7	1.65	1.97	2.10	1.57	1.53	1.64	1.69	1.99	1.95	1.63
8	1.61	1.54	1.63	1.76	1.69	1.91	1.62	1.99	1.62	1.90
9	1.80	1.90	2.00	1.70	1.89	1.89	1.83	1.71	1.66	1.59
10	1.52	1.65	1.59	1.71	1.66	1.82	1.82	1.83	1.67	1.81

	A	B	C	D	E	F	G	H	I	J
1	1.93	1.53	1.83	1.80	1.81	1.64	1.83	1.76	2.05	1.76
2	1.80	1.83	1.63	1.76	1.71	1.58	1.68	1.96	1.78	1.60
3	1.65	1.96	1.55	1.75	1.57	1.68	1.80	1.64	1.72	1.66
4	1.62	1.75	1.79	1.79	1.61	1.86	1.58	1.63	1.81	1.54
5	1.73	1.86	1.57	1.90	1.79	1.90	1.65	1.68	1.56	1.56
6	1.66	1.91	2.14	2.23	1.87	1.60	1.54	1.56	1.72	1.54
7	1.75	1.86	1.86	1.82	1.53	1.57	1.56	1.67	1.55	1.62
8	1.67	1.80	1.91	1.55	1.65	1.86	1.91	1.58	1.76	1.53
9	1.75	1.67	1.53	1.75	1.94	1.86	1.92	1.95	1.82	1.66
10	1.60	1.54	1.60	1.60	1.69	1.93	1.81	1.74	1.58	1.57

Figure 7-7 Roedean access point, Equotip quadrats 3 – 4.

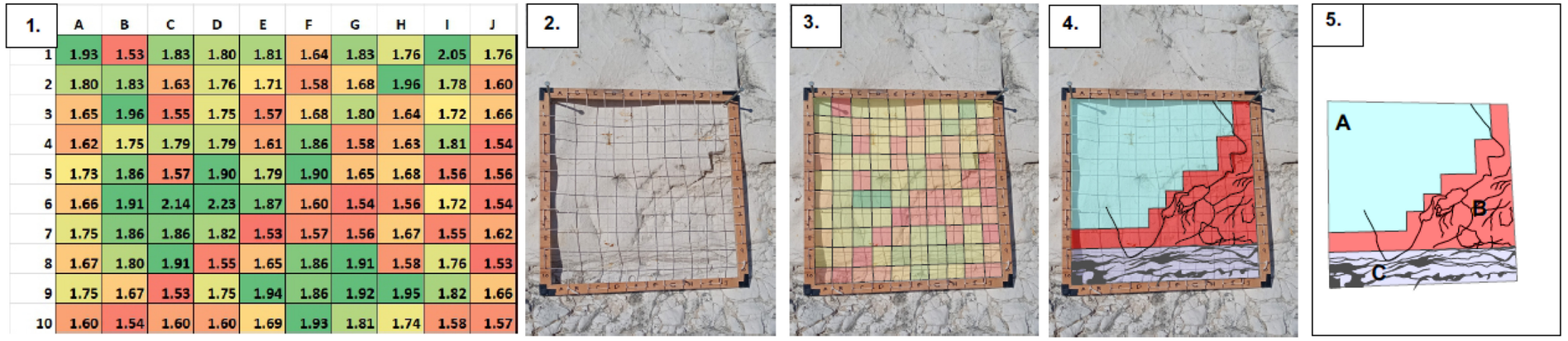
Equotip quadrat 4 (Figure 7-7) is brecciated with a high-angled, flint infilled fault cross-cutting the Newhaven chalk. Discontinuities within this area of brecciation are open >3mm and spaced >20 mm (grade C5). In the right-hand bottom corner of the quadrat, the chalk is graded A2 is significantly discoloured. Measured IDD ranges 1.52 – 3.61 Mg/m^3 with a mean density of 1.78 Mg/m^3 (high CIRIA density grade).

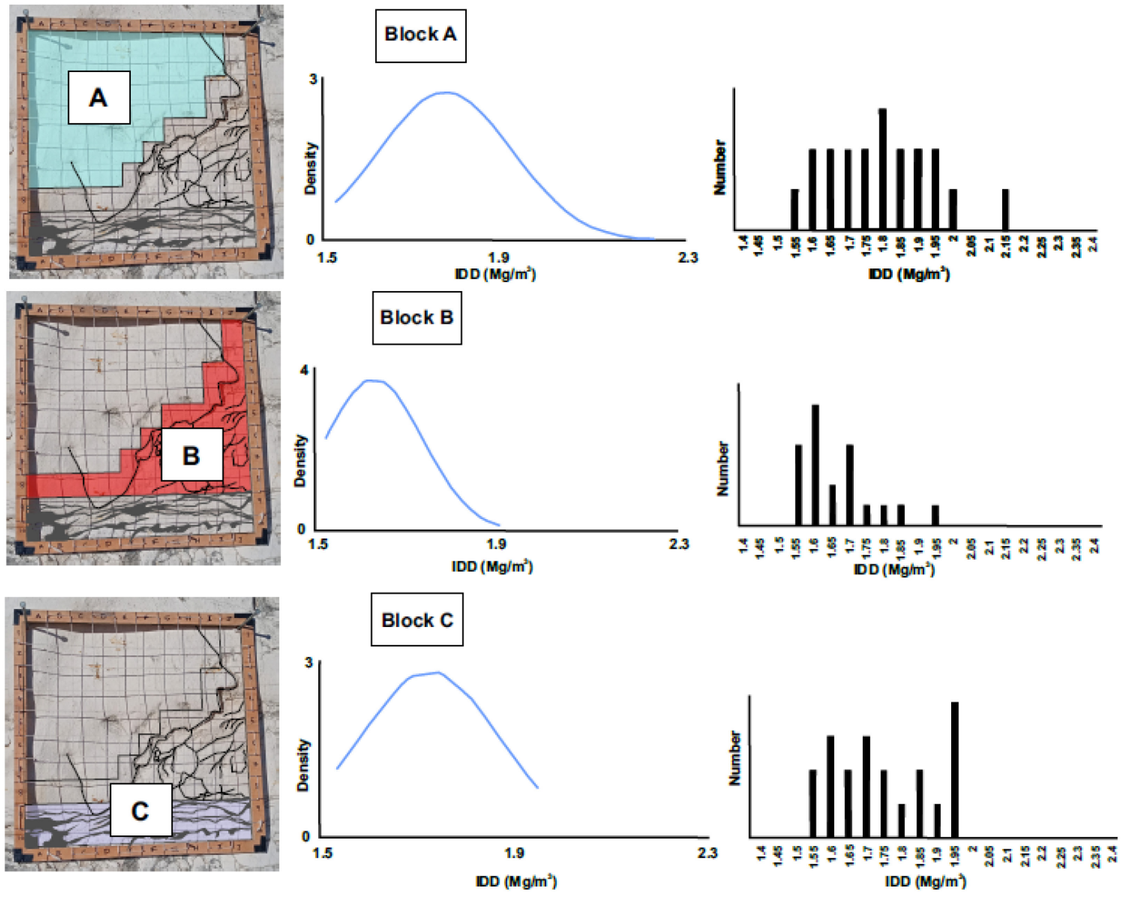
The brecciation is likely to be due to cataclastic processes, leading to small-scale discontinuity generation, which is then further exacerbated by water weakening and wet-dry cycles, leading to material loss. The chalk displays a high density, which would support the angular style of brecciation observed.

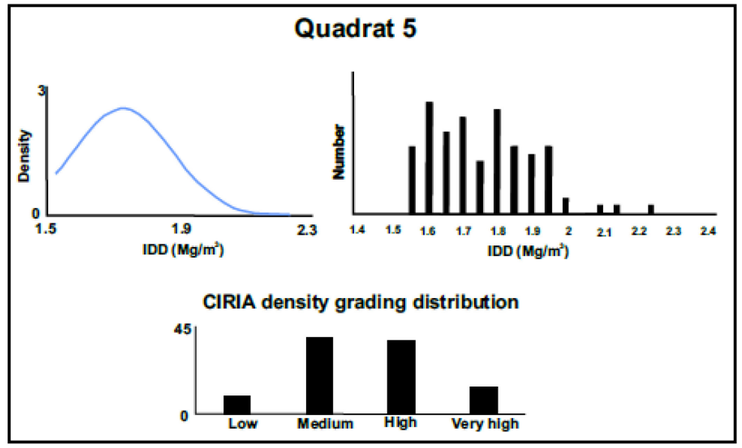
Quadrat 5 (Figure 7-8) is split into three discrete blocks based on the distribution of fractures and a heat map, highlighting the position of lower value readings associated with observed fractures. Block A is characterised as being intact grade A chalk, block B is characterised as brecciated grade B chalk, while block C is defined by a marl horizon with an anastomosing texture, darker in colour than the surrounding chalk.

96 valid readings were taken, with four being invalid due to surface texture. The greatest mean IDD was measured in grade A chalk (block A) at 1.77 Mg/m^3, and the lowest in grade B chalk (block B) at 1.63 Mg/m^3, with the intermediate value of 1.73 Mg/m^3 in the anastomosing marl (block C).

These results can be directly related to CIRIA grades, weathering, fracturing and sedimentology. Block A has the highest IDD and least statistical dispersion and variability from a measured mean value, with a CIRIA grade of A1. Block B has the lowest IDD and greatest dispersion owing to its brecciated nature with a CIRIA grade of B4. Block C with its marl seams causing small-scale textural changes leading to a CIRIA grade of A5 (Figure 7-8).







Descriptive statistics

Roedean Quadrat 5	Block A- grade A	Block B- grade B	Block G- anastomosing marl
Valid readings	51	25	20
Mode	1.567	1.537	1.534
Median	1.783	1.6	1.716
Mean	1.774	1.631	1.725
Range	1.534–2.23	1.525–1.906	1.534–1.948
Standard deviation	0.146	0.107	0.142
Coefficient of variability (%)	2.1	1.2	0.2
Skewness	0.284	1.256	0.75
Kurtosis	1.108	0.859	-1.312

Figure 7-8 Roedean access point, Equotip quadrat 5 and descriptive statistics. Quadrat 5 is split into three discreet blocks based on texture; A – grade A1 competent chalk, B – diagonal discontinuity underlain by a widely spaced anastomosing flaser marl and C – a horizontal band of flaser marl with a tight anastomosing structure. Blocks are described by statistical distribution of IDD.

Block A has a higher range of densities, but high-density readings are sparse in number compared to low density readings within this population. Block A is the least weathered block of the three (Table 7-4). Block B has a smaller number of readings than block A, and has a smaller density range, indicating lower densities can be associated with increased fracture frequency. Block C is the most weathered of the three blocks considered. Block C has a normal distribution, with little skew, indicating that density differences within this block were higher in range and more evenly distributed. Block C is weathered to an intermediate level compared to blocks A and B.

Table 7-4 Roedean access point, quadrat 5 degree of weathering.

EQ quadrat 5	**IDD (Mg/m^3)**	**IDD range (Mg/m^3)**	**CIRIA density grading**	**Fracture spacing (mm)**	**Fracture aperture (mm)**	**CIRIA fracture classification**	**Degree of weathering**
Block A	1.77	1.53 – 2.23	High	>600	Closed	A1	Least
Block B	1.63	1.60 – 1.91	Medium	20 < t < 60	< 3	B4	Most
Block C	1.73	1.53 – 1.94	High	< 20	Closed	A5	Intermediate

In terms of dispersion, the range for block A was the highest at 0.696, block C was the intermediate at 0.414, while block B was the lowest at 0.381. Standard deviation follows this trend (Figure 7-8). The greatest variance is associated with the grade A chalk at 0.021, while the marl is intermediate, and brecciated chalk the lowest, which was unexpected given the quality of the surface textures of each block – that said, this may be an effect of increased sample size related to block A in comparison to blocks B and C. This shows that in relatively unweathered, un-brecciated chalk, there are areas of particularly high IDD, while more weathered, brecciated chalks have more consistent, relatively low values compared to the less weathered.

The distribution of each of the blocks are markedly distinct, with block A showing positively skewed normal distribution, block B to a lesser extent, while block C exhibits near perfect normal distribution. This is reflected in the kurtosis of each of the blocks, with block C being platykurtic at -1.312, indicating that there are significantly less outliers compared to block B at 0.859 and block A at 1.108, which can be observed graphically in the degree of tailedness in Figure 7-8.

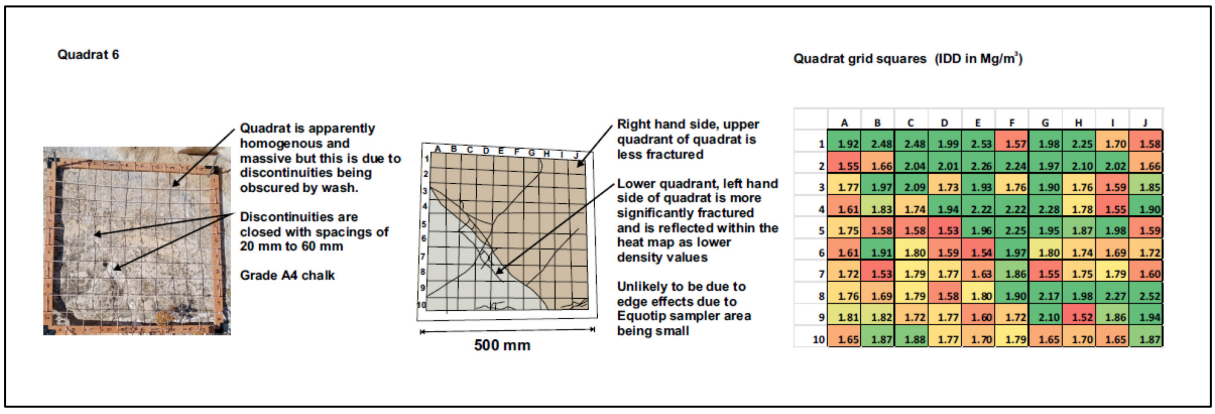
Owing to the disparity in sample size when quadrat 7 is broken down into blocks, a Welch's independent t-test was undertaken to evaluate the equality of averages. Block C was compared against block A, resulting in a t-statistic of -1.3 and a P-value of 0.201, indicating that there are no statistically significant differences between the two groups.

Block A, compared to block B, yields a T-value of 4.81 and a P-value of <0.01. The P-value indicates that there is a statistically significant difference between block A and B, while the T value indicates that block A has a higher mean IDD compared to block B.

When block B is compared with block C, the T-value is -2.447 and the P-value is 0.02, indicating that the mean IDD of block C is greater than block B and the P value of 0.02 indicates a statistically significant difference between the two data sets. These analyses, coupled with the observation of block B (against blocks A and C) allows inference that the degree of weathering is greatest in block B as a function of lower mean IDD and increased fracture intensity.

This analysis supports the hypothesis that the Equotip Leeb is an effective tool for investigation of differing rock textures and degree of weathering, in conjunction with field observations and industry standard grading.

Equotip quadrat 6 (Figure 7-9) initially appears to be the most homogenous quadrat of the six quadrats measured at Roedean. On closer inspection, it is possible to observe closed, fine fractures with a spacing of 20 – 60 mm running diagonally across the bottom left-hand side of the quadrat, resulting in a CIRIA fracture grade of A4.



	A	B	C	D	E	F	G	H	I	J
1	1.92	2.48	2.48	1.99	2.53	1.57	1.98	2.25	1.70	1.58
2	1.55	1.66	2.04	2.01	2.26	2.24	1.97	2.10	2.02	1.66
3	1.77	1.97	2.09	1.73	1.93	1.76	1.90	1.76	1.59	1.85
4	1.61	1.83	1.74	1.94	2.22	2.22	2.28	1.78	1.55	1.90
5	1.75	1.58	1.58	1.53	1.96	2.25	1.95	1.87	1.98	1.59
6	1.61	1.91	1.80	1.59	1.54	1.97	1.80	1.74	1.69	1.72
7	1.72	1.53	1.79	1.77	1.63	1.86	1.55	1.75	1.79	1.60
8	1.76	1.69	1.79	1.58	1.80	1.90	2.17	1.98	2.27	2.52
9	1.81	1.82	1.72	1.77	1.60	1.72	2.10	1.52	1.86	1.94
10	1.65	1.87	1.88	1.77	1.70	1.79	1.65	1.70	1.65	1.87

Figure 7-9 Roedean access point, Equotip quadrat 6.

Quadrat 6 has a mean IDD of 1.85 Mg/m^3, ranging 1.52 – 2.53 Mg/m^3, corresponding to high CIRIA density grading. By plotting IDD against the rock surface texture and applying a heat map, it is possible to observe that higher IDD values are associated with the areas of chalk that do not have significant discontinuities, while lower IDD values are associated with regions of chalk where discontinuities are present, persistent, and-cross cutting.

Splitting the quadrat into two discrete areas (Table 7-5), the upper area with lack of discontinuities has a mean IDD of 1.89 Mg/m^3, ranging 1.52 – 2.53 Mg/m^3 and corresponding high-density CIRIA grade,

while the bottom area of the quadrat has a mean IDD of 1.72 Mg/m^3, ranging 1.53 – 1.91 Mg/m^3 (high-density CIRIA grade).

Table 7-5 Roedean access point, quadrat 6 degree of weathering.

EQ quadrat 6	IDD (Mg/m^3)	IDD range (Mg/m^3)	CIRIA density grade	Fracture spacing (mm)	Fracture aperture (mm)	CIRIA fracture grade	Degre of weathering
Upper unfractured area	1.89	1.52 – 2.53	High	Closed	>600	A1	Least
Lower fractured area	1.72	1.53 – 1.91	High	Closed	<20	A5	Most

While both discrete areas are categorised as high density using the CIRIA method, this demonstrates that the Equotip is sensitive enough to measure small density changes and quantify weathering related to discontinuities.

Table 7-6 presents a summary of CIRIA gradings based on lithological observations, Equotip measured IDD and density estimated from the CIRIA hammer penetration test. Comparing the Equotip measured IDD with CIRIA hammer density estimations shows discrepancy; most hammer estimations fall within the medium - high density classifications, while the Equotip measured densities range from low - high densities. This is likely due to the relative sensitivity of the Equotip providing higher resolution readings compared to the hammer estimation.

Table 7-6 Roedean, Equotip derived IDD against texture and weathering grade.

Equotip quadrat	Texture	IDD (Mg/m^3)	IDD range (Mg/m^3)	Equotip CIRIA density grade	Hammer penetration (mm)	Hammer penetration range (mm)	Hammer CIRIA density grade	CIRIA fracture grade
1	Highly brecciated, open discontinuities	1.65	1.52 – 1.97	Medium	14	11 – 17	Medium	C5
2	Brecciated, closed discontinuities	1.67	1.48 – 2.24	Medium	15.3	12 – 18	Medium	B4
	Brecciated, open discontinuities	1.37	0.0 – 1.97	Low	17.6	15 – 20	Medium	C5
3	Brecciated, open discontinuities	1.70	1.53 – 2.10	High	12.3	11 – 15	Medium	C3
	Brecciated, coalescing around conjugate joint	1.69	1.52 – 2.16	Medium	12.3	11 – 15	Medium	C5
4	Cataclastic; coalescing around fault	1.70	1.52 – 2.54	High	15	12 – 18	Medium	C5
	Homogenous chalk	1.80	1.56 – 2.54	High	13.3	11 – 17	Medium	A2
5	Anastomosing marl	1.73	1.53 – 2.05	High	13	12 – 15	Medium	A1
	Homogenous chalk	1.77	1.54 – 2.23	High	10	10 – 11	High	B4
	Brecciated, closed discontinuities	1.63	1.53 – 1.95	Medium	13.6	12 – 15	Medium	A5
6	Homogenous chalk	1.89	1.52 – 2.53	High	9	8 – 10	High	A4
	Brecciated, closed discontinuities	1.72	1.53 – 1.91	High	10.3	10 – 11	High	A5

All Equotip readings measured at Roedean appear to be within a reasonable range for a medium - high density chalk, apart from quadrat 3, where the highest reading in that range was 3.61 Mg/m^3. This is considered an outlier as it was identified that a sub-vertical sheet flint was measured.

It was identified that within each quadrat, there could be multiple CIRIA grades of chalk, and that other features, such as marl horizons, could skew results and that the Equotip was particularly suitable for investigation of these features, given the tool's sensitivity and small sampling surface area.

7.2.2 Portobello Outfall research site

At Portobello outfall, eight quadrats were set out with the aim of investigating geological features, characterise the Newhaven Chalk Formation and compare both the SilverSchmidt and Equotip Leeb instruments (Figure 7-10). Observation of lithology and heat maps for both the SilverSchmidt-measured UCS and Equotip-measured IDD were generated for each quadrat.

The aim of quadrats 1 – 4 was to investigate the material properties of a highly weathered conjugate fault, where discontinuity-driven weathering has resulted in significant material loss. Quadrats 1 – 4 were distributed on the eastern side of the outfall. At this locality, the SilverSchmidt was used exclusively, with 400 readings undertaken.

The aim of quadrats 5 – 8 was to investigate the properties of the Newhaven Chalk Formation, located on the western side of the outfall. Both the SilverSchmidt and Equotip were used within each quadrat, allowing comparison of each instrument. 400 readings were undertaken for each instrument.

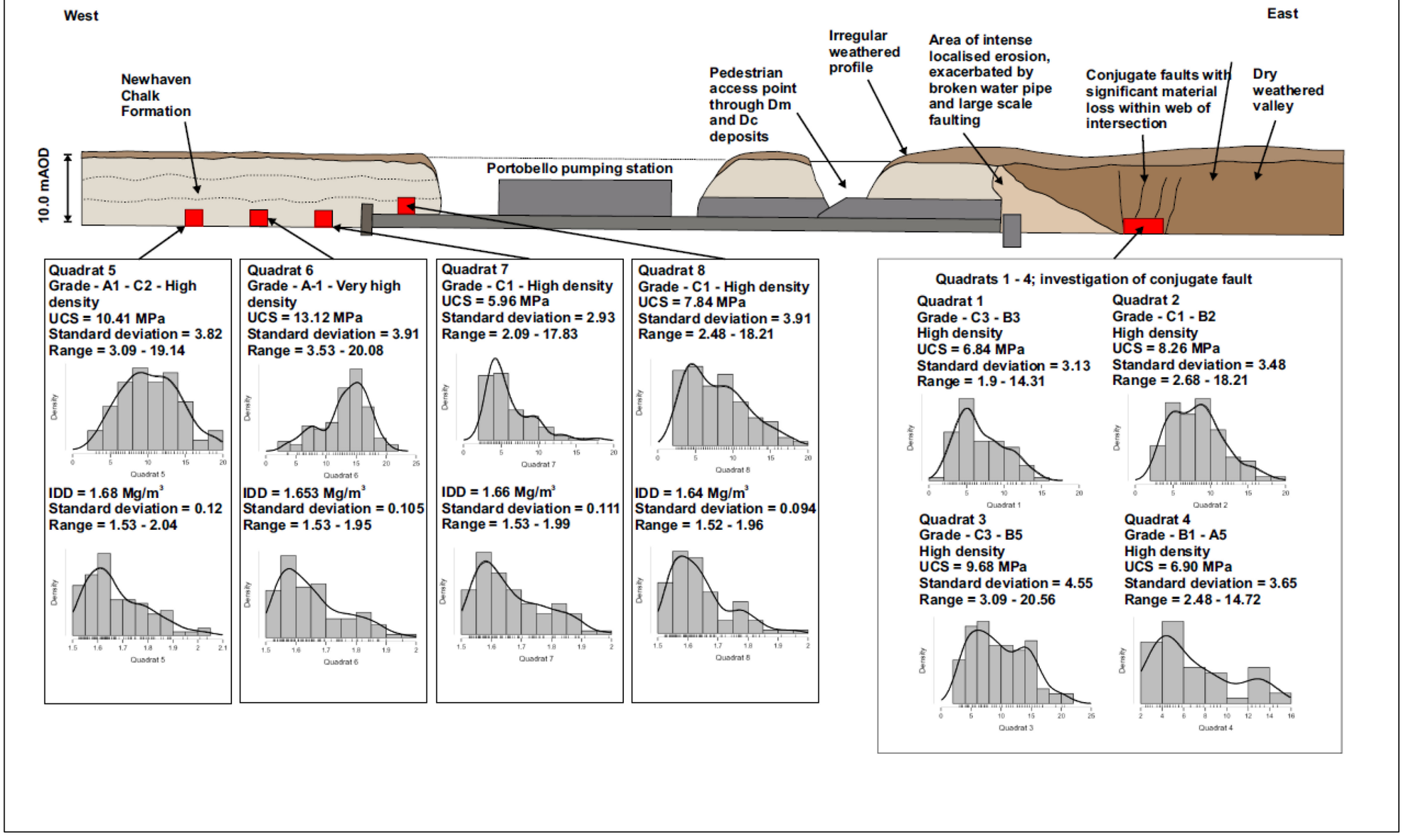
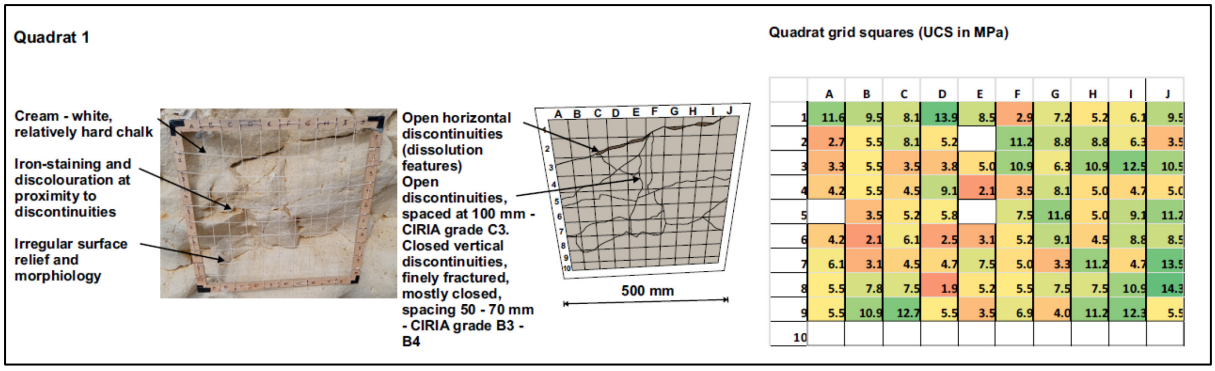


Figure 7-10 Schematic cross section of Portobello Outfall, Telscombe Cliffs.

Quadrats 1 – 4

Quadrat 1 (Figure 7-11) was positioned parallel to the cliff face, on the western limb of a conjugate fault that has undergone significant material loss. The chalk is iron stained, cream to white Newhaven chalk, dominated by open (>3 mm) horizontal discontinuities with 100 mm spacing; with some dissolution observed, classified as CIRIA grade C3. Vertical discontinuities are characterised by 50 – 70 mm spacings and apertures <3mm; assigned CIRIA grade B3 - B4.

87 valid SilverSchmidt readings from 100 were measured. These range from 1.9 – 14.31 MPa, with a mean UCS of 6.84 MPa, corresponding to a high-density chalk. Missing values correspond with high relief areas of chalk where the instrument could not reach (bottom of quadrat) and missing readings in the upper area correspond with discontinuities and dissolution features.

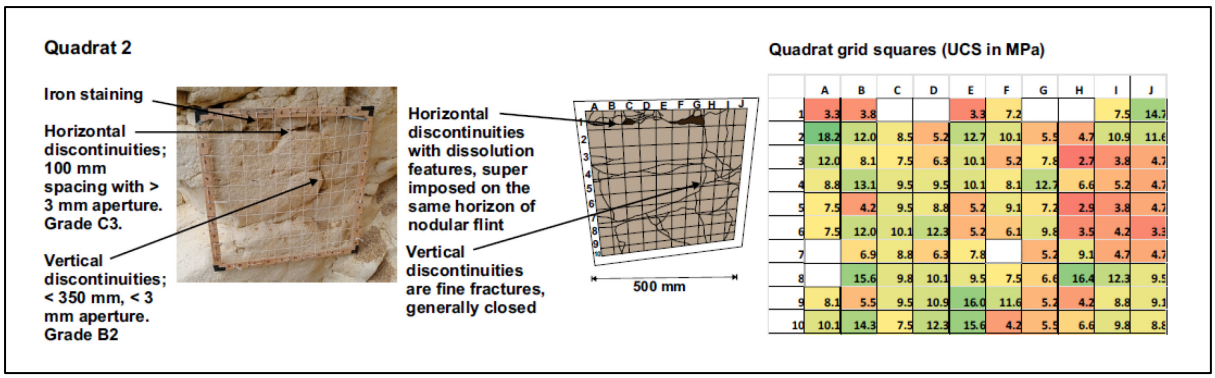


	A	B	C	D	E	F	G	H	I	J
1	11.6	9.5	8.1	13.9	8.5	2.9	7.2	5.2	6.1	9.5
2	2.7	5.5	8.1	5.2		11.2	8.8	8.8	6.3	3.5
3	3.3	5.5	3.5	3.8	5.0	10.9	6.3	10.9	12.5	10.5
4	4.2	5.5	4.5	9.1	2.1	3.5	8.1	5.0	4.7	5.0
5		3.5	5.2	5.8		7.5	11.6	5.0	9.1	11.2
6	4.2	2.1	6.1	2.5	3.1	5.2	9.1	4.5	8.8	8.5
7	6.1	3.1	4.5	4.7	7.5	5.0	3.3	11.2	4.7	13.5
8	5.5	7.8	7.5	1.9	5.2	5.5	7.5	7.5	10.9	14.3
9	5.5	10.9	12.7	5.5	3.5	6.9	4.0	11.2	12.3	5.5
10										

Figure 7-11 Portobello Outfall, quadrat 1 (white squares denote null readings).

Quadrat 2 (Figure 7-12) was positioned on the western internal face of the fault, perpendicular to the cliff face. The chalk is cream to white Newhaven chalk, with iron staining. Horizontal discontinuities are open >3 mm at 100 mm spacing, graded as C3, while vertical discontinuities are up to 350 mm spaced, and open <3 mm, graded B2.

93 valid SilverSchmidt readings were taken from 100, with missing readings corresponding with more significantly brecciated areas. The SilverSchmidt derived UCS range was 1.68 – 18.21 MPa, with a mean UCS value of 8.26 MPa, corresponding to a high-density chalk.

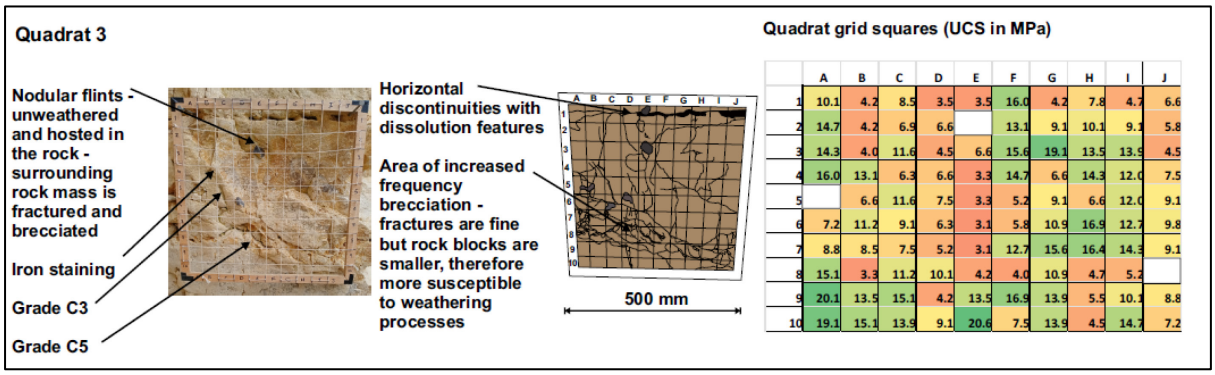


	A	B	C	D	E	F	G	H	I	J
1	3.3	3.8			3.3	7.2			7.5	14.7
2	18.2	12.0	8.5	5.2	12.7	10.1	5.5	4.7	10.9	11.6
3	12.0	8.1	7.5	6.3	10.1	5.2	7.8	2.7	3.8	4.7
4	8.8	13.1	9.5	9.5	10.1	8.1	12.7	6.6	5.2	4.7
5	7.5	4.2	9.5	8.8	5.2	9.1	7.2	2.9	3.8	4.7
6	7.5	12.0	10.1	12.3	5.2	6.1	9.8	3.5	4.2	3.3
7		6.9	8.8	6.3	7.8		5.2	9.1	4.7	4.7
8		15.6	9.8	10.1	9.5	7.5	6.6	16.4	12.3	9.5
9	8.1	5.5	9.5	10.9	16.0	11.6	5.2	4.2	8.8	9.1
10	10.1	14.3	7.5	12.3	15.6	4.2	5.5	6.6	9.8	8.8

Figure 7-12 Portobello Outfall, quadrat 2 (white squares denote null readings).

Quadrat 3 (Figure 7-13) was positioned on the eastern face of the fault, opposite quadrat 2 and perpendicular to the cliff face. There was increased brecciation in the lower left-hand quadrant of the quadrat, with spacings <20 mm and open >3 mm, graded C5, while in the remaining area of the quadrat, discontinuities were more widely spaced at 60 – 200 mm, leading to grade C3.

Quadrat 3 had 97 valid SilverSchmidt readings from a possible 100 attempts, ranging 3.09 – 20.56 MPa, with a mean UCS value of 9.68 MPa, classified as a high-density chalk.



	A	B	C	D	E	F	G	H	I	J
1	10.1	4.2	8.5	3.5	3.5	16.0	4.2	7.8	4.7	6.6
2	14.7	4.2	6.9	6.6		13.1	9.1	10.1	9.1	5.8
3	14.3	4.0	11.6	4.5	6.6	15.6	19.1	13.5	13.5	4.5
4	16.0	13.1	6.3	6.6	3.3	14.7	6.6	14.3	12.0	7.5
5		6.6	11.6	7.5	3.3	5.2	9.1	6.6	12.0	9.1
6	7.2	11.2	9.1	6.3	3.1	5.8	10.9	16.9	12.7	9.8
7	8.8	8.5	7.5	5.2	3.1	12.7	15.6	16.4	14.3	9.1
8	15.1	3.3	11.2	10.1	4.2	4.0	10.9	4.7	5.2	
9	20.1	13.5	15.1	4.2	13.5	16.9	13.9	5.5	10.1	8.8
10	19.1	15.1	13.9	9.1	20.6	7.5	13.9	4.5	14.7	7.2

Figure 7-13 Portobello Outfall, quadrat 3 (white squares denote null readings).

Quadrat 4 (Figure 7-14) is positioned on the eastern limb of the conjugate fault, parallel to the cliff face. The chalk is Newhaven Chalk and has vertical open discontinuities of <3 mm and a spacing of 200 – 600 mm, classified as grade B2. Horizontal discontinuities are closed, with a spacing of 50 – 100 mm, graded as A3.

51 Valid SilverSchmidt readings were recorded, with 49 invalid readings corresponding to areas of material loss in the left-hand region of the quadrat, and with high surface relief and discontinuities in the lower area of the quadrat. The UCS range was 2.48 – 14.72 MPa, with a mean of 6.90 MPa; classified as high-density.

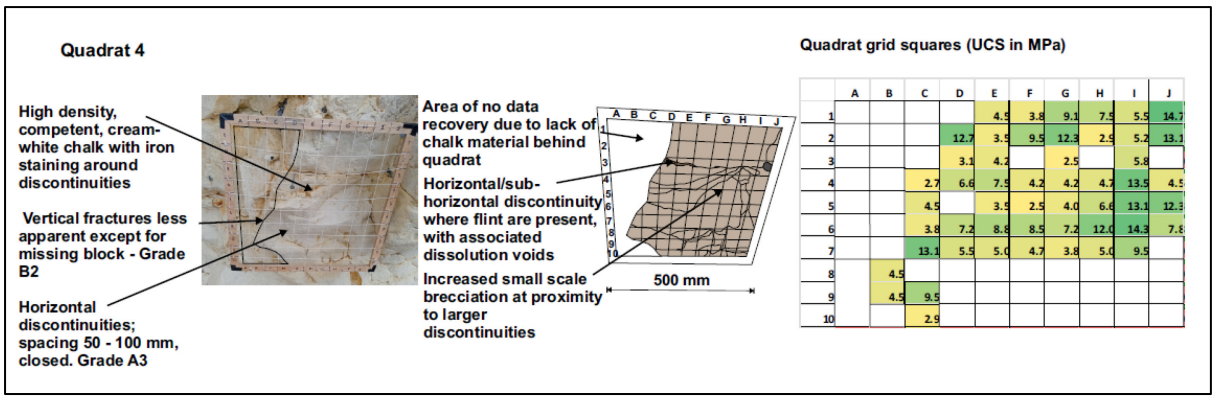


Figure 7-14 Portobello Outfall, quadrat 4 (white squares denote null readings).

Figure 7-15 shows a summary diagram of the analyses undertaken at this fault. It was hypothesised that the chalk that comprises the conjugate fault would be a low-medium strength, medium to high density chalk, which had led to intense brecciation and exacerbated material loss. In terms of CIRIA grade and rock competency, these rock surfaces were graded as C – A grade structured chalk, and previous analysis using hammer pick penetration estimated density as high.

Discontinuity spacing at this fault was in the CIRIA ranges of 1 – 5 on the surfaces parallel to the cliff line (quadrats 1 and 4), and up to grade 5 on the fault surfaces perpendicular to the cliff (quadrats 2 and 3). Grade 5 indicates that the spacing of fractures is <20 mm, which would contribute intense fracturing. Observation of grade 5 fracture spacings occurring perpendicular to one another, is evidence that they intersect, leading to blocky material loss.

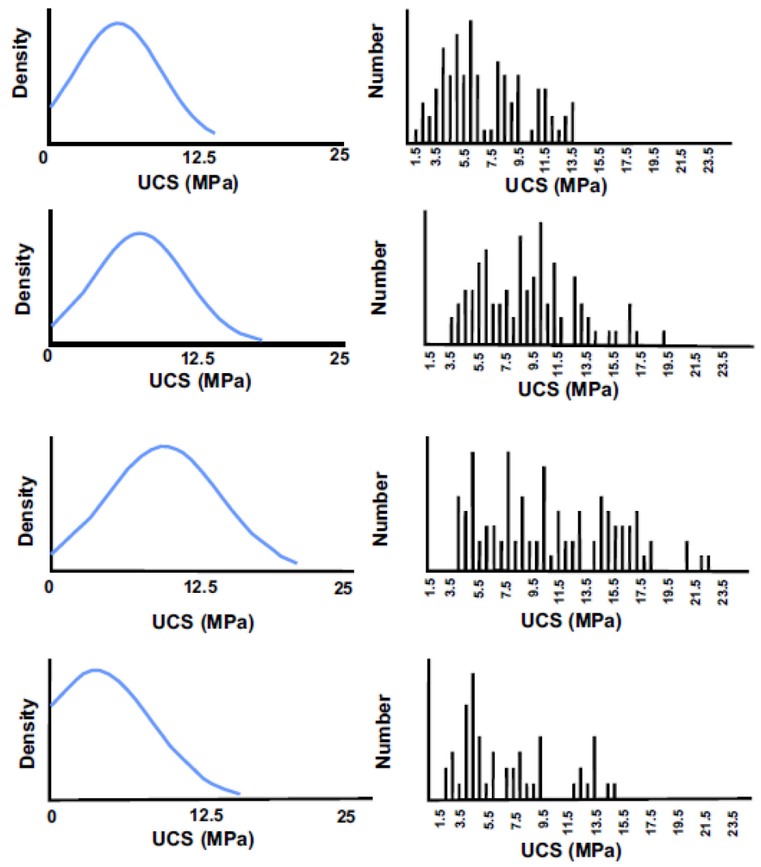


Quadrat 1
Grade - C3 - B3
High density
UCS = 6.84 MPa
Standard deviation = 3.13
Range = 1.9 - 14.31

Quadrat 2
Grade - C1 - B2
High density
UCS = 8.26 MPa
Standard deviation = 3.48
Range = 2.68 - 18.21

Quadrat 3
Grade - C3 - B5
High density
UCS = 9.68 MPa
Standard deviation = 4.55
Range = 3.09 - 20.56

Quadrat 4
Grade - B1 - A5
High density
UCS = 6.90 MPa
Standard deviation = 3.65
Range = 2.48 - 14.72



Conjugate fault, Portobello - Quadrats 1 - 4

Portobello fault investigation	Quadrat 1	Quadrat 2	Quadrat 3	Quadrat 4
CIRIA grade	C1 – B3 high density	C1 – B2 high density	C3 – B5 high density	B1 – A5 high density
Missing	13	7	4	49
Coefficient of variability (%)	45.7	42.1	46.4	52.9
Skewness	0.558	0.581	0.384	0.776
Kurtosis	-0.621	-0.083	-0.824	-0.688

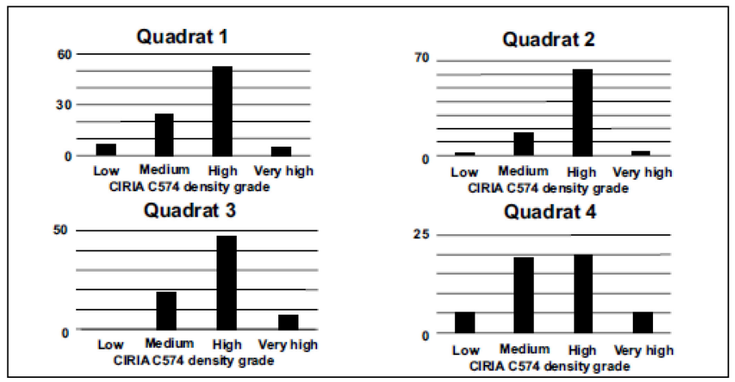


Figure 7-15 Portobello Outfall, quadrats 1 - 4 and descriptive statistics.

Quadrats 3 and 2 have the least invalid readings, with 4 and 7 readings lost from 100 respectively, quadrat 1 is missing 13 readings, while quadrat 4 has significantly more missing readings at 49 lost. When linked to CIRIA gradings, it is possible to observe that of the four quadrats, the highest reading loss corelates to a B1 – A5 grade (Table 7-7). This is because in lower grades of chalk, where fractures are more widely spaced (i.e., grades 1 – 4) and with closed discontinuities, the chalk has increased surface areas without discontinuities where a competent reading can be taken. Similarly, bias occurs where fractures are open (grades B and C), the SilverSchmidt would be preferentially positioned within areas where chalk was competent, whereby the user would avoid open discontinuities. Grade A5 however, results in a significant loss of readings as fractures are closed, and intense in terms of spacings, which leads to rebound energy loss along closed discontinuities.

In quadrats 1 – 4 (Figure 7-15) mean UCS ranges are 6.84 – 9.75 MPa for all four quadrats and are all classified as high density. The ranges of measured values for each quadrat are 1.9 – 20.56 MPa. The greatest individual UCS range of the quadrats is quadrat 3, which is 17.47 MPa, while the lowest is quadrat 4, at 12.24 MPa (Table 7-7).

Table 7-7 Portobello Outfall, quadrats 1 - 4 descriptive statistics for SilverSchmidt.

SilverSchmidt	Quadrat 1	Quadrat 2	Quadrat 3	Quadrat 4
Number of valid readings	87	93	97	51
Mean UCS (MPa)	6.84	8.26	9.68	6.90
Standard deviation	3.13	3.48	4.55	3.65
Range (MPa)	1.9 – 14.31	2.68 – 18.21	3.09 – 20.56	2.48 – 14.72
Variance	9.76	12.08	20.70	13.33
Skewness	0.59	0.58	0.40	0.78
Kurtosis	-0.621	-0.083	-0.827	-0.688
CIRIA density grade	High	High	High	High
CIRIA fracture grade	Horizontal C3, vertical B3-4	Horizontal C3, vertical B2	C5 to C3	Horizontal A3, vertical B4

Quadrats 1 (1.9 – 14.31 MPa) and 4 (2.48 – 14.72 MPa) have lower UCS ranges compared to quadrats 2 (2.68 – 18.21 MPa) and 3 (3.09 – 20.56 MPa). This indicates that the surface of the cliff (more exposed to the elements and weathering processes) has a lower UCS as the result of this exposure, compared to the material behind the cliff face, with UCS increasing into the rock mass away from the cliff face. This supports the hypothesis that a rock mass that is subject to weathering processes and wave action are more weathered and lower in UCS compared to a rock masses internal material that is not.

By comparing quadrats, it is possible to observe that quadrats 1 and 4 (parallel to the cliff face) are more positively skewed than quadrats 2 and 3 (perpendicular to the cliff face – i.e., measured within the cliff), which indicates that quadrats 1 and 4 have a higher distribution of lower density readings.

The results show more intense fracture weathering leads to greater erosive processes at this locality, despite having a relatively high CIRIA density grade and ranging discontinuity grades. Should the rock have been of a lower density, then the likelihood of intense fracturing would have been lower. This is important as a lower density rock would not have been able to have supported an intersecting intense fracture regime, which has led to blocky material loss. This is significant as it identifies that high density deposits are vulnerable to weathering processes due to their intrinsic properties.

Quadrats 5 – 8

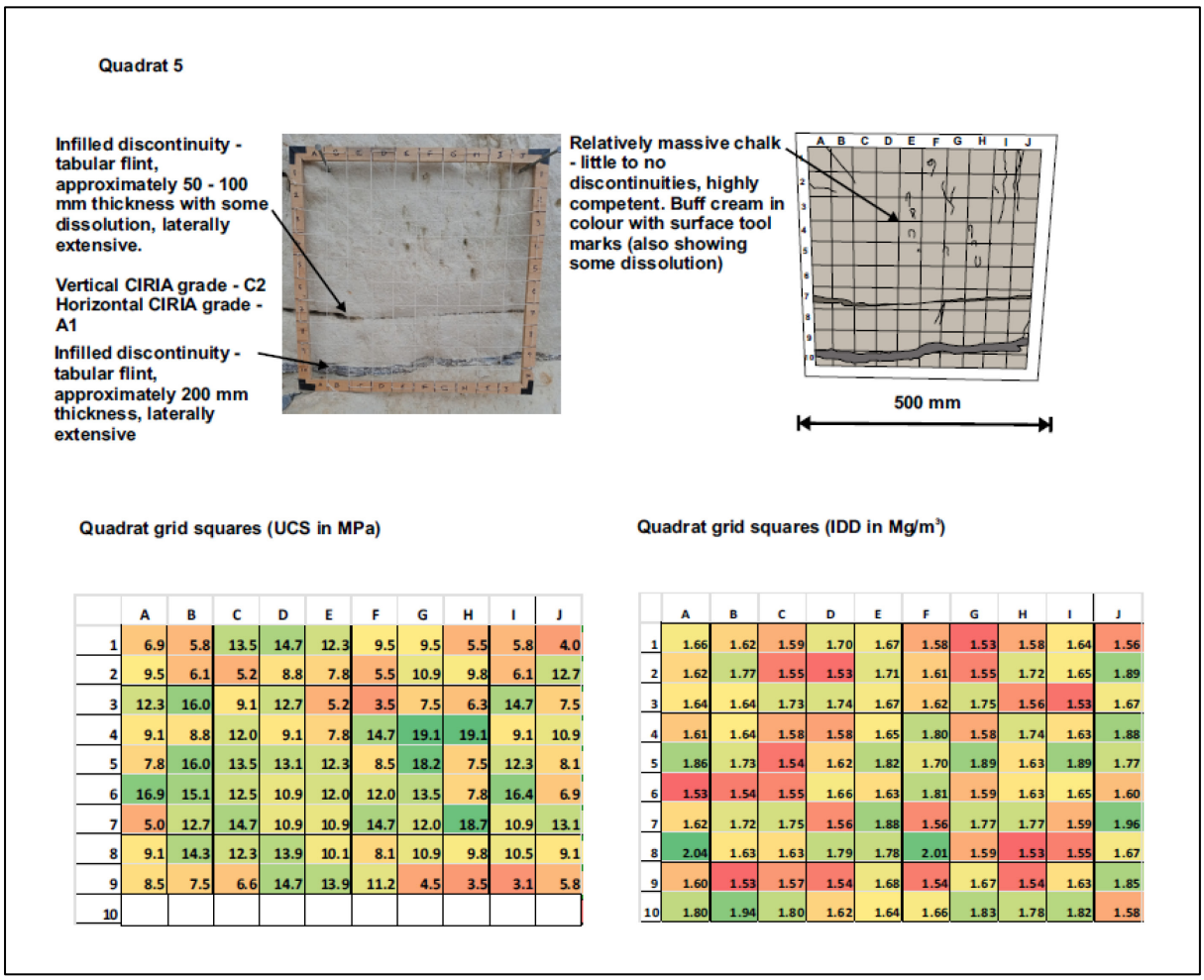
400 readings were recorded using the SilverSchmidt and Equotip over quadrats 5 to 8, with CIRIA C574 grading ranging from medium - high density, and discontinuity gradings of C1 and C2 to A1. The measured SilverSchmidt UCS ranges for all four quadrats are 2.09 – 20.08 MPa, with 15 invalid readings from 400 attempted measurements. For the Equotip, the IDD ranges are 1.522 – 2.035 Mg/m^3, with all measurement attempts valid. The measurements taken from this area reflect the relatively unweathered nature of the section, compared to the measurements taken to the east of the dry valley.

Quadrat 5 was located 100 m west of the outfall infrastructure. The quadrat objective was competent Newhaven Chalk, which was cross-cut by a flint infilled horizon (Figure 7-16). The quadrat had fracture spacings of >600 mm, and the fractures were closed, resulting in a CIRIA grade A1. The quadrat is cross-cut by a horizontal discontinuity, which is open >3 mm due to dissolution, which has resulted in a secondary grade of C1.

100 SilverSchmidt UCS measurements were taken (Figure 7-16), of which 90 were valid. The UCS range was 3.09 – 19.14 MPa, with a mean UCS of 10.41 MPa (high CIRIA density grade). Invalid measurements correspond with the contact between the relatively hard horizon of flint and the overlying chalk, which is interpreted as energy loss through a combination of discontinuity attenuation and irregular surface relief between the chalk and flint, resulting in poor contact between the plunger and rock.

Within the same quadrat, 100 valid IDD measurements were made using the Equotip device. The IDD ranges 1.53 and 2.04 Mg/m^3, with a mean IDD of 1.58 Mg/m^3, corresponding to a medium - high CIRIA density grade. Figure 7-16 shows there appears to be little correlation, with differences within the SilverSchmidt readings relating primarily to discontinuities and surface relief, while the Equotip

differences depend predominantly on surface texture and material properties (i.e., heterogeneous variability in the density of the rock), with some input from discontinuities. This was considered a function of device sensitivity as well as the relative difference of sample surface area between the two devices.



	A	B	C	D	E	F	G	H	I	J
1	6.9	5.8	13.5	14.7	12.3	9.5	9.5	5.5	5.8	4.0
2	9.5	6.1	5.2	8.8	7.8	5.5	10.9	9.8	6.1	12.7
3	12.3	16.0	9.1	12.7	5.2	3.5	7.5	6.3	14.7	7.5
4	9.1	8.8	12.0	9.1	7.8	14.7	19.1	19.1	9.1	10.9
5	7.8	16.0	13.5	13.1	12.3	8.5	18.2	7.5	12.3	8.1
6	16.9	15.1	12.5	10.9	12.0	12.0	13.5	7.8	16.4	6.9
7	5.0	12.7	14.7	10.9	10.9	14.7	12.0	18.7	10.9	13.1
8	9.1	14.3	12.3	13.9	10.1	8.1	10.9	9.8	10.5	9.1
9	8.5	7.5	6.6	14.7	13.9	11.2	4.5	3.5	3.1	5.8
10										

	A	B	C	D	E	F	G	H	I	J
1	1.66	1.62	1.59	1.70	1.67	1.58	1.53	1.58	1.64	1.56
2	1.62	1.77	1.55	1.53	1.71	1.61	1.55	1.72	1.65	1.89
3	1.64	1.64	1.73	1.74	1.67	1.62	1.75	1.56	1.53	1.67
4	1.61	1.64	1.58	1.58	1.65	1.80	1.58	1.74	1.63	1.88
5	1.86	1.73	1.54	1.62	1.82	1.70	1.89	1.63	1.89	1.77
6	1.53	1.54	1.55	1.66	1.63	1.81	1.59	1.63	1.65	1.60
7	1.62	1.72	1.75	1.56	1.88	1.56	1.77	1.77	1.59	1.96
8	2.04	1.63	1.63	1.79	1.78	2.01	1.59	1.53	1.55	1.67
9	1.60	1.53	1.57	1.54	1.68	1.54	1.67	1.54	1.63	1.85
10	1.80	1.94	1.80	1.62	1.64	1.66	1.83	1.78	1.82	1.58

Figure 7-16 Portobello Outfall, quadrat 5 (white squares denote null readings).

Quadrat 5 is further broken down into 3 discrete blocks, which overlie stratigraphically. The aim of splitting the quadrat down further is to observe CIRIA grades and material properties to evaluate the degree of weathering variability within the quadrat (Figure 7-17).

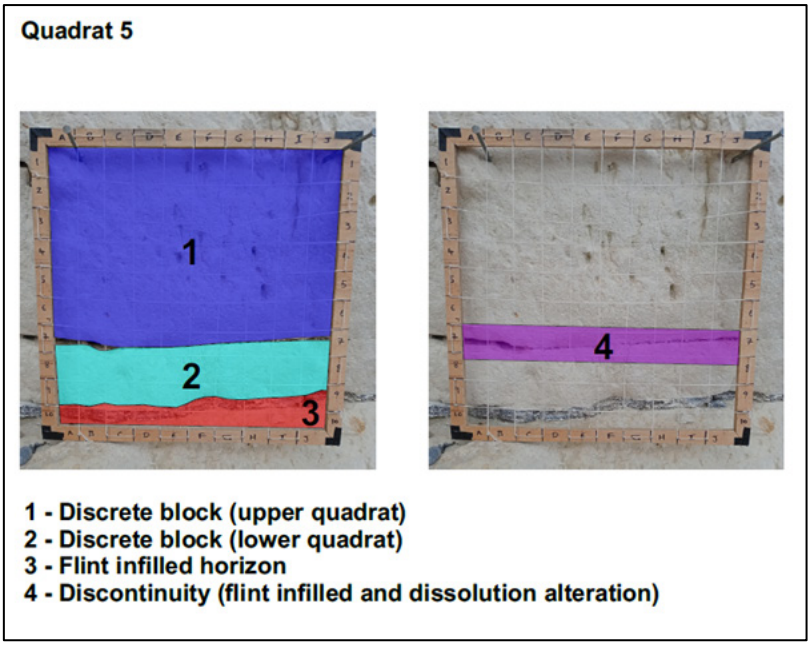


Figure 7-17 Portobello Outfall, quadrat 5 discrete blocks.

Block 1 comprises a competent chalk, with widely spaced, closed discontinuities, grade A1. The block has a mean UCS of 10.71 MPa, ranging from 3.53 – 19.14 MPa, corresponding to high density (Table 7-8). Block 2 comprises a similarly competent chalk, graded A1. The mean UCS for this block is less than block 1 at 9.81 MPa, ranging 3.09 – 14.72 MPa, classified as high-density grade (Table 7-8).

Block 3 (Table 7-8) is visually the most variable block within this quadrat, where competent chalk is cross-cut by a horizontal discontinuity, infilled with tabular flint. The flint is brecciated, resulting in a platy, brecciated texture. The discontinuity is open >3 mm, and its spacing is greater than 600 mm, giving a CIRIA fracture grade of C1. The mean UCS is the highest within this quadrat, at 12.34 MPa. While this feature has been graded using the CIRIA method, the UCS is reflective of the material strength of the flint itself (given that the flints true thickness is observed as 25 – 35 mm) as well as the surrounding chalk, therefore grading this feature with the CIRIA system would be inappropriate.

Blocks 1 and 2 are separated by a horizontal discontinuity that is both partially in-filled with tabular flint and observably altered due to dissolution, with voids left where flint has weathered out. This discontinuity is open <3mm (greater where dissolution has occurred) and is spaced greater than 600 mm, resulting in a grade of C1. The mean UCS of this discontinuity is markedly lower than that of block 3 at 7.93 MPa, ranging 3.09 – 14.72 MPa. The lower values are likely due to the relative thickness of the discontinuity. The discontinuity in block 3 is relatively thick (25 – 35 mm), which means that it is thick enough for the SilverSchmidt to test the flint material exclusively. The discontinuity in block 4 is relatively thin (i.e., open <3mm), with thinner infill that is missing in places. This results in material

heterogeneity (affecting the range of the readings) as well as attenuation of rebound energy via open discontinuities.

Table 7-8 Portobello quadrat 5 - discrete blocks, SilverSchmidt.

SilverSchmidt quadrat 5	UCS (MPa)	UCS range (MPa)	CIRIA density grade	Fracture spacing (mm)	Fracture aperture (mm)	CIRIA fracture grade	Degree of weathering
Block 1	10.71	3.53 - 19.14	High	>600	Closed	A1	Least
Block 2	9.38	3.09 – 14.72	High	>600	Closed	A1	Second least
3 horizontal infilled discontinuity	12.34	4.98 – 18.67	High – very high	>600	>3	B1	Second most
4 infilled and altered fracture	7.93	3.09 – 14.72	High	>600	>3	C1	Most

Using the SilverSchmidt to derive UCS and evaluating the weathering grades of the blocks, it is possible to state that Block 1 is the least weathered block, followed by block 2. The most weathered is block 4, and the second most weathered is block 3. This is not an accurate reflection of the degree of weathering, given that the CIRIA system is not appropriate for measuring flints.

A Welch's independent t-test on blocks 1 and 4 did not show any statistically significant differences in mean SilverSchmidt derived UCS value, however block 1 demonstrated the highest mean UCS values.

In terms of uniformity, Blocks 1 (coefficient of variance (CV) = 0.362) and 2 (CV = 0.375) have similar variances, indicating a consistent degree of weathering between the two blocks, while block 3 has a lower variance (CV = 0.287) compared to block 1, suggesting more uniform weathering. Block 4 has a higher variance (CV = 0.470) compared to block 1, indicating uneven weathering across this quadrat area.

Table 7-9 presents corresponding Equotip IDD measurements of the same blocks. Mean IDD's for blocks 1 and 2 are the same, with exception of the ranges, with block 1 ranging 1.53 – 1.96 Mg/m^3 and block 2 with a greater range of 1.53 – 2.04 $Mg/m^{3.}$, which both give a medium CIRIA density grade. While a direct comparison with the measured UCS cannot be made, their corresponding CIRIA grades can be compared, with the grades derived from UCS being consistently higher than the grades derived from the Equotip measured IDD.

Table 7-9 Portobello quadrat 5 - discrete blocks, Equotip

EQ quadrat 5	IDD (Mg/m^3)	IDD range (Mg/m^3)	CIRIA density grade	Fracture spacing (mm)	Fracture aperture (mm)	CIRIA fracture grade	Degree of weathering
Block 1	1.67	1.53 – 1.96	Medium	>600	closed	A1	Least
Block 2	1.67	1.53 – 2.04	Medium	>600	closed	A1	Least
3 horizontal infilled discontinuity	1.72	1.56 – 1.96	High	>600	>3	C1	Second least
4 infilled and altered fracture	1.68	1.53 – 1.94	Medium	>600	>3	C1	Most

Portobello Quadrat 5 equotip data were tested using a Welch's T-test. When block 1 was compared with block 2, a statistically significant difference between the populations was identified (t-statistic = 2.186, degrees of freedom (df) = 40.292, P-value = 0.035), indicating strong evidence of the mean densities being unequal. Block 2 shows lower variability (CV = 0.046) compared to block 1 (CV = 0.059), indicating block 2 having a more consistently distributed density. When block 1 is compared with block 3, there are no statistically significant differences identified, and variability is similar between the two blocks.

Quadrat 6 was located 50 m west of the pumping station infrastructure. A field photograph was taken but was lost, however measurements for both the SilverSchmidt and Equotip are presented in Figure 7-18. In terms of description, quadrat 6 focused on a relatively unfractured, competent chalk. One fracture was observed, with spacings greater than 600 mm, and was closed, corresponding to a CIRIA grade of A1.

SilverSchmidt derived UCS values were measured, with 95 valid readings from 100 attempts. UCS values range 3.53 – 20.08 MPa, with a mean of 13.12 MPa, corresponding to a very high CIRIA density grade.

IDD was measured using 100 valid Equotip measurements. The range of IDD was 1.53 – 1.95 Mg/m^3, with a mean IDD of 1.53 Mg/m^3. This resulted in a medium CIRIA density grade. This lower grade has disparity with the SilverSchmidt and is likely due to surface texture affecting the Equotip readings.

As the field photograph was lost, it was not possible to interpret textures or structures of quadrat 6 in conjunction with measurements made in the field.

Quadrat 6

Quadrat grid squares (UCS in MPa)

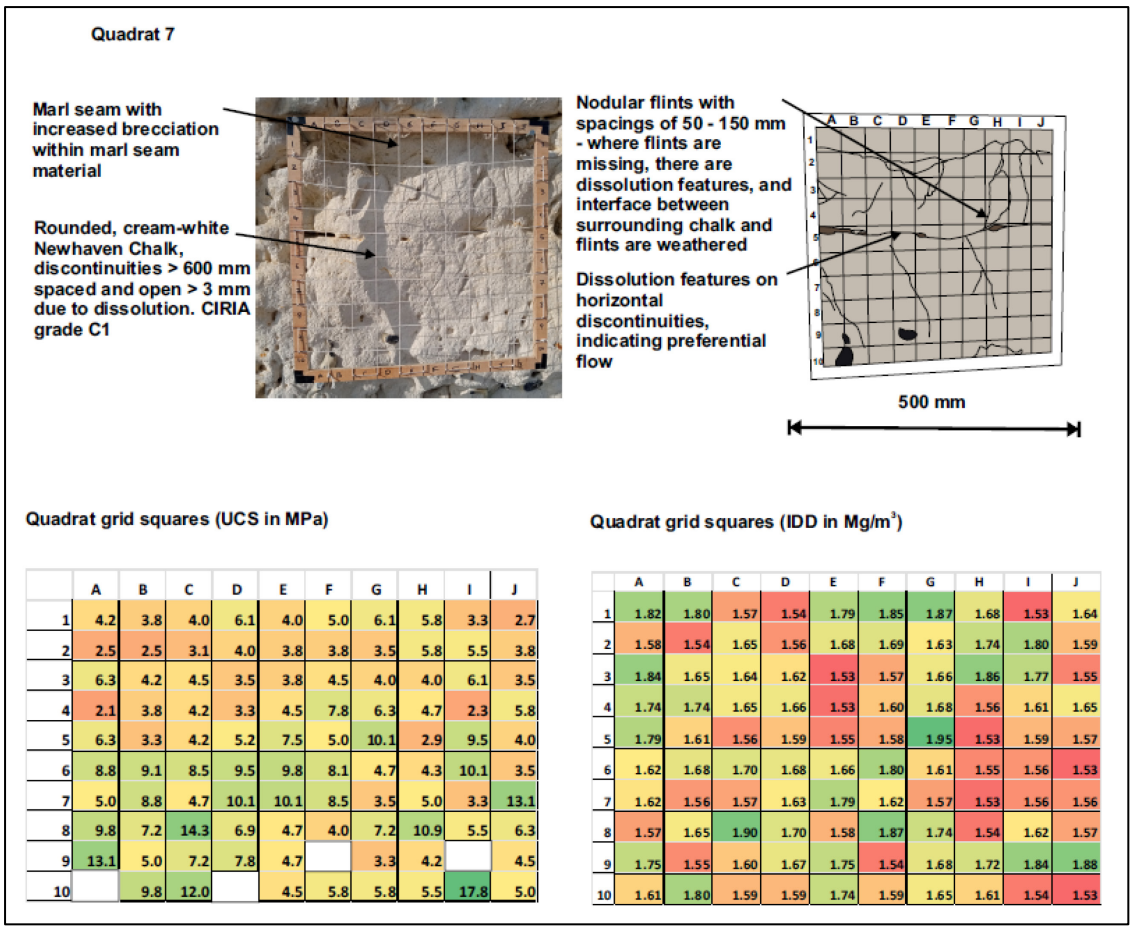
	A	B	C	D	E	F	G	H	I	J
1	13.5	12.7	8.1	5.5	12.3	15.6	17.3	12.3	5.2	8.5
2	16.0	14.7	14.3	12.3	12.3	15.1	13.9	17.3	16.4	16.4
3	13.1	13.5	6.3	11.2	11.6	17.8	15.6	17.3	18.2	17.8
4	11.6	6.3	15.6	16.4	11.6	16.0	7.8	18.2	12.7	15.6
5	15.6	14.7	6.1	14.7	14.7	13.5	13.9	10.5	12.0	17.8
6	7.5	16.4	12.7	14.3	8.5	15.1	13.5	20.1	15.6	12.0
7	16.4	17.3	16.0	12.3	9.5	12.3	10.1	17.8	20.1	13.9
8	14.3	18.7	16.4	11.6		8.1	14.3	14.7	16.0	12.7
9	7.2	7.5	8.1	12.3	9.5		6.6	15.1	13.5	16.0
10			3.5	3.5		3.8	15.6	14.3	18.2	16.0

Quadrat grid squares (IDD in Mg/m^3)

	A	B	C	D	E	F	G	H	I	J
1	1.56	1.81	1.75	1.83	1.55	1.58	1.53	1.58	1.64	1.56
2	1.77	1.69	1.84	1.57	1.69	1.61	1.55	1.72	1.65	1.89
3	1.85	1.69	1.56	1.86	1.53	1.62	1.75	1.56	1.53	1.67
4	1.61	1.74	1.86	1.85	1.99	1.80	1.58	1.74	1.63	1.88
5	1.53	1.56	1.64	1.65	1.58	1.70	1.66	1.63	1.89	1.77
6	1.54	1.66	1.56	1.81	1.76	1.63	1.61	1.60	1.74	1.65
7	1.59	1.56	1.57	1.55	1.61	1.81	1.91	1.66	1.55	1.55
8	1.74	1.58	1.60	1.56	1.59	1.56	1.56	1.60	1.56	1.53
9	1.66	1.59	1.88	1.58	1.58	1.62	1.65	1.63	1.76	1.69
10	1.80	1.53	1.73	1.68	1.54	1.77	1.59	1.74	1.60	1.60

Figure 7-18 Portobello quadrat 6 – heat maps (white squares denote null readings).

Quadrat 7 (Figure 7-19) was located 30 m west of Portobello outfall, and comprised competent, rounded cream-white Newhaven Chalk, with a fine marl seam at the top of the quadrat and cross-cut by a dissolution enhanced discontinuity, with some nodular flints. Horizontal discontinuity spacings were greater than 600 mm, and open >3 mm, owing to dissolution, resulting in a CIRIA grade of C1. Vertical discontinuities were closed, and tightly spaced (50 – 150 mm), and had connectivity with the overlying brecciated marl layer. These were classified as grade A4 – 3.



	A	B	C	D	E	F	G	H	I	J
1	4.2	3.8	4.0	6.1	4.0	5.0	6.1	5.8	3.3	2.7
2	2.5	2.5	3.1	4.0	3.8	3.8	3.5	5.8	5.5	3.8
3	6.3	4.2	4.5	3.5	3.8	4.5	4.0	4.0	6.1	3.5
4	2.1	3.8	4.2	3.3	4.5	7.8	6.3	4.7	2.3	5.8
5	6.3	3.3	4.2	5.2	7.5	5.0	10.1	2.9	9.5	4.0
6	8.8	9.1	8.5	9.5	9.8	8.1	4.7	4.3	10.1	3.5
7	5.0	8.8	4.7	10.1	10.1	8.5	3.5	5.0	3.3	13.1
8	9.8	7.2	14.3	6.9	4.7	4.0	7.2	10.9	5.5	6.3
9	13.1	5.0	7.2	7.8	4.7		3.3	4.2		4.5
10		9.8	12.0		4.5	5.8	5.8	5.5	17.8	5.0

	A	B	C	D	E	F	G	H	I	J
1	1.82	1.80	1.57	1.54	1.79	1.85	1.87	1.68	1.53	1.64
2	1.58	1.54	1.65	1.56	1.68	1.69	1.63	1.74	1.80	1.59
3	1.84	1.65	1.64	1.62	1.53	1.57	1.66	1.86	1.77	1.55
4	1.74	1.74	1.65	1.66	1.53	1.60	1.68	1.56	1.61	1.65
5	1.79	1.61	1.56	1.59	1.55	1.58	1.95	1.53	1.59	1.57
6	1.62	1.68	1.70	1.68	1.66	1.80	1.61	1.55	1.56	1.53
7	1.62	1.56	1.57	1.63	1.79	1.62	1.57	1.53	1.56	1.56
8	1.57	1.65	1.90	1.70	1.58	1.87	1.74	1.54	1.62	1.57
9	1.75	1.55	1.60	1.67	1.75	1.54	1.68	1.72	1.84	1.88
10	1.61	1.80	1.59	1.59	1.74	1.59	1.65	1.61	1.54	1.53

Figure 7-19 Portobello Outfall, quadrat 7 (white squares denote null readings).

SilverSchmidt UCS was measured (Figure 7-19), with 96 of 100 attempts being successful readings. UCS ranged from 2.09 – 17.83 MPa, with a mean value of 5.96 MPa – high density chalk. Invalid readings coincided with minor dissolution and areas of missing chalk material in the lower third of the quadrat, where surface relief has affected the instrument.

100 valid Equotip measurements were taken, with resulting ranges of IDD of 1.53 – 1.99 Mg/m^3, and a mean IDD of 1.66 Mg/m^3, resulting in a medium CIRIA density grade.

Quadrat 7 was split into 3 discrete blocks based on structures observed within the quadrat and observable trends within the heat maps (Figure 7-20). Block 1 is characterised by a marl seam with tightly spaced, open fractures (<3 mm) graded as CIRIA grade B2. This overlies block 2, which is characterised by intermediately spaced (<300 mm) discontinuities which are open <3 mm, (CIRIA grade B2). Block 3 is competent, with closed, widely spaced discontinuities (CIRIA grade A2) and underlies block 2. Blocks 2 and 3 are separated by a horizontal discontinuity, open <3 mm due to dissolution alteration.

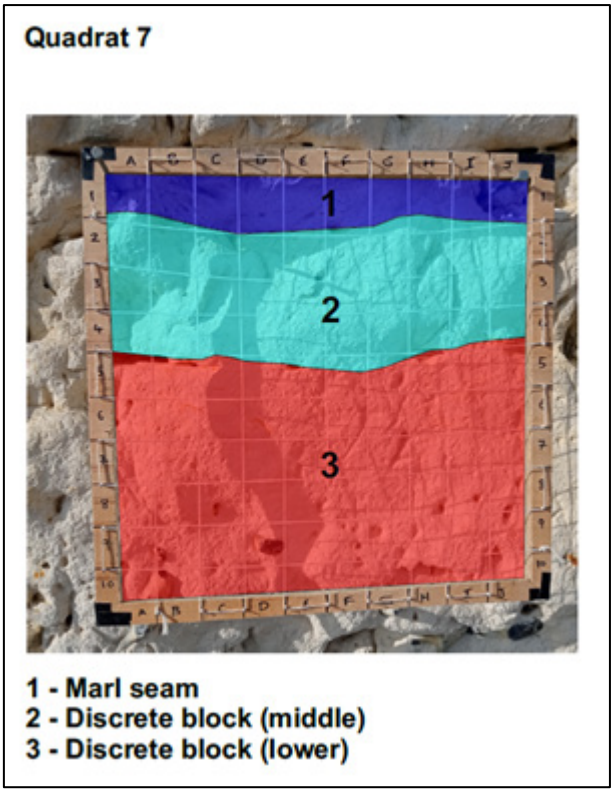


Figure 7-20 Portobello Outfall, quadrat 7 - discrete blocks.

Block 1 had a mean UCS of 4.48 MPa, with a range of 2.68 - 6.10 MPa (medium CIRIA density grade). Block 2 has a slightly lower mean UCS of 4.26 MPa, but with a greater range of 2.10 – 7.83 MPa (graded medium density). The greatest mean UCS is associated with block 3 – 7.13 MPa, with a range of 2.88 – 17.83 MPa (Table 7-10). With density grades, in conjunction with CIRIA fracture grading and observation, it is possible to interpret block 2 as the most weathered, block 3 as the least, and block 2 (the brecciated marl) has an intermediate degree of weathering.

Table 7-10 Portobello quadrat 7 - discrete blocks, SilverSchmidt.

SilverSchmidt quadrat 7	UCS (MPa)	UCS range (MPa)	CIRIA density grade	Fracture spacing (mm)	Fracture aperture (mm)	CIRIA fracture grade	Degree of weathering
Block 1	4.48	2.68 – 6.10	Medium	<300	<3	B2	Intermediate
Block 2	4.26	2.10 – 7.83	Medium	<300	<3	B2	Most
Block 3	7.13	2.88 – 17.83	High	<600	closed	A2	Least

A Welch's independent t-test shows that block 2 compared to block 3 (t-statistic = 4.561, df = 83.661 and P-value of <0.001) results in a statistically significant difference, indicating a difference in degree

of weathering. In terms of variation, block 2 (CV = 0.317) is lower than block 3 (CV = 0.537), suggesting that block 2 has been subject to more uniform weathering but is overall more degraded than block 3.

Block 1 compared to block 3 (t-statistic = -3.66, df = 42.289, P-value = <0.001) also shows a statistically significant difference between mean values, indicating a true difference in degree of weathering. The coefficient of variability of block 3 (CV = 0.537) indicates a grater variability in weathering compared to block 2 (CV = 0.264). In both comparisons, block 3 consistently shows higher values, indicating a lower amount of weathering, but has a greater variability. These results may suggest a progressive decrease in weathering from block 1 to block 3 as a function of stratigraphic position, with the presence of dissolution altered horizons as boundaries indicating chemical disequilibrium and potential water percolation as weathering agents.

Table 7-11 details corresponding Equotip derived IDD. Block 2 has the greatest IDD value of 1.71 Mg/m^3 and a range of 1.53 – 1.99 Mg/m^3, while blocks 1 and 3 present the same mean IDD value of 1.64 Mg/m^3. Block 1 has the lowest range of 1.53 – 1.83 Mg/m^3, while block 3 has the highest range, at 1.53 – 1.91 Mg/m^3.

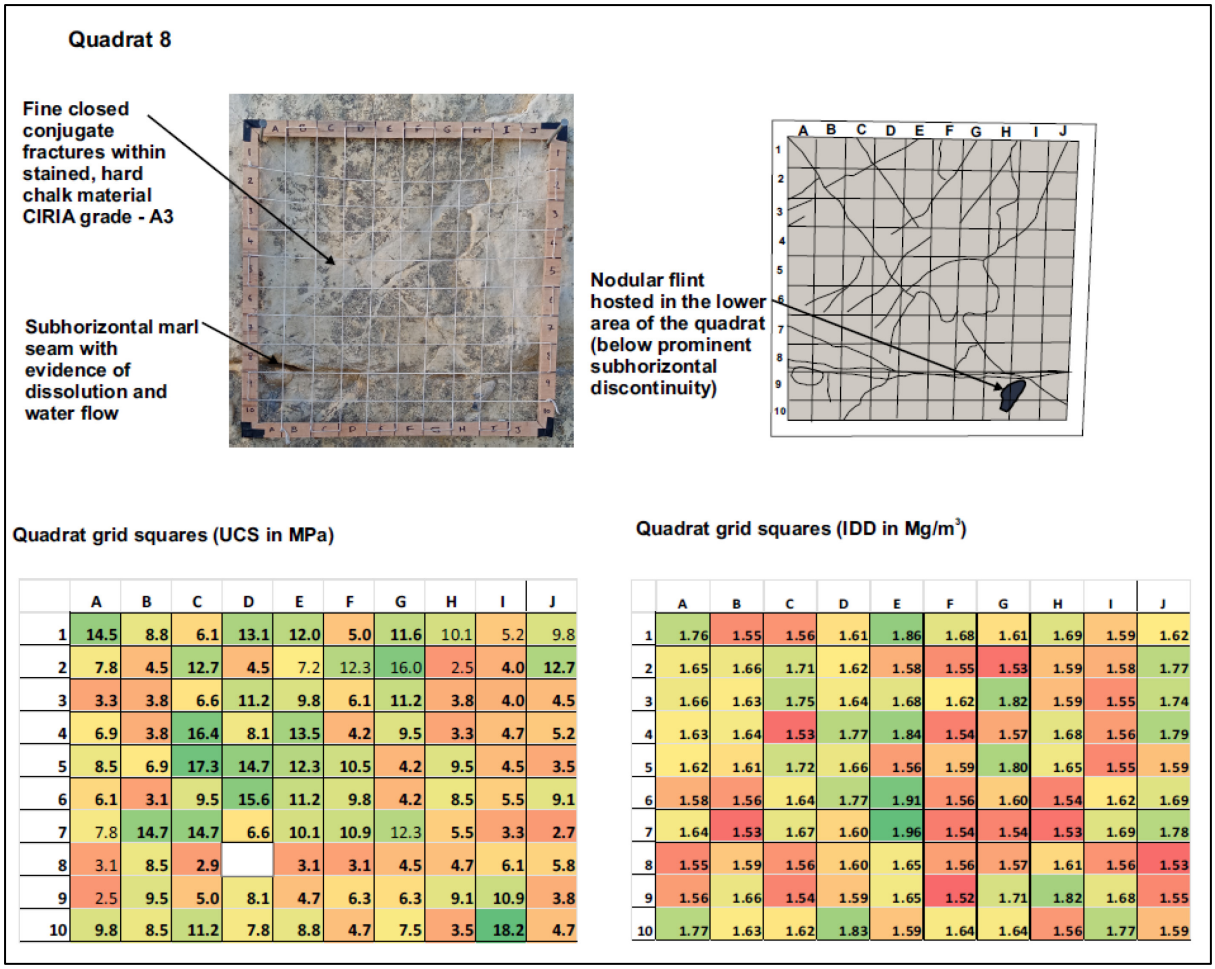
Table 7-11 Portobello quadrat 7 - discrete blocks, Equotip.

EQ quadrat 7	IDD (Mg/m^3)	IDD range (Mg/m^3)	CIRIA density grade	Fracture spacing (mm)	Fracture aperture (mm)	CIRIA fracture grade	Degre of weathering
Block 1	1.64	1.53 – 1.83	Medium	<300	<3	B2	Intermediate
Block 2	1.71	1.53 – 1.99	High	<300	<3	B2	Most
Block 3	1.64	1.53 – 1.91	Medium	<600	closed	A2	Least

There is discrepancy between SilverSchmidt measured UCS and Equotip measured IDD density grades, with the UCS being classified as medium density, while the IDD grade classified as high density. While there is discrepancy, the interpreted degree of weathering is still considered similar. This is because weathering is not wholly defined by one aspect of the CIRIA system and relies upon a combination of density, fracture classification and engineering judgement when undertaking observation.

Quadrat 8 (Figure 7-21) was located 10 m west of Portobello Outfall, and focussed on relatively competent, discoloured Newhaven Chalk, with closed sub-vertical and sub-horizontal discontinuities, resulting in a conjugate diagonal distribution. At the base of the quadrat (directly between grid squares A8 – J8 and A9 – J9), there is a thin wispy marl, which exhibits dissolution alteration.

100 UCS measurements were undertaken, with 99 valid measurements recovered. UCS ranged 2.48 – 8.21 MPa, with a mean UCS of 7.84 MPa, resulting in a high CIRIA density grading. The invalid measurement coincides with a dissolution feature of the wispy marl, indicating that the surface relief has made instrument sampler seating unsteady. IDD was measured with 100 valid Equotip readings. The IDD values ranged 1.52 – 1.96 Mg/m^3, with a mean value of 1.64 Mg/m^3 (medium CIRIA density grading).



	A	B	C	D	E	F	G	H	I	J
1	14.5	8.8	6.1	13.1	12.0	5.0	11.6	10.1	5.2	9.8
2	7.8	4.5	12.7	4.5	7.2	12.3	16.0	2.5	4.0	12.7
3	3.3	3.8	6.6	11.2	9.8	6.1	11.2	3.8	4.0	4.5
4	6.9	3.8	16.4	8.1	13.5	4.2	9.5	3.3	4.7	5.2
5	8.5	6.9	17.3	14.7	12.3	10.5	4.2	9.5	4.5	3.5
6	6.1	3.1	9.5	15.6	11.2	9.8	4.2	8.5	5.5	9.1
7	7.8	14.7	14.7	6.6	10.1	10.9	12.3	5.5	3.3	2.7
8	3.1	8.5	2.9		3.1	3.1	4.5	4.7	6.1	5.8
9	2.5	9.5	5.0	8.1	4.7	6.3	6.3	9.1	10.9	3.8
10	9.8	8.5	11.2	7.8	8.8	4.7	7.5	3.5	18.2	4.7

	A	B	C	D	E	F	G	H	I	J
1	1.76	1.55	1.56	1.61	1.86	1.68	1.61	1.69	1.59	1.62
2	1.65	1.66	1.71	1.62	1.58	1.55	1.53	1.59	1.58	1.77
3	1.66	1.63	1.75	1.64	1.68	1.62	1.82	1.59	1.55	1.74
4	1.63	1.64	1.53	1.77	1.84	1.54	1.57	1.68	1.56	1.79
5	1.62	1.61	1.72	1.66	1.56	1.59	1.80	1.65	1.55	1.59
6	1.58	1.56	1.64	1.77	1.91	1.56	1.60	1.54	1.62	1.69
7	1.64	1.53	1.67	1.60	1.96	1.54	1.54	1.53	1.69	1.78
8	1.55	1.59	1.56	1.60	1.65	1.56	1.57	1.61	1.56	1.53
9	1.56	1.66	1.54	1.59	1.65	1.52	1.71	1.82	1.68	1.55
10	1.77	1.63	1.62	1.83	1.59	1.64	1.64	1.56	1.77	1.59

Figure 7-21 Portobello Outfall, quadrat 8 (white squares denote null readings).

Observation of both the structures and heat maps of quadrat 8 shows that this quadrat is more complex compared to the quadrats 5 and 7. Quadrat 8 is not split by simple horizontal discontinuity planes and comprises 4 discrete blocks. These blocks are inferred by a combination of discontinuity and heat map trends and are separated by discontinuities themselves (Figure 7-22).

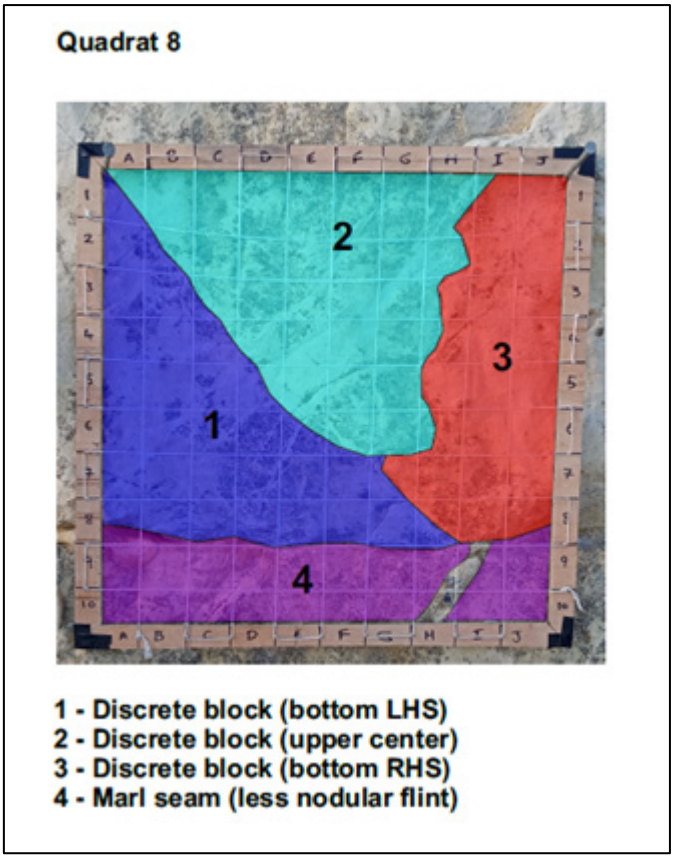


Figure 7-22 Portobello Outfall, quadrat 8 - discrete blocks.

Block 1 has the highest mean UCS of 8.95 MPa and a range of 2.48 – 15.99 MPa. This block was characterised as having widely spaced (<600 mm) closed discontinuities, resulting in a classification of high-density grade A2 chalk (Table 7-12).

Block 2 had the lowest mean UCS of 6.05 MPa, and a range of 2.68 – 2.72 MPa. Discontinuity spacings ranged between 20 – 600 mm and discontinuity apertures were closed, resulting in a high-density grade A2 chalk (Table 7-12).

Block 3 was position to the right-hand edge of the quadrat and had the second lowest mean UCS at 6.64 MPa. The UCS range was 2.48 – 18.21 MPa. Fracture spacings were greater than 600 mm, with discontinuity apertures closed. The grade assigned was high density grade A1 chalk (Table 7-12).

Block 4 framed a more brecciated marl horizon and had the second highest mean UCS of 7.95 MPa, with a range of 2.88 – 17.31 MPa. Discontinuity spacings were the tightest of all blocks within quadrat 8 at 20 mm or less and discontinuity apertures were open <3 mm, resulting in a high-density grade C5 chalk (Table 7-12).

Block 4 was considered the most weathered, followed by block 2. Block 1 was considered the second to least weathered, while block 3 considered the least, with a predominance of A1 - 2 grades. The

interpretation of weathering associated with block 3 is largely dependent on the brecciation of the marl texture and is different to the surrounding A grade chalks observed.

Table 7-12 Portobello quadrat 8 - discrete blocks, SilverSchmidt.

SilverSchmidt quadrat 8	UCS (MPa)	UCS range (MPa)	CIRIA density grade	Fracture spacing (mm)	Fracture aperture (mm)	CIRIA fracture grade	Degree of weathering
Block 1	8.95	2.48 – 15.99	High	<600	Closed	A2	Second least
Block 2	6.05	2.68 – 12.72	High	60 – 200	Closed	A2	Second most
Block 3	6.64	2.48 – 18.21	High	>600	Closed	A1	Least
4 marl horizon	7.95	2.88 – 17.31	High	<20	<3	C5	Most

Table 7-13 presents the Equotip measured IDD values corresponding with the UCS values for quadrat 8. All mean IDD values are similar, between 1.62 and 1.65 Mg/m^3. Block 1 has a mean IDD of 1.63 Mg/m^3 and a range of 1.53 – 1.96 Mg/m^3, block 2 has a mean IDD of 1.65 Mg/m^3, and a range of 1.53 – 1.91 Mg/m^3. Block 3 has a mean IDD of 1.64 Mg/m^3 and a range of 1.53 – 1.79 Mg/m^3, while block 4 has a mean IDD of 1.62 Mg/m^3 and a range of 1.52 – 1.83 Mg/m^3. When compared with the SilverSchmidt derived CIRIA density grade, the IDD derived CIRIA density grade is consistently a single grade lower. This could indicate that one of the instruments may be measuring overly high (in the case of the SilverSchmidt) or overly low (in the case of the Equotip).

Table 7-13 Portobello quadrat 8 - discrete blocks, Equotip.

EQ quadrat 8	IDD (Mg/m^3)	IDD range (Mg/m^3)	CIRIA density grade	Fracture spacing (mm)	Fracture aperture (mm)	CIRIA fracture grade	Degree of weathering
Block 1	1.63	1.53 – 1.96	Medium	<600	Closed	A2	Second least
Block 2	1.65	1.53 – 1.91	Medium	60 – 200	Closed	A2	Second most
Block 3	1.64	1.53 – 1.79	Medium	>600	Closed	A1	Least
4 marl horizon	1.62	1.52 – 1.83	Medium	<20	<3	C5	Most

Table 7-14 presents a summary of the SilverSchmidt derived UCS values, Equotip derived IDD values, CIRIA gradings (including hammer penetration derived CIRIA density grades) in conjunction with textures observed within quadrats 5, 7 and 8.

Table 7-14 Portobello, SilverSchmidt derived UCS and Equotip derived IDD against texture and weathering grade.

Quadrat	Texture	UCS (MPa)	UCS range (MPa)	SilverSchmidt CIRIA density grade	IDD (Mg/m^3)	IDD range (Mg/m^3)	Equotip CIRIA density grade	Hammer penetration (mm)	Hammer penetration range (mm)	Hammer CIRIA density grade	CIRIA fracture grade
5	Competent, widely spaced closed discontinuities	10.71	3.53 - 19.14	High	1.67	1.53 – 1.96	Medium	4.33	2 – 7	High	A1
	Competent, widely spaced closed discontinuities	9.38	3.09 – 14.72	High	1.67	1.53 – 2.04	Medium	5.33	4 – 7	High	A1
	Flint infilled discontinuity; brecciated	12.34	4.98 – 18.67	High – very high	1.72	1.56 – 1.96	High	N/A	N/A	N/A	C1
	Flint infilled; dissolution altered discontinuities	7.93	3.09 – 14.72	High	1.68	1.53 – 1.94	Medium	N/A	N/A	N/A	C1
7	Brecciated; tightly spaced, open fractured marl	4.48	2.68 – 6.10	Medium	1.64	1.53 – 1.83	Medium	5.66	3 – 8	High	B2
	Competent; intermediately spaced, open discontinuities	4.26	2.10 – 7.83	Medium	1.71	1.53 – 1.99	High	6.66	5 – 8	Very high	B2
	Competent, widely spaced, closed discontinuities	7.13	2.88 – 17.83	High	1.64	1.53 – 1.91	Medium	9	3 – 9	High	A2
8	Intermediately spaced, closed discontinuities	8.95	2.48 – 15.99	High	1.63	1.53 – 1.96	Medium	3.33	3 – 4	High	A2
	Intermediately spaced, closed discontinuities	6.05	2.68 – 12.72	High	1.65	1.53 – 1.91	Medium	8	7 – 9	High	A2
	Competent, widely spaced, closed discontinuities	6.64	2.48 – 18.21	High	1.64	1.53 – 1.79	Medium	3.33	3 – 4	High	A1
	Tightly spaced, openly brecciated marl	7.95	2.88 – 17.31	High	1.62	1.52 – 1.83	Medium	5.66	3 – 9	High	C5

By comparing CIRIA density gradings derived from both the SilverSchmidt and Equotip for each quadrat, it is possible to observe some significant differences, indicating that one or both instruments are leading to erroneous grades. Quadrat 5 is graded as high density with the SilverSchmidt and medium high density with the Equotip, with this quadrat being the most consistent between these two gradings. The greatest discrepancy lies with quadrat 6, where the SilverSchmidt provides a grade of very high density, while the Equotip provides a medium density grade.

Both quadrats 7 and 8 have high density grades derived from the SilverSchmidt and medium density grades derived from the Equotip. It is possible that this could be a function of chalk heterogeneity or instrument calibration, and therefore would require further investigation. In terms of accuracy and precision of IDD field measurements, the Equotip Leeb is accurate to +/- 6 HL, but is optimised for steel and other hard metals. Readings may be affected by material properties such as softness and surface effects, such as roughness, which are irregular in chalk surfaces. The equation for estimating IDD produced by Thrower et al. was developed through correlation of laboratory IDD measurements and Equotip testing undertaken on blocks of chalk where the surfaces had been prepared for the test, therefore the precision of the device in the field could be improved by further correlation of IDD tests and field measurements. Further statistical analyses and comparison would give more insight into instrument effectiveness.

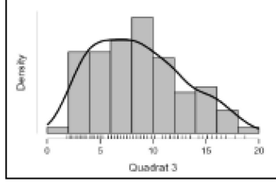
7.2.3 Newhaven Harbour research site

At Newhaven Harbour, five quadrats were measured, resulting in 700 readings, making this site the smallest in terms of data acquisition. The 700 readings comprise 500 SilverSchmidt measurements and 200 Equotip measurements. 300 SilverSchmidt measurements were taken within quadrats 1 -3. Their aim was to evaluate if the chalk is more weathered with a lower density at proximity to fracture systems, given that the CIRIA weathering classification utilises discontinuity character and density as aspects of assessment. The remaining 400 readings were taken from quadrats 4 and 5 (200 SilverSchmidt readings and 200 Equotip readings respectively). The aim of quadrats 4 and 5 was to evaluate if there are any material changes in proximity to a dissolution feature).

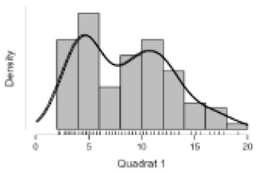
Figure 7-23 shows the relative positions of quadrats 1 – 3 at Castle Hill, Newhaven Harbour, detailing the fracture geometry of the discontinuities investigated and presents statistical data. Figure 7-24 shows the positions of quadrats 4 and 5, also located on Castle Hill, but further west. Figure 7-24 details the position of the quadrats relative to a large-scale fault which has undergone karstic weathering as well as providing SilverSchmidt derived UCS and Equotip derived IDD distributions.

Schematic field sketch 1 of Newhaven Harbour;quadrat locations

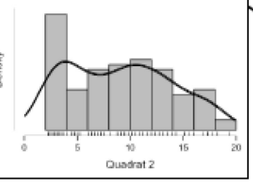
Quadrat 3
Grade - A1 - High density
UCS = 8.59 MPa
Standard deviation = 4.20
Range = 1.90 - 18.67

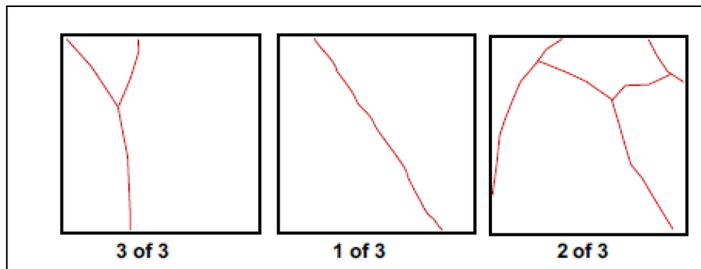


Quadrat 1
Grade - A1- B5 - High density
UCS = 8.43 MPa
Standard deviation = 4.21
Range = 2.09 - 19.14

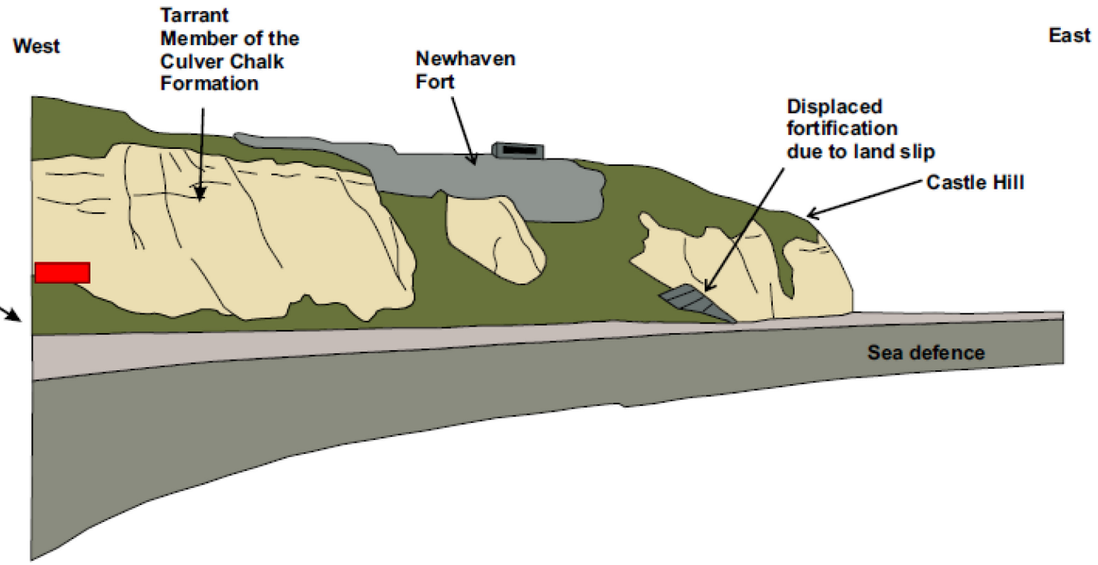


Quadrat 2
Grade - B3 - B2 - High density
UCS = 9.09 MPa
Standard deviation = 4.85
Range = 2.25 - 19.4





Relative quadrat positions with discontinuity patterns



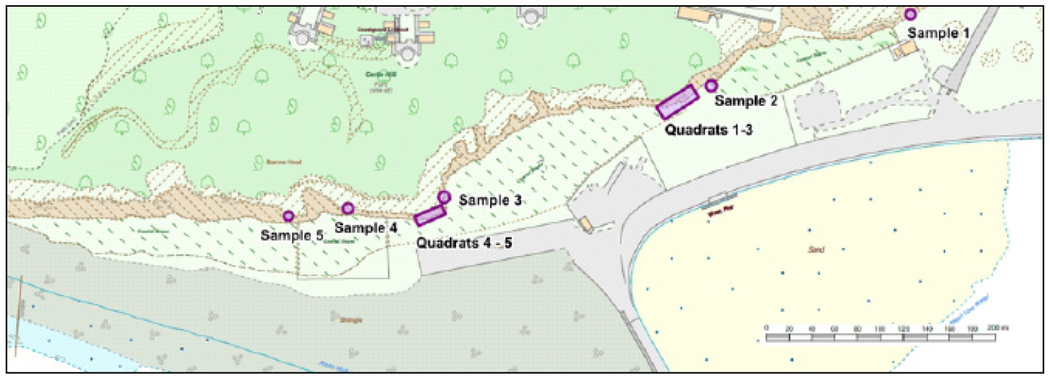


Figure 7-23 Schematic field sketch 1; Newhaven Harbour.

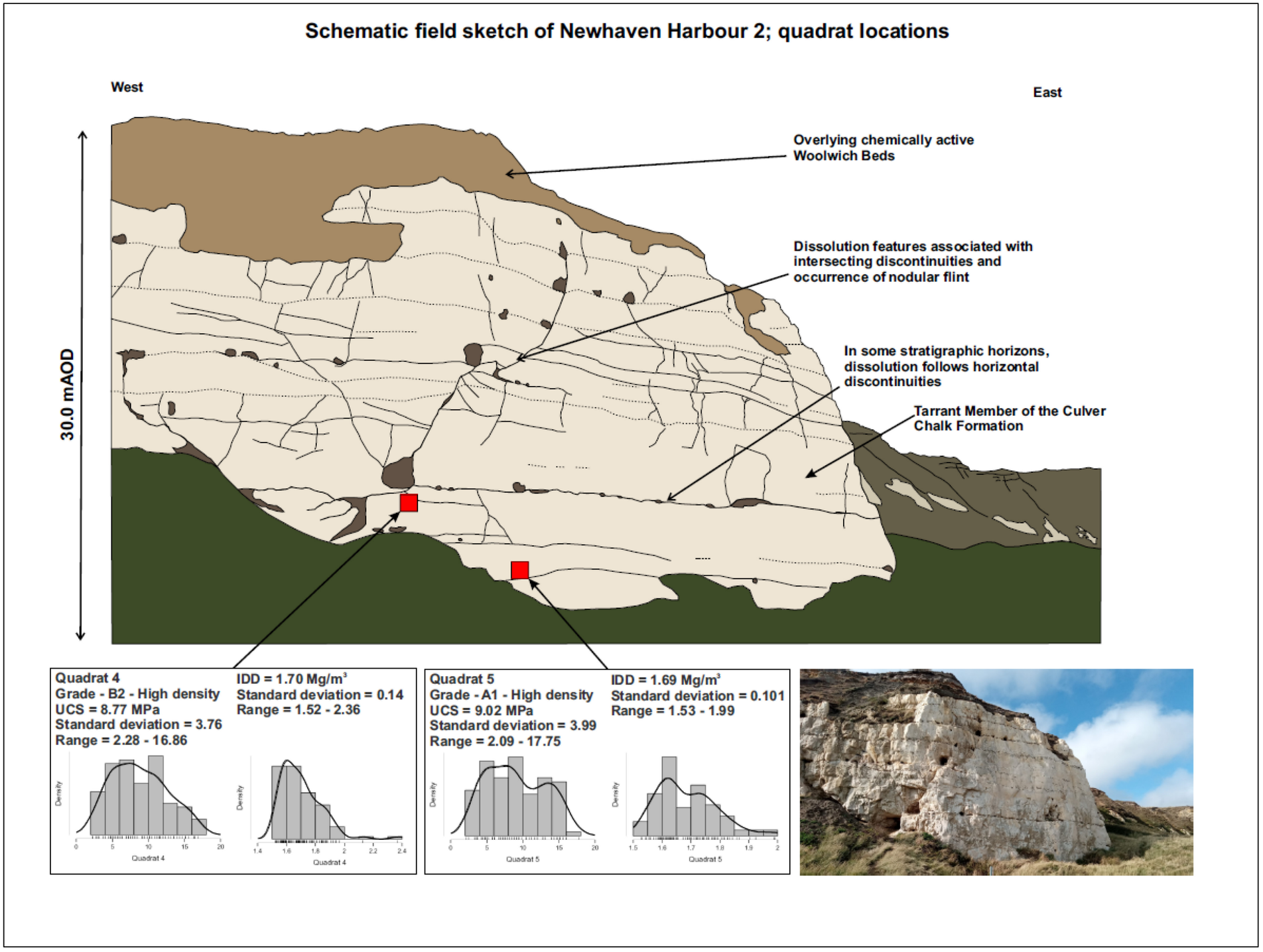


Figure 7-24 Schematic field sketch 2; Newhaven Harbour.

Quadrats 1 - 3

Quadrats 1 - 3 had SilverSchmidt derived mean UCS values ranging from 8.43 – 9.09 MPa (Figure 7-25), resulting in a CIRIA grade of high-density. The standard deviation was similar, ranging from 4.2 – 4.8 MPa, which indicates that dispersion is low. From observation of quadrat positions, it is possible to observe several fractures breaking each quadrat into discrete blocks, meaning that more meaningful analyses could be undertaken.

Figure 7-14 shows each quadrat split into discrete blocks, with quadrat 1 split into two blocks (labelled blocks 1A and 1B). Quadrat 2 is split into five blocks (labelled blocks 2A – 2E inclusively). Quadrat 3 is split into three discrete blocks (with the same convention of 3A – 3C). When a heat map is applied to each quadrat (Figure 7-25), it can be observed that some discrete blocks yield markedly lower readings compared to others, indicating that the mean UCS presented in Figure 7-14 does not uniformly reflect the chalk rock mass of each quadrat.

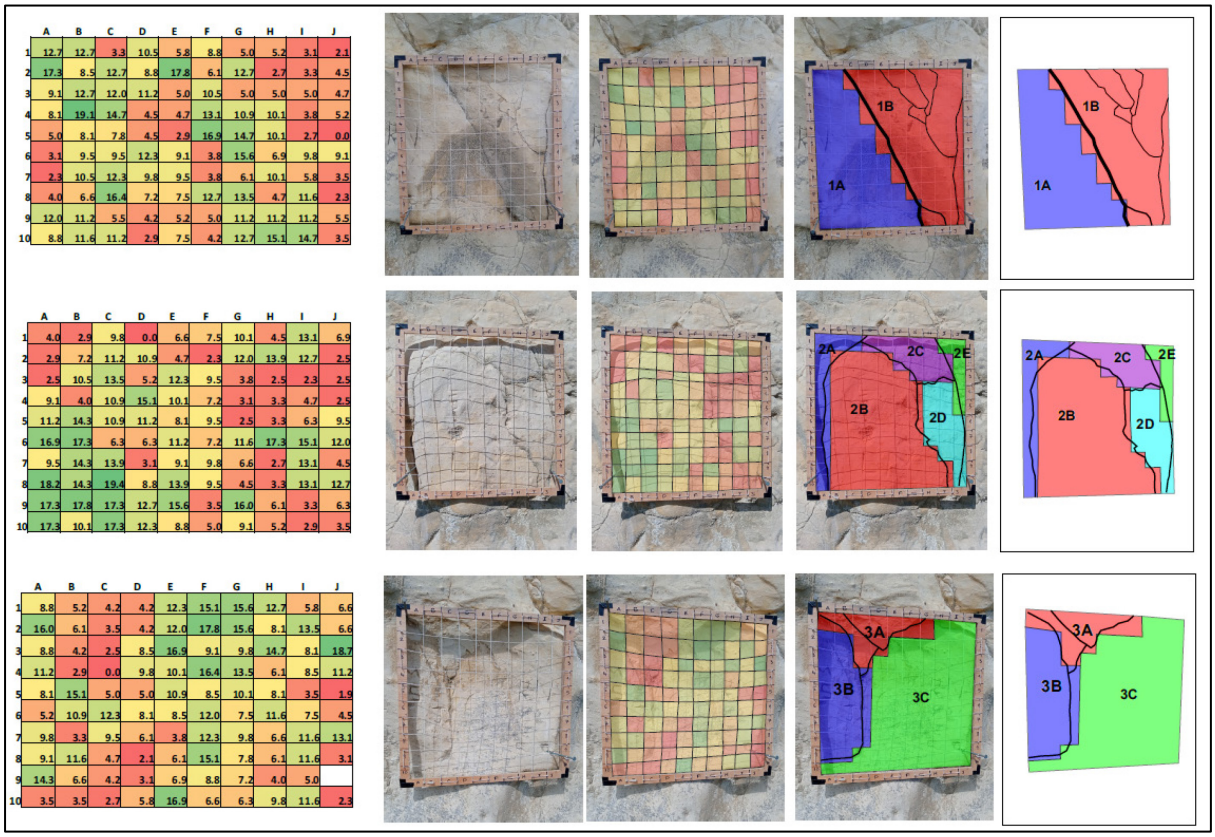


Figure 7-25 Newhaven Harbour, quadrats 1 – 3 (white squares denote null readings).

Quadrat 1 (Figure 7-26) has a mean UCS value of 8.30 MPa and was split into 2 blocks based upon trends observed within the superimposed heat map and discontinuity distribution. Block 1A has a mean UCS value of 9.31 MPa, and ranges 2.28 – 19.14 MPa. Block 1A was considered a massive block

of chalk, with few discontinuities and 46 measurements taken. In terms of CIRIA grading, this was classified as high density, grade A1.

Block 1B had a mean UCS value of 7.30 MPa and ranging 2.48 – 17.75 MPa, with increased fracture frequency in the upper right-hand side of the quadrat. 54 measurements were taken from block 1B. This block was classified as high density, grade C4. Blocks 1A and 1B are separated by a high persistence discontinuity, which was open >3 mm and infilled with wash.

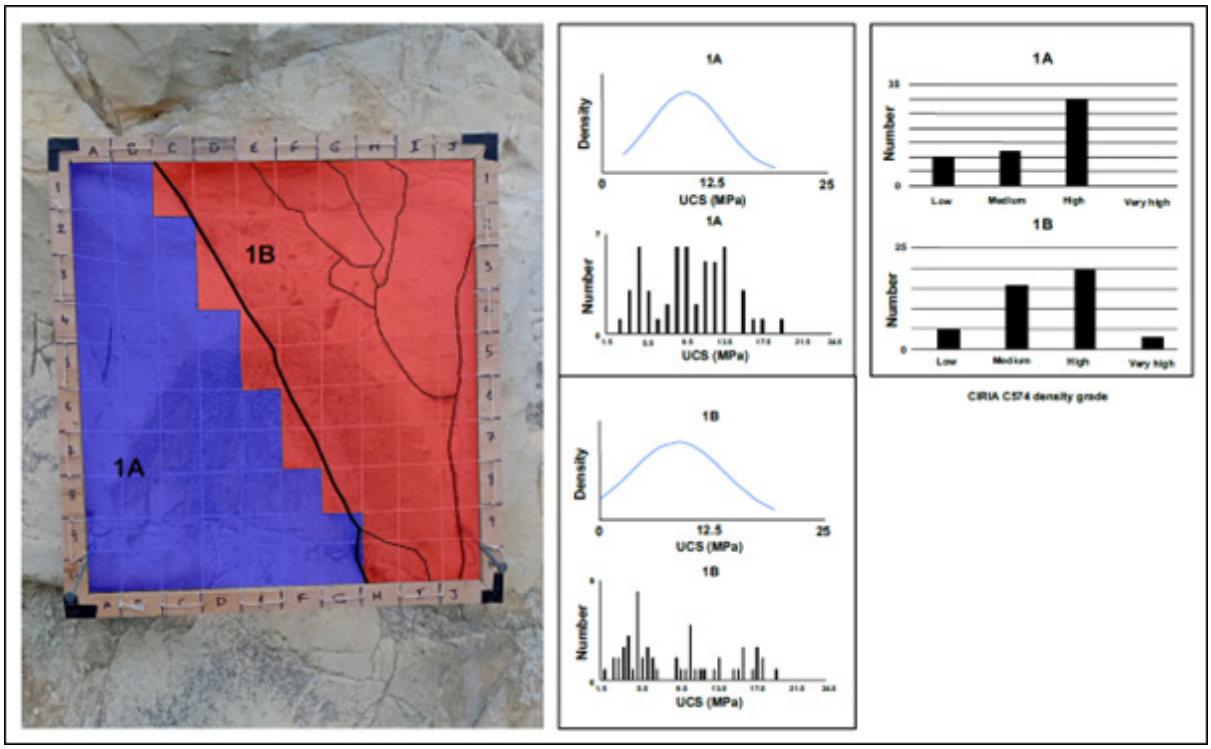


Figure 7-26 Newhaven Harbour, quadrat 1 - discrete blocks.

Table 7-15 shows block 1A compared to block 1B. From this analysis, it is interpreted that block 1A is the least weathered, while block 1B is the most. This is due to the combination of CIRIA grading components, rather than exclusively density or discontinuity characteristics.

Table 7-15 Quadrat 1; SilverSchmidt descriptive statistics and CIRIA grades.

SilverSchmidt quadrat 1	UCS (MPa)	UCS range (MPa)	CIRIA density grade	Fracture spacing (mm)	Fracture aperture (mm)	CIRIA fracture grade	Degree of weathering
Block 1A	9.31	2.28 – 19.14	High	>600	closed	A1	Least
Block 1B	7.30	2.48 – 17.75	High	20 - 60	<3	C4	Most

Both blocks display normal statistical distributions which are positively skewed. Block 1A has a higher range of densities compared to block 1B, however, block 1B has a greater number of lower density readings than block 1A, reflecting block 1B's fractured character.

Quadrat 2 has a mean UCS of 9.0 MPa, ranging 2.28 – 19.4 MPa, giving an overall medium CIRIA density grade. Fracture spacings ranged 200 – 600 mm, and apertures were open <3 mm, resulting in a CIRIA fracture grade of B2. The quadrat was further split into 5 discrete blocks based on structures observed within the quadrat and trends observed within the superimposed heat map.

Block 2A comprised 12 measurements and has the highest UCS of all blocks observed in quadrat 2, resulting in a mean UCS of 10.12 MPa, ranging 2.48 – 18.21 MPa, corresponding to a high-density grade chalk. Discontinuity spacings were >600 mm and apertures were open <3 mm, resulting in a B1 CIRIA fracture grade.

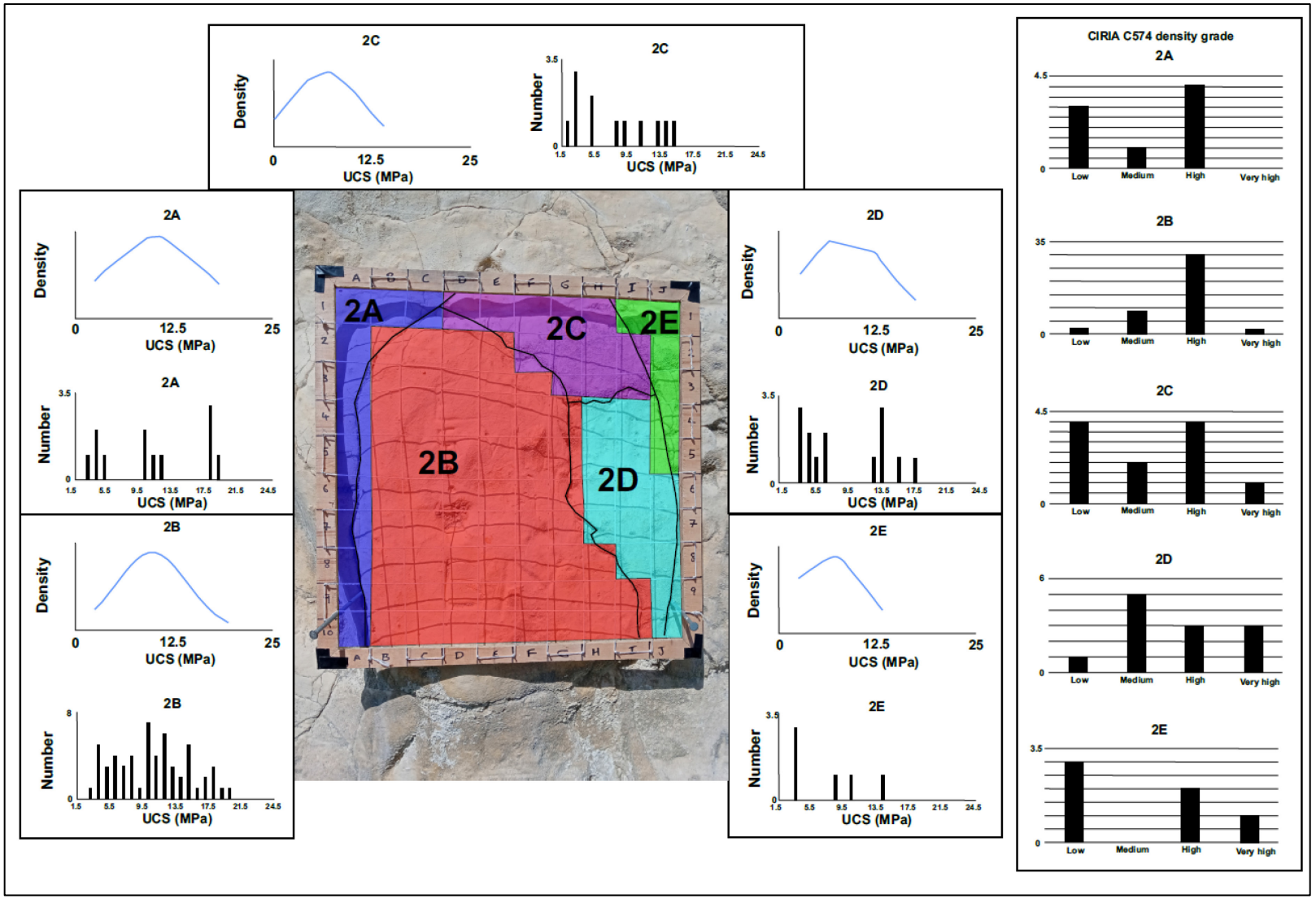


Figure 7-27 Newhaven Harbour, quadrat 2 - discrete blocks.

Block 2B (Figure 7-27) had the largest area of all discrete blocks in this quadrat and had the greatest number of readings at 54. The mean UCS was 9.74 MPa, ranging 2.48 – 19.4 MPa. Fracture spacings and apertures were the same as block 2; >600 mm and open <3 mm, respectively. These resulted in an overall CIRIA grade of high density B2 chalk.

Blocks 2C and 2D each have 14 SilverSchmidt measurement. Block 2C has a mean UCS value of 7.10 MPa, ranging 2.25 – 13.91 MPa. Block 2D has a mean UCS of 8.43 MPa, ranging 2.68 – 17.31 MPa. Discontinuity spacings are between 200 – 600 mm, and fractures are open <3 mm in both quadrats. These values and ranges result in both blocks 2C and 2D being classified as high density, grade B2 chalks.

2E has the lowest number of measurements of all discrete blocks considered in this quadrat. It also yields the lowest mean UCS at 6.15 MPa and a range of 2.48 – 13.11 MPa. Fracture spacings are absent within the block, however, the bounding discontinuities are spaced <150 mm and open <3 mm. This results in a CIRIA classification of B3, high-density chalk. The grading in this block would be inappropriate as block 2E is a discrete, relatively small block with an absence of discontinuities, therefore discontinuity spacings of 4 and 5 are not relevant as they are not present, and spacings of 200 mm or over cannot be applied, as the block is below this in terms of size. The fracture aperture classification also cannot be applied to this individual block as there is an absence of fractures within the main fabric. Table 7-16 provides a summary of CIRIA grading and interpretations of degree of weathering. Block 2A was the least weathered, followed by 2B, 2D, 2C and most weathered was 2E.

Table 7-16 Quadrat 2; SilverSchmidt descriptive statistics and CIRIA grades.

SilverSchmidt quadrat 2	UCS (MPa)	UCS range (MPa)	CIRIA density grade	Fracture spacing (mm)	Fracture aperture (mm)	CIRIA fracture grade	Degree of weathering
Block 2A	10.12	2.48 – 18.21	High	>600	<3	B1	Least (1)
Block 2B	9.74	2.48 – 19.4	High	>600	<3	B1	(2)
Block 2C	7.10	2.25 – 13.91	High	200 – 600	<3	B2	(4)
Block 2D	8.43	2.68 – 17.31	High	200 – 600	<3	B2	(3)
Block 2E	6.15	2.48 – 13.11	High	< 150	<3	B3	Most (5)

All blocks were normally distributed with positive skew, with lower readings associated with discontinuities that had apertures greater than 3 mm. Block 2A had the most consistent distribution; this is attributed to the relatively larger sample size compared to that of blocks 2B – 2E. In terms of

statistical significance, this means that the values presented had relatively little variation and measured values are more consistent across each block.

Quadrat 3 (Figure 7-28) was classified as grade A1, except for the upper left-hand side of the quadrat, which was graded C5 in a discrete area. A mean of UCS 8.59 MPa, ranging 1.9 – 18.67 MPa indicates a high-density chalk. Quadrat 3 was split into three discreet blocks, all of which were graded as C1-3, medium to high density chalk.

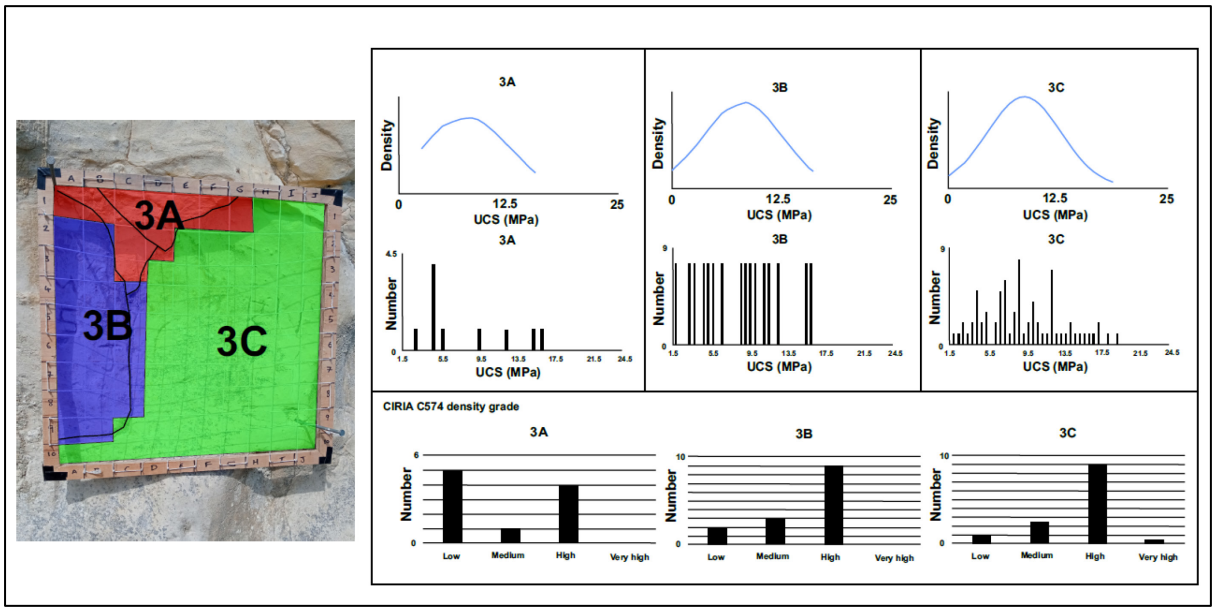


Figure 7-28 Newhaven Harbour, quadrat 3 - discrete blocks.

Quadrat 3A and 3B had similar ranges (Table 7-17), with 3A having a range of 2.48 – 15.56 MPa from nine measurements, while 3B ranging 2.88 – 15.99 MPa from 21 measurements. Block 3C had the greatest range of 1.9 – 18.67 MPa resulting from 70 measurements. Block 3A and 3B display normal distribution and positive skew, while block 3C is normally distributed and not significantly skewed.

Table 7-17 Quadrat 3; SilverSchmidt descriptive statistics and CIRIA grades.

SilverSchmidt quadrat 3	UCS (MPa)	UCS range (MPa)	CIRIA density grade	Fracture spacing (mm)	Fracture aperture (mm)	CIRIA fracture grade	Degree of weathering
Block 3A	7.58	2.48 – 15.56	High	60 - 200	>3	C3	Most (3)
Block 3B	8.03	2.88 – 15.99	High	>600	>3	C1	Intermediate (2)
Block 3C	8.61	1.9 – 18.67	High	>600	>3	C1	Least (1)

From these observations, it is possible to state that blocks 3B and 3C, which have low discontinuity frequencies, have similarities in terms of strength and distribution, with dispersion of the distribution

affected by sample size and limited outliers, demonstrated by block 3A. It is possible to observe that strength measurements are affected by the presence of discontinuities, with lower readings associated with the interface of two blocks (i.e., quadrat 3; lower left-hand side of the quadrat, between the interface of blocks 3B and 3C) and where two or more discontinuities intersect (i.e., quadrat 1; block 1B and quadrat 3; upper left-hand side of the quadrat where 3A, 3B and 3C discontinuities converge). These lower strength measurements are attributed to edge effects and the loss of rebound energy via friction at these discontinuities.

A Welch's independent t-test was undertaken for quadrats 2 and 3 owing to the relatively small sample sizes of the blocks under consideration, however there was no observable statistically significant difference between these.

Quadrats 4 - 5

Quadrats 4 and 5 were positioned to evaluate potential evidence of case hardening or softening at proximity to karstic features within the Tarrant Chalk at Newhaven. Quadrat 4 was positioned at proximity to a discontinuity with significant karstification, while quadrat 5 was situated further down the cliff sequence away from karstic processes for comparison (Figure 7-29).

Quadrat 4

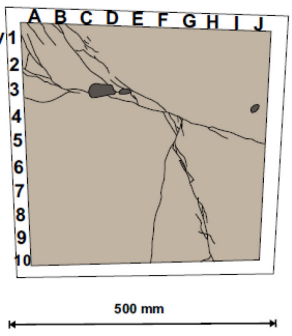
Off white, massive Tarrant chalk, with fine conjugate sinuous discontinuities observed.

Aperture of discontinuities are closed to open < 3 mm, with limited spacing of 200 < t < 600mm; grade B2.



Sinuous, anastomosing whispy fracture pattern

Fracturing at proximity to fault, indicative of shear - secondary fractures are fine and closed



Quadrat grid squares (UCS in MPa)

	A	B	C	D	E	F	G	H	I	J
1	5.5	8.5	9.8	15.1	11.2	5.0	9.5	10.9	13.5	9.1
2	5.0	6.9	4.7	7.8	6.9	13.5	7.8	8.1	10.1	13.5
3	7.8	9.8	10.1	9.1	2.7	4.7	5.2	4.5	14.3	10.5
4	16.4	14.7	11.6	13.9	12.0	8.1	3.8	3.8	15.1	12.3
5	2.3	10.1	15.6	13.1	7.5	11.2	4.0	10.1	7.8	11.2
6	5.2	5.2	6.1	11.5	15.1	11.5	4.0	9.1	7.8	12.0
7	4.7	12.7	6.9	7.8	16.4	14.3	11.6	5.8	9.5	16.3
8	2.3	5.0	6.3	4.0	8.1	16.9	12.7	7.2	10.1	8.1
9	5.5	7.8	7.2	8.5	4.7	5.0	6.3	7.2	11.5	10.9
10	3.1	3.1	2.9	5.8	10.1	7.5	7.2	5.2	5.5	11.6

Quadrat grid squares (IDD in Mg/m^3)

	A	B	C	D	E	F	G	H	I	J
1	1.57	1.71	1.62	1.58	1.74	1.88	1.86	1.71	1.85	1.57
2	1.53	1.62	1.61	1.52	1.74	1.59	1.56	2.13	1.68	1.58
3	1.64	1.57	1.54	1.87	1.60	1.78	1.81	1.79	1.60	1.54
4	1.59	1.96	1.53	1.53	1.65	1.59	1.79	1.87	1.68	1.58
5	1.72	1.56	1.67	1.63	1.59	1.56	1.69	1.62	1.56	1.57
6	1.77	1.67	1.69	1.67	1.74	1.58	1.72	1.68	1.68	1.59
7	1.84	1.59	1.58	1.69	1.76	1.91	1.59	1.83	1.71	1.56
8	1.84	1.76	1.78	1.85	1.66	1.80	1.92	1.58	1.72	1.72
9	1.88	2.37	1.70	1.68	1.84	1.73	1.88	1.56	1.69	1.55
10	1.95	1.63	1.65	1.63	1.77	1.94	1.68	1.61	1.68	1.60

Figure 7-29 Newhaven Harbour, quadrat 4.

Quadrat 4 (Figure 7-29) was classified as grade B2 high density chalk, with a mean UCS of 8.77 MPa, the range of which was 2.28 – 16.68 MPa. The mean IDD was measured as 1.70 Mg/m^3, with a range of 1.52 – 2.38 Mg/m^3. Two further analyses were undertaken to (i) evaluate the degree of weathering due to discontinuities and (ii) evaluate the relative strengths of discoloured areas observed within the quadrat.

Based on the degree of brecciation and positions of discontinuities, quadrat 4 was split into discrete blocks. (Figure 7-30). Block 4A was classed as high density although observably brecciated, with a mean UCS of 6.73 MPa, ranging 4.73 – 9.79 MPa. Block 4B was the largest block, positioned in the bottom left-hand of the quadrat, was high density, with a greater UCS of 8.72 MPa, ranging 2.68 – 15.14 MPa. Block 4C was positioned in the upper right hand of the quadrat and was the second largest block, with a mean UCS of 9.42 MPa and a range of 2.68 – 15.14 MPa. Block 4D had a mean UCS of 9.12 MPa and a range of 3.76 – 16.28 MPa (Table 7-18).

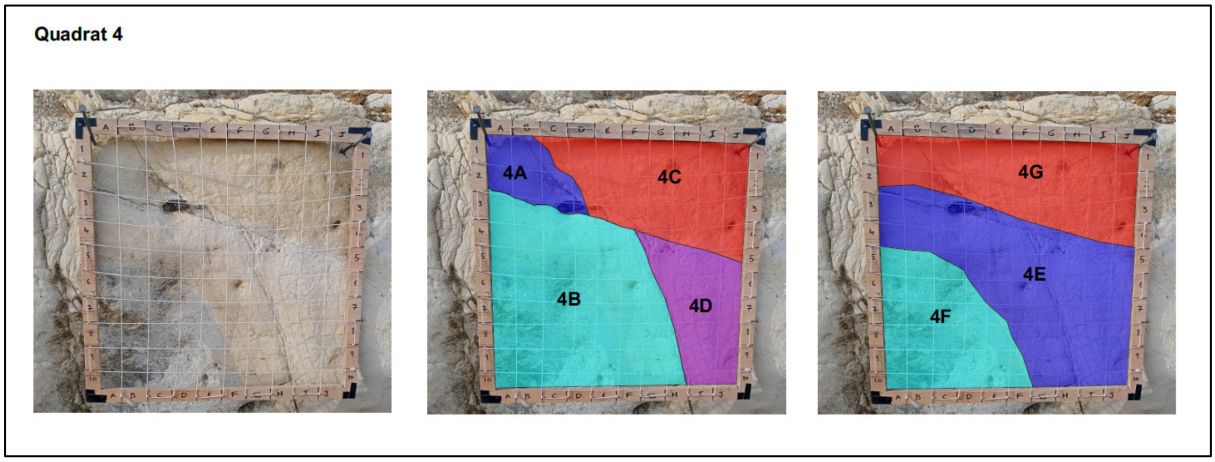


Figure 7-30 Newhaven Harbour, quadrat 4 - discrete blocks.

While there are lower UCS readings associated with discontinuities (such as block 4A and discrete areas) within this quadrat, there are low UCS value areas that coincide with an absence of discontinuities and a distinct change in colour (such as grid squares A8:10 and B8:10). This indicates that while discontinuities do affect the UCS values, there are also other contributory factors in variable strength and density values.

Table 7-18 Newhaven quadrat 4 - degree of weathering based on discontinuities, SilverSchmidt.

SilverSchmidt quadrat 4	UCS (MPa)	UCS range (MPa)	CIRIA density grade	Fracture spacing (mm)	Fracture aperture (mm)	CIRIA fracture grade	Degree of weathering
Block 4A	6.73	4.73 – 9.79	High	<20 mm	<3 mm	B5	Most (1)
Block 4B	8.72	2.68 – 15.14	High	200 – 600	<3 mm	B2	(3)
Block 4C	9.42	2.68 – 15.14	High	200 – 600	<3 mm	B2	(2)
Block 4D	9.12	3.76 – 16.28	High	>600	<3 mm	B1	Least (4)

Areas of significant colour change were considered along with the superimposed heat map to further split quadrat 4 for further analysis, resulting in 3 discrete blocks (Figure 7-30). Block 4E was interpreted as the central lighter coloured chalk within the centre of the quadrat, and had the highest mean UCS of 9.91 MPa, ranging 2.68 – 16.42 MPa. Block 4F was interpreted from discolouration in the bottom left hand of the quadrat, where the chalk is darker in colour, 4F had the lowest mean UCS at 6.08 MPa and a range of 2.28 – 12.74 MPa. Block 4G was interpreted from the discoloured area in the top right hand of the quadrat, where the chalk is slightly more discoloured than 4E but less than 4F. 4G had a similar mean UCS to block 4D at 9.04 MPa, ranging 4.48 – 15.14 MPa (Table 7-19).

Table 7-19 Newhaven, quadrat 4 - degree of weathering based on discolouration, SilverSchmidt.

SilverSchmidt quadrat 4	UCS (MPa)	UCS range (MPa)	CIRIA density grade	Fracture spacing (mm)	Fracture aperture (mm)	CIRIA fracture grade	Degree of weathering
Block 4E	9.91	2.68 – 16.42	High	>600	<3 mm	B1	Least (1)
Block 4F	6.08	2.28 – 12.74	High	>600	<3 mm	B1	Most (3)
Block 4G	9.04	4.48 – 15.14	High	20 - 600	<3 mm	B2-5	Intermediate (2)

While all blocks fall within the high-density CIRIA grade, the discolouration along with measured mean UCS demonstrates relative strength differences. This is interpreted to be chemical weathering, whereby the chalk has been altered by chemically rich ground water, resulting in discolouration of the weaker chalk, and lower UCS values. This chemical weathering, in combination with discontinuities is a significant cause of variability in UCS readings. Table 7-20 presents a summary of SilverSchmidt UCS variability with weathering grade and textures observed.

Table 7-20 Newhaven Harbour, SilverSchmidt derived UCS against texture and weathering grade.

SilverSchmidt quadrat	Texture	UCS (MPa)	UCS range (MPa)	SilverSchmidt CIRIA density grade	Hammer penetration (mm)	Hammer penetration range (mm)	Hammer CIRIA density grade	CIRIA fracture grade
1A	Massive, un-brecciated	9.31	2.28 – 19.14	High	9	8 - 10	High	A1
1B	Brecciated, open fractures	7.30	2.48 – 17.75	High	7.6	6 - 10	High	C4
2	Widely spaced discontinuities	6.15	2.48 – 13.11	High	6.4	3 - 10	High	B1-3
3A	Brecciated,	7.58	2.48 – 15.56	High	4.6	4 – 5	High	C3
3B	un-brecciated	8.03	2.88 – 15.99	High	10	9 – 11	High	C1
3C	Massive, un-brecciated block	8.61	1.9 – 18.67	High	8.8	7 - 10	High	C1
4A	Brecciated,	6.73	4.73 – 9.79	High	8.6	6 – 10	High	B5
4B	Chemically weathered	8.72	2.68 – 15.14	High	10	9 – 10	High	B2
4C	Chemically weathered	9.42	2.68 – 15.14	High	6	6 – 6	High	B2
4D	Chemically weathered	9.12	3.76 – 16.28	High	8	7 – 9	High	B1
4E	Brecciated, chemically weathered	9.91	2.68 – 16.42	High	8.8	7 – 12	High	B1
4F	Chemically weathered	6.08	2.28 – 12.74	High	9.6	7 – 12	High	B1
4G	Chemically weathered	9.04	4.48 – 15.14	High	7.3	6 - 10	High	B2-5
5	Unbrecciated; chemically weathered	9.02	2.09 – 17.75	High	9.8	9 - 14	High	A1

The analysis was repeated using the Equotip to establish trends in IDD related to observed discoloration and the distribution of discontinuities (Table 7-21). The rationale behind this approach is that the Equotip sampler is smaller than the SilverSchmidt, and therefore less likely to be affected by energy loss due to discontinuities being beneath the sample test surface.

Table 7-21 Newhaven, quadrat 4 - degree of weathering based on discontinuities, Equotip.

Equotip quadrat 4	IDD (Mg/m^3)	IDD range (Mg/m^3)	CIRIA density grade	Fracture spacing (mm)	Fracture aperture (mm)	CIRIA fracture grade	Degree of weathering
Block 4A	1.61	1.53 - 1.71	Medium	<20 mm	<3 mm	B5	Most (1)
Block 4B	1.73	1.53 - 2.37	High	200 – 600	<3 mm	B2	Least (4)
Block 4C	1.71	1.52 - 2.13	High	200 – 600	<3 mm	B2	(2)
Block 4D	1.66	1.55 - 1.83	Medium	>600	<3 mm	B1	(3)

Comparing the IDD results with the SilverSchmidt derived UCS results shows discrepancy between the two methods; block 4A has a mean IDD of 1.61 Mg/m^3, and a range of 1.53 – 1.71 Mg/m^3, giving a medium-density CIRIA grade, which is a lower grade than the SilverSchmidt derived UCS values. Block B has a mean IDD of 1.73 Mg/m^3, ranging 1.53 – 2.37 Mg/m^3, which is high density, corresponding to the UCS grade. Block C has a lower IDD of 1.71 Mg/m^3, corresponding to a high CIRIA density grade and matched the SilverSchmidt reported values, while block 4D has a mean IDD of 1.66 Mg/m^3, ranging 1.55 – 1.83 Mg/m^3 (Table 7-22).

Table 7-22 Newhaven, quadrat 4 - degree of weathering based on discolouration, Equotip.

Equotip quadrat 4	IDD (Mg/m^3)	IDD range (Mg/m^3)	CIRIA density grade	Fracture spacing (mm)	Fracture aperture (mm)	CIRIA fracture grade	Degree of weathering
Block 4E	1.66	1.53 - 1.96	Medium	>600	<3 mm	B1	Intermediate (2)
Block 4F	1.76	1.56 - 2.37	High	>600	<3 mm	B1	Least (1)
Block 4G	1.68	1.52 - 2.13	Medium	20 - 600	<3 mm	B2-5	Most (3)

Tables 7-21 and 7-22 show no changes of discontinuity character, but do demonstrate differences between density grades; Block 4E had a mean IDD of 1.66 Mg/m^3, ranging 1.53 – 1.96 Mg/m^3 and block 4G had a mean IDD of 1.68 Mg/m^3, ranging 1.52 - 2.13 Mg/m^3, which correlate to medium-density CIRIA grades. When classified using UCS (Tables 7-18 and 7-19), these grades were high-density. Another observed difference between UCS and IDD is that when measured using IDD, block

4F had the lowest mean UCS of 6.08 MPa, while when IDD is measured, this block has the highest reading of 1.76 Mg/m^3 and a range of 1.56 – 2.37 Mg/m^3. This is likely due to the size of the Equotip sampler face – its small size more suitable for testing the rock material as opposed to the rock mass. Observation of relative IDD differences with discontinuity positions shows a pattern of medium density readings either on the line of discontinuity or slightly below (Figure 7-31).

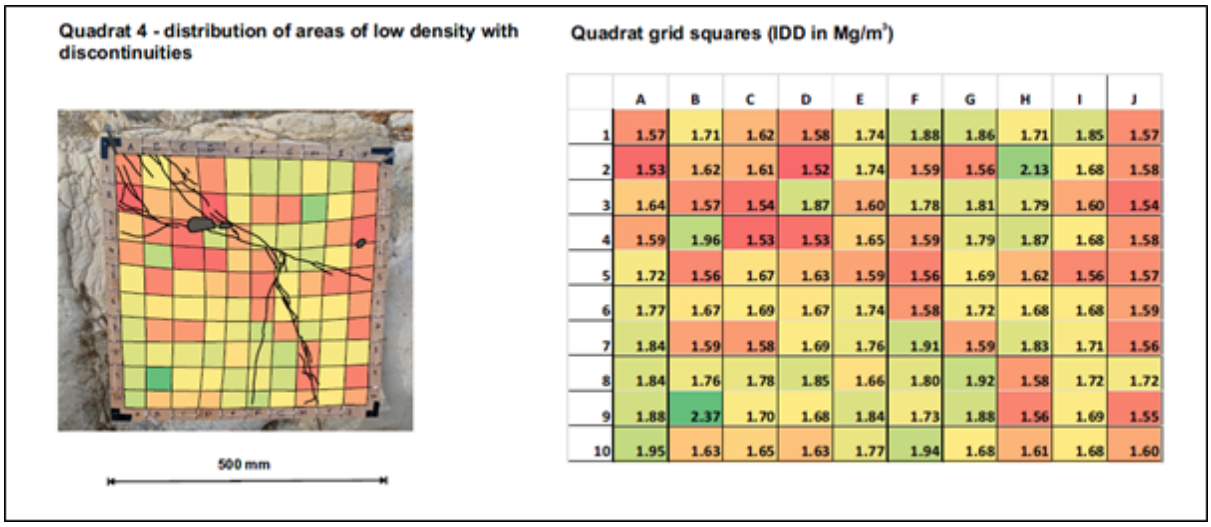


Figure 7-31 Newhaven Harbour, quadrat 4 - discrete line of discontinuity and heat map.

Using the line of discontinuity to position a line of measurement on the quadrat, it is possible to observe a mean IDD of 1.62 Mg/m^3, ranging 1.53 – 1.87 Mg/m^3. Values for mean IDD away from the line of discontinuity are higher, with a mean IDD of 1.72 Mg/m^3 and a range of 1.52 – 2.37 Mg/m^3 (High CIRIA density grade) (Table 7-23).

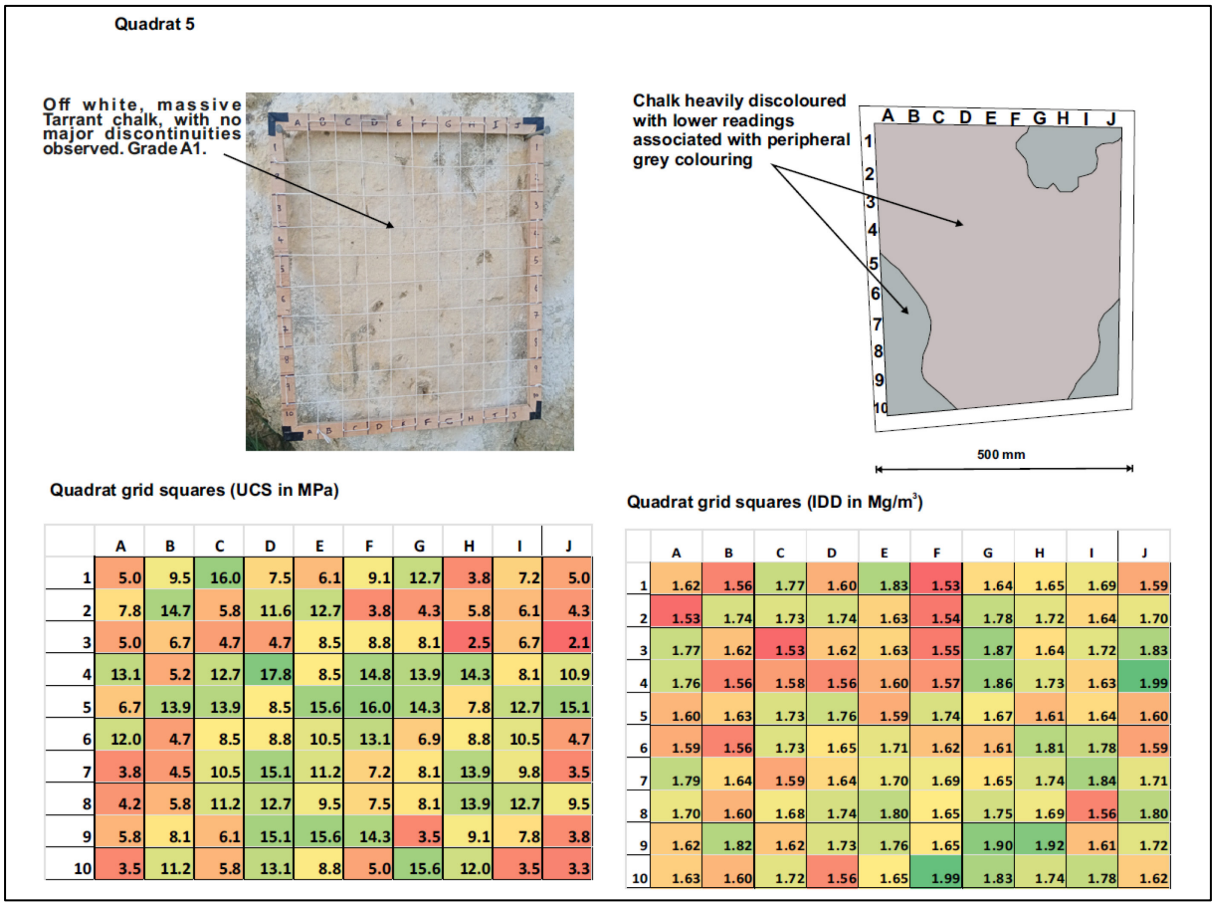
Table 7-23 Newhaven, quadrat 4 - degree of weathering due to discontinuity

EQ quadrat 4;	**IDD (Mg/m³)**	**IDD range (Mg/m³)**	**CIRIA density grade**	**Fracture spacing (mm)**	**Fracture aperture (mm)**	**CIRIA fracture grade**	**Degree of weathering**
Discontinuity line	1.62	1.53 – 1.87	Medium	Variable; <20 - 200	Open <3 mm	B5	Moderate
Remainder of quadrat 4	1.72	1.52 – 2.37	High	Variable; <20 - 200	Open <3 mm	B5	Moderate

From observation, it is possible to infer a mechanism for this localised weakening; the sampler size of the Equotip is small and discrete, therefore the density change is unlikely to be due to rebound energy attenuation through fractures, so the density readings (accurate or not) are likely to be a true reflection of the rock properties as the testing is repeatable. Discolouration indicates chemical alteration of the chalk, while a loss of density supports this, with an inferred loss of microstructure in the chalk due to dissolution. The brecciation associated with discontinuities is likely to cause further weakening and the

and position of weakening on (or below, indicating percolation) discontinuities indicates that the main fault has acted as a preferential pathway for chemically-rich water, which has altered the chalk.

Quadrat 5 produced similar measurements, despite the stratigraphically lower position, with a mean UCS value of 9.02 MPa and range of 2.09 – 17.75 MPa, and a mean IDD value of 1.69 Mg/m^3, and a range of 1.53 – 1.99 Mg/m^3 (Figure 7-32). The chalk is off white, massive Tarrant chalk, significantly discoloured, with no major discontinuities observed, graded as A1 high-density chalk. Without observation of discontinuities, classification by discontinuity aperture is a default grading.



	A	B	C	D	E	F	G	H	I	J
1	5.0	9.5	16.0	7.5	6.1	9.1	12.7	3.8	7.2	5.0
2	7.8	14.7	5.8	11.6	12.7	3.8	4.3	5.8	6.1	4.3
3	5.0	6.7	4.7	4.7	8.5	8.8	8.1	2.5	6.7	2.1
4	13.1	5.2	12.7	17.8	8.5	14.8	13.9	14.3	8.1	10.9
5	6.7	13.9	13.9	8.5	15.6	16.0	14.3	7.8	12.7	15.1
6	12.0	4.7	8.5	8.8	10.5	13.1	6.9	8.8	10.5	4.7
7	3.8	4.5	10.5	15.1	11.2	7.2	8.1	13.9	9.8	3.5
8	4.2	5.8	11.2	12.7	9.5	7.5	8.1	13.9	12.7	9.5
9	5.8	8.1	6.1	15.1	15.6	14.3	3.5	9.1	7.8	3.8
10	3.5	11.2	5.8	13.1	8.8	5.0	15.6	12.0	3.5	3.3

	A	B	C	D	E	F	G	H	I	J
1	1.62	1.56	1.77	1.60	1.83	1.53	1.64	1.65	1.69	1.59
2	1.53	1.74	1.73	1.74	1.63	1.54	1.78	1.72	1.64	1.70
3	1.77	1.62	1.53	1.62	1.63	1.55	1.87	1.64	1.72	1.83
4	1.76	1.56	1.58	1.56	1.60	1.57	1.86	1.73	1.63	1.99
5	1.60	1.63	1.73	1.76	1.59	1.74	1.67	1.61	1.64	1.60
6	1.59	1.56	1.73	1.65	1.71	1.62	1.61	1.81	1.78	1.59
7	1.79	1.64	1.59	1.64	1.70	1.69	1.65	1.74	1.84	1.71
8	1.70	1.60	1.68	1.74	1.80	1.65	1.75	1.69	1.56	1.80
9	1.62	1.82	1.62	1.73	1.76	1.65	1.90	1.92	1.61	1.72
10	1.63	1.60	1.72	1.56	1.65	1.99	1.83	1.74	1.78	1.62

Figure 7-32 Newhaven Harbour, quadrat 5.

With further scrutiny, lower UCS values are observed to correlate with areas of white – grey discolouration at the peripheries of the quadrat, while the central cream coloured area has higher UCS values (Table 7-24).

Table 7-24 Newhaven, quadrat 5 - degree of weathering, SilverSchmidt.

SS quadrat 5;	UCS (MPa)	UCS range (MPa)	CIRIA density grade	Fracture spacing (mm)	Fracture aperture (mm)	CIRIA fracture grade	Degree of weathering
White-grey discoloured areas	6.03	2.09 – 12.72	High	>600 mm	N/A	A1	Most (2)
Buff-cream coloured area	10.36	3.53 – 17.75	High	>600 mm	N/A	A1	Least (1)

Equotip values did not correlate with measured UCS values, with particularly high IDD readings associated with the bottom left-hand corner of the quadrat compared to low UCS readings (Figure 7-32, grid squares A9, A10, B9, B10). As observation of the chalk face was obscured, it was not possible to infer if this was a discrete block. Density differences in the rock face may be due to preferential physical weathering due to exposure to the elements and surface relief of the rock.

While weathering was observed in the features of the rock mass, measurement of UCS and IDD within each quadrat did not correlate. The SilverSchmidt derived UCS trends were interpreted as case hardening and softening due to chemical weathering, however this was not supported by the Equotip IDD values. The IDD values observed were difficult to interpret as the rock face (and potential discontinuities) were obscured, it was not possible to infer their origin.

The nature of the karstification at this locality is attributed to sulphate rich waters from the overlying Woolwich beds (Mortimore, 2014), which is the provenance of the increased chemical content in the groundwater These aggressive ground waters exploited faults as preferential flow pathways causing disequilibrium mixing, leading to karstification (Maurice et al. 2023). The fault itself is a high-angled conjugate fault. Material loss is associated with areas where other discontinuities intersect with this high-angled fault; this is inferred to be due to cataclastic processes disaggregating the chalk in discrete pockets, which is then followed by transport of acidic groundwater which dissolves the breccia, leaving karstic voids at the intersections of discontinuities and bedding planes.

7.2.4 Birling Gap research site

Five quadrats were measured at Birling Gap using both SilverSchmidt and Equotip instruments. This yielded 500 measurements per device respectively. Data collected from Birling Gap are presented in Table 7-25 and Figure 7-33. The quadrats were positioned across the dry valley to evaluate and compare the material properties of structured and D-grade chalk as well as the instrument effectiveness within these two types of deposits.

Figure 7-33 demonstrates that less weathered chalks have higher SilverSchmidt-derived UCS values compared to de-structured Dc and Dm grades, with quadrats 5 and 3 having UCS values of 6.80 and 7.35 MPa respectively. The quadrats which are positioned on the de-structured grades of chalk have lower UCS values; quadrat 4 has a mean UCS of 3.05 MPa, quadrat 1 has a mean UCS of 4.30 MPa and quadrat 2 has a UCS of 5.05 MPa (Table 7-25).

In contrast, Equotip derived IDD values fall within a narrow range of 1.64 – 1.68 Mg/m^3. Quadrat 5 has the greatest IDD value at 1.68 Mg/m^3, quadrat 1 at 1.67 Mg/m^3, quadrats 2 and 3 have the same IDD value of 1.65 Mg/m^3. The lowest mean UCS is quadrat 4 at 1.64 Mg/m^3 (Table 7-25).

Table 7-25 Birling Gap, SilverSchmidt descriptive statistics and CIRIA weathering grades.

Birling Gap	**SS quadrat 1**	**EQ quadrat 1**	**SS quadrat 2**	**EQ quadrat 2**	**SS quadrat 3**	**EQ quadrat 3**	**SS quadrat 4**	**EQ quadrat 4**	**SS quadrat 5**	**EQ quadrat 5**
Valid	71	100	91	100	100	100	80	100	100	100
Mean	4.31 MPa	1.67 Mg/m^3	5.05 MPa	1.65 Mg/m^3	7.35 MPa	1.65 Mg/m^3	3.05 MPa	1.64 Mg/m^3	6.84 MPa	1.68 Mg/m^3
Range	1.9 – 19.5 MPa	1.52 - 2.64 Mg/m^3	1.73 – 13.5 MPa	1.53 - 1.96 Mg/m^3	1.9 – 22.5 MPa	1.53 - 1.9 Mg/m^3	1.73 – 9.79 MPa	1.52 - 1.91 Mg/m^3	2.68 – 17.75 MPa	1.52 - 2.13 Mg/m^3
Standard deviation	2.80	0.14	2.78	0.095	3.33	0.092	3.05	0.097	3.05	0.125
Variance	7.80	0.02	7.74	0.009	11.08	0.008	1.28	0.009	9.32	0.016
Skewness	3.37	3.891	1.261	1.061	1.137	0.86	2.85	0.836	0.969	1.019
Kurtosis	13.88	23.69	0.948	0.996	2.965	-0.134	14.792	-0.287	0.917	0.996
CIRIA discontinuity grade	Dc		C4		A3		B5		A1	
CIRIA density grade	Low - Medium	Low	Medium	Medium	Low - Medium	Medium	Medium	Low	Low - Medium	Medium

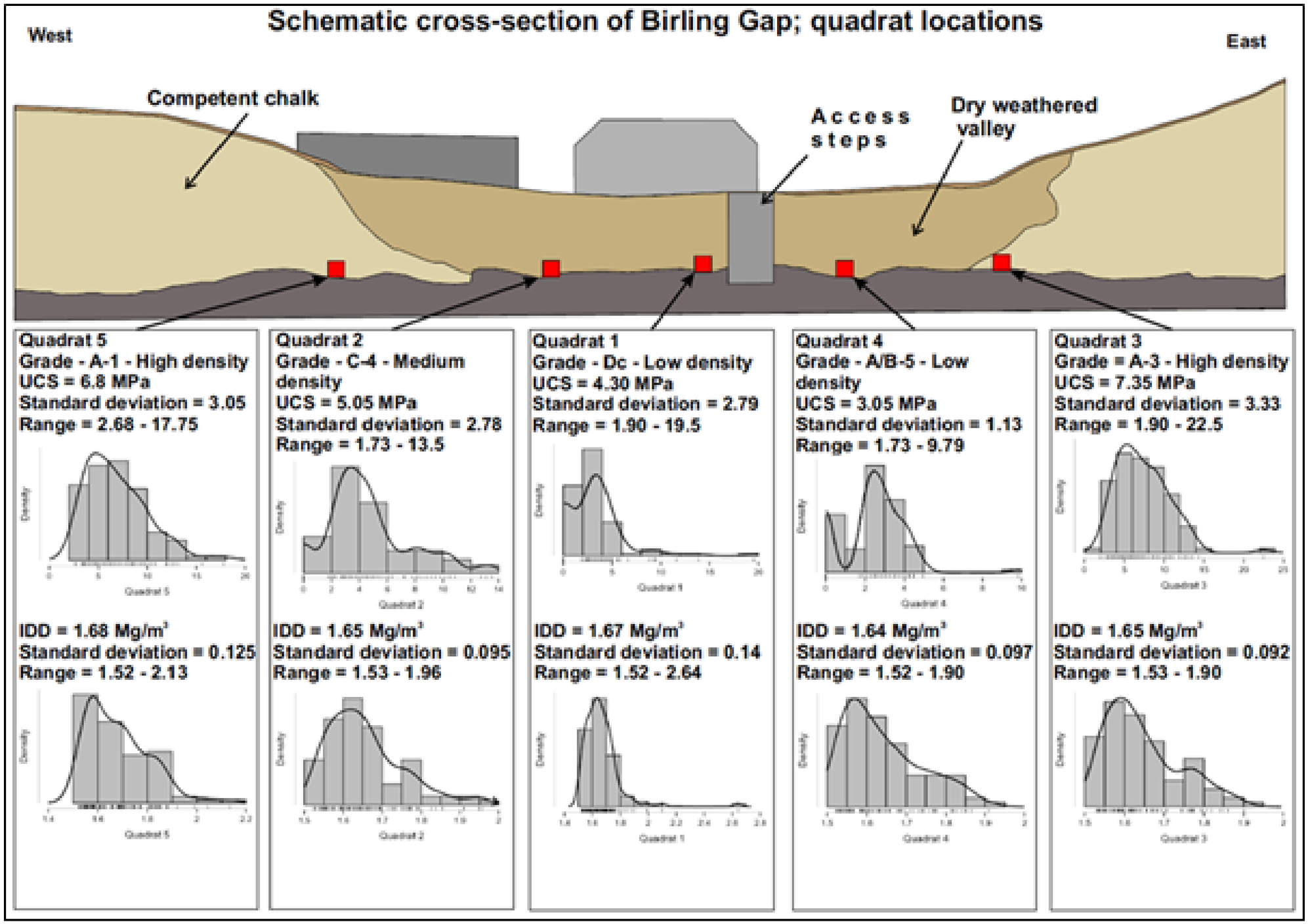


Figure 7-33 Schematic cross-section; Birling Gap, East Dean.

Quadrats 1 and 5

Figure 7-34 shows a comparison of a grade A, Seaford Chalk and grade Dc, Seaford Chalk. Each of the quadrats were measured using the Equotip for IDD and the SilverSchmidt for UCS. Initial measurement showed that all Equotip IDD measurements were valid, with 100% of readings returning a positive value, while with the SilverSchmidt, twenty-nine readings were invalid when measuring the grade Dc chalk. This suggests the Equotip has a greater probability of returning valid readings compared to the SilverSchmidt.

Statistically all data series were normally distributed with a positive skew, indicating that there is a pre-disposal of readings to be at the lower end of the density and strength scales. Quadrat 1 yields the greatest ranges of values for both IDD and UCS, with the greatest kurtosis for both, which indicates that Dc chalk is more variable in terms of material properties compared to structured A1 chalk. This is interpreted as textural heterogeneity due to clasts and matrix.

Comparing the UCS of A1 to Dc grade, the structured A grade chalk has a lower range variability and a higher mean UCS of 6.8 MPa compared to that of Dc – 4.30 MPa. Comparing the IDD of A1 to Dc, the A1 IDD values are similar, with quadrat 5 (grade A1) having an IDD of 1.68 Mg/m^3, while quadrat 1 (grade Dc) is 1.63 Mg/m^3. The likelihood is that the relative discrepancy between UCS and IDD values (i.e., UCS being variable and IDD being similar) is due to instrument type used. The SilverSchmidt imparts a higher amount of energy over a greater surface area compared to that of the Equotip, therefore is likely to have modified the structure of the de-structured chalk. The Equotip imparts a much lower energy, therefore disturbs the de-structured chalk less.

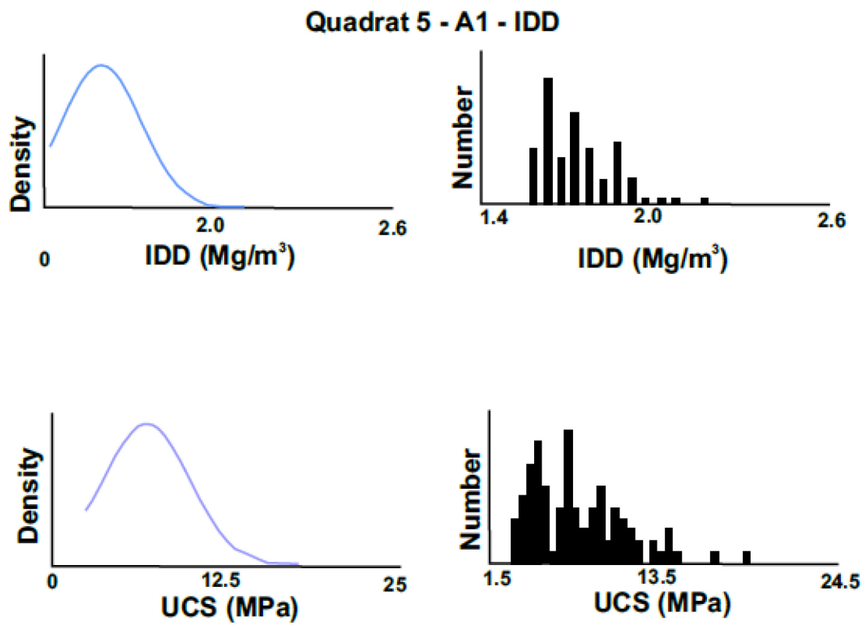
Quadrat 5: grade A1 chalk
CIRIA density based on Equotip derived IDD
Mean = medium density

	A	B	C	D	E	F	G	H	I	J
1	1.56	1.81	1.75	1.83	1.55	1.82	2.13	1.57	1.76	1.83
2	1.77	1.69	1.84	1.57	1.69	1.71	1.69	1.92	1.61	1.69
3	1.85	1.69	1.56	1.86	1.53	1.58	1.59	1.68	1.70	1.57
4	1.61	1.74	1.86	1.85	1.99	1.66	1.88	1.89	2.04	1.77
5	1.53	1.56	1.64	1.65	1.58	1.63	1.68	1.71	1.70	1.66
6	1.54	1.66	1.56	1.81	1.76	1.74	1.85	1.82	1.55	1.54
7	1.59	1.56	1.57	1.55	1.61	1.57	1.58	1.55	1.83	1.62
8	1.74	1.58	1.60	1.56	1.59	1.55	1.69	1.72	1.65	1.68
9	1.66	1.59	1.88	1.58	1.58	1.61	1.59	1.56	1.62	1.75
10	1.80	1.53	1.73	1.68	1.54	1.68	1.71	1.52	1.70	1.57

Quadrat 5: CIRIA density based on Silverschmidt derived UCS
Mean = high density

	A	B	C	D	E	F	G	H	I	J
1	2.7	12.7	8.5	7.8	2.7	12.7	10.5	6.1	2.7	4.5
2	5.0	17.8	3.5	3.5	6.3	4.5	4.7	9.8	8.8	5.5
3	3.3	4.2	7.2	6.6	6.9	12.7	9.5	8.1	9.8	4.5
4	8.5	4.7	9.8	15.6	6.6	5.5	9.5	10.1	4.2	6.1
5	6.3	3.8	7.8	4.7	6.1	10.9	5.8	7.8	10.1	8.5
6	3.5	10.9	3.3	5.8	9.8	6.1	3.8	4.2	12.0	13.1
7	3.5	3.3	12.0	4.5	7.8	6.3	4.0	4.0	9.1	5.2
8	8.8	6.3	9.5	8.5	7.5	12.3	6.3	6.9	6.6	7.2
9	3.8	6.3	4.5	3.3	4.5	3.3	9.1	8.1	4.5	5.0
10	4.5	6.3	7.2	3.3	4.7	6.1	2.7	5.8	4.7	8.1





Quadrat 1: grade Dc chalk
CIRIA density based on Equotip derived IDD
Mean = medium density

	A	B	C	D	E	F	G	H	I	J
1	1.55	1.72	1.70	1.67	1.61	1.60	1.70	1.59	1.53	1.59
2	1.56	1.63	1.64	1.67	1.59	1.74	1.83	1.71	1.55	1.55
3	1.66	1.72	1.62	1.57	1.61	1.66	1.80	1.90	1.73	1.65
4	1.64	1.69	1.99	1.55	1.65	1.72	1.76	1.76	1.59	1.85
5	1.58	1.55	1.65	1.62	1.58	1.74	1.59	1.70	1.61	1.77
6	2.64	1.61	1.64	1.72	1.53	1.69	1.52	1.56	1.63	1.66
7	1.53	1.60	1.71	1.64	1.53	1.73	2.10	1.57	1.88	1.75
8	1.70	1.71	1.62	1.64	1.66	1.62	1.62	1.53	1.66	1.56
9	1.69	1.61	1.68	1.74	1.79	1.63	1.74	1.67	1.55	1.76
10	1.53	1.63	1.68	1.62	1.53	1.68	1.54	1.58	1.56	1.67

Quadrat 1: CIRIA density based on Silverschmidt derived UCS
Mean = medium density

	A	B	C	D	E	F	G	H	I	J
1	5.5	2.9	8.8	3.8	5.0		3.5			4.5
2	3.8		4.7				2.5	4.0		3.1
3	4.0	4.0	1.9	5.8		3.5	2.5	4.5	4.2	3.3
4	5.8	1.9		5.8	3.1	2.3	4.3	2.7	2.5	3.5
5		3.3	2.5	2.9	6.6	9.1		3.5	2.7	2.7
6		4.5	11.6	13.9	3.5		4.0		3.8	9.5
7	3.8		5.0	3.3	4.0		4.7	2.9	5.0	10.5
8	2.9	2.1	2.9	3.1	2.5					
9	2.7	3.1	4.5	2.9	2.9	3.5	4.0			
10		3.1	2.7		2.5	3.3	4.0	3.8		



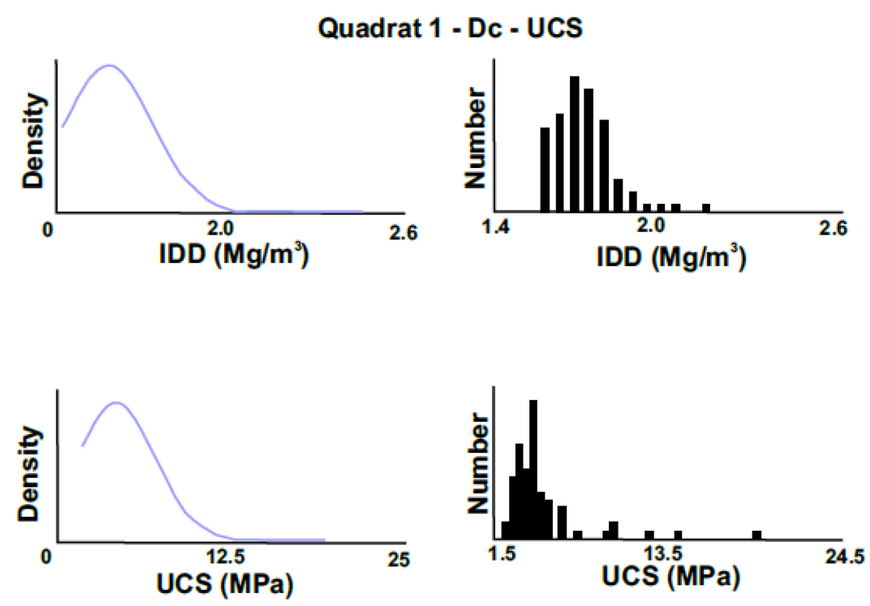


Figure 7-34 Birling Gap, quadrat 1 versus quadrat 5 (de-structured chalk versus structured chalk – white squares denote null readings).

Quadrat 2

Quadrat 2 (Figure 7-35) is a medium density, highly brecciated chalk. Discontinuities are open >3mm and are tightly spaced between 20 – 60 mm, resulting in a grade C4 chalk. The chalk is discoloured, which is characteristic of a dry valley setting due to rubification (as observed at other locations, such as Portobello).

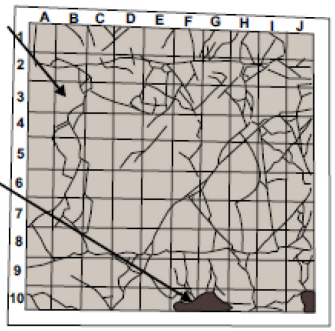
Quadrat 2

Medium density grade C4 Seaford Chalk, with some areas of grade B discontinuity aperture openings. Buff to cream colour with discontinuities that are angular.



Fractures appear to control slabby or blocky material loss

Nodular flints



Quadrat grid squares (UCS in MPa)

	A	B	C	D	E	F	G	H	I	J
1	10.5	5.2	3.3	8.8	10.1	4.7	3.3	2.9	2.9	
2	5.0	2.7	3.8	3.1	5.8	4.7	2.7	3.8	3.8	5.5
3	4.0	2.3	3.1	2.1		4.5	8.1	2.7		
4	4.5	0.0	5.2	4.5	7.2	9.1	4.5	2.3		
5	6.3	2.9	2.7	2.9	6.1	7.8	2.9	3.5		
6	5.0	3.1	5.2	7.2	10.9	13.1	4.2	4.2	4.7	4.5
7	5.0	6.3	8.5	12.7	13.5	7.8	5.5	1.7	4.5	3.3
8	1.9	3.8	9.5	10.5	10.5	4.5	3.3	3.1	3.3	3.3
9	3.3	3.3	8.1	2.1	2.1	4.5	4.0	2.3	4.2	3.8
10	5.0	9.8	8.1	3.1	3.1	4.5	2.3	6.1	1.9	1.9

Quadrat grid squares (IDD in Mg/m^3)

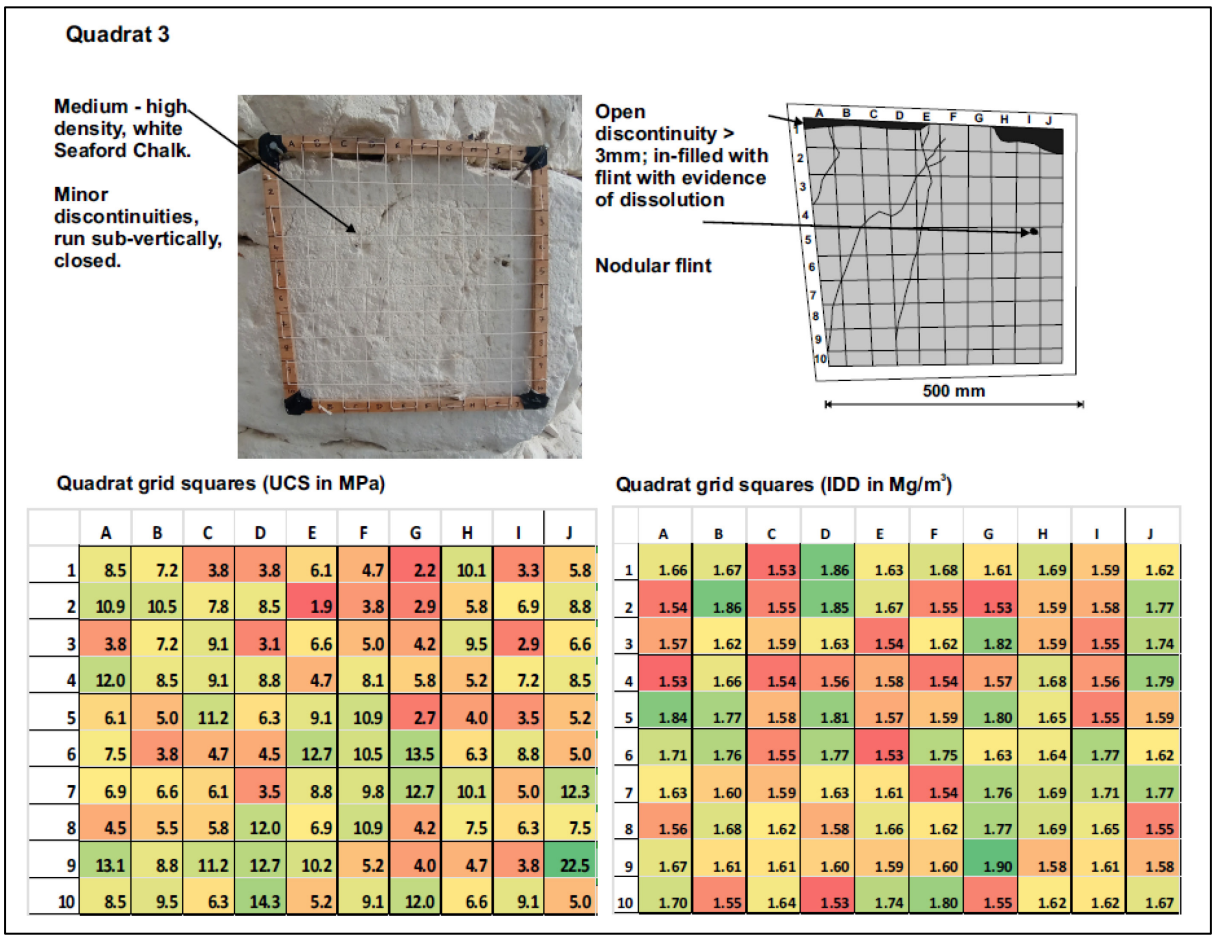
	A	B	C	D	E	F	G	H	I	J
1	1.64	1.68	1.66	1.67	1.60	1.95	1.64	1.75	1.54	1.53
2	1.86	1.70	1.70	1.79	1.66	1.59	1.57	1.55	1.73	1.64
3	1.60	1.73	1.53	1.54	1.54	1.79	1.76	1.70	1.58	1.57
4	1.65	1.80	1.78	1.60	1.69	1.69	1.60	1.55	1.60	1.64
5	1.70	1.58	1.67	1.62	1.59	1.59	1.74	1.57	1.68	1.62
6	1.62	1.61	1.72	1.66	1.56	1.76	1.55	1.56	1.61	1.86
7	1.58	1.56	1.64	1.77	1.91	1.65	1.66	1.71	1.62	1.58
8	1.64	1.53	1.67	1.60	1.96	1.66	1.63	1.75	1.64	1.68
9	1.55	1.59	1.56	1.60	1.65	1.63	1.64	1.53	1.77	1.84
10	1.56	1.66	1.54	1.59	1.65	1.77	1.63	1.62	1.83	1.59

Figure 7-35 Birling Gap, quadrat 2 (white squares denote null readings).

The mean UCS is 5.05 MPa, ranging from 1.9 – 15.5 MPa, giving a medium CIRIA density grade. The corresponding mean IDD is 1.65 Mg/m^3, giving a medium CIRIA density and ranging 1.53 – 1.96 Mg/m^3. In terms of invalid readings, there are a significant number of zero readings using the SilverSchmidt which are associated with closely-spaced, open discontinuities. The IDD measurements are not affected by these closely spaced fractures.

Quadrat 3

Quadrat 3 (Figure 7-36) is less weathered Seaford chalk, brilliant white in hue. This quadrat focuses on a relatively unweathered section of chalk, however, there are discontinuities in-filled with flint and subject to discrete dissolution and weathering, resulting in a CIRIA discontinuity grade of A3.



Quadrat grid squares (UCS in MPa)

	A	B	C	D	E	F	G	H	I	J
1	8.5	7.2	3.8	3.8	6.1	4.7	2.2	10.1	3.3	5.8
2	10.9	10.5	7.8	8.5	1.9	3.8	2.9	5.8	6.9	8.8
3	3.8	7.2	9.1	3.1	6.6	5.0	4.2	9.5	2.9	6.6
4	12.0	8.5	9.1	8.8	4.7	8.1	5.8	5.2	7.2	8.5
5	6.1	5.0	11.2	6.3	9.1	10.9	2.7	4.0	3.5	5.2
6	7.5	3.8	4.7	4.5	12.7	10.5	13.5	6.3	8.8	5.0
7	6.9	6.6	6.1	3.5	8.8	9.8	12.7	10.1	5.0	12.3
8	4.5	5.5	5.8	12.0	6.9	10.9	4.2	7.5	6.3	7.5
9	13.1	8.8	11.2	12.7	10.2	5.2	4.0	4.7	3.8	22.5
10	8.5	9.5	6.3	14.3	5.2	9.1	12.0	6.6	9.1	5.0

Quadrat grid squares (IDD in Mg/m^3)

	A	B	C	D	E	F	G	H	I	J
1	1.66	1.67	1.53	1.86	1.63	1.68	1.61	1.69	1.59	1.62
2	1.54	1.86	1.55	1.85	1.67	1.55	1.53	1.59	1.58	1.77
3	1.57	1.62	1.59	1.63	1.54	1.62	1.82	1.59	1.55	1.74
4	1.53	1.66	1.54	1.56	1.58	1.54	1.57	1.68	1.56	1.79
5	1.84	1.77	1.58	1.81	1.57	1.59	1.80	1.65	1.55	1.59
6	1.71	1.76	1.55	1.77	1.53	1.75	1.63	1.64	1.77	1.62
7	1.63	1.60	1.59	1.63	1.61	1.54	1.76	1.69	1.71	1.77
8	1.56	1.68	1.62	1.58	1.66	1.62	1.77	1.69	1.65	1.55
9	1.67	1.61	1.61	1.60	1.59	1.60	1.90	1.58	1.61	1.58
10	1.70	1.55	1.64	1.53	1.74	1.80	1.55	1.62	1.62	1.67

Figure 7-36 Birling Gap, quadrat 3.

The mean UCS of quadrat 3 was 7.35 MPa, ranging from 1.9 – 22.5 MPa, resulting in a CIRIA density of high, while the measured IDD was 1.65 Mg/m^3, ranging of 1.53 – 1.90 Mg/m^3. The measured IDD puts this as being a medium density chalk, the measured UCS value is close to the boundary between medium and high-density grades.

Quadrat 4

Quadrat 4 (Figure 7-37) frames a heavily brecciated, blocky, rubbly, disturbed, brown to buff Seaford Chalk. Discontinuities are open <3 mm and spaced <20 mm, giving this chalk a CIRIA discontinuity grade of B5. The chalk is cross-cut by a horizontal discontinuity that is open >3 mm and infilled with sheet flint. The discontinuity flint is also highly brecciated and disturbed. Below the sheet flint, the chalk appears to consist of larger sized blocks than those above the discontinuity.

Quadrat 4

Highly brecciated and disturbed Seaford Chalk; buff brown discolouration.

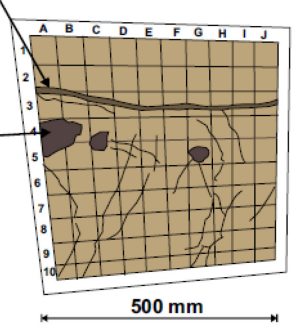
Rubbly, blocky surface texture.

Grade B5



Highly brecciated and disturbed infilled flint horizon

Nodular flint



Quadrat grid squares (UCS in MPa)

	A	B	C	D	E	F	G	H	I	J
1	2.7	3.1	2.1	2.3	4.0	4.0	4.5	3.1	3.1	2.5
2		2.1	2.1	2.3	3.8	2.9	1.9	1.7	3.1	
3					4.0	3.1	5.0		2.3	1.9
4	9.8	3.8	2.1	2.9	2.1	2.5	2.3	2.1	3.3	2.7
5	1.9	1.9	2.1	2.5	3.8	4.0	3.1	1.9	4.5	2.7
6			2.5	2.5	1.7	3.3	2.5	2.9	5.0	2.7
7		3.1	2.9	2.5	2.1		2.5	2.7	2.7	2.9
8	3.5	2.1	2.9	3.3	3.5	4.2	2.3	4.2	3.5	4.5
9	4.2		3.3	3.3			3.8	2.5		4.5
10						2.1	2.7	4.0	4.0	1.9

Quadrat grid squares (IDD in Mg/m^3)

	A	B	C	D	E	F	G	H	I	J
1	1.56	1.60	1.54	1.62	1.69	1.63	1.61	1.60	1.74	1.65
2	1.54	1.54	1.53	1.69	1.78	1.81	1.91	1.66	1.55	1.55
3	1.56	1.57	1.61	1.56	1.53	1.56	1.56	1.60	1.56	1.53
4	1.52	1.71	1.82	1.68	1.55	1.62	1.65	1.63	1.76	1.69
5	1.64	1.64	1.56	1.77	1.59	1.77	1.59	1.74	1.60	1.60
6	1.55	1.73	1.86	1.68	1.84	1.78	1.59	1.58	1.54	1.68
7	1.83	1.85	1.59	1.74	1.82	1.66	1.55	1.63	1.75	1.54
8	1.53	1.53	1.68	1.56	1.68	1.59	1.57	1.66	1.59	1.65
9	1.77	1.56	1.72	1.65	1.55	1.63	1.77	1.55	1.61	1.82
10	1.56	1.56	1.70	1.53	1.59	1.62	1.68	1.61	1.85	1.56

Figure 7-37 Birling Gap, quadrat 4 (white squares denote null readings).

Quadrat 4 was split into 2; above the flint filled discontinuity and the area below. The measured mean UCS for the discontinuity and above was 2.8 MPa, ranging 1.7 – 6.5 MPa, which gives a low CIRIA density grade, while below, the mean UCS was 3.1 MPa and ranged 1.7 – 9.8 MPa, giving a medium CIRIA density grade. For IDD the mean UCS above the flint filled discontinuity was 1.61 Mg/m^3 ranging 1.53 – 1.91 Mg/m^3, resulting in a medium density grade, while below the discontinuity, the measured IDD mean was 1.65 Mg/m^3, ranging 1.52 – 1.86 Mg/m^3.

Table 7-26 presents SilverSchmidt-derived UCS values, comparing these against CIRIA density grades derived from hammer penetration tests and textures. From this it is possible to observe that the hammer derived density grades are consistently higher than the SilverSchmidt derived density grades.

Table 7-26 Birling Gap, SilverSchmidt derived UCS against texture and weathering grade.

SilverSchmidt quadrat	Texture	UCS (MPa)	UCS range (MPa)	SilverSchmidt CIRIA density grade	Hammer penetration (mm)	Hammer penetration range (mm)	Hammer CIRIA density grade	CIRIA fracture grade
1	Competent clasts hosted in a puttified matrix	4.31	1.9 – 19.5	Low – medium	29.7	10 - 60	Low	Dc
2	Highly brecciated with tightly spaced discontinuities	5.05	1.73 – 13.5	Medium	6.8	5 - 9	High	C4
3	Un-brecciated, competent Seaford Chalk	7.35	1.9 – 22.5	High	7.5	5 – 12	High	A3
4 – above discontinuity	Heavily brecciated chalk and flint horizon	2.8	1.7 – 9.8	Low	10.83	5 – 14	Medium/high	B5
4 below discontinuity	Heavily brecciated, rubbly chalk	3.1	1.53 – 1.91	Low – medium	11	8 – 16	Medium	B5
5	Competent, un-brecciated Seaford Chalk	6.84	2.68 – 17.75	High	7.4	7 - 9	High	A1

7.3 Regional data summary

SilverSchmidt and Equotip data was collected and mapped at four locations, as shown in Figure 7-38. Of the four locations, Roedean has the greatest number of total readings at 1400, followed by Portobello outfall with 1200 readings, Birling Gap with 1000 readings and Newhaven with 700 readings.

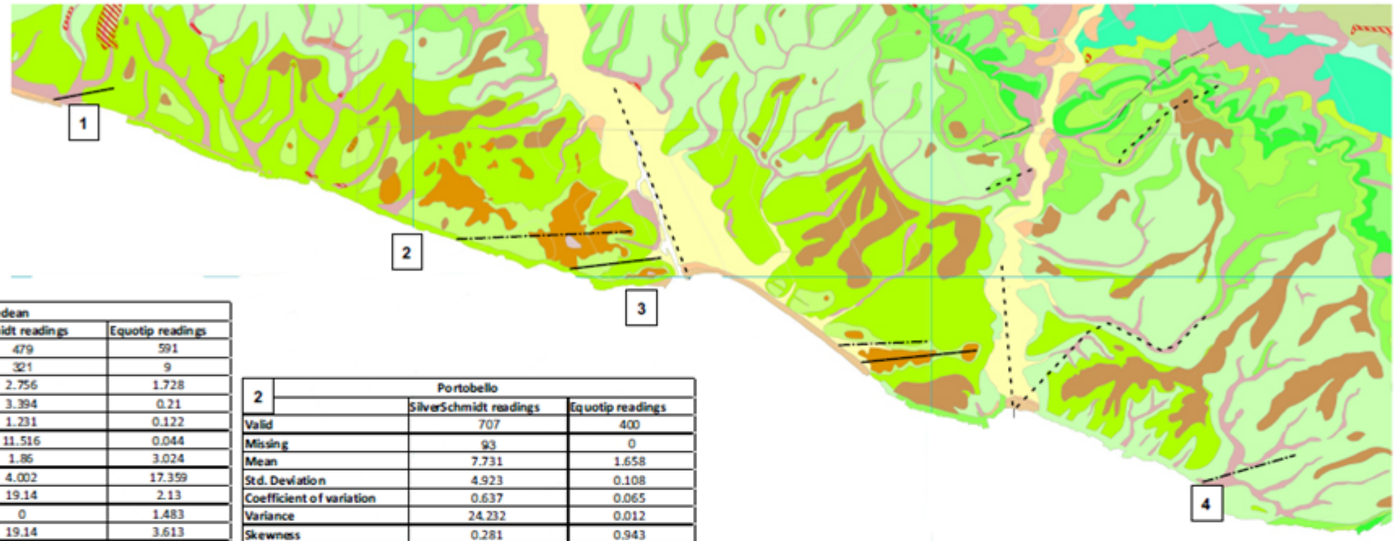
At Roedean, 800 SilverSchmidt readings were taken, of which, 479 were valid, giving a mean UCS value of 2.76 MPa corresponding to a low-density chalk by C574 standards, while 600 Equotip readings were undertaken, of which 591 were valid. This yielded an IDD value of 1.73 Mg/m^3, corresponding to a high-density chalk (Figure 7-38).

Portobello has the second highest number of SilverSchmidt readings, 800 of which 707 are valid, giving a mean UCS value of 7.73 MPa – high CIRIA chalk density grading. 400 valid readings (of an attempted 400 measurements) were recorded using the Equotip device resulting in a regional grading of medium density with a mean IDD value of 1.66 Mg/m^3 (Figure 7-38).

Newhaven has the lowest number of readings comprising of 497 valid SilverSchmidt readings and 3 invalid readings. The regional UCS value here corresponds to a high CIRIA density grade at 8.71 MPa, while based on 500 valid Equotip readings (of 500 attempted), regional IDD is 1.69 Mg/m^3 giving a medium CIRIA density grade (Figure 7-38).

At Birling Gap, 442 valid SilverSchmidt values were collected with 58 unrecovered. The mean UCS at this site was 4.86 MPa (Medium density CIRIA grade). 500 Equotip readings were valid, resulting in a mean regional IDD value of 1.66 Mg/m^3, which corresponds with a medium density Chalk (Figure 7-38).

Geological map of East Sussex showing site location, SilverSchmidt derived UCS and Equotip derived IDD.



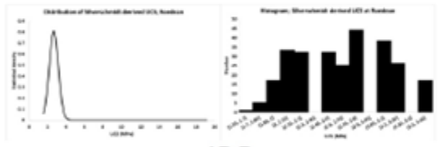
1	Roedean	
	SilverSchmidt readings	Equotip readings
Valid	479	591
Missing	321	9
Mean	2.756	1.728
Std. Deviation	3.394	0.21
Coefficient of variation	1.231	0.122
Variance	11.516	0.044
Skewness	1.86	3.024
Kurtosis	4.002	17.359
Range	19.14	2.13
Minimum	0	1.483
Maximum	19.14	3.613
CIRIA density equivalent	Low density	High density

2	Portobello	
	SilverSchmidt readings	Equotip readings
Valid	707	400
Missing	93	0
Mean	7.731	1.658
Std. Deviation	4.923	0.108
Coefficient of variation	0.637	0.065
Variance	24.232	0.012
Skewness	0.281	0.943
Kurtosis	-0.686	0.185
Range	20.56	0.513
Minimum	0	1.522
Maximum	20.56	2.035
CIRIA density equivalent	High density	Medium density

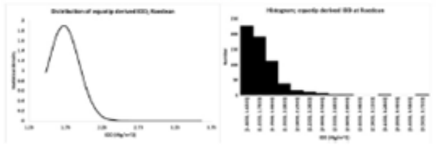
3	Newhaven	
	SilverSchmidt	Equotip
Valid	497	200
Missing	3	400
Mean	8.71	1.692
Std. Deviation	4.264	0.122
Coefficient of variation	0.49	0.072
Variance	18.178	0.015
Skewness	0.289	1.453
Kurtosis	-0.812	4.371
Range	19.4	0.846
Minimum	0	1.522
Maximum	19.4	2.368
CIRIA density equivalent	High density	Medium density

4	Birling Gap	
	SilverSchmidt	Equotip
Valid	442	500
Missing	58	100
Mean	4.855	1.658
Std. Deviation	3.477	0.112
Coefficient of variation	0.716	0.068
Variance	12.09	0.013
Skewness	1.068	2.195
Kurtosis	1.778	12.219
Range	22.5	1.119
Minimum	0	1.522
Maximum	22.5	2.641
CIRIA density equivalent	Medium density	Medium density

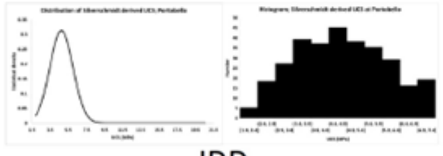
UCS



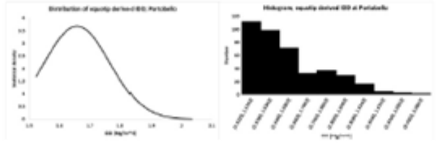
IDD



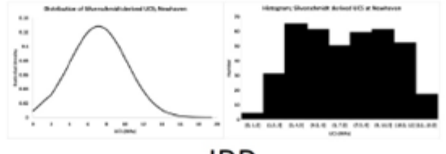
UCS



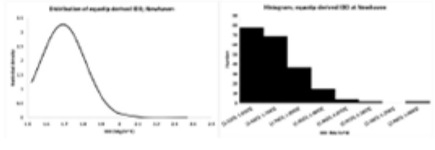
IDD



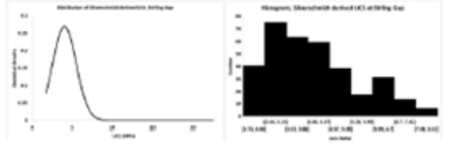
UCS



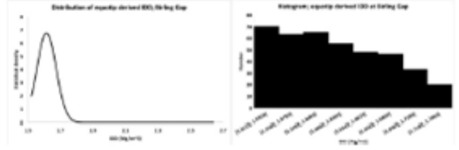
IDD



UCS



IDD



Trace of syncline axis

Trace of anticline axis

1 Roedean

2 Portobello Outfall, Peacehaven

3 Newhaven Harbour

4 Birling Gap, East Dean

5.0 km

Figure 7-38 Statistical summary of data by area.

Comparing values in literature and laboratory measurements, the SilverSchmidt-derived UCS values were consistently higher for structured chalk. Equotip values were relatively similar and consistent with both the literature as well as lab-measured values.

The reason for the consistent high values from the SilverSchmidt is likely due to calibration as the tool was calibrated for low strength concrete, therefore the curve used to extrapolate values was developed for this purpose. A retrospective correction can be applied by comparing the SilverSchmidt measured UCS values with values found in literature and values measured in the laboratory.

Table 7-27 presents the mean values of each chalk formation; the Culver, Newhaven, and Seaford Chalk Formations respectively. These are compared against mean grades reported from measured laboratory values. As the SilverSchmidt-derived UCS values were considered erroneously high but consistent, they were corrected using the established values by applying a ratio.

Table 7-27 SilverSchmidt correction ratio (data taken from Mider (2017), Lau (2018) and (Lawrence et al. 2013)).

Formation	Laboratory measured mean UCS (MPa) (B)	Laboratory measured UCS range (MPa)	CIRIA density grade	SS derived mean UCS (MPa) (C)	SS derived mean range (MPa)	CIRIA density grade	Correction ratio
Culver	3.03	2.46 - 3.47	Low - medium	8.78	1.90 – 19.14	High	2.89
Newhaven	3.32	3.12 - 3.51	Medium	7.62	1.73 – 20.56	High	2.3
Seaford	4.02	2.4 - 6.55	Low - medium	5.51	1.73 – 13.5	High	1.37

Table 7-28 summarises SilverSchmidt derived UCS of the Tarrant Member of the Culver Chalk Formation, which had a mean value of 8.78 MPa, ranging 1.9 – 19.14 MPa. With a correction factor of 2.89, corrected UCS values have a mean of 3.03 MPa, ranging 2.91 – 3.15 MPa.

Table 7-28 SilverSchmidt correction ratio – Culver Chalk Formation.

Location	Formation	Quadrat	Mean UCS (MPa)	UCS range (MPa)	Correction factor	Corrected UCS	Corrected CIRIA density grade
Newhaven harbour	Culver	1	8.43	2.09 – 19.14	2.89	2.91	Low
		2	9.09	2.25 – 19.4	2.89	3.15	Medium
		3	8.59	1.9 – 18.67	2.89	2.97	Low
		4	8.77	2.28 – 16.86	2.89	3.03	Medium
		5	9.02	2.09 – 17.75	2.89	3.12	Medium
Location mean			8.78	1.9 – 19.4	2.89	3.03	Medium

Table 7-29 summarises SilverSchmidt derived UCS of the Newhaven Chalk Formation (taken from Roedean access point and Portobello Outfall). This data has a mean value of 7.62 MPa, ranging 1.73 – 20.56 MPa. With a correction factor of 0.37, corrected UCS values have a mean of 3.31 MPa, ranging 1.30 – 5.70 MPa.

Table 7-29 SilverSchmidt correction ratio - Newhaven Chalk Formation.

Location	Formation	Quadrat	Mean UCS (MPa)	UCS range (MPa)	Correction factor	Corrected UCS	Corrected CIRIA density grade
Roedean access point	Newhaven	5	2.99	1.73 – 5.78	2.3	1.3	Low
		6	6.32	1.9 – 15.99	2.3	2.75	Low
		7	5.83	1.73 – 19.14	2.3	2.53	Low
		8	7.1	1.9 – 17.31	2.3	3.08	Medium
Portobello Outfall	Newhaven	1	6.84	1.9 – 14.31	2.3	2.97	Low
		2	8.26	2.68 – 18.21	2.3	3.59	Medium
		3	9.86	3.09 – 20.56	2.3	4.29	Medium
		4	6.9	2.48 – 14.72	2.3	3.0	Medium
		5	10.41	3.09 – 19.14	2.3	4.53	Medium
		6	13.12	3.53 – 20.08	2.3	5.70	High
		7	5.96	2.09 – 17.83	2.3	2.59	Low
		8	7.84	2.48 – 18.21	2.3	3.41	Medium
Formation mean			7.62	1.73 – 20.56	2.3	3.31	Medium

Table 7-30 summarises SilverSchmidt derived UCS for the Seaford Chalk Formation, which had a mean value of 5.51 MPa, ranging 1.73 – 22.5 MPa. With a correction factor of 1.37, corrected UCS values have a mean of 4.02 MPa, ranging 2.22 – 35.36 MPa.

Table 7-30 SilverSchmidt correction ratio - Newhaven Chalk Formation.

Location	Formation	Quadrat	Mean UCS (MPa)	Range (MPa)	Correction factor	Corrected UCS	Corrected CIRIA density grade
Birling Gap	Seaford	5	6.6	2.68 – 17.75	1.37	4.82	Medium
		2	5.05	1.73 – 13.5	1.37	3.69	Medium
		3	7.35	1.9 – 22.5	1.37	5.36	High
		4	3.05	1.73 – 9.79	1.37	2.22	Low
Locality mean			5.51	1.73 – 22.5	1.37	4.02	Medium

After the correction is applied, the values for UCS for each formation are closer to laboratory tested values, and are reflective of each formations' typical density, with the corrected values for Culver Chalk falling within the low-medium density grade, Newhaven chalk falling within the low-medium grade and Seaford falling within the medium-high density grade. It is also possible to observe that of the three chalk types, the Seaford chalk has the most consistent values between quadrats, while the Newhaven and Culver have more variability.

7.4 Chapter summary

Four research sites were selected and visited for extensive survey and study. Field observations of weathering features and products were undertaken, initially using first principal geological techniques, and later using specialised instruments to estimate material properties of the chalk and their variation in relation to weathering. From initial geological fieldwork, the identification of weathering types was possible at each field location, with particular emphasis on the physical indicators of weathering, which allowed proposed mechanisms to be hypothesised.

In summary, Culver, Newhaven, and Seaford chalks were tested. For the Culver chalk, four quadrats were tested using the SilverSchmidt, resulting in a mean UCS of 8.78 MPa, and range of 1.9 – 19.4 MPa for the site, which characterises the chalk erroneously as high density. This measurement was considered excessively high (compared to laboratory data and values within the literature) - after correction, the mean UCS was 3.03 MPa, which is considered a low – medium CIRIA density grade, which is more in line with previously presented values. Two quadrats were tested with the Equotip, resulting in a mean IDD of 1.70 Mg/m^3, ranging 1.52 – 1.99 Mg/m^3, characterising the chalk as ranging low to high density, with the mean IDD being medium to high.

For the Newhaven Chalk, 12 quadrats were tested using both the SilverSchmidt and Equotip. The SilverSchmidt derived UCS mean for the Newhaven Chalk was 7.62 MPa, ranging 1.73 – 20.56 MPa, corresponding to a high CIRIA density grade. After correction the mean UCS was 3.31 MPa, which is medium density. The mean IDD derived from Equotip measurements was 1.70 Mg/m^3, ranging 1.53 – 3.61 Mg/m^3, resulting in a high CIRIA density grade.

Five quadrats were measured for the Seaford Chalk, comprising one de-structured chalk and four structured chalks of varying grades. The mean UCS was 5.51 MPa for the structured chalks, ranging from 1.73 – 22.5 MPa, corresponding to a high CIRIA density grade. After correction, the mean value was 4.02 MPa, resulting in a density grade of medium. The mean density of the de-structured chalk was 4.3 MPa before correction (medium density), with a range of 2.5 – 19.5 MPa. After correction the mean UCS was 1.87 MPa, corresponding to a low-density CIRIA grade. The mean IDD for the Seaford Chalk was 1.66 Mg/m^3 with a range of 1.52 – 2.64 Mg/m^3, corresponding to a low to high range, with the mean IDD being medium density.

Density grades were assessed using two specialist tools; the Equotip Leeb hardness tester and the SilverSchmidt low-strength rebound hammer, measuring IDD and UCS respectively. The generation of a statistically significant number of data allowed characterisation of each research site on a regional

scale, while the use of quadrats allowed spatial constraint. This constraint enabled the discrete analysis of weathering features and products to be measured.

Key outcomes include;

- Both UCS and IDD have been observed to increase with depth from ground-level, which is inferred to be a decrease in the effects of weathering.
- Both UCS and IDD were observed to increase away from the cliff face and into the rock mass, indicating that surface weathering weakens the cliff face.
- The SilverSchmidt is not suitable for measuring the UCS of crushable material, such as de-structured chalk as it modifies the soil structure.
- Brecciation, fractures and discontinuities affect measurements made by the SilverSchmidt and Equotip, with the SilverSchmidt being particularly sensitive due to sampler surface area.
- The Equotip is effective in identification and quantification of chemical weathering, such as karstic case hardening and softening, such as observed at Newhaven Harbour.
- The Equotip is sufficiently sensitive to register small scale density changes at proximity to discontinuities and can be used to infer block boundaries.
- Competent, solid chalk tends to produce a uniform normal distribution and has high associated values. Brecciated chalk tends to produce a positively skewed normal distribution, where the bulk of the readings are associated with lower UCS and IDD ranges, however, there are high value outliers.
- Using a quadrat to constrain area and the SilverSchmidt and Equotip to undertake physical measurements, it is possible to identify and quantify the different degrees of weathering within a study area.
- It was identified that it was possible for several differing CIRIA grades to occur any one quadrat and that the Equotip was particularly suitable for quantifying this.
- Field estimations of grade using a hammer pick are consistently higher than SilverSchmidt derived grades, and SilverSchmidt derived grades are consistently higher than laboratory measured grades, although there is no correlation between hammer pick derived grade and laboratory measured grades.

This Chapter contributes to this scientific field by presenting a viable strategy to quantify weathering systematically, which can be applied to any geological setting. Weathering has never been studied statistically on this scale, nor to this detail previously and there are no other weathering studies such as this exist within current literature, making this novel. Practitioners who will find this approach and

data useful include early career geologists and engineers who wish to develop their experience and knowledge of weathering, geotechnical engineers and geologists who log and grade weathered chalk, as well as geomorphologists concerned with weathering studies in a field setting. Engineers and geologists may use this data as a baseline degree of weathering at each of the research sites, as well as use trends within the data concerning geomorphological features to infer similar data patterns within other geographical locations.

8 Laboratory results

8.1 Introduction

A laboratory-based investigation was undertaken to better understand the geomechanical and hydrogeological properties of chalk, and to identify and evaluate the causes and processes of weathering in the Seaford and Newhaven Chalk Formations. The investigation was designed to underpin and compliment the fieldwork undertaken in Chapters 6 and 7 by validating field measurements of UCS and IDD, testing the durability of CIRIA graded chalk, to establish a baseline of chalk material properties of chalks from the Southern Province formations, undertake artificial weathering of structured chalk from the Seaford and Newhaven Chalk Formations and to characterise de-structured (CIRIA D-grade) chalks.

Chapter 4 described the methods used for data and sample collection to enable characterisation of structured chalk, de-structured chalk and weathering products within a field setting. Chapter 4 also detailed the development of a sampling methodology for de-structured grade chalks producing samples compatible with standard laboratory testing.

Chapter 5 details laboratory methods used to characterise both structured and de-structured chalks collected from targeted sample sites, and includes adaptations of traditional methods to assess de-structured chalk. The aim of this laboratory work is to underpin field studies and further augment the CIRIA C574 grading system, while developing techniques to characterise sampled de-structured grade chalk to reflect field conditions. This laboratory work does not aim to characterise homogenous chalk putties prepared in controlled laboratory settings as an idealised geoengineering material, but to characterise undisturbed, heterogeneous de-structured grade chalks. Chapter 8 partially satisfies objectives 2, 3, 4, 5 and 6, with particular emphasis on the development of sampling (objective 2), methodologies for characterising rock material and mass properties (objective 3) and quantifying chalk weathering (objective 4).

This Chapter comprises the results of index testing in Section 8.2. Slake durability and artificial weathering tests of CIRIA graded chalk in Section 8.3, permeability testing of D-grade chalks in Section 8.4, geomechanical strength testing (including UCS, tensile and triaxial testing) in Section 8.5. An analysis of chalk microtexture in Section 8.6. Section 8.7 summarises and concludes this Chapter. A full breakdown of tests is provided in Table 8-1.

Table 8-1 List of tests undertaken to characterise weathering in chalk.

Test	Property	Section
Intact dry density	IDD	8.2.1
Natural moisture content	NMC	8.2.3
Saturated moisture content	SMC	8.2.3
Voids ratio and porosity	Void ratio, porosity	8.2.4
Water weakening	Observation	8.2.5
Particle size distribution	Quantification of particle distribution	8.2.6
Bushinsky technique	Quantification of fabric	8.2.7
Slake durability	Durability of chalk	8.3.1
Permeability	Permeability	8.4
UCS	UCS, Young's modulus	8.5.1
Brazilian tensile test	Tensile strength	8.5.2
Triaxial test	Strength, angle of friction, cohesion	8.5.3
SEM	Quantification of microtexture	8.6

The objectives of the laboratory testing programme is to:

- Test and evaluate the hypothesis of this study.
- Assess which of the Southern Province Chalk formations are most susceptible to weathering by undertaking artificial weathering tests.
- Assess if gradings given in accordance with C574 correlate with degree of weathering and durability.
- Evaluate water weakening and salt weakening processes on chalk by using an adapted slake durability methodology with prepared slaking fluids.
- Adapt methods of geotechnical testing for Dc and Dm graded chalk.
- Develop a strategy of geotechnical testing that compliments the C574 grading methodology and quantifies the degree of intactness of de-structured chalks.
- Undertake microscopy to evaluate if weathering has any effect on the microstructure of chalk, and if so, can this be used to rapidly identify the grade of weathering?

The importance of laboratory testing of both structured and de-structured chalk cannot be overstated; laboratory testing allows the characterisation of soil and rock properties required for geotechnical analyses, the development of geotechnical models and allows some prediction of the materials engineering behaviour under working conditions. This is significant as weathering processes alter the physical properties of the parent rock, resulting in insitu chalks that have varying physical properties. De-structured chalks also pose challenges in terms of characterisation as to whether they should be

approached as a very weak rock, or a stiff soil. Currently, there are little data of the physical properties of Dm and Dc chalks within the literature, therefore the testing undertaken in this chapter in novel. This research project aims to develop a classification strategy and begin the development of a database of physical properties of Dm and Dc chalks as an engineering material.

8.2 Baseline index testing to establish the effects of weathering on chalk properties

Primary data of all Southern Province chalk formations were collated from MSc dissertations at Imperial College London supervised by the author and from the literature. This section focuses on IDD, NMC and SMC, as these have been demonstrated to correlate well together and with UCS (Lamont-Black and Mortimore, 1996). These parameters are considered as the most important in this study in terms of increasing weathering (i.e., brecciation and de-structuration) of competent chalk. Changes in competency is reflected in both the density and moisture contents of a chalk, and these tests allow repeatable quantification of these changes, unlike other qualitative methods, such as field observation. All index test methods are described in Chapter 5.2.

8.2.1 Intact dry density testing results

A total of 103 IDD tests were collated from data from previous MSc researchers work for structured chalk (Mider, 2017, Lau, 2018, Zadeh, 2018, Marley, 2020, Harman, 2020). 40 de-structured (weathered) chalk IDD tests were undertaken by the author. Table 8-2 shows the ranges and mean values of IDD and corresponding CIRIA density gradings for each formation of the Southern Chalk Province, less the Portsdown Chalk Formation – this is due to this formation not being present within the study area.

Table 8-2 IDD for Southern Province Chalks (less the Portsdown Chalk Formation).

Formation	**IDD range (Mg/m^3)**	**IDD mean (Mg/m^3)**	**Standard deviation**	**CIRIA grade based on range**	**CIRIA grade based on mean**
Culver Chalk	1.45 – 1.59	1.53	0.05	Low – medium	Low
Newhaven Chalk	1.64 – 1.86	1.74	0.06	High	High
Seaford Chalk	1.46 – 1.86	1.69	0.08	Low – high	High
Lewes Nodular Chalk	1.52 – 1.94	1.75	0.12	Low – high	High
New Pit Chalk	1.68 – 2.11	1.81	0.17	Medium – very high	High
Holywell Nodular Chalk	2.13 – 2.22	2.17	0.04	Very high	Very high
Zig Zag Chalk	1.88 – 2.23	2.10	0.11	High – very high	Very high
West Melbury Marly Chalk	1.92 – 2.32	2.08	0.17	High – very high	Very high

These values are graphically presented in Figure 8-1. The highest mean is 2.17 Mg/m^3 for the Holywell Nodular Chalk Formation, with a range of 2.13 – 2.22 Mg/m^3, graded as high density using the CIRIA grading system. The lowest is the Culver Chalk Formation, with a mean IDD of 1.53 Mg/m^3, a range of 1.45 – 1.59 Mg/m^3, corresponding to a low-density CIRIA grade.

In general, it can be observed that the average IDD increases with formation age and stratigraphic depth, except for the Holywell Nodular Chalk Formation, which is markedly higher that the preceding and succeeding formations. The increase in density is attributed to induration and consolidation due to overburden during burial (Clayton and Matthews, 1987). The marked increase in IDD of the Holywell Nodular Chalk Formation is attributed to the relatively high clay content with volcanic and terrigenous origins during the period of deposition (Cenomanian – Turonian) (Mortimore, 2018).

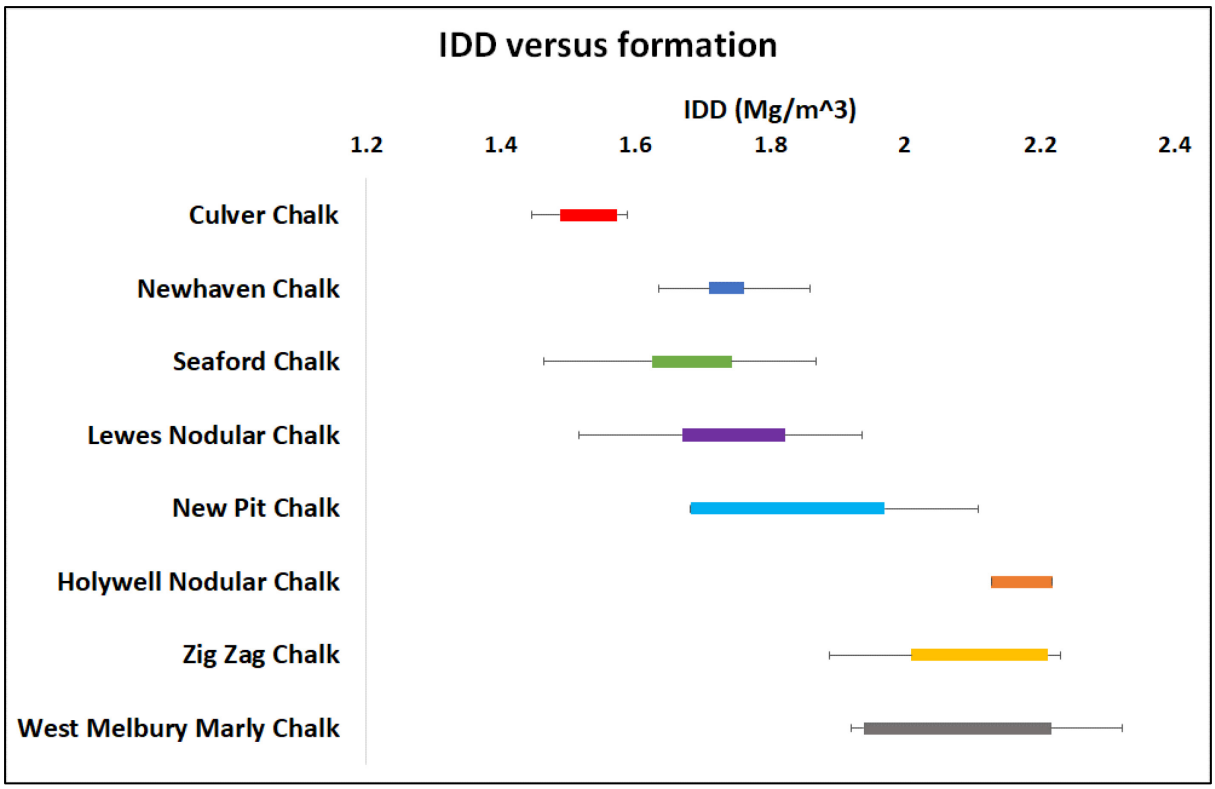


Figure 8-1 IDD versus formation.

The implications of high IDD values are increased strength as well as a reduced ability to hold moisture within pore space. (Lord et al. 2002). This means that chalks with higher IDD values are stronger, more durable and are less susceptible to water weakening processes, chemical weathering, cryoclasty and mechanical disaggregation (i.e., abrasion and erosional processes).

Chalks with lower IDD values (below 1.70 Mg/m^3) have been demonstrated to take on and lose moisture content more readily (Mortimore, 1997). This means that chalks with lower IDDs are potentially more susceptible to water weakening processes, chemical weathering (by virtue of water being a mode of transport for chemicals) as well as cryoclasty from ice expansion of water within pore structures. This has further informed the focus of this thesis on relatively younger Southern Province chalk formations, i.e., the Seaford and Newhaven Chalks, given their geographical distribution.

Table 8-3 compares IDD values of both structured and de-structured Seaford and Newhaven Chalk Formations. The table presents structured chalk as a reference to compare the de-structured IDD values against. These values are presented graphically in Figure 8-2.

Table 8-3 Comparison of IDD between structured and de-structured Newhaven and Seaford Chalk Formation.

Formation and grade	**IDD range (Mg/m^3)**	**IDD mean (Mg/m^3)**	**Standard deviation**	**CIRIA grade based on range**	**CIRIA grade based on mean**	**% lower than reference value**
Newhaven Chalk Formation	1.64 – 1.84	1.74	0.068	Medium – high	High	Reference value
Newhaven Dc grade	1.46 – 1.67	1.56	0.08	Low – medium	Low/medium	10.34
Newhaven Dm grade	1.41 – 1.60	1.50	0.06	Low – medium	Low	13.8
Seaford Chalk Formation	1.46 – 1.87	1.68	0.01	Low – high	Medium	Reference value
Seaford Dc grade	1.43 – 1.65	1.54	0.07	Low – medium	Low	8.33
Seaford Dm grade	1.54 – 1.57	1.56	0.06	Low – medium	Low	7.14

The structured Newhaven chalk had the highest IDD at 1.74 Mg/m^3 and a range of 1.64 – 1.84 $Mg/m^{3,}$ resulting in a high CIRIA density grade. The structured Seaford Chalk was lower, with a mean IDD of 1.68 Mg/m^3, and a range of 1.46 – 1.87 Mg/m^3, resulting in a medium CIRIA density grade (Figure 8-2).

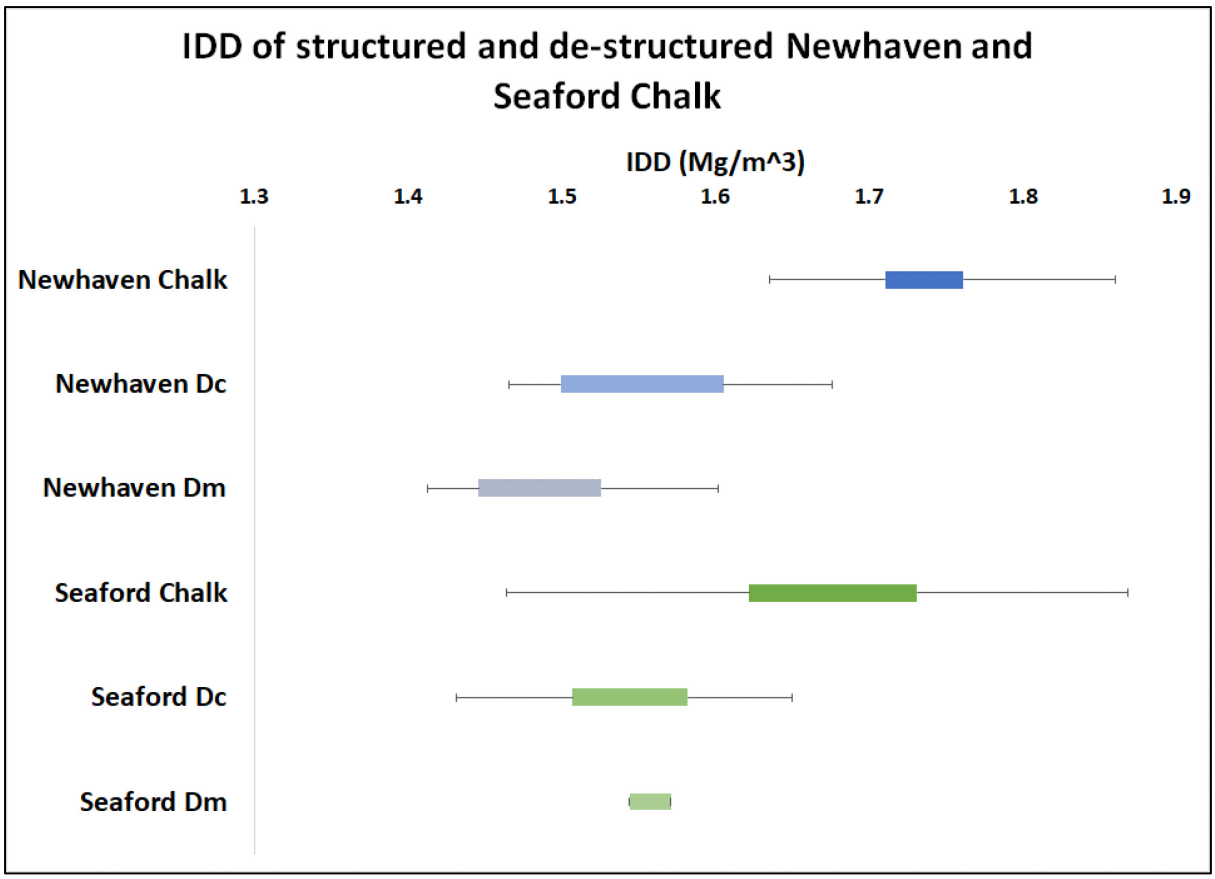


Figure 8-2 IDD of structured and de-structured Newhaven and Seaford chalk.

The de-structured chalk grades had lower IDD values compared to structured counterparts (Figure 8-2); Newhaven grade Dc was 10.34% lower than the structured Newhaven, at 1.56 Mg/m^3 (low CIRIA density) while Newhaven Dm was 13.8% lower at 1.50 Mg/m^3 (also low CIRIA density). Seaford Dc was 8.33% lower than the structured Seaford Chalk at 1.54 Mg/m^3 (low CIRIA density) while the Seaford grade Dm, was 7.14% lower than the structured Seaford chalk, but slightly higher than the Dc, at 1.56 Mg/m^3 (borderline of low-medium CIRIA density grade).

The differences between mean IDD's of the structured chalk are likely due to lithological differences within the samples, however, it would be expected that Newhaven chalk had a lower IDD compared to Seaford This difference is likely due to one or more outliers within the data or the local site characteristics of the chalk.

The IDD values for Newhaven chalk follow expectations, whereby Dc would yield a higher IDD, given that the samples contain an increased number of competent clasts (>65%) compared to that of the Dm grade (<65% clasts). The Seaford chalk, however, does not follow this trend, with the Dm grade slightly higher than the Dc grade chalk – this is likely due to statistical representation, with a single Dm grade being tested (due to sampling difficulties). The differences between the constituents of the two

de-structured chalk types are discussed in more detail later in this chapter (section 8.2.6; particle size distribution), however, it was identified that clasts within the Newhaven Dc chalk were greater in size than clasts observed in the Seaford Dc chalk, which accounts for the differences between the respective Dc grades. In terms of sampling, Dm chalk was difficult to identify in a field setting, which resulted in a limited number of Dm grade chalks being collected, thus reducing the sample size, and this could have resulted in misidentification of Dm or Dc grades, leading to erroneous results. On average the mean CIRIA grade is one grade lower in de-structured chalk than structured chalk, although the differences between the weathering grades are inconclusive and minor.

8.2.2 Laboratory measured IDD versus Equotip derived IDD results

Table 8-4 presents laboratory IDD values for Seaford and Newhaven structured and de-structured chalks (grades Dc and Dm) compared against Equotip derived IDD values for structured chalks at the research sites Roedean, Portobello Outfall and Birling Gap. These Equotip data are presented in Chapter 7. Comparison between lab measured and Equotip derived data is graphically presented in Figure 8-3.

The highest values are associated with laboratory tests of structured chalk, with laboratory IDD values for Newhaven chalk at 1.74 Mg/m^3 (high density), while the structured Seaford chalk was measured as 1.68 Mg/m^3 (medium density). The lowest IDD values are associated with de-structured chalks.

Table 8-4 Laboratory measured IDD and Equotip measured IDD values.

Measurement type	**Mean IDD (Mg/m^3)**	**Range (Mg/m^3)**	**Standard deviation**	**CIRIA density grade**
Newhaven Chalk				
IDD - Newhaven Chalk	1.74	1.64 - 1.86	0.06	High
Equotip derived IDD – Roedean	1.73	1.48 - 3.60	0.21	High
Equotip derived IDD – Portobello	1.66	1.52 - 2.04	0.11	Medium
Lab IDD - Newhaven Dc	1.56	1.47 - 1.68	0.07	Medium
Lab IDD - Newhaven Dm	1.50	1.41 - 1.60	0.06	Low
Seaford Chalk				
Lab IDD - Seaford Chalk	1.68	1.46 - 1.87	0.08	Medium
Equotip derived IDD - Birling Gap	1.66	1.52 - 2.64	0.11	Medium
Lab derived IDD - Seaford Dc	1.54	1.43 - 1.65	0.06	Low
Lab derived IDD - Seaford Dm	1.56	1.54 - 1.57	0.01	Medium

Laboratory densities are consistently higher for both the Seaford and Newhaven chalks in comparison to Equotip derived densities. For the Newhaven chalk, Equotip derived densities measured at Roedean are very similar to the lab derived IDD at 1.73 Mg/m^3 (high density), while the IDD measured at Portobello are lower at 1.66 Mg/m^3 (medium density). The Equotip derived IDD measured at Birling

Gap is similar, but slightly lower than the laboratory IDD for Seaford chalk, differing by 0.02 Mg/m^3 at 1.66 Mg/m^3 (medium density).

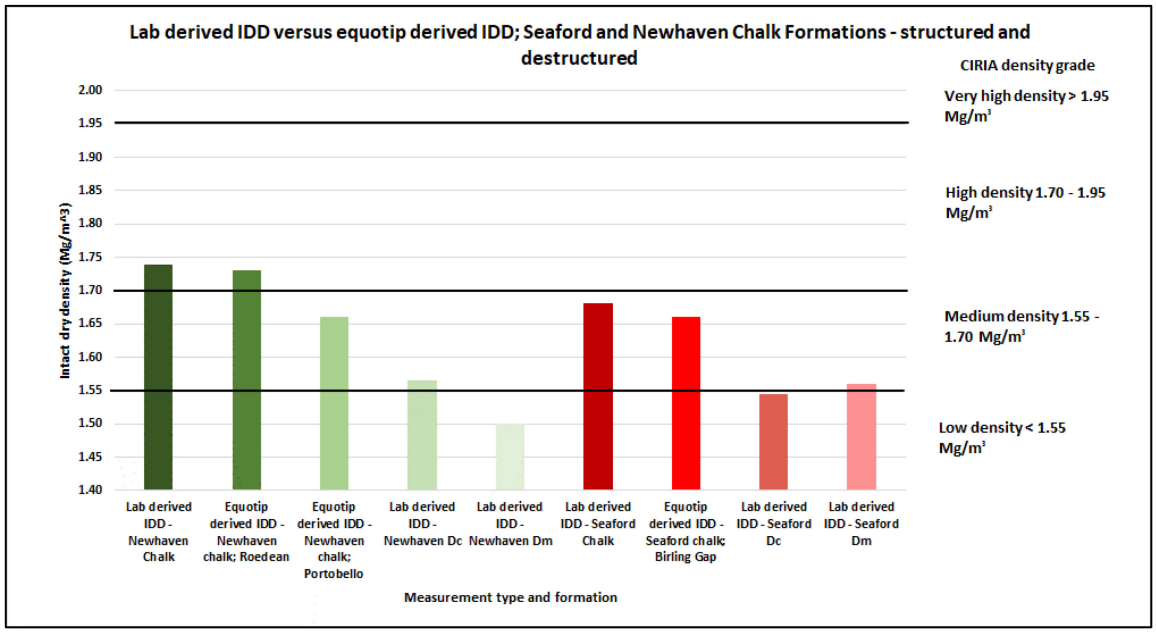


Figure 8-3 Lab derived IDD versus Equotip derived IDD; de-structured Newhaven and Seaford chalk formations.

De-structured chalks are consistently lower in terms of laboratory IDD versus the IDD of structured chalks, with associated CIRIA grades of low – medium (Figure 8-4). During field studies, one quadrat was used to measure the IDD of Dc grade Seaford Chalk. Newhaven Chalk was not measured owing to challenges in recovering readings. Figure 8-4 and Table 8-5 shows a comparison between laboratory IDD and Equotip derived IDD for Dc grade Seaford Chalk. Lab derived IDD was lowest at 1.54 Mg/m^3 (low density), while Equotip derived IDD was highest at 1.67 Mg/m^3 (medium density).

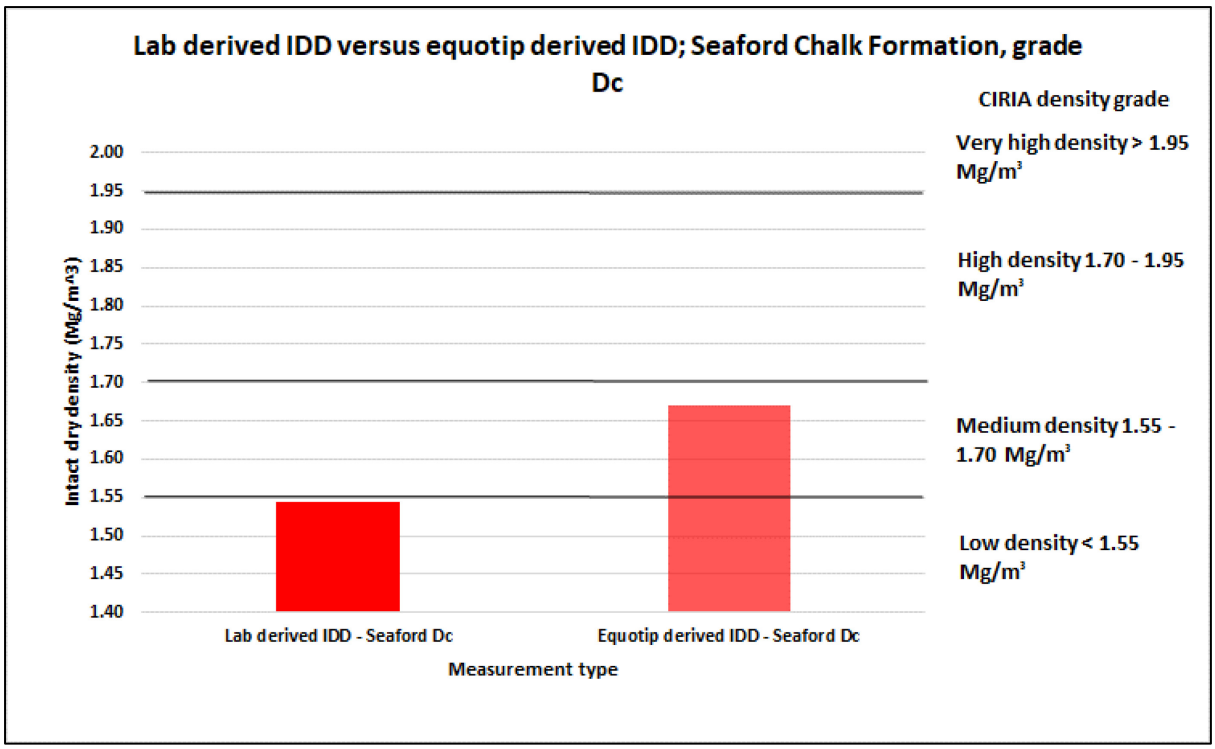


Figure 8-4 Lab derived IDD versus Equotip derived IDD; Seaford Chalk Formation, grade Dc.

Table 8-5 IDD of Dc grade Seaford Chalk.

Measurement type	Mean IDD (Mg/m^3)	Range (Mg/m^3)	Standard deviation	CIRIA density grade
Lab measured IDD - Seaford Dc	1.54	1.43 - 1.65	0.06	Low
Equotip derived IDD - Seaford Dc (Birling Gap, Quadrat 1)	1.67	1.52 - 2.64	0.14	Medium

Laboratory IDD values for structured chalks are slightly higher than those derived in the field using the Equotip. In both the Seaford and Newhaven (Roedean) chalk formations the Equotip correctly measured the IDD as medium and high density retrospectively, when compared to the laboratory tests. Although the Equotip results were lower for the Portobello samples this was marginal. The results show that the Equotip can be used as a reliable field test to establish the IDD of structured chalk. The laboratory IDD values are likely to be more representative compared to the Equotip field results as the material prepared in the laboratory is subject to greater scrutiny when selecting test samples and field samples have more variability in terms of material properties.

IDD values for de-structured chalks are characteristically lower than structured, both in laboratory and field tests, which is expected owing to their de-structured properties. In terms of reliability of results, it is reasoned that the Equotip measured IDD values are more representative of true Dc grade chalk given their inherent material property variability. Field measurements are higher than laboratory

measurements, which is likely due to a sample size factor – samples tested in the laboratory have a mass of 40 - 60 g (relatively small), while samples measured in the field are spread over an area measuring 0.5 m^2 (larger surface area). The implications of this are that the laboratory samples have less material variability by virtue of their size, and are therefore more representative of rock material (such as rock matrix material), while field measured IDD values taken from quadrats have a larger sample surface area, therefore -capture more variability within the rock mass (such as observed in Figure 7-8, quadrat 5), which is significantly important for describing overall weathering. This would imply that testing methods for de-structured weathered chalks would need upscaling, and to prescribe samples greater than 40 g to be more effective at representing the heterogeneity inherent with D-grade chalks. It is likely that this upscaling would be beneficial in all index tests described within Chapter 5, such as NMC and SMC, given D-grade chalk's dual-property nature.

8.2.3 Moisture content

Chalk as an engineering material has the capacity to retain a high NMC (close to saturation) (Higginbottom, 1966), which has implications for engineering applications, such as the use of chalk as an engineering fill and use in embankments (Lord et al. 2002). Chalks with a high moisture content are observed to be more susceptible to frost action, more easily reduced to putty during engineering works and weaker (in terms of strength) due to water weakening effects (Section 8.2.5) (Lord et al. 2002). Moisture content tests of de-structured chalk have been undertaken and compared with structured chalk with the aim of examining the effect of weathering on degree of saturation. A method for measuring NMC is presented in Section 5.2.1 and SMC in section 5.2.2.

NMC was plotted against formation to ascertain if any trend could be identified based on formation material properties. Figure 8-5 presents NMC against formation. The formation with the highest NMC is the Newhaven Chalk Formation at 21.98%, while the lowest is the Holywell Nodular Chalk Formation at 2.87%.

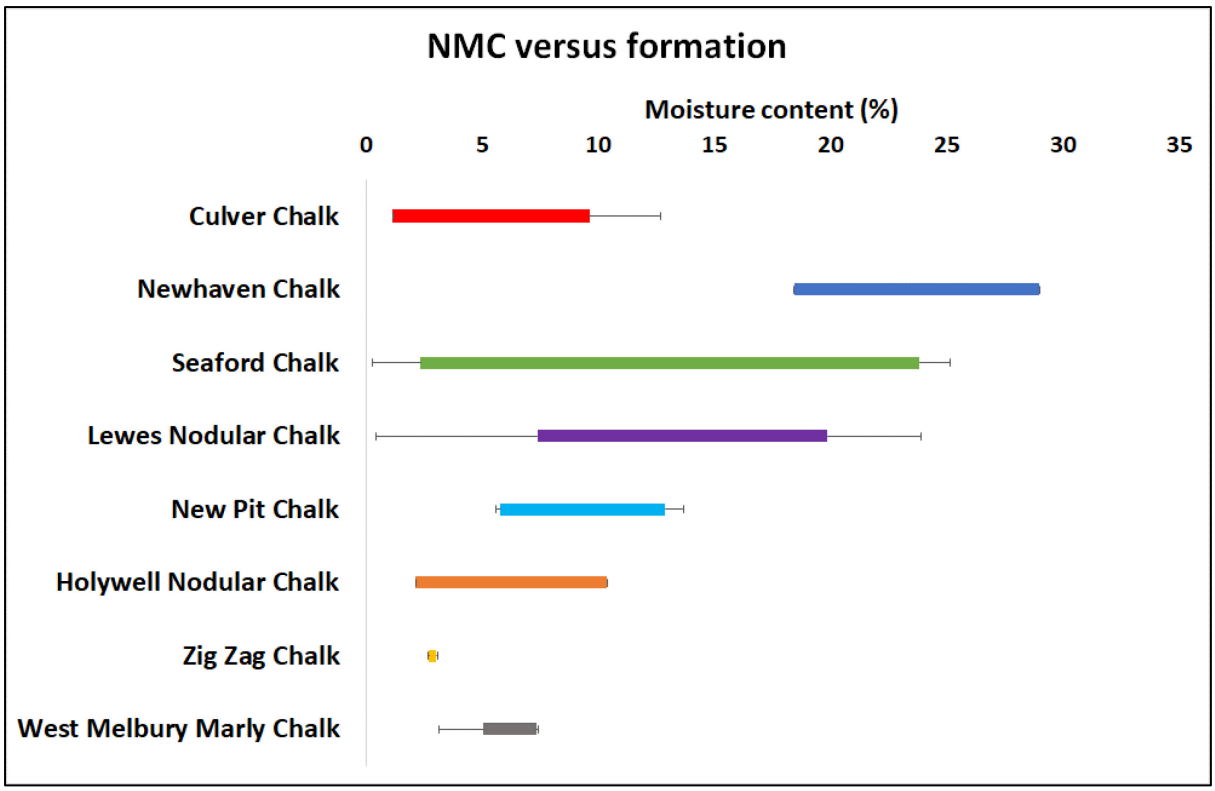


Figure 8-5 NMC versus formation.

When compared, mean NMC values are observed to reduce with stratigraphic depth and increasing formation age, which is likely a function of increasing IDD. NMC ranges also reduce with IDD (Table 8-6), except the Culver Chalk, which is considered to be erroneously low at 8.61% moisture content (speculated to be due to poor sample handling), and the Holywell and Zig Zag Chalks, which are significantly lower at 2.54% and 2.87% respectively. The differences in these two chalks are inferred to be due to increasing clay content within the chalk matrix.

Table 8-6 Mean IDD and NMC of Southern Province Chalks (less the Portsdown Chalk Formation).

Formation	**Mean IDD (Mg/m^3)**	**Mean NMC (%)**	**NMC range (%)**
Culver Chalk	1.53	8.61	4.54 - 12.68
Newhaven Chalk	1.74	21.98	18.43 - 29.00
Seaford Chalk	1.69	18.10	1.87 - 25.16
Lewes Nodular Chalk	1.75	15.81	6.35 - 23.88
New Pit Chalk	1.81	10.16	5.59 - 13.70
Holywell Nodular Chalk	2.17	2.54	2.14 - 2.94
Zig Zag Chalk	2.10	2.87	2.67 - 3.03
West Melbury Marly Chalk	2.09	6.12	3.15 - 7.43

The range of moisture content per formation is significant as this is controlled by IDD – chalks with an IDD of less than 1.70 Mg/m^3 lose and gain moisture more easily (Lord et al. 2002), which has implications for water weakening and slaking (i.e., wetting and drying cycles), as this has been observed to further weaken chalk (Risnes et al. 2003). By plotting mean NMC values against formation, it is possible to infer formational differences, such as overburden compaction due to burial and diagenetic processes in the White Chalk supergroup and the addition of increasing clay content in the Grey Chalk supergroup, that will affect weathering susceptibility – for example, the Newhaven Chalk Formation is likely more susceptible compared to that of the Holywell Nodular Chalk Formation (supported by a combination of index testing and slake durability testing**,** Sections 8.2 and 8.3).

SMC was calculated from IDD and was plotted against formation (Figure 8-6). This allowed the calculation of mean SMC values and ranges of samples tested. In terms of trends, these values plotted inversely to the IDD values plotted, with SMC decreasing with stratigraphic depth and increasing formation age due to IDD being used to derive saturated moisture content. SMC is more effective when interpreting burial history as NMC is dependent upon environmental input and conditions at the time of sampling.

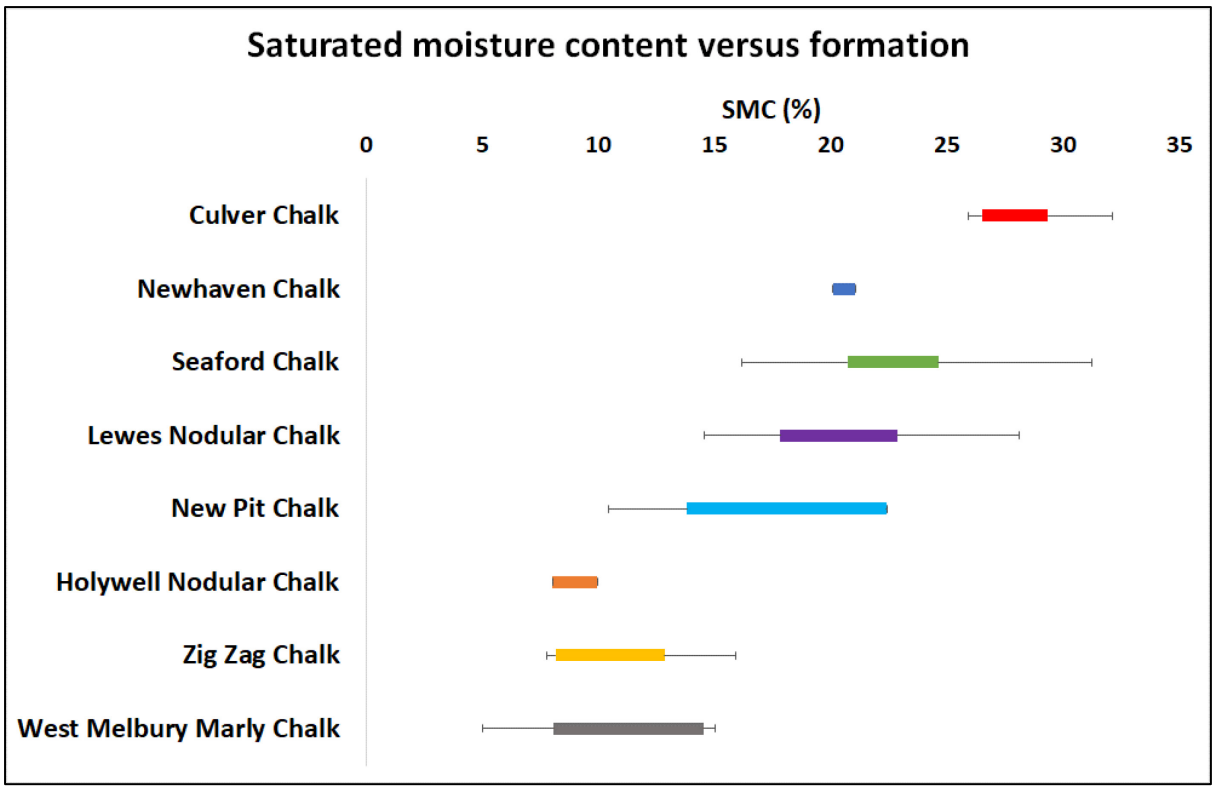


Figure 8-6 SMC versus formation.

NMC values were plotted against calculated SMC values to evaluate the degree of saturation of the samples and the effectiveness of sample handling and storage. Individual NMC data was plotted against SMC data for structured and de-structured Seaford and Newhaven Chalk to investigate how the de-structured grades differed to their structured counterparts in terms of saturation.

By averaging each sub-data set (Table 8-7), it is possible to observe that SMC values range from 1.04 – 1.15 times greater than NMC values and that all formations considered lie above 85% saturation and below 100% saturation (Figure 8-7).

Table 8-7 Moisture contents of de-structured Newhaven and Seaford Chalks against structured counterparts (– data taken from Mortimore and Fielding, 1990).*

Formation	Location/beds	Average NMC (%)	Average SMC (%)	NMC range (%)	SMC range (%)	NMC:SMC ratio	Degree of saturation (%)
Newhaven	Telscombe Cliffs	18.48	20.85	18.43 - 18.52	20.63 - 21.07	0.89	88.63
Newhaven grade Dc	Telscombe Cliffs	24.57	27.60	21.60 - 28.27	22.62 - 33.13	0.89	89.02
Newhaven grade Dm	Telscombe Cliffs	25.48	29.20	19.54 - 29.11	22.69 - 33.76	0.87	87.26
Seaford	Birling Gap	22.47	22.80	14.65 - 25.163	18.67 - 26.74	0.99	98.55
Seaford grade Dc	Birling Gap	25.00	27.84	22.01 - 27.86	23.56 - 32.82	0.90	89.79
Seaford grade Dm	Birling Gap	24.38	27.08	22.49 - 25.78	26.62 - 27.72	0.90	90.00
Newhaven	Meeching Beds (*)	20.9	21.20	18.25 - 23.4	19.14 - 23.20	0.99	98.58
Newhaven	Old Nore Beds (*)	27.12	28.21	23.0 - 29.5	26.66 - 30.53	0.96	96.13
Newhaven	Castle Hill Beds (*)	20.05	20.83	19.8 - 25.9	21.10 - 25.46	0.96	96.25
Seaford	Cuckmere Beds (*)	22.68	24.17	15.5 - 24.5	14.78 - 25.07	0.94	93.83

Structured Seaford chalk is observed to plot higher than Newhaven Chalk both for NMC and SMC and has a greater spread, which indicates a greater range for both NMC and SMC in comparison. In general, de-structured chalk have a higher SMC, but NMC's at a percentage of SMC is lower. This is also true in comparison to the NMC values for structured chalk – as previously mentioned, NMC values are generally close to saturation for structured chalks, however weathered chalk NMC values are not close to saturation.

In terms of saturation of structured chalk, the Meeching Beds, Newhaven Chalk is the highest at 98.58%, Followed by Seaford Chalk tested at Imperial College at 98.55%, Castle Hill Beds, Newhaven Chalk at 96.25%, Old Nore Beds, Newhaven at 93.83%, Cuckmere beds of the Seaford chalk at 93.83% and the structured chalk with the lowest saturation was the Newhaven Chalk tested at Imperial College, at 88.63 % (Figure 8-7).

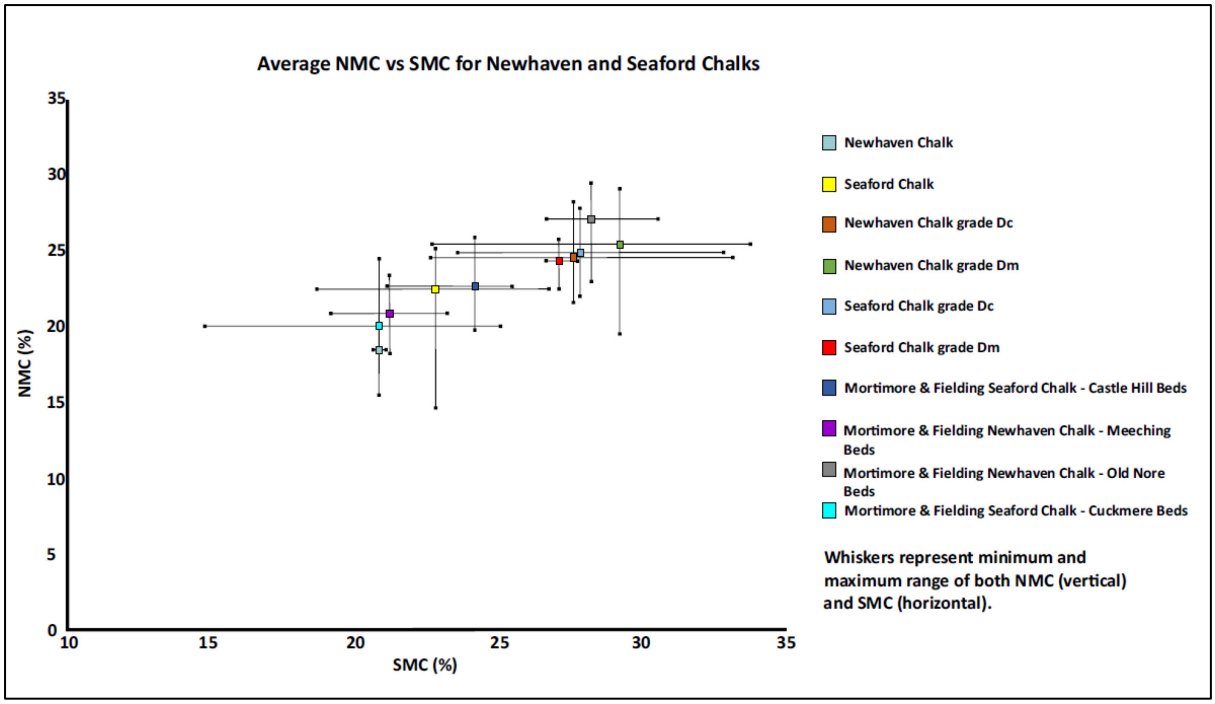


Figure 8-7 Average NMC versus SMC for Newhaven and Seaford de-structured chalk.

De-structured chalk has a lower degree of saturation compared to their parent members, with Seaford Dm having the highest degree of saturation at 90%, followed by Seaford Dc at 89.79%. The average of all Seaford Chalks was 96.19%, meaning that the average saturation of weathered, de-structured Seaford chalk material (both Dc and Dm at 89.88%) was 6.31% lower. The Newhaven de-structured material had lower saturation compared to the de-structured Seaford chalk, with Newhaven Dc being 89.02% saturated, and the Newhaven Dm being 87.26%. When compared to an average degree of saturation of 94.90%, it is possible to observe that the de-structured Newhaven chalk is 6.76% lower, at 88.14% saturation (Figure 8-7). All structured grades (less the Old Nore Beds) plot within the medium to high-density regions of the plot, with the majority falling below the SMC-IDD line, indicating NMC is very close to saturation.

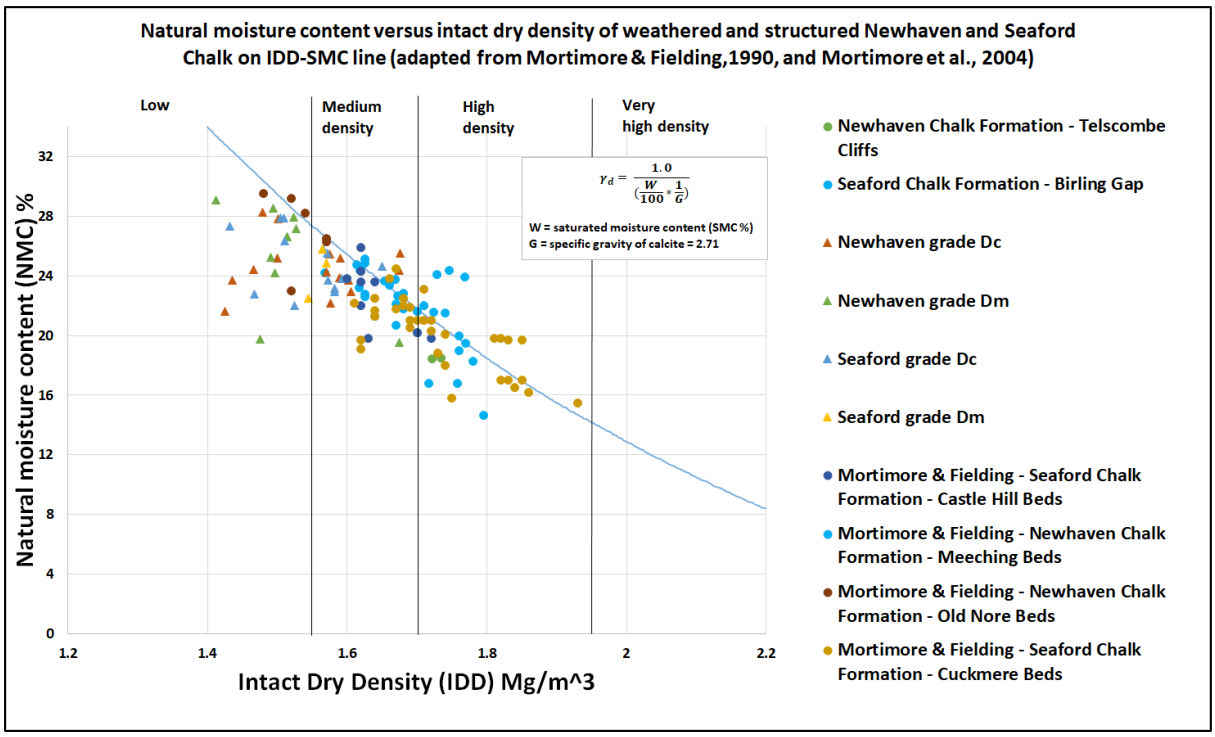


Figure 8-8 Natural moisture content of naturally occurring structured and de-structured chalks plotted into the IDD-SMC line (adapted from (Mortimore and Fielding, 1990)).

By plotting the grades on the SMC-IDD line (Figure 8-8), it is possible to observe that de-structured chalks fall within the low-density category of IDD and have a greater range of NMC compared to that of structured chalks, which plot within the medium to high-density regions.

8.2.4 Void ratio and porosity

Void ratio is the ratio of voids to solid material within a sample, while porosity is the ratio of voids to the total volume of a sample mass. A method for calculating both parameters is presented in Section 5.2.4. Table 8-8 presents calculated voids ratio and porosity for all formations of the Southern Province chalk (less the Portsdown Chalk). Data used was compiled from previous MSc projects (Mider, 2017, Lau, 2018, Zadeh, 2018, Marley, 2020, Harman, 2020), as per Section 8.2.1.

Table 8-8 Voids ratios and porosities of Southern Province Chalks.

Formation	Voids ratio (e)	Voids ratio range (e)	Average porosity (%)	Porosity range (%)
Culver Chalk	0.763	0.700 – 0.867	43.21	41.17 – 46.44
Newhaven Chalk	0.567	0.543 – 0.584	36.18	35.19 – 36.85
Seaford Chalk	0.616	0.445 – 0.844	37.99	30.81 – 45.78
Lewes Nodular	0.549	0.394 – 0.781	35.15	28.26 – 43.85
New Pit Chalk	0.501	0.281 – 0.605	32.93	21.93 – 37.70
Holywell Nodular Chalk	0.279	0.217 – 0.392	21.65	17.81 – 28.15
Zig Zag Chalk	0.385	0.210 – 1.169	25.65	17.39 – 53.89
West Melbury Marly Chalk	0.320	0.162 – 0.406	23.88	13.96 – 28.85
CIRIA C574 range	N/A	0.1 – 1.10	N/A	9.0 – 52.0

Average voids ratio reduces with stratigraphic depth, with the highest ratio being Culver Chalk at 0.763, and the lowest being 0.279 for the Holywell Nodular Chalk. Voids ratio for all formations ranges from 0.162 to 0.867 Which falls within the range highlighted for void ratios (Lord et al. 2002)**,** the only exception being the Zig Zag Chalk, which is slightly higher at 1.169, with an average value of 0.385. Similarly, all porosity ranges fall within the ranges provided by CIRIA guidance, except the Zig Zag Chalk, with an upper porosity range of 53.89%.

Table 8-9 shows calculated void ratios and porosities for the Seaford and Newhaven Chalk, both structured and de-structured. Newhaven Dc chalk has a voids ratio of 0.749, with a range of 0.611 – 0.895, which is greater than the structured Newhaven Chalk. Newhaven grade Dm is greater than Dc, with a void's ratio of 0.788, with a range of 0.613 – 0.911. Seaford Dm has a voids ratio of 0.751 (similar to Newhaven Dc) and a range of 0.636 – 0.886, while Seaford Dm has a larger voids ratio of 0.731 and a range of 0.719 – 0.749. Generally de-structured chalk voids ratios are higher than their structured parent material, and of the two grades, Dm grades are the highest.

Newhaven grade Dm has a calculated porosity of 43.99%, with a range of 37.99 – 47.68%, while Newhaven Dc has a porosity of 42.72% and a range of 37.91 – 47.22%. Seaford Dc has a porosity of 42.83%, with a range of 38.88 – 46.98%, while Seaford Dm has a porosity of 42.23%, with a range of 41.82 – 42.81%. Calculated porosities follow a similar trend to calculated voids ratios, with de-structured chalks having higher porosities than their structured parent chalks.

Table 8-9 Voids ratios and porosities of D-grade Newhaven and Seaford chalk.

Formation	Voids ratio (e)	Voids ratio range (e)	Average porosity (%)	Porosity range (%)
Newhaven Chalk	0.567	0.543 – 0.584	36.18	35.19 – 36.85
Newhaven – grade Dc	0.749	0.611 – 0.895	42.72	37.91 – 47.22
Newhaven – grade Dm	0.788	0.613 – 0.911	43.99	37.99 – 47.68
Seaford Chalk	0.616	0.445 – 0.844	37.99	30.81 – 45.78
Seaford – grade Dc	0.751	0.636 – 0.886	42.83	38.88 – 46.98
Seaford – grade Dm	0.731	0.719 – 0.749	42.23	41.82 – 42.81

Voids ratios and porosity ranges for de-structured chalks are higher than the parent material (Table 8-9). This is significant as the calculation used assumes the material is homogenous. In reality, the material ranges from solid competent clasts to de-structured puttified sediment material, each of which have differing voids ratios and porosities by virtue of their respective micro-structure, therefore being a dual-property material. An attempt to quantify these constituents was undertaken by splitting down both voids ratio and porosity by the ratio of clasts to matrix as they are classified by CIRIA standards in this fashion. This attempt however, led to unrealistic values for clast and matrix components, therefore the analysis was abandoned.

Previous studies on idealised chalk putty materials (which correspond to the matrix component in these samples), have been reported as 0.543 – 0.565 (Spearing-Bundy, 2013), which is lower than the total calculated void ratios for Dc and Dm chalks (Table 8-9). Experimental work undertaken by Alvarez-Borges (2019) yielded voids ratio values of 0.666 – 0.738 for laboratory prepared Seaford Chalk putties, which compare more favourably to the total calculated void ratios of de-structured chalk. These chalk putties do not form a suitable analogy for de-structured, weathered chalk because putty chalks have a finer matrix due to their microtexture.

The implication of this analysis is that traditional calculation of voids ratio and porosity are not suitable for de-structured chalk as a material due to its heterogeneity and subsequent dual properties. By splitting down the two constituent materials (i.e., clasts and putty), voids ratio and porosity for both structured chalk and idealised chalk putty cannot be accurately calculated, nor accurately validated.

8.2.5 Water weakening of D-grade Chalk

Index testing of weathered chalk identified that when dry, the weathered chalk material appeared to be brittle, however, when moisture content approached that of NMC, the weathered chalk matrix was putty-like in texture and behaviour. To test the extent of the weakening of the material, de-structured chalk was saturated and observed.

Upon inundation with water under atmospheric conditions (i.e., without vacuum or confinement), the de-structured chalk slakes and shedded material within a matter of seconds, with 38 mm core samples collapsing upon themselves. This experiment was repeated several times to confirm that the disintegration of the initial core sample was not due to defects inherent in that one core.

Figure 8-9 shows a core of D-grade Newhaven chalk disintegrating when submerged in water at time intervals. At 0 seconds, the core retained a cylindrical shape, however, axial cracks were observed to form instantaneously. At 10 seconds, the core began to shed material as a debris flow, losing material from the sides and base. At 15 seconds, the core had lost over approximately 50% of its cylindrical shape and debris flows of slaked material surrounded the cores original position. At 15 seconds, the debris flows continued, and the core retained little of the original shape. At 30 seconds, the core had disintegrated into a cone of chalk powder material and by 60 seconds, the chalk had reached equilibrium and was no longer shedding.

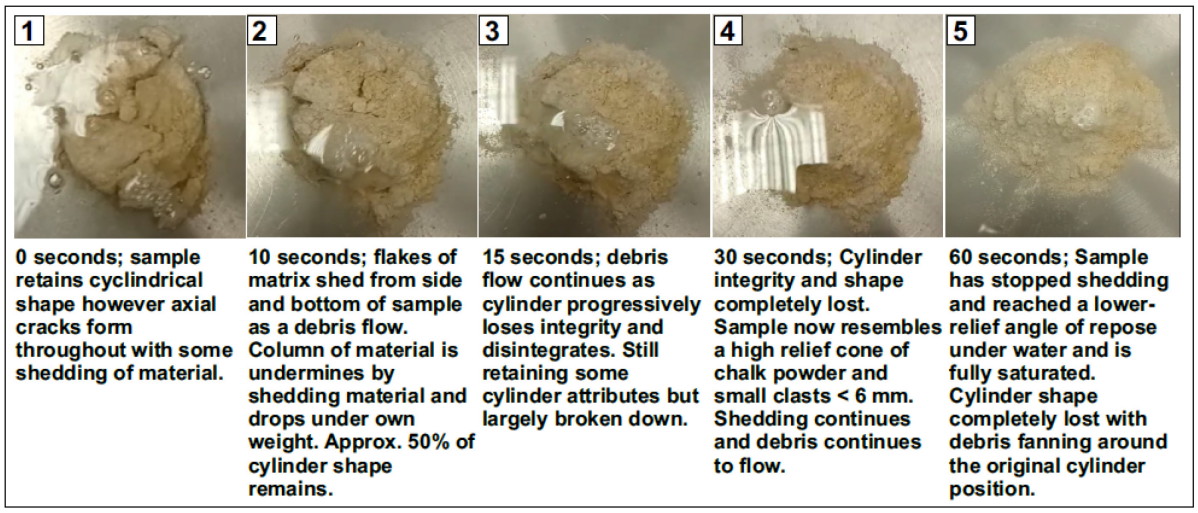


Figure 8-9 Collapse of D-grade material when submerged in water.

When this experiment was repeated with ethylene glycol-water mix, collapse still occurred, however at a much slower rate. This suggests that Dm and Dc chalks are extremely vulnerable to water weakening. The implications of this experiment are that weathered, de-structured chalks are liable to collapse under complete saturation, which may affect areas where Dm and Dc grades are observed (i.e., dry valleys) as well as where construction activity reduces the chalk to putty.

8.2.6 Particle size distribution of D-grade chalk

Particle size distribution (PSD) of de-structured chalk was undertaken to ascertain if there were differences between Dm and Dc grades of chalk. The method for undertaking this test is presented in Section 5.6. Figure 8-10 shows PSD of Newhaven chalk, grade Dm, samples from the dry valley at Portobello Outfall and Seaford Chalk, grade Dc, sampled from the dry valley at Birling Gap.

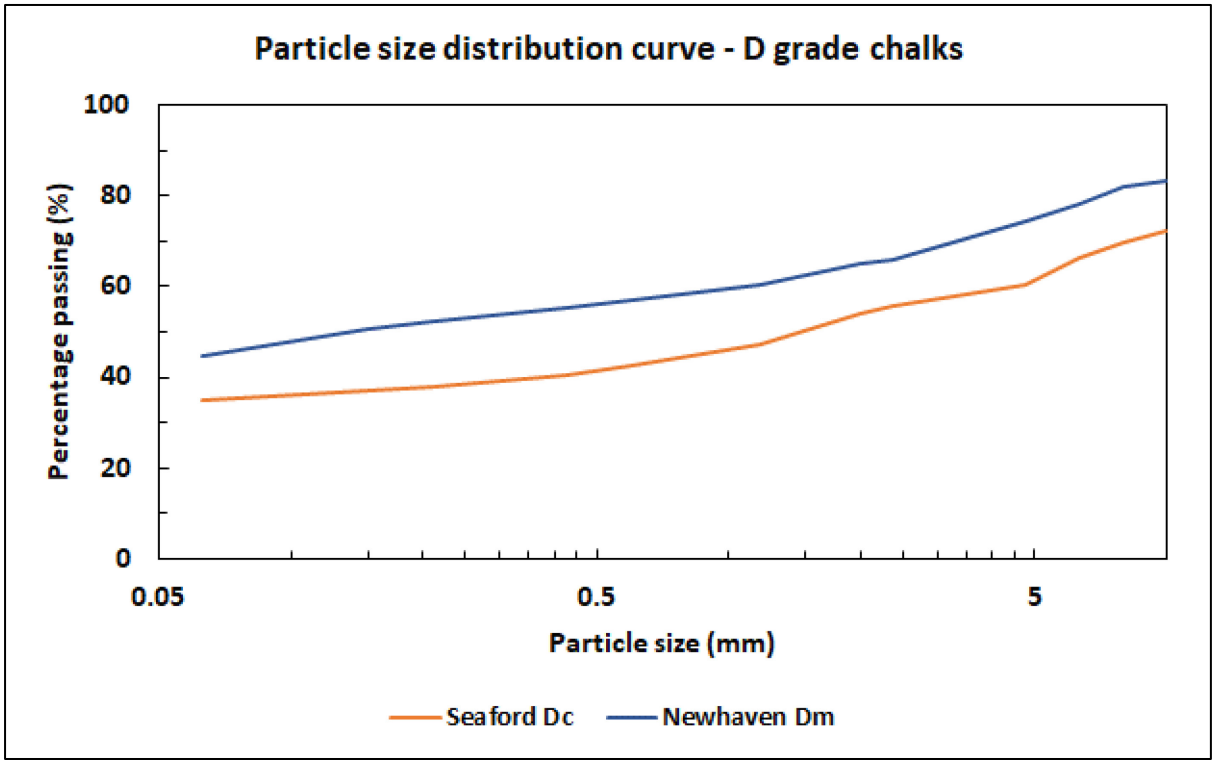


Figure 8-10 PSD curve for Seaford chalk, grade Dc and Newhaven chalk, grade Dm.

From the PSD curve, it is possible to observe that Newhaven Chalk has >40% particles <625 µm, while Seaford comprised 35% particles <625 µm. The curves show a good representation of all grain sizes of material, and therefore are classified as well graded soils. The Newhaven Chalk, being a matrix dominated grade, has more fines compared to the clast dominated grade Dc Seaford chalk. Figure 8-11 presents chalk clasts after PSD was undertaken.



Figure 8-11 Particles after PSD completion.

The implication of the grain size distribution (Figure 8-11) is that at least 35% of the weathered, dry valley composition could be of this grain size and therefore more prone to erosion through natural processes such as rainfall and winnowing.

8.2.7 Modification of the Bushinsky technique

The Bushinsky Oil technique and the development of a modified technique for de-structured chalk is described in Section 5.5. Upon undertaking intact dry density measurements of weathered chalk samples, it was observed that when immersed in paraffin wax, weathered samples tended retained the paraffin wax more readily in the matrix compared to the intact clasts, which led to a colour and contrast change elucidating the weathered chalks internal structure. This modified Bushinsky oil technique (Lawrence et al. 2018a, Bushinsky, 1947), along with image processing software has allowed further semi-quantified grading of de-structured chalk. Figure 8-12 shows an example of Seaford chalk, grade Dc.



Figure 8-12 Modified Bushinsky technique using wax; Seaford chalk, grade Dc.

This approach was considered to be appropriate for weathered D-grade samples as the paraffin wax had has a similar colour to WD40 (as used within the current Bushinsky technique for structured chalk), when applied to the sample, the wax gave additional support to the sample structure, and the degree of penetration of wax and viscosity could be controlled by temperature.

From initial observation of samples, it is possible to observe that while a 65:35% ratio of clasts and matrix can be applied, the range of clast sizes are gradational, ranging from large clasts (>10 mm) to matrix (<63 µm). This is supported by the PSD results presented in Section 8.2.6. Table 8-10 provides

a summary of measurements of the internal structure of various weathered chalks utilising this modified Bushinsky technique, ImageJ and JMicrovision image processing software.

Table 8-10 Quantification of clasts versus putty matrix.

Sample	Formation	Field grade	Clasts (%)	Matrix (%)	Applied grade from image processing	Clast length range (mm)	Average clast length (long axis) (mm)	Number of clasts	Comments
1	Newhaven	Dc (1)	86.3	13.7	Dc	0.75 – 18.74	3.86	44	Some very large clasts, separated by fractures, with little matrix infill.
2	Newhaven	Dc (2)	83.5	16.5	Dc	0.87 – 15.28	6.27	33	Core section mainly comprises large clasts separated by fractures with a matrix filled void within the main body.
3	Newhaven	Dc	62.6	37.4	Dm	0.47 – 14.92	3.14	76	One large clast with length of 14.92 mm – fabric is then dominated by relatively mid-sized clasts and pockets of putty matrix.
4	Seaford	Dc	80.6		Dc	0.2 – 14.27	2.35	143	Apparent shear zone within core, bimodal grain size distribution.

N.B. Sample 4 was re-classified based on CIRIA C574 guidance and the calculated ratio if clasts to matrix. It must be noted that the image processing software is 2-D, therefore this may be an erroneous classification.

From Table 8-10 and Figure 8-13, it is possible to observe differences between Dm and Dc grades of Seaford and Newhaven Chalk. For the purpose of this experiment, the matrix is defined as being <63 µm, with large clasts being >10 mm and small clasts >63 µm but <10 mm. Newhaven Dc is characterised as having larger clasts that are separated by fractures as opposed to matrix, although matrix is still present. Newhaven Dm has larger clasts with fractures, however at least 50% of the core section is represented by smaller clasts hosted within a putty matrix. Seaford Dc has on average smaller grains compared to the Newhaven grades, and they are more numerous. The clasts within the Seaford chalk are hosted within the matrix, which also shows some evidence of shearing and mobilisation of putty, leading to the alignment of larger clasts. At least one of these samples was erroneously graded within a field setting, however it was possible to calculate representative clasts and matrix ratio, leading to a revised laboratory grade.

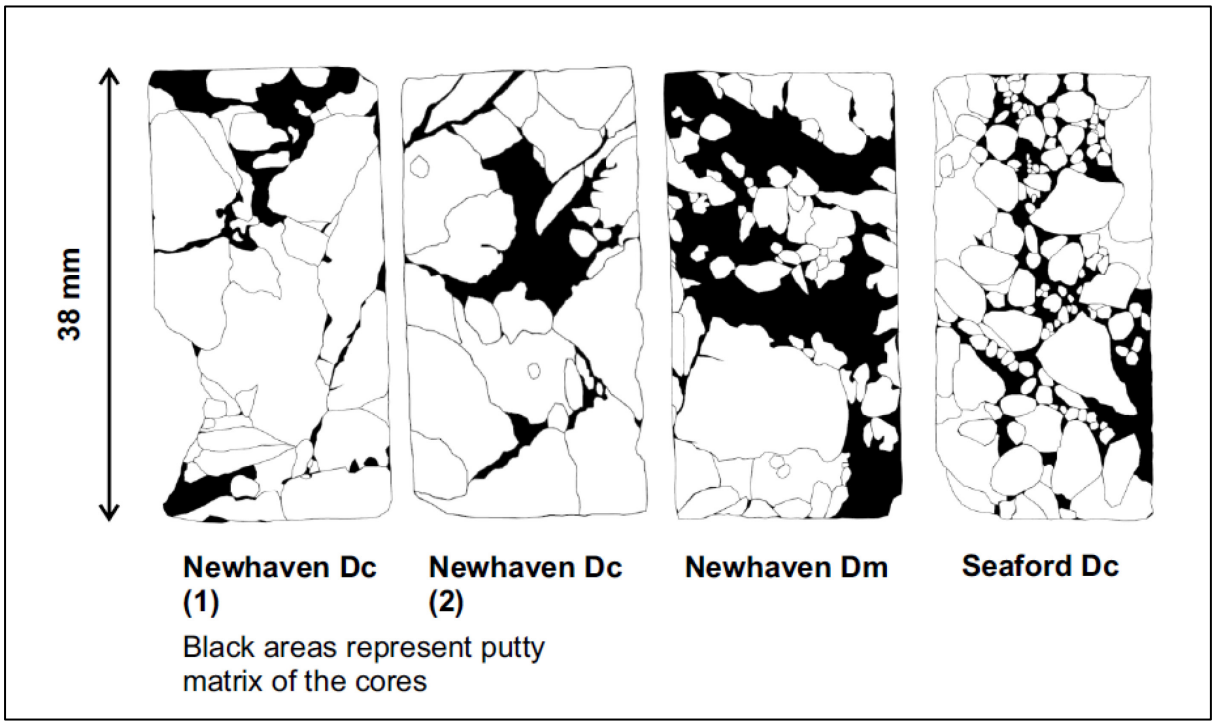


Figure 8-13 Image binarisation for quantification of grade based on putty matrix/clast ratio.

It is possible to observe considerable differences between these samples, and the implication is that these differences will likely affect the engineering behaviour of these weathered chalks. The application of this modified Bushinsky technique and the presented strategy in quantifying clast and putty ratios may reduce uncertainty in characterising engineering behaviour of weathered chalk.

Four samples were measured using the modified Bushinsky technique, and this was not applied to samples which had been tested for permeability or under triaxial conditions. This was due to the timing of development of the technique occurring after permeability testing being undertaken. That

said, the application of this technique may have merit in the identification of changes within internal microstructure modified by consolidation, shearing and fluid flow.

This technique relies upon the chalk samples being fully dried for at least 24 hours prior to cutting, shaping and sanding, with the samples being highly friable. This fragility can lead to samples becoming broken if not handled with care.

Another consideration would be the degree of heterogeneity associated with the samples; owing to the destructive nature of the modified Bushinsky technique, it is not possible to examine each sample pre and post-test (i.e., permeability or triaxial), therefore it would be necessary to select representative control samples to build a statistically significant data set for full appreciation of the microstructure modification due to other forms of testing.

8.3 Slake durability of Southern Province chalks

Slake durability was undertaken to characterise the susceptibility of Southern Province Chalks to weathering due to wetting and drying cycles with periods of disaggregation and is described in Chapter 5, Section 5.3. Different slaking fluids were used to examine water weakening and haloclasty effects, and CIRIA graded chalk was tested to examine if different weathering grades were more susceptible to this artificial weathering process.

Slake durability data of chalk are limited within the current geotechnical literature, with CIRIA reporting values of 13 – 96% for all chalks at 2nd cycle (I_d2), with no formation specified Bell (1977) reports values for the Lower Chalk (92.4 – 97.2%, with a mean value of 95.5%), Middle Chalk (94.7 – 96.6%, mean of 95.9%) and Upper Chalk (79.3 – 84.4%, mean of 82.6%). More recent work by Magalhaes et al. (2018) on the Burnham Chalk Formation, evaluated for use as a sub-base in road construction, yielded similarly high values of 94.9% for the first cycle of slake durability (I_d1) and 94.1% for I_d2. The implication of this limited data is while there is some indication of the durability of chalk, the effects of heterogeneities and rock characteristics of chalk and how they affect chalk durability have not previously been elucidated. As this is a simulated weathering test, it is sensible to postulate that the factors which affect slake durability would likely affect the chalk in terms of weathering resistance and susceptibility.

The degradation of argillaceous rocks due to slaking has been interpreted as mass loss through fracturing (Gamble, 1971), however the wetting phase of slake durability has been established to have the greatest effect on rock strength. Van Eeckhout (1976) studied water weakening of shales and their subsequent strength reduction when tested wet, listing five processes in which rocks weaken during the wetting phase of slake durability; (i) fracture surface energy reduction, whereby absorption of water reduces fracture strength, (ii) capillary tension decrease, where water menisci are lost upon moisture increase, (iii) pore fluid pressure increase, where pore fluids are pressurised, creating an outward pressure gradient and reducing the strength of the rock, (iv) reduction of friction and (v) chemical deterioration, where there are mineralogical changes or chemical processes, such as dissolution, active within the rock in association with water content increase.

The capillary effect is likely to play a critical role when saturated. When the moisture content in rock progressively increases, the curved menisci of water is lost (as reported by Heggheim et al. 2005), which increases the radius of curvature, which is inversely proportionate to capillary tension. The capillary tension then decreases at grain contacts and at the tips of micro-cracks. These capillary forces

are likely to also squeeze the air out, leading to increase in pore water pressure, with potential to damage the microstructure of the rock.

Olivier (1979) states that irreversible anisotropic swelling and shrinkage occurs respectively during wetting and drying cycles, and further exacerbates slaking. This volume change promotes the formation of microfractures, which in turn provides more conduits for moisture redistribution, thus resulting in further deterioration via slaking – this could be analogous to areas weathered areas that are already affected by discontinuities.

Material properties that have been reported to correlate with slake durability include UCS, porosity, grain characteristics (i.e., grain size and angularity), fractal shape and the degree of microfractures within the rock matrix itself.

8.3.1 Standard slake durability procedure

Slake durability was developed for assessing the durability (essentially the weatherability) of weak mudstones and shales (Franklin and Chandra, 1972), which while similar in terms of grainsize to chalk, they are chemically different, and therefore have the capacity to absorb water molecules, unlike chalk. To assess moisture loss in chalk, a preliminary assessment on drying times at 105 °C for structured Seaford and Newhaven Chalk Formations was undertaken over eight hours to refine slake durability testing of chalk. 10 pieces of 40 – 60 g of material per sample type were tested as per ASTM guidelines for the slake durability test (ASTM, 2008).

From this assessment (Table 8-11), it was possible to observe that moisture loss ceased after 3 hours, and therefore a 4-hour period was required to dry the samples. This provided a basis for a minimum drying period, and fell in line with the ASTM standard of 4 – 6 hours (ASTM, 2008).

Table 8-11 Drying times of Newhaven and Seaford chalk.

Sample	**Initial sample weight (g)**	**Drying time (hours)**								**Moisture content (%)**
		1	**2**	**3**	**4**	**5**	**6**	**7**	**8**	
Newhaven 1	85.5	71.5	67.0	67.0	67.0	67.0	67.0	67.0	67.0	29.07
Newhaven 2	79.5	64.5	61.5	61.0	61.0	61.0	61.0	61.0	61.0	33.0
Seaford 1	38.57	33.72	32.95	31.31	31.31	31.31	31.31	31.31	31.31	26.74
Seaford 2	140.0	139.1	115.7	113.7	113.7	113.7	113.7	113.7	113.7	24.49

Testing for an initial database of Southern Province Chalks was undertaken at the University of Leeds to provide a basis for study of these formation. Samples were collected during the reconnaissance

phase of this investigation (described in Chapter 3); these chalks were ungraded by CIRIA standards and IDD was measured. A total of 35 samples were tested during this period over 4 cycles of wetting, drying and abrasion (Table 8-12).

Samples were collected from the Culver, Newhaven, Seaford, Lewes, New Pit, Holywell Nodular, Zigzag and West Melbury Marly Chalk Formations to capture the variability of these chalk formations already identified in other material properties by index testing.

Table 8-12 Slake durability of structured Southern Province chalks.

Sample number	Formation	Location	I_D1 (%)	I_D2 (%)	I_D3 (%)	I_D4 (%)
CC-NH-01	Culver Chalk	Newhaven	76.60	73.40	64.31	63.30
CC-NH-02	Culver Chalk	Newhaven	21.45	10.43	8.74	7.25
CC-NH-03	Culver Chalk	Newhaven	33.86	14.13	10.31	6.61
CC-SP-01	Culver Chalk	Splash Point	78.58	60.43	49.49	41.60
CCF-01	Culver Chalk	Splash Point	66.21	31.47	20.63	13.33
CCF-02	Culver Chalk	Splash Point	71.00	46.04	32.70	25.28
NH-RC-01	Newhaven Chalk	Roedean	86.36	79.34	65.50	58.26
NH-RC-02	Newhaven Chalk	Roedean	85.59	75.67	65.53	61.26
NH-RC-03	Newhaven Chalk	Roedean	93.54	89.52	85.11	80.90
NH-RC-04	Newhaven Chalk	Roedean	94.50	91.05	89.54	84.84
NH-RC-05	Newhaven Chalk	Roedean	84.11	70.32	59.37	44.63
NHCF-01	Newhaven Chalk	Roedean	81.21	72.99	69.05	63.28
NHCF-03	Newhaven Chalk	Roedean	79.68	78.64	67.26	50.52
NHCF-02	Newhaven Chalk	Roedean	91.54	85.41	72.83	66.05
SCF-BG-01	Seaford Chalk	Birling Gap	85.71	72.78	64.03	56.83
SCF-BG-02	Seaford Chalk	Birling Gap	86.29	73.79	64.92	62.70
SCF-BG-03	Seaford Chalk	Birling Gap	81.19	67.54	61.03	53.35
SCF-01	Seaford Chalk	Birling Gap	91.06	75.91	67.09	58.51
SCF-02	Seaford Chalk	Birling Gap	80.75	75.11	66.10	58.77
LNC-BG-01	Lewes Nodular Chalk	Birling Gap	98.32	88.24	81.37	79.24
LNC-BG-02	Lewes Nodular Chalk	Birling Gap	84.22	73.42	71.86	65.52
LNC-BG-03	Lewes Nodular Chalk	Birling Gap	89.97	78.54	74.72	69.11
LNCF-01	Lewes Nodular Chalk	Birling Gap	93.48	85.53	77.26	63.11
LNCF-02	Lewes Nodular Chalk	Birling Gap	79.68	76.24	64.72	58.24
NPC-BH-01	New Pit Chalk	Beachy Head	92.98	89.92	83.01	80.75
NPC-BH-02	New Pit Chalk	Beachy Head	95.13	91.42	87.82	83.43
NPCF-01	New Pit Chalk	Beachy Head	90.75	74.16	57.00	45.41
NPCF-02	New Pit Chalk	Beachy Head	92.54	88.90	83.81	78.90
HNC-HB-01	Holywell Nodular	Holywell Beach	97.61	96.47	94.28	93.35
HNCF-01	Holywell Nodular	Beachy Head	96.07	94.42	86.05	83.95
HNCF-02	Holywell Nodular	Beachy Head	97.76	96.56	95.52	93.80
ZZCF-HB-01	Zig Zag Chalk	Holywell Beach	95.44	85.75	77.47	60.24
ZZCF-01	Zig Zag Chalk	Holywell Beach	96.64	95.55	92.70	86.99
ZZCF-02	Zig Zag Chalk	Holywell Beach	96.70	95.09	91.62	87.78
WMMCF-01	West Melbury Chalk	Beachy Head	92.96	91.78	82.94	80.59

By plotting percentage of material retained against cycle number and utilising Franklin and Chandra's (1972) durability classification (Figure 8-14), it is possible to observe slake indices for I_d1 to I_d4. I_d1 is disregarded as per the ASTM standard. During this initial cycle, angular edges left by sample preparation and natural shape irregularity are broken away by mechanical action, resulting in excess material loss.

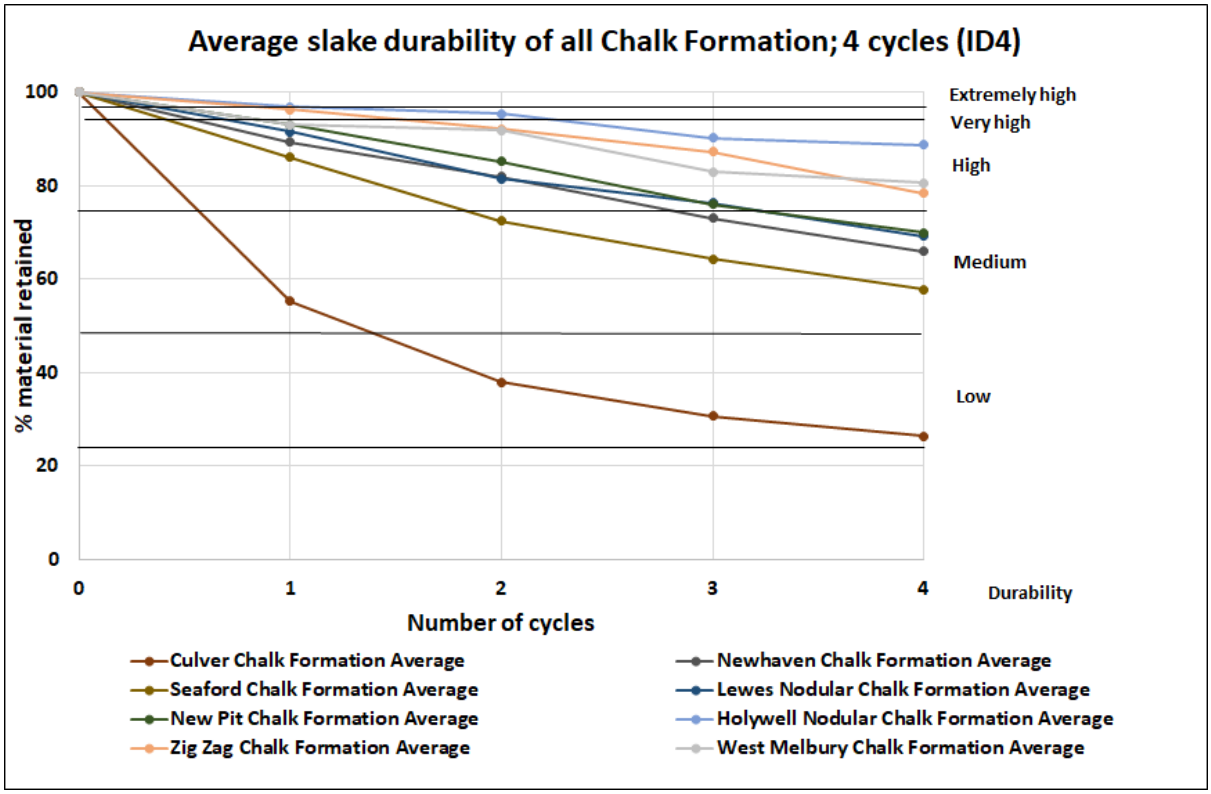


Figure 8-14 Average slake durability of Southern Chalk Formations (less the Portsdown Chalk Formation).

Table 8-12 shows the orders of sequence for each index, starting with the lowest first. Consistently, the Culver Chalk retains the lowest material, followed by Seaford, Lewes and Newhaven, the New Pit, Zig Zag, West Melbury and finally Holywell Nodular Chalks retained the most material. All chalks follow the same order, except the Zig Zag and West Melbury Chalks, which, given their initial close values, switch positions between I_d2 and I_d4.

Table 8-13 presents a classification for slake durability by Franklin and Chandra (1972).

Table 8-13 Slake durability classification (Franklin and Chandra, 1972).

Slake durability I_D (%)	**Classification**	**Geomaterial type**
0 – 25	Very low	Soil
25 – 50	Low	Soil
50 – 75	Medium	Soil
75 – 90	High	Soil
90 – 95	Very high	Rock
95 – 100	Extremely high	Rock

Franklin and Chandra's slake durability classification (Table 8-13) states that material types which retain a percentage <90% are classified as a soil, therefore, of the eight chalks tested for two cycles, the West Melbury, Zig Zag and Holywell Chalks are classed as rock material, with the formations that retain lower being classified as soils. At four cycles, none of the chalks tested reach Franklin and Chandra's criteria for rock. This is by comparing material loss from initial mass to 4th cycle, therefore this does not accurately represent the material. Table 8-14 presents classification results of geomaterial based on slake durability.

Table 8-14 Slake durability and classification of geomaterial based on Franklin and Chandra's methodology.

Chalk type	**Average I_d2 (% retained)**	**Durability classification (Franklin and Chandra)**	**Geomaterial type (Franklin and Chandra)**	**Order of durability (1 = low, 8 = high)**	**Average I_d4 (% retained)**	**Durability classification (Franklin and Chandra)**	**Geomaterial type (Franklin and Chandra)**	**Order of durability (1 = low, 8 = high)**
Culver	37.97	Low	Soil	1	26.41	Low	Soil	1
Newhaven	81.88	High	Soil	4	65.99	Medium	Soil	4
Seaford	75.51	High	Soil	2	57.85	Medium	Soil	2
Lewes	81.43	High	Soil	3	65.24	Medium	Soil	3
New Pit	85.17	High	Soil	5	69.86	Medium	Soil	5
Holywell	95.44	Extremely high	Rock	8	88.65	High	Soil	8
Zig Zag	92.13	Very high	Rock	7	78.33	High	Soil	6
West Melbury	91.78	Very high	Rock	6	80.59	High	Soil	7

The implications of this, given that the classification was initially developed for mudstone, is that it may not be suitable for chalk, but there may be merit in adapting this method for the classification of susceptibility of chalk weathering with further research.

Slake durability is a test to estimate the resistance of a rock to a combination of wetting, drying and abrasion, and should be used comparatively between rock types or formations. It does not predict the rate of weathering nor the state of weathering of the rock being tested, but does give an indication of the weatherability of a rock. These results show that older chalk formations (established by index testing to be harder) are more durable to weathering, therefore further testing will focus on the relatively young Seaford and Newhaven Chalk Formations.

8.3.2 Comparison of Seaford and Newhaven Chalk Formations from baseline testing

By comparing both the Seaford and Newhaven Chalk slake durability results from initial testing, it is possible to observe differences in slaking materials of each formation.

From eight initial slake durability tests of Newhaven Chalk, three were omitted from analysis due to departure from standard testing procedures. Of the five remaining tests (Table 8-15), at I_d1, there was a range of 84.11 - 94.50% (10.39% difference) and a mean percent material retained of 88.82%. At I_d2, there was material retention in the range of 70.32 - 91.05% (20.73% difference) and a mean material retention of 81.18%, which is classified as a high durability material. For I_d3, the range is 59.37 - 89.54% (30.17 % difference), with a mean retention of 73.01%; a medium durability material. At I_d4, the material retention range was reduced to 44.63 - 84.84% (40.21% difference), while the mean percent retention was 65.98%, corresponding to a medium durability material.

Table 8-15 Slake durability of Newhaven chalk.

Sample number	**Sample**	**I_d (%)**			
		1	**2**	**3**	**4**
NH-RC-01	Newhaven Chalk - Roedean	86.36	79.34	65.50	58.26
NH-RC-02	Newhaven Chalk - Roedean	85.59	75.67	65.53	61.26
NH-RC-03	Newhaven Chalk - Roedean	93.54	89.52	85.11	80.90
NH-RC-04	Newhaven Chalk - Roedean	94.50	91.05	89.54	84.84
NH-RC-05	Newhaven Chalk - Roedean	84.11	70.32	59.37	44.63
NH mean	Newhaven Chalk Formation	88.82	81.18	73.01	65.98
Range of material loss per I_D (%)	Newhaven Chalk Formation	84.11 – 94.50	70.32 - 91.05	59.37 - 89.54	44.63 - 84.84

Similarly for the Seaford Chalk, five tests were undertaken (Table 8-16). At I_d1, 80.75 - 91.06% of material was retained (10.31% difference) and a mean retention of 86.06%. At I_d2, there was material

retention range of 67.54 - 75.91% (8.37% difference) and a mean material retention of 72.51%, which is classified as a medium durability material. For I_d3, the range reduces to 61.03 - 66.10% (a range of 5.07%), with a mean retention of 64.27%, which is a medium durability material. At I_d4, the material retention range was reduced to 53.35 - 62.70% (7.03% difference), while the mean percent retention was 57.85%, corresponding to a low durability material.

Table 8-16 Slake durability of Seaford chalk.

Sample number	Sample	I_d (%)			
		1	2	3	4
SCF-BG-01	Seaford Chalk - Birling Gap	85.71	72.78	64.03	56.83
SCF-BG-02	Seaford Chalk - Birling Gap	86.29	73.79	64.92	62.70
SCF-BG-03	Seaford Chalk - Birling Gap	81.19	67.54	61.03	53.35
SCF-01	Seaford Chalk - Birling Gap	91.06	75.91	67.09	58.51
SCF-02	Seaford Chalk – Birling Gap	80.75	75.11	66.10	58.77
SCF mean	Seaford Chalk Formation	86.06	72.51	64.27	57.85
Range of material loss per I_D (%)	Seaford Chalk Formation	80.75 – 91.06	67.54 - 75.91	61.03 - 66.10	53.35 - 62.70

Initial average material lost from I_d0 to I_d1 was greatest for the Seaford Chalk at 13.06% lost, compared to the Newhaven Chalk at 11.18%. Figure 8-15 shows these results compared graphically.

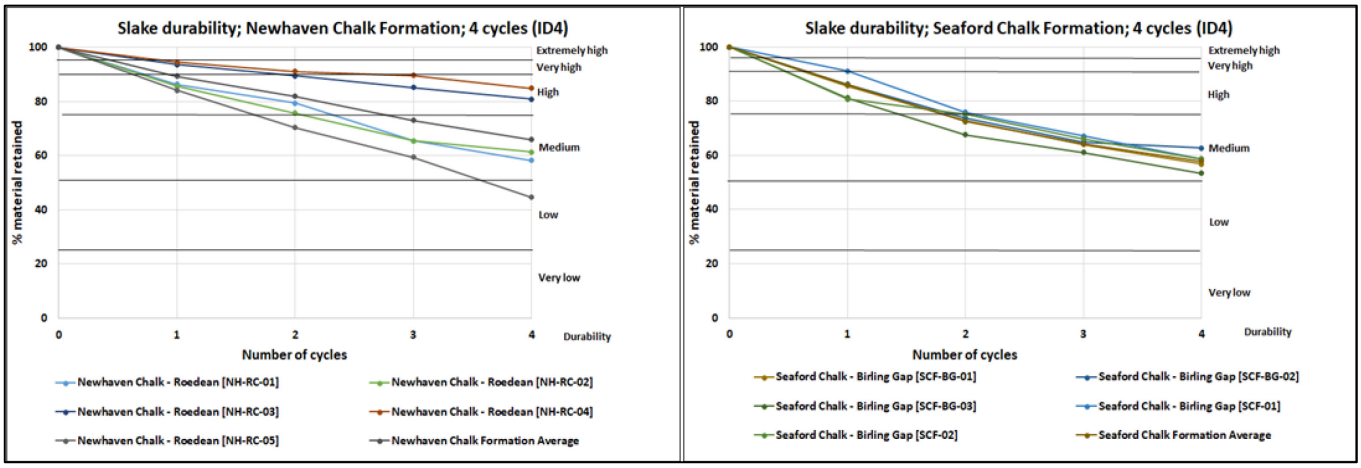


Figure 8-15 Slake durability of Newhaven and Seaford chalk formations (4 cycles).

From the comparison, it is possible to observe that the Newhaven Chalk retains more material on average at I_d2 compared to the Seaford Chalk Formation. The Newhaven Chalk also has a greater range of material retained compared to the Seaford Chalk at I_d2. As cycles progress, the range of material lost by the Newhaven Chalk increases at approximate 10% intervals, with the greatest range

associated with I_d4, while the range for the Seaford Chalk are lower than 10% and remain relatively consistent in comparison.

The higher percentage of material retained by the Newhaven Chalk at I_d2 could suggest that the Newhaven Chalk is more durable than the Seaford. The Newhaven Chalk results are far more variable with a material retention range at I_d2 of 20.73% compared to the Seaford Chalk, which is 8.37%, this difference continues to increase through to I_d5.

The variability in the Newhaven Chalk results indicates that it is more heterogeneous in terms of material properties than the Seaford Chalk. The increasing range over further cycles indicates that the Newhaven Chalk is more durable than the Seaford Chalk but more susceptible to breakdown through wetting and drying samples, with periods of abrasion as a rock mass, probably due to a greater number of micro-fractures. Figure 8-16 demonstrates that at I_d2, the Newhaven chalk has fractured into more fragments compared to the Seaford Chalk, while maintaining a similar mass of material.

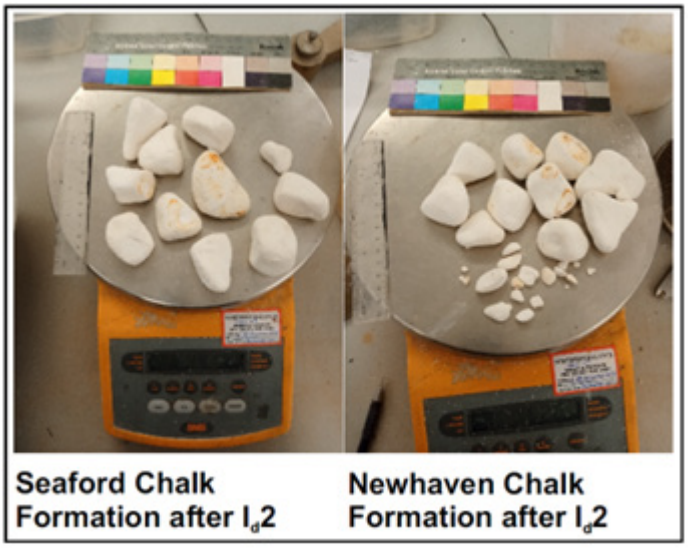


Figure 8-16 Comparison of Seaford and Newhaven chalk clasts after I_d2.

8.3.3 The effects of slaking fluid and moisture content on artificial chalk weathering

Nine tests were undertaken (three tests of Newhaven, Seaford, and Holywell Nodular Chalk Formations each) to examine the effects of three different slaking fluids; distilled water, artificial sea water and ethylene glycol. Each formation sub-set of samples were cut from the same block to reduce heterogeneity, the results are shown in Table 8-17.

Table 8-17 Slake durability using different slaking fluids.

Slaking fluid	**Sample**	**Location**	**I_d1 (%)**	**I_d2 (%)**	**I_d3 (%)**	**I_d4 (%)**	**Durability classification at I_d2**
Distilled water	Newhaven	Roedean	90.76	74.50	66.30	59.65	Medium durability soil
Distilled water	Seaford	Birling Gap	87.14	74.94	66.89	59.84	Medium durability soil
Synthetic seawater	Newhaven	Roedean	82.41	71.83	63.51	55.0	Medium durability soil
Synthetic seawater	Seaford	Birling Gap	93.17	77.27	71.96	61.92	High durability soil
Ethylene glycol	Newhaven	Roedean	98.16	95.34	91.34	81.27	Extremely high durability rock
Ethylene glycol	Seaford Newhaven	Birling Gap	94.74	87.86	79.97	72.84	High durability soil

When plotted graphically, it is possible to observe the relative differences of each slaking fluid on the selected chalk formations. Figure 8-17 (A) shows that at I_d2 chalk slaked in ethylene glycol retains 95.34% of material, while chalk slaked in distilled water retains 20.84% less material, retaining 74.5%. The most slaking fluid associated with most material loss for the Newhaven Chalk was synthetic seawater, retaining 71.83%, which is 2.67% lower than distilled water slaking fluid and 23.51% lower than ethylene glycol slaking fluid.

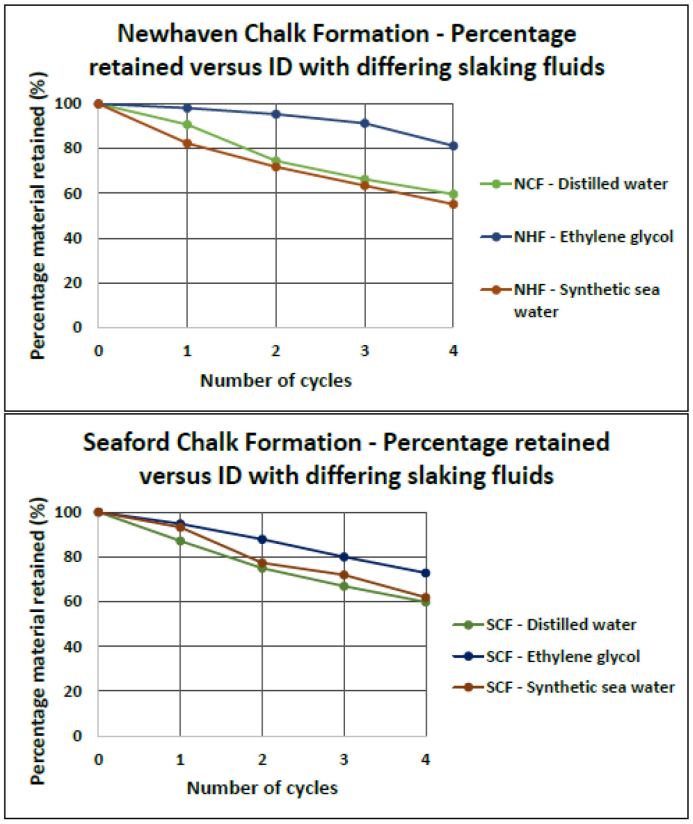


Figure 8-17 Slake durability using differing slaking fluids (A) Newhaven Chalk Formation, (B) Seaford Chalk Formation.

The Seaford Chalk (Figure 8-17 - B) shows at I_d2, ethylene glycol slaking fluid tests retain 87.86% of chalk material, followed by synthetic seawater slaking fluid, retaining 77.27% (10.59 % lower than ethylene glycol), which is then followed by distilled water slaking fluid, which retains 74.94%. This is 12.92% less retained than samples slaked in ethylene glycol and 2.33% less than samples slaked in distilled water.

Table 8-17 shows I_d1 to I_d4 of all samples tested with different slaking fluids. It is possible to observe that the distilled water and synthetic seawater caused the most slaking of the samples regardless of formation. Owing to the variability observed within the Newhaven Chalk Formation within Figure 8-15, and the limited number of tests presented in Figure 8-17, it is not possible to draw any conclusions on the variability with differing slaking fluids for the Newhaven Chalk Formation at this time. This would require testing of more samples with differing slaking fluids to build a statistically significant and robust data set in terms of repeatability. For the Seaford Chalk, the repeatability demonstrated in Figure 8-15 shows that both fresh water and salt water may weather the Seaford chalk in a coastal setting.

Observations of fracture character, arisings and turbidity of slaking fluid

For all slaking fluids, samples of the Seaford Chalk Formation were vacuum saturated prior to testing within a pressure vessel at 1 MPa. During this time within distilled water and synthetic seawater, air bubbles were observed exsolving from the samples. For the Seaford Chalk Formation, test samples within distilled water and synthetic seawater tended to round by I_d2 and take on a mottled, golf ball-like texture, pitted by small surface indentations. The synthetic seawater samples further disaggregated into relatively smaller but angular fragments after I_d2. Samples tested within the ethylene glycol retained angularity when compared to the other slaking fluids.

Arisings produced were suspended within the slaking fluid (estimated as <63 µm), increasing turbidity, with a significant amount settling to the bottom of the slaking tank (<2 mm), forming a chalk sludge (Figure 8-18). In terms of turbidity, I_d1 was the most turbid cycle with turbidity gradually reducing each cycle. While turbidity was not measured, physical observation allowed estimation that of the 3 slaking fluids, distilled water was most turbid and ethylene glycol was least turbid, supporting earlier observations of the weakening action of water on chalk. This has implications for weathering in that the material lost was of the <63 µm grain size, and therefore material loss insitu would be very gradual.

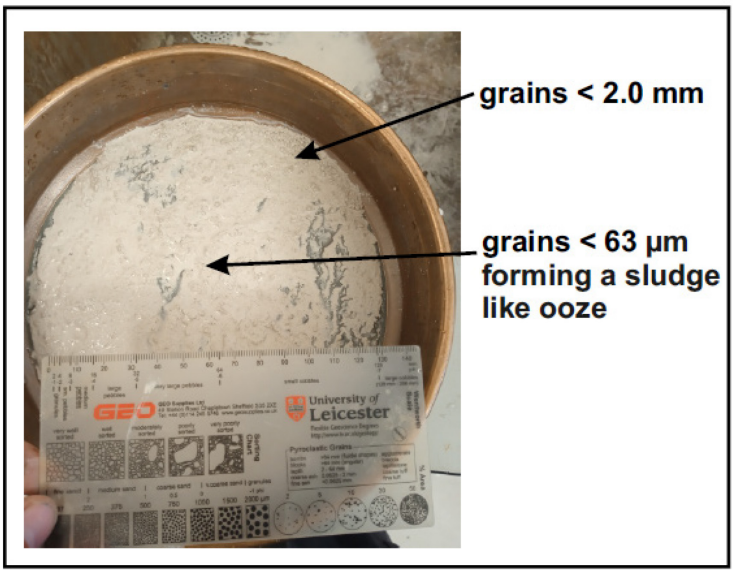


Figure 8-18 Newhaven chalk arisings after slaking (<2 mm).

The Newhaven Chalk Formation tested in ethylene glycol and distilled water resulted in individual rounded blocks, but when slaked in synthetic seawater, the blocks disintegrated into numerous smaller angular fragments, presumably caused by halite nucleation during drying periods within the microfractures. Arisings components comprised a fine (<63 µm) and coarse fraction (63 µm – 2 mm). After slaking with ethylene glycol, there was some faint discolouration of microfractures within the Newhaven Chalk however, these could not be photographed owing to camera resolution and subtle

hue. Figure 8-19 shows the Newhaven chalk when slaked in freshwater (top) compared to increased disaggregation of Newhaven Chalk when subject to synthetic seawater (bottom). It is speculated that microfracturing is caused by haloclasty, and therefore this would have implications for chalks subject to sea spray or immersion in sea water.



Figure 8-19 Newhaven Chalk Formation disaggregation in response to slaking water change – upper figures show samples slaked in fresh water, lower figures show samples slaked in synthetic salt water.

8.3.4 Slake durability of CIRIA chalk grades

Graded Seaford and Newhaven chalk slake durability results

Samples selected, graded and collected by the author were tested using the slake durability method by Shi (2022) as part of an MSc project supervised by the author. 15 samples of Newhaven Chalk, graded A1 to Dm were tested, and 16 samples of Seaford Chalk, graded A1 to Dm, were tested (Table 8-18). The majority of CIRIA grades were tested but some have been missed because of the challenges obtaining representative samples.

Table 8-18 Formations and grades of Seaford and Newhaven chalk tested.

Formation and grades tested	
Newhaven A1	Seaford A1
Newhaven A5	Seaford B2
Newhaven B3	Seaford B4
Newhaven B4	Seaford B5
Newhaven C3	Seaford C3
Newhaven C4	Seaford C4
Newhaven C5	Seaford C5
Newhaven Dc	Seaford Dc
Newhaven Dm	Seaford Dm

Newhaven Chalk Formation

Table 8-19 presents results for graded Newhaven Chalk, including grades from conjugate fractures and three samples which deviated from the slake durability procedure. Table 8-19 represents all grades of Newhaven chalk plotted at I_d2 to I_d5 and can be further split down into samples that follow standard procedures and those samples which were tested saturated to evaluate wetting and drying cycles. At I_d2, of the samples that were tested per procedure, the greatest durability is grade A1 at 89.52%. Grade C4 and B4 showed similar curves and at I_d2 retained 86.70% and 86.60% of material respectively. Grade B4 retained the next greatest amount of material, however, this sample was taken at proximity to a conjugate fracture, meaning that the material may be compromised by microfractures, at 71.71%. This was followed by grade C5 at 67.24%, grade B3 at 57.83% and then C3 at 50.90%. Material retained then significantly reduced with grade A5, at 33.46%. D-grade chalks retain the lowest material, with grade Dc retaining 12.42% and grade Dm at 4.59%.

Table 8-19 CIRIA graded Newhaven chalk slake durability results (graded by Maher, slake testing by Shi, 2022).

Sample and grade	**I_d1 (%)**	**I_d2 (%)**	**I_d3 (%)**	**I_d4 (%)**	**I_d5 (%)**	**IDD (Mg/ m^3)**
Newhaven Chalk, Roedean B4 (sampled from conjugate fracture)	85.71	71.71	53.14	39.66	28.91	1.64
Newhaven Chalk, Roedean A5	74.51	33.46	18.09	14.59	12.26	-
Newhaven Chalk, Roedean B3	75.00	57.83	38.40	36.98	24.03	1.76
Newhaven Chalk, Roedean B4	92.25	86.60	79.07	71.32	66.56	1.78
Newhaven Chalk, Roedean C3	76.77	50.90	27.90	15.33	11.86	1.73
Newhaven Chalk, Roedean C4	92.38	86.70	78.11	68.56	59.12	1.86
Newhaven Chalk, Roedean C5	85.89	67.24	33.87	19.39	13.74	1.69
Newhaven Chalk, Roedean B3 (saturated - undried at slaking)	92.97	85.66	79.68	74.07	68.85	-
Newhaven Chalk, Roedean B4 (saturated - undried at slaking)	97.53	92.18	86.83	83.13	79.01	-
Newhaven Chalk, Roedean C3 (saturated - undried at slaking)	88.86	79.29	70.84	62.95	56.82	-
Newhaven Chalk, Roedean A1	93.54	89.52	85.11	80.90	75.34	1.72
Newhaven Chalk, Portobello Dm	9.08	4.59	4.59	4.59	4.59	1.46
Newhaven Chalk, Portobello Dc	16.24	12.42	12.42	12.42	12.42	1.05
Newhaven Chalk, A1 (saltwater saturated - slaked in synthetic seawater)	73.84	61.13	54.59	-	-	-
Newhaven Chalk, A1 (salt saturated - slaked in distilled water)	76.28	64.36	58.16	-	-	-

Five cycles were undertaken to observe the effects of repeated slaking cycles on the same chalk samples to assess the degree of material loss. Newhaven grade A1 continued to retain the most material at 79.01%, followed by grade B4 (66.56%), grade C4 (59.12%). Material retained again significantly drops, with grade B4 retaining 28.93%, grade B3 retaining 24.03% and C5 retaining 13.74%. D-grade chalks retain the same value from I_d2.

Figure 8-20 presents slake durability against CIRIA discontinuity aperture grade for the Newhaven Chalk Formation. The resulting order of grades are A, B, C, B, B, C, B, C, A, D, D with grade A coinciding with most durable samples, while D-grades are least durable samples. Figure 8-19 presents slake durability against CIRIA discontinuity spacing grade for the Newhaven Chalk Formation. The resulting order of grades is 1, 4, 4, 4, 5, 3, 3, 5, clasts and matrix, with grade 1 coinciding with the most durable sample, and clasts and matrix coinciding with the least durable.

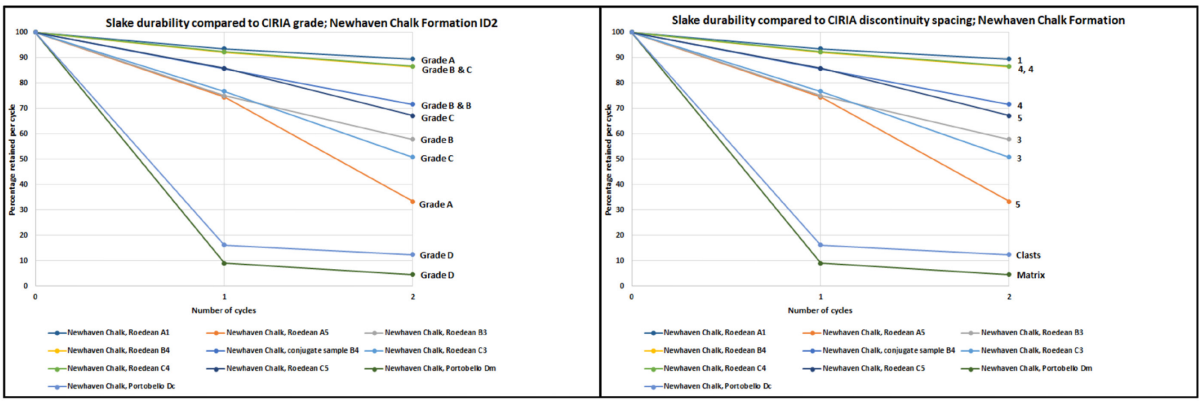


Figure 8-20 Slake durability of CIRIA graded Newhaven chalk.

Seaford Chalk Formation

Table 8-20 is a summary of all grades of Seaford Chalk Formation tested during this work package. 16 tests were undertaken. Table 8-20 represent all grades of Seaford chalk plotted I_d2 to I_d5 and is further broken down into saturated and unsaturated chalks, which were tested to evaluate wetting and drying cycles. At I_d2, the greatest amount of material retained by a chalk tested under standard procedures was in-land grade A1 Chalk from Tarring Neville, at 89.51% and coastal grade A1 at 80.71% (Birling Gap). This was followed by grade B4 (73.94%), then by grade B3 samples from the base of Birling Gap at a wave cut notch, at 73.0%. Grade B2 (72.51%), grade C4 (72.23%), grade B5 (70.58%), grade C3 (70.57%) and grade C5 (66.82%) follow. De-structured grades retain the lowest material, with grade Dc retaining 22.59% and grade Dm retaining 12.12%. This material comprised small chalk clasts, with the matrix component dispersed within the slaking fluid.

Table 8-20 CIRIA graded Seaford chalk slake durability results (graded by Maher, slake testing by Shi, 2022).

Sample and grade	**I_d1 (%)**	**I_d2 (%)**	**I_d3 (%)**	**I_d4 (%)**	**I_d5 (%)**	**IDD (Mg/ m^3)**
Seaford Chalk, Tarring Neville A1 (Inland)	94.04	89.51	84.98	80.81	76.40	*
Seaford Chalk, Birling Gap A1	89.17	80.71	73.22	65.31	60.54	1.78
Seaford Chalk, Birling Gap B2	81.03	72.51	61.82	55.46	49.58	1.77
Seaford Chalk, Birling Gap B4	83.59	73.94	62.48	55.73	49.34	1.69
Seaford Chalk, Birling Gap B5	81.89	70.58	57.85	50.82	44.68	*
Seaford Chalk, Birling Gap C3	81.03	70.57	56.90	48.05	41.72	1.70
Seaford Chalk, Birling Gap C4	83.92	72.23	61.51	56.03	48.84	1.72
Seaford Chalk, Birling Gap C5	81.06	66.82	54.00	46.59	40.00	1.69
Seaford Chalk, Birling Gap Dc	27.12	22.59	20.85	19.69	18.53	0.99
Seaford Chalk, Birling Gap Dm	16.66	12.12	12.12	12.12	12.12	1.48
Seaford Chalk, B3 (saturated)	88.78	79.36	71.04	64.13	57.72	*
Seaford Chalk, B5 (saturated)	83.59	70.69	61.93	52.17	48.34	*
Seaford Chalk, C3 (saturated)	83.51	73.26	64.48	57.08	52.85	*
Seaford Chalk, C4 (saturated)	89.92	81.25	73.79	67.64	62.40	*
Wave cut notch, Birling Gap B3	85.37	73.00	59.45	52.53	43.55	1.71
Wave cut notch, Birling Gap B3 (saturated)	86.23	76.79	68.73	61.85	55.56	*

Of the non-standard slaking tests, grade B3 at 79.36% retained the most material, followed by a grade B3 sampled from the base of cliff at Birling Gap, saturated on testing, at 76.97%. Saturated grade B4 follows at 73.94%, saturated grade C3 (73.26%) and finally saturated grade B5 at 70.69% retained the least material.

Samples tested to I_d5 broadly follow similar trends; at I_d5, the in-land Seaford grade A1 retains the greatest amount of material at 76.41%, followed by coastal grade A1, at a lower amount of 60.54%. Grade B2 retains 49.58%, followed by B4 (49.34%), C4 (48.84%) and grade B5 (44.68%). Grade B3 (sampled from the wave cut notch at the base of cliff at Birling Gap) retained 43.55%, followed by C3 at 41.72% and C5 at 40.0%. De-structured grades remained the same as I_d2 values.

Figure 8-21 presents slake durability against CIRIA discontinuity aperture grade for the Seaford Chalk Formation. The resulting order is A (in-land chalk), A (coastal chalk), B, B, C, C, C, D, and D, with grade A (in-land) coinciding with the most durable chalk and D-grades being the least durable. Figure 8-21 (right) presents slake durability against CIRIA discontinuity spacing grade for the Seaford Chalk Formation. The resulting order is grade 1, 4, 5, 4, 3, 5, 2, clasts and matrix, with grade 1 coinciding with the most durable chalk and clasts and matrix coinciding with the least durable.

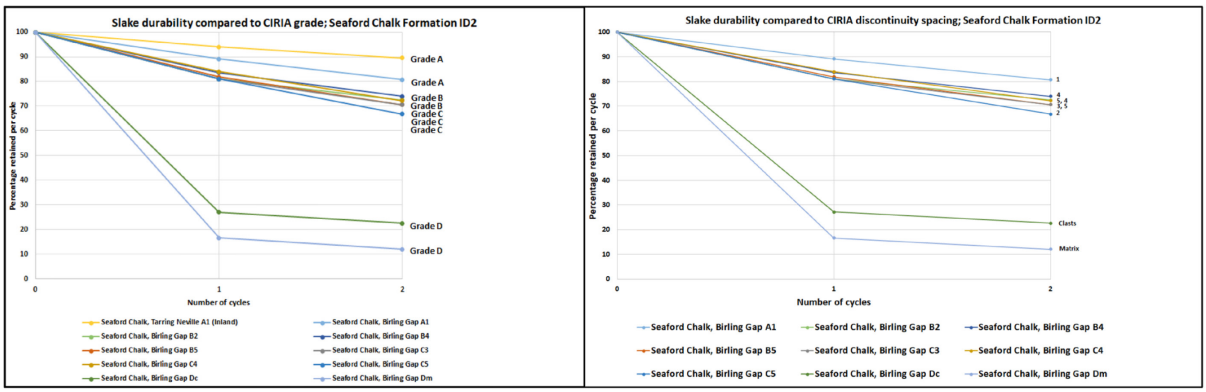


Figure 8-21 Slake durability of CIRIA graded Seaford Chalk.

8.3.5 Slake durability at I_d2 versus IDD

Figure 8-22 plots percentage of material retained against IDD for the Seaford and Newhaven Chalk, Franklin and Chandra's durability index (1972) and the CIRIA density grade are also shown. I_d2 was selected as it is considered the most representative stage of durability within the literature.

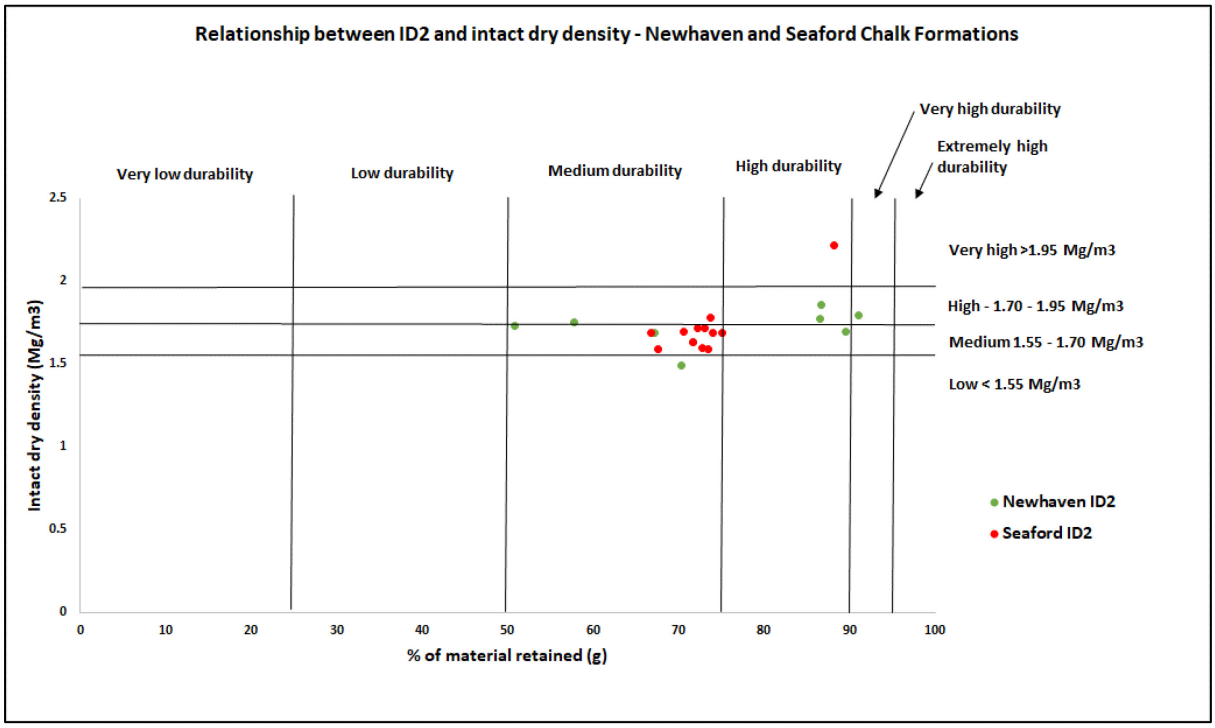


Figure 8-22 Relationship between I_d2 and intact dry density - Newhaven and Seaford Chalk Formations.

The Newhaven Chalk Formation shows The highest IDD was 1.86 Mg/m^3, corresponding to 86.70% chalk material retained while the lowest IDD was 1.49 Mg/m^3, corresponding to 70.32% chalk material retained. It is possible to observe that broadly, medium durability chalks correlate with medium dry densities and high durability chalks correlate with high dry density values.

Figure 8-22 shows IDD plotted against I_d2 for the Seaford Chalk Formation. The highest IDD was 2.22 Mg/m^3, corresponding to 88.24% chalk material retained, while the lowest IDD was 1.59 Mg/m^3, which corresponded to 75.24% chalk material retained. The majority of data points cluster within the medium durability and medium density ranges, and the highest IDD, considered a very high-density chalk by CIRIA standards coincides with a classification of a high durability chalk as per Franklin and Chandra. This has implications in that it suggests that IDD could be an indicator of the durability (and susceptibility to weathering) of a chalk.

8.4 Permeability of de-structured chalk

Accelerated permeability testing was undertaken (described in Chapter 5.4), 22 samples were test of D-grade, de-structured chalk but only 11 tested were successfully completed. Of these successful tests three were Newhaven Dm, four were Newhaven Dc, two were Seaford Dm and two were Seaford Dc (Table 8-21). Newhaven Dm samples had permeability values which ranged 1.18 – 5.99 x 10^{-8} m/s. Newhaven Dc permeability values ranged 9.69 x 10^{-9} to 7.76 x 10^{-8} m/s, Seaford Dm ranged 4.22 – 7.10 x 10^{-8} m/s and Seaford Dc had permeability values that ranged 7.78 x 10^{-9} to 2.67 x 10^{-8} m/s.

Table 8-21 Permeability of de-structured Newhaven and Seaford chalks.

Sample	**Stage 1 (m/s) 120 kPa**	**Stage 2 (m/s) 240 kPa**	**Stage 3 (m/s) 360 kPa**	**Pre-test MC (%)**	**Post-test MC (%)**	**IDD (Mg/m^3)**	**SMC (%)**
NewhavenDm_21022023	1.56 x 10^{-8}	1.57 x 10^{-8}	1.18 x 10^{-8}	27.18	28.69	1.52	28.48
NewhavenDc_14022023	1.16 x 10^{-8}	1.19 x 10^{-8}	1.12 x 10^{-8}	27.81	27.53	2.05	11.67
SeafordDm_29012023	7.10 x 10^{-8}	5.29 x 10^{-8}	4.22 x 10^{-8}	25.77	29.74	1.56	26.89
NewhavenDc_15012023	2.32 x 10^{-8}	1.42 x 10^{-8}	9.76 x 10^{-9}	25.19	26.69	1.88	16.04
SeafordDc_20122022	2.67 x 10^{-8}	2.63 x 10^{-8}	2.11 x 10^{-8}	22.79	27.61	1.47	31.14
NewhavenDm_11122022	5.99 x 10^{-8}	3.47 x 10^{-8}	2.42 x 10^{-8}	26.62	30.92	1.51	29.03
NewhavenDc_05122023	1.55 x 10^{-8}	1.19 x 10^{-8}	1.11 x 10^{-8}	28.27	28.33	1.59	25.54
SeafordDm_22112022	5.56 x 10^{-8}	5.13 x 10^{-8}	-	22.49	28.47	1.54	27.72
NewhavenDm_24102022	5.88 x 10^{-8}	5.64 x 10^{-8}	5.04 x 10^{-8}	25.18	26.79	1.52	28.86
SeafordDc_24092022	1.38 x 10^{-8}	8.43 x 10^{-9}	7.78 x 10^{-9}	27.86	27.59	1.68	22.16
NewhavenDc_07102022	2.38 x 10^{-8}	1.35 x 10^{-8}	9.69 x 10^{-9}	24.27	28.47	1.63	24.13

By plotting the mean values of permeability, it is possible to observe that Dm grades have higher permeabilities than Dc grades, and that Seaford Chalks have higher permeabilities compared to Newhaven chalks. Permeabilities decrease with increasing effective stress. The highest permeabilities correspond to Seaford Dm at 4.48 x 10^{-8} m/s reducing to 2.28 x 10^{-8} m/s with Newhaven Dm permeabilities approximately 30% lower at 6.33 x 10^{-8} m/s reducing to 4.23 x 10^{-8} m/s. Dc grades follow a similar pattern in that Seaford Dc chalk has higher permeabilities at 6.3 x 10^{-8} m/s reducing to 4.23 x 10^{-8} m/s and Seaford Dc chalks at 1.86 x 10^{-8} m/s reducing to 1.04 x 10^{-8} m/s (approximately 9 – 28% lower). These values are similar to structured chalks which have been reported as 10^{-8} m/s by

Mider and Lawrence (2018) for Seaford chalk, and 10^{-7} to 10^{-8} m/s for Seaford by Molyneux (2012). Permeabilities of 10^{-5} – 10^{-9} m/s for Dc grades described as 'soft chalks', 10^{-3} and 10^{-7} – 10^{-9} m/s for Dm chalks were reported by Preene and Roberts (2017) and Spearing-Bundy (2013) reported values for lab-produced, homogenised putty chalks of 2.5 – 12.5 x 10^{-9} m/s at confining pressures of 0 – 400 kPa.

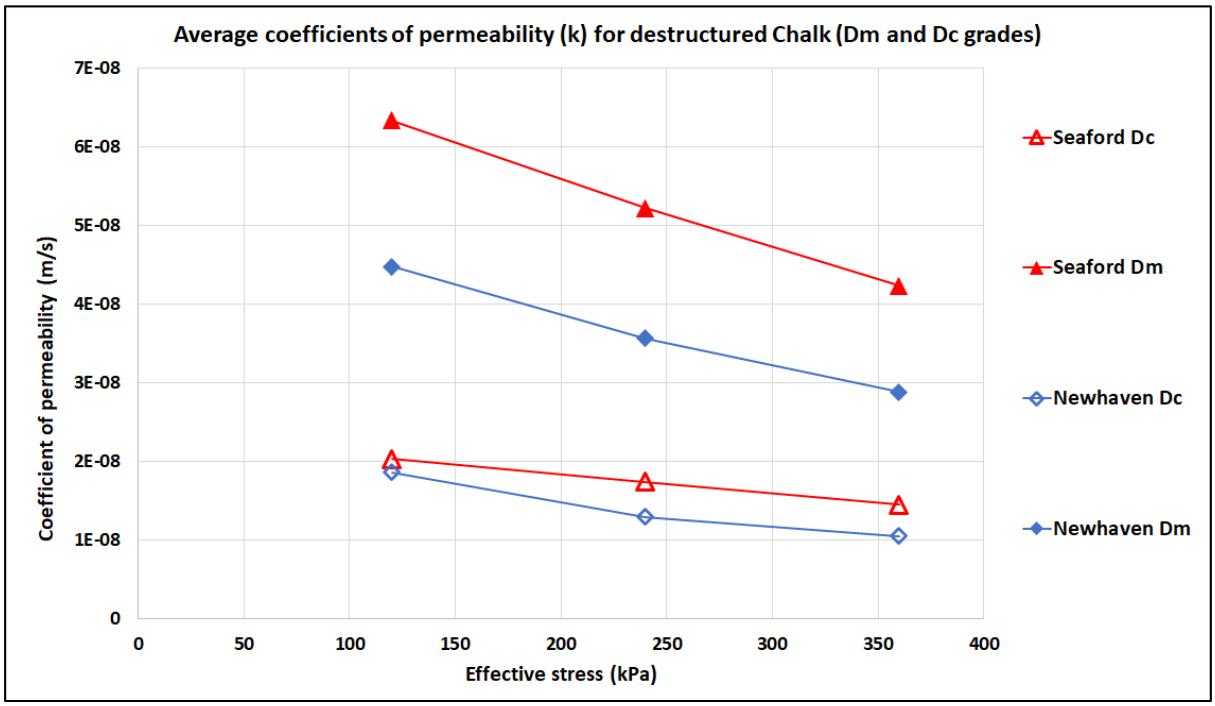


Figure 8-23 Permeability of Seaford and Newhaven de-structured chalk.

In all cases permeability decreases with increasing effective stress (Figure 8-23), with decreases being greater in Dm samples, compared to Dc samples. This is likely due to structural changes within the matrix component, which in Dm samples is more pronounced (Figure 8-23). Decreases in permeability with increasing effective stress was also reported by Spearing-Bundy, whereby the reduction in permeability was attributed to changes in void ratio, porosity and specific volume of a granular material (Spearing-Bundy, 2013). This has implications for the geological setting of these samples; extensive and deep dry valleys will likely have higher permeabilities at the surface (i.e., close to ground level) where confining pressure is lower, while permeability would be expected to decrease with depth (and increase in effective stress). Hadlow et al. (Hadlow, 2014, Hadlow et al. 2018) reports that at 20.0 mbgl, there are improvements in both CIRIA grade and seismic velocities, while Molyneux (2012) suggests that at 20.0 mbgl, the effects of relaxation are nullified and dilation of discontinuities ceases, with permeability becoming equivalent to matrix permeability. This is supported by the phenomena observed of reducing permeability with increasing effective stress observed during this permeability testing.

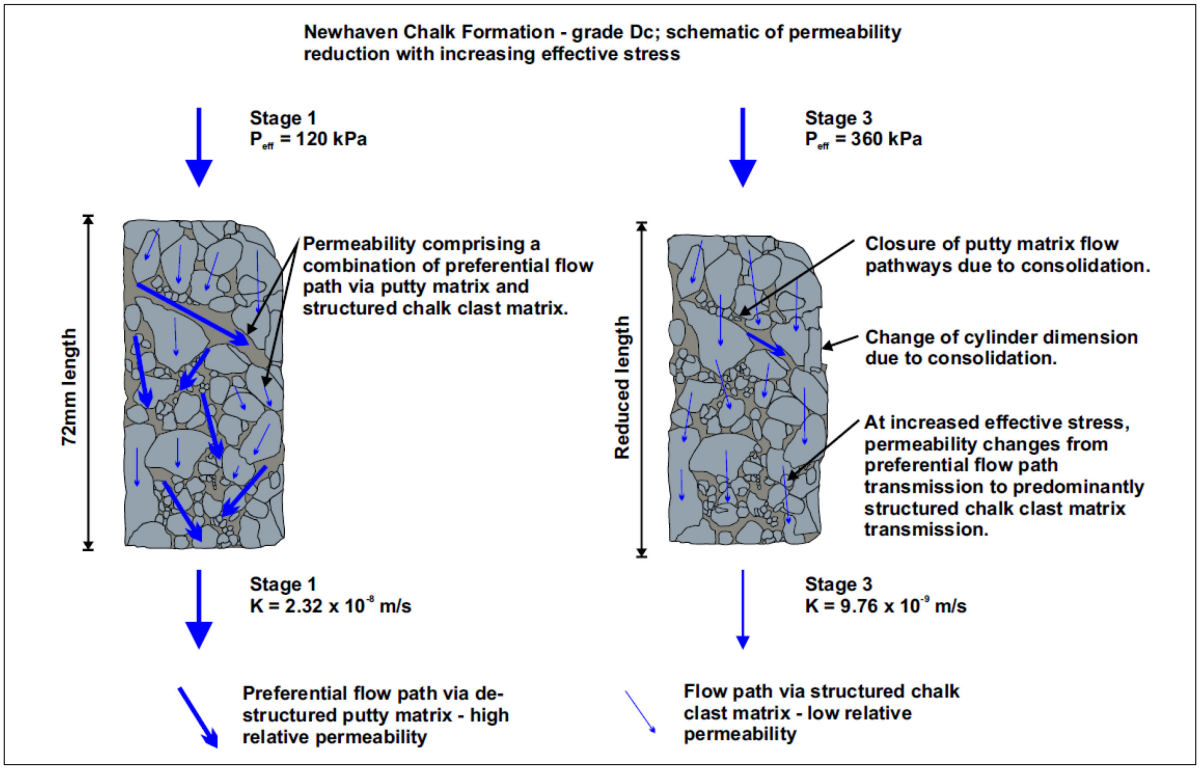


Figure 8-24 Schematic of permeability reduction with increasing effective stress (arrows with greater thickness indicate higher flow rate).

The distinct difference between Formations is postulated to be due to inherent parent material properties. Mider and Lawrence (2018) demonstrated that Seaford Chalk had higher permeabilities, at 2.4 0 x 10^{-8} m/s – 2.50 x 10^{-8} m/s, compared to Newhaven Chalk, at 1.07 x 10^{-8} m/s – 1.10 x 10^{-8} m/s, which supports this. The higher permeabilities associated with the Dm grades are interpreted to be due to a loss of pore networks due to de-structuration with flow being advective, while the lower permeabilities associated with the Dc grades are attributed to the increased presence of competent chalk clasts, which contain structured pore networks where flow is diffusive, as well as the constriction of putty matrix preferential pathways (Figure 8-24). The increase in effective stress, degree of consolidation and reduction of permeability in Dc samples, also supports Molyneux's hypothesis that with depth, the effects of the dilation of discontinuities (in this case, matrix filled conduits) is nullified and permeability becomes equivalent to a structured matrix.

8.5 Geomechanical properties of de-structured chalk

8.5.1 Unconfined compressive strength

15 samples of de-structured chalks were tested for UCS using a stiff testing frame (25 kN) (described in Chapter 5.4.9). Data was measured using axially mounted LVDT's with an accuracy of 5 µm, and recorded using TRIAX software.

Samples comprised seven Newhaven grade Dc, two Newhaven grade Dm and six Seaford Dc. The omission of Seaford grade Dm was due to the challenges of sampling this grade of Seaford Chalk in a field setting. Of these samples, two Newhaven Dc samples were tested at NMC, five Newhaven Dc samples were tested in a dry state, one Newhaven Dm sample was tested at NMC, one Newhaven Dm sample was tested completely dry, three Seaford Dc samples were tested at NMC, and three Seaford Dc samples were tested completely dry (Table 8-22).

Newhaven Dc has a UCS range of 0.18 – 0.59 MPa, and a mean UCS of 0.26 MPa, which has the lowest strength of all sample types tested. Newhaven Dm has a UCS range of 0.25 – 0.50 MPa and a mean strength of 0.37 MPa, which is the highest of all material types tested. Seaford Dc is the intermediate with a range of UCS values of 0.22 – 0.43 MPa, and a mean strength of 0.32 MPa (Table 8-22). These mean strength values however comprise both dry samples, and samples with a natural moisture content, which therefore require consideration. From initial observation, it is possible to state that both de-structured Seaford and Newhaven chalks have a much lower strength compared to that of structured chalks, with Lawrence et al. (2013) reporting values of 1.5 – 3.8 MPa for structured Newhaven Chalk, and 2.4 – 3.12 MPa for structured Seaford Chalk. Clayton and Matthews (1987) have previously reported strengths for dry chalk <32 MPa. The lower values of the D-grade chalks are likely due to the loss of cementation, de-structuration of chalk fabric and sedimentary nature of the chalk putty components.

For total Young's modulus, Seaford Dc ranges 8.75 – 243.90 MPa and has the highest mean of 118.39 MPa, while Newhaven Dc is observed to have a range of 14.89 – 19.86 MPa and the lowest, with a mean Young's modulus of 17.38 MPa. Young's modulus was not calculated for Newhaven Dm. (Table 8-22). Young's modulus for structured chalk has been established to vary as a function of induced stresses in structured chalks, with Bell reporting a mean Youngs modulus of 5.7 MPa, with a range of 3.9 – 8.3 MPa (Bell et al. 1999). This is likely to be similar for de-structured chalks given that de-structured chalk is metastable and a composite material of chalk putty and clasts, and therefore would have a wide variability in terms of range. Poisson's ratio could not be calculated due to instrument error.

Table 8-22 UCS of D-grade Seaford and Newhaven chalk.

Sample name	Formation	Grade	UCS (MPa)	Youngs modulus (MPa)	MC at test (%)	IDD (Mg/m³)	Dimension ratio
NewhavenDcUCS_19032023A	Newhaven Chalk Formation	Dc	0.29	141.83	Dry	1.93	2.01
NewhavenDcUCS_19032023 [NCDC6]	Newhaven Chalk Formation	Dc	0.25	153.09	Dry	1.70	1.99
NewhavenDcUCS_14032023	Newhaven Chalk Formation	Dc	0.26	67.13	Dry	1.47	2.01
NewhavenDcUCS_15102022	Newhaven Chalk Formation	Dc	0.59	98.01	Dry	1.44	1.99
NewhavenDcUCS_19032023A	Newhaven Chalk Formation	Dm	0.24	107.98	Dry	1.18	2.04
NewhavenDcUCS_04042023A	Newhaven Chalk Formation	Dc	0.32	14.89	23.29	2.07	2.01
NewhavenDcUCS_22032023	Newhaven Chalk Formation	Dc	0.18	19.86	26.31	1.68	2.02
NewhavenDmUCS_15102022	Newhaven Chalk Formation	Dm	0.50	-	Dry	1.57	1.98
NewhavenDmUCS_31102022	Newhaven Chalk Formation	Dm	0.25	-	23.09	1.40	2.05
SeafordDcUCS_14032023	Seaford Chalk Formation	Dc	0.26	217.32	Dry	1.57	2.01
SeafordDcUCS_01032023	Seaford Chalk Formation	Dc	0.43	243.90	Dry	1.57	1.98
SeafordDcUCS_16102022	Seaford Chalk Formation	Dc	0.22	99.63	Dry	1.42	1.98
SeafordDcUCS_04042023	Seaford Chalk Formation	Dc	0.30	8.75	22.62	1.80	2.03
SeafordDcUCS_22032023	Seaford Chalk Formation	Dc	0.33	73.91	26.74	1.43	2.03
SeafordDcUCS_26102022	Seaford Chalk Formation	Dc	0.38	66.8	19.47	1.66	2.01

By splitting down the samples by moisture content (Table 8-23), it is possible to observe dry Newhaven Dc having a UCS of 0.33 MPa, while Newhaven Dc with a NMC content has a mean UCS of 0.25 MPa, Dry Newhaven Dm has a mean UCS of 0.50 MPa, while Newhaven Dm with NMC has a UCS of 0.25 MPa. Dry Seaford Dc has a mean UCS of 0.46 MPa, while Seaford Dc with NMC has a mean UCS of 0.34 MPa.

Table 8-23 UCS of de-structured Newhaven and Seaford chalks; dry and NMC.

Material type and MC state	**Number of samples**	**UCS range (MPa)**	**Mean UCS (MPa)**	**Young's modulus range (e)**	**Mean Young's modulus (e)**
Newhaven Dc NMC	5	0.18 – 0.32	0.25	14.89 – 19.86	17.38
Newhaven Dc dry	2	0.26 – 0.29	0.27	67.13 – 153.09	113.60
Newhaven Dm NMC	1	0.25	0.25	-	-
Newhaven Dm dry	1	0.24 – 0.50	0.40	-	-
Seaford Dc NMC	3	0.30 – 0.38	0.34	8.75 – 73.91	41.33
Seaford Dc dry	3	0.22 – 0.43	0.30	99.63 – 243.90	186.95

Figures 8-25 and 8-26 shows the results presented in Table 8-22 graphically. Figure 8-25 shows axial stress versus axial strain for nine dried samples in total, comprising five Newhaven Dc, one Newhaven Dm and three Seaford Dc chalk samples.

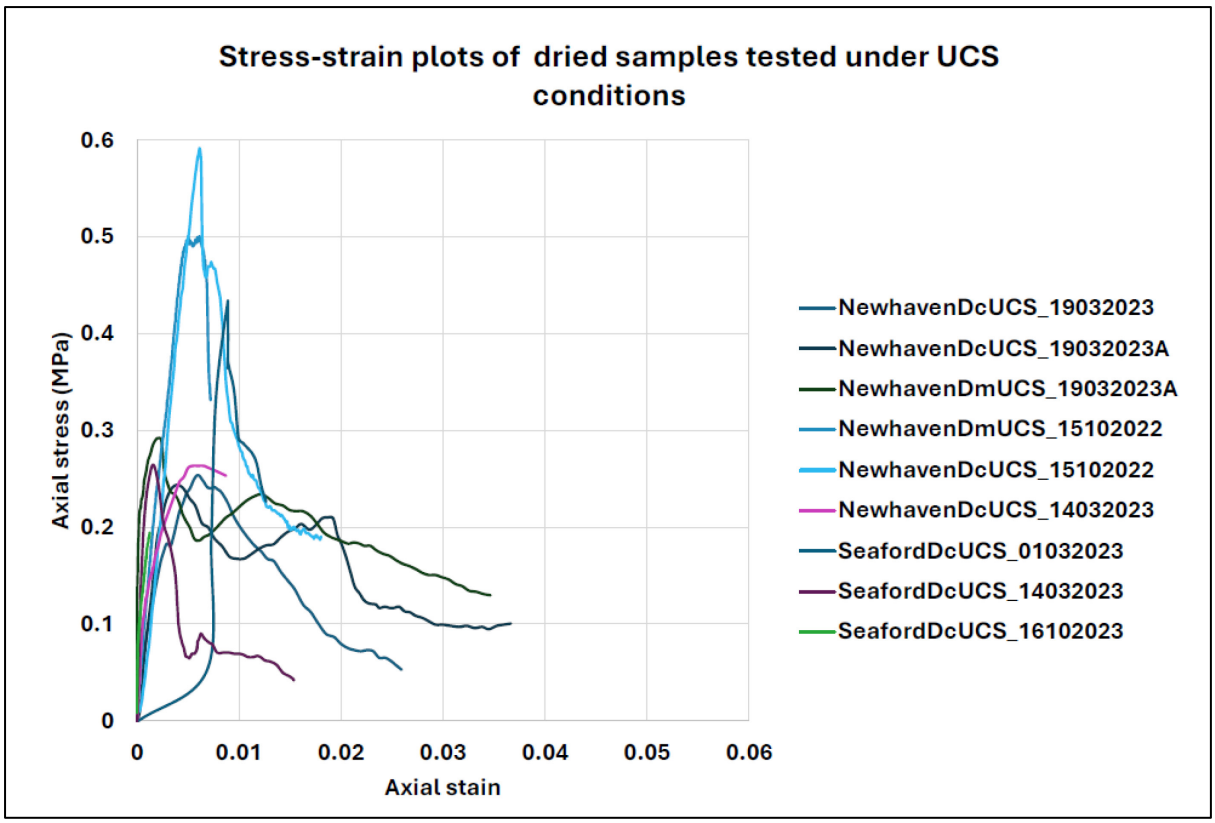


Figure 8-25 Stress-strain plots of dried samples tested under UCS conditions.

Figure 8-26 shows axial stress versus axial strain for six samples at natural moisture content in total, comprising two Newhaven Dc, one Newhaven Dm and three Seaford Dc chalk samples.

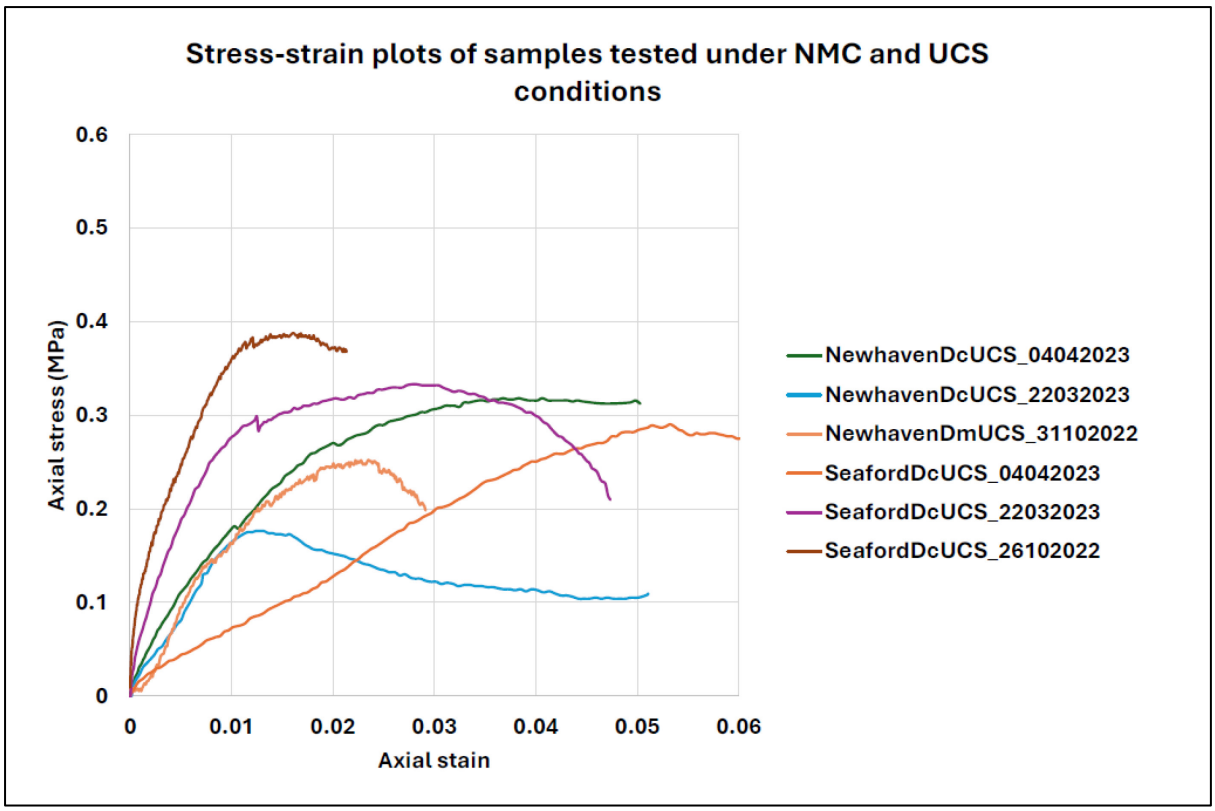


Figure 8-26 Stress-strain plots of samples tested under NMC and UCS conditions.

When stress-strain curves are plotted, it is possible to observe that dry samples are stronger than samples with NMC, and that the modes of failure differ. Samples which are dry have relatively high stress-low strain elastic phases and a defined yield point, while samples tested with natural moisture content have relatively long, shallow elastic phases, indicative of increasing plastic strain. The jaggedness of each of the curves is speculated to be due to the heterogeneous composition of clasts and matrix within each sample, whereby localised failure of individual clasts surrounded by matrix results in undulations within the curve. This is also speculated to similarly affect residual strength in dry samples (Figures 8-25 and 8-26).

The two curve types observed indicate that there are differences between dried samples and those with a natural moisture content. Owing to the limited number of samples, it was not possible to accurately correlate mode of failure with moisture content, demonstrating that our knowledge of the engineering behaviour of de-structured chalk is incomplete, and that further study is required.

It was expected that dry samples would have higher mean UCS values compared to those with a NMC because of water weakening, whilst this is the case for both the Dm and Dc Newhaven Chalks, the Dc Seaford Chalks' strength increases when tested when under NMC conditions compared to dry. Seaford

Dc (NMC) has a greater UCS compared to Newhaven Dc (both dry and natural moisture content) and Newhaven Dm (NMC).

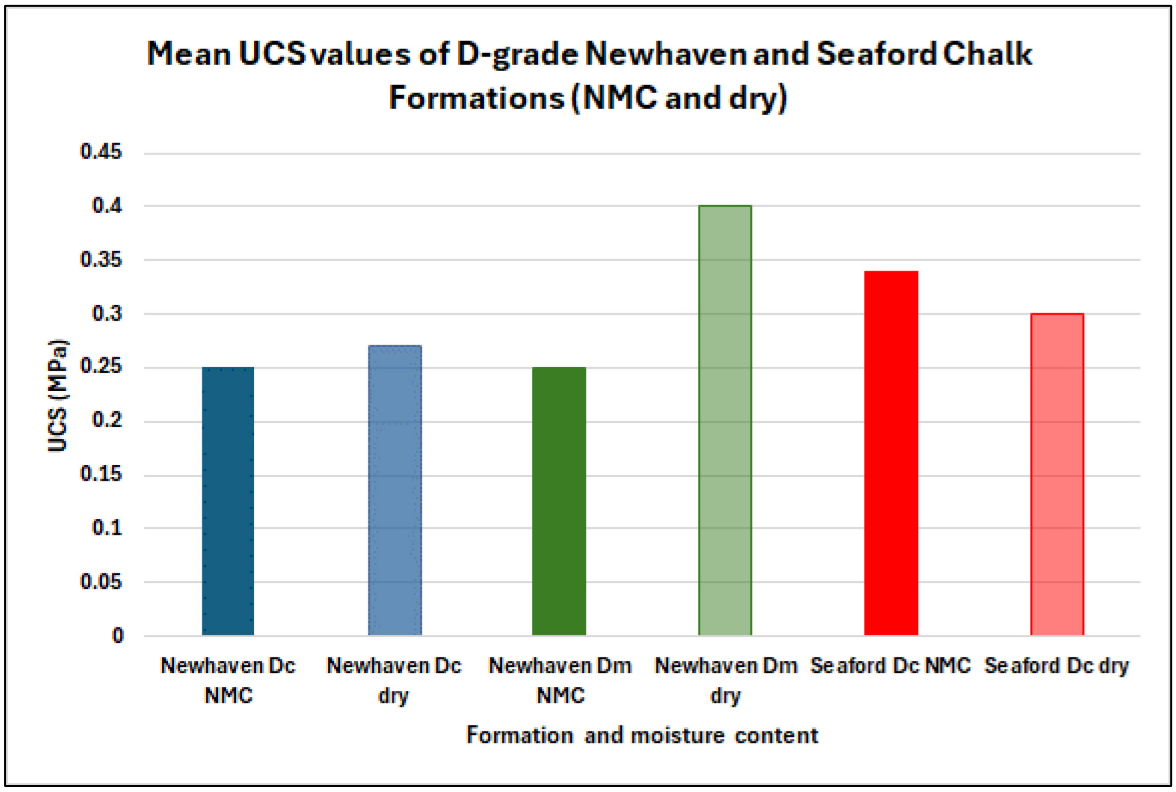


Figure 8-27 Mean UCS of D-grade Newhaven and Seaford Chalk.

Figure 8-27 shows that dry Dm grade Newhaven chalk has the highest UCS, with Newhaven Dm at NMC being equal to Newhaven Dc at NMC. Dry Newhaven Dc is higher relative to the two Newhaven grades at NMC. Conversely, Seaford Dm NMC has a higher UCS relative to dry Seaford Dc.

When compared to structured chalk (Figure 8-28), it is possible to observe that laboratory derived UCS values for de-structured values were all significantly lower. D-grade Seaford chalk is approximately 12 times lower than structured Seaford Chalk in terms of UCS and D-grade Newhaven Chalk is approximately 11 times lower than its structured counterpart.

When compared against SilverSchmidt derived UCS values, UCS values derived within a laboratory setting are lower. The discrepancies of UCS values between lab tested UCS for structured chalk and SilverSchmidt derived UCS for structured chalk are likely due to the SilverSchmidt not being calibrated for the material tested (Figure 8-28).

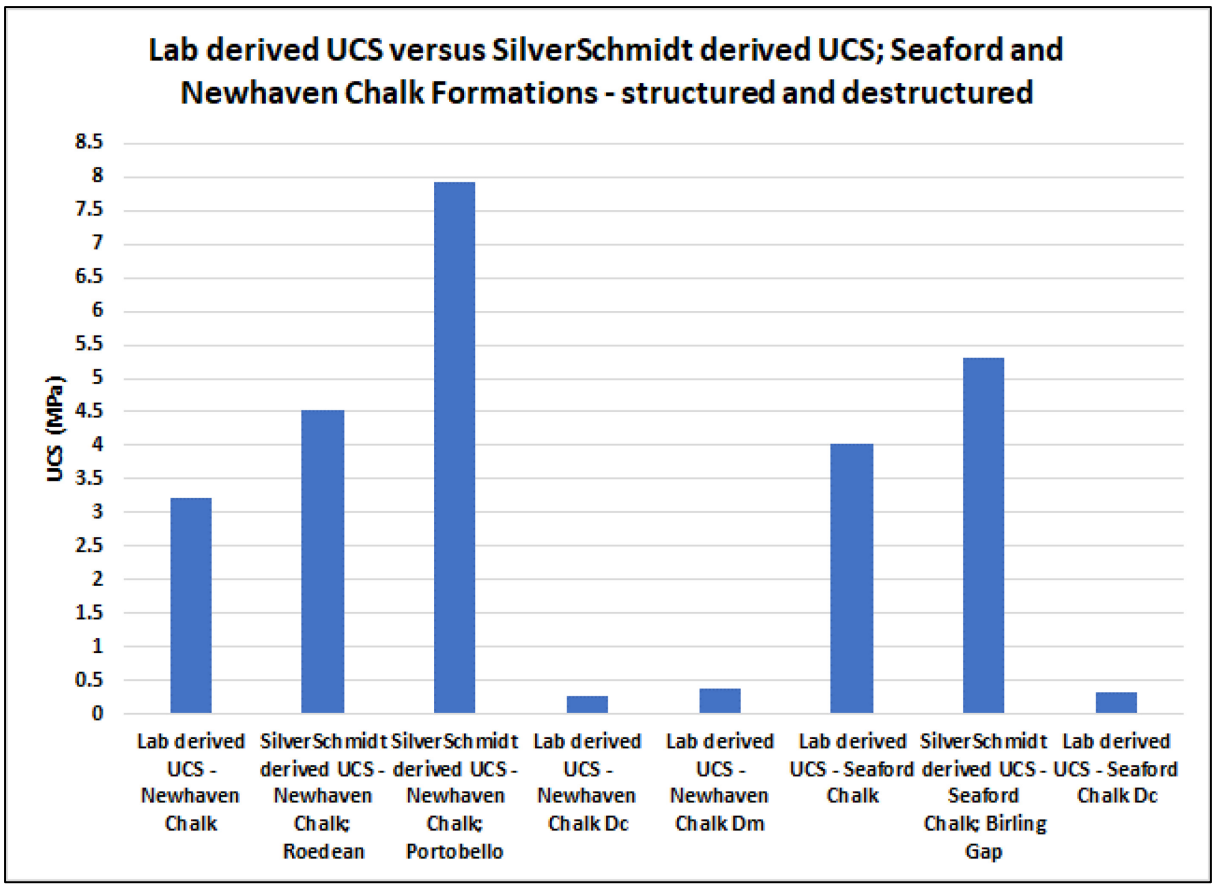


Figure 8-28 Lab derived UCS versus SilverSchmidt derived UCS (Structured chalk data taken from Lawrence et al. (2013)).

The UCS test induces a shear failure mechanism in samples under test conditions. During testing, the Dm and Dc chalk samples were observed to fail initially through matrix-clast interaction, with deformation beginning within the matrix, with the putty matrix offering less resistance to shear compared to the clasts. Cracking of the matrix in dried samples was observed, with failure occurring on matrix-clast interfaces. As the load and shear stress increases, the cores were observed to spall, with brittle failure occurring in dry samples (Figure 8-25) and ductile, plastic failure observed in samples with a higher moisture content (Figure 8-26). In samples with natural moisture content, clast rotation was observed with increased shear. In both dry samples and those with NMC, grain crushing was not observed, however, fractures were observed to propagate vertically through the clasts.

The differing failure modes are attributed to the heterogeneous fabric of the samples, comprising a matrix and a clast component – in terms of texture, these samples are similar to that of a breccia or a conglomerate. The matrix-clast interaction and failure occurring initially in the matrix indicates that the matrix is weaker than the clasts (as reported by Clayton, detailed within Chapter 2; friction angles of 31 - 33° and apparent cohesion values of 0 – 30 kPa), leading to differential stress distribution within the sample and localised shear distribution. This is supported by failures observed at matrix-clast interfaces, indicating localised increased stress at these surfaces. In samples with NMC, plastic strain

is observed and is reflected in ductile failure, whereby clasts are observed to rotate and preferentially align in response to shear.

When comparing the UCS of dry samples against those with natural moisture content, it must be noted that there are nine tests for dry material against six tests for material at a natural moisture content. Furthermore, when broken down by formation and CIRIA grade, there are three dry Newhaven dc against two Newhaven Dc at NMC, two dry Newhaven Dm against one Newhaven Dm at NMC and three dry Seaford Dc against three Seaford Dc at NMC. The implications of these limited numbers of samples are that (i) the data presented suggests behavioural differences between dry samples and those at NMC but as a data set are limited in size and (ii) the number of samples at NMC are limited compared to dry samples, therefore could not be considered wholly representative. To address these discrepancies and further build knowledge of these materials, it would be recommended that further UCS testing is undertaken.

In terms of accuracy, the LVDT's used are limited to an accuracy of 5 µm (due to the calibration equipment), which allows a measurement of up to two significant figures. Owing to the heterogeneous composition of cores tested (i.e., clasts and matrix), and subsequent differential distribution of stress, the UCS results obtained are unlikely to be a true reflection of compressive stress within de-structured chalks, and further testing would be required to build a statistically significant dataset.

8.5.2 Brazilian tensile strength of D-grade chalk

A total of 12 Brazilian tensile tests were undertaken to characterise the tensile strength of Seaford and Newhaven chalks graded Dc and Dm. Three samples of each grade and chalk were tested, with one test undertaken at normal moisture content, and two tests dry, to establish the effects of moisture content on tensile strength. Data is summarised in Table 8-24. A methodology for this test is presented in Section 5.6.

Samples of Newhaven Dm ranged 0.041 – 0.057 MPa, with the NMC sample yielding the lowest tensile strength of 0.041 MPa. Newhaven Dc samples ranged 0.058 – 0.09 MPa, with the NMC sample having an intermediate tensile strength of 0.1 MPa. Seaford Dm tensile strengths ranged 0.044 – 0.058 MPa, with the NMC value corresponding to a strength value of 0.052 MPa. Seaford Dc tensile strengths ranged 0.044 – 0.314 MPa, with the NMC corresponding to an intermediate strength value of 0.053 MPa.

Table 8-24 Tensile strength of de-structured Newhaven and Seaford chalk.

Sample	Moisture content (%)	Diameter D (mm)	Thickness t (mm)	t/D ratio	Rate of displacement (mm/min)	Time to failure (s)	Maximum Load (N)	Tensile strength (MPa)	Failure mode
Newhaven grade Dm - Sample 1	19.00	37.48	14.99	0.40	0.51	22	36.16	0.041	Tensile
Newhaven grade Dm - Sample 2	0.0	37.56	8.92	0.24	0.51	10	27.13	0.052	Tensile – punching
Newhaven grade Dm - Sample 3	0.0	37.54	10.72	0.29	0.51	8	36.16	0.057	Clast/putty interface
Seaford grade Dm - Sample 1	24.36	37.61	17.28	0.46	0.51	16	59.39	0.058	Tensile
Seaford grade Dm - Sample 2	0.0	37.63	16.53	0.44	0.51	42	54.22	0.056	Punching shear
Seaford grade Dm - Sample 3	0.0	37.44	16.39	0.44	0.51	24	42.61	0.044	Tensile
Seaford grade Dc - Sample 1	21.54	38.30	15.09	0.39	0.51	14	47.79	0.053	Tensile
Seaford grade Dc - Sample 2	0.0	37.95	12.28	0.32	0.51	62	229.78	0.314	Non-conforming
Seaford grade Dc - Sample 3	0.0	37.38	11.54	0.31	0.51	6	29.70	0.044	Tensile
Newhaven grade Dc - Sample 1	20.92	37.47	16.95	0.45	0.51	20	99.4	0.100	Non-conforming
Newhaven grade Dc - Sample 2	0.0	36.93	14.10	0.38	0.51	16	73.59	0.090	Tensile
Newhaven grade Dc - Sample 3	0.0	37.68	14.19	0.38	0.51	14	89.07	0.106	Non-conforming

In terms of failure modes, all samples failed in a tensile mode except for Newhaven Dm sample 3, Seaford Dm sample 2, Seaford Dc sample 2 and Newhaven Dc samples 1 and 3, which demonstrated punching shear failure and failure along clast puttied matrix interface, with larger clasts influencing failure within the discs (Figure 8-29).

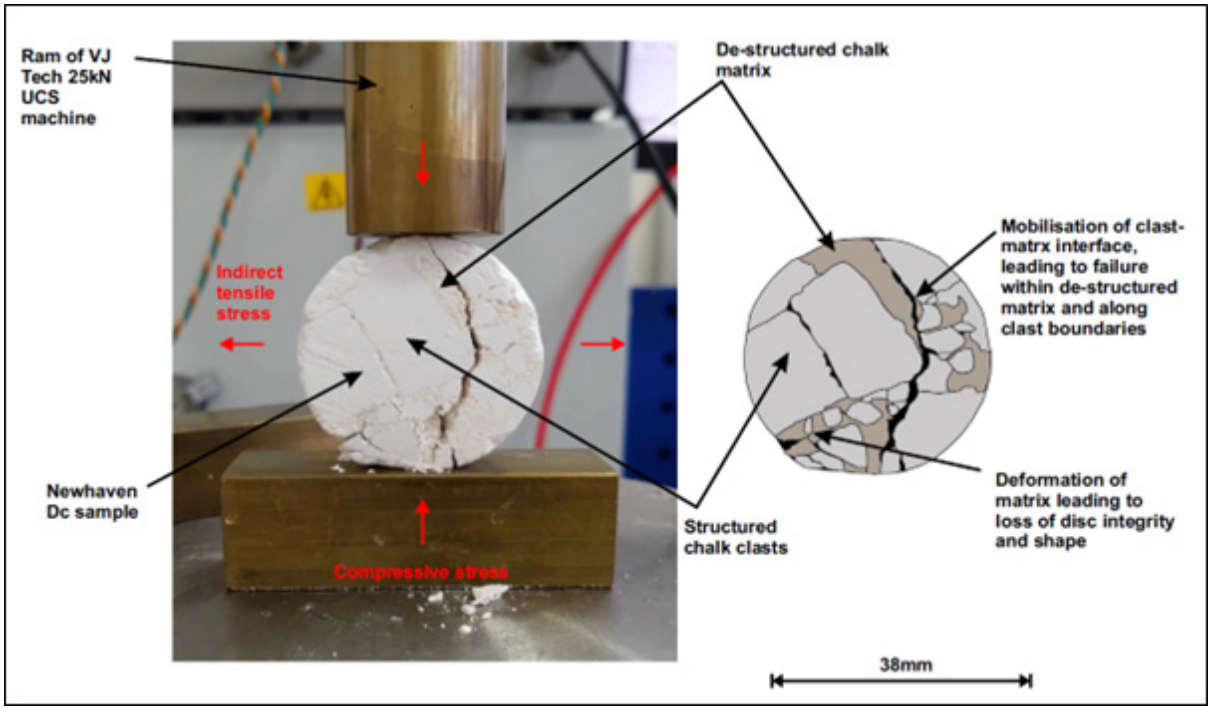


Figure 8-29 Tensile test of Newhaven Dc.

Figure 8-29 shows the failure pattern of a disk of Newhaven Dc at 0% moisture content. Failure has occurred via matrix mobilisation and along the clast/matrix interface, with some deformation of localised areas of matrix. During this test, microfracturing of clasts was not observed, however clast alignment did change owing to damage to the matrix.

Figure 8-30 presents a comparison of tensile strengths of structured Seaford and Newhaven chalk taken from literature (Lord et al. 2002, Marley, 2020, Lau, 2018, Mider and Lawrence, 2018), against de-structured Seaford and Newhaven Chalks tested during this study.

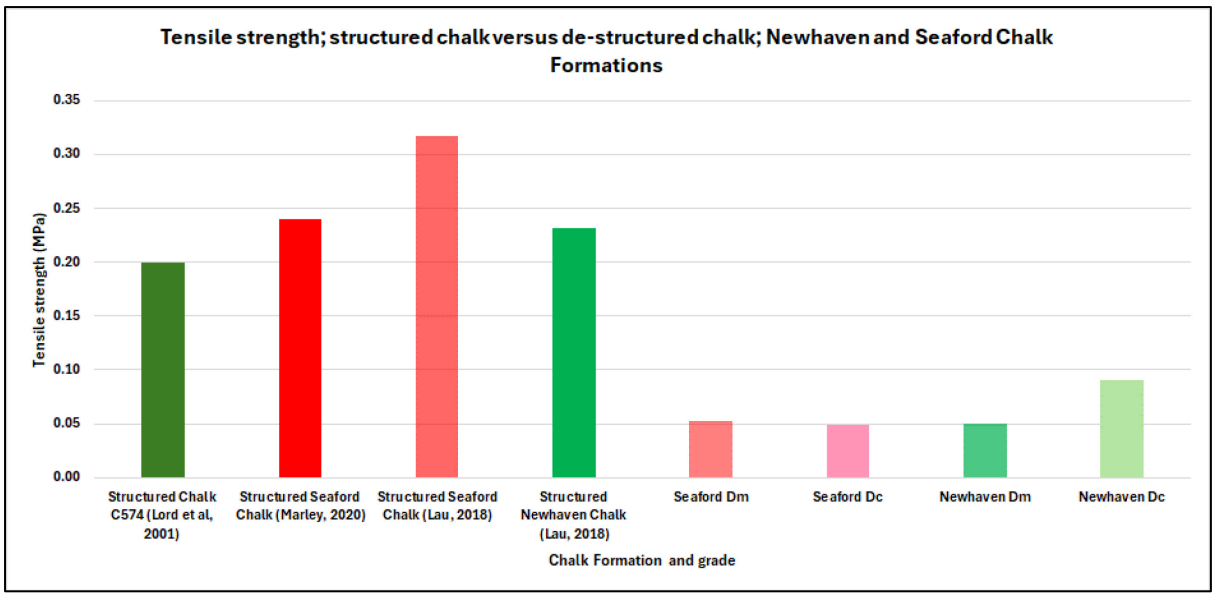


Figure 8-30 tensile strength; structured chalk versus de-structured chalk, Newhaven and Seaford Chalk Formations (Structured chalk data taken from (Lord et al. 2002, Marley, 2020, Lau, 2018, Mider and Lawrence, 2018)).

Figure 8-30 shows that all de-structured chalks have lower tensile strengths than their structured counterparts, with Seaford Dm and Dc being 4 – 4.6 times lower than structured Seaford Chalk. Newhaven Dc is 2 – 2.5 times lower than structured Newhaven, and Newhaven Dm is lower still at 4 – 4.6 times lower. This demonstrates the effects of weathering on chalk strength and de-structured chalk material properties overall.

Table 8-25 shows a comparison of D-grade UCS values against D-grade tensile strengths.

Table 8-25 UCS versus tensile strength; de-structured Newhaven and Seaford chalk.

Formation	Mean UCS (MPa)	Mean tensile strength (MPa)
Seaford Dc	0.32	0.14
Seaford Dm	Not tested	-
Newhaven Dc	0.26	0.05
Newhaven Dm	0.33	0.1

From this comparison it is possible to observe that the tensile strength of Seaford Dc is 2.3 time less than the corresponding UCS. Seaford Dm was not tested for UCS due to sampling challenges. The tensile strength of Newhaven Dc is 5.2 times lower than the corresponding UCS, and Newhaven Dm is 3.3 times lower than the corresponding UCS of the same material type. This follows similar trends to the ratio of UCS to tensile strength in structured chalk These strength differences have implications when considering degradation, particularly due to water saturation, with already lower strength D-grade deposits being subject to further weakening, owing to water weakening effects and higher SMC potential.

8.5.3 Triaxial strength testing of D-grade chalk

Triaxial testing of weathered chalk was undertaken as part of an MSc study by Maclean (2023), supervised by the author of this thesis, as part of supplementary work to this PhD (described in Chapter 5.7). Previous triaxial testing of D-grade chalk has not been undertaken, which allows for a degree of novelty for both the MSc and this PhD. Four samples of weathered Newhaven Chalk and one sample of weathered Seaford Chalk were undertaken to evaluate whether this material acted as a very weak rock or a highly stiff soil depending upon the degree of de-structuration due to weathering. one sample of Newhaven Chalk (WNC3) was discounted due to instrumentation error (Table 8-26).

Table 8-26 Triaxial test schedule of de-structured Newhaven and Seaford chalk.

Sample	**Formation**	**Strain rate (% /day)**	**Maximum strain (%)**	**Comments**
WNC1	Newhaven	5	23	Load cell fluctuation after 15%
WNC2	Newhaven	5	17.5	Load cell fluctuation after 14%
WNC3	Newhaven	1	4	Test aborted
WNC4	Newhaven	50	25	Test complete
WSC1	Seaford	5	20	Test complete

The test comprises three stages; saturation, consolidation and shearing. This section will focus on the shearing, within the context of the strength and material properties. All samples were saturated to an average B-value of 0.93, and all samples were consolidated to an effective stress of 50 kPa, with a back pressure of 500 kPa and a cell pressure of 550 kPa. This was achieved at a rate of 50 kPa/hr.

8.5.4 Mohr-Coloumb parameters

Each of the four tests show different behaviour in terms of material response to shearing. Figure 8-31 (A) shows deviatoric stress versus axial strain for de-structured Newhaven chalk WNC1. In terms of response, the load peaks at 250 – 270 kPa at an axial strain of 2.5 – 3.0%. After this point, deviatoric stress decreases as axial strain increases. Initial deformation is apparently elastic, with further elastic behaviour post-peak.

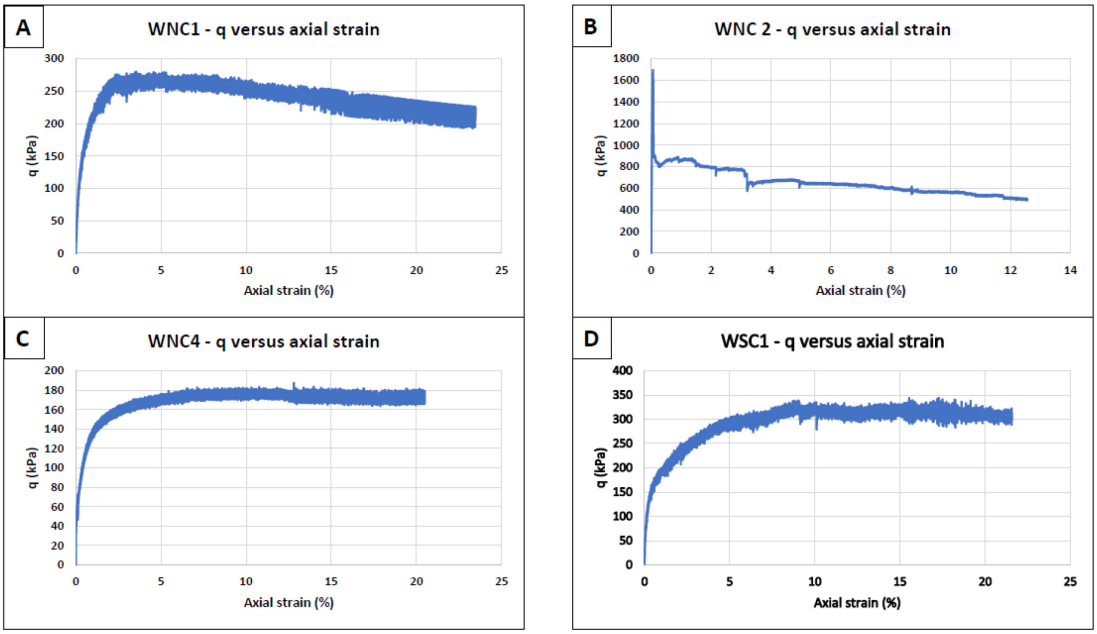


Figure 8-31 Deviatoric stress versus axial strain plots for WNC1 (A), WNC2 (B), WNC4 (C) and WSC1 (D).

Figure 8-31 (B) shows deviatoric stress against axial strain for WNC2. Deviatoric stress peaks at 1669 kPa at <1% axial strain, then sharply falls to values between 800 – 900 kPa. At this point, the deviatoric stress reduces as axial strain increases, which would be reflective of a brittle failure mode, indicating that unlike WNC1, this material is behaving more like an intact chalk sample. In post peak deformation, the sample appears to reduce in residual strength, indicative of apparent work-softening of the material.

Figure 8-31 (C) shows deviatoric stress versus axial strain for WNC4. Deviatoric stress peaks at 160 – 180 KPa with a relatively high, axial strain of 7 – 7.5%, when compared to the previous two tests. The post peak deviatoric stress is maintained at approximately 160 – 180 kPa as axial strain increases. While this behaviour is reflective of a clay or a sand, the deviatoric stress values are lower than those observed in tests WNC1 and WNC2. Even with differences in strength, this sample behaves in a similar fashion as WNC1. While strain softening can occur within rocks, given the relatively low confining pressures and observation of the material fabric, it is likely that this strain softening behaviour is indicative of a soil, rather than intact chalk.

Deviatoric stress versus axial strain for Seaford chalk (WSC1) are presented in Figure 8-31 (D). Deviatoric stress peaks later than the Newhaven samples at 8 – 9% axial strain, at a value of 300 kPa. At approximately 17% axial strain, deviatoric stress begins to drop. This behaviour is reflective again of a soil, and compared to Newhaven, this sample has greater deviatoric stress peaks than WNC 1 and WNC4 but not for WNC2.

Structured Seaford chalk was compared against the weathered samples, demonstrating the significantly lower values of deviatoric stress for de-structured grade chalk. Figure 8-32 shows deviatoric stress against axial strain for structured, intact chalk, with peak deviatoric stresses of up to 2300 kPa at less than 0.2% axial strain. Similarly, work presented by Vinck et al. (2018) demonstrated deviatoric stress peaks <3000 kPa over 10% axial strain for structured chalks.

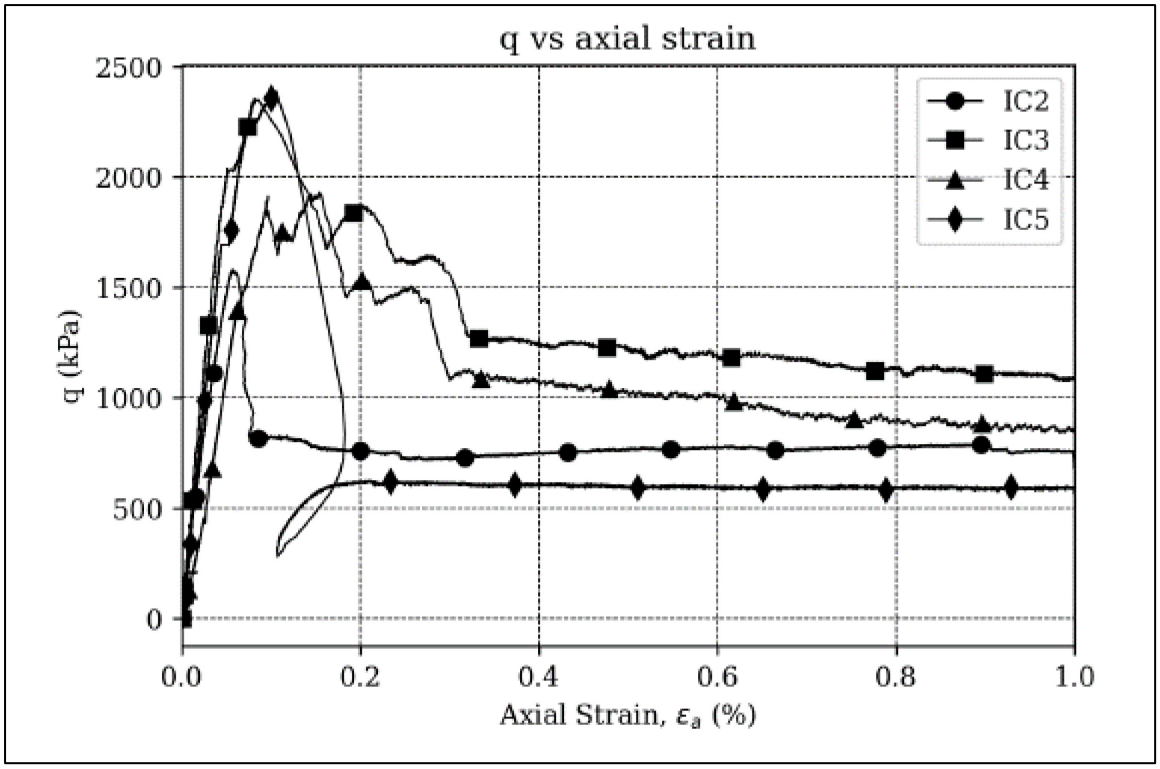


Figure 8-32 Deviatoric stress versus axial strain of structured chalk by Maclean (2023).

The varying behaviours observed between the four weathered samples is likely due to varying grade within the chalk samples. After testing, The samples were dried and split to apply the modified Bushinsky technique described in Section 5.5. The laboratory classification of WNC1 and WSC1 were Dm grade chalk and behaved more like a soil, whilst WNC2 and WNC4 were classified as Dc grade chalk, however there was discrepancy between the behaviour of the two samples under shear. This grading would account for the peak observed in WNC2, with the sample interpreted to act more like a rock, although WNC4 behaved similar to that of WNC1 and WSC1. Figure 8-33 shows WNC4 and WSC1, photographs were not undertaken for WNC1 and WNC2.

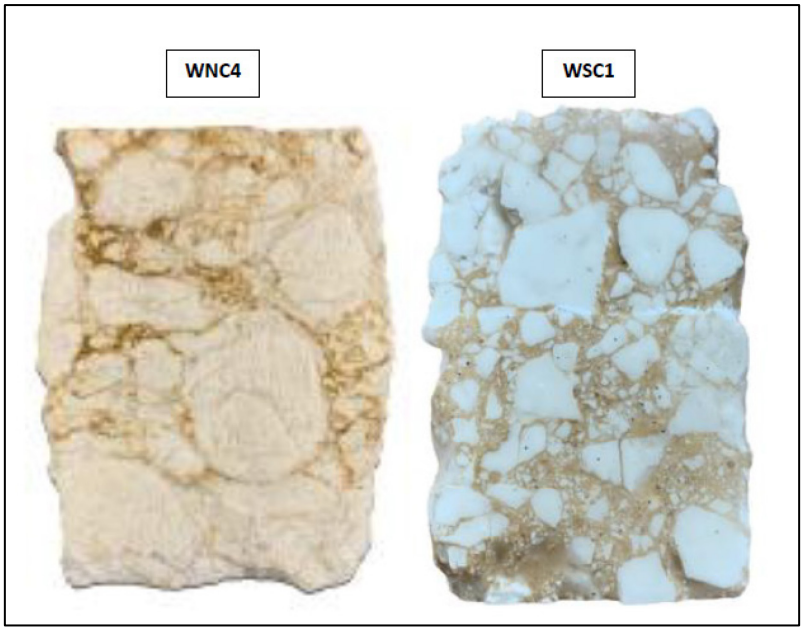


Figure 8-33 modified Bushinsky technique on Newhaven (WNC4) and Seaford Chalk (WSC1) after triaxial testing (Maclean, 2023).

By combining both the UCS data for Newhaven chalk and triaxial data, it was possible to undertake a principal stress analysis to calculate cohesion (c) and angle of friction (τ) using Mohr-Coloumb parameters (Table 8-27).

Table 8-27 Triaxial test results for de-structured Newhaven and Seaford chalk.

Test number	**Formation**	**Minor principal stress σ_3 (MPa)**	**Major principal stress σ_1 (MPa)**	**Effective stress (MPa)**	**Poisson's ratio (v)**	**Small strain Young's modulus (e) (MPa)**
UCS weathered NCF (average)	Newhaven	0	0.277	0.277	-	17.38
UCS weathered SCF (average)	Seaford	0	0.338	0.338	-	49.82
WNC1	Newhaven	0.55	0.710	0.160	0.39	90.93
WNC2	Newhaven	0.65	1.265	0.615	-	119.12
WNC3	Newhaven	0.55	0.643	0.093	-	336.65
WNC4	Newhaven	0.55	0.658	0.108	-	70.4
WSC1	Seaford	0.55	0.710	0.160	0.4	219.45

NB. All UCS tests for this analysis were at NMC.

Figure 8-34 shows Mohr circles of triaxial, UCS and tensile data with failure envelope, resulting in a cohesion value of 110 KPa and an angle of friction of 11 – 12 °.

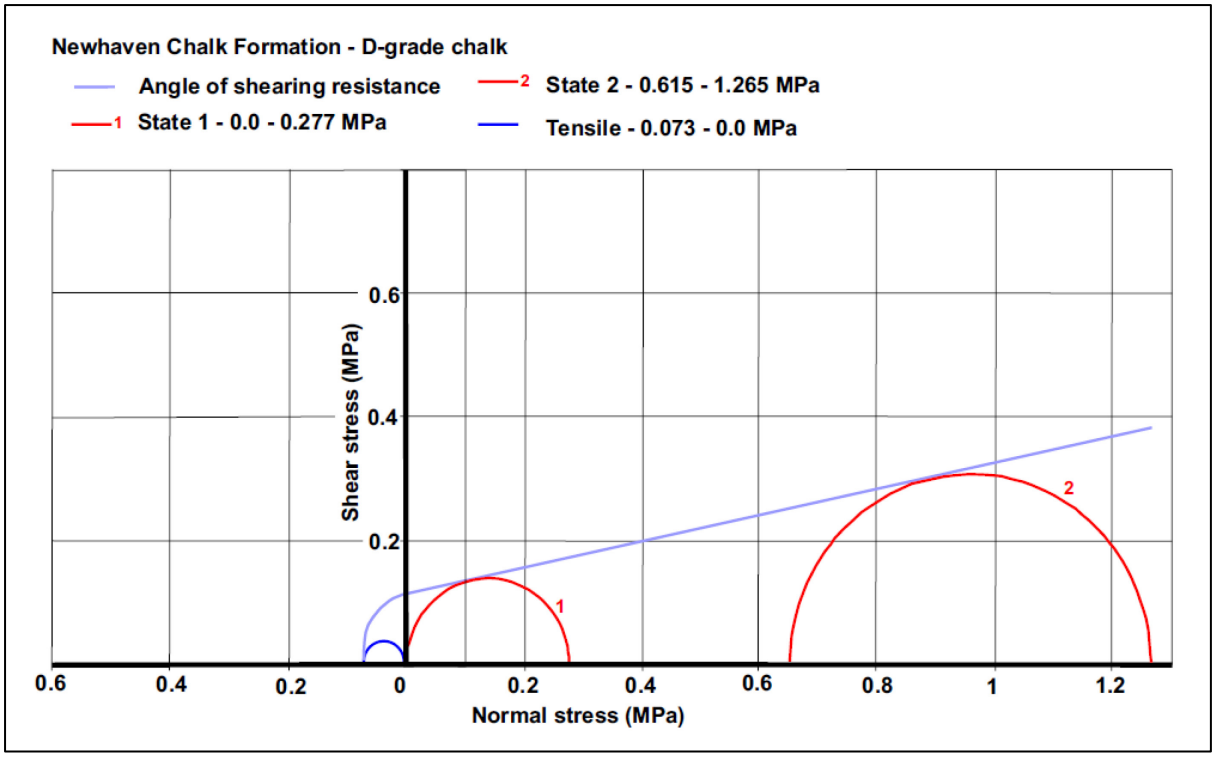


Figure 8-34 Mohr circle and failure envelope of de-structured Newhaven chalk.

These data are limited, and therefore this analysis is not definitive of both cohesion and angle of friction for weathered chalk. These measured values are significantly lower than values reported for intact chalk (detailed in Chapter 2), with cohesion values of 0.49 MPa and friction angles of 39.6 ° (reported by Vinck et al. 2018) and chalk putties, with cohesion values of 0 – 0.03 MPa (Spearing-Bundy, 2013) and friction values of 29 – 34 °, assuming a cohesion value of zero (tests by Clayton and Matthews (1987)). When cohesion was set at zero, and using WNC2, the angle of friction for weathered chalk increases to 18 °.

The WNC sample series were sampled from the same deposit, within 0.5 – 1.0 m distance of each other, which indicates the significant variability of de-structured chalk. The UCS results presented earlier in this chapter and the triaxial results suggest that currently it is difficult to differentiate between Dm and Dc grades in terms of material properties, and further work would be required in this area.

The failure modes of weathered chalk are significantly different to intact chalk. No brittle failure was observed but samples visibly spalled and bulged around the mid-point of the core. The degree of barrelling was uneven due to clasts mobilising within the matrix and being pushed out of position, with some rotation (identified by the modified Bushinsky technique). This implies that clast distribution controls the cylinder evenness and shape of the sample deformation, while the amount of matrix controls the material properties of the core and clast alignment, with matrix dominant

samples deforming more evenly, with little clast alignment (as demonstrated by WSC 1) (Figure 8-33). In terms of deformation, the Newhaven Chalk (WNC1) was calculated to have a Poisson's ratio of 0.39, while the Seaford Chalk (WSC1) was 0.40 (Table 8-27). Figure 8-35 shows a schematic of how a Dc sample is interpreted to consolidate and deform during triaxial testing.

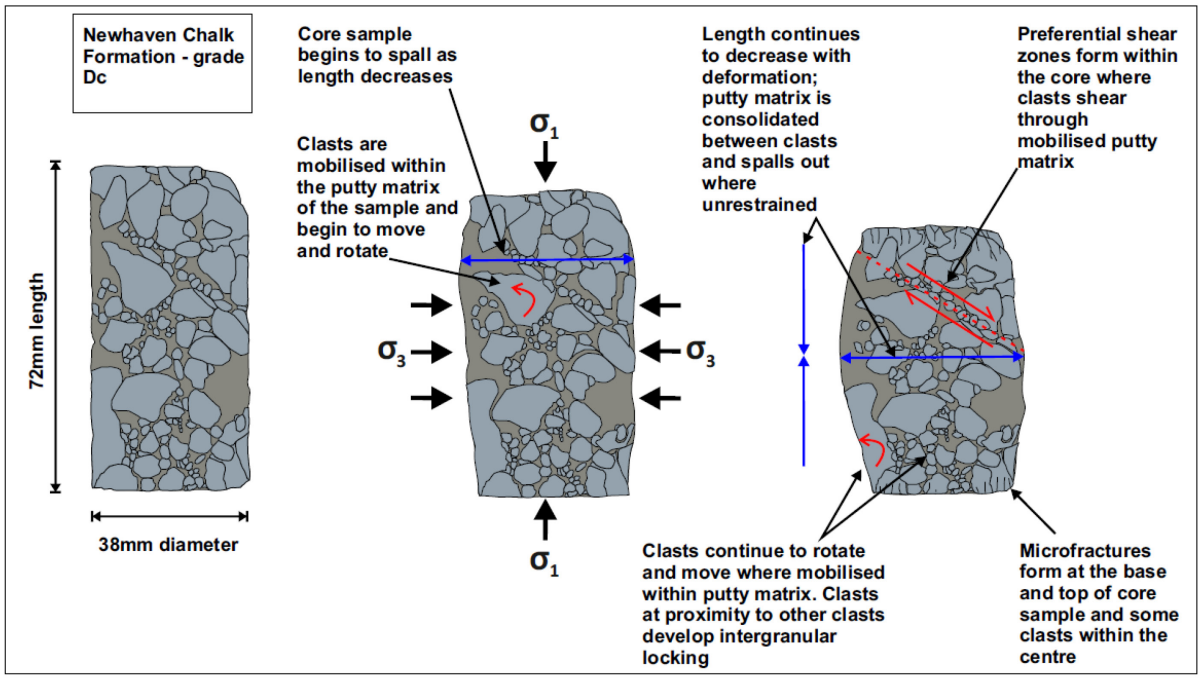


Figure 8-35 Schematic of consolidation and deformation of a D-grade chalk sample.

To summarise triaxial testing of weathered chalk, it is possible to state that D-grade chalk behaviour under triaxial conditions is different to that of intact chalk. D-grade chalks reach peak deviatoric stresses at <400 kPa, except for WNC2. This is likely due to the dominance of clasts in WNC2 (i.e., Dc grade) eliciting a similar response to that of intact chalk. Of the four tests, all except for WNC2 demonstrated linear elastic deformation with increasing axial strain, which is likely due to matrix dominance (i.e., Dm grade) in these samples and deformation mobilising the matrix.

Dm grade chalk appears to behave like a soil and Dc grade more like a rock, however, given the limited amount of data presented in this study, more testing would be required. Table 8-28 demonstrates the difference between structured and de-structured chalk and shows a comparison of structured Seaford and Newhaven chalk (sampled from Peacehaven) against D-grade Newhaven Chalk (sampled from the same locality).

Table 8-28 Mohr-Coloumb parameters (structured data taken from (Mortimore et al. 2004b).

	Structured Seaford Chalk	Structured Newhaven Chalk	D-grade Newhaven Chalk
Angle of friction (°)	28 (sat) – 34.5 (dry)	24 (sat) – 43.5 (dry)	10 – 11
Cohesion (kPa)	600 (sat) – 2600 (dry)	600 (sat) – 2400 (dry)	110

The D-grade Newhaven Chalk has a friction angle of 10 - 11 °, which is approximately 50% lower than that of saturated structured Newhaven chalk at 24° and approximately four times lower than dry at 43.5 °. D-grade Newhaven chalk cohesion is approximately five and a half times lower than that of saturated Newhaven and approximately 22 times lower than that of dry saturated Newhaven chalk.

8.6 SEM analysis

SEM analysis was undertaken to evaluate the effects of weathering on the microscale and to develop a texture map in aiding the identification of weathering types, however this proved to be ineffective. Full methodology and results can be found in Appendix H.

In terms of analysis, the following parameters were considered;

- Number of grains
- Dimensions of grains
- Binarisation and % of pore space to estimate porosity
- Identification of coccolith taxa
- Fabric description
- Contact description

While the use of SEM techniques was not suitable for elucidating weathering, it was possible to identify formational differences;

- Analysis of microstructure using SEM showed little in terms of weathering, however, it was possible to observe differences between each chalk formation.

- Porosity was estimated for all formations, with the Seaford Chalk having a porosity of 29.77% and the Newhaven Chalk having a porosity of 28.70%.

- Identification of coccolith taxa was possible in samples where preservation was exceptional.

Further SEM analysis could be of merit, with further quantification of other aspects of the chalk, such as grain contacts, degree and type of cementation and tortuosity allowing characterisation. This would be of benefit when evaluating de-structured chalk counterparts, where there is a matrix component and a clast component.

Tortuosity characterisation could be applied to both the pore space within the matrix component on the coccolith scale as well as the areas of de-structured matrix within Dm and Dc samples, which are anticipated to have a different permeability and porosity compared to the structured clast components. Owing to the complexity of D-grade chalk, an analysis of microstructure and macrostructure of matrix would be required, whereby void space between coccoliths and matrix was measured in terms of tortuosity, as well as the void space between larger clasts (i.e., the matrix component) as both would have significant effect on the transmission of fluid through a D-grade chalk. Such a study would be considered beyond the remit of this thesis, but could / should be considered as future work in characterising D-grade material.

Chalk samples taken from areas where weathering through chemical disequilibrium and karstification could benefit from analysis using X-ray dispersive spectroscopy, whereby it may be possible to identify the species of chemical agents resulting in weathering.

8.7 Chapter summary

In this chapter, a range on methods have been used to establish some field and laboratory contrasts between structured and de-structured chalk. In addition, the work has compared results to establish the most effective means of quantifying de-structured chalk. Lastly the work has quantified the degree of weathering, especially in relation to the CIRIA Dm and Dc grading system.

Key outcomes include;

Index testing, the results of which are novel in that index testing of D-grade chalk deposits have never been quantified comprehensively or in such depth;

IDD

- Seaford Dm has an IDD of 1.56 mg/m^3, Seaford Dc has an IDD of 1.54 Mg/m^3, Newhaven Dm has an IDD of 1.50 Mg/m^3, while Newhaven Dc has an IDD of 1.56 Mg/m^3.
- The mean CIRIA density grade is observed to be one grade lower in de-structured chalk than in structured chalk. The differences between weathering grade were inconclusive and minor.
- Laboratory densities of structured chalk are consistently higher than densities measured with the Equotip Leeb in a field setting, however, in grade Dc Seaford Chalk, laboratory densities were lower than those obtained using the Equotip.

Moisture content

- Except for chalks sampled at Telscombe Cliffs, D-grade chalks are not close to saturation like their structured parent material. This is novel as this has never been established previously.
- The NMC of Seaford Dc was 25.0%, while Seaford Dm had an NMC of 24.36%. Newhaven Dc had an NMC of 24.57% and Newhaven Dm had an NMC of 25.48%.
- SMC for Seaford Dc was 27.60%, Seaford Dm was 29.20%, while Newhaven Dc was 27.84% and Newhaven Dm was 27.08%.
- When moisture content is plotted against IDD, D-grade chalks fall into the low-medium CIRIA classification.
- D-grade chalks have higher SMC values compared to structured chalks, but comparably lower NMC values. SMC values for D-grade chalks are 1 – 1.15 times higher than NMC values.

Voids ratio and porosity

- Values for both voids ratio and porosity were significantly higher for de-structured chalk compared to structured, and due to their dual property nature (and subsequent heterogeneity), cannot be relied upon.

- Newhaven Dc chalk has a voids ratio of 0.749, with a range of 0.611 – 0.895. Newhaven Chalk. Newhaven grade Dm is greater than Dc, with a voids ratio of 0.788, with a range of 0.613 – 0.911. Seaford Dm has a voids ratio of 0.751 and a range of 0.636 – 0.886, while Seaford Dm has a larger voids ratio of 0.731 and a range of 0.719 – 0.749.
- Newhaven grade Dm has a calculated porosity of 43.99%, with a range of 37.99 – 47.68%, Newhaven Dc has a porosity of 42.72% and a range of 37.91 – 47.22%. Seaford Dc has a porosity of 42.83%, with a range of 38.88 – 46.98%, Seaford Dm has a porosity of 42.23%, with a range of 41.82 – 42.81%.

Water weakening of D-grade chalk

- D grade chalk collapses upon itself and forms debris flows when immersed in water within 30 seconds. The rate of collapse was observed to decrease when water was substituted for ethylene glycol, suggesting a water weakening effect.

Particle size distribution

- D-grade chalks tested showed that D-grade Newhaven comprised 40% particles <625 µm and 60% particles >625 µm, while D-grade Seaford chalk comprised 35% particles <625 µm and 65% particles >625 µm, leading to a classification of a well-graded soil.

Modified Bushinsky technique

- This technique is novel in that it allowed the 2-D quantification of the internal structure of a D-grade chalk, leading to a more refined grading.
- This demonstrated that there are differences in clast number, clast dimensions, percentage of clasts depending on their grain size and identified differences in matrix fabric.
- Demonstrated that field grades could be erroneous, however must be used with caution owing to 2-D representation.

Slake durability testing

- Durability was observed to broadly correlate with formation age, with older formations being more durable, indicating older formations are more susceptible to weathering.
- De-structured chalk has a far lower durability than that of structured chalk, which demonstrates the effects of weathering on material properties.
- In Seaford Chalks, the CIRIA weathering grades correlate with durability, meaning that slake durability can be used to measure weathering; D grades are the least durable and grades A-C appear to follow a broad pattern.
- Newhaven chalk appeared more resistant to slaking compared to Seaford Chalk, however, the range of material retained was greater in the Newhaven Chalk but was more readily

disaggregated. This suggests the presence of microfractures in the Newhaven Chalk not present in the Seaford Chalk.

- IDD has been demonstrated to correlate with Franklin and Chandra's durability classification at the 2nd cycle, meaning that IDD is a good indicator for a chalk's resistance against weathering.
- As a slaking fluid, distilled water was associated with lower durability compared to synthetic seawater and ethylene glycol, suggesting a water weakening effect.

Hydrogeological parameters measured;

Permeability testing

- Dm grades have higher permeabilities compared to Dc grades, with Seaford Dm having the highest permeability at 4.22 – 7.10 x 10^{-8} m/s, compared to Newhaven Dm at 1.18 – 5.99 x 10^{-8} m/s. Similarly, Seaford Dc has a lower permeability, at 7.78 x 10^{-9} to 2.67 x 10^{-8} m/s, compared to Newhaven Dm, but had a higher permeability than Newhaven Dc, at 9.69 x 10^{-9} to 7.76 x 10^{-8} m/s. This is interpreted to be the presence of increased clasts within Dc grades.
- The Seaford Formation D-grade chalks have higher permeabilities compared to the Newhaven D-grade Chalks, which is inferred to be due to inherent Formational attributes. This is supported by a similar pattern in structured chalk as reported within the literature.
- Seaford Dm has 30% higher permeabilities compared to Newhaven Chalk across all effective stresses, while Seaford Dc chalk has permeability 9% higher than Newhaven Dc at 120 kPa, however this increases to 26 – 28% for the final two stages.

Characterisation of geomechanical properties;

UCS testing

- When split by moisture content, dry Newhaven Dc has a UCS of 0.33 MPa, while Newhaven Dc with a NMC content has a mean UCS of 0.25 MPa, Dry Newhaven Dm has a mean UCS of 0.50 MPa, while Newhaven Dm with NMC has a UCS of 0.25 MPa. Dry Seaford Dc has a mean UCS of 0.46 MPa, while Seaford Dc with NMC has a mean UCS of 0.34 MPa.
- Dry Newhaven Dm and Dc chalks have higher UCS values compared to those of natural moisture content. Seaford chalk, conversely, has a higher UCS with NMC compared to dry samples tested.
- D-grade chalks have a lower strength compared to their parent material, with D-grade Seaford chalk being approximately 12 times lower than structured and D-grade Newhaven Chalk being approximately 11 times lower that its structured counterpart.
- Failure modes differ between samples, grades and moisture contents, with some failing in a ductile fashion and others in a brittle fashion. The implication of this is that our knowledge of the engineering behaviour of weathered, D-grade chalk is incomplete.

Brazilian tensile testing

- Newhaven Dc had the lowest tensile strength at 0.04 MPa, while Seaford Dm and Dc each had tensile strength at 0.05 MPa. Newhaven Dm had the highest tensile strength of 0.1 MPa.
- Tensile strengths of Seaford Dm were 2.3 times lower than the corresponding UCS, while Newhaven Dc was 5.2 times lower, and Newhaven Dm was 3.3 times lower than their corresponding UCS counterparts. Seaford Dm was not tested for UCS, therefore could not be compared.

Triaxial testing

- Four weathered samples were tested under triaxial conditions; three Newhaven Chalk samples and one Seaford Chalk sample.
- Each of the four tests show differing failure modes, indicative of both soil-like behaviour and rock-like behaviour.
- Of the four samples, three were Newhaven; WNC1 peaked at 250 – 270 kPa at a strain rate of 2.5 – 3%, WNC2 peaked at 1669 kPa at a strain <1%, WNC4 peaked at 160 – 180 kPa at a strain rate of 7 – 7.5% and the Seaford sample, WSC1, peaked at 300 kPa at a strain rate of 8 – 9%.
- It was observed that samples deform and mobilise, with the putty matrix being the controlling attribute of failure.

- Cohesion of weathered Newhaven chalk was 110 kPa, which is approximately 50% lower than structured Newhaven chalk.
- The angle of friction was 11 – 10°, which is approximately 4 times lower than dry, structured Newhaven chalk and 2 times lower than saturated Newhaven chalk.

This chapter is novel in that it has characterised CIRIA D-grade chalks using industry standard test methodologies, which have never been undertaken previously. Novelty also lies in the design of the program in that it has comprehensively compared D-grade weathered chalk against structured counterparts, including index testing, permeability testing and geomechanical testing, which also have never been undertaken. This work will be of interest to scientists and engineers who are concerned with weathered chalk as an engineering challenge and will assist in the identification of chalk weathering by material properties.

9 Summary and conclusions

9.1 Introduction

As stated in Chapter 1, the aim of this thesis is to further understand and characterise the development and distribution of weathering (and stages of weathering) in the Newhaven and Seaford Chalk Formations. This aim has been achieved by a program of significant field investigation, underpinned by laboratory work, and has led to novel sampling and testing techniques, identifying significant gaps within the current knowledge of the behaviour of de-structured grade chalk;

The original research objectives were to:

1. Qualitatively assess existing methods of grading of weathered chalk through practice within the field and comparison with differing localities.
2. Develop sampling and testing methodologies for weathered chalk.
3. Develop methodologies to measure the material and rock mass properties of weathered chalk.
4. Quantify chalk weathering and changes of grade through destructive and non-destructive field and laboratory techniques.
5. Develop a microtexture index or texture map for identification of chalk weathering types by correlating SEM analysis with field macrostructures.
6. Develop a predictive toolbox to assess weathering profiles in the chalk and provide consistency between engineers of varying levels of experience.

This Chapter discusses how these research objectives have been met, and where they were not, examines why this was the case. Table 9-1links the meeting of objectives to relevant chapters and the techniques used to meet them.

Table 9-1 Research objectives; techniques and Chapters demonstrating satisfaction.

Objective	Chapter	Techniques used
1	3, 4, 5, 6, 7	Field observation, CIRIA grading methodology
2	4, 5, 6, 7, 8	CIRIA grading methodology, SilverSchmidt, Equotip, index testing, slake durability testing, geomechanical strength testing, permeability testing
3	7	SEM analysis, image processing
4	5, 6, 7, 8	CIRIA grading methodology, SilverSchmidt, Equotip, index testing, slake durability testing, geomechanical strength testing, permeability testing
5	6, 7, 8, Appendix	Sampling -- Chapters 6 and 7, validation - Chapter 8, results - appendix
6	4, 5, 6, 7, 8, Appendix H	CIRIA grading methodology, SilverSchmidt, Equotip, index testing, slake durability testing, geomechanical strength testing, permeability testing

This Chapter concludes the thesis by collating the main findings of the research and discussing their implications for the study of chalk as an engineering material, and appraises the research undertaken, the methodologies developed as part of this study and makes recommendations for future research in this area.

9.2 Summary discussion and conclusion of main findings

9.2.1 Fieldwork summary and conclusions

Chapter 6 established that field observation identifies weathering types, weathering products and predisposing conditions of weathering vulnerability in Chalk. There are several different concurrent and competing weathering processes active, with evidence of overprinting relationships from historic weathering episodes, and continuous contemporary weathering evidenced in Section 6.2. Weathering is observed to be predominantly the result of Quaternary ground freezing, leaving characteristic patterns of brecciation and de-structuration of competent chalk to grades Dm and Dc, such as brecciation observed at Roedean Access Point (Section 6.2.1). Sedimento-tectonic modification of the chalk leads to increased weathering vulnerability, with increasing depth from the cliff top coinciding with reduced fracture intensity (observed at Roedean; Section 6.2.1 and Newhaven Harbour; Section 6.2.3).

Hydrogeology of the chalk mass is modified by the induction of secondary permeability (resultant preferential flow pathways) where there are high persistence and high frequency fractures leading to increased vulnerability to water weakening and chemical weathering. Where three or more closely spaced discontinuity sets exist, (such as those observed at Roedean (Section 6.2.1) and Portobello Outfall (Section 6.2.2)), accelerated weathering and material loss is more likely. Discontinuities in hydraulic conductivity with overlying chemically active soils are associated with significant karst features (as reported in Section 6.2.3 at Newhaven Harbour) with a distribution controlled by the transport of water via fracture networks and horizontal discontinuities, such as impermeable beds.

Metastable, de-structured chalk deposits (dry valleys) lose constituent material upon water inundation via entrainment and run-off (observed at Portobello Outfall, Section 6.2.2). The orientation of dry valleys coincides with low topographical relief and their axes run parallel to the strikes of measured discontinuities (Section 6.3.1, Figure 6-24), suggesting that the distribution of dry valleys is controlled by tectonics, fracturing and resulting structural geology. Dry valleys extend into the shore platform (Section 6.2.3, Figure 6-20), away from the cliff face, with differential erosion rates of platform and cliff faces leading to truncation of dry valleys. This observation is novel and requires further investigation within future studies.

In terms of practical application, Chapter 6 demonstrates that the application of scanline surveys compliment the CIRIA C574 grading system, allowing further quantification of discontinuities. C574 allows quantification of the discontinuity aperture and spacings, while scanline surveys quantify fracture character further, allowing geological context and interpretation. A full summary of practical applications is presented in Table 6-24, Section 6.3.1.

Fieldwork conclusions;

- Younging relationships are vital in the identification of weathering types and their sequence in geological history, as well as identifying if some beds or formations are more susceptible to weathering than others. This approach is novel in that it has never been undertaken in the context of chalk weathering.
- There are several different concurrent and competing weathering processes ongoing at any location at any one time and differ between locations. Weathering can be divided into historic and contemporary processes.
- Fracture intensity reduces with depth from cliff tops through the chalk unsaturated zone (CUZ), which indicates a top-down weathering process. This is interpreted to be periglacial

ground freezing, which also controls the distribution of laterally extensive brecciation patterns in the upper 3.0 m of chalk.

- Chalk horizons with aquiclude layers stratigraphically above and below have entrapped water, which is inferred to have allowed localised, acute cryoclasty during periods of ground freezing – both historic (i.e., periglacial) and contemporary. This then makes the horizon more susceptible to later weathering processes, such as slaking during wetting and drying episodes.
- Areas which have significant cover in the form of superficial deposits are likely to have less pronounced periglacial weathering effects owing to the overlying deposits protecting the chalk from permafrost conditions.
- Chalk deposits with large-scale faults in hydraulic continuity with overlying chemically active soils give rise to sub-vertical and sub-horizontal karstic features, with chalk discolouration acting as a significant indicator of chemical weathering.
- Dry valleys are observed to extend out into the shore platform; a difference between platform and cliff erosion rates explains truncation of the dry valley, leading to cliff formation. This is novel in that this has not been reported in previous literature and merits more investigation.

9.2.2 Uniformity Survey summary and conclusions

Chapter 7 demonstrated that both UCS and IDD could be measured in a field setting using NDT techniques, and that weathering causes variation in these measurements, meaning that weathering can be effectively quantified in a field setting. This has implications for the engineering practitioner in that CIRIA C574 provides an approximation, while the techniques presented in this thesis allow for repeatability and precision, effectively reducing uncertainty in data collection.

In terms of trends, Chapter 7 established that both UCS (measured by SilverSchmidt) and IDD (measured by Equotip) increased with depth, as the effects of weathering decrease. Table 9-2 presents mean Equotip-measured IDD and SilverSchmidt-measured UCS values where D-grade chalks are positioned at the cliff top and structured chalk is representative of unweathered chalk at an increased depth. This supports observations of decreasing weathering with depth made in Chapter 6, where fracture frequency and persistence reduce with depth.

Chapter 7 demonstrated the suitability of both the SilverSchmidt and the Equotip Leeb in measuring UCS and IDD respectively. In terms of statistical distribution, solid, competent, less weathered chalk produces uniform, normal distributions comprising relatively high UCS and IDD values, while brecciated and de-structured chalks produce positively skewed normal distributions comprising relatively lower UCS and IDD values. The degree of variability within the measurements and distinct

lack of obvious physical changes indicated some stochasticity, suggesting that our current understanding of weathering processes is incomplete.

Table 9-2 IDD and UCS of structured and de-structured Seaford and Newhaven Chalk.

Formation and grade	**Mean IDD (Mg/m^3)**	**Mean UCS (MPa)**
Structured Seaford chalk	1.69	5.87
Seaford grade Dc	1.54	0.32
Seaford grade Dm	1.56	Not tested
Structured Newhaven chalk	1.74	5.32
Newhaven grade Dc	1.56	0.26
Newhaven grade Dm	1.50	0.33

The Equotip was particularly suited to measuring changes within the chalk owing to its sensitivity and resolution, and capability of measuring small changes in IDD. The Equotip was sensitive enough to measure small scale density changes at proximity to discontinuities and was also effective in measuring density changes in chalk subject to chemical weathering and case hardening.

For the Newhaven Chalk, at Roedean (Section 7.2.1) and Portobello Outfall (Section 7.2.2), a total of 12 quadrats were measured. The mean IDD for Newhaven chalk was 1.70 Mg/m^3, with a range of 1.53 – 3.61 Mg/m^3, resulting in a high CIRIA density grade. For the Culver chalk at Newhaven Harbour (Section 7.2.3), 2 quadrats were tested with the Equotip, resulting in a mean IDD of 1.70 Mg/m^3, ranging 1.52 – 1.99 Mg/m^3, characterising the chalk as ranging low to high density, with the mean IDD being medium to high**.** Five quadrats were measured at Birling Gap (Section 7.2.4) for the Seaford Chalk, comprising one de-structured chalk and four structured chalks of varying grades. The mean IDD was 1.66 Mg/m^3 (medium density) with a range of 1.52 – 2.64 Mg/m^3 (low to high density).

Limitations of the Equotip were due to the size of the tungsten carbide indentor, which became clogged with chalk dust in dry conditions, exacerbated in wet conditions where this dust became a putty and required periodic cleaning. This meant that measurement of de-structured chalk was significantly challenging.

The SilverSchmidt allowed measurement of compressive strength in a field setting, but required a correction due to repeated, consistently high results. The SilverSchmidt derived UCS mean for the Newhaven Chalk for both Roedean and Portobello outfall (Sections 7.2.1 – 7.2.2) was 7.62 MPa, ranging 1.73 – 20.56 MPa, corresponding to a high CIRIA density grade. After correction the mean UCS was 3.31 MPa (medium density). At Newhaven (Section 7.2.3), four quadrats were measured, resulting in a mean UCS of 8.78 MPa, and range of 1.9 – 19.4 MPa. This characterises the chalk erroneously as high density. This measurement was considered excessively high (compared to

laboratory data and values within the literature) - after correction, the mean UCS was 3.03 MPa, a low – medium CIRIA density grade. The mean UCS of Seaford chalk (sampled at Birling Gap – Section 7.2.4) was 5.51 MPa for structured chalks, ranging from 1.73 – 22.5 MPa (high CIRIA density grade). The corrected mean value was 4.02 MPa, resulting in a density grade of medium. The mean density of the de-structured chalk was 4.3 MPa before correction, with a range of 2.5 – 19.5 MPa. After correction, mean UCS was 1.87 MPa (low-density CIRIA grade).

This study highlighted the limitations of using the SilverSchmidt; The device is only effective in the range of 5 – 30 MPa, therefore anything below or above this range could not be considered reliable. Secondarily, the SilverSchmidt was not suitable to measure the UCS of de-structured, crushable material. This is because repeated sampling of one area modifies the material due to exertion of pressure, effectively crushing de-structured chalk.

In terms of statistical distribution, solid, competent, less weathered chalk produces uniform, normal distributions comprising relatively high UCS and IDD values, while brecciated and de-structured chalks produce positively skewed normal distributions comprising relatively lower UCS and IDD values. The degree of variability within the measurements and distinct lack of obvious physical changes indicated a degree of stochasticity, suggesting that both understanding of weathering processes and data collected is incomplete.

Uniformity survey conclusions;

- Both UCS and IDD increase with depth from ground-level, inferred to be a decrease in the effects of weathering.
- The SilverSchmidt is not suitable for measuring de-structured, crushable chalk as it modifies the soil structure.
- Brecciation, fractures and discontinuities affect measurements made by both the SilverSchmidt and Equotip.
- The Equotip is effective in identification and quantification of chemical weathering, such as karstic case hardening and is sufficiently sensitive to register small scale density changes at proximity to discontinuities and can be used to infer block boundaries.
- It was identified that it was possible for several differing CIRIA grades to occur any one quadrat and that the Equotip was particularly suitable for quantifying this.
- Field estimations of grade using a hammer pick are consistently higher than SilverSchmidt derived grades, and SilverSchmidt derived grades are consistently higher than laboratory measured grades, and no correlation between hammer pick derived grade and

laboratory measured grades.

9.2.3 Laboratory testing summary and conclusions

Index testing summary and conclusions

Chapter 8 presented several novel techniques to characterise both the geomechanical and hydrogeological properties of weathered and de-structured grades of chalk. Previously these techniques had not been undertaken on weathered and destructed chalk, this allowed identification of several aspects of chalk behaviour that were not previously understood.

In terms of characterisation, Chapter 8 achieved several outcomes. Initially, a database of material properties for each chalk formation in the southern province (less the Portsdown Chalk) was developed (Section 8.2) from previous studies and further testing, which allowed comparison with de-structured counterparts as well as contributed to an understanding of weathering susceptibility of each formation.

Sections 8.2.1 and 8.2.2 presented the results of IDD testing, where structured chalk was characterised and then compared against de-structured chalk; Seaford grade Dm has a mean IDD of 1.56 mg/m^3, Seaford grade Dc has an IDD of 1.54 Mg/m^3, Newhaven grade Dm has an IDD of 1.50 Mg/m^3, while Newhaven Dc has an IDD of 1.56 Mg/m^3. The mean CIRIA density grade is observed to be one grade lower in de-structured chalk than in structured chalk. The differences between weathering grade were minor. When compared, laboratory densities of structured chalk are consistently higher than densities measured with the Equotip Leeb, however, in grade Dc Seaford Chalk, laboratory densities were lower than those obtained using the Equotip.

Moisture content testing (Section 8.2.3) showed that with the exception of Newhaven D-grade chalk sampled at Portobello Outfall, D-grade chalks are not close to saturation like their structured counterparts. This is novel as this has never been established before. NMC values for Seaford Dc was 25.0%, while Seaford Dm had an NMC of 24.36%. Newhaven Dc had an NMC of 24.57% and Newhaven Dm had an NMC of 25.48%. SMC for Seaford Dc was 27.60%, Seaford Dm was 29.20%, while Newhaven Dc was 27.84% and Newhaven Dm was 27.08%. When moisture content is plotted against IDD (Section 8.2.2, Figure 8-7), D-grade chalks fall into the low-medium CIRIA classification. D-grade chalks have higher SMC values compared to structured chalks, but comparably lower NMC values. SMC values for D-grade chalks are 1 – 1.15 times higher than NMC values.

Voids ratio and porosity were calculated for D-grades of Newhaven and Seaford chalk in Section 8.2.4; Newhaven Dc chalk has a voids ratio of 0.749, with a range of 0.611 – 0.895. Newhaven Chalk. Newhaven grade Dm is greater than Dc, with a voids ratio of 0.788, with a range of 0.613 – 0.911.

Seaford Dm has a voids ratio of 0.751 and a range of 0.636 – 0.886, while Seaford Dm has a larger voids ratio of 0.731 and a range of 0.719 – 0.749.

Newhaven grade Dm has a calculated porosity of 43.99%, with a range of 37.99 – 47.68%, Newhaven Dc has a porosity of 42.72% and a range of 37.91 – 47.22%. Seaford Dc has a porosity of 42.83%, with a range of 38.88 – 46.98%, Seaford Dm has a porosity of 42.23%, with a range of 41.82 – 42.81%. Values for both voids ratio and porosity were significantly higher for de-structured chalk compared to structured, and due to their dual property nature (and subsequent heterogeneity), cannot be relied upon. It would be necessary to measure these values via other means, such as measuring these properties in matrix and clasts individually.

Water weakening experiments (Section 8.2.5) were undertaken to observe the behaviour of D-grade chalks when submerged in water. D-grade chalk forms debris flow when immersed in water within 30 seconds. The rate of collapse decreased when water was substituted for ethylene glycol, suggesting a water weakening effect.

Efforts to characterise D-grade material comprised a modified PSD test (Section 8.2.6) and a modified Bushinsky technique (Section 8.2.7). These allowed quantification of clasts to matrix ratios. PSD testing showed that D-grade Newhaven comprised 40% particles <625 µm and 60% particles >625 µm, while D-grade Seaford chalk comprised 35% particles <625 µm and 65% particles >625 µm, leading to a classification of a well-graded soil. The number of PSD tests were limited and therefore more study should be undertaken in this area.

The modified Bushinsky technique allowed elucidation of D-grade chalks internal structure and fabric. This technique demonstrated that there are differences in clast number, clast dimensions, percentage of clasts depending on their grain size and identified differences in matrix fabric, such as shear zones and disturbance of clasts when this technique was applied to post-test samples. This technique is novel in that it allowed the 2-D quantification of the internal structure of a D-grade chalk, leading to a more refined grading, although the 2-D aspect dictates that caution should be used when applying a grade based on observed clast-matrix ratio. It would be advised that this observational method was supported by PSD testing to quantify clasts.

Index testing Conclusions;

IDD

- The IDD of D-grade chalk is consistently classified as low CIRIA density grade.
- Mean CIRIA density grades are observed to be one grade lower in de-structured chalk than in structured chalk.
- Laboratory densities of structured chalk are consistently higher than densities measured with the Equotip Leeb in a field setting, however, in grade Dc Seaford Chalk, laboratory densities were lower than those obtained using the Equotip.

Moisture content

- With the exception of chalks sampled at Telscombe Cliffs, D-grade chalks are not close to saturation like their structured parent material. This is novel as this has never been established previously.
- When moisture content is plotted against IDD, D-grade chalks fall into the low-medium CIRIA classification.
- D-grade chalks have higher SMC values compared to structured chalks, but comparably lower NMC values. SMC values for D-grade chalks are 1 – 1.15 times higher than NMC values.

Voids ratio and porosity

- Values for both voids ratio and porosity were significantly higher for de-structured chalk compared to structured. The dual property nature of matrix hosting clasts (and subsequent heterogeneity) means that these values are not reliable.

Water weakening of D-grade chalk

- D grade chalk collapses upon itself and forms debris flows when immersed in water within 30 seconds. The rate of collapse was observed to decrease when water was substituted for ethylene glycol, suggesting a water weakening effect.

Particle size distribution

- PSD demonstrated that D-grade Newhaven comprised 40% particles <625 µm and 60% particles >625 µm, while D-grade Seaford chalk comprised 35% particles <625 µm and 65% particles >625 µm, leading to a classification of a well-graded soil.

Modified Bushinsky technique

- This technique is novel in that it allowed the 2-D quantification of the internal structure of a D-grade chalk.
- This technique is novel as it is not reported within current literature.

- This technique demonstrated the differences in clast number, clast dimensions, percentage of clasts depending on their grain size and identified differences in matrix fabric.

9.2.4 Slake durability Summary and conclusions

Significant slake durability testing allowed the evaluation of each chalk formation in terms of durability and established that the more weathered the chalk by CIRIA grading standards, the less durable. By changing slaking fluid to that of ethylene glycol and saltwater, it was possible to observe the weakening effects of both water and that of haloclasty on the Newhaven and Seaford Chalk Formations.

Durability was observed to broadly correlate with formation age, with older formations being more durable, indicating younger formations are more susceptible to weathering. In Seaford Chalks, the CIRIA weathering grades correlate with durability, meaning that slake durability can be used to measure weathering; D grades are the least durable and grades A - C appear to follow a broad pattern, with A grades being the most durable and C, the least. Newhaven chalk appeared more resistant to slaking, however, the range of material retained was greater in the Newhaven Chalk but was more readily disaggregated. This suggests the presence of microfractures in the Newhaven Chalk not present in the Seaford Chalk.

De-structured chalk has a far lower durability than that of structured chalk, which demonstrates the effects of weathering on material properties and IDD has been demonstrated to correlate with Franklin and Chandra's durability classification at the 2nd cycle, meaning that IDD is a good indicator for a chalk's resistance against weathering. This is novel in that IDD has never been correlated with weathering and provides a method for quantifying weathering susceptibility.

Slake Durability Conclusions

- Durability was observed to broadly correlate with formation age, with older formations being more durable, indicating older formations are more susceptible to weathering.
- De-structured chalk has a far lower durability than that of structured chalk, which demonstrates the effects of weathering on material properties.
- In Seaford Chalks, the CIRIA weathering grades correlate with durability, meaning that slake durability can be used to measure weathering.
- IDD has been demonstrated to correlate with Franklin and Chandra's durability classification at the 2nd cycle, meaning that IDD is a good indicator for a chalk's resistance against weathering.

9.2.5 Permeability summary and conclusions

The development of novel sampling techniques for de-structured chalk as part of this study allowed the undertaking of industry standard testing, which is also novel as this has previously not been undertaken on de-structured grades of chalk. Accelerated permeability, UCS, Brazilian, and triaxial testing were undertaken to establish permeabilities and strength parameters of de-structured chalks. When compared to structured chalks, it was possible to observe, unsurprisingly, that de-structured chalks were markedly weaker and had lower permeabilities.

Accelerated permeability testing (Section 8.4) demonstrated that de-structured chalks had a decreasing permeability with increasing effective stress, attributed to modification of pore structures within the matrix element of the cores, and that de-structured chalks had significantly lower permeability than structured chalks. Dm grades of Newhaven and Seaford Chalks had higher permeabilities than their Dc grade counterparts, with Seaford Dm having the highest permeability at 4.22 – 7.10 x 10^{-8} m/s, compared to Newhaven Dm at 1.18 – 5.99 x 10^{-8} m/s. Seaford Dc has a lower permeability, at 7.78 x 10^{-9} to 2.67 x 10^{-8} m/s, compared to Newhaven Dm, but had a higher permeability than Newhaven Dc, at 9.69 x 10^{-9} to 7.76 x 10^{-8} m/s (Section 8.4, Figure 8-22). This is interpreted to be due to the presence of increased clasts within Dc grades.

The Seaford Formation D-grade chalks have higher permeabilities compared to the Newhaven D-grade Chalks, which is inferred to be due to inherent formational attributes. This is supported by a similar pattern in structured chalk as reported within the literature. Comparatively, Seaford Dm has 30% higher permeabilities than Newhaven Chalk across all effective stresses, while Seaford Dc chalk has permeability 9% higher than Newhaven Dc at 120 kPa, however this increases to 26 – 28% for the final two stages. The reduction in permeability in Dc grades is attributed to consolidation, whereby matrix filled fractures are closed by effective stress, and the flow of fluid within the sample becomes diffusive through competent chalk clasts, as opposed to advective via the de-structured matrix (Section 8.4, Figure 8-23).

This is novel in that this type of permeability testing on de-structured chalk has never been undertaken before and has implications for engineering works where geological rockhead comprises Dc and Dm chalks, and by virtue of low confining stress, increased moisture content.

Permeability conclusions;

- Dm grades have higher permeabilities compared to Dc grades.

- The Seaford Formation D-grade chalks have higher permeabilities compared to the Newhaven D-grade Chalks, which is inferred to be due to inherent Formational attributes. This is supported by a similar pattern in structured chalk as reported within the literature.
- This technique is novel as permeability testing on D-grade chalks has not been undertaken previously.

9.2.6 Geomechanical testing summary and conclusions

UCS

UCS test results are presented in Section 8.5.1. When split by moisture content (Table 8-23), it is possible to observe dry Newhaven Dc having a UCS of 0.33 MPa, while Newhaven Dc with a NMC content has a mean UCS of 0.25 MPa, Dry Newhaven Dm has a mean UCS of 0.50 MPa, while Newhaven Dm with NMC has a UCS of 0.25 MPa. Dry Seaford Dc has a mean UCS of 0.46 MPa, while Seaford Dc with NMC has a mean UCS of 0.34 MPa. Compared to structured chalk, D-grade chalks have a lower strength, with D-grade Seaford chalk being approximately 12 times lower and D-grade Newhaven Chalk being approximately 11 times lower.

Failure modes differ between samples, grades and moisture content, with samples with a natural moisture content failing plasticly in a ductile fashion, while dry fail in a brittle fashion. The implication of this is that our knowledge of the engineering behaviour of weathered, D-grade chalk is incomplete.

In terms of UCS (Section 8.5.1) and Brazilian strengths (Section 8.5.2), the failure of de-structured chalks differed with CIRIA grade and moisture content. Desiccated chalks tended to fail plastically, with a defined failure peak, while chalks tested with an NMC failed in creep. Tests between Dc and Dm grades were unpredictable and controlled by the ratio of clasts to matrix and also clast size, demonstrating that currently, there is insufficient data to fully understand the behaviour of these deposits. It is possible that an increased moisture content attributes its strength to partial saturation and some frictional resistance, and desiccated chalks rely predominantly on friction and secondary minor, water-soluble cementation.

UCS testing conclusions;

- Overall, de-structured Newhaven chalk has a higher mean UCS compared to de-structured Seaford Chalk.
- Dry Newhaven Dm and Dc chalks have higher UCS values compared to those of natural moisture content. Seaford chalk has a higher UCS with NMC compared to dry samples.
- D-grade chalks have a lower strength compared to structured chalk, with D-grade Seaford chalk being approximately 12 times lower than structured and D-grade Newhaven Chalk being approximately 11 times lower that its structured counterpart.
- Failure modes differ between samples, grades and moisture contents, with some failing in a ductile fashion and others in a brittle fashion.
- This testing was novel in that UCS values for D-grade chalk have not been reported within the literature.

Brazilian tensile testing

Brazilian tensile testing (Section 8.5.2) showed that Newhaven Dc had the lowest tensile strength at 0.04 MPa, while Seaford Dm and Dc each had tensile strength at 0.05 MPa. Newhaven Dm had the highest tensile strength of 0.1 MPa. Tensile strengths of Seaford Dm were 2.3 times lower than the corresponding UCS, while Newhaven Dc was 5.2 times lower, and Newhaven Dm was 3.3 times lower than their corresponding UCS counterparts. Seaford Dm was not tested for UCS, therefore could not be compared.

Brazilian tensile testing conclusions;

- Newhaven Dc had the lowest tensile strength at 0.04 MPa, while Seaford Dm and Dc each had tensile strength at 0.05 MPa. Newhaven Dm had the highest tensile strength of 0.1 MPa.
- Tensile strengths of Seaford Dm were 2.3 times lower than structured Seaford chalk. Newhaven Dc was 5.2 times lower, and Newhaven Dm was 3.3 times lower than structured Newhaven chalk.
- This testing was novel in that tensile testing has not been reported in the literature previously.

Triaxial testing

Triaxial testing is presented in Section 8.5.3, with derived Mohr Coloumb parameters presented in Section 8.5.4. Four weathered samples were tested under triaxial conditions; three Newhaven Chalk samples and one Seaford Chalk sample. Each of the four tests show differing failure modes, indicative of both soil-like behaviour and rock-like behaviour It was observed that samples deform and mobilise, with the putty matrix being the controlling attribute of failure – this is significant as it means that there is a degree of uncertainty as to how a D-grade chalk will behave when tested triaxially. Of the four samples, three were Newhaven; WNC1 peaked at 250 – 270 kPa at a strain rate of 2.5 – 3%, WNC2 peaked at 1669 kPa at a strain <1%, WNC4 peaked at 160 – 180 kPa at a strain rate of 7 – 7.5% and the Seaford sample, WSC1, peaked at 300 kPa at a strain rate of 8 – 9%. Cohesion of weathered Newhaven chalk was 110 kPa, which is approximately 50% lower than structured Newhaven chalk, and the angle of friction was 11 – 10°, which is approximately 4 times lower than dry, structured Newhaven chalk and 2 times lower than saturated Newhaven chalk.

Sections 8.5.3 and 8.5.4 established that de-structured grade chalks can be tested triaxially, with samples yielding significantly lower strengths compared to structured chalk. In terms of consistency, no two samples of de-structured chalk failed in the same mode, with one sample exhibiting brittle failure (reflective of an intact chalk), and three samples exhibiting failure in creep but at significantly different strengths (reflective of an over-consolidated clay). This is attributed to the angularity and size

of chalk clasts as well as amount of putty within each sample. This indicates that currently, the understanding of behaviour of de-structured chalk under triaxial conditions is limited, with further research required.

Triaxial testing conclusions;

- Each of the triaxial four tests show differing failure modes, indicative of both soil-like behaviour and rock-like behaviour.
- It was observed that samples deform and clasts mobilise within the matrix, which is the controlling attribute of failure.
- Cohesion of weathered Newhaven chalk was 110 kPa, which is approximately 50% lower than structured Newhaven chalk.
- The angle of friction was 11 – 10°, which is approximately 4 times lower than dry, structured Newhaven chalk and 2 times lower than saturated Newhaven chalk.
- Triaxial testing of D-grade material is novel as it is not reported within previous literature.

9.2.7 SEM summary and conclusions

An attempt to link weathering with microstructure using SEM techniques was made, however, this was proved to be ineffective. SEM techniques, however, were effective in identifying definition between different Chalk Formations. Porosity was estimated using ImageJ for all formations, with the Seaford Chalk having a porosity of 29.77% and the Newhaven Chalk having a porosity of 28.70%. Image processing also allowed the quantification of grains and the identification of coccolith taxa, where well-preserved. EDS work undertaken on chalk was limited but did identify haloclasty within salt-weathered chalks. Full results for SEM testing is found in Appendix G.

SEM conclusions;

- Analysis of microstructure using SEM showed little in terms of weathering, however, it was possible to observe differences between each chalk formation.
- Porosity was estimated for all formations, with the Seaford Chalk having a porosity of 29.77% and the Newhaven Chalk having a porosity of 28.70%.
- Identification of coccolith taxa was possible in samples where preservation was exceptional.

9.3 Strength and limitations of research

9.3.1 Strengths

The comprehensive research presented in this thesis has advanced scientific knowledge on the distribution, development and identification of chalk weathering in a field setting. The research has also advanced knowledge by developing a significant laboratory-based data set of the behavioural properties of structured and de-structured weathered chalk, which in itself is novel, as this has never been undertaken to this depth. New methodologies had to be developed to test this weathered material in both settings.

This thesis has set out a novel, statistically significant and robust approach in quantifying the degree of weathering in the field by adapting the CIRIA C574 approach with non-destructive testing and first principal geological techniques. This allowed effective identification of various stages of weathering and weathering products, which would be of value to both industry and academic practitioners by providing precision and repeatability. The significance of this part of the research is that by characterising the distribution of weathering in terms of depth below ground level and lateral extent, this thesis allows reduction of engineering uncertainty for engineering geologists when operating in Chalk geologies.

Laboratory work was similarly impactful in terms of advancing scientific knowledge, however, to achieve laboratory testing, a viable sampling technique was required to be developed to produce

samples of industry standard dimensions. Research undertaken as part of this thesis led to a viable, novel sampling technique, which over the course of the project was further refined in terms of material use in sampling tubes and methods of driving tubes.

Novel developments for field sampling integral to sampling strategy success include;

- Section 4.2.3 – Development of a strategy to constrain and measure weathering in a field setting by selecting suitable tools (i.e., SilverSchmidt and Equotip) and using non-geological techniques (use of a quadrat for constraint).
- Section 4.2.4 – Adaptation of the CIRIA C574 density grades for use with the SilverSchmidt test hammer and the Equotip Leeb device.
- Section 4.3.2 – Modification and development of U38 core retrieval.
- Section 4.3.3 - Refinement of this technique using several different metal types, core sizes and methods of driving samplers.
- Section 4.3.3 – Development of a method of in-field sample extrusion into a membrane and subsequent strategy for preserving moisture content.

9.3.2 Limitations

Initially it was planned to produce a textural map and predictive toolbox and link these to measured physical properties of weathered chalk. While physical testing of different grades of weathered chalk was robust, it was not possible to link this to a range of microtextures. The microtexture of the chalks observed did not vary with the degree of weathering of the samples.

SEM work undertaken during this research project was limited. Ideally, a more extensive SEM-EDS works package could have provided evidence of chemical weathering in a variety of environments. Given the relative purity of chalk in terms of $CaCO_3$ content, it would be sensible to postulate that an EDS study of chalk would likely yield positive results where chemical weathering is indicated from physical observation.

9.4 Future work

By evaluating the main findings and considering the limitations of this research, it is possible to identify recommendations for future work. A proposal for a workflow model for a predictive toolbox is presented and recommendations are broken down into (i) future fieldwork, (ii) future laboratory work and (iii) future modelling work.

9.4.1 Proposed workflow classification as a predictive toolbox

In Section 5.9.4**,** a proposed workflow diagram for the classification of de-structured chalks was presented. In this section, five interconnected workflows are presented to provide a strategy for classifying and then validating weathering in chalk, providing fulfilment of objective 6. Full size workflow diagrams are presented in Appendix I.

Classification 1 (Figure 9.1) is a workflow for stages of field investigation, detailing preliminary desk study, field observations, scanline surveys and the application of the CIRIA C574 grading system, sample selection for laboratory testing of field derived samples and specialised field tools required to undertake a regional uniformity survey, effectively mirroring the work undertaken in this thesis.

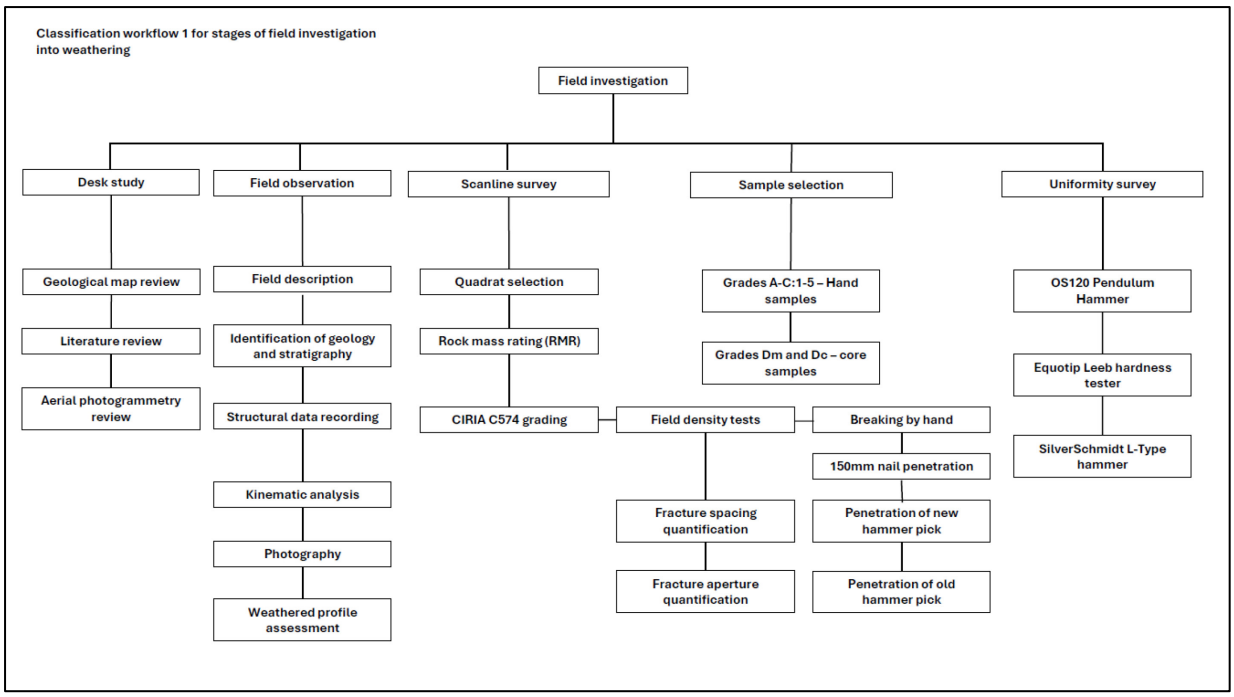


Figure 9-1 Classification workflow for stages of field investigation of weathering.

Classification 2 (Figure 9-2) provides a flowchart of weathering features related to geomorphology based on observations within this thesis. This workflow should act as a non-exhaustive aide memoire when undertaking observations within a research site setting and allow the user to identify styles of weathering so they can be put into context along with CIRIA gradings and other field observations.

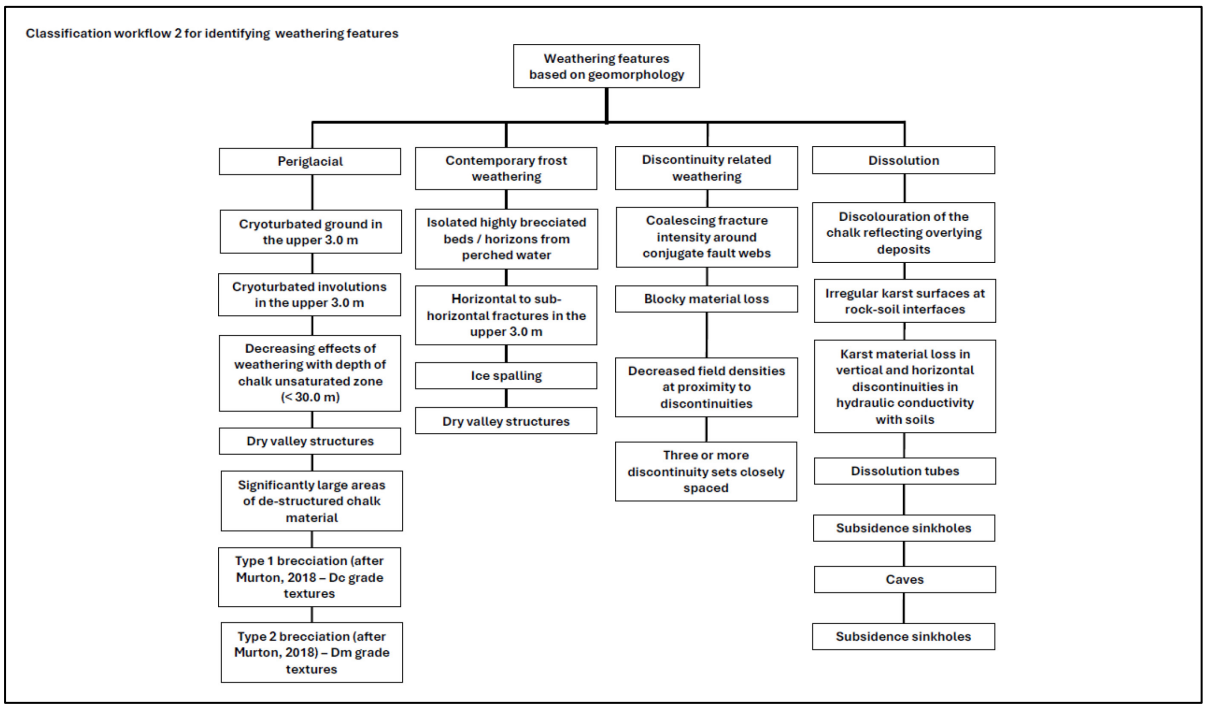


Figure 9-2 Classification workflow for identifying weathering features.

Classification 3 (Figure 9-3) shows a methodology for classifying grades A1 – C3 structured chalks (as per CIRIA C574) but also utilises slake durability as a validation tool for CIRIA discontinuity spacing and aperture grades (presented in Chapter 8). This workflow also details how a regional density and strength survey using the Equotip Leeb and SilverSchmidt rebound hammer can be validated with laboratory methods.

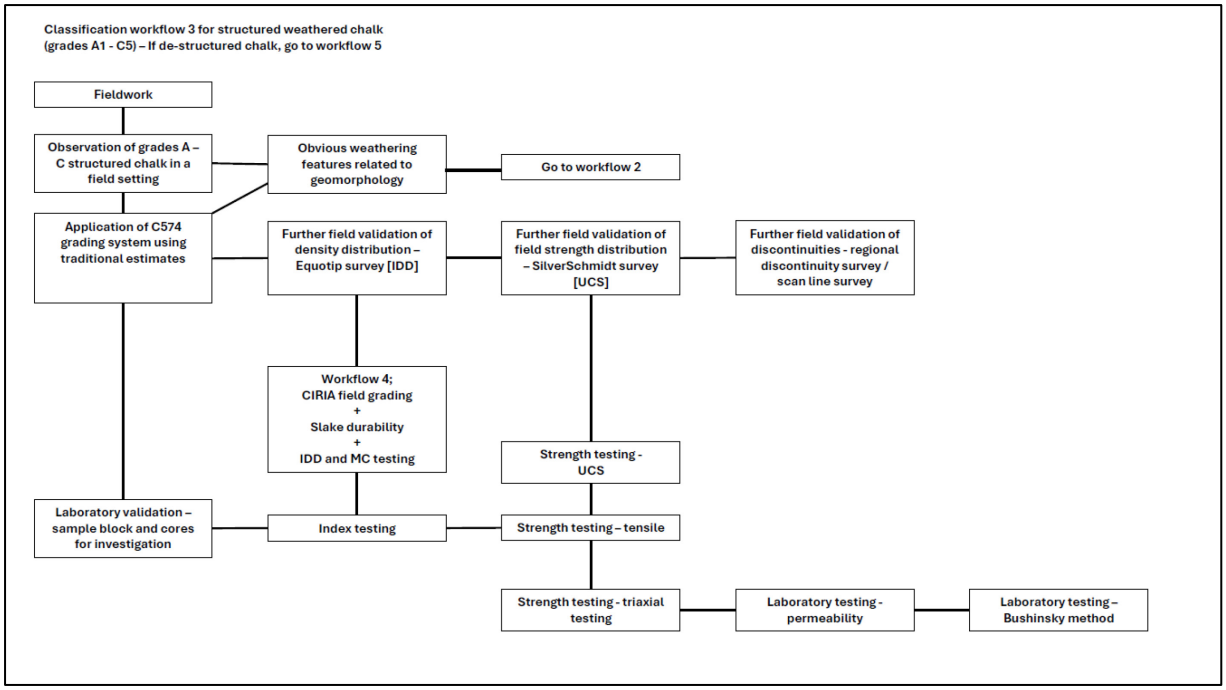


Figure 9-3 Classification workflow for structured chalks, grades A1-C5.

Classification workflow 4 (Figure 9-4) details how the slake durability method can be used to validate weathering grades using 2nd cycle slake durability and IDD results plotted against the CIRIA density grades as well as Franklin and Chandra's durability index (as per Section 8.3.4). This methodology ultimately validates in-field measurement or estimation of density to CIRIA C574 standards and allows chalk to be quantified in terms of durability.

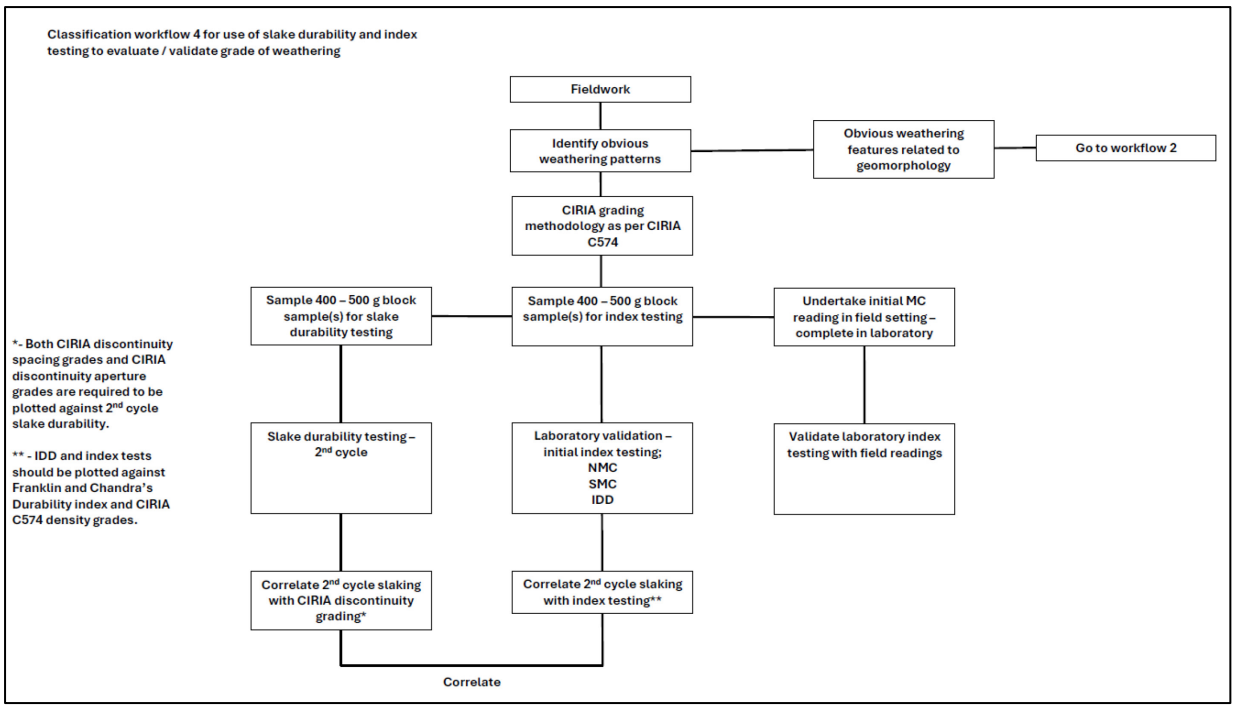


Figure 9-4 Classification workflow for use of slake durability and index testing to validate weathering in chalk.

Classification workflow 5 (Figure 9-5) is a refinement of the workflow presented in Section 5.9.4. In terms of refinement, index testing are now a stand-alone column within the workflow as initial tests that should be performed as a minimum. Permeability and triaxial testing are now both validated by the destructive, modified Bushinsky technique, where samples are dried after permeability or triaxial testing and then assigned a CIRIA D-grade based on the observed clast to matrix ratio. Similarly, the destructive UCS and tensile test methods are validated with the modified PSD test in order to quantify the material in terms of grain size.

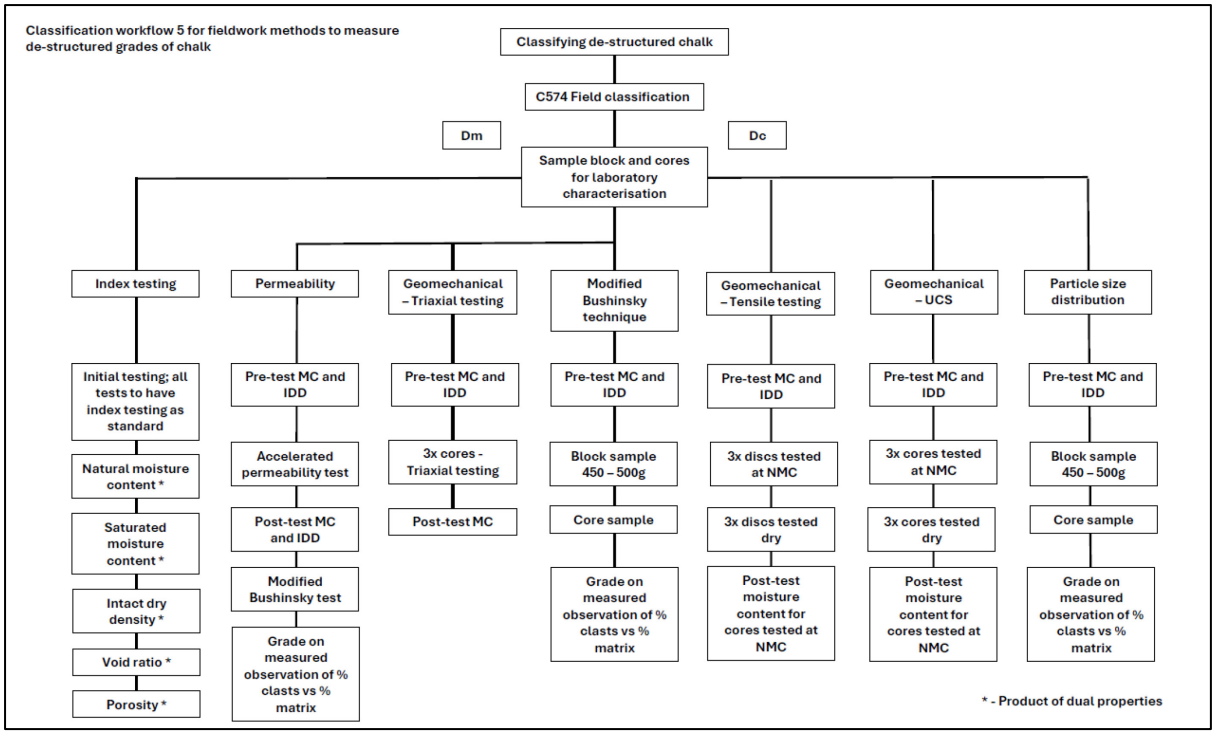


Figure 9-5 Classification workflow 5.

By proposing this workflow based on the work undertaken in this thesis, a predictive toolbox to assess weathering profiles has been produced and inconsistency between engineers of varying levels of experience has been addressed by more robust field and laboratory methods, demonstrating that objective 6 has been fulfilled. It is envisioned that this workflow will be further refined by industry and academic practice.

9.4.2 Future fieldwork

Future fieldwork should be undertaken in the context of quantifying density and compressive strength of representative weathering types using the SilverSchmidt and Equotip devices. Similarly, further work on these instruments in conjunction with laboratory testing is required to reconcile the variety in field measurements with index tests and would further refine precision.

It is recommended that the developed core sampling procedure for de-structured chalk (described in Section 4.3.2) is further developed, with emphasis placed upon press-in sampling rather than percussive methods to avoid modification of the sample microstructure. Should this not be possible in a field setting, it is recommended that sufficiently large block samples are collected so that push-in sampling can be developed in a laboratory.

9.4.3 Future laboratory work

This thesis has established methods for characterising D-grade samples in the laboratory and has quantified index properties (Section 8.2), however, strength testing has produced some inconsistent results, which is largely a function of the limited number of samples tested and a limited knowledge of laboratory testing of D-grade chalks

Geomechanical testing of D-grade chalk material produced results that were variable in terms of failure modes and strengths (Section 8.5). Further work is required which should include more samples to understand the controls on this mechanical behaviour of the D grade chalk, which is likely to be related to moisture content and the characteristics of the matrix and clasts within the sample. Similarly, the behaviour of D-grade chalk material under triaxial conditions during this study demonstrates that the behaviour is not well understood. This is due to the limited number of tests undertaken, and it is therefore recommended that more research and testing is conducted to increase knowledge and understanding of these materials.

Image processing techniques used with the SEM micrographs and modified Bushinsky techniques yielded limited quantification of the chalk in that only 2-D surfaces were considered. To fully characterise clasts at macroscale and grains on the microscale then a 3-D approach would be required, such as use of CT scanning to explain constituent grain characteristics and their positions within 3-D space.

9.4.4 Future modelling work

As discussed in Section 9.6, data presentation is limited when describing the distribution of weathered chalk and the degree to which the chalk is weathered. To date, 3-D modelling of weathered chalk has been limited, with some work undertaken by Hadlow, et al. (2014, 2018) and further built on by Cullen (2021) while supervised by the author. Cullen produced promising digital terrain models to visualise weathering, however these could not be used as a predictive tool owing to a lack of data, which led to unrealistic predictive models. To that end, further data collection and 3-D modelling is recommended.

9.4.5 Future applications and implications for industry and academia

The results of this research are impactful in several ways and have implications for industry. From a hydrogeological perspective, this research is significant in that weathering has been established as modifying permeability of chalk – both matrix permeability (established in Section 8.4) and secondary fracture permeability. By establishing trends of weathering, such as decreasing weathering with depth (reduction of fracture spacings and aperture and an increase in density) and typical permeabilities of

weathered chalk, it would be possible to make more informed estimates on permeability or validation of measured permeability at depth.

Identification of weathering, at the intersection of major discontinuities has implications for subterranean excavation in that this weathering may be present at depth, and only manifest once an underground space is excavated and the stresses redistributed around the void. By understanding the distribution of discontinuity sets and their interplay, an estimation of the likelihood of encountering these pockets of weathering (and indeed their frequency) can be made. Newman and Hadlow (2021) identified extensive faulting and discontinuities in London when undertaking investigation for the Thames Tideway tunnel. They reported that these were sub-parallel geological faults with systems of strike-slip displacement, which would suggest similar patterns of weathering as what is observed on the Sussex coast (Chapter 6.3).

In engineering geology terms, this research has implications in estimating and identifying true engineering rockhead. By quantifying and characterising weathered chalks properties and developing ranges for these properties in weathered chalk, and by understanding trends in weathering distribution with depth, it is possible to make the distinction between weathered structured chalk more easily. This is especially true of the Dc grades of weathered chalk, which may act more like a weak rock, as opposed to the matrix dominated Dm grades of chalk, which behave like a stiff soil. The estimation of rockhead is particularly important when designing foundations or sinking shafts, as it denotes the depth at which competent chalk is achieved.

9.5 Conclusion

In conclusion, this thesis presents a comprehensive investigation which has provided a thorough understanding of weathering and resulting material properties of the Seaford and Newhaven Chalk Formations.

As established in Chapter 1 and 2, there are significant omissions in the knowledge of weathering and the distribution of weathering within current literature. This is due to a number of factors, such as the lack of sampling methods of weathered chalk, the lack of scientific methods to quantify weathering in chalk and the lack of studies exclusive to weathering, with the commentary of weathering being periphery to other main topics. This thesis is significant in that it has identified these omissions and filled in these knowledge gaps.

Chapter 4 demonstrated the development of novel sampling techniques to industry-standards (enabling experimentation described in Chapter 5) and a novel strategy for quantifying chalk weathering in a field setting. Chapter 5 presented the adaptation of industry-standard techniques in order to measure weathered chalk, which is novel in that these techniques had never been undertaken on CIRIA D-grade chalk material previously.

Fieldwork (Chapter 6) highlighted the complex effects of weathering processes, identifying Quaternary ground freezing as a predominant factor leading to brecciation and de-structuration of competent chalk within the upper 30 m of strata (the CUZ). The study identified the influence of hydrogeology and discontinuities on weathering, particularly through secondary permeability induced by fractures. The observation of dry valleys and their relation to structural geology presents a novel geomorphological research opportunity.

Uniformity surveys presented in Chapter 7 demonstrated the effectiveness of non-destructive testing techniques in quantifying weathering effects in a field setting, allowing both discrete measurement and characterisation of weathering on a site-scale. The uniformity surveys emphasised the limitations of certain methods, such as the SilverSchmidt for de-structured chalk, while highlighting the effectiveness of Equotip in identifying chemical weathering and fracture-related changes.

Chapter 8 presented laboratory work which expanded on and underpinned field findings by characterising index properties, geomechanical and hydrogeological properties of weathered Seaford and Newhaven chalks. Novel techniques provided insights into the behaviour of de-structured chalk, identifying significant differences in properties compared to structured chalk, such as distinct lower values of IDD, moisture content, UCS and tensile strength. Permeability testing highlighted the differences between structured and de-structured chalk, with further distinction between Dc and Dm

grades. Triaxial testing revealed varying failure modes and strengths indicative of the current uncertainties of knowledge of weathered chalk. SEM techniques, though ineffective in linking weathering with microstructure, provided valuable insights into formation identification and porosity estimation.

Overall, this thesis contributes to a more comprehensive understanding of chalk weathering processes and their implications for engineering practices. The study suggests further research directions, particularly in exploring the relationships between weathering, structural geology, and hydrogeology, as well as the development of more robust testing techniques for de-structured chalk.

References

ADRIANO, D. 2023. *Screenshot of aerial drone footage; Birling Gap* [Online]. Drone Adriano. Available: https://www.youtube.com/watch?v=2Kz3qvv9D-s [Accessed 01 November 2023].

AL-JAF, P., SMITH, M. & GUNZEL, F. 2022. Measurement of the hydraulic properties of chalk using centrifuge permeameter; the study of chalk hydraulic properties under accelerated gravitational force. *The Quarterly Journal of Engineering Geology and Hydrogeology,* 55.

AL-JAF, P., SMITH, M. & GUNZEL, F. 2021. Unsaturated zone flow processes and aquifer response time in the Chalk Aquifer, Brighton, South East England. *Groundwater,* 59**,** 381-395.

ALVAREZ-BORGES, F. J. A. 2019. The shaft capacity of small displacement piles in chalk. Southampton: University of Southampton (Unpublished PhD Thesis).

AOKI, H. & MATSUKURA, Y. 2007. A new technique for non-destructive field measurement of rock-surface strength: an application of the Equotip hardness tester to weathering studies. *Earth Surface Processes and Landforms: The Journal of the British Geomorphological Research Group,* 32**,** 1759-1769.

ARMAN, H., HUSSEIN, S., ABOUHALIGAH, H. E. Y., OSMAN, M., BALOCH, M. A., HAG, D. B. A. & ALGAISHI, H. A. A. Predicting weathering characteristics of carbonate rocks under different geo-environmental conditions. IOP Conference Series: Earth and Environmental Science, 2019. IOP Publishing, 012016.

ASONI, G. A., STAVROU, A. & LAWRENCE, J. A. Erosion of the chalk coastal cliffs at Birling Gap, Sussex, UK. Correlation between rate of coastal retreat, geotechnical rocks properties and precipitation. *In:* LAWRENCE, J. A., PREENE, M., LAWRENCE, U. L. & BUCKLEY, R., eds. Engineering in Chalk: Proceedings of the Chalk 2018 Conference, 2018 London. ICE Publishing, 361 - 367.

ASTM 2008. ASTM D4644-08 Standard Test Method for Slake Durability of Shales and Similar Weak Rocks.

BARTON, N. R., LIEN, R. & LUNDE, I. 1974. Engineering classification of rock masses for the design of tunnel supports. *The Journal of Rock Mechanics,* 6.

BELL, F. G. 1977. A note on the physical properties of the chalk. *Engineering Geology,* 11**,** 217-225.

BELL, F. G., CULSHAW, M. G. & CRIPPS, J. C. 1999. A Review of Selected Engineering Geology Characteristics of English Chalk. *Engineering Geology,* 54**,** 237-269.

BERRY, T. W., FISH, P. F., PRICE, S. J. & HADLOW, N. W. 2020. Chapter 10 Periglacial geohazards in the UK. *In:* GILES, D. P. & GRIFFITHS, J. S. (eds.) *Geological Hazards in the UK: Their Occurrence, Monitoring and Mitigation Engineering Group Working Party Report.* London.

BGS-EARTHWISE 2015. Chalk of the UK - History of research.

BGS(A). 2022. *The BGS Lexicon of Named Rock Units - West Melbury Marly Chalk Formation* [Online]. Available: https://webapps.bgs.ac.uk/lexicon/lexicon.cfm?pub=WMCH [Accessed 01 April 2022 2022].

BGS(B). 2022. *The BGS Lexicon of Named Rock Units - Zig Zag Chalk Formation* [Online]. Available: https://webapps.bgs.ac.uk/lexicon/lexicon.cfm?pub=ZZCH [Accessed 01 April 2021].

BGS(C). 2022. *The BGS Lexicon of Named Rock Units - Holywell Nodular Chalk Formation* [Online]. Available: https://webapps.bgs.ac.uk/lexicon/lexicon.cfm?pub=HCK [Accessed 01 April 2022 2022].

BGS(D). 2022. *The BGS Lexicon of Named Rock Units - New Pit Chalk Formation* [Online]. Available: https://webapps.bgs.ac.uk/lexicon/lexicon.cfm?pub=NPCH [Accessed 01 April 2022 2022].

BGS(E). 2022. *The BGS Lexicon of Named Rock Units - Lewes Nodular Chalk Formation* [Online]. Available: https://webapps.bgs.ac.uk/lexicon/lexicon.cfm?pub=LECH [Accessed 01 April 2022 2022].

BGS(F). 2022. *The BGS Lexicon of Named Rock Units - Seaford Chalk Formation* [Online]. Available: https://webapps.bgs.ac.uk/lexicon/lexicon.cfm?pub=SECK [Accessed 01 April 2022 2022].

BGS(G). 2022. *The BGS Lexicon of Named Rock Units - Newhaven Chalk Formation* [Online]. Available: https://webapps.bgs.ac.uk/lexicon/lexicon.cfm?pub=NCK [Accessed 01 April 2022 2022].
BGS(H). 2022. *The BGS Lexicon of Named Rock Units - Culver Chalk Formation* [Online]. Available: https://webapps.bgs.ac.uk/lexicon/lexicon.cfm?pub=CUCK [Accessed 01 April 2022 2022].
BGS(I). 2022. *The BGS Lexicon of Named Rock Units - Portsdown Chalk Formation* [Online]. Available: https://webapps.bgs.ac.uk/lexicon/lexicon.cfm?pub=PCK [Accessed 01 April 2022 2022].
BIALOWAS, G. A. 2017. Time and stress dependent mechanical properties of reconstituted chalk. Bristol: University of Bristol (Unpublished PhD Thesis).
BIENIAWSKI, Z. T. Geomechanics classification of rock masses and its applications in tunnelling. . Proceedings of the 3rd conference of the International Society of Rock Mechanics, 1974 Denver, United States of America.
BLOOMFIELD, J. P., BREWERTON, L. J. & ALLEN, D. J. 1995. Regional trends in matrix porosity and dry density of the Chalk of England. *The Quarterly Journal of Engineering Geology,* 28**,** 131-142.
BOSWELL, P. G. H. 1948. A preliminary examination of the thixotropy of some sedimentary rocks. *The Quarterly Journal of Engineering Geology and Hydrogeology,* civ**,** 499-526.
BOWDEN, A. J. 2013. Geological controls on tunnelling in the chalk of Southwick Hill, Brighton. *The Quarterly Journal of Engineering Geology and Hydrogeology,* 46**,** 203-213.
BRADFORD, R. D. 2002. Controls on the discharge of chalk streams of the Berkshire Downs, UK. . *Science of the Total Environment,* 282-283**,** 65-80.
BRISTOW, R., MORTIMORE, R. N. & WOOD, C. 1997. Lithostratigraphy for mapping the Chalk of southern England. *Proceedings of the Geological Association,* 108**,** 293-315.
BRITISH GEOLOGICAL SURVEY - STRANGE, P. J. 2006. *Lewes and Eastbourne. England and Wales. Bedrock and Superficial Deposits Sheet 319/334*, 1:50 000. Keyworth, Nottingham: British Geological Survey - Falvey, D.A.
BROMLEY, R. G. 1981. Enhancement of visibility of structures in marly chalk: modification of the Bushinsky oil technique. *Bulletin of the Geological Society of Denmark,* 29**,** 111-118.
BROMLEY, R. G. & GALE, A. S. 1982. The lithostratigraphy of the English Chalk Rock. *The Journal of Cretaceous Research,* 3**,** 273-306.
BSI 1990. BS 1377-2:1990 Methods of test for soils for civil engineering purposes. Classification tests. London: BSI.
BSI 2015. BS5930 Code of practice for site investigations. London: BSI.
BSI 2016. BS EN ISO 17892-4:2016 Geotechnical investigation and testing. Laboratory testing of soil. Determination of particle size distribution London: BSI.
BSI 2018. BS EN ISO 17892-9:2018 Geotechnical investigation and testing. Laboratory testing of soil. Consolidated triaxial compression tests on water saturated soils. London: BSI.
BSI 2022a. Geotechnical investigation and testing — Laboratory testing of soil. Part 1: Determination of water content London: BSI.
BSI 2022b. Methods of test for soils for civil engineering purposes. Classification tests and determination of geotechnical properties London: BSI.
BUSHINSKY, G. I. 1947. Textures and structures of Cretaceous chalk and flints (Russian with English Summary). *Bulletin of the Moscow Society of Naturalists,* 52**,** 37-43.
CATT, J. A. & HODGESON, J. M. 1976. Soils and geomorphology of the chalk of south-east England. *The Journal of Earth Surface Processes and Landforms,* 1**,** 181-193.
CLAYTON, C. 1983. The influence of diagenesis on some index properties of chalk in England. *Geotechnique,* 33**,** 225-241.
CLAYTON, C. R. I. 1978. Chalk as Fill Surrey: University of Surrey (Unpublished PhD Thesis).
CLAYTON, C. R. I. & MATTHEWS, M. C. 1987. Deformation, diagenesis and the mechanical behaviour of chalk. *In:* JONES, M. E. & PRESTON, R. M. F. (eds.) *Deformation of Sediments and Sedimentary Rocks, Special Publication.* London: Geological Society.

COLLINGS, A. V. J. 2018. Periglacial weathering and disturbance below valley bottoms. *In:* LAWRENCE, U. L., PREENE, M., LAWRENCE, J. & BUCKLEY, D. K. (eds.) *Engineering in Chalk.* London: ICE Publishing.

CONYBEARE, W. & PHILLIPS, W. 1822. *Outlines of the Geology of England and Wales. ,* London, Phillips, W.

CRAIG, R. F. & KNAPPET, J. A. 2012. *Craig's Soil Mechanics,* London, Spon Press.

CULLEN, E. 2021. The Potential of Interactive Ground Models: A focus on coastal erosion in East Sussex London: Imperial College London (Unpublished MSc thesis).

DE VARGAS, C., AUBRY, M.-P., PROBERT, I. & YOUNG, J. 2007. Chapter 12 - Origin and Evolution of Coccolithophores: From Coastal Hunters to Oceanic Farmers. *In:* FALKOWSKI, P. G. & KNOLL, A. H. (eds.) *Evolution of Primary Producers in the Sea.* Academic Press.

DELAGE, P., SCHRODER, C. & CUI, Y. J. Subsidence and capillary effects in chalks. Proceedings of EUROCK '96, Prediction and Performance on Rock Mechanics and Rock Engineering, 1996 Turin, Italy,. ISRM, 1291-1298.

DIGIMAP, E. 2023. Map of East Sussex. Tony Maher.

DOUGHTY, L. 2016. Laboratory testing of chalk. (Unpublished MSc Thesis). London: Imperial College London

DUNHAM, R. J. 1962. Classification of Carbonate Rocks According to Depositional Texture. *In:* HAM, W. E. (ed.) *Classification of Carbonate Rocks—A Symposium.* AAPG.

DUPERRET, A., TAIBI, S., MORTIMORE, R. N. & DAIGNEAULT, M. 2005. Effect of groundwater and sea weathering cycles on the strength of chalk rock from unstable coastal cliffs of NW France. *Engineering Geology,* 78**,** 321-343.

EMBRY, A. F. & KLOVAN, J. E. 1971. A Late Devonian Reef Tract on the North Western Banks Island, North West Territories. *Bulletin of Canadian Petroleum Geologists,* 19**,** 730-781.

FA-GOMORD, O., SOETE, J., DAVY, C. A., JANSSENS, N., TROADEC, D., CAZAUX, F., CALINE, B. & SWENNEN, R. 2017. Tight chalk: Characterization of the 3D pore network by FIB-SEM, towards the understanding of fluid transport. *The Journal of Petroleum Science and Engineering,* 156**,** 67-74.

FLETCHER, M. & MIZON, D. Paper 14: Piles in chalk for Orwell Bridge. Piling and ground treatment, 1984 London. Thomas Telford Publishing, 203-209.

FOLK, R. L. 1959. Practical Petrographic Classification of Limestones. *AAPG Bulletin,* 43**,** 1–38.

FRANKLIN, J. A. & CHANDRA, R. 1972. The slake-durability test. . *The International Journal of Rock Mechanics and Mining Sciences* 9**,** 325-328.

GALE, A. S. 2012. Late Cretaceous to Early Palaeogene Pelagic Deposits: Deposition on Greenhouse Earth. *In:* WOODCOCK, N. & STRACHAN, R. (eds.) *Geological History of Britain and Ireland.* London: Blackwell Publishing Ltd.

GALE, A. S., WOOD, C. J. & BROMLEY, R. G. 1987. The lithostratigraphy and marker bed correlation in the White Chalk (Cenomanian - Campanian) of Southern England. *The Journal of Mesozoic Research,* Vol 1**,** 107-118.

GALLOIS, R. 2006. Large-scale partial dissolution of the Chalk of the Devon coast and its engineering significance. *Geoscience in south-west England: proceedings of the Ussher Society,* 11**,** 123-131.

GAMBLE, J. C. 1971. *Durability-Plasticity; Classification of Shales and Other Argillaceous Rocks.* PhD, University of Illinois.

GIBBARD, P. L. & CLARK, C. D. 2011. Chapter 7 - Pleistocene Glaciation Limits in Great Britain. *In:* EHLERS, J., GIBBARD, P. L. & HUGHES, P. D. (eds.) *Developments in Quaternary Sciences.* London: Elsevier,.

GOOGLE-EARTH. 2021. *Map of East Sussex* [Online]. Available: https://earth.google.com/web/search/Birling+Gap,+Eastbourne/@50.79337249,0.11318966,82.20676349a,42786.96390964d,35y,0h,0t,0r/data=CoIBGlgSUgolMHg0N2RmNzc0M2NmOTAwZDkxOjB4ZTRlNzE1YWQ3OTA4ZGM1NBmieJW1TV9JQCFzu5f75CjKPyoXQmlybGluZyBHY

XAsIEVhc3Rib3VybmUYAiABIiYKJAnHiMOEG2M1QBHFiMOEG2M1wBnzX9e2slE2QCFpv7FXXkdUwDoDCgEw [Accessed 2021].
GOUDIE, A. 2006. The Schmidt hammer in geomorphological research. *Progress in Physical Geography,* 30**,** 703 - 718
GOUDIE, A. S., BULL, P. A. & MAGEE, A. W. 1989. Lithological control of Rillenkarren development in the Napier range, Western Australia. *Zeitschrift für Geomorphologie Supplementband,* 75**,** 95 - 114.
HADLOW, N. W. 2014. *Conceptual and digital geological models of Chalk catchments in Northern France and Southern England* PhD, University of Brighton (Unpublished PhD thesis).
HADLOW, N. W., LAWRENCE, J. A. & MORTIMORE, R. N. Evaluation and prediction of anticipated depths of weathering (engineering rockhead) as a function of geomorphology in areas of chalk outcrop in southern England and northern France. Engineering in Chalk: Proceedings of the Chalk 2018 Conference, 2018 London. ICE Publishing., 711-720.
HANCOCK, J. M. 1975. The petrology of the Chalk. *Proceedings of the Geologists' Association,* 86**,** 499-535.
HARMAN, E. 2020. Understanding the mechanismc leading to coastal cliff instability in Hunstyanton, Norfolk. London: Imperial College London Unpublished MSc.
HEAD, K. H. 2006. *Manual of soil laboratory testing Vol 1, Soil classification tests,* Dunbeath, Whittles.
HEGGHEIM, T., MADLAND, M. V., RISNES, R. & AUSTAD, T. 2005. A chemical induced enhanced weakening of chalk by seawater. *The Journal of Petroleum.,* 46**,** p171–181.
HIGGINBOTTOM, I. E. The Engineering Geology of Chalk. Chalk in Earthworks and Foundations Proceeds of Symposioum of the Institution of Cilvil Engineers, 1966 London. Institution of Civil Engineers, 1-13.
HOEK, E. 1994. Strength of rock and rock masses. *ISRM News Journal,* 2**,** 4-16.
HOEK, E. & BROWN, E. T. 2019. The Hoek-Brown failure criterion and GSI - 2018 edition. *The Journal of Rock Mechanics and Geotechnical Engineering,* 11**,** 445-463.
JORDAN, R. W. 2009. Coccolithophores. *In:* SCHAECHTER, M. (ed.) *Encyclopedia of Microbiology (Third Edition).* Academic Press.
KATZ, O., RECHES, Z. & ROEGIERS, J.-C. 2000. Evaluation of mechanical rock properties using a Schmidt Hammer. *The International Journal of Rock Mechanics and Mining Services* 37**,** 723-728.
KAWASAKI, S., TANIMOTO, C., KOIZUMI, K. & ISHIKAWA, M. 2002. An attempt to estimate mechanical properties of rocks using the Equotip hardness tester. *The Journal of the Japan Society of Engineering Geology,* 43**,** 244-248.
KIRUMAKKI, N. 1977. Some Aspects of Lithification in Chalk. *Transactions of the Nebraska Academy of Science,* 449**,** 229-231.
KOMPATSCHER, M. Equotip-rebound hardness testing after D. Leeb. Conference on hardness measurements theory and application in laboratories and industries, 2004 Washington DC, USA. 1-12.
KORSNES, R. I., MADLAND, M. V. & AUSTAD, T. Impact of brine composition on the mechanical strength of chalk at high temperature. *In:* COTTHEM, A. V., CHARLIER, R., THIMUS, J. F. & TSHINBANGU, J. P., eds. EUROCK '06, Multiphysics coupling and Long Term Behaviour in Rock Mechanics. Proceedings of the International Society for Rock Mechanics, 2006 Liege, Belgium. Taylor & Francis, p133 – 140.
LAKE, L. 1975. Engineering Properties of Chalk with Special Reference to Foundation Design and Performance. Surrey: University of Surrey (Unpublished PhD Thesis).
LAMONT-BLACK, J. & MORTIMORE, R. N. 1996. Determination of the intact dry density of irregular chalk lumps: a new method. *The Quarterly Journal of Engineering Geology and Hydrogeology,* 29**,** 241-248.

LAU, C. C. 2018. Coastal Weathering and Weakening of Chalk. London: Imperial College London (Unpublished MSc thesis).
LAWRENCE, J. A. 2007. Engineering Properties of chalk in relation to coastal cliff instability Brighton: University of Brighton (Unpublished PhD Thesis).
LAWRENCE, J. A., MORTIMORE, R. N., STONE, K. & BUSBY, J. P. 2013. Sea saltwater weakening of chalk and the impact on cliff instability. *Geomorphology,* 191**,** 14-22.
LAWRENCE, J. A., MORTIMORE, R. N. & THROWER, A. Macro and micro fabrics in chalk identified using the Bushinsky Oil Technique: an updated method and new applications for an old experimental technique. *In:* LAWRENCE, U. L., PREENE, M., LAWRENCE, J. A. & BUCKLEY, R., eds. Engineering in chalk: proceedings of the chalk 2018 conference, 2018a London. ICE Publishing, 549-555.
LAWRENCE, J. A., SPENCE, R., MORTIMORE, R. N., EADE, M. & BOTTRELL, S. H. 2018b. Coastal cliff rock mass weakening of Chalk and the impact of salt water. *Proceedings of the Institution of Civil Engineers – Geotechnical Engineering,* 171**,** 545-555.
LE, T., EIKSUND, G. & STRØM, P. Characterisation of Residual Shear Strength at the Sheringham Shoal Offshore Wind Farm. *In:* ASME, ed. Proceedings of the ASME 2014 33rd International Conference on Ocean, Offshore and Arctic Engineering, 2014 San Francisco, California. ASME.
LEEB, D. 1979. New dynamic method for hardness testing of metallic materials. *Revista de Metalurgia,* 15**,** 57-63.
LEWIS, P. 2022. The mechanical stratigraphy and fault zone deformation of the Austin Chalk in ten Mile Creek, Desoto, Texas. Texas Christian University (Unpublished BSc thesis).
LIU, T., AHMADI-NAGHADEH, R., VINCK, K., JARDINE, R. J., KONTOE, S., BUCKLEY, R. M. & BYRNE, B. W. 2021. An experimental investigation into the behaviour of destructured chalk under cyclic loading. *Géotechnique,* 0**,** 1-13.
LOKIER, S. & AL JUNAIBI, M. 2016. The petrographic description of carbonate facies: are we allspeaking the same language? *Sedimentology,* 63**,** 1843–1885.
LORD, J. A., CLAYTON, C. R. I. & MORTIMORE, R. N. 2002. *C574; Engineering in Chalk,* London, Construction Industry Research and Information Association (CIRIA).
MACDONALD, A. M. & ALLEN, D. J. 2001. Aquifer properties of the Chalk of England. *The Quarterly Journal of Engineering Geology and Hydrogeology,* 34**,** 371-384.
MACLEAN, S. 2023. *On the Strain Rate Dependence of Chalk.* MSc, Imperial College London (Unpublished MSc thesis).
MAGALHAES, T., AKHTAR, S. & GILBERT, P. 2018. Use of chalk on the A160 Port of Immingham Improvement scheme. *Engineering in Chalk.* ICE Publishing.
MAHER, A. 2019. The chalk of East Sussex as an analogue for Harwell, Oxfordshire - An evaluation of the CIRIA C574 density field identification method. Imperial College London (Unpublished MRes thesis).
MAHER, A. 2021a. *Newhaven sample locations May 2021*, 1:2500. London: Edina Digimap.
MAHER, A. 2021b. *Portobello quadrats May 2021*. London: Edina Digimap.
MAHER, A. 2021c. *Roedean, East Sussex*, 1:1250. London: Edina Digimap.
MAHER, A. 2022a. *Birling Gap quadrats May 2021*. Edina Digimap.
MAHER, A. 2022b. *Birling Gap, East Dean*, 1:2500. London: Edina Digimap.
MAHER, A. 2022c. *Portobello Outfall, Telscombe*, 1:2500. London: Edina Digimap.
MANTELL, G. 1822. *The Fossils of the South Downs; Or Illustrations of the Geology of Sussex.,* London, Lupton Relfe.
MARLEY, S. 2020. Correlation of the Lithostratigraphic and Geomechanical Properties of the Chalk Rock in the Transitional Province. London: Imperial College London (Unpublished MSc thesis).
MATTHEWS, J. A. & WINKLER, S. 2022. Schmidt-hammer exposure-age dating: A review of principles and practice. *Earth-Science Reviews,* 230**,** 104038.

MAURICE, L., FARRANT, A. R., MATHEWSON, E. & ATKINSON, T. 2023. Karst hydrogeology of the Chalk and implications for groundwater protection. *In:* FARRELL, R. P., MASSEI, N., FOLEY, A. E., HOWLETT, P. R. & WEST, L. J. (eds.) *Special Publication: The Chalk Aquifers of Northern Europe.* London: Geological Society.

MAURICE, L. D., ATKINSON, T. C., BARKER, J. A., BLOOMFIELD, J. P., FARRANT, A. R. & WILLIAMS, A. T. 2006. Karstic behaviour of groundwater in the English Chalk. *The Journal of Hydrology,* 330**,** 63-70.

MIDER, G. & LAWRENCE, J. A. Anisotropic permeability of chalk. *In:* PREENE, M., LAWRENCE, U. L., BUCKLEY, R. & LAWRENCE, J. A., eds. Engineering in Chalk, 2018 London. ICE Publishing, 481-487.

MIDER, M. 2017. Anisotropic permeability of chalk. London: Imperial College London (Unpublished MSc thesis).

MOLYNEUX, I. 2012. *Hydrogeological characterisation of the Chalk: with specific reference to the unsaturated zone* Brighton, University of Brighton (Unpublished PhD. Thesis).

MORSE, J. W. 2003. 7.03 - Formation and Diagenesis of Carbonate Sediments. *In:* HOLLAND, H. D. & TUREKIAN, K. K. (eds.) *Treatise on Geochemistry.* Pergamon.

MORTIMORE, R. 1997. *The Chalk of Sussex and Kent. No. 57,* London, The Geologists' Association.

MORTIMORE, R. 2014. *Logging the chalk,* Caithness, Whittles Publishing.

MORTIMORE, R. 2021. *The Chalk of the South Downs of Sussex and Hampshire and the North Downs of Kent*

MORTIMORE, R. N. 1986. The stratigraphy of the upper cretaceous white chalk of Sussex. *Proceedings of the Geologists Association,* 97**,** 79-139.

MORTIMORE, R. N. 2013. Geoconservation and the advancement of geosciences: lessons from the Chalk of England. *Proceedings of the Geologists' Association,* 124**,** 593-611.

MORTIMORE, R. N. & FIELDING, P. M. 1990. The relationship between texture, density and strength of chalk. *In:* MORTIMORE, R. N., ROBERTS, L. D. & JONES, D. L. (eds.) *Chalk International Symposium.* London: Thomas Telford Publishers - Institution of Civil Engineers.

MORTIMORE, R. N., LAWRENCE, J., POPE, D., DUPERRET, A. & GENTER, A. 2004a. Coastal cliff geohazards in weak rock: the UK Chalk cliffs of Sussex. *Geological Society, London, Engineering Geology Special Publications,* 20**,** 3-31.

MORTIMORE, R. N., STONE, K. J., LAWRENCE, J. A. & DUPERRET, A. 2004b. Chalk physical properties and cliff instability. *In:* MORTIMORE, R. N. & DUPERRET, A. (eds.) *Coastal Chalk cliff instability.* London: The Geological Society.

MORTIMORE, R. N., WOOD, C. J. & GALLOIS, R. W. 2001. *Geological Conservation Review Series - British Upper Cretaceous stratigraphy*, Joint Nature Conservation Committee (JNCC).

MOSES, C. 2014. Chapter 4 - The rock coast of the British Isles: shore platforms. *Geological Society, London, Memoirs,* 40**,** 39-56.

MOSES, C. & ROBINSON, D. 2011. Chalk coast dynamics: Implications for understanding rock coast evolution. *Earth Science Reviews,* 109**,** 63-73.

MOSES, C. & WILLIAMS, R. 2008. Weathering and durability of the Goldsworthy Chalk Stones, South Downs, West Sussex, England. *The Journal of Environmental Geology,* 56**,** 495–506.

MOSES, C. A., ROBINSON, D. A., WILLIAMS, R. B. G. & MARQUES, F. M. S. F. 2006. Predicting rates of platform downwearing from rock geotechnical properties and laboratory simulation of weatheirng and erosion processes. *Zeitschrift fur Geomorphologie, Supplementband,* 144**,** 19-37.

MURRAY, E. J. 2003. *Procedure for the determination of the permeability of clayey soils in a triaxial cell using the accelerated permeability test*, Environment Agency.

MURTON, J. Testing: in situ and laboratory: Frost weathering of chalk. *In:* LAWRENCE, J. A., PREENE, M., LAWRENCE, U. L. & BUCKLEY, R., eds. Engineering in Chalk – Proceedings of the Chalk 2018 Conference, 2018a London. ICE Publishing, 497-502.

MURTON, J. B. 2018b. Frost weathering of chalk. *Engineering in Chalk.*

MURTON, J. B. & BALLANTYNE, C. K. 2017. Chapter 5 - Periglacial and permafrost ground models for Great Britain. *Geological Society, London, Engineering Geology Special Publications,* 28**,** 501-597.
NEWELL, A. J., WOODS, M. A., FARRANT, A. R., SMITH, H. & HASLAM, R. B. 2018. Chalk thickness trends and the role of tectonic processes in the Upper Cretaceous of southern England. *Proceedings of the Geologists' Association,* 129**,** 610-628.
NEWMAN, T. G. & HADLOW, N. W. 2021. Geological structures beneath the River Thames in London: findings from the Thames Tideway Tunnel investigations. *The Quarterly Journal of Engineering Geology and Hydrogeology,* 54.
OLIVIER, H. J. 1979. A new engineering geological rock durability classification. *The Journal of Engineering Geology,* 14**,** 255-279.
OLSEN, T., BORELLA, J. & STAHL, T. 2020. Clast transport history influences Schmidt hammer rebound values. *The Journal of Earth Surface Processes and Landforms,* 45**,** 1392–1400.
PERRAS, M. & DIEDERICHS, M. The importance of classification for carbonates and mudrocks in engineering. 2011 Pan-Am CGS Geotechnical Conference, 2011 Toronto.
PHILLIPS, W. 1818. *A selection of facts from the Best Authorites so as to form an Outline of the Geology of England and Wales.,* London, Phillips, W.
PREENE, M. Introduction to Engineering in Chalk: the Chalk 2018 conference. *In:* LAWRENCE, J. A., PREENE, M., LAWRENCE, U. L. & BUCKLEY, R., eds. Engineering in Chalk - Proceedings of the Chalk 2018 Conference, 2018 London. ICE, 1 - 6.
PREENE, M. & ROBERTS, T. O. L. 2017. Construction dewatering in chalk. *Proceedings of the Institution of Civil Engineers, Geotechnical Engineering,* 170**,** 367-390.
PRICE, D. 1995. Weathering and weathering processes. *The Quarterly Journal of Engineering Geology,* 28**,** 243-252.
PRICE, M., LOW, R. G. & MCCANN, C. 2000. Mechanisms of water storage and flow in the unsaturated zone of the Chalk aquifer. . *The Journal of Hydrology,* 233**,** 54-71.
PROCEQ. 2021. *SilverSchmidt* [Online]. Available: https://www.screeningeagle.com/en/products/silver-schmidt-os8200 [Accessed 2021].
PROCEQ. 2023. *Schmidt OS120 pendulum hammer* [Online]. Available: https://www.screeningeagle.com/en/products/schmidt-os120 [Accessed 2023].
RAWSON, P., ALLEN, P. & GALE, A. 2001. The Chalk Group - A Revised Lithostratigraphy. *Geoscientist,* 11**,** 21.
RAZOAKI, R. N. 2000. Effect of ageing on mechanics of chalk slurries. Portsmouth: University of Portsmouth (Unpublished PhD Thesis).
RIGBY-JONES, J., CLAYTON, C. R. I. & MATTHEWS, M. C. 1994. 7. Dissolution features in the chalk: from hazard to risk. *In:* SKIPP, B. O. (ed.) *Risk and reliability in ground engineering.* London: Thomas Telford Publishing.
RISNES, R., HAGHIGHI, H., KORSNES, R. I. & NATVIK, O. 2003. Chalk-fluid interactions with glycol and brines. *Tectonophysics,* 370**,** 213-226.
RISNES, R., MAADLAND, M. V., HOLE, M. & KWABIAH, N. K. 2005. Water weakening of chalk – mechanical effects of water-glycol mixtures. *The Journal of Petroleum Science and Engineering,* 48**,** 21-36.
ROBINSON, D. A. 2020. The Chalk Coast of Sussex. *In:* GOUDIE, A. & MIGOŃ, P. (eds.) *Landscapes and Landforms of England and Wales. World Geomorphological Landscapes.* Cham. Switzerland: Springer.
SCHMIDT, E. 1950. Der Beton-Prufhammer. *Schweizer Baublatt,* 68**,** 378.
SCHOLLE, P. A. 1977. Chalk diagenesis and its relation to petroleum exploration: oil from chalks, a modern miracle? *AAPG Bulletin,* 61**,** 982-1009.
SCOTESE, C. R., VERARD, C., BURGENER, L., ELLING, R. P. & KOCSIS, A. T. 2025. *The Cretaceous world: plate tectonics, palaeogeographhy and palaeoclimate,* London, Geological Society, Special Publication.

SHI, T. 2022. Development of a slake durability database and correlation to other material properties London: Imperial College London (Unpublished MSc thesis).
SPEARING-BUNDY, S. P. 2013. Geotechnical Properties of Chalk Putties Portsmouth: University of Portsmouth (Unpublished PhD. Thesis).
SPINK, T. W. & NORBURY, D. R. The engineering geological description of chalk'. 1st Ed. , C. *In:* BURLAND, J. B., MORTIMORE, R. N., ROBERTS, L. D., JONES, B. L. & CORBETT, B. O., eds. Chalk. Proceedings of the International Chalk Symposium, 1990 London. Thomas Telford Publishing, 153-159.
STAVROU, A., LAWRENCE, J. A., MORTIMORE, R. N. & MURPHY, W. 2011. A geotechnical and GIS based method for evaluating risk exposition along coastal cliff environments: a case study of the chalk cliffs of southern England. *The Journal of Natural Hazards and Earth System Sciences,* 11**,** 2997-3011.
SUMNER, P. & NEL, W. 2002. The effect of rock moisture on Schmidt hammer rebound: tests on rock samples from Marion Island and South Africa. *The Journal of Earth Surface Processes and Landforms,* 27**,** 1137-1142.
THROWER, A., BARLOW, J., MOORE, R. & CANE, T. 2022. A pilot study investigating the rapid estimation of intact dry density of chalk using low impact energy hardness measurements taken with an Equotip Leeb hardness tester. *The Quarterly Journal of Engineering Geology and Hydrogeology,* 55.
TUDOR, D. 2019. Victorian chalk mine stability assessment in Reading, UK: influence of brittle geological structures. London: Imperial College London (Unpublished MSc thesis).
TWINE, D. & WRIGHT, R. 1991. Farmers Avenue Road Crossing, Castle Mall development, Norwich. *In:* INSTITUTE, D. F., ed. 4th International Conference on Piling and Deep Foundations, 1991 Stresa, Italy. Rotterdam, Brookfield: A.A. Balkema, 147-155.
TWISS, R. J. & MOORES, E. M. 2006. *Structural Geology*, W.H. Freeman.
TYRRELL, T. & YOUNG, J. R. 2009. Coccolithophores. *In:* STEELE, J. H. (ed.) *Encyclopedia of Ocean Sciences (Second Edition).* Academic Press.
VAN EECKHOUT, E. M. 1976. The mechanisms of strength reduction due to moisture in coal mine shales. *The International Journal of Rock Mechanics and Mining Sciences & Geomechanics,* 13**,** 61-67.
VERWAAL, W. & MULDER, A. 1993. Estimating rock strength with the Equotip hardness tester. . *The International Journal of Rock Mechanics and Mining Sciences and Geomechanics,* 30**,** 659-662.
VILES, H., GOUDIE, A., GRAB, S. & LALLEY, J. 2011. The use of the Schmidt Hammer and Equotip for rock hardness assessment in geomorphology and heritage science: a comparative analysis. *The Journal of Earth Surface Processes and Landforms,* 36**,** 320 - 333.
WAKELING, T. R. M. 1970. A comparison of the results of standard site investigation methods against the results of a detailed geotechnical investigation in Middle Chalk at Munford, Norfolk. In situ investigation in soil and rocks. *British Geotechnical Society***,** 17-22.
WARD, W. H., BURLAND, J. B. & GALLOIS, R. W. 1968. Geotechnical assessment of a site at Mundford, Norfolk, for a large proton accelerator. *Geotechnique,* 18**,** 399-431.
WILLIAMSON, M. & SOLERA, S. Engineering challenges building on Grade D chalk in East Anglia. *In:* LAWRENCE, J. A., PREENE, M., LAWRENCE, U. L. & BUCKLEY, R., eds. Engineering in Chalk, 2018 London. ICE Publishing, 297-302.
WOODWARD, S. 1833. *An outline of the Geology of Norfolk. ,* London, John Stacy; Longman & Co.
YAALON, D. H. & SINGER, S. 1974. Vertical variation in strength and porosity of calcrete (nari) on chalk, Shefela, Israel and interpretation of its origin. *The Journal of Sedimentary Petrology,* 44**,** 1016-1023.
ZADEH, A. 2018. Correlation of the lithostratigraphic and geomechanical properties of the white Chalk subgroup. London: Imperial College London (Unpublished MSc thesis).

Appendix A - CIRIA grading

App A-1 Cryoturbated lobe CIRIA gradings; Roedean.

Involution	Involution length (m)	Involution width (m)	Hammer pick penetration range (mm)	Average penetration (mm)	CIRIA Density grade
Cryoturbated involution 1	0.8	0.4	28 – 35	30	Low
Separating material 1	-	0.1	15 – 25	19.8	Medium
Cryoturbated involution 2	0.85	0.4	25 – 33	31.8	Low
Separating material 2	-	0.3	11 – 20	15.1	Medium
Cryoturbated involution 3	0.75	0.6	25 - 34	32.1	Low
Separating material 3	-	0.4	10 - 22	18	Medium
Cryoturbated involution 4	0.6	0.25	20 - 30	27	Medium
Separating material 4	-	0.2	12 - 25	19	Medium
Cryoturbated involution 5	0.4	0.35	24 - 38	31.5	Low
Separating material 5	-	0.3	12 - 32	22.3	Medium

App A-2 CIRIA weathering grades six sample points in structured chalk; Roedean

Section length (m)	Hammer penetration range (mm)	Average penetration (mm)	CIRIA density grade	Discontinuity spacing (mm)	Discontinuity aperture (mm)	CIRIA discontinuity grade
5.0	5 – 24	17.1	high	20 - 60	>3	C 4
10.0	9 – 24	13.5	high	20 - 60	>3	C 4
15.0	5 – 20	14.4	high	20 - 60	>3	C 4
20.0	5 – 12	8.1	high	20 - 60	>3	B 4
25.0	3 – 19	14.4	high	20 - 60	<3	B 4
30.0	5 – 12	8	high	20 - 60	Closed	A 4

App A-3 CIRIA weathering grades; east side of Portobello outfall – Culver Chalk Formation;

Section length (m)	Hammer penetration range (new pick) (mm)	Average penetration (mm)	CIRIA density grade	Discontinuity spacing (mm)	Discontinuity aperture (mm)	CIRIA Discontinuity grade
2.0	3 – 8	6.8	High	20 – 100	>3	C 3-4
4.0				20 – 300	>3	C 2-4
6.0				200 – 300	Closed	A 2
8.0	3 – 7	4.66	High	200 – 600	>3	C 2
10.0				<600	>3	C 2
12.0				>600	<3	B 1
14.0	3 – 6	3.66	High	<600	<3	B 2
16.0				<600	<3	B 2
18.0				20 – 100	>3/closed	C 3-4
20.0	6 – 11	7.83	High	200 – 300	<3	B 2
22.0				200 – 600	<3	B 2
24.0				>600	<3	B 1
26.0	3 – 6	3.8	High	600 – 1000	>3	C 1
28.0				20 – 300	<3	B 2-4
30.0	2 – 6	3.8	High	20 – 400	Closed	A 2-4

App A-4 CIRIA weathering grades; west side of Portobello outfall – Newhaven Chalk Formation;

Section length (m)	Hammer penetration range (new pick) (mm)	Average penetration (mm)	CIRIA density grade	Discontinuity spacing (mm)	Discontinuity aperture (mm)	CIRIA Discontinuity grade
5.0	2 – 7	4.8	high	200 – 600	closed	A 2
10.0	4 – 9	6.4	high	60 – 200	>3 mm	C 3
15.0	3 – 9	5.2	high	200 – 600	>3 mm	C 2
20.0	3 – 9	5	high	200 – 600	>3 mm	C 3

App A-5 CIRIA weathering grades; Portobello dry valley – east flank

Length along section (m)	**Hammer (new pick) penetration range (mm)**	**Average penetration (mm)**	**CIRIA Density**	**Hammer (used pick) penetration range (mm)**	**Average penetration (mm)**	**CIRIA Density**	**Nail penetration range (mm)**	**Average penetration (mm)**	**CIRIA Density**	**Grade**
2.0	26 - 42	34.33	low/med	22 - 54	39.66	low	45 - 62	52.66	low	Dm
4.0	25 - 32	28.1	medium	18 - 35	25.5	medium	28 - 44	35.5	low	Dm
6.0	11 - 26	19.8	medium	16 - 35	21.8	medium	22 - 30	24.2	low/medium	Dm
8.0	18 - 21	19	medium	11 - 24	17	medium	22 - 35	26.2	low	Dm
9.0	11 - 20	18	medium	15 - 21	17.5	medium	20 - 26	23.8	medium	Dm
11.0	11 - 16	14.16	high	12 - 19	15.5	medium	14 - 19	16.6	medium	Dc
13.0	11 - 20	15.16	high	11 - 20	14.8	medium	14 - 18	16	medium	Dc
14.0	10 - 18	13.33	high	9 - 16	12.8	medium	15 - 20	17	medium	Dm
16.0	9-17	14.33	high	14 - 20	16.33	medium	18 - 22	21.5	medium	Dm
18.0	11 - 19	14.33	high	13 - 21	16.5	medium	18 - 21	21.25	medium	Dc
20.0	18 - 31	23.5	medium	15 - 22	18.66	medium	19 - 27	21.75	medium	Dc
22.0	14 - 22	17.5	medium/high	14 - 22	18.8	medium	10 - 15	12.25	medium	Dc

App A-6 CIRIA weathering grades; Portobello dry valley – west flank

Length along section (m)	Hammer (new pick) penetration range (mm)	Average penetration (mm)	CIRIA Density	Hammer (used pick) penetration range (mm)	Average penetration (mm)	CIRIA Density	Nail penetration range (mm)	Average penetration (mm)	CIRIA Density	Grade
2.0	16 - 21	17.33	high	10 - 14	12	medium	16 - 21	18.25	medium	Dm
4.0	11 - 16	14.7	high	10 - 14	11.7	medium	11 - 17	13.75	high	Dc
6.0	14 - 24	19	medium	14 - 21	15.5	medium	18 - 22	20.25	medium	Dc
8.0	11 - 16	14	high	11 - 15	12.2	medium	14 - 21	17.75	medium	Dm
10.0	16 - 21	17.8	high	12 - 16	14.3	medium	14 - 24	19.75	medium	Dm
12.0	17 - 25	20.5	medium	12 - 19	14.3	medium	20 - 24	21.75	medium	Dm

App A-7 CIRIA weathering grades – Newhaven Harbour;

Sample point	Hammer penetration range (new pick) (mm)	Average penetration (mm)	CIRIA density grade	Discontinuity spacing (mm)	Discontinuity aperture (mm)	CIRIA Discontinuity grade
1	9 - 14	11	Low	<600	<3	A-1 to B-5
2	8 - 15	11.41	Low	60 - 200	<3	B-3 to B-2
3	9 - 12	11.16	Low	>600	Closed	A-1
4	6 - 12	8.01	Medium	200 - 600	<3	B-2
5	6 - 14	10.03	Medium	>600	Closed	A-1

App A-8 CIRIA weathering grades, Birling gap, West of valley axis

Length along section (m)	Hammer (New) range (mm)	Average	CIRIA density	Hammer (Old) range (mm)	Average	CIRIA density	Nail range (mm)	Average	CIRIA density	Discontinuity spacing (mm)	Discontinuity aperture (mm)	Discontinuity grade
5.0	7-11	18.16	medium	5-9	7	high	10-15	12.75	high	20-500	<3mm	B 2 - 4
10.0	6-10	9	High	6-11	9.66	high	8-16	11.5	med/high	20-30	>3mm	C 4
15.0	15-23	18.66	medium	12-14	12.8	medium	9-22	17.75	medium	20-30	>3mm	C 4
20.0	8-15	12.4	High	12-15	13	medium	13-18	16.5	medium	20-30	>3mm	C 4

App A-8 CIRIA weathering grades, Birling gap, East of valley axis

Length along section (m)	Hammer (New) range (mm)	Average	CIRIA density	Hammer (Old) range (mm)	Average	CIRIA density	Nail range (mm)	Average	CIRIA density	Discontinuity spacing (mm)	Discontinuity aperture (mm)	Discontinuity grade
5.0	6-14	9.66	High	7-14	10.16	high	12-24	16.5	medium	100	<3mm	B 3
10.0	16-22	19.33	medium	12-20	15.66	medium	8-20	13	high	20	>3mm	C 4-5
15.0	6-14	9.5	High	7-12	8.83	high	9-13	10.75	high	20	>3mm	C 4-5
20.0	3-7	5	High	6-11	10.16	high	4-7	5.75	high	100-150	<3mm	B 3

App A-8 CIRIA weathering grades, Birling gap, centre of valley axis

Length along section (m)	Hammer (new pick) penetration range (mm)	Average penetration (mm)	CIRIA Density	Hammer (used pick) penetration range (mm)	Average penetration (mm)	CIRIA Density	Nail penetration range (mm)	Average penetration (mm)	CIRIA Density	Grade
4.0	25 - 32	28.1	medium	22 - 54	39.66	low	22 - 30	24.2	low/medium	Dc
9.0	11 - 20	18	medium	15 - 21	17.5	medium	19 - 27	21.75	medium	Dc
14.0	10 - 16	14.33	high	14 - 20	16.33	medium	14 - 19	16.6	medium	Dc
18.0	11 - 19	14.33	high	18 - 35	25.5	medium	18 - 22	21.5	medium	Dm
22.0	14 - 24	18.2	medium/high	14 - 22	18.8	medium	18 - 21	21.25	medium	Dc

Appendix B - Quadrat photographs

Birling Gap

Quadrat 1



Quadrat 2



Quadrat 3



Quadrat 4



Quadrat 5



Roedean

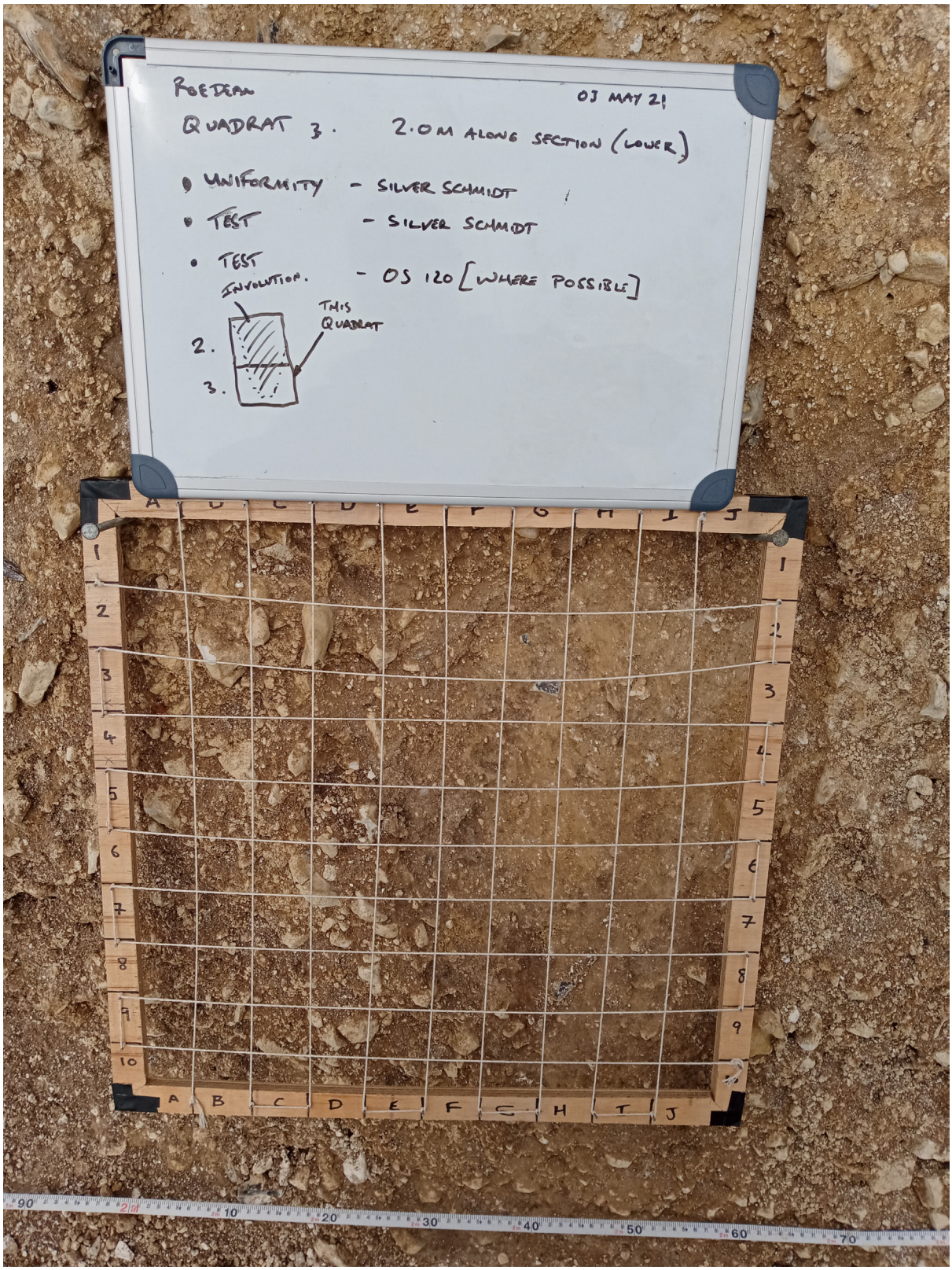
Quadrat 1



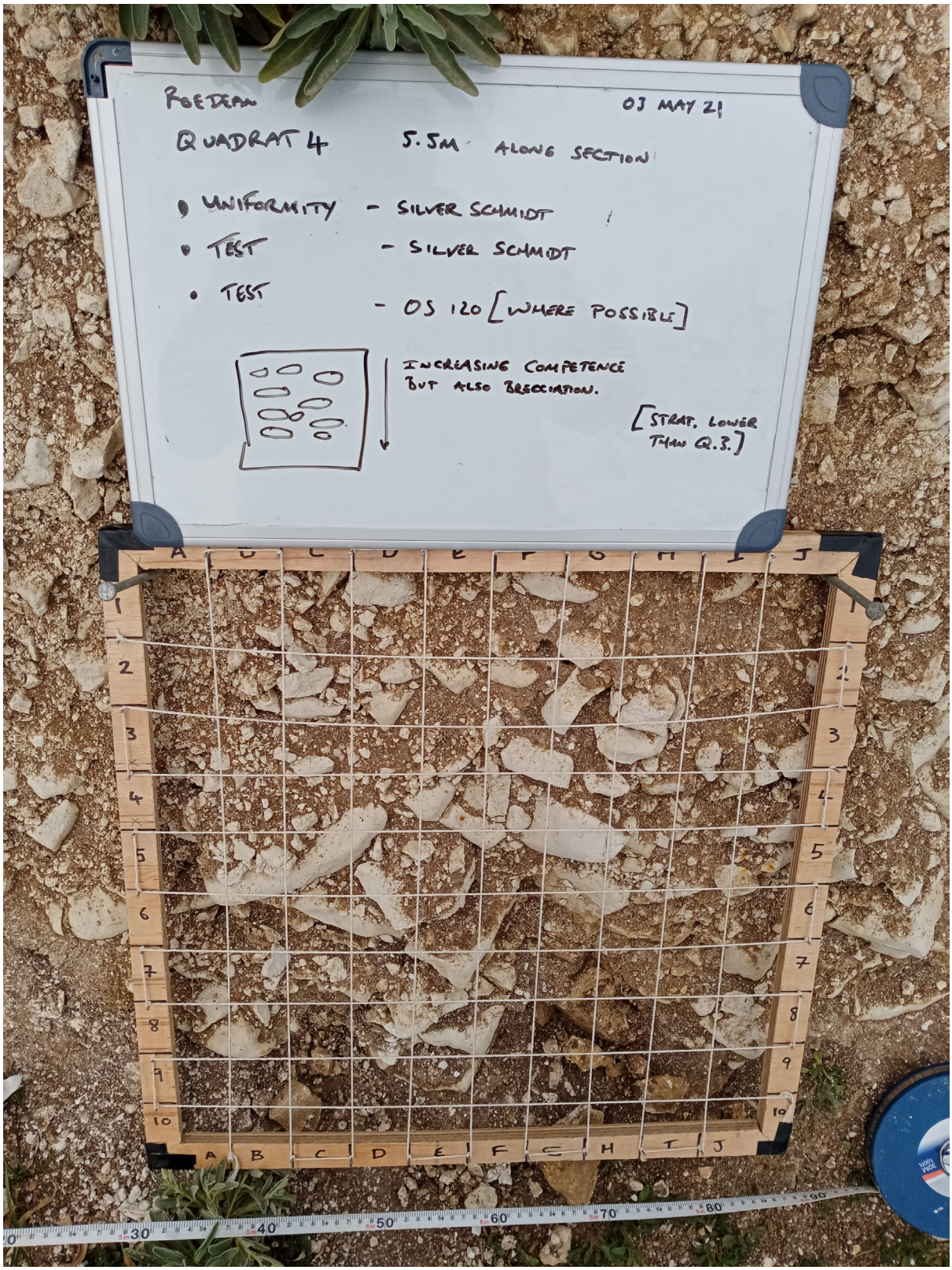
Quadrat 2


ROEDEAN
03 MAY 21
QUADRAT 2. 2.0M ALONG SECTION (UPPER)
• UNIFORMITY - SILVER SCHMIDT
• TEST - SILVER SCHMIDT
• TEST INVOLUTION. - OS 120 [WHERE POSSIBLE]
THIS QUADRAT
A B C D E F G H I J
1 2 3 4 5 6 7 8 9 10

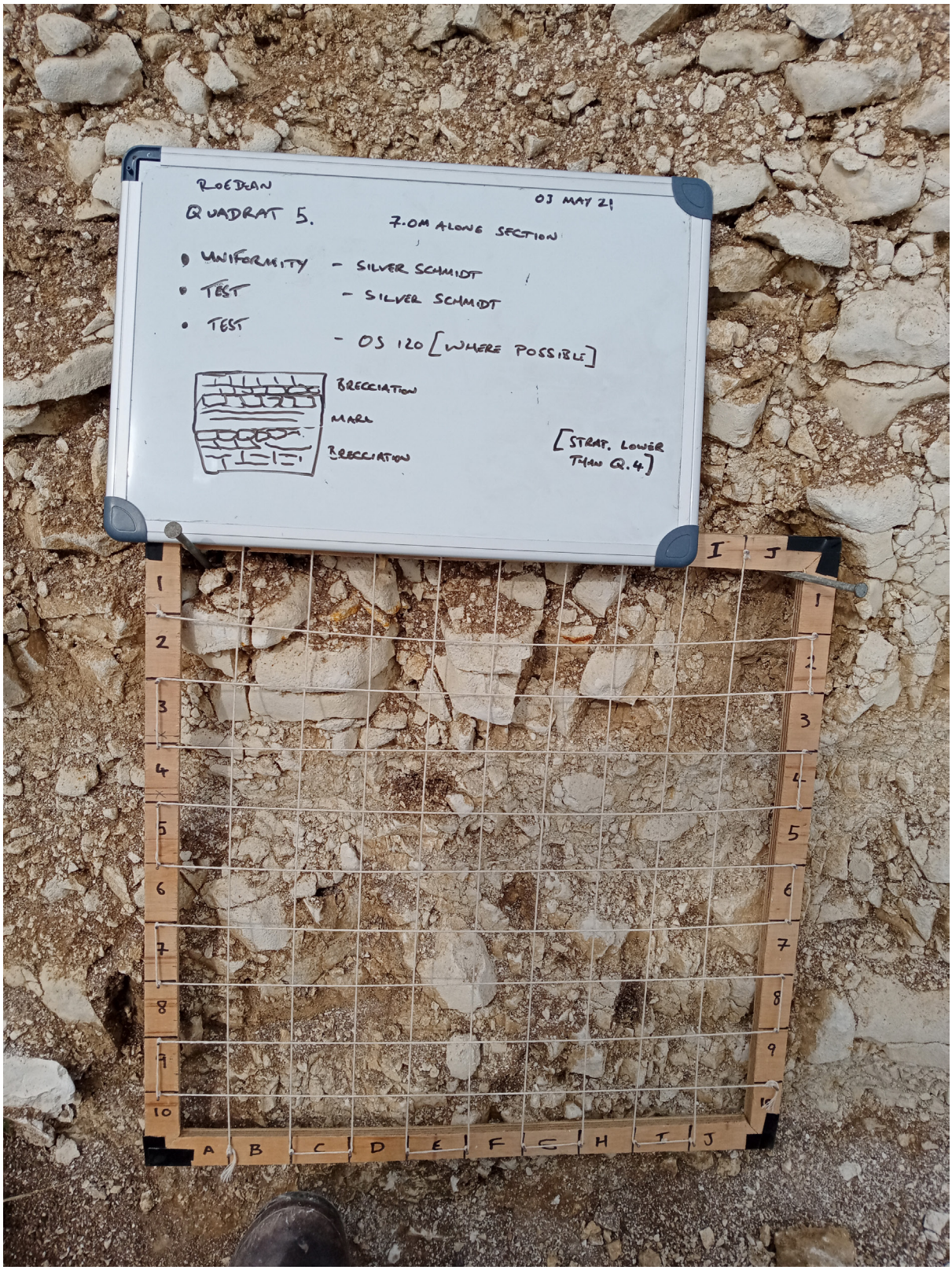
Quadrat 3


ROEDEAN
03 MAY 21
QUADRAT 3. 2.0M ALONG SECTION (LOWER)
• UNIFORMITY - SILVER SCHMIDT
• TEST - SILVER SCHMIDT
• TEST - OS 120 [WHERE POSSIBLE]
INVOLUTION.
THIS QUADRAT
2.
3.
A B C D E F G H I J
1 2 3 4 5 6 7 8 9 10

Quadrat 4


ROEDEAN
03 MAY 21
QUADRAT 4
5.5M ALONG SECTION
• UNIFORMITY - SILVER SCHMIDT
• TEST - SILVER SCHMIDT
• TEST - OS 120 [WHERE POSSIBLE]
INCREASING COMPETENCE
BUT ALSO BRECCIATION.
[STRAT. LOWER THAN Q.3.]

Quadrat 5


ROEDEAN
03 MAY 21
QUADRAT 5.
7.0M ALONG SECTION
• UNIFORMITY - SILVER SCHMIDT
• TEST - SILVER SCHMIDT
• TEST - OS 120 [WHERE POSSIBLE]
BRECCIATION
MARL
BRECCIATION
[STRAT. LOWER THAN Q.4]
I J
1 2 3 4 5 6 7 8 9 10
A B C D E F G H I J

Quadrat 6


REEDEAN
07 MAY 21
QUADRAT 6
13.0 M ALONG SECTION
• UNIFORMITY - SILVER SCHMIDT
• TEST - SILVER SCHMIDT
• TEST - OS 120 WHERE POSSIBLE
HIGHER COMPETENCY.
LESS WEATHERED.

Quadrat 7



Quadrat 8



Newhaven

Quadrat 1



Quadrat 2



Quadrat 3



Quadrat 4



Quadrat 5



Portobello

Quadrat 1



Quadrat 2



Quadrat 3



Quadrat 4



Quadrat 5



Quadrat 6

NO PHOTOGRAPH

Quadrat 7



Quadrat 8



Appendix C – Quadrat raw data

SilverSchmidt data

Roedean research site

Quadrat 1

	A	B	C	D	E	F	G	H	I	J
1	12.5	9.5	9	13	9	10.5	11.5	14	7.5	0
2	10	14	13	12	12	8	17.5	7	0	0
3	10	11.5	11.5	10.5	9.5	8.5	11	10	7	14
4	11	7.5	12.5	12.5	8	11.5	7.5	11.5	10	12
5	7.5	6.5	10.5	11.5	10.5	11	7.5	9	10	11.5
6	8.5	11	9	10	8.5	0	0	7	10	8
7	9.5	7.5	8	10	0	0	9	7	10.5	10.5
8	11	15.5	9.5	12.5	0	11.5	10.5	8.5	10	9.5
9	11	12	12	8	7.5	10.5	6.5	11	15.5	9.5
10	7.5	8.5	10.5	9.5	6.5	10	7	11.5	11	7.5

Quadrat 2

	A	B	C	D	E	F	G	H	I	J
1	0	0	13.5	8.5	0	7.5	7.5	9	0	7.5
2	9	5.5	9	10	7	8	9	7.5	0	7
3	11	11.5	7	12	6.5	7	10	7.5	8	9.5
4	0	0	8	7	0	9.5	10.5	9.5	8.5	8
5	0	10.5	11	11	6	6.5	7.5	6.5	11	12.5
6	11.5	9	9.5	0	0	6.5	8.5	7.5	7	8
7	10.5	0	8	0	6.5	9	9	9	7	7
8	0	10	9.5	0	10	17.5	9	7	7	6.5
9	0	10	0	10	8.5	9	9	6.5	10	11
10	0	7	9.5	10	12	9	0	12	12	11

Quadrat 3

	A	B	C	D	E	F	G	H	I	J
1	7	0	0	8	9	6.5	9	7.5	8	6.5
2	8.5	0	0	8.5	9	6	8	8.5	10	9.5
3	0	0	0	8	9	9.5	12.5	10.5	10.5	13
4	0	0	0	0	0	7.5	9	7.5	0	8.5
5	0	0	0	0	0	9.5	9	11.5	0	0
6	0	0	0	0	0	11	11.5	12.5	10.5	7.5
7	0	0	0	0	0	0	9.5	9	8	8.5
8	0	0	0	0	0	0	7.5	10.5	9	0
9	0	0	0	0	0	9	8	10	9.5	0
10	0	0	0	0	10	9	0	10	12	9

Quadrat 4

	A	B	C	D	E	F	G	H	I	J
1	0	0	0	0	0	0	0	0	0	10
2	0	0	0	0	0	0	0	0	0	0
3	0	0	0	0	0	0	0	0	0	0
4	0	0	0	0	0	0	0	0	0	0
5	0	9.5	0	0	0	0	0	9.5	0	0
6	0	0	8	0	0	0	0	0	0	0
7	0	0	0	0	0	0	14.5	0	0	0
8	0	0	0	0	0	0	0	0	0	20
9	21.5	0	0	0	0	0	0	0	0	10
10	0	0	0	0	18.5	0	0	0	0	0

Quadrat 5

	A	B	C	D	E	F	G	H	I	J
1	0	0	0	0	0	0	8.5	0	7.5	7
2	0	9.5	12	12	9	0	0	0	7.5	7
3	14	15	9.5	15	13	0	0	0	7.5	7
4	7	7.5	8	0	9	8	7.5	7	7.5	6
5	8.5	0	6.5	8.5	8.5	7	6	7.5	7.5	8
6	9	9	8	0	0	0	0	0	0	0
7	9	9	0	0	0	0	0	0	0	0
8	0	0	0	0	0	0	0	0	0	0
9	0	0	0	0	0	0	0	0	0	0
10	0	0	0	0	0	0	0	13	13	13

Quadrat 6

	A	B	C	D	E	F	G	H	I	J
1	0	0	20	23	27.5	15	18.5	0	0	0
2	13	0	20	20	14.5	22	17.5	0	0	0
3	22	24	24.5	17.5	20.5	20.5	22.5	9	0	23
4	21	11.5	625	14.5	29.5	18.5	17	11.5	0	9.5
5	9	10	11	20.5	10	17	0	7	8	13.5
6	0	10	12	13	8	9	0	7.5	9	8.5
7	0	10	11	9	23.5	21	20	19	20	7
8	0	0	0	9	21.5	9	0	7.5	16	17
9	0	0	0	0	0	0	0	0	16	7
10	0	0	0	0	10	27	16	16	16	7

Quadrat 7

	A	B	C	D	E	F	G	H	I	J
1	12.5	22.5	12.5	10	25.5	23.5	14	33	30.5	10
2	10	18.5	19	17.5	29	13.5	9	13	10	0
3	9.5	9.5	14	21.5	28	26.5	21.5	8	20.5	11
4	12.5	9	9.5	17.5	17.5	6.5	6.5	10.5	9	10.5
5	0	11	6.5	8.5	8	0	0	0	0	0
6	0	0	0	0	0	0	0	0	0	0
7	0	0	0	0	0	0	0	0	0	0
8	0	0	0	6	0	7	0	0	0	0
9	0	0	0	0	0	0	0	9	9	0
10	0	0	0	0	0	0	0	9	9	0

Quadrat 8

	A	B	C	D	E	F	G	H	I	J
1	6.5	7.5	6	18	16	16	18	0	0	0
2	7	9.5	8	8	0	0	0	0	9.5	9.5
3	9.5	20.5	11	24.5	24.5	15.5	18	25	21	17.5
4	28	23.5	26.5	8	12.5	16.5	10	31	30.5	22
5	10.5	28	23.5	19	16	22.5	23	28	10	14
6	9	8.5	10	22.5	20.5	17.5	14	23.5	14.5	8
7	0	20.5	15	14	22	26.5	0	9	7	7
8	0	29	12.5	21.5	9	21.5	8.5	8.5	10	12.5
9	0	11	20	27.5	11.5	21	7	12	8	18
10	9.5	2.5	22	30.5	24.5	17	11	11	10	14.5

Portobello Outfall research site

Quadrat 1

	A	B	C	D	E	F	G	H	I	J
1	24	21	19	27	19.5	9	17.5	14	15.5	21
2	8.5	14.5	19	14	0	23.5	20	20	16	10.5
3	10.5	14.5	10.5	11	13.5	23	16	23	25	22.5
4	12	14.5	12.5	20.5	7	10.5	19	13.5	13	13.5
5	0	10.5	14	15	0	18	24.5	13.5	200.5	25.5
6	12	7	15.5	8	9.5	14	20.5	12.5	20	19.5
7	15.5	9.5	12.5	13	18	13.5	10	23.5	13	26.5
8	14.5	18.5	18	6.5	14	14.5	7	18	23	27.5
9	14.5	23	25.5	14.5	10.5	17	11.5	23.5	25	14.5
10	0	0	0	0	0	0	0	0	0	0

Quadrat 2

	A	B	C	D	E	F	G	H	I	J
1	10	11	0	0	10	17.5	0	0	18	28
2	32	24.5	19.5	14	25.5	22	14.5	13	23	24
3	24.5	19	18	16	22	14	18.5	8.5	16	22
4	18	12	21	15	14	20.5	17.5	9	11	13
5	20	26	21	21	22	19	25.5	16.5	14	13
6	18	24.5	27.5	25	14	15.5	21.5	10.5	12	10
7	0	17	20	16	18.5	0	14	20.5	13	13
8	0	29	21.5	22	21	18	16.5	30	25	21
9	19	14.5	21	23	29.5	24	14	12	15	20.5
10	22	27.5	18	25	29	12	14.5	16.5	21.5	20

Quadrat 3

	A	B	C	D	E	F	G	H	I	J
1	22	12	19.5	10.5	10.5	29.5	19.5	18.5	13	16.5
2	28	12	17	16.5	0	26	20.5	22	20.5	15
3	27.5	11.5	24	12.5	16.5	29	33	26.5	27	12.5
4	29.5	26	16	16.5	16	28	27	27.5	24.5	18
5	0	16.5	24	18	10	14	20.5	16.5	24.5	20.5
6	17.5	23.5	20.5	16	9.5	15	23	30.5	25.5	21.5
7	20	19.5	18	14	12	25.5	29	30	27.5	20.5
8	28.5	10	23.5	22	14	11.5	23	13	14	0
9	34	27.5	28.5	12	26.5	30.5	27	14.5	22	20
10	33	28.5	27	20.5	34.5	18	27	12.5	28	17.5

Quadrat 4

	A	B	C	D	E	F	G	H	I	J
1	0	0	0	0	12.5	11	20.5	18	14.5	28
2	0	0	0	25.5	10.5	21	25	9	14	26
3	0	0	0	9.5	12	0	8	0	15	0
4	0	0	8.5	16.5	18	12	12	13	26.5	12.5
5	0	0	12.5	0	10.5	8	11.5	16.5	26	25
6	0	0	11	17.5	20	19.5	17.5	24.5	27.5	18.5
7	0	0	26	14.5	13.5	13	11	13.5	21	0
8	0	17.5	0	0	0	0	0	0	0	0
9	0	13.5	21	0	0	0	0	0	0	0
10	0	0	9	0	0	0	0	0	0	0

Quadrat 5

	A	B	C	D	E	F	G	H	I	J
1	17.5	15	26.5	28	25	21	21	14.5	15	11.5
2	21	15.5	14	20	18.5	14.5	23	21.5	15.5	25.5
3	25	29.5	20.5	25.5	14	10.5	18	16	28	18
4	20.5	20	24.5	20.5	18.5	28	33	33	20.5	23
5	18.5	29	26.5	26	25	19.5	32	18	25	19
6	30.5	28.5	25	28.5	23	24.5	26.5	18.5	30	17
7	13.5	25.5	28	23	23	28	24.5	32.5	23	26
8	20.5	27.5	25	27	22	19	23	21.5	22.5	20.5
9	19.5	18	16.5	28	27	23.5	12.5	10.5	9.5	15
10	0	0	0	0	0	0	0	0	0	0

Quadrat 6

	A	B	C	D	E	F	G	H	I	J
1	26.5	25.5	19	14.5	25	29	31	25	14	19.5
2	29.5	28	27.5	25	25	28.5	27	31	30	30
3	26	26.5	16	23.5	24	31.5	29	31	32	31.5
4	24	16	29	30	24	29.5	18.5	32	25.5	29
5	29	28	15.5	28	28	26.5	27	22.5	24.5	31.5
6	18	30	25.5	27.5	27.5	28.5	26.5	34	29	24.5
7	30	31	29.5	25	25	25	22	31.5	34	27
8	27.5	32.5	30	24	24	19	27.5	28	29.5	25.5
9	17.5	18	19	25	25	0	16.5	28.5	26.5	29.5
10	0	0	10.5	10.5	0	11	29	27.5	32	29.5

Quadrat 7

	A	B	C	D	E	F	G	H	I	J
1	0	11	11.5	15.5	11.5	13.5	15.5	15	10	8.5
2	8	8	9.5	11.5	11	11	10.5	15	14.5	11
3	16	12	12.5	10.5	11	12.5	11.5	11.5	15.5	10.5
4	7	11	12	10	12.5	18.5	16	13	7.5	15
5	16	10	12	14	18	13.5	22	9	21	11.5
6	20	20.5	19.5	21	21.5	19	13	12	22	10.5
7	13.5	20	13	22	22	19.5	10.5	13.5	10	26
8	21.5	17.5	27.5	17	13	11.5	17.5	23	14.5	16
9	26	13.5	17.5	18.5	13	0	10	12	0	12.5
10	0	21.5	24.5	0	12.5	15	15	14.5	14.5	13.5

Quadrat 8

	A	B	C	D	E	F	G	H	I	J
1	27.5	20	15.5	26	24.5	13.5	24	22	14	21.5
2	18.5	12.5	25.5	12.5	17.5	25	29.5	8	11	25.5
3	10	11	16.5	23.5	21.5	15.5	23.5	11	11.5	12.5
4	17	11	30	19	26.5	12	21	10	13	14
5	19.5	17	31	28	25	22.5	12	21	12.5	10.5
6	15.5	9.5	21	29	23.5	21.5	12	19.5	14.5	20.5
7	18.5	28	28	16.5	22	23	25	14.5	10	8.5
8	9.5	19.5	9	0	9.5	9.5	12.5	13	15.5	15
9	8	21	13.5	19	13	16	16	20.5	23	11
10	21.5	19.5	23.5	18.5	20	13	18	10.5	32	13

Newhaven research site

Quadrat 1

	A	B	C	D	E	F	G	H	I	J
1	25.5	25.5	10	22.5	15	20	13.5	14	9.5	7
2	31	19.5	25.5	20	31.5	15.5	25.5	8.5	10	12.5
3	20.5	22.5	24.5	23.5	13.5	22.5	13.5	13.5	13.5	13
4	19	33	28	27.5	13	28.5	23	22	11	14
5	13.5	19	18.5	12.5	9	30.5	28	22	8.5	0
6	9.5	21	21	25	20.5	11	29	17	21.5	20.5
7	7.5	22.5	25	21.5	21	11	15.5	22	15	10.5
8	11.5	16.5	30	17.5	16	25.5	26.5	13	24	7.5
9	24.5	23.5	14.5	12	14	13.5	23.5	23.5	23.5	14.5
10	20	24	23.5	9	18	12	25.5	28.5	28	10.5

Quadrat 2

	A	B	C	D	E	F	G	H	I	J
1	11.5	9	21.5	0	16.5	18	22	12.5	26	17
2	9	17.5	23.5	23	13	7.5	24.5	27	28.5	8
3	8	22.5	26.5	14	25	21	11	8	7	8
4	20.5	11.5	23	28.5	22	17.5	9.5	10	13	8
5	23.5	27.5	23	23.5	19	21	8	10	16	21
6	30.5	31	16	16	23.5	17.5	24	31	28.5	24.5
7	21	27.5	27	9.5	20.5	21.5	16.5	8.5	26	12.5
8	32	27.5	33	20	27	21	12.5	10	26	25.5
9	31	31.5	31	23.5	29	10.5	29.5	15.5	10	16
10	31	22	31	25	20	13.5	20.5	14	9	10.5

Quadrat 3

	A	B	C	D	E	F	G	H	I	J
1	20	14	12	12	25	28.5	29	25.5	15	16.5
2	29.5	15.5	10.5	12	24.5	31.5	29	19	26.5	16.5
3	20	12	8	19.5	30.5	20.5	21.5	28	19	32.5
4	23.5	9	0	21.5	22	30	26.5	15.5	19.5	23.5
5	19	28.5	13.5	13.5	23	27	22	19	10.5	6.5
6	14	23	25	19	19.5	24.5	18	24	18	12.5
7	21.5	10	21	15.5	11	25	21.5	16.5	16.5	26
8	20.5	24	13	7	15.5	28.5	18.5	15.5	24	19.5
9	27.5	16.5	12	9.5	17	20	17.5	11.5	13.5	0
10	10.5	20.5	8.5	15	30.5	16.5	16	21.5	24	7.5

Quadrat 4

	A	B	C	D	E	F	G	H	I	J
1	14.5	19.5	21.5	28.5	23.5	13.5	21	23	26.5	20.5
2	13.5	17	13	18.5	17	26.5	18.5	19	22	26.5
3	18.5	21.5	22	20.5	8.5	13	24	12.5	27.5	22.5
4	30	28	24	27	24.5	19	11	11	28.5	25
5	7.5	22	29	26	18	25	13.5	22	18.5	23.5
6	14	14	15.5	24.5	28.5	24.5	11.5	20.5	18.5	24.5
7	13	23.5	17	18.5	30	27.5	24	15	21	30.5
8	7.5	13.5	16	11.5	19	30.5	25.5	17.5	22	19
9	14.5	18.5	17.5	19.5	13	13.5	16	16.5	24.5	23
10	9.5	10	9	15	22	18	17.5	14	14.5	24

Quadrat 5

	A	B	C	D	E	F	G	H	I	J
1	13.5	21	29.5	18	15.5	20.5	25.5	11	17.5	13.5
2	18.5	28	15	24	25.5	11	12	15	15.5	12
3	13.5	16.5	13	13	19.5	20	19	8	16.5	7
4	26	14	25.5	31.5	19.5	28	27	27.5	19	23
5	16.5	27	27	19.5	29	29.5	27.5	18.5	23.5	28.5
6	24.5	13	19.5	20	22.5	26	17	20	22.5	13
7	11	12.5	22.5	28.5	23.5	17.5	19	27	21.5	10.5
8	12	15	23.5	25.5	21	18	19	22	25.5	21
9	15	19	15.5	28.5	29	27.5	10.5	20.5	18.5	11
10	10.5	25.5	15	26	20	13.5	29	24.5	10.5	10

Birling Gap research site

Quadrat 1

	A	B	C	D	E	F	G	H	I	J
1	14.5	9	20	11	13.5	0	10.5	0	0	12.5
2	11	0	13	0	0	0	8	11.5	0	9.5
3	11.5	11.5	6.5	15	0	10.5	8	12.5	12	10
4	15	6.5	0	15	9.5	7.5	12	8.5	8	10.5
5	0	10	8	9	16.5	20.5	0	10	8.5	8.5
6	0	12.5	24	27	10.5	0	11.5	0	11	8.5
7	11	0	13.5	10	11.5	0	13	9	13.5	21
8	9	7	9	9.5	8	0	0	0	0	0
9	8.5	9.5	12.5	9	10	10.5	11.5	0	0	0
10	0	9.5	8.5	0	8	10	11.5	12	0	0

Quadrat 2

	A	B	C	D	E	F	G	H	I	J
1	22.5	14	10	20	22	21	13	10	9	0
2	13.5	8.5	11	9.5	15	0	13	8.5	11	14.5
3	11.5	7.5	9.5	7	0	11.5	19	7.5	0	0
4	12.5	0	14	12.5	17.5	20.5	12.5	10	0	0
5	16	9	8.5	9	15.5	18.5	9	10.5	0	0
6	13.5	9.5	14	17.5	23	26	12	12	13	12.5
7	13.5	16	19.5	25.5	26.5	18.5	14.5	6	12.5	10
8	20.5	11	21	22.5	17	12.5	10	9.5	10	10
9	10	10	19	7	8.5	12.5	11.5	7.5	12	11
10	13.5	21.5	19	9.5	10	12.5	7.5	15.5	6.5	6.5

Quadrat 3

	A	B	C	D	E	F	G	H	I	J
1	19.5	17.5	11	11	15.5	13	14	22	10	15
2	23	22.5	18.5	19.5	6.5	11	9	15	17	20
3	11	17.5	20.5	9.5	16.5	13.5	12	21	9	16.5
4	24.5	19.5	20.5	20	13	19	15	14	17.5	19.5
5	15.5	13.5	23.5	16	20.5	23	18.5	11.5	10.5	14
6	18	11	13	12.5	25.5	22.5	26.5	16	20	13.5
7	17	16.5	15.5	10.5	20	21.5	25.5	22	13.5	25
8	12.5	14.5	15	24.5	17	23	12	18	16	18
9	26	20	23.5	25.5	22	14	11.5	13	11	22.5
10	19.5	21	16	27.5	14	20.5	24.5	16.5	20.5	13.5

Quadrat 4

	A	B	C	D	E	F	G	H	I	J
1	8.5	9.5	7	7.5	11.5	11.5	12.5	9.5	9.5	8
2	0	7	7	7.5	11	9	6.5	6	9.5	0
3	0	0	0	0	11.5	9.5	13.5	0	7.5	6.5
4	21.5	11	7	9	7	8	7.5	7	10	8.5
5	6.5	6.5	7	8	11	11.5	9.5	6.5	12.5	8.5
6	0	0	8	8	6	10	8	9	13.5	8.5
7	0	9.5	9	8	7	0	8	8.5	8.5	9
8	10.5	7	9	10	10.5	12	7.5	12	10.5	12.5
9	12	0	10	10	0	0	11	8	0	12.5
10	0	0	0	0	0	7	6.5	11.5	11.5	6.5

Quadrat 5

	A	B	C	D	E	F	G	H	I	J
1	8.5	25.5	19.5	18.5	8.5	25.5	22.5	15.5	8.5	12.5
2	13.5	31.5	10.5	10.5	16	12.5	13	21.5	20	14.5
3	10	12	17.5	16.5	17	25.5	21	19	21.5	12.5
4	19.5	13	21.5	29	16.5	14.5	21	22	12	15.5
5	16	11	18.5	13	15.5	23	15	18.5	22	19.5
6	10.5	23	10	25	21.5	15.5	11	12	24.5	26
7	10.5	10	24.5	12.5	18.5	16	11.5	11.5	20.5	14
8	20	16	21	16.5	18	25	16	17	16.5	17.5
9	11	16	12.5	10	12.5	10	20.5	19	12.5	13.5
10	12.55	16	17.5	10	13	15.5	8.5	15	13	19

Equotip data

Roedean research site

Quadrat 1

	A	B	C	D	E	F	G	H	I	J
1	200	202	262	222	245	248	220	244	246	206
2	201	220	211	210	283	330	222	202	229	213
3	244	324	225	224	217	285	204	211	237	204
4	221	260	248	277	259	217	292	207	311	312
5	252	247	334	248	235	261	212	243	214	236
6	212	287	221	202	202	205	271	211	201	254
7	210	214	204	220	210	230	209	223	219	219
8	250	340	239	253	232	242	225	243	254	200
9	282	349	206	275	249	208	286	310	313	331
10	203	247	221	298	202	204	251	225	263	203

Quadrat 2

	A	B	C	D	E	F	G	H	I	J
1	236	205	202	255	293	202	249	220	308	274
2	192	212	292	275	191	187	281	250	278	222
3	235	295	251	207	201	273	200	240	268	345
4	296	236	312	206	203	208	205	244	251	287
5	218	206	386	326	212	240	238	202	205	201
6	203	217	245	439	211	349	234	232	206	259
7	348	303	201	224	239	276	243	300	310	270
8	267	245	201	231	200	289	206	283	215	255
9	209	257	295	226	266	247	306	341	220	205
10	209	0	0	0	0	0	0	0	0	0

Quadrat 3

	A	B	C	D	E	F	G	H	I	J
1	258	236	230	240	413	267	279	256	241	232
2	238	264	233	289	227	205	294	327	282	212
3	206	233	259	302	242	202	244	253	293	243
4	209	227	215	299	213	214	236	284	207	239
5	205	241	208	256	236	234	210	212	207	243
6	203	207	257	266	256	235	301	255	203	225
7	242	348	391	217	203	238	255	357	342	235
8	230	207	236	279	256	330	234	355	233	327
9	291	325	359	260	324	323	303	263	246	222
10	200	244	221	263	246	299	300	303	249	295

Quadrat 4

	A	B	C	D	E	F	G	H	I	J
1	243	212	213	779	632	257	214	223	298	209
2	222	256	257	218	296	279	221	202	263	319
3	220	277	218	897	242	246	235	274	217	239
4	208	220	214	227	229	219	300	409	213	346
5	208	242	264	274	298	257	276	291	273	285
6	224	213	212	471	538	245	253	292	308	257
7	232	245	302	527	238	411	337	283	250	225
8	200	297	355	248	292	312	263	221	212	227
9	220	270	322	219	234	220	246	239	328	249
10	267	326	359	371	414	260	259	346	396	276

Quadrat 5

	A	B	C	D	E	F	G	H	I	J
1	337	204	304	291	297	239	303	279	377	280
2	292	301	235	280	263	220	252	346	287	226
3	243	346	210	276	215	252	292	239	267	247
4	232	275	288	289	229	312	220	237	295	205
5	269	314	215	325	288	326	244	253	211	212
6	247	328	407	436	317	226	205	213	266	205
7	277	313	313	298	201	215	211	250	210	231
8	248	293	329	209	243	314	328	219	278	201
9	275	249	204	277	338	312	334	342	299	245
10	225	206	227	226	256	335	295	273	219	215

Quadrat 6

	A	B	C	D	E	F	G	H	I	J
1	334	519	519	357	536	216	354	441	258	218
2	209	245	373	364	445	439	349	392	365	247
3	282	350	390	269	336	280	325	280	221	309
4	229	302	271	340	432	433	454	287	208	327
5	276	220	218	202	345	441	341	316	351	221
6	229	328	291	224	206	348	294	273	255	267
7	266	204	290	283	237	314	210	275	290	226
8	280	256	289	220	291	325	415	352	448	531
9	296	298	265	281	226	267	393	200	311	340
10	244	316	318	282	259	290	242	258	241	315

Portobello research site

Quadrat 5

	A	B	C	D	E	F	G	H	I	J
1	247	232	222	260	250	220	202	220	238	213
2	233	284	208	203	263	230	209	267	244	323
3	238	239	270	271	248	231	275	213	204	249
4	229	239	220	218	242	294	220	271	236	320
5	313	269	205	232	299	260	323	236	322	283
6	201	207	210	247	235	297	224	237	241	226
7	234	266	276	212	319	211	283	283	223	345
8	371	237	235	289	286	362	221	201	208	248
9	225	201	215	207	254	207	250	205	236	310
10	293	339	291	232	240	245	302	287	300	220

Quadrat 6

	A	B	C	D	E	F	G	H	I	J
1	211	297	276	304	209	220	202	220	238	213
2	284	255	306	217	256	230	209	267	244	323
3	308	257	212	311	204	231	275	213	204	249
4	230	273	311	309	356	294	220	271	236	320
5	203	213	238	244	220	260	247	236	322	283
6	207	246	214	295	280	237	228	226	273	242
7	222	213	216	209	230	297	329	245	209	209
8	272	219	227	212	224	211	212	226	213	202
9	246	222	319	219	218	232	244	236	279	255
10	293	201	269	251	206	284	223	272	226	226

Quadrat 7

	A	B	C	D	E	F	G	H	I	J
1	299	294	215	206	288	309	317	253	201	239
2	220	206	243	212	252	257	237	274	293	222
3	307	244	238	231	201	217	246	311	281	208
4	273	272	243	246	203	225	253	212	229	241
5	288	228	211	224	208	218	344	202	221	217
6	234	253	258	251	245	294	229	209	212	201
7	232	213	216	237	288	234	215	203	211	212
8	215	241	326	258	220	316	271	205	233	216
9	276	210	225	250	277	206	253	265	306	318
10	228	294	221	221	274	224	243	228	206	201

Quadrat 8

	A	B	C	D	E	F	G	H	I	J
1	280	209	211	230	311	254	230	257	224	233
2	241	246	264	233	218	209	203	222	218	282
3	246	236	277	240	254	233	299	221	210	274
4	236	240	202	283	305	206	216	252	213	290
5	233	229	267	247	213	223	292	244	208	222
6	218	212	239	282	329	211	225	207	232	255
7	240	202	250	227	345	205	207	203	255	285
8	208	224	211	226	241	214	215	228	211	201
9	213	247	207	223	242	200	262	298	251	208
10	284	235	231	301	223	238	238	212	283	221

Newhaven research site

Quadrat 4

	A	B	C	D	E	F	G	H	I	J
1	217	262	231	218	272	319	312	261	309	215
2	201	233	230	200	271	223	214	402	254	218
3	239	216	206	316	227	287	296	289	226	206
4	224	347	202	204	242	222	289	315	254	218
5	266	213	248	237	224	211	255	232	213	215
6	282	249	257	249	273	219	266	252	251	223
7	306	223	220	256	280	329	224	302	263	213
8	307	278	285	310	247	294	333	220	265	267
9	320	482	259	253	306	268	319	211	256	210
10	341	237	242	235	284	339	254	230	251	226

Quadrat 5

	A	B	C	D	E	F	G	H	I	J
1	231	211	284	225	301	202	239	242	257	223
2	203	273	268	273	236	207	286	265	238	260
3	283	231	202	233	237	208	315	240	266	302
4	279	211	219	213	225	216	312	268	236	356
5	227	235	270	280	224	272	250	228	239	226
6	224	211	268	242	263	231	230	296	287	221
7	289	239	222	238	258	255	242	273	307	263
8	259	226	253	274	291	244	277	255	211	294
9	234	298	232	270	280	243	327	334	230	266
10	235	227	265	213	244	355	304	274	287	234

Birling Gap research site

Quadrat 1

	A	B	C	D	E	F	G	H	I	J
1	210	267	260	249	230	225	259	223	202	221
2	214	237	240	250	223	271	301	261	209	209
3	247	266	233	217	230	247	293	326	268	243
4	239	256	357	209	243	266	279	280	224	309
5	220	208	241	233	218	273	224	258	228	281
6	573	230	240	265	201	257	200	213	237	246
7	204	227	262	239	202	269	392	216	319	275
8	258	261	234	238	246	234	233	202	246	211
9	255	228	253	272	289	237	271	248	208	278
10	202	237	251	231	201	254	205	218	211	248

Quadrat 2

	A	B	C	D	E	F	G	H	I	J
1	240	253	246	248	227	342	238	276	205	202
2	311	259	259	288	246	223	216	210	268	238
3	226	270	201	207	206	289	279	259	218	215
4	244	291	285	225	256	257	225	209	227	240
5	258	218	250	231	224	221	271	216	251	231
6	233	229	267	247	213	280	209	211	230	311
7	218	212	239	282	329	241	246	264	233	218
8	240	202	250	227	345	246	236	277	240	254
9	208	224	211	226	241	236	240	202	283	305
10	213	247	207	223	242	284	235	231	301	223

Quadrat 3

	A	B	C	D	E	F	G	H	I	J
1	245	250	204	313	237	254	230	257	224	233
2	206	313	208	309	249	209	203	222	218	282
3	216	232	224	237	206	233	299	221	210	274
4	202	245	205	211	218	206	216	252	213	290
5	306	284	220	295	217	223	292	244	208	222
6	262	278	209	283	203	275	235	240	282	232
7	235	225	221	235	230	205	280	257	262	281
8	214	253	232	218	245	231	282	257	244	208
9	248	229	230	226	224	225	326	220	229	220
10	260	210	239	203	274	292	208	234	231	249

Quadrat 4

	A	B	C	D	E	F	G	H	I	J
1	211	225	207	232	255	237	228	226	273	242
2	205	207	203	255	285	297	329	245	209	209
3	214	215	228	211	201	211	212	226	213	202
4	200	262	298	251	208	232	244	236	279	255
5	238	238	212	283	221	284	223	272	226	226
6	210	269	314	254	306	285	221	220	207	253
7	302	309	222	272	300	246	209	235	275	205
8	203	203	254	212	253	221	215	245	224	242
9	282	211	265	241	208	236	282	209	228	298
10	214	212	258	204	222	231	253	229	310	211

Quadrat 5

	A	B	C	D	E	F	G	H	I	J
1	211	297	276	304	209	298	404	216	280	301
2	284	255	306	217	256	262	257	332	229	257
3	308	257	212	311	204	220	224	251	259	217
4	230	273	311	309	356	247	318	321	374	283
5	203	213	238	244	220	235	253	261	260	247
6	207	246	214	295	280	272	309	298	209	207
7	222	213	216	209	230	216	219	210	303	232
8	272	219	227	212	224	208	256	267	243	254
9	246	222	319	219	218	228	221	213	234	275
10	293	201	269	251	206	253	264	200	260	217

Appendix D - Index tests

IDD

IDD by formation (collated from previous MSc research projects by (Mider, 2017, Lau, 2018, Zadeh, 2018, Marley, 2020, Harman, 2020);

App D-1 Culver Chalk Formation;

Formation	Location	SMC (%)	IDD (Mg/m^3)	NMC (%)	Mean SMC (%)	Mean IDD (Mg/m^3)	Mean NMC (%)
Culver Chalk Formation	Newhaven Harbour	27.69	1.50	8.61			
Culver Chalk Formation	Newhaven Harbour	32.11	1.45	12.68			
Culver Chalk Formation	Newhaven Harbour	25.92	1.59	4.54			
Culver Chalk Formation	Newhaven Harbour	28.44	1.53				
Culver Chalk Formation	Newhaven Harbour	26.76	1.57				
Culver Chalk Formation	Newhaven Harbour	26.70	1.57		27.94	1.53	8.61

App D–2 Newhaven Chalk Formation;

Formation	Location	SMC (%)	IDD (Mg/m^3)	NMC (%)	Mean SMC (%)	Mean IDD (Mg/m^3)	Mean NMC (%)
Newhaven Chalk Formation	Telscombe Cliffs	20.11	1.75	29.00			
Newhaven Chalk Formation	Telscombe Cliffs	21.07	1.72	18.43			
Newhaven Chalk Formation	Telscombe Cliffs	20.63	1.73	18.52			
Newhaven Chalk Formation	Roedean		1.64				
Newhaven Chalk Formation	Roedean		1.76				
Newhaven Chalk Formation	Roedean		1.78				
Newhaven Chalk Formation	Roedean		1.73				
Newhaven Chalk Formation	Roedean		1.86				
Newhaven Chalk Formation	Roedean		1.69				
Newhaven Chalk Formation	Roedean		1.72		20.60	1.74	21.98

App D-3 Seaford Chalk Formation;

Formation	Location	SMC (%)	IDD (Mg/m^3)	NMC (%)	Mean SMC (%)	Mean IDD (Mg/m^3)	Mean NMC (%)
Seaford Chalk Formation	Shoreham Quarry	21.89	1.68				
Seaford Chalk Formation	Shoreham Quarry	19.26	1.78				
Seaford Chalk Formation	Shoreham Quarry	21.06	1.72				
Seaford Chalk Formation	Shoreham Quarry	24.48	1.63				
Seaford Chalk Formation	Shoreham Quarry	16.19	1.81				
Seaford Chalk Formation	Shoreham Quarry	19.36	1.77				
Seaford Chalk Formation	Shoreham Quarry	21.13	1.72				
Seaford Chalk Formation	Shoreham Quarry	20.64	1.73				
Seaford Chalk Formation	Shoreham Quarry	21.13	1.72				
Seaford Chalk Formation	Birling Gap	29.18	1.57	24.21			
Seaford Chalk Formation	Birling Gap		1.64				
Seaford Chalk Formation	Birling Gap		1.76				
Seaford Chalk Formation	Birling Gap		1.78				
Seaford Chalk Formation	Birling Gap		1.73				
Seaford Chalk Formation	Birling Gap		1.86				
Seaford Chalk Formation	Birling Gap		1.69				
Seaford Chalk Formation	Birling Gap		1.72				
Seaford Chalk Formation	Birling Gap	20.23	1.75	24.37			
Seaford Chalk Formation	Birling Gap	24.77	1.62	24.39			
Seaford Chalk Formation	Birling Gap	19.52	1.77	23.95			
Seaford Chalk Formation	Birling Gap	20.83	1.73	24.11			
Seaford Chalk Formation	Birling Gap	23.44	1.65	23.63			
Seaford Chalk Formation	Birling Gap	24.46	1.63	24.88			
Seaford Chalk Formation	Birling Gap	22.76	1.67	22.64			
Seaford Chalk Formation	Birling Gap	24.74	1.62	24.61			
Seaford Chalk Formation	Birling Gap	19.83	1.76	16.81			
Seaford Chalk Formation	Birling Gap	16.49	1.87				
Seaford Chalk Formation	Birling Gap	18.68	1.80	14.65			

Seaford Chalk Formation	Birling Gap	25.79	1.59				
Seaford Chalk Formation	Birling Gap	31.27	1.46				
Seaford Chalk Formation	Birling Gap	27.47	1.55				
Seaford Chalk Formation	Birling Gap	24.82	1.62				
Seaford Chalk Formation	Birling Gap	24.18	1.62				
Seaford Chalk Formation	Birling Gap	23.08	1.68				
Seaford Chalk Formation	Birling Gap	24.93	1.61	24.77			
Seaford Chalk Formation	Birling Gap	21.77	1.70	20.17			
Seaford Chalk Formation	Birling Gap	21.22	1.72	16.81			
Seaford Chalk Formation	Birling Gap	24.52	1.63	25.16			
Seaford Chalk Formation	Birling Gap	20.97	1.72	21.58			
Seaford Chalk Formation	Birling Gap	22.86	1.67	23.74			
Seaford Chalk Formation	Birling Gap	24.81	1.62	23.24			
Seaford Chalk Formation	Birling Gap	22.49	1.68	22.82			
Seaford Chalk Formation	Birling Gap	24.50	1.63	22.77			
Seaford Chalk Formation	Birling Gap	24.46	1.63	22.59	22.68	1.69	22.47

App D-4 Lewes Nodular Chalk Formation;

Formation	Location	SMC (%)	IDD (Mg/m^3)	NMC (%)	Mean SMC (%)	Mean IDD (Mg/m^3)	Mean NMC (%)
Lewes Nodular Chalk Formation	Shoreham Quarry	20.01	1.67	14.01			
Lewes Nodular Chalk Formation	Shoreham Quarry	17.80	1.82	11.90			
Lewes Nodular Chalk Formation	Shoreham Quarry	23.43	1.65	15.77			
Lewes Nodular Chalk Formation	Shoreham Quarry	19.91	1.76	11.98			
Lewes Nodular Chalk Formation	Shoreham Quarry	28.10	1.54	16.37			
Lewes Nodular Chalk Formation	Shoreham Quarry	18.06	1.82				
Lewes Nodular Chalk Formation	Shoreham Quarry	19.68	1.76				
Lewes Nodular Chalk Formation	Shoreham Quarry	18.16	1.81	8.12			
Lewes Nodular Chalk Formation	Shoreham Quarry	26.64	1.57	3.44			
Lewes Nodular Chalk Formation	Shoreham Quarry	14.89	1.93	2.20			
Lewes Nodular Chalk Formation	Shoreham Quarry	14.58	1.94	4.24			
Lewes Nodular Chalk Formation	Shoreham Quarry	15.32	1.91	6.35			
Lewes Nodular Chalk Formation	Birling Gap	22.07	1.69	22.19			
Lewes Nodular Chalk Formation	Birling Gap	14.75	1.93	15.61			
Lewes Nodular Chalk Formation	Birling Gap	17.84	1.82	14.26			
Lewes Nodular Chalk Formation	Hope Gap	22.77	1.67	20.59			
Lewes Nodular Chalk Formation	Hope Gap	19.01	1.78	15.68			
Lewes Nodular Chalk Formation	Hope Gap	22.95	1.67	22.43			
Lewes Nodular Chalk Formation	Hope Gap	26.94	1.52	17.63			

Lewes Nodular Chalk Formation	Hope Gap	19.08	1.78	20.37			
Lewes Nodular Chalk Formation	Hope Gap	20.83	1.73	23.88			
Lewes Nodular Chalk Formation	Hope Gap	22.84	1.67	19.71	20.26	1.75	14.34

App D-5 New Pit Chalk Formation;

Formation	Location	SMC (%)	IDD (Mg/m^3)	NMC (%)	Mean SMC (%)	Mean IDD (Mg/m^3)	Mean NMC (%)
New Pit Chalk Formation	Beachy Head	22.41	1.68	5.59			
New Pit Chalk Formation	Beachy Head	19.48	1.77	5.88			
New Pit Chalk Formation	Beachy Head	21.83	1.70	12.39			
New Pit Chalk Formation	Beachy Head	22.40	1.68	12.62			
New Pit Chalk Formation	Birling Gap	14.94	1.92	13.70			
New Pit Chalk Formation	Birling Gap	10.46	2.11	10.80	18.59	1.81	10.16

App D-6 Holywell Nodular Chalk Formation;

Formation	Location	SMC (%)	IDD (Mg/m^3)	NMC (%)	Mean SMC (%)	Mean IDD (Mg/m^3)	Mean NMC (%)
Holywell Nodular Chalk Formation	Cow Gap	8.04	2.22	2.94			
Holywell Nodular Chalk Formation	Cow Gap	8.94	2.18	2.14			
Holywell Nodular Chalk Formation	Birling Gap	9.95	2.13		8.98	2.17	2.54

App D-7 Zig Zag Chalk Formation;

Formation	Location	SMC (%)	IDD (Mg/m^3)	NMC (%)	Mean SMC (%)	Mean IDD (Mg/m^3)	Mean NMC (%)
Zig Zag Chalk Formation	Cow Gap	11.97	2.13	2.89			
Zig Zag Chalk Formation	Cow Gap	13.14	1.99	3.03			
Zig Zag Chalk Formation	Cow Gap	15.94	1.89	2.88			
Zig Zag Chalk Formation	Cow Gap	9.91	2.13	3.02			
Zig Zag Chalk Formation	Cow Gap	7.83	2.23	2.71			
Zig Zag Chalk Formation	Cow Gap	7.80	2.23	2.67			
Zig Zag Chalk Formation	Cow Gap	9.21	2.16	2.88			
Zig Zag Chalk Formation	Birling Gap	11.53	2.06		10.92	2.10	2.87

App D-8 West Melbury Marly Chalk Formation;

Formation	Location	SMC (%)	IDD (Mg/m^3)	NMC (%)	Mean SMC (%)	Mean IDD (Mg/m^3)	Mean NMC (%)
West Melbury Marly Chalk Formation	Birling Gap	8.79	2.18	7.43			
West Melbury Marly Chalk Formation	Birling Gap	5.01	2.32	3.15			
West Melbury Marly Chalk Formation	Birling Gap	8.08	2.22	7.32			
West Melbury Marly Chalk Formation	Southerham	14.54	1.94	5.70			
West Melbury Marly Chalk Formation	Southerham	14.25	1.95	7.00			
West Melbury Marly Chalk Formation	Southerham	15.02	1.92	6.12	10.95	2.09	6.12

App D-9 Equotip measured IDD versus laboratory measured IDD data

Measurement	Formation	Average IDD	Min	Max	SD
Newhaven Chalk	Newhaven Chalk Formation	1.74	1.64	1.86	0.06
Newhaven Dc	Newhaven Chalk Formation	1.56	1.47	1.68	0.07
Newhaven Dm	Newhaven Chalk Formation	1.50	1.41	1.60	0.06
Equotip derived IDD - Roedean	Newhaven Chalk Formation	1.73	1.48	3.60	0.21
Equotip derived IDD - Portobello	Newhaven Chalk Formation	1.66	1.52	2.04	0.11
Seaford Chalk	Seaford Chalk Formation	1.68	1.46	1.87	0.08
Seaford Dc	Seaford Chalk Formation	1.54	1.43	1.65	0.06
Seaford Dm	Seaford Chalk Formation	1.56	1.54	1.57	0.01
Equotip derived IDD - Birling Gap	Seaford Chalk Formation	1.66	1.52	2.64	0.11

App D-10 Equotip versus laboratory data – grade Dc Seaford Chalk Formation

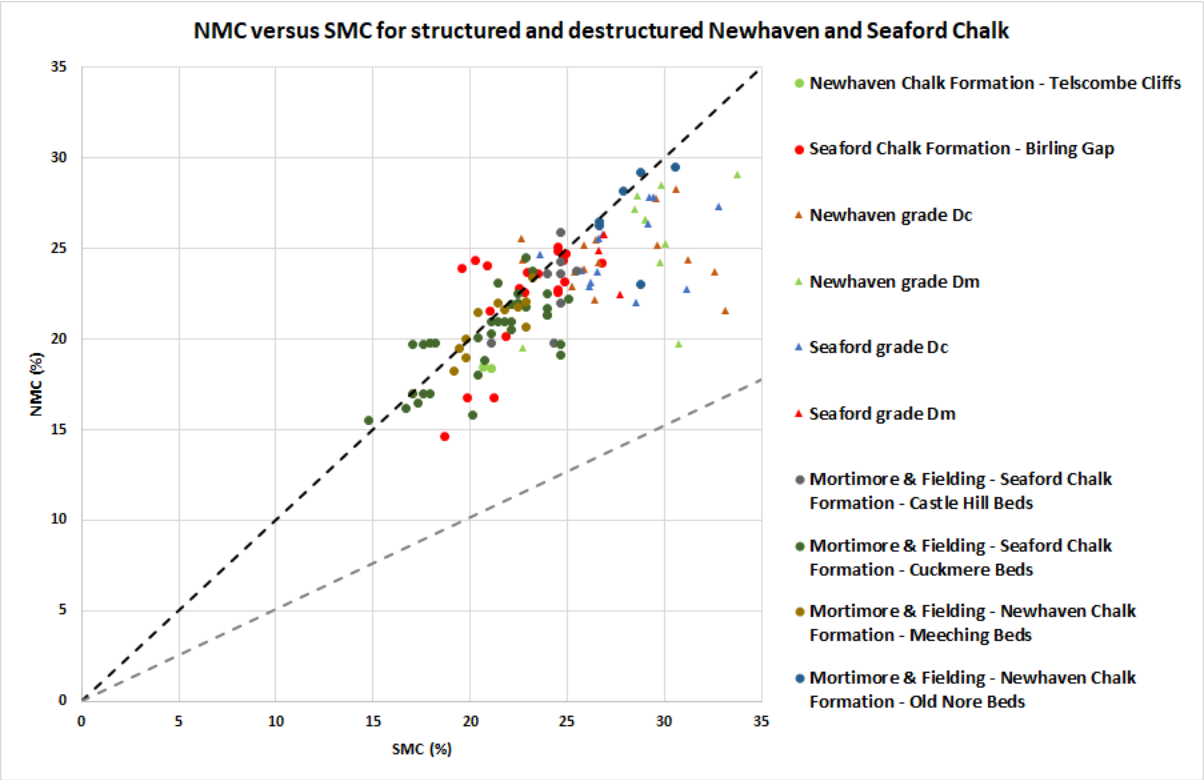
	Average IDD	Min	Max	SD
Lab derived IDD - Seaford Dc	1.54	1.43	1.65	0.06
Equotip derived IDD - Seaford Dc	1.67	1.52	2.64	0.14

App D-11 IDD of D-grade Seaford and Newhaven Chalk;

Sample name	Formation	Grade	IDD
Seaford Dc	Seaford Chalk Formation	Dc	1.57
SeafordDc_22012023	Seaford Chalk Formation	Dc	1.58
SeafordDc_20122022	Seaford Chalk Formation	Dc	1.47
SeafordDc_24092022	Seaford Chalk Formation	Dc	1.51
SCDC4	Seaford Chalk Formation	Dc	1.51
SCDC5	Seaford Chalk Formation	Dc	1.57
SCDC6	Seaford Chalk Formation	Dc	1.57
SeafordDc_24092022	Seaford Chalk Formation	Dc	1.51
SCDC1 UCS	Seaford Chalk Formation	Dc	1.43
SeafordDcUCS_04042023	Seaford Chalk Formation	Dc	1.59
SeafordDcUCS_26102022	Seaford Chalk Formation	Dc	1.65
SeafordDcUCS_16102023	Seaford Chalk Formation	Dc	1.58
SeafordDcBTS	Seaford Chalk Formation	Dc	1.52
Seaford Dm	Seaford Chalk Formation	Dm	1.56
SeafordDm_22112022	Seaford Chalk Formation	Dm	1.54
SeafordDmBTS	Seaford Chalk Formation	Dm	1.57
Newhaven Dc	Newhaven Chalk Formation	Dc	1.50
NewhavenDc_15012023	Newhaven Chalk Formation	Dc	1.50
NewhavenDc_05122022	Newhaven Chalk Formation	Dc	1.48
NewhavenDc_24102022	Newhaven Chalk Formation	Dc	1.59
NewhavenDc_07102022	Newhaven Chalk Formation	Dc	1.57
NHDC4	Newhaven Chalk Formation	Dc	1.47
NHDC5	Newhaven Chalk Formation	Dc	1.58
NHDC6	Newhaven Chalk Formation	Dc	1.57
NHDC1 UCS	Newhaven Chalk Formation	Dc	1.68
NewhavenDcUCS_04042023	Newhaven Chalk Formation	Dc	1.61
NewhavenDcUCS_04042023A	Newhaven Chalk Formation	Dc	1.67
Newhaven Dm	Newhaven Chalk Formation	Dm	1.53
NewhavenDm_11122022	Newhaven Chalk Formation	Dm	1.51
NHDM4	Newhaven Chalk Formation	Dm	1.52
NHDM5	Newhaven Chalk Formation	Dm	1.41
NewhavenDm_17092022	Newhaven Chalk Formation	Dm	1.49
NewhavenDm_07102022	Newhaven Chalk Formation	Dm	1.50
NewhavenDcUCS_15102022	Newhaven Chalk Formation	Dc	1.59
NewhavenDmUCS_15102022	Newhaven Chalk Formation	Dm	1.49
NewhavenDc_15102022	Newhaven Chalk Formation	Dc	1.44
NewhavenDcUCS_16102022	Newhaven Chalk Formation	Dc	1.60
NewhavenDmBTS	Newhaven Chalk Formation	Dm	1.48
NewhavenDcBTS	Newhaven Chalk Formation	Dc	1.43

Moisture content

App D-12 NMC plotted against SMC;



PSD

App D-13 PSD

Newhaven Dm		Seaford Dc	
Sieve size (mm)	% passing	Sieve size (mm)	% passing
15	100	15	100
10	83.47	10	72.29
8	81.94	8	69.82
6.3	78.23	6.3	66.34
4.75	74.41	4.75	60.56
2.36	65.93	2.36	55.59
2	64.96	2	53.96
1.18	60.24	1.18	47.44
0.6	56.86	0.6	42.76
0.425	55.13	0.425	40.48
0.212	52.47	0.212	38.09
0.15	50.67	0.15	37.09
0.063	44.60	0.063	35.07

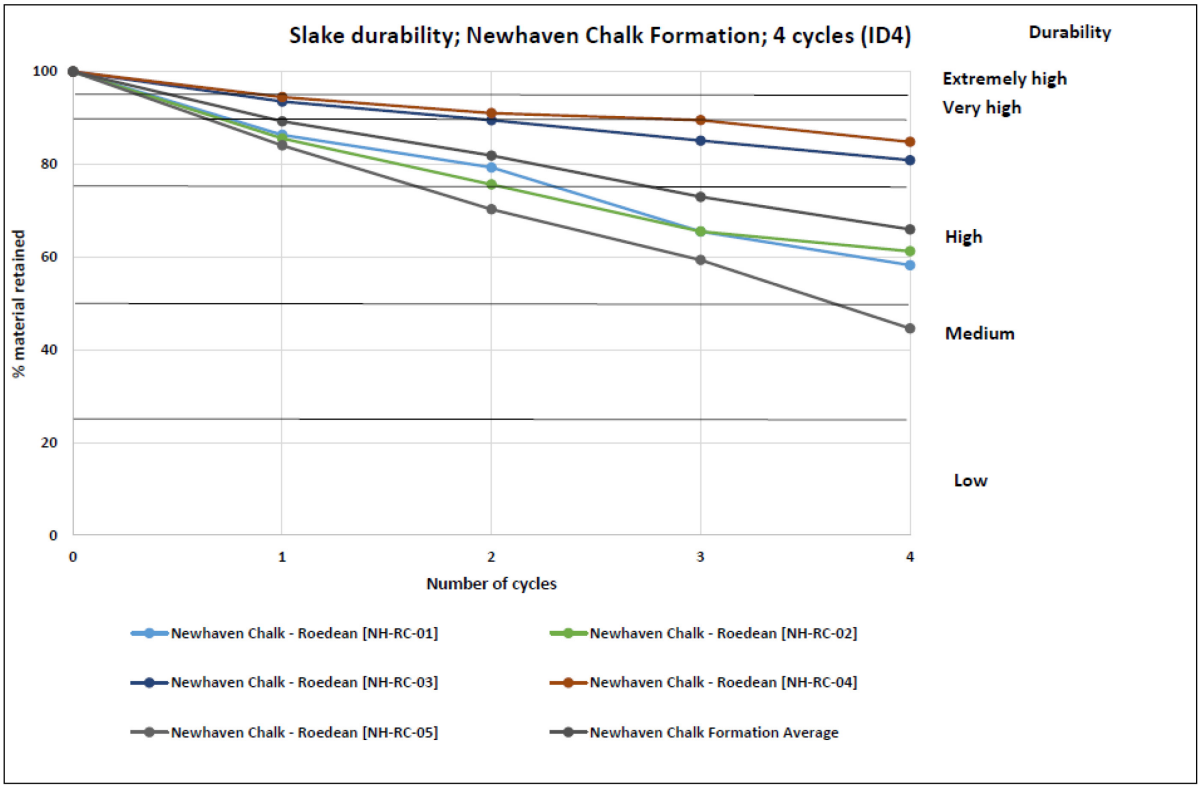
App D-14 PSD Newhaven chalk

NewhavenDm_24102022		**132.07g = dry core weight**	**1% = 1.32**
Sieve size (mm)	**Weight retained (g)**	**Percentage retained**	**Percentage passing**
10	21.82	16.53	83.47
8	2.02	1.53	81.94
6.3	4.9	3.71	78.23
4.75	5.04	3.82	74.41
2.36	11.2	8.48	65.93
2	1.29	0.97	64.96
1.18	6.23	4.72	60.24
0.6	4.46	3.38	56.86
0.425	2.29	1.73	55.13
0.212	2.52	2.66	52.47
0.15	2.38	1.8	50.67
0.063	8.02	6.07	44.6
	73.17	55.4	44.6

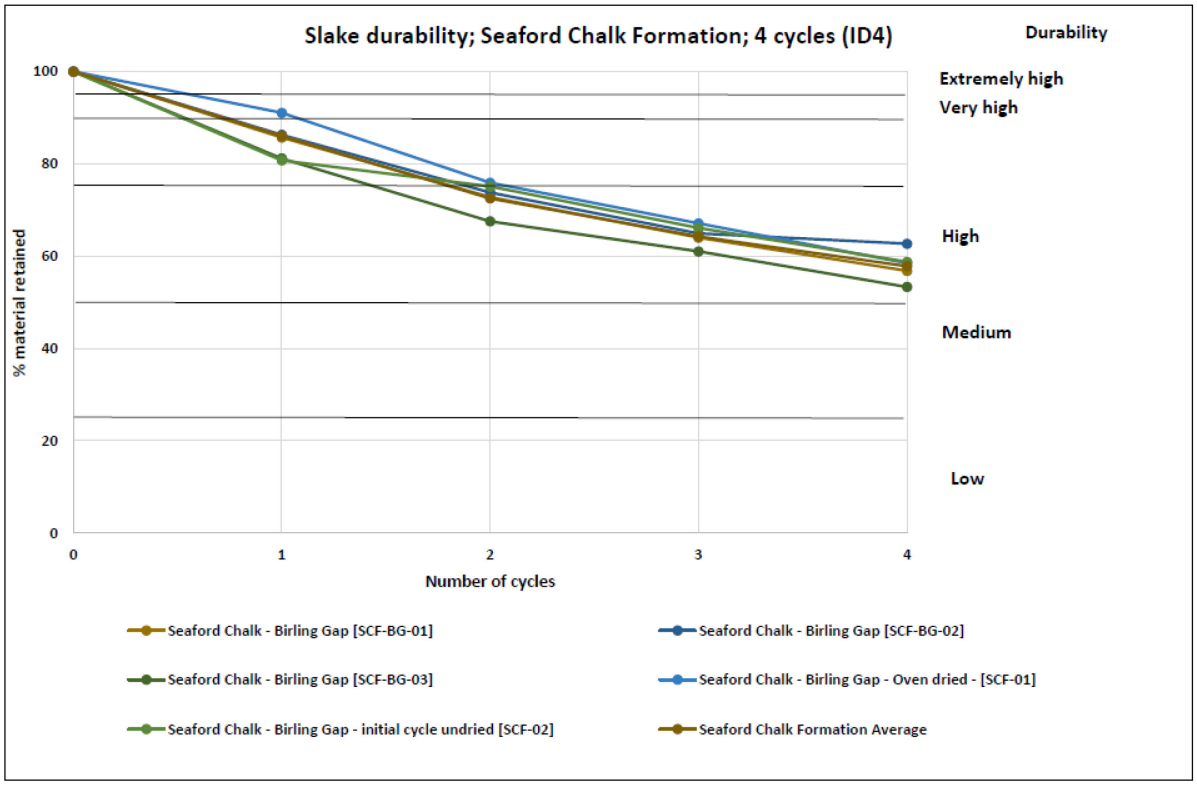
SeafordDc - Sample 2		**98.28g = dry core weight**	**1% = 0.98**
Sieve size (mm)	**Weight retained (g)**	**Percentage retained**	**Percentage passing**
10	21.28	27.71	72.29
8	2.42	2.47	69.82
6.3	3.41	3.48	66.34
4.75	5.67	5.78	60.56
2.36	4.88	4.97	55.59
2	1.6	1.63	53.96
1.18	6.39	6.52	47.44
0.6	4.59	4.68	42.76
0.425	2.24	2.28	40.48
0.212	2.35	2.39	38.09
0.15	0.98	1	37.09
0.063	1.98	2.02	35.07
	57.79	64.93	35.07

Appendix E - Slake durability

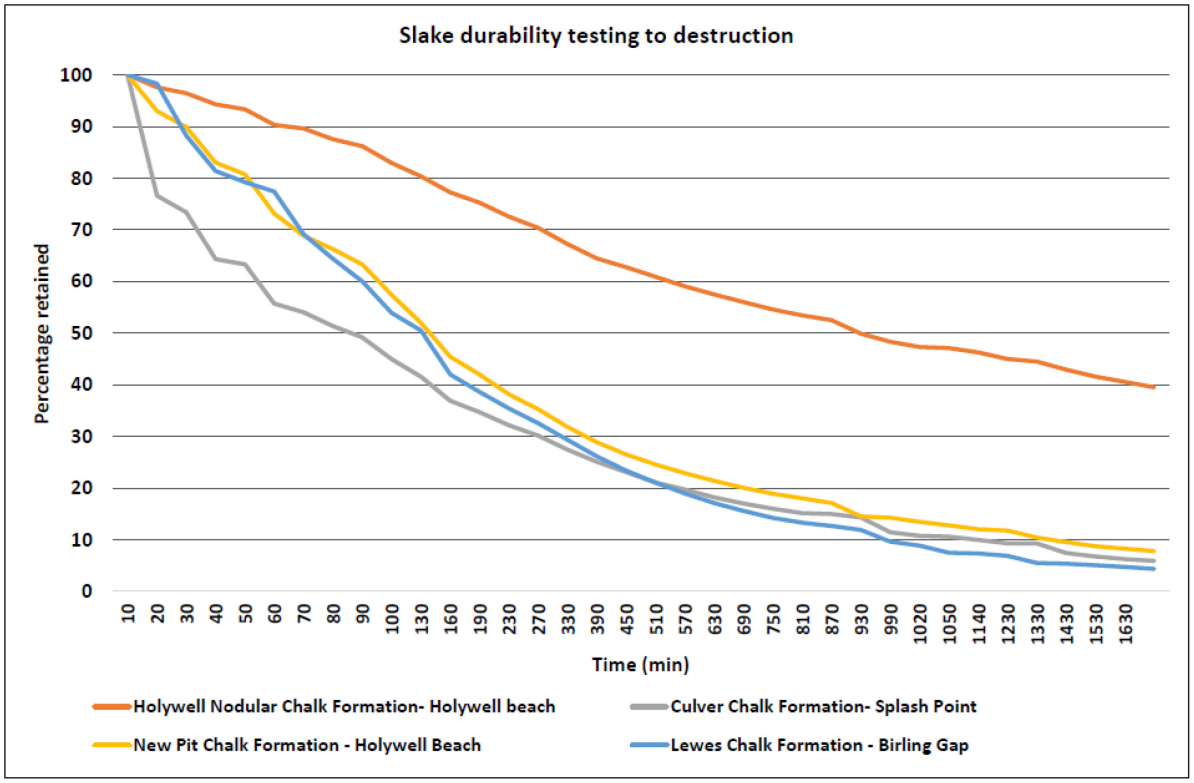
App E-1 Plot of I_d4 cycles for Newhaven structured chalk;



App E-2 Plot of I_d4 cycles for Seaford structured chalk;

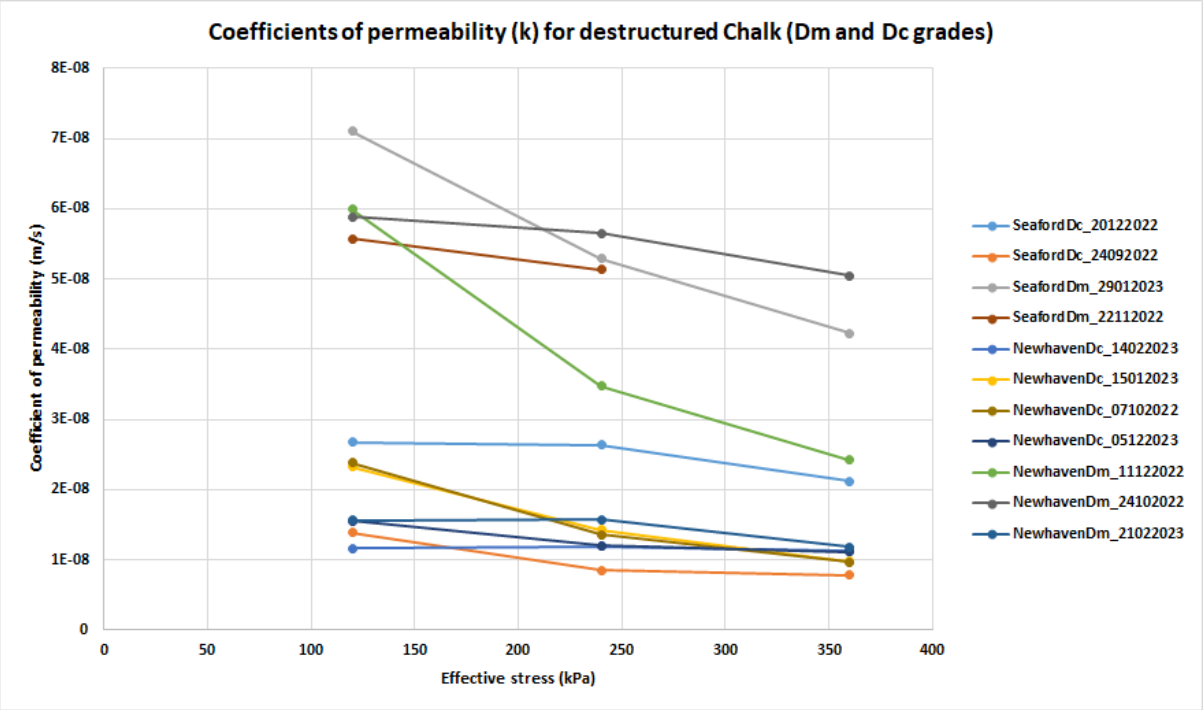


App E-3 Slake durability to destruction over time;



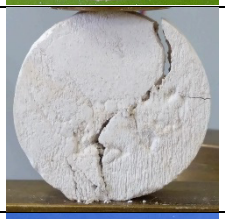
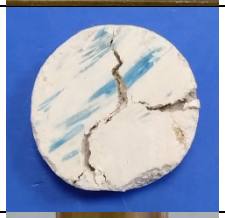
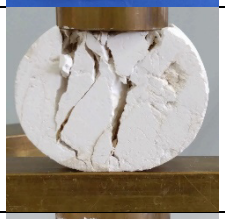
Appendix F - Permeability

App F-1 Plot of individual permeability tests;

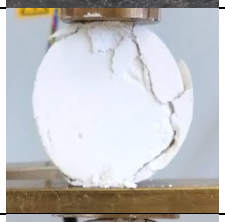
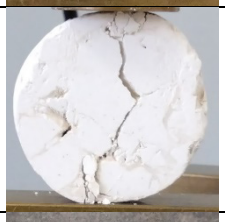
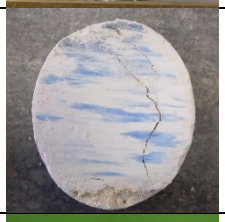


Appendix G - Brazilian tensile testing

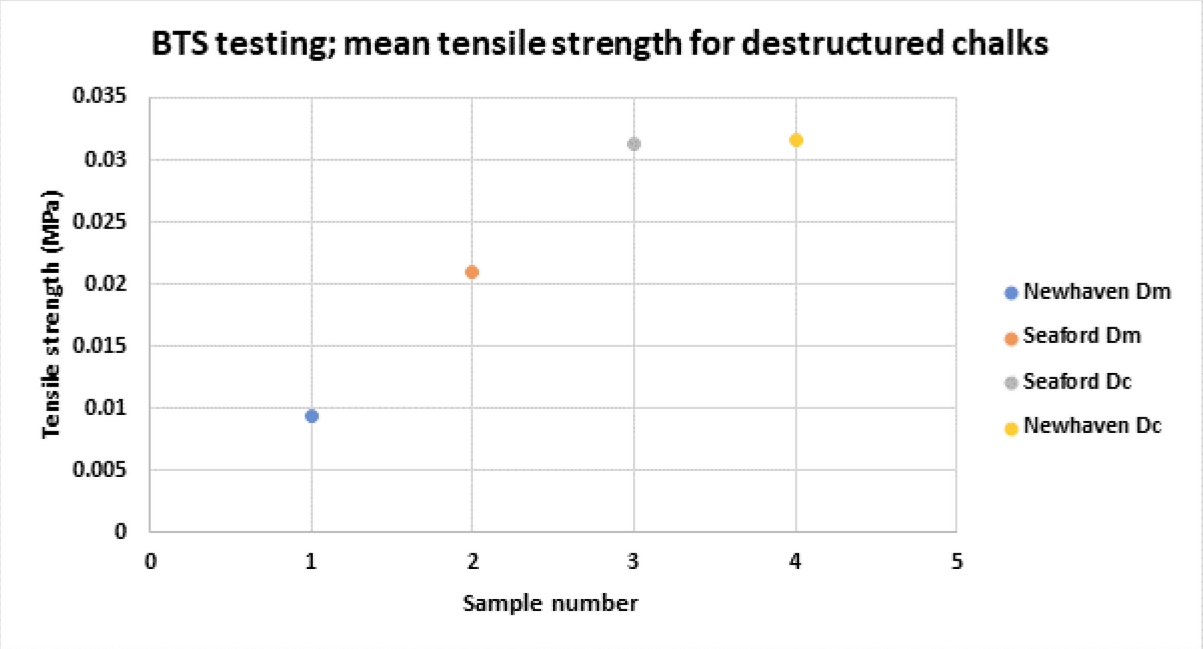
App G-1 Dm grade Seaford and Newhaven chalk;

Sample	MC %	IDD (Mg/m^3)	Tensile strength (MPa)	Fracture pattern
NewhavenDm - Sample 1 NMC	18.1	1.23	0.04	
NewhavenDm - Sample 2 Desiccated	20.6	1.23	0.05	
NewhavenDm - Sample 3 Desiccated	18.23	1.23	0.06	
SeafordDm - Sample 1 NMC	24.36	1.57	0.06	
SeafordDm - Sample 2 Desiccated	23.31	1.57	0.05	
SeafordDm - Sample 3 Desiccated	21.33	1.57	0.04	

Dc grade Seaford and Newhaven chalk;

Sample	MC %	IDD (Mg/m^3)	Tensile strength (MPa)	Fracture pattern
SeafordDc - Sample 1 NMC Desiccated	21.54	1.13	0.05	
SeafordDc - Sample 2 Desiccated	23.50	1.13	0.31	
SeafordDc - Sample 3 Desiccated	22.25	1.13	0.04	
NewhavenDc - Sample 1 NMC	20.92	1.35	0.09	
NewhavenDc - Sample 2 Desiccated	20.84	1.35	0.09	
NewhavenDc - Sample 3 Desiccated	20.58	1.35	0.11	

App G-2 Mean tensile strengths of D-grade Seaford and Newhaven Chalk;



Appendix H - SEM Analysis

App H-1 SEM analysis

To elucidate and make observations of the microstructure of chalk, SEM techniques were applied, followed by image processing techniques. This Appendix describe the equipment and procedure for making observations and analyses, as well as results.

Sampling

Sampling of material for SEM analysis was undertaken on a regional scale to reflect as many Formations within the Southern Chalk Province framework as possible. A detailed itinerary of samples is provided in Table H-1.

Table H-1 Sample locations for SEM analysis.

Formation	Location	Grid
Culver Chalk Formation	Splash Point, Seaford	548807, 98204
Newhaven Chalk Formation	Roedean Access Point, Roedean	534618, 103106
Seaford Chalk Formation	Birling Gap, East Dean	555318, 96034
Lewes Chalk Formation	Foyle Way, Holywell	559975, 96901
New Pit Chalk Formation	Beachy Head, East Sussex	558713, 95597
Holywell Nodular Chalk Formation	Holywell Beach Promenade, Holywell	560321, 97232
Zig Zag Chalk Formation	Falling Sands, Beachy Head	559197, 95525
West Melbury Marly Chalk Formation	Falling Sands, Beachy Head	559340, 95518

Samples were collected from Roedean Access Point for Newhaven Chalk and Birling Gap for Seaford Chalk. At Roedean, the chalk was sampled down a chalk cliff section, with CIRIA weathering grade differing with depth, while at Birling Gap, chalk sampled across a weathered valley.

The material was collected in the field in small cobble sized lumps of chalk. The samples are wrapped twice in aluminium foil (to retain natural moisture content), labelled, and then wrapped in cellophane or zip-lock bags, where permissible.

Equipment and software

To undertake scanning electron microscopy and acquisition of images, a Hitachi TM4000Plus tabletop scanning electron microscope (SEM) is used to undertake observations (Figure I-1).

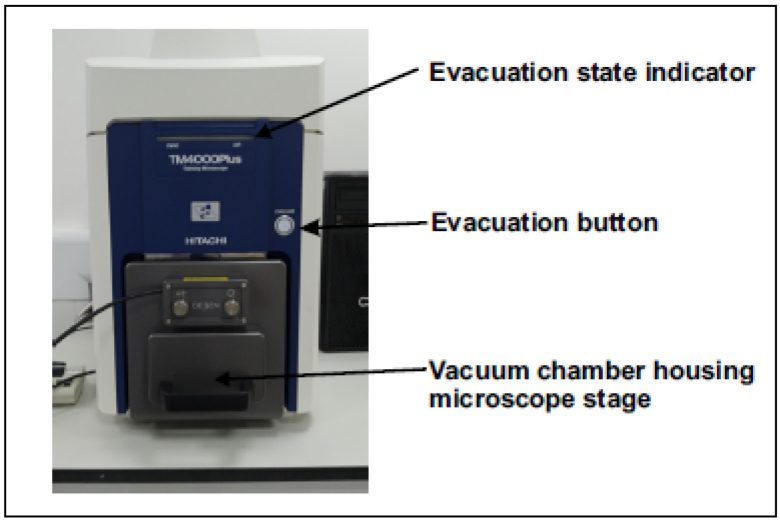


Figure I-1 Hitachi TM4000Plus Scanning electron microscope.

Further analysis of the acquired images is undertaken using image processing software; ImageJ, which allow image manipulation and quantification of objectives within the images.

Sample preparation

Samples must be desiccated prior to use as the SEM undertakes imaging within a vacuum.

1. Oven dry sample for a period of 24 hours.
2. Break the sample to a sufficiently small size to be mounted upon SEM specimen stubs.
3. Take an aluminium specimen stub and place a carbon adhesive disk onto the objective stage.
4. Fix sample to the carbon adhesive disk on the specimen stub.
5. Place the specimen stub in the specimen holder and height gauge, adjust the specimen holder to the correct clearance.

Image processing

Chalk was characterised using the following criteria, informed by the approach of previous authors;

- Coccoliths – quantity and size.
- Disaggregated coccoliths – number and length of long axes of grain.
- Appearance of pore space.
- Binarization of SEM images and quantification of interpreted pore space.
- Inclusion and interpretation of clay minerals.
- Inclusion and interpretation of other minerals (such as halite).

ImageJ analysis

The use of ImageJ allows image processing of SEM micrographs. Methods used for this include

- Sharpening of micrograph images.
- Removal of noise from images.
- Adjustment of contrast and brightness.
- Binarisation and segmentation of images for the estimation and inference of porosity.
- Manual point counting of grains.
- Measurement of objectives within micrographs.

SEM analysis results

Scanning electron microscopy was employed to evaluate if weathering could be identified within the microtexture of a chalk, then linked to weathering grade In terms of microtexture mapping, each formation was analysed, with the exceptions of the Portsdown Chalk Formation. A methodology is presented in earlier in Appendix H. The Lewes Nodular Chalk was analysed but there was significant halite growth which obscured the matrix, rendering this analysis incomplete. Microtexture was defined by a threshold porosity estimation, coccolith character, grain dimension characteristics, fabric, grain habit and contact character. It was not possible to correlate CIRIA grading with microtexture, however it was possible to discern textural differences between each chalk formation. A summary of microtexture mapping is given in Tables H-2 and H-3.

The formation with the highest estimated porosity using image processing software was the Seaford Chalk at 29.77% (Table H-2 column C), while the lowest porosity was the West Melbury Chalk at 20.01% (Table H-3 column C). The Newhaven Chalk had an estimated porosity of 28.70% (Table H-2 column C).

Coccolith character varies across the formation, with some formations having more well preserved coccoliths than others. The Newhaven Chalk Formation displays well-preserved *Prediscosphaera cretacea (*or *spinosa)* coccoliths, while the Seaford Chalk has more disarticulated, poorly preserved coccoliths, whose taxa are not readily identifiable.

In terms of grain dimensions, the West Melbury Chalk has the greatest estimated number of grains within the field of view at 799, with a mean grain length of 1.88 µm. The Culver Chalk Formation has the lowest number of grains within the field of view at 330, with a mean grain length of 2.93 µm. The Newhaven Chalk had an estimated 596 grains, with a mean grain length of 2.10 µm, while the Seaford Chalk had an increased number of estimated grains at 764, with a smaller mean grain length of 1.95 µm.

Newhaven Chalk fabric character was observed to have vuggy pore space distribution. The ground mass was highly bioclastic with well-preserved coccoliths and spines that appear poorly cemented.

The Seaford Chalk fabric was characterised as vuggy, with angular pore spaces (<1.5 μm) in areas. The groundmass comprised relatively large $CaCO_3$ grains, disaggregated coccoliths and smaller overgrowths. Grains for both formations were generally euhedral, with punctic contacts and some evidence of suturing.

Table H-2 Microtexture index table 1.

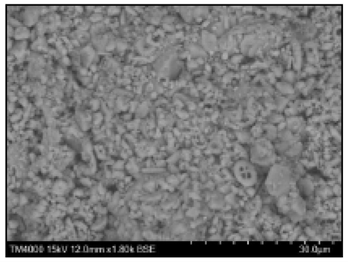
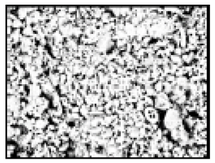
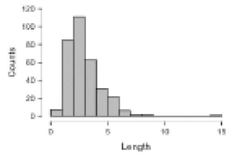
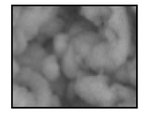
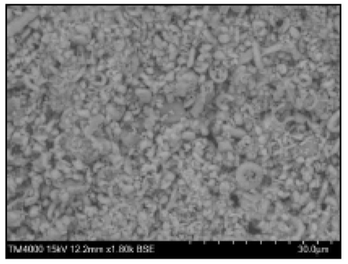
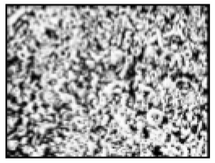
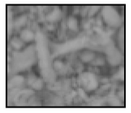
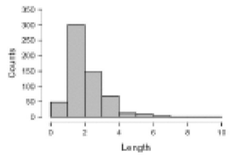
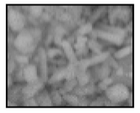
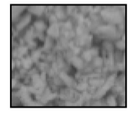
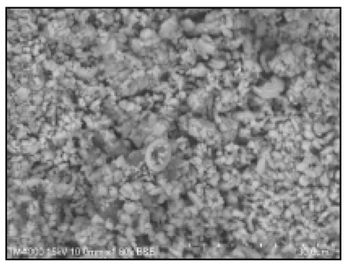
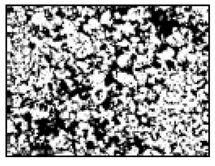
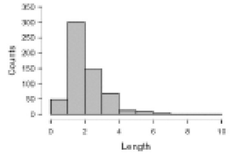
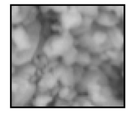
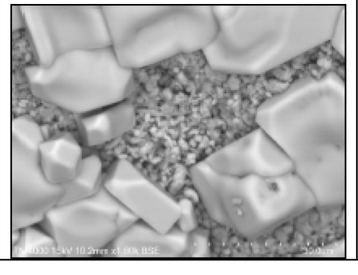
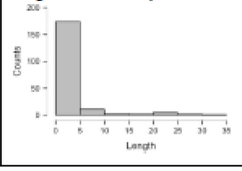
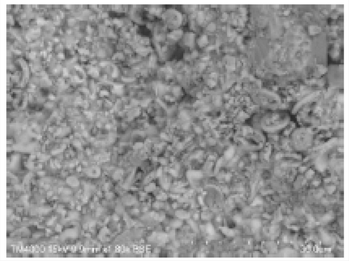
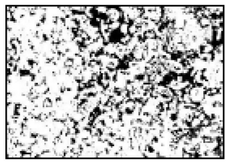
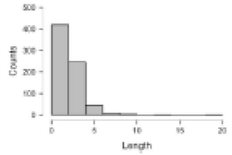
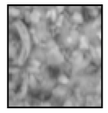
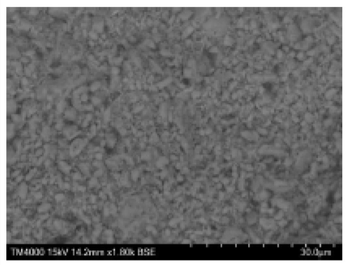
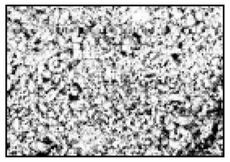
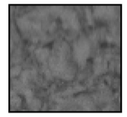
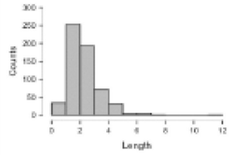
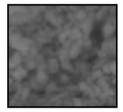
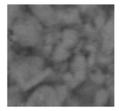
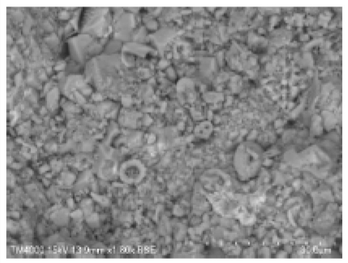
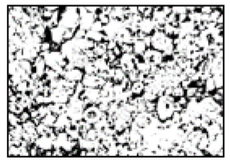
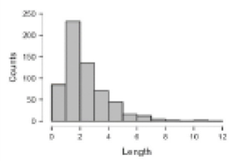
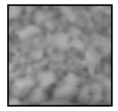
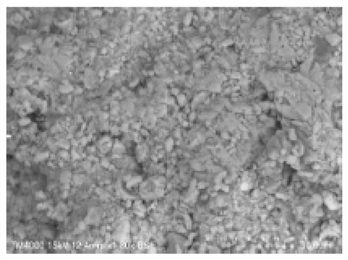
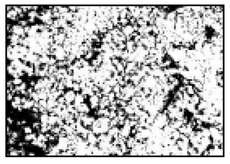
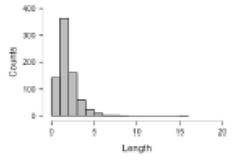
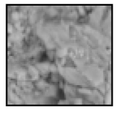
Formation (a)	Micrograph (b)	Threshold estimate of porosity % (c)	Coccolith character (d)	Grain dimension character (e)	Fabric character (f)	Grain habit (g)	Contact character (h)
Culver Chalk Formation		23.36 	Moderately well preserved, some disaggregated. 6 whole *Prediscosphaera cretacea (*or *spinosa)* placolith observed (elliptical, cruciform crossbars) < 6 µm. 	Number of grains – 330. Distribution – Unimodal, normal. Mean grain length – 2.93 µm Standard deviation – 1.54 Range – 0.76 – 14.35 µm 	Semi-vuggy; some voids, not consistent over micrograph. 	Some euhedral, relatively large grains (< 6 µm long axis), sitting within a matrix comprising amorphous, anhedral sub-spherical grains (< 1 µm), sporadic occurrence of acicular grains, disaggregated and whole coccoliths (< 7 µm long axis).	Punctic contacts – defined, with little coalescence. or sutured contacts. 
Newhaven Chalk Formation		28.7 	Well preserved coccoliths. 7 whole *Prediscosphaera cretacea (*or *spinosa)* placolith observed, elliptical with cruciform crossbars and preservation of coccolith spine(s), < 9 µm. 	Number of grains – 596 Distribution – Unimodal, normal. Mean grain length – 2.10 µm Standard deviation – 1.13 Range – 0.38 – 9.03 µm 	Vuggy pore space distribution. Highly bioclastic with well-preserved coccoliths and spines. Poorly cemented, resembling an assemblage of ovoid and acicular grains, with coccoliths. 	Largely sub-angular re-precipitated CaCO3 grains (< 8 µm), some acicular grains (< 6 µm in length). Well preserved coccoliths (< 6 µm).	Punctic contacts - little evidence of coalescence or suturing. 
Seaford Chalk Formation		29.77 	Poor preservation of coccoliths; 1 whole coccolith observed, elliptical in morphology but obscured by re-precipitated calcite – taxa not identifiable. 	Number of grains – 764 Distribution – Unimodal, normal. Mean grain length – 1.95 µm Standard deviation – 1.11 Range – 0.14 – 9.88 µm 	Vuggy. Large angular pore spaces (< 1.5 µm) in areas. Groundmass comprises large CaCO3 grains, disaggregated coccoliths and smaller overgrowths, appearing fine-grained. 	Larger CaCO3 grains are sub-angular to spherical (< 5-6 µm), while disaggregated coccoliths are < 3 µm. Significant CaCO3 overgrowths on the surface of larger calcite grains and coccoliths are 0.5 – 1.5 µm, with a tabular to cubic habit, with well-defined angles.	Punctic contacts with little evidence of coalescence or suturing. 
Lewes Chalk Formation		Not possible due to significant NaCL overgrowth. 	Absence of whole coccoliths – some disaggregated coccoliths observed. Taxa not identifiable. 	Number of grains – 198. Distribution – Bimodal – large NaCL crystals. Mean grain length – 3.35 µm Standard deviation – 5.22 Range – 0.60 – 30.33 µm 	Non-vuggy, bimodal groundmass; large halite grains, with fine CaCO3 ground mass. 	Characterised by relatively large, euhedral, cubic to dodecahedral grains, observed to be growing out of the groundmass < 30 µm). Ground mass comprises acicular, rather like grains, sub-angular to spherical CaCO3 grains and disaggregated coccoliths (< 3 µm).	Contacts are generally long lined and punctic – defined with little coalescence or suturing. 

Table H-3 Microtexture index, table 2.

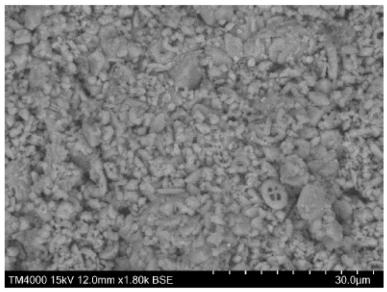
Formation (a)	Micrograph (b)	Threshold estimate of porosity % (c)	Coccolith character (d)	Grain dimension character (e)	Fabric character (f)	Grain habit (g)	Contact character (h)
New Pit Chalk Formation		25.39 	Moderate preservation of coccoliths; 4 whole coccoliths observed, obscured by re-precipitated calcite. Taxa not identifiable. 	Number of grains – 723. Distribution – Unimodal, normal. Mean grain length – 2.15 µm Standard deviation – 1.49 Range – 0.08 – 18.37 µm 	Vuggy in areas. Grains appear cemented. 	High observable degree of bioclastic grains comprising whole and disaggregated coccoliths, with some alteration to their definition (< 6 µm). The underlying groundmass appears coalesced or cemented by reprecipitated CaCO3.	Some large areas of re-precipitated CaCO3. Contacts appear poorly defined and coalesced. 
Holywell Nodular Chalk Formation		23.68 	Absence of whole coccoliths, disaggregated particles - taxa cannot be identified. 	Number of grains – 597. Distribution – Unimodal, normal. Mean grain length – 2.25 µm Standard deviation – 1.12 Range – 0.16 – 11.28 µm 	Groundmass is fine grained and densely packed, with small pore spaces – not particularly vuggy. 	Grains vary in size and largely sub-angular to spherical. There is little bioclastic components observed, those that are, have been disaggregated and subsequently altered. Larger re-precipitated grains of CaCO3 are observed growing within the groundmass.	Grain contacts are interlocked and long, but fuzzy and poorly defined, suggesting coalescence. 
Zig Zag Chalk Formation		21.99 	Moderately well preserved coccoliths; 2 whole coccoliths observed – 1x *Watznaueria Britannica* and 1x *Prediscosphaera cretacea (or spinosa).* Some disaggregated coccoliths preserved. 	Number of grains – 607. Distribution – Unimodal, normal. Mean grain length – 2.38 µm Standard deviation – 1.58 Range – 0.28 – 11.99 µm 	Crystalline grains make up the bulk of the fabric, with groundmass comprising re-precipitated calcite, angular and well formed. Vuggy in areas, pore space is generally tight. 	Relatively large, euhedral re-precipitated calcite < 9 µm. Well defined coccoliths < 7 µm and a component of smaller, granular sub-angular to rounded calcite mineral < 3 µm. Coccoliths are subject to calcite overgrowths.	Some areas of well defined, punctic contacts, while some are coalesced and sutured. 
West Melbury Marly Chalk Formation		20.01 	Disaggregated coccoliths. *Emiliania huxleyi.* < 6 µm. Partial placolith observed. 	Number of grains – 799. Distribution –Unimodal, normal. Mean grain length – 1.88 µm Standard deviation – 1.20 Range – 0.29 – 15.33 µm 	Highly crystalline with lamellar minerals – secondary clay mineral growth. Disaggregated coccoliths observed. Tightly spaced pores, densely packed. 	Underlying secondary clay minerals are lamellar and massive < 15 µm – some microfractures observed within the fabric of these minerals. Some coccoliths are completely altered with secondary calcite granular coatings. Smaller component of calcite grains < 1.5 µm are sub-angular.	Some areas of well defined, punctic contacts, while some are coalesced and sutured. 

SEM analysis summary

- Analysis of microstructure using SEM showed little in terms of weathering, however, it was possible to observe differences between each chalk formation.
- Porosity was estimated for all formations, with the Seaford Chalk having a porosity of 29.77% and the Newhaven Chalk having a porosity of 28.70%.
- Identification of coccolith taxa was possible in samples where preservation was exceptional.

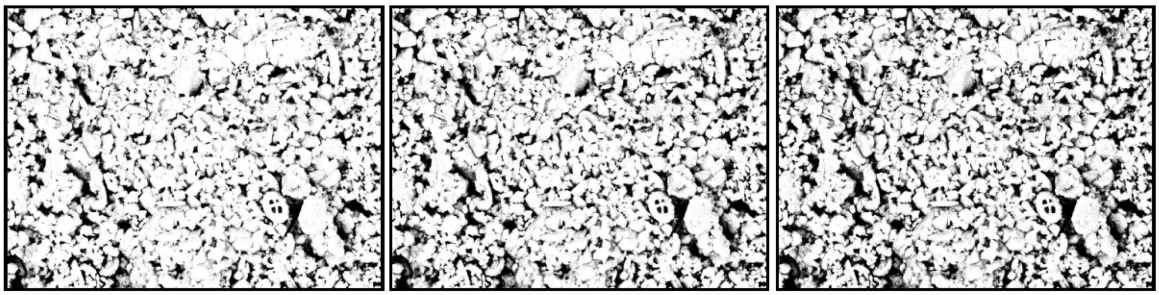
App H-4 Porosity estimation;

Culver Chalk Formation



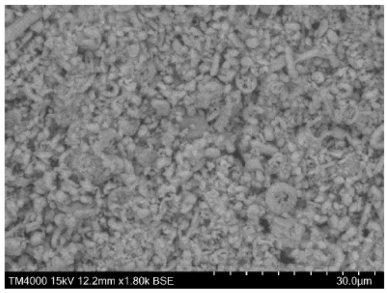
Tarrant Chalk Member of the Basal Culver Chalk Formation
Sampled at Newhaven Harbour, East Sussex
Grid: TV 4404 9999

Porosity estimation via binarisation (thresholding) of SEM images of freshly broken surfaces



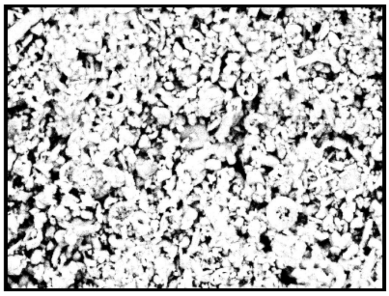
19.59 % **23.59 %** **26.92 %**

Newhaven Chalk Formation

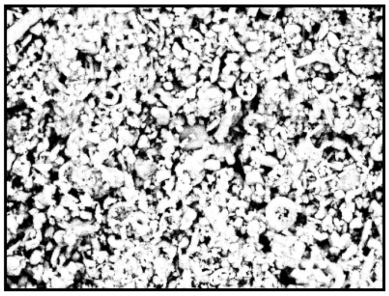


Newhaven Chalk Formation
Sampled at Roedean Café access point, East Sussex
Grid: TQ 3458 0309

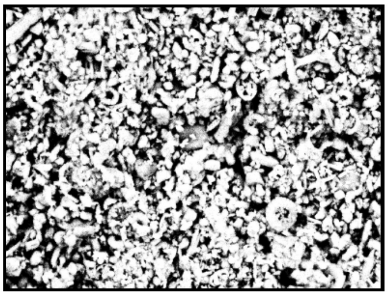
Porosity estimation via binarisation (thresholding) of SEM images of freshly broken surfaces



23.79 %

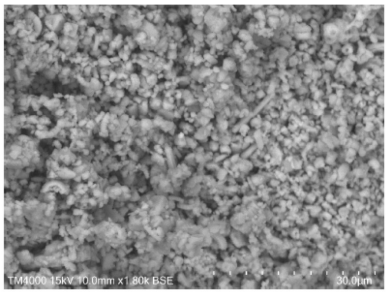


27.28 %



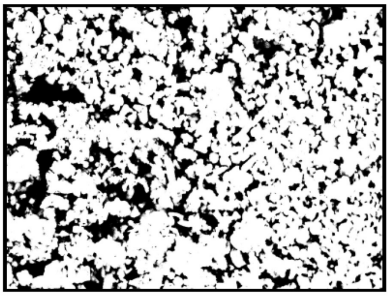
35.04 %

Seaford Chalk Formation

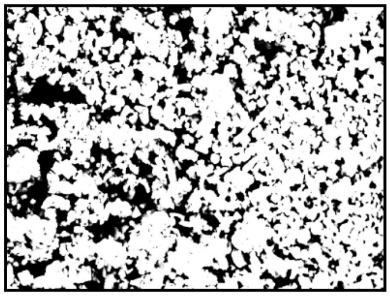


Seaford Chalk Formation
Sampled at Birling Gap, East Sussex
Grid: TV 5528 9609

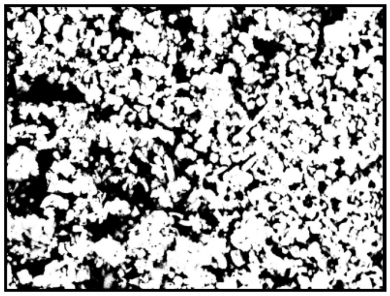
Porosity estimation via binarisation (thresholding) of SEM images of freshly broken surfaces



26.10 %

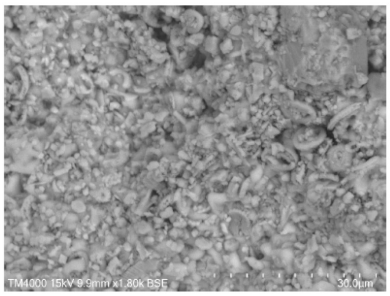


27.73 %



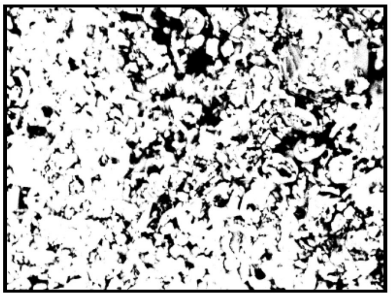
35.49 %

New Pit Chalk Formation

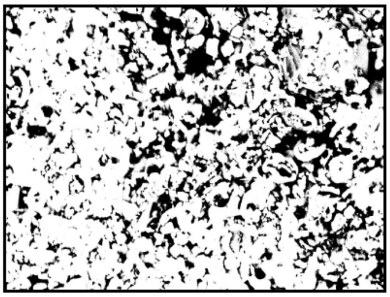


New Pit Chalk Formation
Sampled at Beachy Head, East Sussex
Grid: TV 5927 9561

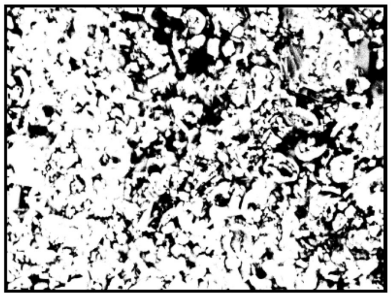
Porosity estimation via binarisation (thresholding) of SEM images of freshly broken surfaces



23.52 %

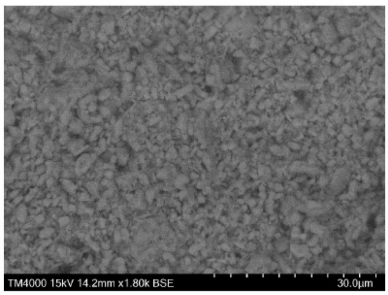


24.56 %



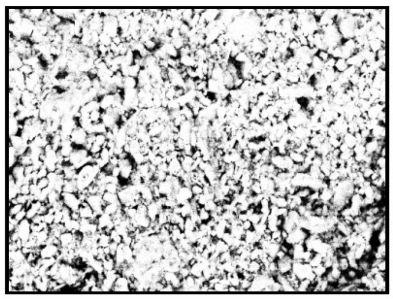
28.09 %

Holywell Nodular Chalk Formation

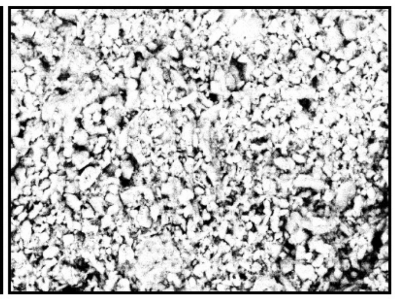


Holywell Nodular Chalk Formation
Sampled at Holywell Beach, East Sussex
Grid: TV 6006 9682

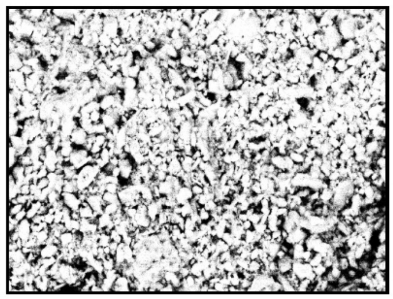
Porosity estimation via binarisation (thresholding) of SEM images of freshly broken surfaces



22.09 %

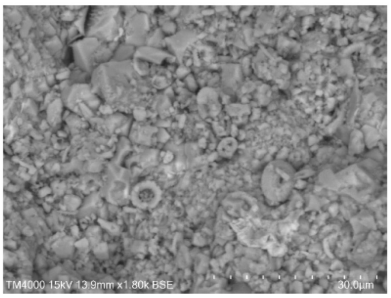


23.61 %



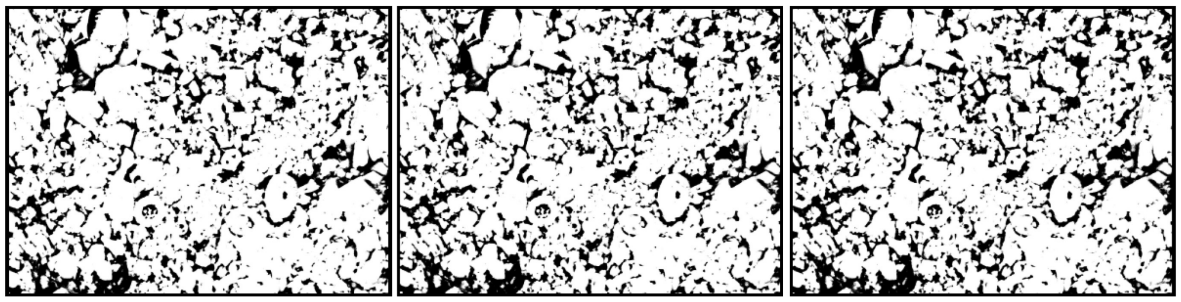
25.36 %

Zig Zag Chalk Formation



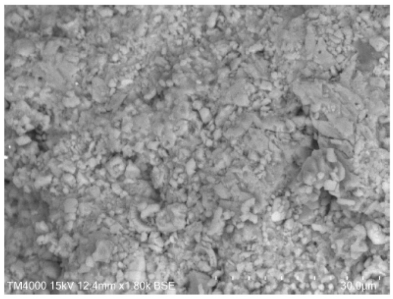
Zig Zag Chalk Formation
Sampled at Falling Sands, East Sussex
Grid: TV 5929 9553

Porosity estimation via binarisation (thresholding) of SEM images of freshly broken surfaces



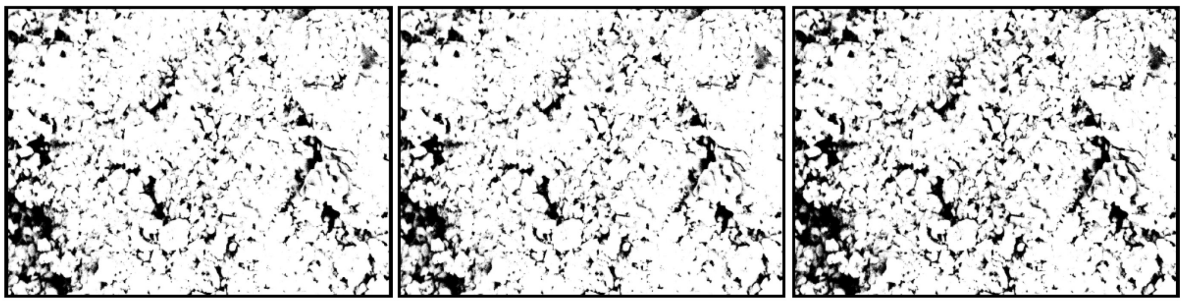
20.35 % 22.48 % 23.44 %

West Melbury Marly Chalk Formation



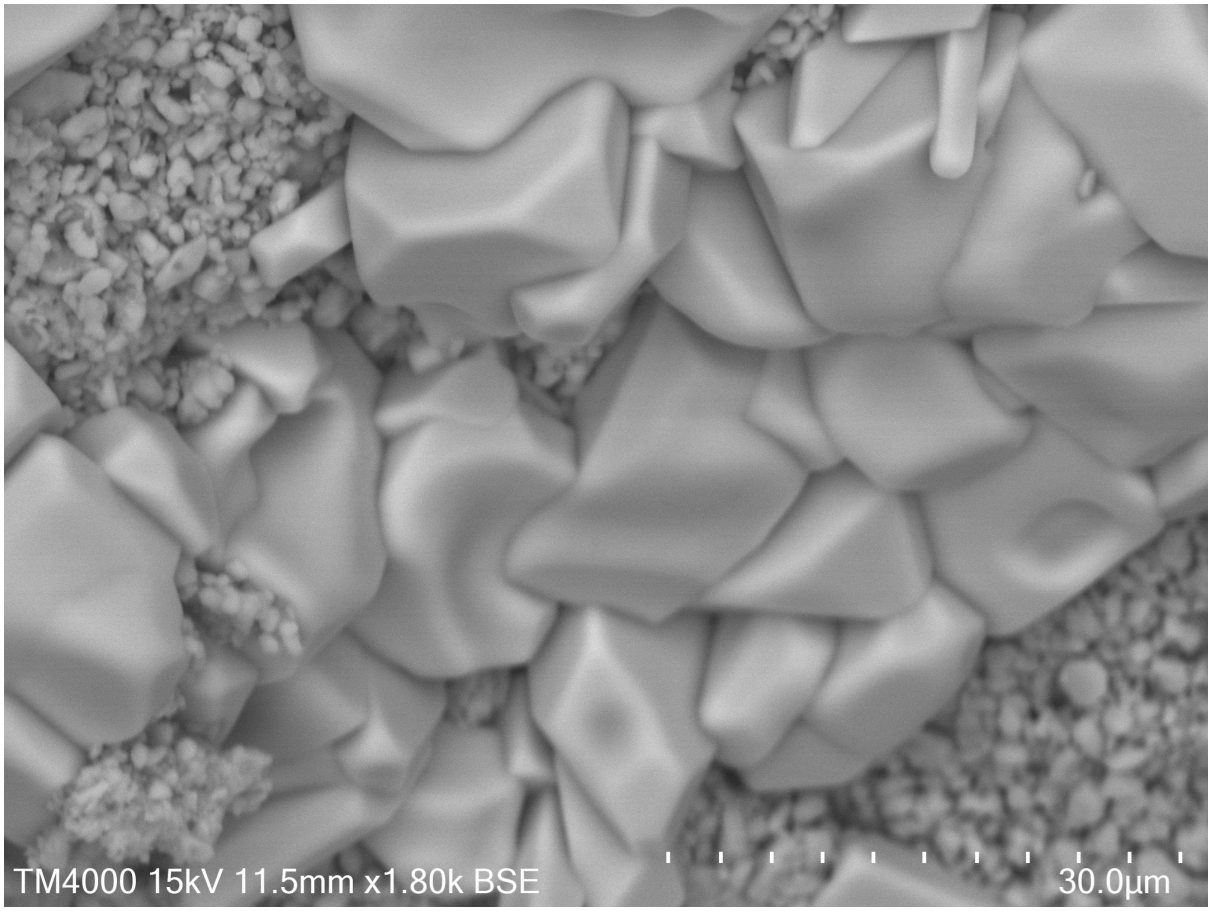
West Melbury Marly Chalk Formation
Sampled at Falling Sands, East Sussex
Grid: TV 5929 9553

Porosity estimation via binarisation (thresholding) of SEM images of freshly broken surfaces



14.13 % 21.37 % 24.55 %

App G-3 micrograph of Lewes Nodular Chalk Formation demonstrating haloclasty;


TM4000 15kV 11.5mm x1.80k BSE
30.0µm

Project 1_Site1_2020-11-24-09-43-06

Sample site

Cliff at base platform level; east of Portobello Outfall access point; below weathered valley

MED – HIGH DENSITY GRADE A CHALK

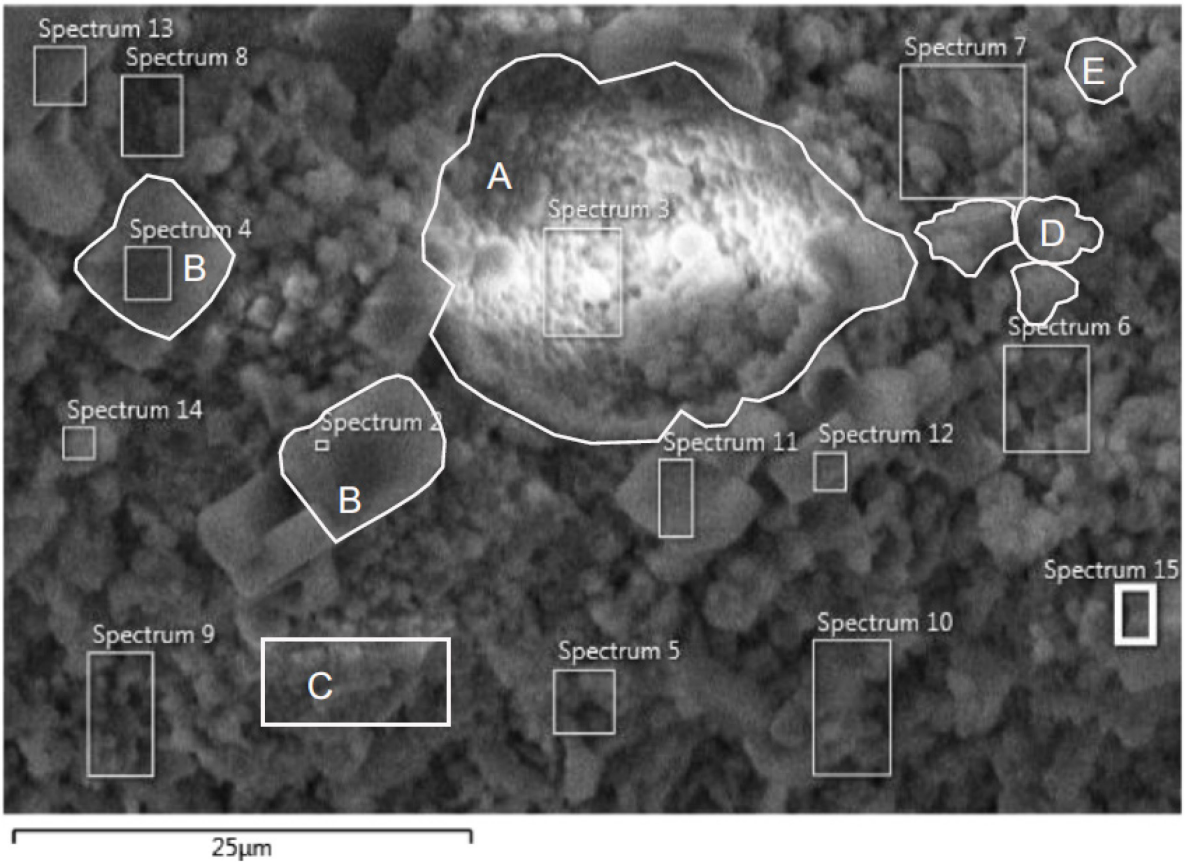
Subject to salt spray and saltwater immersion of the cliff surface by sea water

Analysed at x2000

Description of EDS/SEM plate – [only SEM micrograph available as the EDS image is not of high quality]

Ground mass appears to be flaky and rounded, with little to no discernible coccoliths. Ground mass could be considered granular. There are tabular/cubic, relatively larger crystals, hosted within the ground mass. These are on the scale of approximately 1-8µm. Their cubic habit could be indicative of salt crystals (Na) with provenance from haloclasty.

In the upper centre of the micrograph, there is a semi-circular/hemispherical concave depression within the ground mass. Here, the ground mass is finer with grain on the scale of <2µm. This concave depression is not fully understood, but could be the remnant of a foraminiferal test. Increased lighter areas and contrast indicates electron interference with the microtopography/stereography of the chalk surface.



A – Hemispherical depression; low stereographic relief region, finer ground mass – high electron interference

B – Cubic crystal habit – high Na values; interpreted as haloclasty/salt crystal growth

C – finer ground mass; poorly defined boundaries, high C, Ca and O values, indicative of calcite (either disaggregated coccoliths, reprecipitation or secondary growth)

D – Flaky, poorly defined grains, high C, Ca and O chemical signatures

E – Potentially a poorly defined coccolith

Spectrum 1 – not present

Spectrum 2 – focusses on cubic/tabular mineral previously described; mineral grain/crystal is approximately 5-7µm in the long axis and 2-4µm in the short axis. EDS chemical analysis indicates that this is a salt crystal with Na Wt% of 52.8. O = 17.9Wt%, C = 12.5 Wt%, Ca = 12.1 Wt%, S = 2.5 W%, with minimal values of Fe (0.1 Wt%), Mg (0.5 Wt%) and Si (0.1 Wt%).

Spectrum 3 – focussed on hemispherical depression with high electron interference and fine ground mass. Highest chemical concentrations are Ca (44.8 Wt%), O (39.2 Wt%), C (9.2 Wt%) and Na (5.2 Wt%). The relative %s could be indicative of degradation of $CaCO_3$ to CaO with the loss of CO_2, however more study would be required. The morphology (i.e. the depression) could support this in a physical sense – such as the loss of physical material. A secondary hypothesis is that this is a remnant/artefact of a foraminiferal test, given its size and morphology, with varying degrees of degradation. Minor elements include S (0.7 Wt%), Mg (0.3 Wt%), K (0.3 Wt%) and Al (0.1 Wt%). One outlying feature is that O has a signature of 0.0 Wt% with a standard deviation (S.D.) of 24.7 Wt%.

Spectrum 4 – focussed on a cubic mineral; indicative of a sodium-based crystal. Na (58.8 Wt%), Ca (23.8 Wt%), O (12.8Wt%) and S (3.0 Wt%). Minor chemical elements = Si (1.3 Wt%), K (0.2 Wt%), Al (0.1 Wt%)

Spectrum 5 – focussed on fine, flakey ground mass; high amounts of Ca and O (44.0 and 43.6 Wt% respectively) with C at 9.4 Wt%. Minor chemical constituents of Na (2.0 Wt%), S (0.5 Wt%), Si (0.4 Wt%) and Mg (0.3 Wt%).

Spectrum 6 – 10 focussed on ground mass.

Spectrum 11 – 13 focussed on cubic sodium minerals.

Spectrum 14 – 15 focussed on ground mass.

Interpretation

High values of Ca, O and C were expected given the constituents of chalk. Most spectra corresponded with a chalk with other minor elements. The chemical element wight percentages are not accurate enough for true quantitative analysis as (i) both oxygen and carbon elements/molecules are relatively light and therefore may interfere with the electron beam on an atomic scale and (ii) there would need to be an idealised, actual control sample (i.e. a 'perfect' representative sample of the chalk) to effectively and accurately gauge against. Samples are also broken surfaces and therefore not prepared using a conductive material, making quantitative analysis difficult.

Difficulties in ascertaining/quantifying the % of $CaCO_3$ arise without the use of an acid insolubility test, therefore it is not possible to quantify clay based or silica-based fractions. Chemical constituents likely

to be presented as chemical signatures of clay or silica-based minerals are relatively extremely low, indicating a particularly pure chalk.

There is a distinct lack of observable coccoliths, however these may have lost their distinct morphology due to the chalk being samples physically from the cliff face.

Sample site - Telscombe Cliffs Grade A

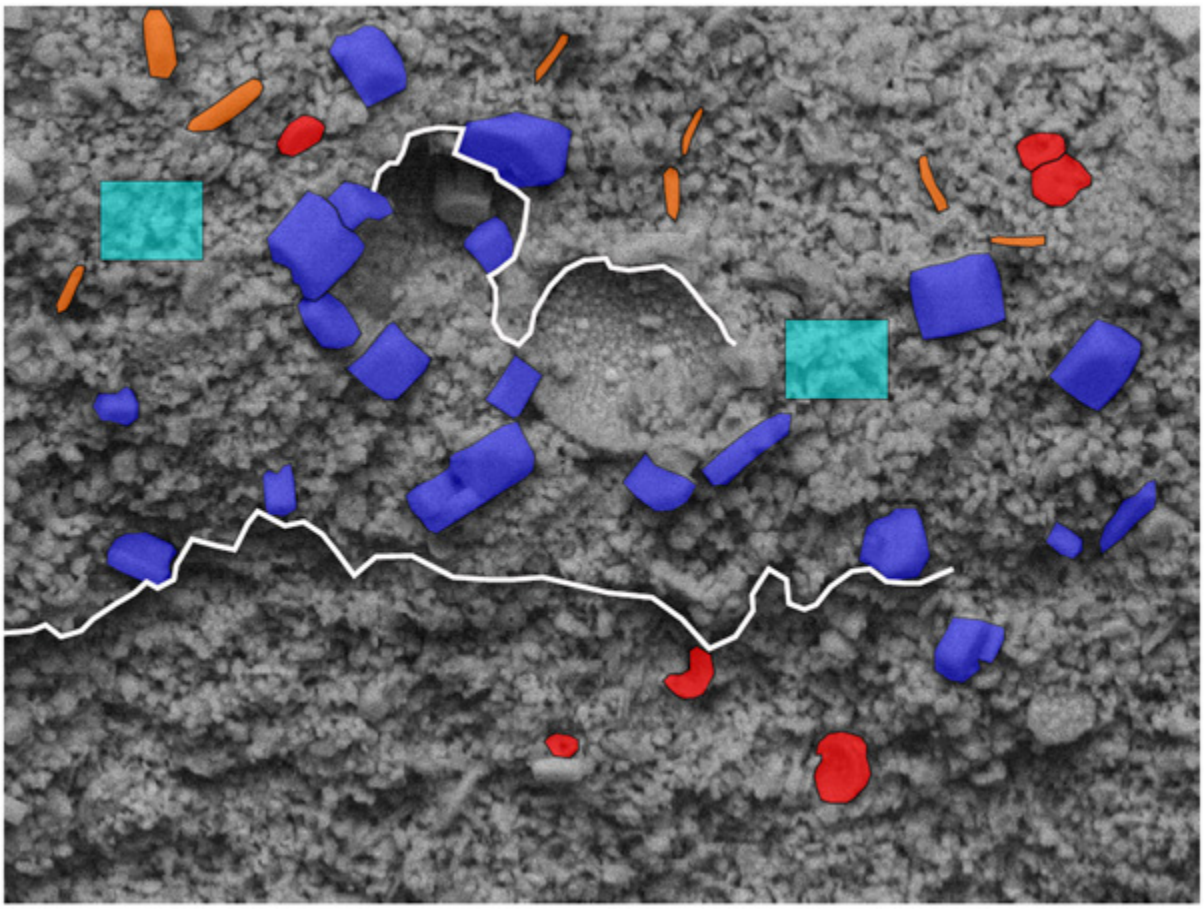
Cliff at base platform level; east of Portobello Outfall access point; below weathered valley

MED – HIGH DENSITY GRADE A CHALK

Subject to salt spray and saltwater immersion of the cliff surface by sea water

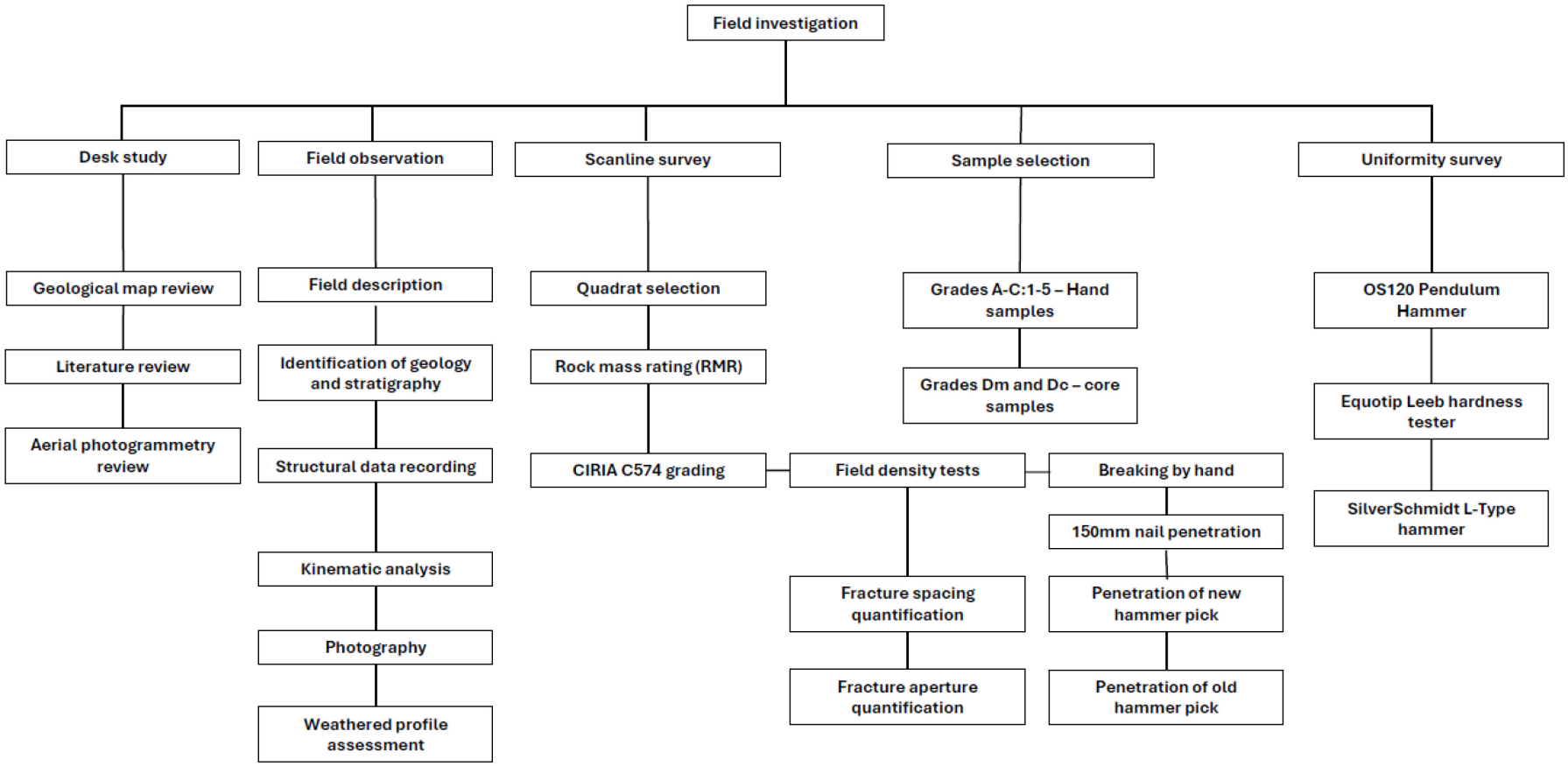
Analysed at x1000

Supplementary image – taken July 2019; No EDS data.

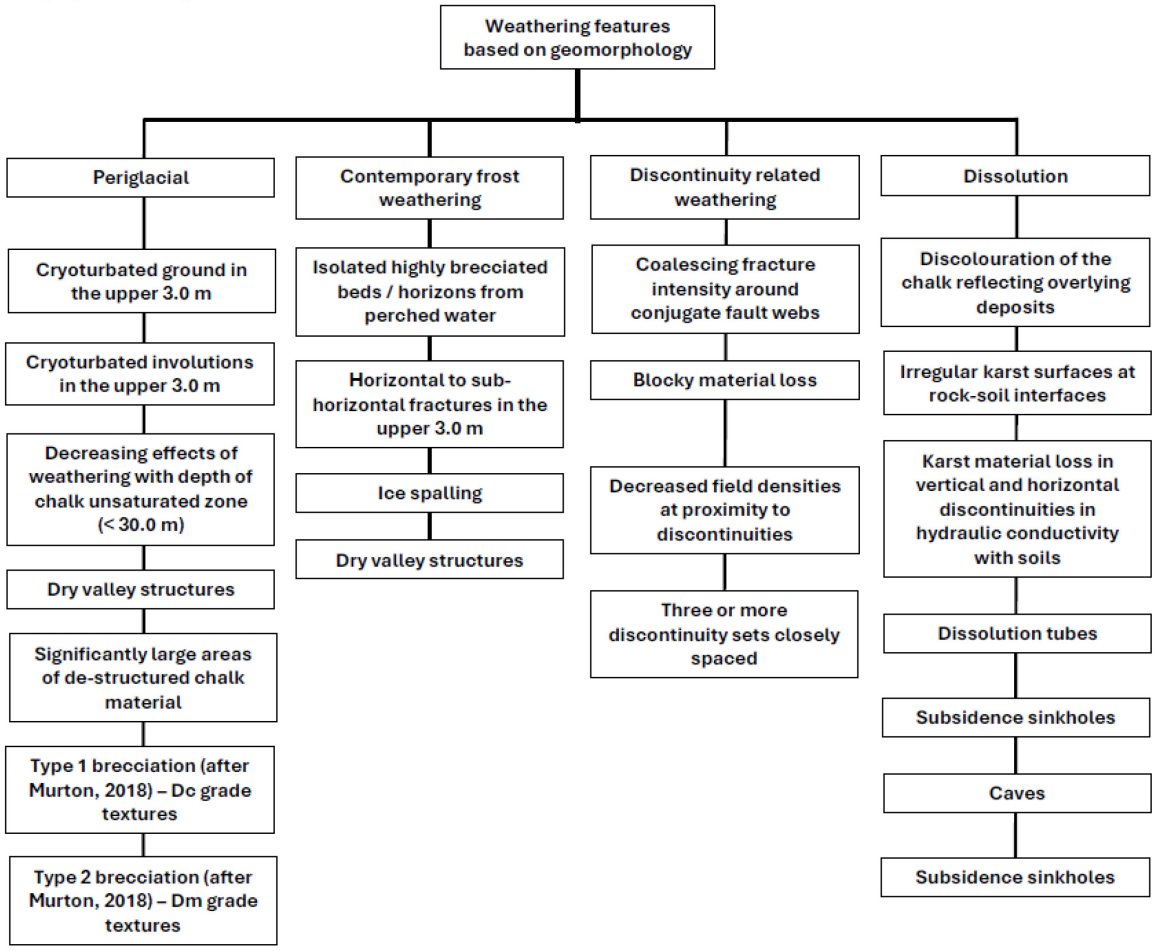


Appendix I – Classification workflows

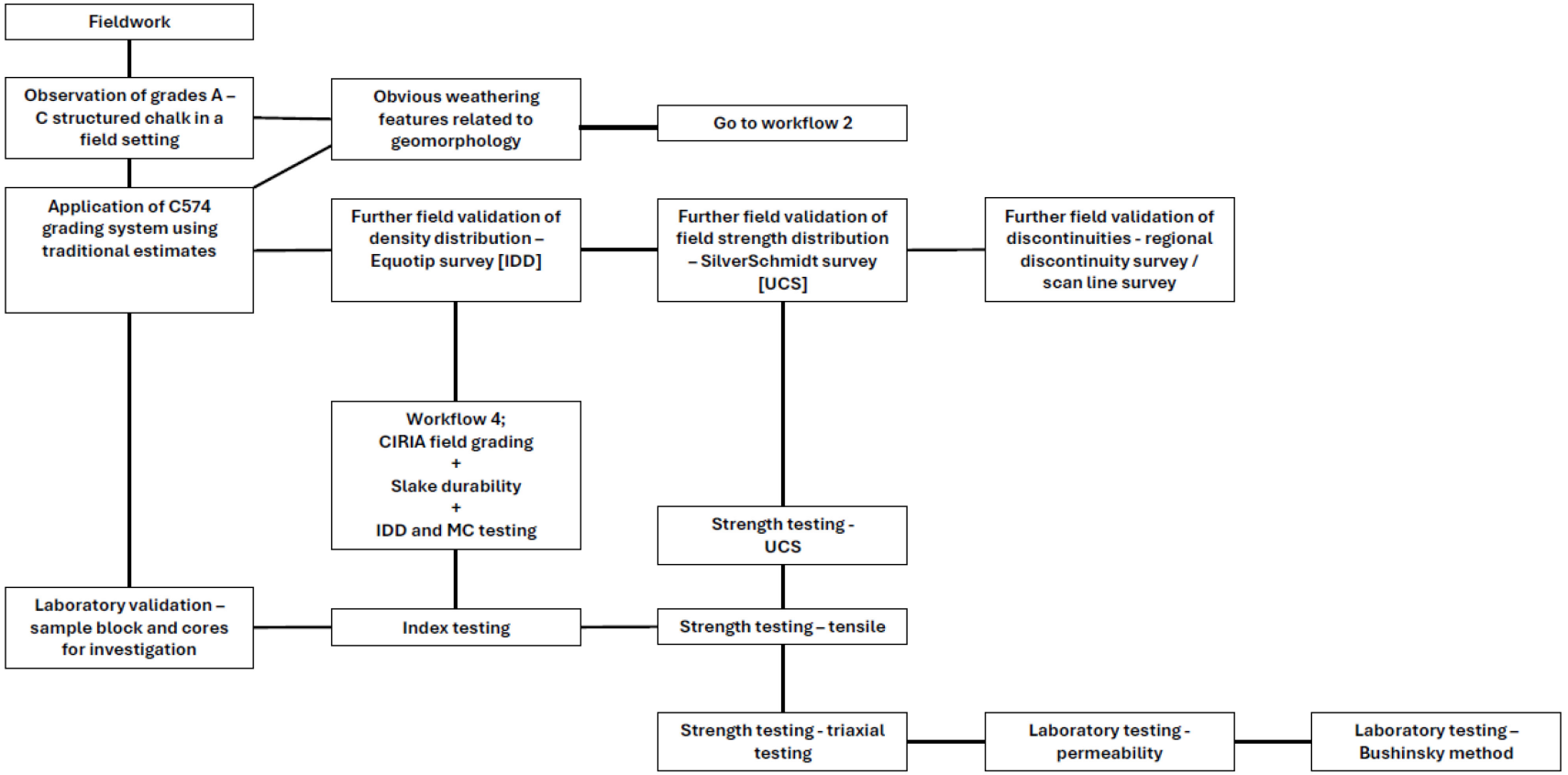
Classification workflow 1 for stages of field investigation into weathering



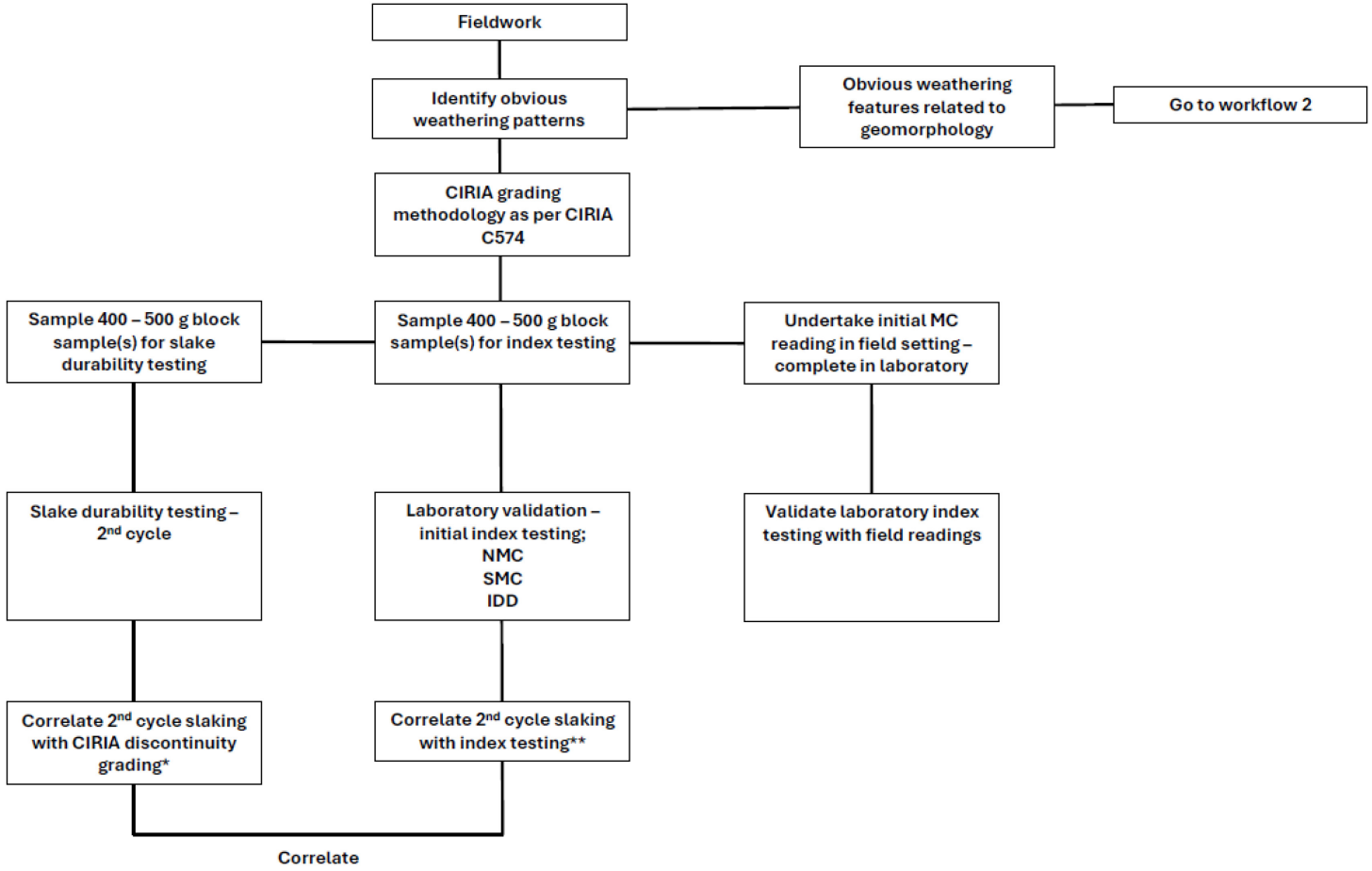
Classification workflow 2 for identifying weathering features



Classification workflow 3 for structured weathered chalk (grades A1 - C5) – If de-structured chalk, go to workflow 5



Classification workflow 4 for use of slake durability and index testing to evaluate / validate grade of weathering



*- Both CIRIA discontinuity spacing grades and CIRIA discontinuity aperture grades are required to be plotted against 2nd cycle slake durability.

** - IDD and index tests should be plotted against Franklin and Chandra's Durability index and CIRIA C574 density grades.

Classification workflow 5 for laboratory work methods to measure de-structured grades of chalk

